An Approach to Mechanical Heart-Lung Interaction

Jon-Emile S. Kenny M.D., M.Sc.

An Approach to Mechanical Heart-Lung Interaction

First Edition

Jon-Emile S. Kenny M.D., M.Sc.

Kenny, JE. An Approach to Mechanical Heart-Lung Interaction. 1st ed. Toronto: Spectral Envelope Publishing House. 2020. pg(s).

Published by Spectral Envelope Publishing House

SE
Publishing
House

325 Front Street W.
4th Floor
Toronto, ON. Canada
M5V 2Y1
se-ph.org

ISBN #: 978-1-7773232-0-2

ISBN 978-1-7773232-0-2
9 781777 323202 >

The typeset is Big Caslon

For Mum & Dad

“Does the ‘knowledge’ of pre-reflective self-consciousness really know?”

-Emmanuel Levinas

Foreword

I initially wrote the first 8 chapters of this book in the final year of my pulmonary & critical care medicine fellowship. Each chapter was composed before I recorded its corresponding lecture at heart-lung.org. Given the subject nature and my distended style of explanation, I created the videos as supplements for the reader. The reasons why it has taken so long to complete the book are many, but generally boil down to life itself: finishing my fellowship, living in a secluded cabin for a bit, starting an ultrasound company, moving back to New York City, simultaneously beginning a job and a Master's Degree and now the extensive travel that comes with start-up life. It only took a pandemic for me to sit down in one place and finish this book.

The initial motivation was a small 'eureka' moment that I had somewhere between an Ike's Sandwich in the Stanford Engineering building and a beach bench in Santa Monica. How to visualize and understand the mechanical link between the heart and the lungs? Arthur Guyton recognized that because the venous return curve and the Frank-Starling relationship share an abscissa, they could be superimposed to generate a useful explanatory model of the cardiovascular system. In a similar fashion, the goal of these chapters [especially the first 4] is to conceptually couple the cardiovascular and the respiratory pumps. Again, the abscissa [pressure] ties the heart and the lungs together; linking physiology figures unites the vessels and ventricles with the thorax.

Yet, a lot has happened in critical care physiology since I initially wrote the first 8 chapters! Because my pulmccm.org contributions have covered some of the intervening literature, I have reorganized some of the 'ICU Physiology in 1000 Words' series into 2 additional chapters. Hence, the topics covered in chapters 9 & 10 will not be new to those familiar with my on-line work. Nevertheless, my hope is that by rearranging and reworking 6 years of the '1000 Words' series, the reader will absorb something new.

In clinical medicine, I believe that we all have 'conflicts of interest.' Each of us are biased towards one practice or another based on our training, mentors, experiences and the literature we have imbibed. This was certainly true for me before I helped start an ultrasound company; I had a Doppler ultrasound bias because it is a quantitative, non-invasive, decision-support tool. I have since carried Doppler ultrasound from a clinical interest to a commercial one. I co-founded Flosonics Medical and I am proud of the wireless, wearable Doppler ultrasound we have built. It was invented to help clinicians better understand hemodynamics. While there is no mention of this device in the chapters below, my clinical and commercial interests deserve declaration.

The cover photo was taken in late 2018 at the Cimitero di Portofino.

Contents

Chapter One

The Mechanics of Ventilation: a graphical analysis with emphasis on the qualitative assessment of the pleural pressure

Abstract

To understand pleural pressure, the clinician should appreciate the static and dynamic properties of the respiratory system; these concepts are nicely visualized via the Campbell diagram. The Campbell diagram parses the pleural pressure into that which is required to affect thoracic volume, as well as drive airflow. This representation also dissects the loads placed upon the respiratory system, and the compensatory mechanisms in response to these loads. Additionally, the Campbell diagram illustrates work of breathing both in the spontaneously breathing patient and the passive, mechanically ventilated one. Ultimately, knowledge of breathing mechanics focuses the clinician upon the pleural pressure and lung volume which are key mediators of mechanical heart-lung interaction.

Key Words: Campbell diagram, pleural pressure, thoracic compliance, airway resistance, elastic work of breathing, static work of breathing, mechanical ventilation, dynamic hyperinflation

Introduction

As the heart is loaded and unloaded within the thorax, the shifting pressure and volume of breathing inexorably marry the respiratory and cardio-circulatory systems in sickness and in health. Because the pleural pressure is the approximate pressure surrounding the heart and great vessels, it is an important variable affecting cardiovascular function. Additionally, pleural pressure is a determinant of lung volume. Importantly, lung expansion alters surface interface pressures and pulmonary capillary volume, which both impact bi-ventricular loading conditions. Consequently, it is imperative that the clinician understand the genesis of both pleural pressure and lung volume as these are key mediators of heart-lung interaction. This chapter provides an overview of the mechanics of ventilation - initially, in the spontaneously breathing patient and then in the patient receiving mechanical support. As elaborated, pleural pressure is essentially a function of both dynamic and static properties of the lung's physiology in the spontaneously

breathing patient, but secondary to the ratio of lung and chest wall compliances in the passive, mechanically ventilated patient.

Static and Dynamic Pressures

With inspiration, the thorax generates a pressure difference that creates and maintains lung volume as well as drives gas flow[1]. The pressure gradient that creates the former is the static pressure while the latter pressure differential is the dynamic pressure. One way to help illustrate these two types of pressure is the 'bag and tube' model of the lung - drawn from the equation of motion [1]. In this model, the bag represents the volume that is generated when a pressure within a distensible object is referenced to the pressure surrounding the object [i.e. the transmural pressure]. Importantly, the relationship between the transmural distending pressure and the change in volume is mediated by the compliance of the object.

$$(1)\quad compliance = \frac{\Delta\ volume}{\Delta\ transmural\ pressure}$$

or

$$(2)\quad \Delta\ transmural\ pressure = \frac{\Delta\ volume}{compliance}$$

Equations 1 & 2: Static respiratory system pressure

In the lung, this transmural pressure gradient is the pressure within the alveolus less the pleural pressure and is also known as the transpulmonary pressure. Importantly, this pressure makes no statement about gas flow. For consistency in this book, the transpulmonary pressure is, by definition, made in states of no flow, or static conditions.

Dynamic pressure within the lung refers to the pressure dedicated to moving gas and tissues. For simplicity, we will ignore pressure dedicated to tissue frictional loses. The dynamic pressure difference is created between the alveolus and mouth; the pressure at the mouth is equivalent to the body surface pressure or atmospheric pressure. The dynamic pressure gradient is directly proportional to airflow and airway resistance - a recapitulation of Ohm's law describing electric current.

$$(3)\quad Pressure\ gradient = flow\ x\ resistance$$

Equation 3: Dynamic respiratory system pressure

[1]Liquid flows down an energy gradient, not a pressure gradient per se. Pressure is used clinically as a surrogate for energy, so this book may colloquially imply that pressure is the primum movens of flow. Nevertheless, it is possible for flow to occur from low to high pressure [e.g. at the exit of a stenosis].

In the 'bag and tube' model of the lung, the dynamic pressure gradient is represented by the tube [figure 1]. The static and dynamic components of respiration are considered in more detail in subsequent sections. As above, the equation of motion integrates both the static and dynamic pressures of the respiratory system as follows [1]:

$$(4)\quad airway\ pressure = \frac{\Delta\ volume}{compliance\ of\ respiratory\ system} + [flow\ x\ resistance]$$

Equation 4: The equation of motion

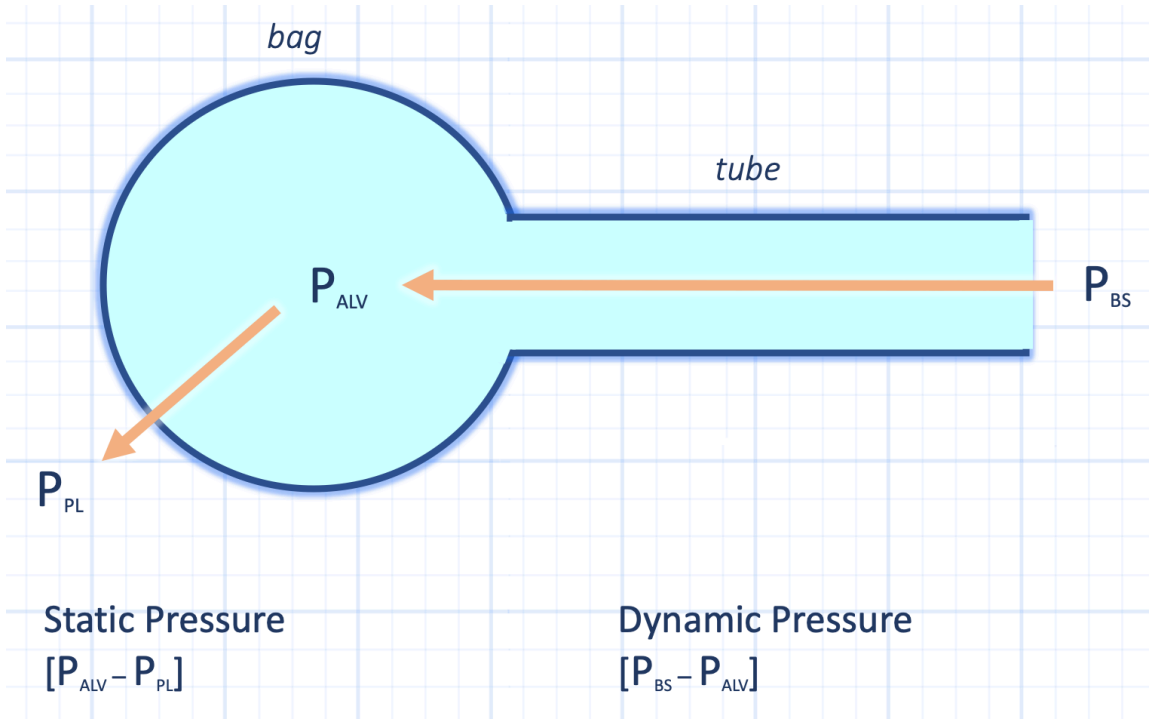

Figure 1: Bag and tube model of the lung. Ppl is pleural pressure; Pbs is body surface pressure; Palv is alveolar pressure

Static Properties of the Lung and Chest Wall

The Lung

If one were to sequentially increase the transpulmonary pressure of the lung and take serial lung volume measurements, a static pressure-volume relationship curve is constructed [2] [see also chapter 9]. A comparable clinical situation is evacuating a pneumothorax with a chest tube. The chest tube and pneunovac apparatus lower the pleural pressure below body surface pressure so the transpulmonary pressure increases; consequently so too does lung volume. A graph of this curve with pleural pressure on the x-axis and lung volume on the y-axis describes pulmonary compliance [3]. Each point of the curve marks a unique pleural pressure - [transpulmonary pressure when referenced to the alveolus] lung volume

relationship in the absence of airflow. Note how the slope of the curve [i.e. the compliance] changes with volume. At high lung volume, greater transpulmonary pressure [or a lower pleural pressure] is required for a given change in volume. Therefore at high lung volume, the lung is less compliant [4]. Also note that the lung has an equilibrium volume that is not zero [2, 5]. This is because a negative transpulmonary pressure [when pleural pressure supersedes airway pressure] favours airways collapse and air-trapping within the lung. Pleural pressure may supersede airway pressure at the base of the lungs especially in clinical states marked by intra-abdominal hypertension [6]. Additionally, when expiration is forced there is tendency for airway collapse, especially when there is reduced elastic recoil; this phenomenon is elaborated upon below [7].

A shift of this pulmonary compliance curve down to the left represents an overall decreased compliance [8], while up to the right is increased lung compliance [9, 10]. The inverse of compliance is elastance and so the shape of this curve is also a description of the elastic recoil of the lung [figure 2].

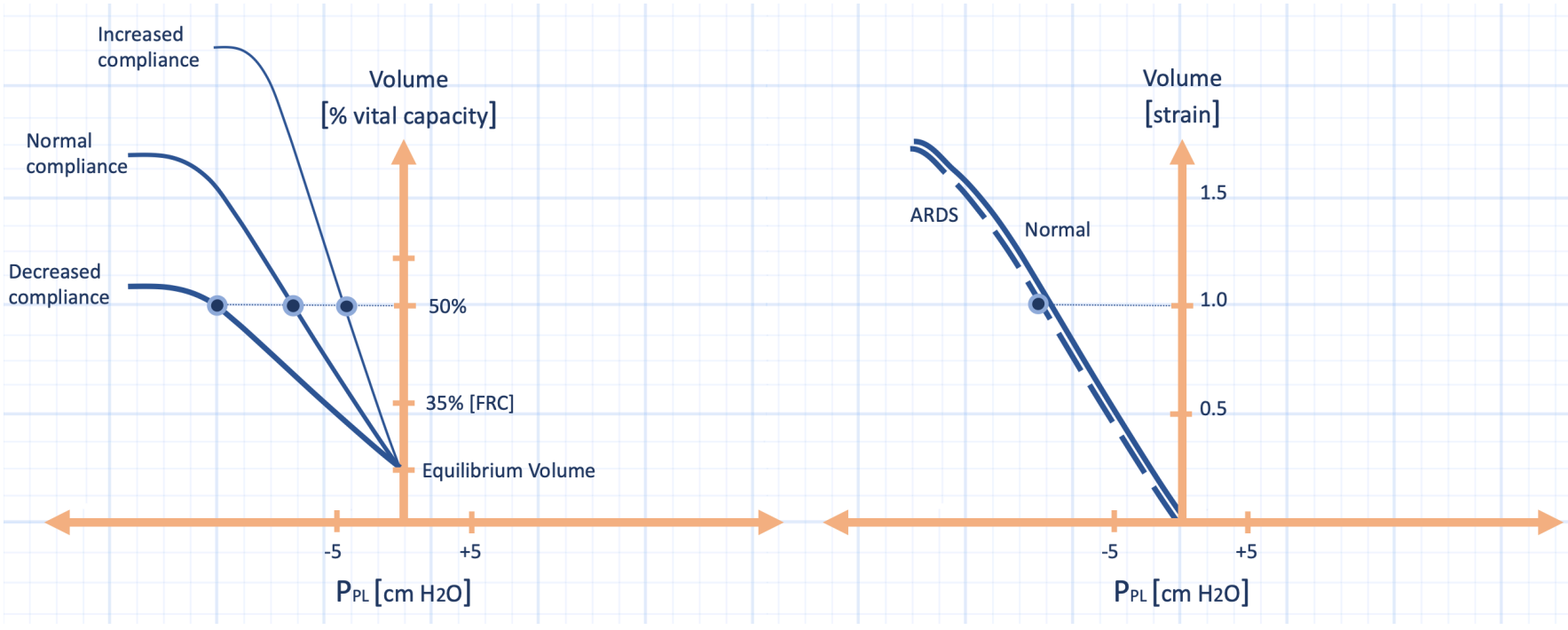

Figure 2: Lung compliance [elastance is the inverse of compliance]. Left panel: Note that for the same volume [50% vital capacity], different pleural pressure is generated in different states of lung compliance. Right panel: The 'baby lung' of ARDS [see also chapter 4 & 9]. The slope, or specific elastance, is the same, but strain rises as a function of smaller 'baby lung'. Strain is the volume of the lung relative to its baseline volume [i.e. tidal volume divided by FRC]. Ppl is pleural pressure and FRC is functional residual capacity. The origin of the graph is atmospheric pressure or body surface pressure.

The compliance [or elastance] of the lung and, therefore, the slope of static pressure-volume curve is predominantly determined by two important physical properties: 1. interstitial collagen and elastin composition and 2. surface tension.

While collagen has large tensile strength, it is only able to distend a small fraction of its length. Conversely, elastin has relatively poor tensile strength, but is able to distend over 100% of its equilibrium length [11]. At low lung volume, elastin contributes more to lung recoil, while at high lung volumes collagen plays a greater role [12, 13]. Loss of elastin and collagen, as seen in emphysema, results in a more compliant lung with less elastic recoil [14].

When air and water meet at a surface, tension along the liquid interface develops as water molecules are preferentially attracted to each other rather than to air. In an air-water interface that forms a sphere, as in an alveolus, the surface tension generates a collapsing pressure that is directly related to the surface tension and inversely related to the radius; this is described by LaPlace's law:

$$(5)\quad transmural\ pressure\ =\ \frac{2\ x\ surface\ tension}{radius\ of\ sphere}$$

Equation 5: LaPlace equation

In a bubble with the approximate radius of an alveolus, the pressure required to maintain any given volume would be so great that the lungs would be too stiff to sustain life. Further, alveolar instability would rapidly occur because alveoli with smaller radii would have large surface pressures; these would then empty into larger alveoli [with lower surface pressure] until one large alveolus is formed [15]. Pulmonary surfactant abrogates both of the aforementioned phenomena. Surfactant is a group of amphipathic [detergent-like] biomolecules that intercalate into the air-water interface, mitigate the attractive forces between water molecules and, consequently, decrease surface tension [16]. Additionally, surfactant directly relates alveolar radius to surface tension which stabilizes surface pressure between alveoli of different radii. In other words, as the radius of a surfactant-containing alveolus decreases, the surface tension also decreases which attenuates any change in surface pressure, and vice versa [17].

While surfactant both decreases surface tension and physiologically links surface tension to alveolar radius, there is still a difference in the inflation and deflation pressure-volume relationships and this is known as hysteresis [18, 19]. Hysteresis occurs primarily for two reasons. First, a fully collapsed alveolus requires greater pressure to overcome the attractive forces between water molecules. Second, as the radius of the alveolus expands, greater energy of activation is required to recruit surfactant from just below the air-water interface to the surface. Thus, the hysteresis curve explains why atelectasis readily occurs and why positive end-expiratory pressure [PEEP] is often needed to maintain alveolar recruitment. Altered surfactant activity can be prominent in states such as ARDS, pneumonia and pulmonary edema; alveolar surfactant deficiency diminishes lung compliance and enhances collapse [20, 21].

Chest Wall

Like the isolated lung, the chest wall also has a static pressure-volume relationship. Importantly, this relationship is obtained when the muscles of respiration are completely passive [22]. If one were to alter the internal pressure of a 'lung-less' chest wall and measure sequential chest wall volumes at states of zero airflow, a static pressure-volume relationship of the passive chest wall is described [figure 3].

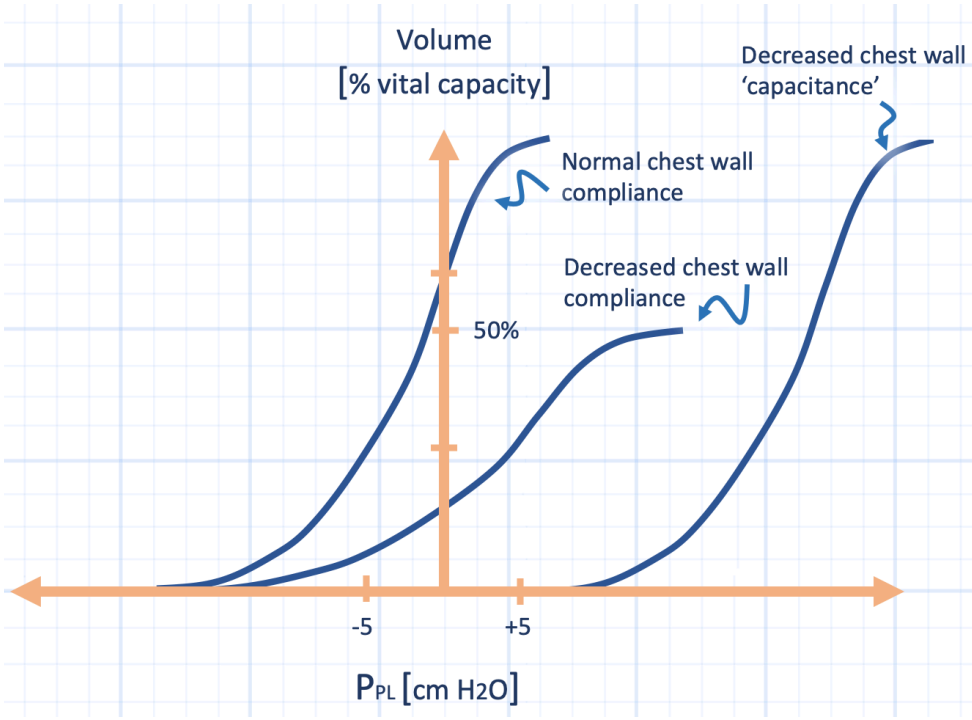

Figure 3: Compliance or elastance of the passive chest wall. The decreased slope of the stiff chest wall means that greater pleural pressure change must occur to affect any given volume change. The whole curve can also shift rightwards, which is likely the predominant mechanism in obesity.

Note that as the internal pressure of this hypothetical 'lung-less' chest wall is lowered below atmospheric pressure [i.e. comparable to negative pleural pressure] the passive chest wall collapses as body surface pressure supersedes the internal pressure. Further, the equilibrium volume of the passive chest wall is much higher than that of the lung; the equilibrium volume of the passive chest wall is roughly 1 litre above FRC [22]. Like the lung, changes in compliance of the passive chest wall shifts its curve. There are a number of mechanisms and disease states that change chest wall compliance. In the ICU, impaired compliance is common. Typically, external loads placed upon the chest shift the compliance curve rightwards [e.g. intra-abdominal hypertension, obesity]. As well, there may be downward displacement of the curve [e.g. supine to prone positioning] [23-26] while age-related changes in chest wall compliance are marked by a rightward, but upshift in the curve [27, 28].

Integration of Passive Lung and Chest Wall Mechanics

Superposition of the static pressure-volume curves of both the lung and chest wall is known as a Campbell diagram [figure 4] [29].

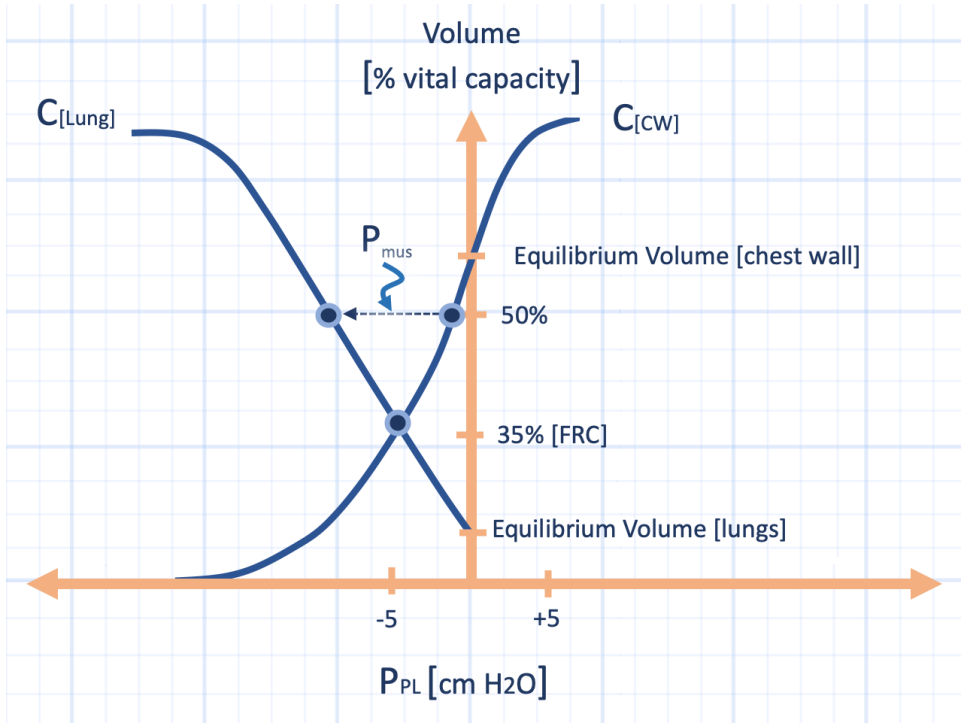

Figure 4: Combination of the static lung and chest wall compliance curves. Their intersection defines functional residual capacity [FRC]. At any given volume, the lateral distance between the two curves represents the pressure the muscles of respiration must generate to maintain that particular volume [i.e. Pmus]. Ppl is pleural pressure and cmH2O is centimetres of water. C[Lung] is lung compliance, C[CW] is chest wall compliance.

The point of intersection of the two curves occurs when the outward recoil of the chest wall [towards its equilibrium volume] is balanced by the inward recoil of the lungs [towards their equilibrium volume]; this point is functional residual capacity [FRC]. At any given volume on the Campbell diagram, the horizontal distance between the two curves represents the absolute pressure that must be generated by the muscles of inspiration to maintain that volume in the absence of airflow [30]. The pleural pressure required to maintain a given static volume follows the pulmonary compliance curve. Consequently an isolated decrement in chest wall compliance increases the absolute amount of pressure that must be generated by the inspiratory muscles as the curves have greater separation, but the end-inspiratory pleural pressure will change little if the lung compliance is unaffected [29]. An isolated reduction in chest wall compliance is an uncommon clinical scenario in the ICU as patients with diminished chest wall compliance usually have excess lung water and atelectasis which reduce lung compliance as well [e.g. ascites] [31]. Decreasing both lung and chest wall compliance 'afterload' the muscles of inspiration [figure 5]; these patients often adopt rapid-shallow breathing to minimize elastic breathing work [29]. This is described in further detail below.

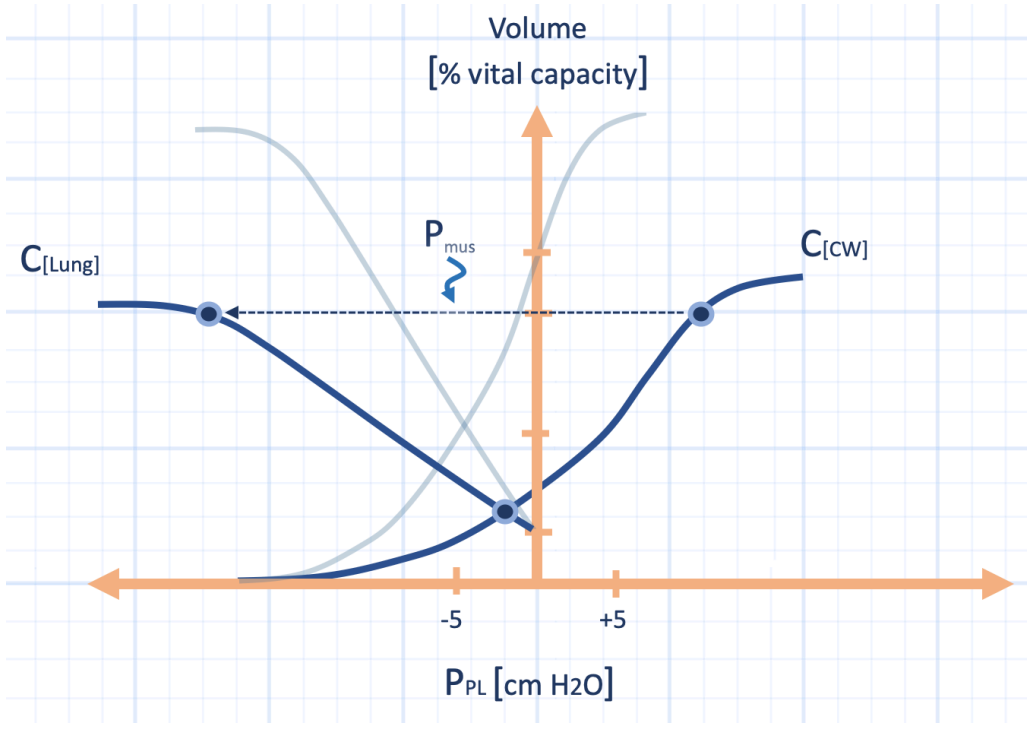

Figure 5: Combination of reduced pulmonary and chest wall compliances. Notice the reduction in functional residual capacity [the intersection of the new pulmonary and chest wall compliance curves] as well as the increased muscle pressure [Pmus] required to achieve the same thoracic volume [50% vital capacity] as figure 4. Ppl is pleural pressure and cm H2O is centimetres of water. C[Lung] is lung compliance, C[CW] is chest wall compliance.

Dynamic Properties of the Respiratory System

The previous sections analyzed the respiratory system in terms of static characteristics only. Returning to the 'bag and tube' model of the lung, the dynamic properties of the respiratory system are illustrated by the tube; this is an additional amount of pressure created by the inspiratory muscles to overcome the inertial elements of gas flow within the airways. While there is also a small amount of pressure dedicated to the frictional loses of tissue sliding over each over [so called 'tissue resistance'] during inspiration, the dynamic properties of lung focus primarily on the frictional loses of flowing gas within the airways [32].

Airway Resistance and the Pressure-Flow Relationship

Gas flow in the tracheobronchial tree may be modelled after Ohm's law of electrical current [1]. Resistance is a physical property that is defined mathematically by the relationship of pressure and flow, that is, if a small pressure gradient is accompanied large flow, then resistance is said to be low and vice versa. By rearranging:

(6) $$pressure\ gradient = gas\ flow\ x\ resistance$$

or

$$(7)\quad resistance = \frac{pressure\ gradient}{gas\ flow}$$

Equations 6 & 7: Dynamic pressure in the respiratory system

This equation for resistance predicts a linear relationship between pressure and flow but, in reality, the pressure-flow relationship 'bends' at high flows because transitional and turbulent patterns are generated. Transitional and turbulent flow have higher effective resistances than laminar flow [33]. Laminar flow is an orderly flowing motion of gas molecules in concentrically arranged parabolas with the innermost molecules moving with the highest velocity [34]. Laminar flow does have a linear pressure-flow relationship and likely only exists in the smallest of airways beyond the terminal bronchioles. Turbulent flow, by contrast, does not have a linear pressure-flow relationship but instead an exponential one. The reason is because turbulent flow does not move in orderly parabolas; instead gas molecules move chaotically, often at 90 degrees to the direction of flow which increases frictional loses. Therefore, when gas flow becomes turbulent, increasing flow accompanies large pressure gradients; thus, the 'effective resistance' increases in concert with flow [35]. Transitional flow is a pattern of gas movement that is a hybrid – between that of turbulent and laminar flow. Transitional flow makes up the bulk of flow within the tracheobronchial tree. One way to predict which kind of flow pattern is present is to use the dimensionless Reynold's number [Re]:

$$(8)\quad Re = \frac{gas\ density\ x\ tube\ diameter\ x\ gas\ flow}{gas\ viscosity}$$

Equation 8: Reynolds number

If Re is less than 2000, then flow is likely laminar; if it is above 4000, then flow is prone to turbulence. When Re is between 2000 and 4000, then flow is likely transitional. The problem with applying this analysis to the tracheobronchial tree is that Reynold's number was derived in relatively long, smooth, branchless tubes while the airways of the lung are quite the opposite. It is therefore estimated that in the airways of the lungs that Reynold's number must be extremely low [less than 1] in order to predict laminar flow [33, 36]. The reason that Reynold's number is so low in the smallest of airways is because gas velocity is very low there. With each successive airway generation, the cumulative cross-sectional area increases exceedingly. Then, at a given flow, great cross-sectional area reduces gas velocity. While all patterns of airflow are exquisitely sensitive to changes in tube diameter, one key distinction between turbulent and laminar flow is that the former is directly proportional to gas density, while the latter is directly proportional to gas viscosity [33].

A relevant clinical correlate of the aforementioned physiology relates to helium-oxygen gas mixture - typically 80% helium and 20% oxygen [37]. Importantly, the density of helium-oxygen is less than air, but its viscosity is greater than air. Because of its lower density, helium-oxygen reduces the tendency for turbulent

flow and also the effective resistance of existent turbulent flow. This is important in the central airways where turbulent flow dominates. Thus, helium-oxygen is often used for patients with large airway obstruction [38]. The benefit of helium-oxygen in diseases that affect the small airways is less physiologically intuitive because helium-oxygen is more viscous than air which effectively increases the resistance of gas flow with a laminar pattern. As above, laminar airflow may only exist in the most distal airways, so helium-oxygen might diminish the effective resistance in the majority of the tracheobronchial tree, especially if there are secretions in the large airways that facilitate turbulent flow patterns. This reasoning explains some of the mixed data for helium-oxygen in patients with small airways disease [39-41]. There is additional material on helium-oxygen mixtures in chapter 9 where airway resistance is discussed in the context of mechanical power.

In the spontaneously breathing patient, understanding the pressure-flow relationship of the lung is paramount. As gas flow and resistance are components of the equation of motion [equation 4], changes in airways resistance or flow pattern alter absolute values of pleural pressure and this is visualized on the Campbell diagram [figure 6] [29].

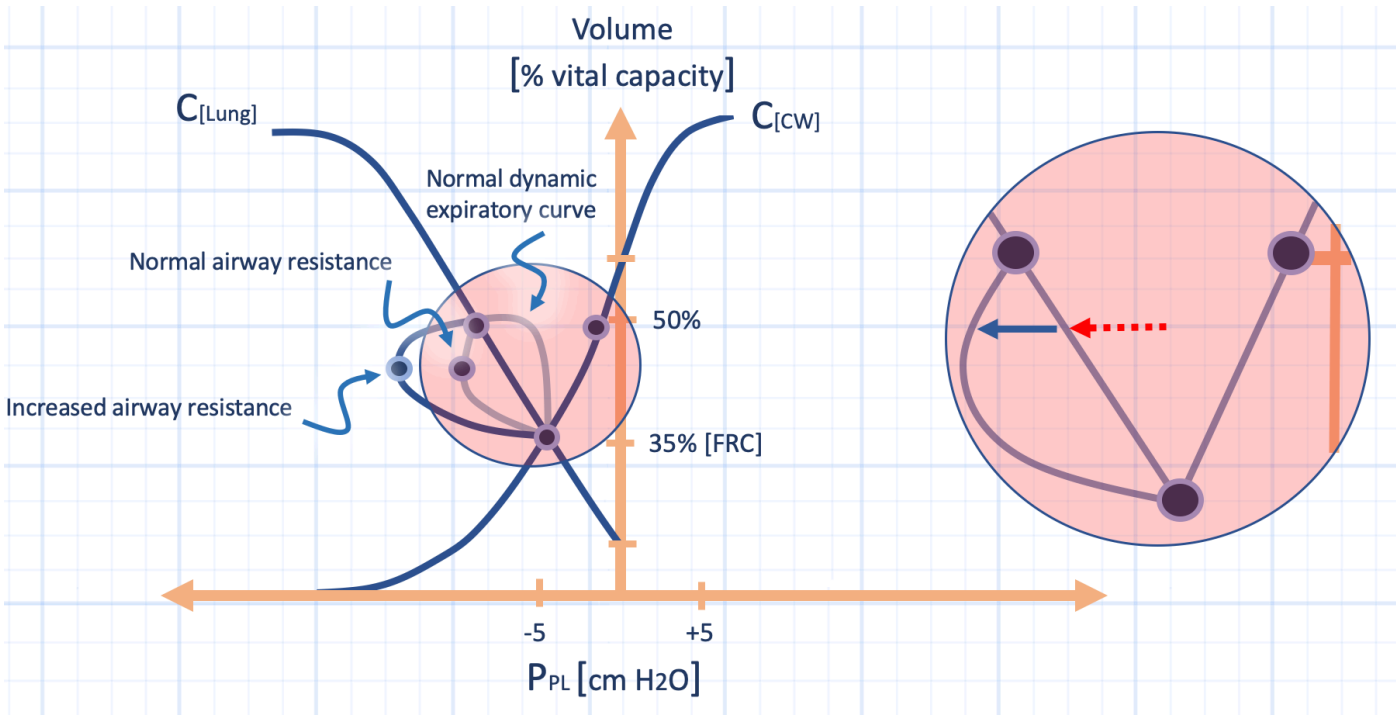

Figure 6: The addition of the dynamic component of pleural pressure to the Campbell diagram. Note the difference between normal and increased airways resistance – lower pleural pressure accompanies gas flow when airway resistance is increased. The normal, passive expiratory pressure volume curve is illustrated. The inset demonstrates that during normal inspiration, at any instantaneous lung volume, a portion of the pleural pressure is dedicated to generating lung volume [dashed, red arrow] while another portion is dedicated to airways resistance [solid, blue arrow]. The relative contributions of pleural pressure to lung volume and gas flow vary from the initiation to inspiration to termination of inspiration. Ppl is pleural pressure and cm H_2O is centimetres of water. C[Lung] is lung compliance, C[CW] is chest wall compliance.

In the spontaneously breathing patient, dynamic pressure properties are depicted as a curve to the left of the static pressure-volume relationship of the lung. Inspiration normally begins at FRC and terminates at a higher lung volume [FRC + tidal volume]. Expiration is passive and the curve is drawn to the right of the static pulmonary pressure-volume relationship. Because the energy used to drive expiratory flow is obtained from the pulmonary elastic recoil under tidal conditions,

the expiration curve lies within the elastic pressure-volume envelope described by the static lung and chest wall curves. By contrast, when expiration is active, the dynamic properties of expiration are depicted beyond the elastic pressure-volume envelope and may result in positive pleural pressure [30, 42] [see figure 9 below].

Integrating Static and Dynamic Components of the Respiratory System

As observed on the Campbell diagram, during tidal inspiration, the degree to which the pleural pressure falls below its value at FRC is a summation of both the static [or elastic] properties of the lung and dynamic properties of air flow [figure 6]. When pleural pressure initially declines during inspiration, much of this is invested into pulling down the alveolar pressure. Because the pleural pressure and alveolar pressure initially drop together, there is little increase in transpulmonary pressure [i.e. volume], but a large difference between alveolar pressure and body surface [mouth] pressure; this latter pressure gradient reflects the energy investment for gas flow. As the lungs fill, alveolar pressure rises towards atmospheric pressure and the gradient for airflow diminishes. However, the pleural pressure remains below alveolar pressure during inspiration; thus, the transpulmonary pressure increases as the alveolar pressure rises relative to the pleural pressure. Note on the Campbell diagram that as inspiration proceeds less of the pleural pressure decrement is invested in the dynamic aspects of inspiration [i.e. airflow] and more is invested in the static aspect [i.e. volume]. Then, at the end of inspiration, the whole of the diminished pleural pressure is dedicated to the transpulmonary pressure; end-inspiration is, therefore, a static state [29, 30].

Work of Breathing

With a firm understanding of the Campbell diagram and how it visually relates normal and pathological states of lung volume and pleural pressure, a discussion on breathing work flows naturally [29, 43]. Work of breathing may have direct mechanical implications for heart-lung interaction [see 'veno-cardiac coupling' in chapter 10]. Further, work of breathing relates to oxygen cost. As well, work of breathing explains abnormal respiratory patterns such as rapid shallow breathing, high volume breathing and auto-positive end-expiratory pressure [auto-PEEP] - all of which have significance for heart-lung interactions [44-46]. Lastly, work over time is power and recent avenues of research in the acute respiratory distress syndrome [ARDS] have focused on mechanical power as a mediator of lung injury [see chapter 9].

Work is defined as the force required to move an object over a distance; the unit of work is the joule which is a quantification of energy.

(9) $Work = force\ x\ distance$

Because pressure is a force applied over a given area, and because volume is an area applied over a distance the following may be derived:

$$(10)\quad work = [pressure\ x\ area]\ x\ \frac{volume}{area}$$

or

$$(11)\quad work = pressure\ x\ volume$$

Equations 9-11: Relating work to the pressure-volume curves on the Campbell diagram

During spontaneous ventilation, work is being done to expand the lung as well as the chest wall. Additionally, work is done to drive gas flow and overcome tissue resistance. Work is visualized as the area bounded by the curves of the Campbell diagram [29]. Note that work can be partitioned into two types: resistive work of breathing and elastic work of breathing [figure 7].

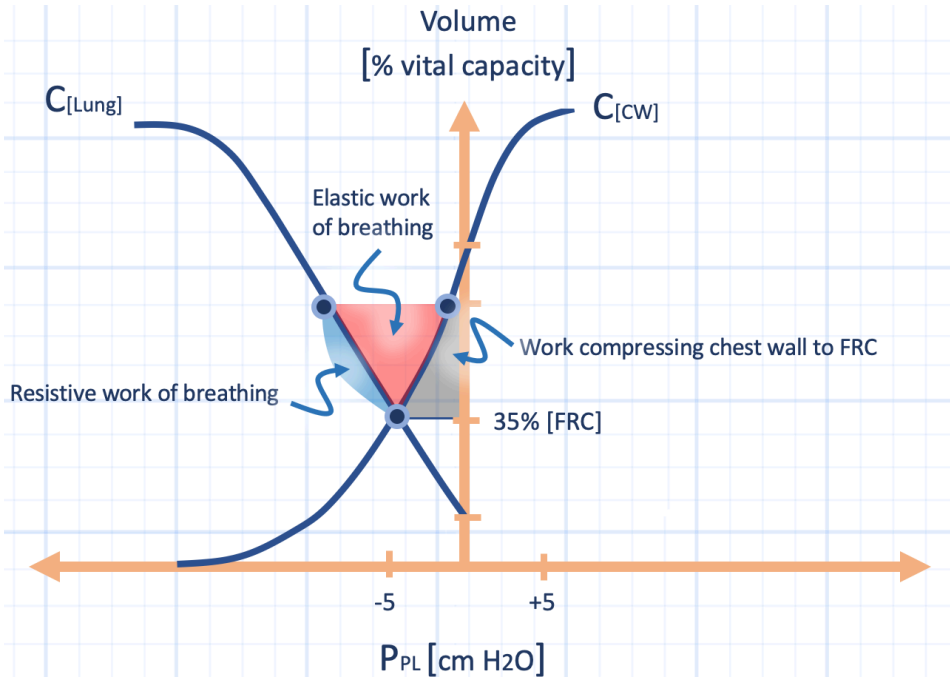

Figure 7: The work of breathing as depicted on the Campbell diagram. See also figures 4-6. Ppl is pleural pressure and cm H_2O is centimetres of water. FRC is functional residual capacity; C[Lung] is lung compliance; C[CW] is chest wall compliance.

The resistive work of breathing is described by the area of the envelope that demarcates dynamic pressure, that is, the area to the left of the pulmonary static pressure volume curve and to the right of the dynamic pressure-volume curve [47]. As described above, the shape and area of this resistive envelope is determined by the pressure-flow relationship of the tracheobronchial tree [29]; the energy dedicated to this portion of breathing work is dissipated as heat. By contrast, the elastic work of breathing is defined by the envelope between the static pressure-volume relationships of the lung and chest wall. This energy is stored as an elastic

recoil within the lung which is a form of potential energy. It is reclaimed during passive expiration. One potential limitation to the Campbell diagram is that it does not take into consideration the work of breathing required to change abdominal volume; thus it may underestimate total breathing work [48].

Elastic Work of Breathing

The elastic work of breathing for both the lung and chest wall is represented as the area to the left of the y-axis [volume] and to the right of the respective static pressure-volume relationship curve [43]. Note that work is required to expand the lung from FRC to the end of a tidal breath; yet within this same volume range, work is required to compress the chest wall because normal, tidal breathing is below the equilibrium volume of the chest wall. Therefore, work is not required to expand the chest wall during normal tidal volumes; this area is not considered as a part of tidal volume breathing. Consequently, it is the triangular area between the two static pressure-volume curves that quantifies elastic work. Interestingly, the work used to compress the chest wall facilitates thoracic expansion during tidal breathing as the chest wall recoils outwards towards its equilibrium volume [29].

A selective decline in lung compliance increases the distance between the two curves. As above, at any given volume the muscles of inspiration must generate greater pressure to achieve and maintain the volume of interest. Clearly, this also relates to the work of breathing which is the area of the envelope bounded by the static pressure-volume curves. Also, as noted above, a selective fall in pulmonary compliance lowers absolute pleural pressure [49].

A similar situation occurs with a specific drop in chest wall compliance [50]. The area between the static pressure-volume relationships of the chest wall and lung increases; consequently, so too does the work of breathing. Notably, the large increase in elastic work that accompanies impaired lung and chest wall compliance is compensated for by rapid-shallow breathing [51]. By taking smaller breaths, the area of the elastic work envelope is minimized and so too is the work of breathing [figure 8]; to maintain minute ventilation, the patient breaths more rapidly. While shallow breathing minimizes elastic work, it has other, important physiological complications. For example, smaller tidal volume [Vt] effectively increases dead space fraction [Vd/Vt]. Because anatomical dead space [Vd] remains constant, the dead space fraction [Vd/Vt] increases when the patient is breathing with a small Vt [52]. Dead space is a subtype of Va/Q mismatch that favours hypoxemia and hypercapnia [53]. Additionally, the rapid breathing may impair alveolar emptying, especially if expiratory airway resistance is high [54]. This phenomenon can cause alveolar pressure that is above atmospheric pressure at end-expiration; the details of this auto-PEEP are detailed in subsequent sections of this chapter [55]. As well, these topics are covered in chapter 9, couched within discussions on high-flow oxygen therapy and helium-oxygen in mechanical power. Lastly, as described next, low lung volume breathing increases airways resistance and, therefore, resistive work of breathing [56].

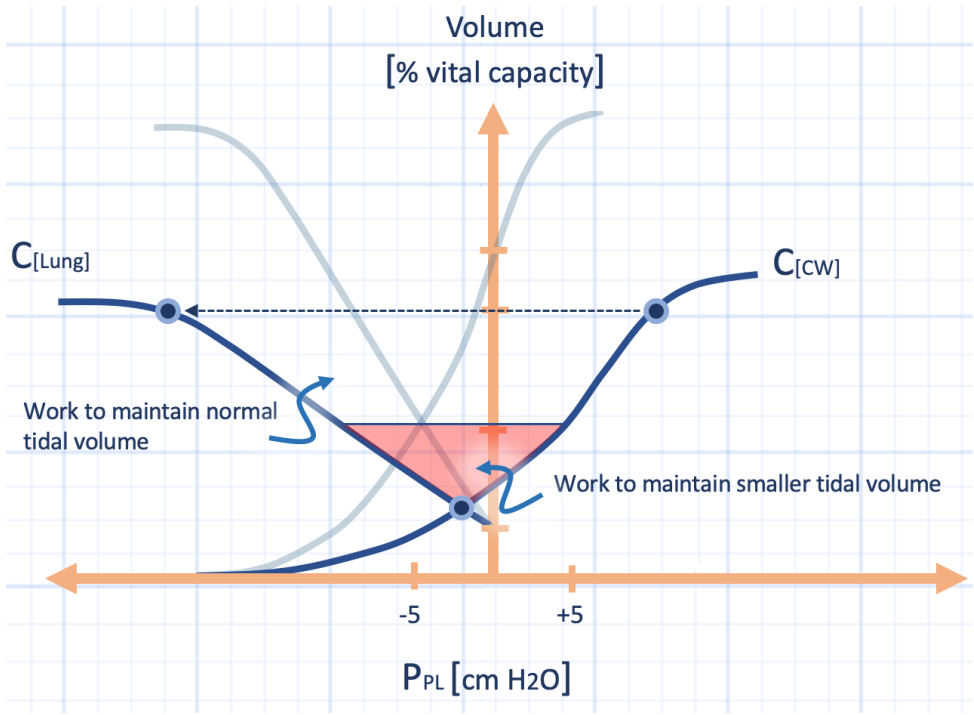

Figure 8: The work of breathing with diminished pulmonary and chest wall compliance. Note that breathing at a smaller tidal volume minimizes the elastic work of breathing [shaded triangle] compared with the work required to achieve a tidal volume of 50% vital capacity [triangle defined by dotted arrow as base]. To maintain minute ventilation, the patient will breathe rapidly. Ppl is pleural pressure and cm H_2O is centimetres of water. C[Lung] is lung compliance; C[CW] is chest wall compliance.

Resistive Work of Breathing

While elastic work of breathing is done to stretch open the lung and chest wall, resistive work of breathing is done to overcome the viscous and inertial components of breathing [29]. This includes the flow of gas, but also the frictional resistance between tissues sliding over one another. The resistive work of breathing, unlike the elastic work of breathing, is dissipated as heat. The area to the right of the dynamic pressure volume curve and the left of the static pressure volume curve defines the inspiratory resistive work of breathing [figure 7]. When the resistance to airflow rises, so too does the area of this envelope [29, 30, 42]. As above, this can occur when physical airway resistance increases [e.g. acute broncho-obstruction, or emphysema] or when turbulent flow patterns are established [33, 34]. Similarly, if expiration is active, an envelope to the right of the static pressure volume relationship of the lung is formed. This additional area further loads the muscles of respiration with work during expiration [29].

During exacerbations of airways disease, inspiratory and expiratory work of breathing can become great [figure 9].

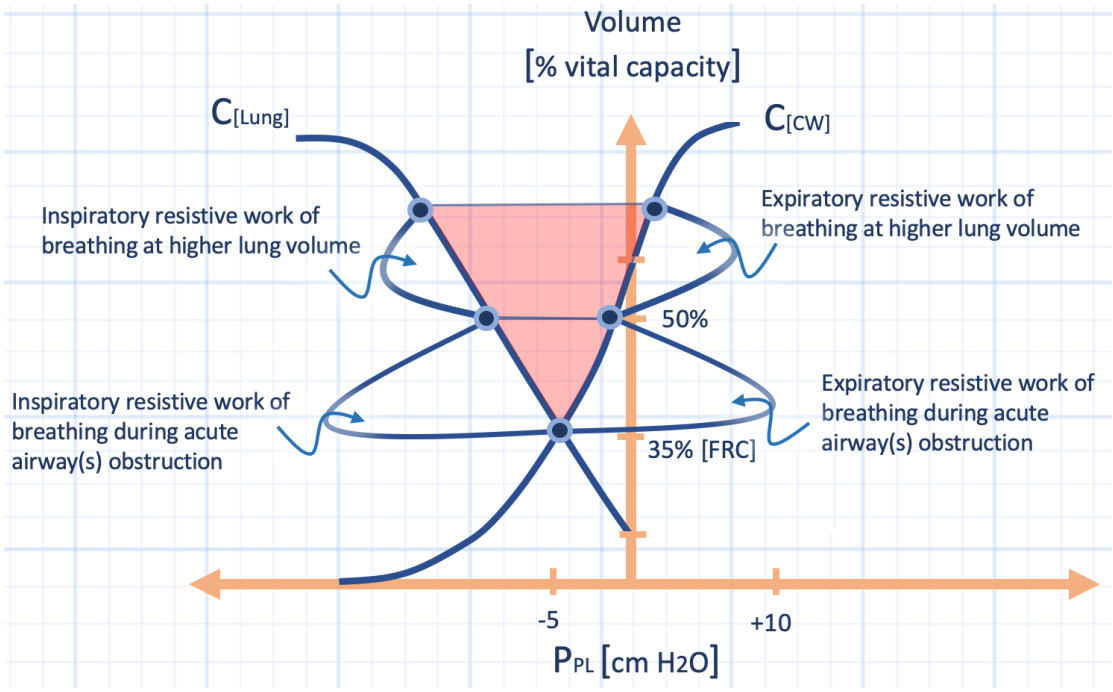

Figure 9: Inspiratory and expiratory resistive work of breathing during an acute attack of airway(s) obstruction. Note that at high lung volume, resistive work of breathing decreases, but elastic work of breathing increases somewhat [shaded areas]. The patient will try to seek the lowest ratio of resistive to elastic work of breathing. Ppl is pleural pressure and cm H_2O is centimetres of water. C[Lung] is lung compliance; C[CW] is chest wall compliance; FRC is functional residual capacity.

This is particularly true during forced expiration, where positive pleural pressure favours airway collapse – especially at low lung volumes when small airways are less tethered-open [56]. Indeed, at small lung volumes, the pressure-flow relationship quickly plateaus such that additional pressure provides no further increase in flow [57, 58]. This type of pressure-flow relationship is said to be 'effort-independent' because no further increment in effort augments flow. The mechanism of effort-independent expiratory flow is described by the equal pressure point hypothesis [59]. This phenomenon occurs when pleural pressure supersedes airway pressure and dynamic airways collapse occurs. In this situation, further increase in effort [i.e. pleural pressure] will simply maintain and/or augment airway resistance so flow will not rise. Dynamic airway collapse is favoured in disease states that erode the elastin fibres maintaining airway patency [e.g. emphysema], but also when lung volumes are low because low lung volume minimizes mechanical tethering of the small airways [60].

Ostensibly, as a mechanism to mitigate this additional work, patients breathe at high lung volumes [10, 42]. At higher lung volumes, large airways dilate as are the small airways which are mechanically tethered to the surrounding alveoli [61]. As seen in the supplemental on-line material, superimposition of the pressure – flow relationships at different lung volumes illustrates how high-volume breathing shrinks expiratory resistive work. Further, inspiratory pressure-flow relationships at different lung volumes is similar, but of smaller magnitude to that of expiratory pressure-flow [56]. Therefore, at high lung volume, inspiratory resistive work is also diminished.

As low volume breathing reduces elastic load, but raises resistive load, high volume breathing reduces resistive load, but increases elastic load [figure 9]. In other words, the high volume breathing tends to increase elastic work, but this is a trade-off for improving airflow during periods of broncho-obstruction. Additionally, high

volume favours West zone I and II physiology which may cause Va/Q mismatch and dead space and further impair gas-exchange, especially in the face of exogenous oxygen administration [62, 63].

Oxygen Cost

Whether elastic work of breathing, resistive work of breathing or both are increased, respiratory oxygen cost rises [45, 51, 54, 64-66] [see also chapters 4 and 9]. While the muscles of respiration typically require only a small portion of the cardiac output at rest, dyspnea from resistive or elastic loads can increase the fraction of cardiac output dedicated to the respiratory pump to 20-25% [67]. Increased oxygen utilization [VO_2] by the respiratory muscles depletes hemoglobin of oxygen so that central and mixed venous blood returning to the right heart is abnormally low [68, 69]. Low mixed venous blood may exacerbate Va/Q mismatch resulting in hypoxemia, respiratory muscle fatigue and myocardial ischemia [70-72].

Mechanical Ventilation

While the first portion of this chapter focused entirely on the patient who is breathing spontaneously, this section focuses on the passive patient [i.e. not making spontaneous respiratory efforts] receiving mechanical ventilation. Crucially, mechanical ventilation is not simply the reverse of spontaneous breathing. During spontaneous breathing, the pleural pressure is the effector of both the static and dynamic components of respiration. During passive mechanical ventilation, pleural pressure is somewhat of a physiological bystander. Equally important, in mechanical ventilation the pleural pressure is steps removed from the proximal tracheal pressure. Thus, there may be little or no relationship between the peak, plateau and pleural pressures [73]; these important concepts are explored below.

Static Components of the Respiratory System

In the spontaneously breathing patient, the static pressure-volume relationship of the respiratory system is parsed into the lungs and chest wall separately. In the passive, mechanically ventilated patient, the lungs are chest wall are considered together as the respiratory system [74]. This is because the lung and chest wall are being moved in unison by a volume, or pressure, applied via an endotracheal tube. This respiratory system compliance curve for the combined lung and chest wall is classically illustrated on the Rahn diagram [figure 10] [74].

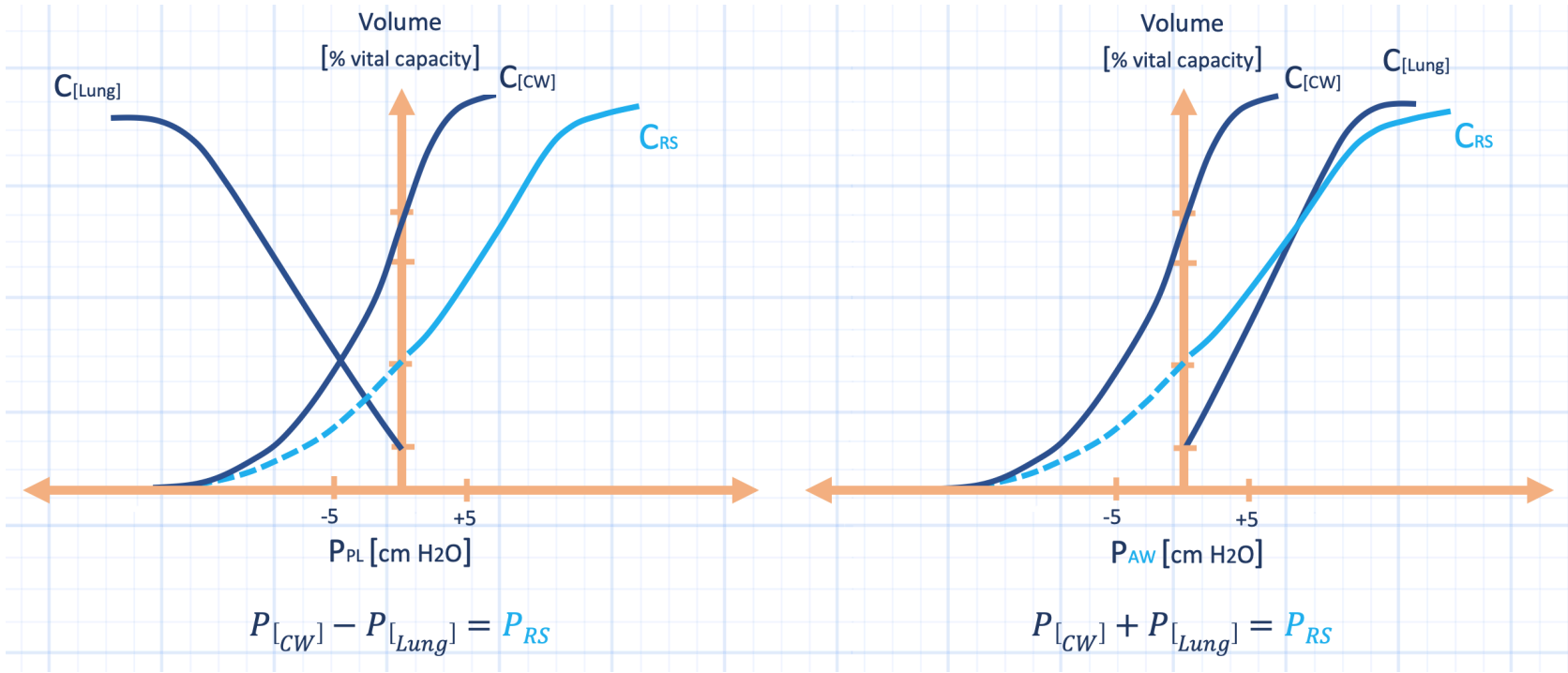

Figure 10: The Campbell & Rahn diagrams. Left panel: The Campbell diagram 'looks' at the lung from the perspective of the pleural space, thus the abscissa is pleural pressure [Ppl]. To generate the pressure required to open the respiratory system [Prs], the pleural pressure [Plung] is subtracted from the chest wall pressure [Pcw] at any given volume. For example, at FRC, both the Plung and Pcw are - 3 cm H_2O, thus Prs is zero or atmospheric pressure. Right panel: The Rahn diagram 'looks' at the lung from the perspective of the airway, thus the abscissa is airway pressure [Paw]. To generate the pressure required to open the respiratory system [lung and chest wall together], the chest wall [Pcw] and lung [Plung] pressures are added. For example, at FRC, the Pcw is - 3 cm H_2O while the Plung is +3 cm H_2O and the Prs is also zero or atmospheric pressure. In some figures and in the lectures on-line, the dotted portion of the respiratory system compliance curve [Crs, light blue] is omitted. cm H_2O is centimetres of water; C[Lung] is lung compliance; C[CW] is chest wall compliance. Values on the y-axis keep the same scale as all previous figures.

There is a straightforward relationship between the Campbell diagram and the Rahn diagram [2, 30, 75]. The difference between the two is whether the lung compliance curve is reflected with a negative [Campbell] or positive [Rahn] slope. When generating the compliance curve of the respiratory system, the pressure of the pulmonary and chest wall curves at any given volume are added to each other in the Rahn diagram and subtracted from each other in the Campbell diagram; the result is mathematically identical. Recall from the Campbell diagram that, for any given volume, the distance between the lung and chest wall curves represents the pressure generated by the muscles of inspiration to create and maintain thoracic volume in the absence of airflow. In the passive, ventilated patient, the distance between the lung and the chest wall curves, therefore, represents the static pressure applied by the ventilator to affect the same volume. Accordingly, if proximal airway pressure is increased step-wise and plotted against volume, the resultant curve depicts the static pressure-volume relationship of the respiratory system, as seen on the modified Campbell diagram [figure 11].

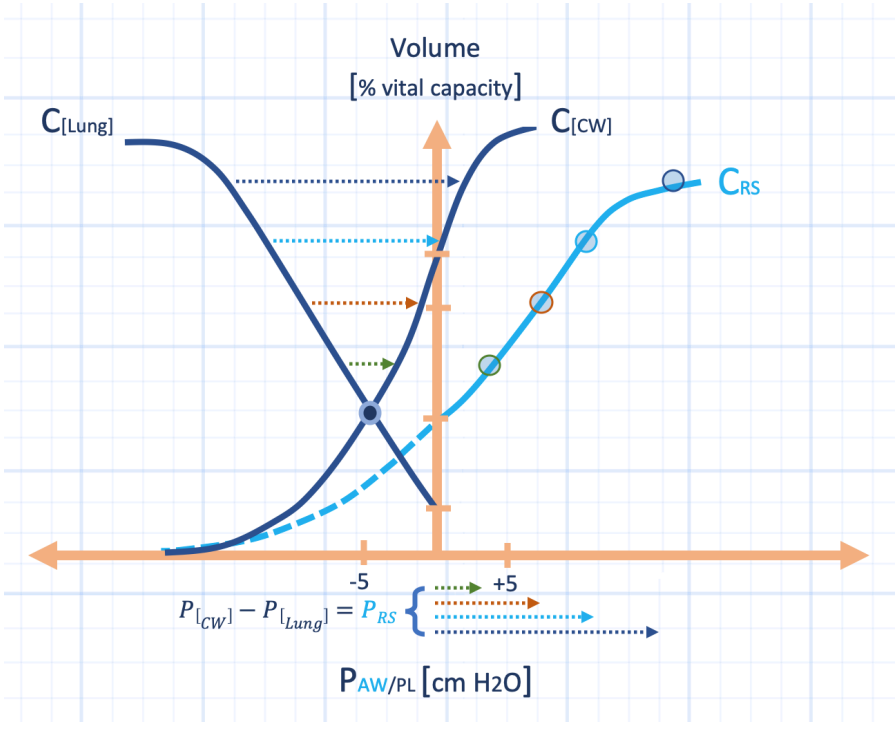

Figure 11: The modified Campbell diagram. Note that the lateral distance between the lung and chest wall compliance curves of the Campbell diagram [previously labeled Pmus] is equivalent to the airway pressure applied to the respiratory system to affect any particular volume. Thus, the Crs [light blue] is the compliance curve of the respiratory system and describes a series of plateau pressures from the ventilator [see figure 10 & text for details]. Ppl is pleural pressure; Paw is airway pressure and cm H_2O is centimetres of water; C[Lung] is lung compliance; C[CW] is chest wall compliance.

The Plateau Pressure

The plateau pressure is another name for the static proximal airway pressure in a mechanically ventilated patient [76]. Consequently, the airway pressure on the x-axis of the respiratory system compliance curve is, more specifically, the plateau pressure because this is achieved in the absence of airflow. A plateau pressure is obtained on a ventilator by instituting an end-inspiratory pause which ceases airflow. The result is the proximal airway pressure relative to body surface pressure [77]. If the plateau pressure is envisioned as a static column of air from the mouth to the alveolus, it then represents alveolar pressure [78]. This technique is analogous to the way by which left ventricular end-diastolic pressure is measured by occluding blood flow with a pulmonary artery catheter. Importantly, the plateau pressure does not record the transpulmonary pressure unless the pleural pressure is also measured [e.g. with an esophageal balloon]. Instead, the plateau pressure gives a trans-respiratory pressure which includes both the lung and chest wall. In the absence of an esophageal balloon, the plateau pressure is the closest approximation of the end-inspiratory pleural pressure; however, the degree to which the plateau pressure relates to the pleural pressure is dependent upon the relative compliances of the lungs and chest wall [79, 80]. This may be qualitatively estimated by the following equation:

$$(12)\quad \Delta\, pleural\ pressure \;=\; plateau\ pressure\ x\ \frac{lung\ compliance}{lung\ compliance \;+\; chest\ wall\ compliance}$$

Equation 12: Estimating the change in pleural pressure from plateau pressure and the lung and chest wall compliances

As evidenced from this equation, if the chest wall and lung compliances are roughly equal [as they are in health] then about 50% of the plateau pressure is experienced by the pleural space. If, however, the lung compliance is much less than the chest wall compliance, then less than 50% of the plateau pressure is achieved in the pleural space. With the corollary, when the lung compliance is much greater than chest wall compliance, more of the plateau pressure is felt in the pleural space [79].

The relationship between the plateau and pleural pressures is visualized graphically when inspecting the the lung, chest wall and respiratory system compliance curves. Note that for the respiratory system, the x-axis is airway pressure, while for the lung and chest wall curves, the x-axis is pleural pressure. During passive, mechanical ventilation, the pleural pressure tracks the curve of the static chest wall pressure-volume relationship [81]. Analysis of these curves reveals that a selective decrease in either the lung or chest wall compliance increases the distance between the individual compliance curves of the lung and chest wall. Consequently, the static [plateau] pressure required to achieve any given volume is also increased; this is reflected in a down and rightward shift of the respiratory system compliance curve [figure 12].

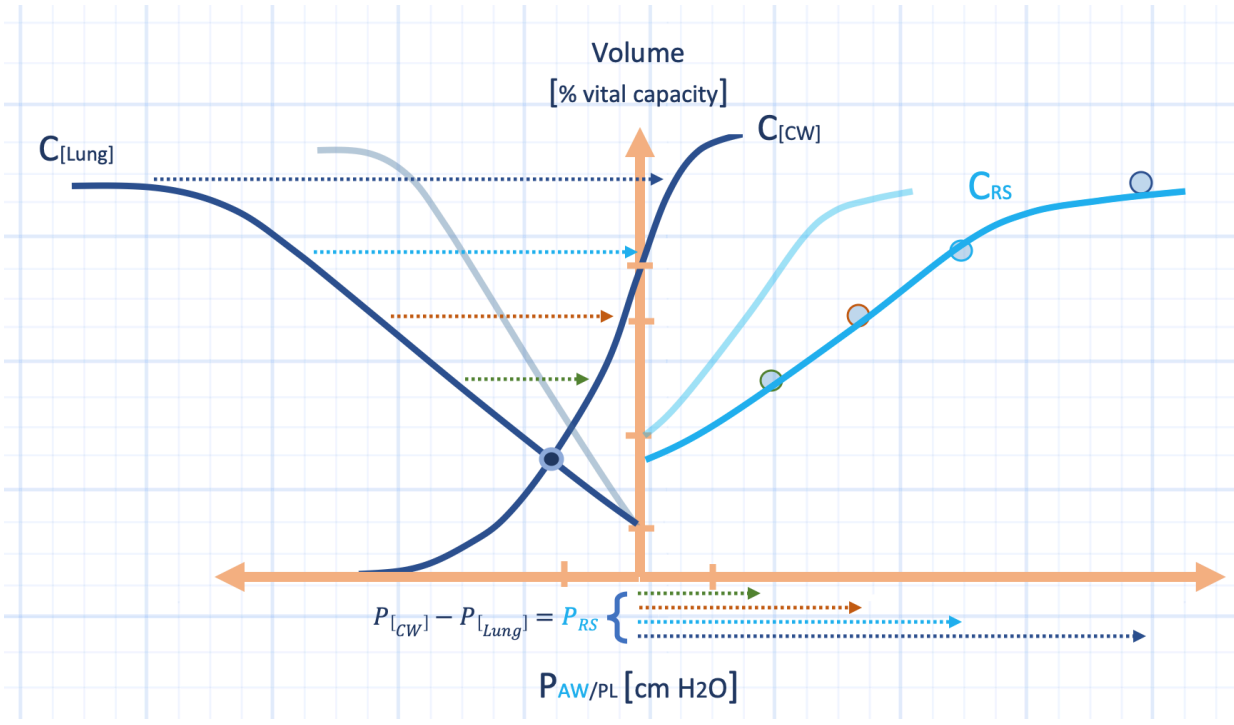

Figure 12: A selective decrease in pulmonary compliance [CLung] decreases respiratory system compliance [Crs]. The drop in Crs is a function of the lateral distance between the lung and chest wall compliance curves [dashed arrows]. As a result, plateau pressure rises, but with no change in chest wall compliance, the pleural pressure does not change for any given volume in the passive, ventilated patient; see also figure 11. Ppl is pleural pressure; Paw is airway pressure and cm H2O is centimetres of water. C[Lung] is lung compliance; C[CW] is chest wall compliance.

However, because the pleural pressure approximates the chest wall compliance curve during mechanical ventilation, a large decrease in pulmonary compliance will not affect the pleural pressure. By contrast, a decrease in chest wall compliance increases pleural pressure [82, 83].

The principles of pressure generation within the pleural space have important hemodynamic implications; further, they are fundamental when managing acute

respiratory distress syndrome [ARDS]. Pulmonary ARDS classically has a decline in calculated lung compliance [84]; thus, the plateau pressure is used as a surrogate for transpulmonary pressure. Because a typical transpulmonary pressure of 30-35 cm H_2O is required to reach TLC in spontaneously breathing healthy subjects, this was chosen as the target transpulmonary pressure in the ARDSNet trial [85]. However, in the ARDSNet trial, the patients were assumed to have lung compliance considerably less than chest wall compliance; this assumption provides the rationale for using plateau pressure as a substitute for transpulmonary pressure [86]. Yet, when the chest wall compliance curve is shifted down or rightwards [e.g. obesity, massive ascites], a larger portion of the plateau pressure is required to 'lift' the chest wall and this elevates the pleural pressure. Consequently, assuming that the plateau pressure is a surrogate for transpulmonary pressure is invalidated [87].

As the plateau pressure is a static pressure, it can be used to estimate compliance if the volume is known. When a patient is receiving a volume-targeted mode of ventilation, the compliance of the respiratory system is calculated as the tidal volume divided by the driving pressure as follows:

$$(13)\quad compliance\ of\ respiratory\ system\ =\ \frac{tidal\ volume}{[plateau\ pressure]\ -\ [end-expiratory\ pressure]}$$

Equation 13: Respiratory system compliance

The denominator of this equation [i.e. the driving pressure] is specifically discussed in chapter 9. Normal compliance values for the lung, chest wall and respiratory system are 200 mL/cm H_20, 150 mL/cm H_2O and 85 mL/cm H_2O. The units translate into the rise in thoracic volume per each cm of H_2O applied [76].

Table 1: Changes in Respiratory System Compliance

	Pulmonary Compliance	Chest Wall Compliance
Increased	Emphysema	Thoracotomy Paralysis
Decreased	Atelectasis Hyperinflation Pulmonary edema Consolidation Pulmonary ARDS++ Pneumothorax Fibrotic lung processes	Extra-pulmonary ARDS Abdominal hypertension Supine relative to upright Prone relative to supine Obesity* Chest wall edema/air Thoracic eschars

*the obese chest wall compliance curve may be shifted rightwards more than a decrease in slope - see figure 3; ++ the specific elastance is minimally changed in pulmonary ARDS - see figure 2.

Dynamic Components of the Respiratory System

As in the spontaneously breathing patient, additional pressure is required to overcome frictional loses that accompany air flow and tissue movement. This additional pressure, in the mechanically ventilated patient, is provided by the ventilator and recorded as an increase in the peak proximal airway pressure. On the Campbell diagram, this is represented by an additional curve to the right of the respiratory system compliance curve [figure 13]. At any given volume, the horizontal distance from the static [plateau] pressure to the peak pressure represents the dynamic pressure contribution [88].

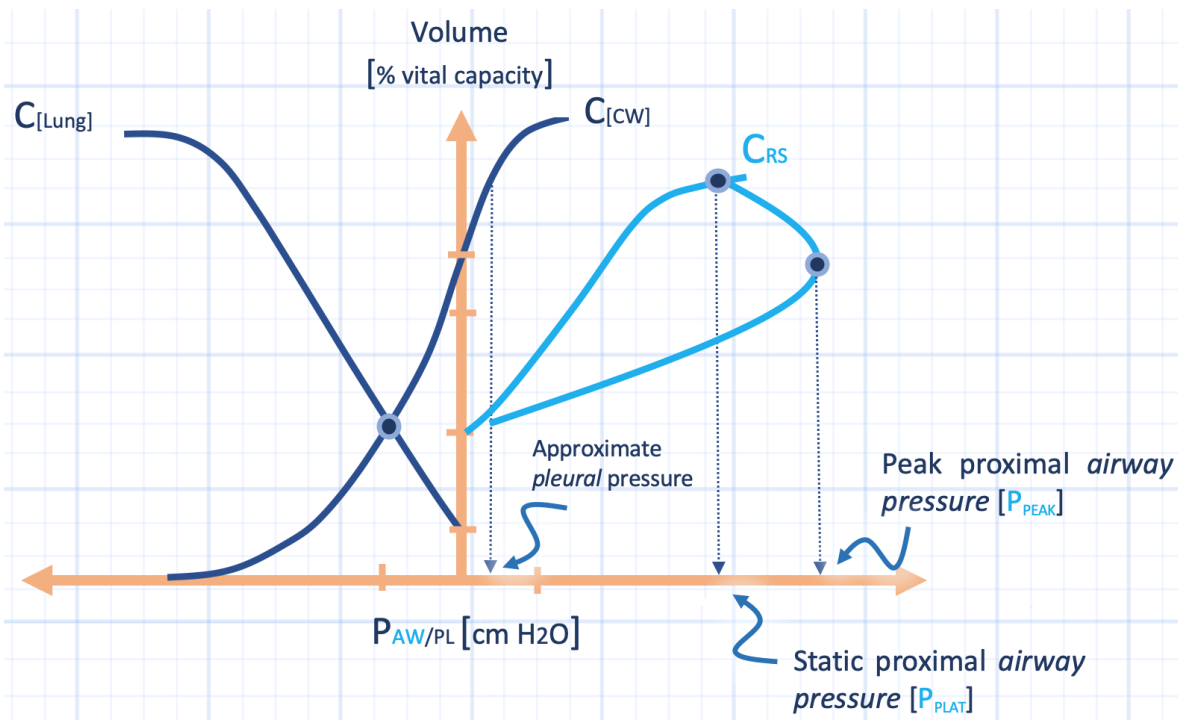

Figure 13: The dynamic pressure of a passive, mechanically-ventilated patient is depicted by the curve to the right of the static respiratory system compliance curve [Crs]. The dynamic pressure defines the peak proximal airway pressure while the Crs curve defines the static proximal airway pressure [i.e. the plateau

pressure]. Recall that the chest wall compliance curve [Ccw] defines the pleural pressure [Ppl] in the passive, ventilated-patient. Paw is airway pressure and cm H_2O is centimetres of water. C[Lung] is lung compliance, C[CW] is chest wall compliance.

The Peak and Dynamic Pressures

The peak proximal airway pressure during volume-targeted mechanical ventilation represents the summation of the static pressure required to maintain thoracic volume plus dynamic pressure required to overcome resistance to air flow.

(14) $$peak\ pressure = plateau\ pressure + dynamic\ pressure$$

or

(15) $$dynamic\ pressure = peak\ pressure - plateau\ pressure$$

Equations 14 & 15: Dynamic airway pressure

As with spontaneous ventilation, the dynamic pressure gradient is proportional to air flow and airway resistance [76]. On a mechanical ventilator, certain modes [e.g. volume-targeted modes] allow direct control of the flow delivered to the patient as well as the pattern by which flow is delivered. In order to best analyze the ventilator pressure waveform, it is most helpful to deliver a constant flow [or square wave] pattern so that this variable remains constant during inspiration [88]. If the delivered volume and airflow are constant, then the peak pressure changes based on respiratory system compliance and/or airway resistance by expansion of the equation of motion [33, 35]:

(16) $$peak\ pressure = \frac{tidal\ volume}{respiratory\ system\ compliance} + [airflow\ x\ airway\ resistance]$$

Equation 16: The peak airway pressure as described by the equation of motion

Parsing out the relative contributions of the plateau and dynamic pressures to an elevated peak pressure requires an end-inspiratory pause [88]. A large drop from the peak to the plateau pressure reveals an elevated dynamic pressure due to either high airflow and/or high inspiratory airway resistance [either within the lungs or the ventilator circuit] [89]. However, a small difference between an elevated peak pressure and the plateau pressure illustrates an excessive static contribution - either from large tidal volume, poor respiratory system compliance, or both [88].

Inspiratory airway resistance can be calculated from the dynamic pressure by the following equation.

(17) $$[peak\ pressure - plateau\ pressure] = airflow\ x\ airway\ resistance$$

or

$$(18)\quad airway\ resistance\ =\ \frac{[peak\ pressure\ -\ plateau\ pressure]}{airflow}$$

Equations 17 & 18: Calculating airway resistance.

A normal airway resistance is less than 4.0 cm H2O/L/second and most of this normal resistance comes from the oropharynx and large airways [90]. This value may increase roughly two-fold in a ventilated patient secondary to the increased resistance provided by the endotracheal tube [91].

As can be seen on the Campbell diagram with the respiratory system compliance curve included, increased dynamic pressure in the mechanically-ventilated patient only increases peak proximal airway pressure [figure 13]. Without a change in the lung and chest wall compliance, the pleural pressure is not exposed to the high proximal pressure. This is not to say, however, that disease states typified by high airflow and airway resistance [and therefore dynamic pressure] do not affect pleural pressure; they commonly do, but because of auto-PEEP, as described below [92].

Work of Breathing in the Mechanically Ventilated Patient

Like the spontaneously breathing patient, mechanical work of breathing is separated into elastic work, which is temporarily stored in the elastic tissues, and resistive work, which is dissipated against friction as heat [29]. The pressure waveform provides information about both elastic and resistive work when an end-inspiratory pause maneuver is undertaken [88]. Of note, work of breathing is estimated from the pressure waveform when flow is a constant, square waveform. The reason for this is that when flow is constant, volume and time become linear analogs [76]. Recall that work is the area under the pressure-volume curve and not the pressure-time curve. If flow has a decelerating, or changing rate, then the assumption of volume and time co-variance is erroneous and work cannot be derived from the pressure waveform. Work of breathing in the mechanically-ventilated patient has emerging relevance because work over time is power and the total power felt by the lungs may mediate acute respiratory distress syndrome. This is discussed further in chapter 9.

An inspiratory pause introduces a well-recognized pattern into the pressure waveform [93]. A line drawn from the initiation of inspiration to the beginning of the plateau pressure forms the hypotenuse of a right triangle; the area of this triangle approximates elastic work of breathing [88]. Above this triangle, a parallelogram is formed and bounded by the outline of the pressure waveform, the peak pressure and the onset of the plateau pressure [figure 14]. The area of this parallelogram represents the resistive work of breathing. Interestingly, if one were to invert the axes of this diagram, by placing volume on the y-axis and pressure on the x-axis, the resulting diagram closely mimics the static and dynamic pressure-volume relationships described above by the static and dynamic curves of the

respiratory system. The hypotenuse of the right triangle mirrors the static pressure-volume relationship of the respiratory system and the outline of the pressure waveform beyond the hypotenuse demarcates the dynamic pressure required to overcome airflow resistance. Consequently, the areas of static and resistive work of breathing are completely analogous to the pictorial descriptions used to calculate work of breathing in the spontaneous patient.

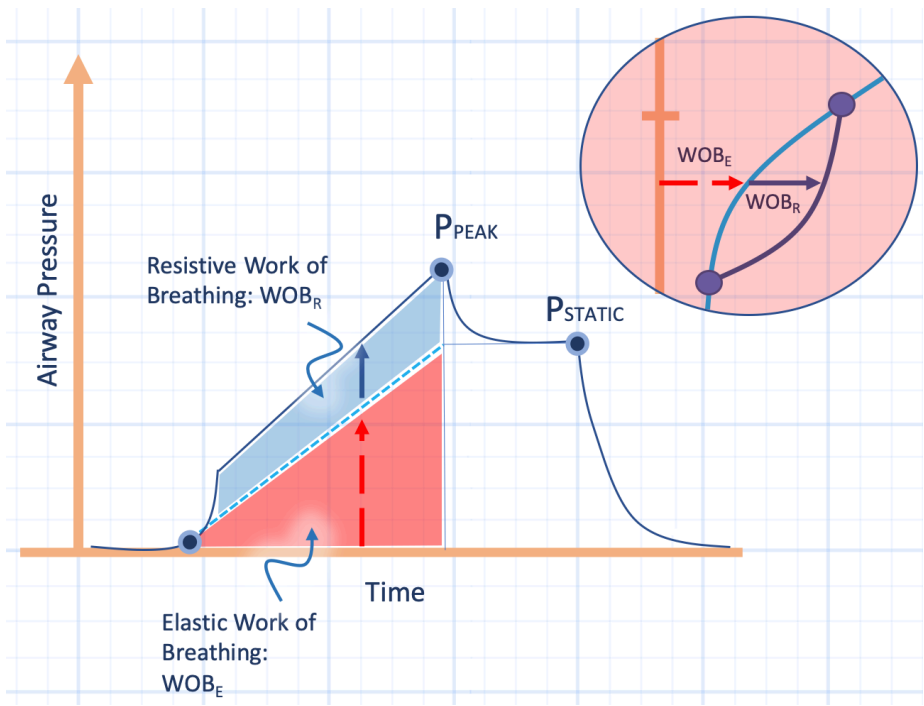

Figure 14: Work of breathing from an end-inspiratory hold on the ventilator. The patient must be receiving volume-targeted, constant-flow mechanical ventilation. The onset of the end-inspiratory hold creates the difference between the peak pressure [Ppeak] and plateau pressure [Pstatic]. The work of breathing is demarcated by the shaded areas. When there is constant flow, time and volume become linear-analogs such that it becomes a pressure-volume graph. If the ventilator graph is inverted [with pressure on the x-axis and volume/time on the y-axis], the ventilator graphic approximates the modified Campbell diagram [inset]. The elastic work of breathing [WOBe] and dynamic or resistive work of breathing [WOBr] are visualized on the inset [see also figure 13].

The Mechanically Ventilated Patient with Active Respiratory Efforts

Determining the pleural pressure in a ventilated patient making spontaneous respiratory efforts is difficult without direct measurement via an esophageal balloon [88, 94]. Sometimes excessive respiratory effort can be judged clinically, by the airway pressure waveform [95] or by evaluation of pulmonary artery occlusion pressure tracings, though these techniques can only suggest the direction of pleural pressure change, rather than the actual value of the pleural pressure [96]. Respiratory effort invalidates most of the assumptions put forth above. Accurate estimation of the pleural pressure cannot be made with actively changing chest wall compliance - as occurs with inspiratory and expiratory muscle activation [97]. An essential detail is that during modes of ventilation that require patient effort [e.g. non-invasive positive pressure, assisted breaths and pressure support] the pleural pressure can be, and often is, sub-atmospheric despite mechanical ventilation [94]. In this situation, the mechanical ventilation is unloading the muscles of respiration; the application of positive pressure at the mouth, however, does not equate to a

positive pleural pressure. Recognition of this seeming paradox is crucial when considering the hemodynamic sequelae of mechanical ventilation [73]. Aspects of this physiology are described in chapter 9 in the context of positive end-expiratory pressure during an asthma exacerbation.

Auto-PEEP

Normally, during passive expiration, the energy stored in the elastic tissue of the lung is briefly distributed to the alveolus which drives airflow out of the lung [98, 99]. At end-expiration, alveolar pressure equates with atmospheric pressure and flow ceases. However, when flow does not terminate at end-expiration, pressure remains in the alveolus and this is termed positive end-expiratory pressure [PEEP] [100]. When PEEP occurs as a result of a pathological process, it is often termed 'intrinsic,' 'occult,' or 'auto' PEEP to distinguish it from PEEP that is applied to a ventilator circuit, or 'extrinsic' PEEP [101, 102].

Formation of Auto-PEEP

Auto-PEEP forms when the alveolus is unable to empty by end-expiration. This is favoured when pulmonary time constants are prolonged and/or the time allowed for expiration is short [103]. A pulmonary time constant is the time required to inflate or deflate a lung unit. Mathematically, the time constant is the product of compliance and resistance. Accordingly, elevated expiratory resistance and/or lung compliance prolong emptying time [100]. If lung units with prolonged time constants are exposed to a short expiratory time [e.g. tachypnea], auto-PEEP is likely to occur [101]. Thus, patients with emphysema are at particular risk for auto-PEEP. During an exacerbation of emphysema, lung units - which have high compliance secondary to elastin and collagen destruction - experience elevated expiratory resistance. The elevation in expiratory airway resistance is due to the underlying exacerbation trigger, airway secretions and also dynamic collapse of the small airways during forced expiration [104]. As respiratory rate increases to maintain minute ventilation, expiratory time diminishes; auto-PEEP is the result [105].

Heterogeneity of Auto-PEEP

Unlike extrinsic PEEP applied by a ventilator, auto-PEEP is not uniformly distributed throughout the lung because auto-PEEP tends to form in areas where airway collapse [and therefore high expiratory resistance] is present. Accordingly, auto-PEEP is commonly encountered in the dependent portions of the lungs where pleural pressure is relatively high [106]. Dependent airway closure can occur in healthy patients but is accentuated in recumbency, emphysema, lung injury and

obesity [107-109]. Pooling of secretions in the dependent airways also elevates airway resistance and enhances auto-PEEP [100].

Dynamic Hyperinflation

Dynamic hyperinflation refers to increased end-expiratory lung volume secondary to auto-PEEP. Note that dynamic hyperinflation refers to pathologically elevated thoracic volume, whereas auto-PEEP is a pressure. Therefore the presence of auto-PEEP encourages dynamic hyperinflation, but the actual increase in thoracic volume is related to the compliance of the lungs and chest wall [100].

Consequences of Auto-PEEP and Dynamic Hyperinflation

Auto-PEEP has a multitude of consequences for both pulmonary and cardio-circulatory physiologies [55, 92, 110]. First, auto-PEEP presents an inspiratory load upon the muscles of respiration [42, 110]. In the spontaneously breathing patient, alveolar end-expiratory pressure above atmospheric pressure must be overcome to generate inspiratory airflow. Second, if dynamic hyperinflation occurs, the lungs and chest wall move to the less compliant portions of their pressure-volume curves. Consequently, pleural pressure must be dragged downwards to a greater degree [and more breathing work performed] to exchange gas [30, 42, 111]. Third, dynamic hyperinflation of the lungs is strongly correlated with subjective dyspnea [54, 64, 90, 112, 113]. Fourth, because auto-PEEP loads the respiratory muscles, this can lead to patient-ventilator asynchrony during triggered and spontaneous breathing [95]. Additionally, auto-PEEP may interfere with pressure-targeted ventilation modes [114].

As mentioned, auto-PEEP hinders the initiation of inspiration because elevated alveolar pressure must be pulled below mouth pressure [atmospheric pressure] to generate inspiratory flow. Whether a ventilator is triggered by a drop in mouth pressure or an inspiratory flow deflection, the presence of auto-PEEP retards breath-triggering. What may be less apparent is that the treatment of auto-PEEP in the ventilated patient – spontaneously triggering breaths – includes applying extrinsic-PEEP [115]. By elevating the pressure at the mouth, the pressure gradient at end-expiration from the alveolus to the mouth narrows; this facilitates breath trigger.

The presence of auto-PEEP especially impairs pressure-targeted modes of ventilation because applying constant pressure [rather than volume] is confounded by the auto-PEEP. If auto-PEEP is neglected by the clinician, administering a pressure-targeted mode of ventilation may provide insufficient volume and flow because of a smaller-than-anticipated pressure gradient from mouth to alveolus. Unexpectedly low tidal volumes may appear with compensatory tachypnea [114]. This can produce a vicious cycle because shortened expiratory time from high respiratory rate worsens auto-PEEP which, in turn, reduces the mouth-to-alveolus

pressure gradient and, therefore, tidal volume. Thus, reduction in respiratory rate may unexpectedly increase tidal volume in pressure-targeted ventilation with auto-PEEP [100].

The hemodynamic consequences of auto-PEEP are thought to be secondary to increased lung volume [dynamic hyperinflation] rather than the alveolar pressure per se [55]; however, elevated trans-pulmonary pressure itself is hypothesized to tax the cardiovascular system [116]. Auto-PEEP and dynamic hyperinflation generate Starling resistors within the pulmonary circulation [117]. This effect creates Va/Q mismatch and afterloads the right-ventricle. Further, dynamic hyperinflation of the lower lobes can raise the pressure around the heart and induce constrictive cardiac physiology [118, 119]. Additionally, depending on the relative compliances of the lungs and chest wall, the degree to which the auto-PEEP alters pleural pressure may retard ingress of blood to the thorax [82]. However, in patients with exacerbation of obstructive airways disease, the pleural pressure may still be significantly negative during inspiration, even in the presence of severe auto-PEEP [120, 121].

Detection of Auto-PEEP

Measurement of auto-PEEP requires a high index of suspicion by the clinician. Excessive auto-PEEP may present dramatically as in a patient with acute broncho-obstruction and cardiovascular collapse secondary to right ventricular failure. Much more often, however, auto-PEEP is subtle [100]. A ventilator expiratory flow tracing that does not reach zero prior to inspiration is one clue to the presence of auto-PEEP [122]. Importantly, there is no correlation between the degree of end-expiratory flow limitation and amount of auto-PEEP [76]. Classically, auto-PEEP is measured via an end-expiratory hold which, like an end-inspiratory hold, approximates alveolar pressure via cessation of air flow. The end-expiratory pressure obtained by this method will reflect the summation of both auto-PEEP and ventilator-applied extrinsic PEEP [101]. However, an end-expiratory hold will measure the 'average' amount of pressure remaining in lung units that are open to the central airways. If auto-PEEP occurs behind collapsed airways at end-expiration [e.g. in the dependent lung zones] then the PEEP in these units will be truly occult and auto-PEEP is underestimated [Figure 15] [100]. If, during a prolonged end-expiratory hold, there is a slow rise in the pressure trace, then this indicates flow from behind collapsed lung units leaking into the central airways.

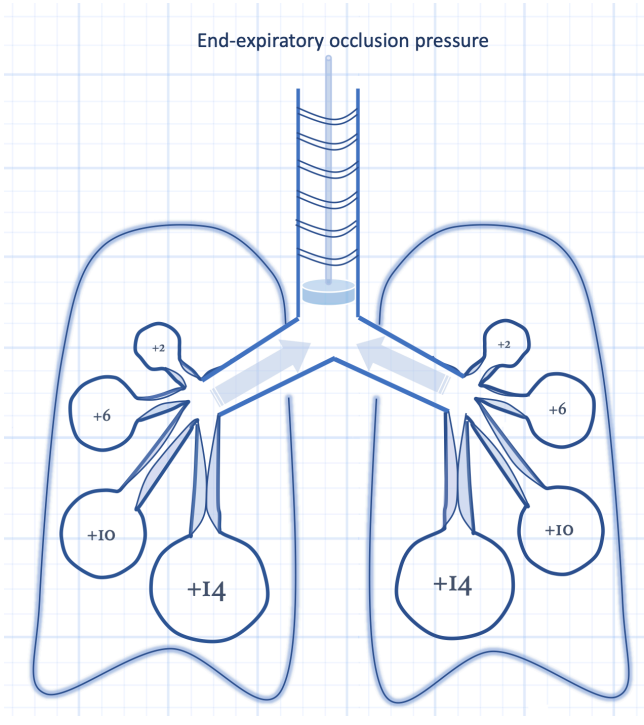

Figure 15: The end-expiratory hold may underestimate total PEEP when auto-PEEP is 'hidden' behind collapsed airways. Here, an end-expiratory hold may read 8 cm H_2O when in actuality the amount of auto-PEEP is much higher. Detecting this 'hidden' auto-PEEP may be achieved by following end-inspiratory holds or the stress index [see text and figure 16].

An end-inspiratory hold may therefore be useful; at end-inspiration all of the lung units should be open to the central airways. If there is a significant drop in the plateau pressure after a prolonged expiration, or ventilator disconnect, then this may indicate occult PEEP as a cause of poor pulmonary compliance [100]. Lastly, in a volume-targeted, constant-flow mode of ventilation, the terminal portion of the pressure waveform may suggest auto-PEEP. If volume, flow and airway resistance are constant through a breath, then the terminal portion of the pressure waveform reflects changes in end-inspiratory compliance [figure 16] [123].

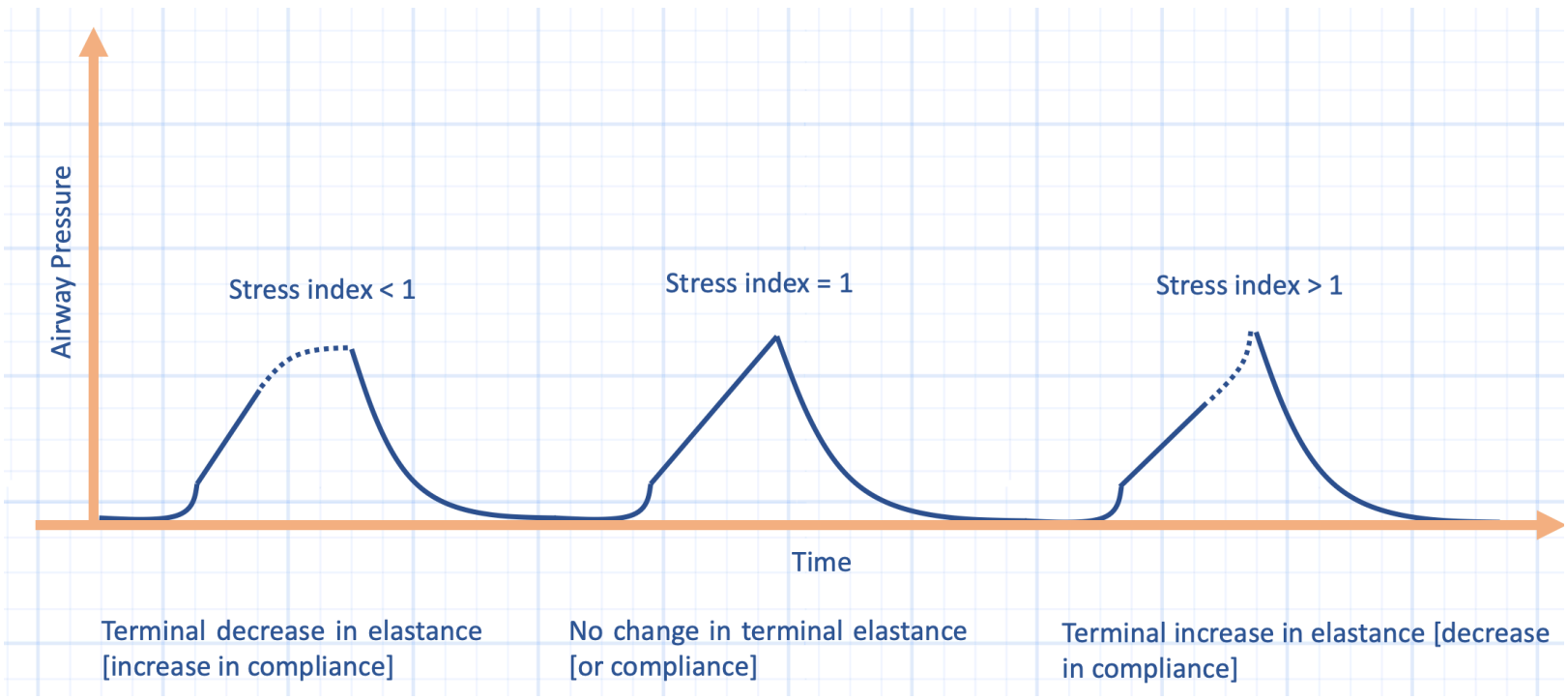

Figure 16: The stress index may detect auto-PEEP. When the stress index is less than 1, there is a suggestion of alveolar recruitment at end-inspiration, such a patient may need more extrinsic-PEEP. When the stress index is more than 1, it suggests alveolar over-distention at the end of the breath. This may be due to auto-PEEP. Importantly, the stress-index may only be derived during volume-targeted, constant-flow [square wave flow] mechanical ventilation.

If there is excessive auto-PEEP, then alveolar over-distention at end-inspiration causes a terminal upwards concavity of the pressure waveform [an increase in elastance or decrease in compliance]. Conversely, if recruitment of atelectatic lung units occurs at end-inspiration, without over-distention, then the terminal portion of the pressure waveform is marked by a terminal convexity. In this latter situation, application of extrinsic PEEP may optimize lung compliance and alveolar recruitment [123]. The physiology of the terminal portion of the pressure waveform, or 'stress index,' is further discussed in chapter 9 in the context of the pressure-volume curve and driving pressure.

Conclusion

Respiratory mechanics are nicely illustrated by the Campbell diagram during spontaneous breathing. When a patient is passive with the ventilator, a modified Campbell diagram that depicts the lung and chest wall compliances, in addition to the combined compliance of the respiratory system, is helpful. Because these analyses highlight thoracic volume and pleural pressure as functions of lung and chest wall mechanics, the reader is well-positioned for qualitative study of heart-lung interactions in sickness and in health.

References

1. Lucangelo, U., F. Bernabe, and L. Blanch, Lung mechanics at the bedside: make it simple. Curr Opin Crit Care, 2007. 13(1): p. 64-72.
2. Gibson, G.J., Lung volumes and elasticity. Clin Chest Med, 2001. 22(4): p. 623-35, vii.
3. Harris, R.S., Pressure-volume curves of the respiratory system. Respir Care, 2005. 50(1): p. 78-98; discussion 98-9.
4. Fenn, W.O., Mechanics of respiration. Am J Med, 1951. 10(1): p. 77-90.
5. Inoue, H., C. Inoue, and J. Hildebrandt, Temperature effects on lung mechanics in air- and liquid-filled rabbit lungs. J Appl Physiol Respir Environ Exerc Physiol, 1982. 53(3): p. 567-75.
6. Ruff, F., et al., Regional lung function in patients with hepatic cirrhosis. J Clin Invest, 1971. 50(11): p. 2403-13.
7. Guerin, C., et al., Small airway closure and positive end-expiratory pressure in mechanically ventilated patients with chronic obstructive pulmonary disease. Am J Respir Crit Care Med, 1997. 155(6): p. 1949-56.
8. Matamis, D., et al., Total respiratory pressure-volume curves in the adult respiratory distress syndrome. Chest, 1984. 86(1): p. 58-66.
9. Hogg, J.C., et al., Elastic properties of the centrilobular emphysematous space. J Clin Invest, 1969. 48(7): p. 1306-12.
10. Dhand, R., Ventilator graphics and respiratory mechanics in the patient with obstructive lung disease. Respir Care, 2005. 50(2): p. 246-61; discussion 259-61.
11. Stromberg, D.D. and C.A. Wiederhielm, Viscoelastic description of a collagenous tissue in simple elongation. J Appl Physiol, 1969. 26(6): p. 857-62.
12. Snider, G.L., et al., Respiratory mechanics in hamsters following treatment with endotracrael elastase or collagenase. J Appl Physiol Respir Environ Exerc Physiol, 1977. 42(2): p. 206-15.
13. Stamenovic, D., Micromechanical foundations of pulmonary elasticity. Physiol Rev, 1990. 70(4): p. 1117-34.
14. Hogg, J.C., Pathophysiology of airflow limitation in chronic obstructive pulmonary disease. Lancet, 2004. 364(9435): p. 709-21.
15. Clements, J.A., E.S. Brown, and R.P. Johnson, Pulmonary surface tension and the mucus lining of the lungs: some theoretical considerations. J Appl Physiol, 1958. 12(2): p. 262-8.
16. Frerking, I., et al., Pulmonary surfactant: functions, abnormalities and therapeutic options. Intensive Care Med, 2001. 27(11): p. 1699-717.
17. Lopez-Rodriguez, E. and J. Perez-Gil, Structure-function relationships in pulmonary surfactant membranes: from biophysics to therapy. Biochim Biophys Acta, 2014. 1838(6): p. 1568-85.
18. Mead, J., J.L. Whittenberger, and E.P. Radford, Jr., Surface tension as a factor in pulmonary volume-pressure hysteresis. J Appl Physiol, 1957. 10(2): p. 191-6.
19. Radford, E.P., Jr., Method for estimating respiratory surface area of mammalian lungs from their physical characteristics. Proc Soc Exp Biol Med, 1954. 87(1): p. 58-61.
20. Schmidt, R., et al., Alteration of fatty acid profiles in different pulmonary surfactant phospholipids in acute respiratory distress syndrome and severe pneumonia. Am J Respir Crit Care Med, 2001. 163(1): p. 95-100.
21. Gunther, A., et al., Surfactant alterations in severe pneumonia, acute respiratory distress syndrome, and cardiogenic lung edema. Am J Respir Crit Care Med, 1996. 153(1): p. 176-84.
22. Agostoni, E. and R. Hyatt, Static behaviour of the respiratory system. Handbook of physiology, Section, 1986. 3: p. 113-130.
23. Behazin, N., et al., Respiratory restriction and elevated pleural and esophageal pressures in morbid obesity. J Appl Physiol (1985), 2010. 108(1): p. 212-8.
24. Pelosi, P., et al., Total respiratory system, lung, and chest wall mechanics in sedated-paralyzed postoperative morbidly obese patients. Chest, 1996. 109(1): p. 144-51.
25. Pelosi, P., et al., Effects of the prone position on respiratory mechanics and gas exchange during acute lung injury. Am J Respir Crit Care Med, 1998. 157(2): p. 387-93.
26. Ranieri, V.M., et al., Impairment of lung and chest wall mechanics in patients with acute respiratory distress syndrome: role of abdominal distension. Am J Respir Crit Care Med, 1997. 156(4 Pt 1): p. 1082-91.
27. Janssens, J.P., J.C. Pache, and L.P. Nicod, Physiological changes in respiratory function associated with ageing. Eur Respir J, 1999. 13(1): p. 197-205.
28. Turner, J.M., J. Mead, and M.E. Wohl, Elasticity of human lungs in relation to age. J Appl Physiol, 1968. 25(6): p. 664-71.
29. Banner, M.J., M.J. Jaeger, and R.R. Kirby, Components of the work of breathing and implications for monitoring ventilator-dependent patients. Crit Care Med, 1994. 22(3): p. 515-23.
30. Loring, S.H., M. Garcia-Jacques, and A. Malhotra, Pulmonary characteristics in COPD and mechanisms of increased work of breathing. J Appl Physiol (1985), 2009. 107(1): p. 309-14.
31. Duranti, R., et al., Respiratory mechanics in patients with tense cirrhotic ascites. Eur Respir J, 1997. 10(7): p. 1622-30.

32. Hildebrandt, J., Dynamic properties of air-filled excised cat lung determined by liquid plethysmograph. J Appl Physiol, 1969. 27(2): p. 246-50.
33. Pedley, T. and J.M. Drazen, Aerodynamic theory. Compr Physiol, 2011.
34. Yellin, E.L., Laminar-turbulent transition process in pulsatile flow. Circ Res, 1966. 19(4): p. 791-804.
35. Rodarte, J.R. and K. Rehder, Dynamics of respiration. Compr Physiol, 1986.
36. Ma, B. and C. Darquenne, Aerosol deposition characteristics in distal acinar airways under cyclic breathing conditions. J Appl Physiol (1985), 2011. 110(5): p. 1271-82.
37. Wigmore, T. and E. Stachowski, A review of the use of heliox in the critically ill. Crit Care Resusc, 2006. 8(1): p. 64-72.
38. Curtis, J.L., et al., Helium-oxygen gas therapy. Use and availability for the emergency treatment of inoperable airway obstruction. Chest, 1986. 90(3): p. 455-7.
39. Maggiore, S.M., et al., A multicenter, randomized trial of noninvasive ventilation with helium-oxygen mixture in exacerbations of chronic obstructive lung disease. Crit Care Med, 2010. 38(1): p. 145-51.
40. Kumar, D. and R.K. Saksena, Best evidence topic report. Use of Heliox in the management of acute exacerbation of COPD. Emerg Med J, 2007. 24(1): p. 45-8.
41. Rodrigo, G., et al., Heliox for nonintubated acute asthma patients. Cochrane Database Syst Rev, 2006(4): p. CD002884.
42. Vassilakopoulos, T., Understanding wasted/ineffective efforts in mechanically ventilated COPD patients using the Campbell diagram. Intensive Care Med, 2008. 34(7): p. 1336-9.
43. Roussos, C. and E. Campbell, Respiratory muscle energetics. Handbook of physiology, Section, 1986. 3: p. 481-509.
44. Christie, R.V., Dyspnoea in relation to the visco-elastic properties of the lung. Proc R Soc Med, 1953. 46(5): p. 381-6.
45. Roussos, C. and A. Koutsoukou, Respiratory failure. Eur Respir J Suppl, 2003. 47: p. 3s-14s.
46. O'Donnell, D.E., et al., Qualitative aspects of exertional breathlessness in chronic airflow limitation: pathophysiologic mechanisms. Am J Respir Crit Care Med, 1997. 155(1): p. 109-15.
47. Guenette, J.A., et al., Sex differences in the resistive and elastic work of breathing during exercise in endurance-trained athletes. Am J Physiol Regul Integr Comp Physiol, 2009. 297(1): p. R166-75.
48. Goldman, M.D., G. Grimby, and J. Mead, Mechanical work of breathing derived from rib cage and abdominal V-P partitioning. J Appl Physiol, 1976. 41(5 Pt. 1): p. 752-63.
49. Bachofen, H. and J. Hildebrandt, Area analysis of pressure-volume hysteresis in mammalian lungs. J Appl Physiol, 1971. 30(4): p. 493-7.
50. Sharp, J.T., et al., Effects of Mass Loading the Respiratory System in Man. J Appl Physiol, 1964. 19: p. 959-66.
51. Cournand, A., et al., The oxygen cost of breathing. Trans Assoc Am Physicians, 1954. 67: p. 162-73.
52. Luce, J.M., Respiratory complications of obesity. Chest, 1980. 78(4): p. 626-31.
53. Young, I.H. and P.T. Bye, Gas exchange in disease: asthma, chronic obstructive pulmonary disease, cystic fibrosis, and interstitial lung disease. Compr Physiol, 2011. 1(2): p. 663-97.
54. O'Donnell, D.E. and K.A. Webb, The major limitation to exercise performance in COPD is dynamic hyperinflation. J Appl Physiol (1985), 2008. 105(2): p. 753-5; discussion 755-7.
55. Berlin, D., Hemodynamic consequences of auto-PEEP. J Intensive Care Med, 2014. 29(2): p. 81-6.
56. Bouhuys, A. and B. Jonson, Alveolar pressure, airflow rate, and lung inflation in man. J Appl Physiol, 1967. 22(6): p. 1086-100.
57. Fry, D.L., et al., The mechanics of pulmonary ventilation in normal subjects and in patients with emphysema. Am J Med, 1954. 16(1): p. 80-97.
58. Fry, D.L. and R.E. Hyatt, Pulmonary mechanics. A unified analysis of the relationship between pressure, volume and gasflow in the lungs of normal and diseased human subjects. Am J Med, 1960. 29: p. 672-89.
59. Mead, J., et al., Significance of the relationship between lung recoil and maximum expiratory flow. J Appl Physiol, 1967. 22(1): p. 95-108.
60. DeGraff, A.C., Jr. and A. Bouhuys, Mechanics of air flow in airway obstruction. Annu Rev Med, 1973. 24: p. 111-34.
61. Brusasco, V. and F. Martinez, Chronic obstructive pulmonary disease. Compr Physiol, 2014. 4(1): p. 1-31.
62. Aubier, M., et al., Effects of the administration of O2 on ventilation and blood gases in patients with chronic obstructive pulmonary disease during acute respiratory failure. Am Rev Respir Dis, 1980. 122(5): p. 747-54.
63. Austin, M.A., et al., Effect of high flow oxygen on mortality in chronic obstructive pulmonary disease patients in prehospital setting: randomised controlled trial. BMJ, 2010. 341: p. c5462.
64. Lougheed, M.D., T. Fisher, and D.E. O'Donnell, Dynamic hyperinflation during bronchoconstriction in asthma: implications for symptom perception. Chest, 2006. 130(4): p. 1072-81.
65. Vogiatzis, I., et al., Intercostal muscle blood flow limitation during exercise in chronic obstructive pulmonary disease. Am J Respir Crit Care Med, 2010. 182(9): p. 1105-13.
66. Levison, H. and R.M. Cherniack, Ventilatory cost of exercise in chronic obstructive pulmonary disease. J Appl Physiol, 1968. 25(1): p. 21-7.

67. Aaron, E.A., et al., Oxygen cost of exercise hyperpnea: measurement. J Appl Physiol (1985), 1992. 72(5): p. 1810-7.
68. Shibutani, K., et al., Critical level of oxygen delivery in anesthetized man. Crit Care Med, 1983. 11(8): p. 640-3.
69. Krafft, P., et al., Mixed Venous Oxygen-Saturation in Critically Ill Septic Shock Patients - the Role of Defined Events. Chest, 1993. 103(3): p. 900-906.
70. Cain, S.M., Peripheral oxygen uptake and delivery in health and disease. Clin Chest Med, 1983. 4(2): p. 139-48.
71. Kasnitz, P., et al., Mixed venous oxygen tension and hyperlactatemia. Survival in severe cardiopulmonary disease. JAMA, 1976. 236(6): p. 570-4.
72. Simmons, D.H., et al., Hyperlactatemia due to arterial hypoxemia or reduced cardiac output, or both. J Appl Physiol Respir Environ Exerc Physiol, 1978. 45(2): p. 195-202.
73. Pinsky, M.R., Cardiovascular issues in respiratory care. Chest, 2005. 128(5 Suppl 2): p. 592S-597S.
74. Rahn, H., A.B. Otis, and et al., The pressure-volume diagram of the thorax and lung. Am J Physiol, 1946. 146(2): p. 161-78.
75. Leith, D.E. and R. Brown, Human lung volumes and the mechanisms that set them. Eur Respir J, 1999. 13(2): p. 468-72.
76. Bekos, V. and J.J. Marini, Monitoring the mechanically ventilated patient. Crit Care Clin, 2007. 23(3): p. 575-611.
77. Gottfried, S.B., et al., Interrupter technique for measurement of respiratory mechanics in anesthetized humans. J Appl Physiol (1985), 1985. 59(2): p. 647-52.
78. Jonson, B., et al., Monitoring of ventilation and lung mechanics during automatic ventilation. A new device. Bull Physiopathol Respir (Nancy), 1975. 11(5): p. 729-43.
79. Jardin, F., et al., Influence of lung and chest wall compliances on transmission of airway pressure to the pleural space in critically ill patients. Chest, 1985. 88(5): p. 653-8.
80. O'Quin, R.J., et al., Transmission of airway pressure to pleural space during lung edema and chest wall restriction. J Appl Physiol (1985), 1985. 59(4): p. 1171-7.
81. Hess, D.R. and L.M. Bigatello, The chest wall in acute lung injury/acute respiratory distress syndrome. Curr Opin Crit Care, 2008. 14(1): p. 94-102.
82. Jardin, F. and A. Vieillard-Baron, Right ventricular function and positive pressure ventilation in clinical practice: from hemodynamic subsets to respirator settings. Intensive Care Med, 2003. 29(9): p. 1426-34.
83. Mutoh, T., et al., Abdominal distension alters regional pleural pressures and chest wall mechanics in pigs in vivo. J Appl Physiol (1985), 1991. 70(6): p. 2611-8.
84. Bigatello, L.M., K.R. Davignon, and H.T. Stelfox, Respiratory mechanics and ventilator waveforms in the patient with acute lung injury. Respir Care, 2005. 50(2): p. 235-45; discussion 244-5.
85. Hager, D.N., et al., Tidal volume reduction in patients with acute lung injury when plateau pressures are not high. Am J Respir Crit Care Med, 2005. 172(10): p. 1241-5.
86. Ventilation with lower tidal volumes as compared with traditional tidal volumes for acute lung injury and the acute respiratory distress syndrome. The Acute Respiratory Distress Syndrome Network. N Engl J Med, 2000. 342(18): p. 1301-8.
87. Talmor, D., et al., Mechanical ventilation guided by esophageal pressure in acute lung injury. N Engl J Med, 2008. 359(20): p. 2095-104.
88. Truwit, J.D. and J.J. Marini, Evaluation of thoracic mechanics in the ventilated patient Part II: applied mechanics. Journal of critical care, 1988. 3(3): p. 199-213.
89. Maung, A.A. and L.J. Kaplan, Waveform analysis during mechanical ventilation. Curr Probl Surg, 2013. 50(10): p. 438-46.
90. O'Donnell, D.E. and P. Laveneziana, Dyspnea and activity limitation in COPD: mechanical factors. COPD, 2007. 4(3): p. 225-36.
91. Wright, P.E., J.J. Marini, and G.R. Bernard, In vitro versus in vivo comparison of endotracheal tube airflow resistance. Am Rev Respir Dis, 1989. 140(1): p. 10-6.
92. Tobin, M.J. and R.F. Lodato, PEEP, auto-PEEP, and waterfalls. Chest, 1989. 96(3): p. 449-51.
93. Lucangelo, U., F. Bernabe, and L. Blanch, Respiratory mechanics derived from signals in the ventilator circuit. Respir Care, 2005. 50(1): p. 55-65; discussion 65-7.
94. Marini, J.J., J.S. Capps, and B.H. Culver, The inspiratory work of breathing during assisted mechanical ventilation. Chest, 1985. 87(5): p. 612-8.
95. Gilstrap, D. and N. MacIntyre, Patient-ventilator interactions. Implications for clinical management. Am J Respir Crit Care Med, 2013. 188(9): p. 1058-68.
96. Hoyt, J.D. and J.W. Leatherman, Interpretation of the pulmonary artery occlusion pressure in mechanically ventilated patients with large respiratory excursions in intrathoracic pressure. Intensive Care Med, 1997. 23(11): p. 1125-1131.
97. de Chazal, I. and R.D. Hubmayr, Novel aspects of pulmonary mechanics in intensive care. Br J Anaesth, 2003. 91(1): p. 81-91.
98. Marini, J.J. and S.A. Ravenscraft, Mean airway pressure: physiologic determinants and clinical importance--Part 2: Clinical implications. Crit Care Med, 1992. 20(11): p. 1604-16.
99. Marini, J.J. and S.A. Ravenscraft, Mean airway pressure: physiologic determinants and clinical importance--Part 1: Physiologic determinants and measurements. Crit Care Med, 1992. 20(10): p. 1461-72.

100. Marini, J.J., Dynamic hyperinflation and auto-positive end-expiratory pressure: lessons learned over 30 years. Am J Respir Crit Care Med, 2011. 184(7): p. 756-62.
101. Rossi, A., et al., Intrinsic positive end-expiratory pressure (PEEPi). Intensive Care Med, 1995. 21(6): p. 522-36.
102. Pinsky, M.R., Through the past darkly: ventilatory management of patients with chronic obstructive pulmonary disease. Crit Care Med, 1994. 22(11): p. 1714-7.
103. Bergman, N.A., Intrapulmonary gas trapping during mechanical ventilation at rapid frequencies. Anesthesiology, 1972. 37(6): p. 626-33.
104. O'Donnell, D.E. and C.M. Parker, COPD exacerbations . 3: Pathophysiology. Thorax, 2006. 61(4): p. 354-61.
105. Calverley, P.M. and N.G. Koulouris, Flow limitation and dynamic hyperinflation: key concepts in modern respiratory physiology. Eur Respir J, 2005. 25(1): p. 186-99.
106. Craig, D.B., et al., "Closing volume" and its relationship to gas exchange in seated and supine positions. J Appl Physiol, 1971. 31(5): p. 717-21.
107. Salome, C.M., G.G. King, and N. Berend, Physiology of obesity and effects on lung function. J Appl Physiol (1985), 2010. 108(1): p. 206-11.
108. Gattinoni, L., et al., Lung structure and function in different stages of severe adult respiratory distress syndrome. JAMA, 1994. 271(22): p. 1772-9.
109. Shim, C., et al., Positional effects on distribution of ventilation in chronic obstructive pulmonary disease. Ann Intern Med, 1986. 105(3): p. 346-50.
110. Smith, T.C. and J.J. Marini, Impact of PEEP on lung mechanics and work of breathing in severe airflow obstruction. J Appl Physiol (1985), 1988. 65(4): p. 1488-99.
111. Mead, J., Respiration: pulmonary mechanics. Annu Rev Physiol, 1973. 35: p. 169-92.
112. Stevenson, N.J., et al., Lung mechanics and dyspnea during exacerbations of chronic obstructive pulmonary disease. Am J Respir Crit Care Med, 2005. 172(12): p. 1510-6.
113. O'Donnell, D.E., Hyperinflation, dyspnea, and exercise intolerance in chronic obstructive pulmonary disease. Proc Am Thorac Soc, 2006. 3(2): p. 180-4.
114. Marini, J.J., P.S. Crooke, 3rd, and J.D. Truwit, Determinants and limits of pressure-preset ventilation: a mathematical model of pressure control. J Appl Physiol (1985), 1989. 67(3): p. 1081-92.
115. Ranieri, V.M., et al., Physiologic effects of positive end-expiratory pressure in patients with chronic obstructive pulmonary disease during acute ventilatory failure and controlled mechanical ventilation. Am Rev Respir Dis, 1993. 147(1): p. 5-13.
116. Venus, B., L.E. Cohen, and R.A. Smith, Hemodynamics and intrathoracic pressure transmission during controlled mechanical ventilation and positive end-expiratory pressure in normal and low compliant lungs. Crit Care Med, 1988. 16(7): p. 686-90.
117. Lopez-Muniz, R., et al., Critical closure of pulmonary vessels analyzed in terms of Starling resistor model. J Appl Physiol, 1968. 24(5): p. 625-35.
118. Butler, J., The heart is in good hands. Circulation, 1983. 67(6): p. 1163-8.
119. Butler, J., et al., Cause of the raised wedge pressure on exercise in chronic obstructive pulmonary disease. Am Rev Respir Dis, 1988. 138(2): p. 350-4.
120. Freedman, S., A.E. Tattersfield, and N.B. Pride, Changes in lung mechanics during asthma induced by exercise. J Appl Physiol, 1975. 38(6): p. 974-82.
121. Stalcup, S.A. and R.B. Mellins, Mechanical forces producing pulmonary edema in acute asthma. N Engl J Med, 1977. 297(11): p. 592-6.
122. Pepe, P.E. and J.J. Marini, Occult positive end-expiratory pressure in mechanically ventilated patients with airflow obstruction: the auto-PEEP effect. Am Rev Respir Dis, 1982. 126(1): p. 166-70.
123. Grasso, S., et al., Airway pressure-time curve profile (stress index) detects tidal recruitment/hyperinflation in experimental acute lung injury. Crit Care Med, 2004. 32(4): p. 1018-27.

Chapter Two

The Mechanics of Blood Flow: a graphical analysis with emphasis on the intersection of venous return and cardiac function

Abstract

The static and dynamic pressures of the cardiovascular system are determinants of vascular volume and blood flow, respectively. Comparable to the examination of respiratory physiology, graphical analysis of the cardiovascular system is achieved by relating pressure, flow and volume. The pressure-flow relationship of the cardiovascular system entails separate consideration for venous return to the heart from venous capacitance beds, in addition to cardiac output. While venous return is determined by multiple variables including mean systemic pressure, right atrial pressure and the resistance to venous return, so too is cardiac output - by preload, afterload, contractility and heart rate. The circuit function curve and cardiac function curve are both pressure-flow relationships that are gross representations of these aforementioned variables. Examining the determinants and morphologies of these curves provide physiological insight into cardiovascular function and facilitate deep appreciation for heart-lung interaction.

Key Words: Venous return, mean systemic pressure, cardiac output, Guyton, Frank-Starling, Sagawa, impedance, pulmonary vascular resistance, heart-lung interaction.

Introduction

Much like the respiratory system, the cardiovascular system is understood in terms of pressures, volumes and flows. As graphical representation of these concepts via the Campbell diagram assist with respiratory physiology, so too will visual aids advance cardiovascular physiology. Unlike the Campbell diagram, which focused on the relationship between pressure and volume, cardiovascular physiology is most often analyzed by the relationship between pressure and flow. This is because cardiac output [i.e. flow] is clinically relevant and cardiac filling pressures are relatively easily obtained. Nevertheless, pressure-volume relationships are also important when dissecting the cardiovascular system because one critical component of cardiac function - the preload - is a volume, despite the commonly used surrogate, right atrial pressure.

Consequently, this chapter encourages analysis of cardiovascular function initially proposed by Guyton and subsequently expanded upon by Magder and others [1]. Simply, this approach maintains that blood flow within the cardiovascular system is determined by the relationship between venous return from the venous capacitance beds and cardiac function via the Frank-Starling mechanism – henceforth referred to as 'circuit function' and 'cardiac function,' respectively. Importantly, the right atrial pressure acts as an intermediary between circuit function and cardiac function with reversed effects on venous return and cardiac output. Accordingly, the value of the right atrial pressure is completely determined neither by circuit function nor cardiac function alone, but by the intersection of both vascular and cardiac physiologies. Additionally, this chapter provides more detailed analysis of both circuit and cardiac function. The latter is examined within the framework of the cardiac pressure-volume curve, as initially proposed by Sagawa [2, 3], as well as its corollaries, i.e. time-varying elastance [4, 5] and ventricular-vascular coupling [6].

Pressure within the Cardiovascular system

The principles outlined in chapter 1 pertaining to pressure within the respiratory system are similarly applied to the cardiovascular system. There are two general origins of pressure within the blood vessels and these are static and dynamic in nature [figure 1]. The static pressure in a blood vessel is the transmural pressure which is the pressure within the vessel less the vessel's surrounding pressure. As in the respiratory system, this pressure determines the tendency to distend or collapse, but the relationship between change in volume and pressure depends upon vascular compliance.

$$(1)\quad vascular\ compliance = \frac{\Delta\ vascular\ volume}{\Delta\ vascular\ pressure}$$

Equation 1: Vascular compliance

If applied to a blood vessel, the transmural pressure determines its radius, while in the ventricle the transmural pressure determines volume - again dependent upon compliance. The transmural pressure difference is sometimes referred to as the 'radial pressure' as this is the vector in which the pressure acts [7].

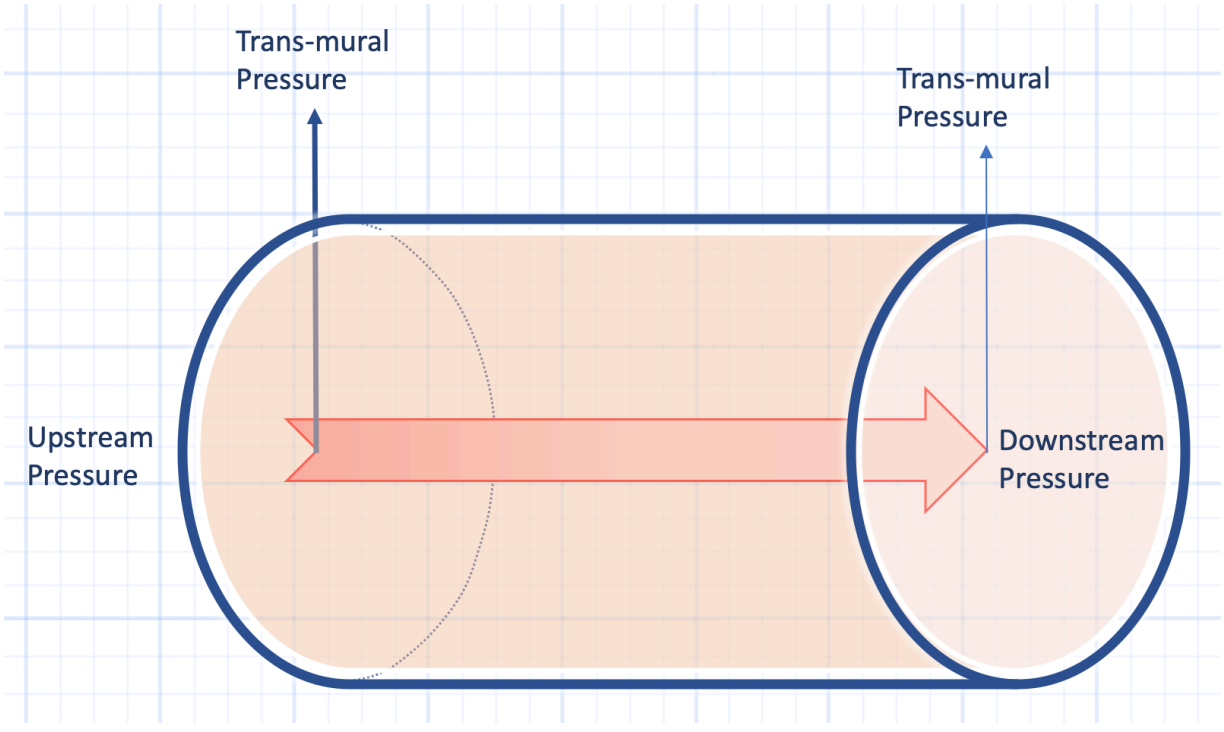

Figure 1: Static versus dynamic pressure within the cardiovascular system. The static pressure, or transmural pressure, is a determinant of vascular volume [as a function of compliance]. The transmural pressure is the pressure within the vessel less the pressure outside the vessel. By contrast, the dynamic pressure is the gradient associated with flow along the length of the blood vessel.

Conversely, the dynamic pressure of the vascular system is sometimes called the 'axial pressure' as the viscous resistance of blood causes the pressure difference when there is moving blood along the axis of the blood vessel; the axial pressure differential is completely analogous to the dynamic pressure of airflow within the tracheo-bronchial tree. Under conditions of constant, laminar flow, the pressure difference along a blood vessel is directly proportional to the magnitude of flow and its resistance as explained by Poiseulle's law [8].

(2) $$axial\ pressure\ difference\ =\ blood\ flow\ x\ resistance$$

Equation 2: The change in blood pressure as a function of flow and resistance

Much like airflow within the airways, blood flow within blood vessels does not relate linearly with the pressure difference as is predicted by the aforementioned equation. Indeed, turbulent flow and physiological coupling between intravascular pressure, vessel radius and resistance all make the vascular pressure – blood flow relationship more complicated, as detailed below.

Lastly, gravity mediates pressure within the vascular system [9]. For example, the pressure within the thoracic aorta compared to the tibial artery is much greater in the standing position compared to supination. Importantly, the difference between the arterial pressure and venous pressure remains the same regardless of body position. The reason for the pressure difference is the effect of gravity on the blood within the vascular tree. While these effects are typically neglected in the prostrate ICU patient, this phenomenon is important when considering vascular monitoring

in relationship to the phlebostatic axis and why 'zeroing' a pressure transducer must occur with changes in patient position.

Importantly, respiratory physiologists and cardiovascular physiologists have used different units to measure pressure. Centimetres of water [cmH_2O] is used when measuring pressure as it pertains to the lung and pleural space, while millimetres of mercury [mmHg] is used for intravascular pressures. The reason for the difference is historical. Centimetres of H_2O was more sensitive measuring pressure differentials within the relatively low-pressure pulmonary milieu; conversely, the high vascular pressures [at least within the arterial tree] demanded dense liquid to track pressure change. These units of measurement have persisted and must be kept in careful consideration when analyzing the effects of airway and pleural pressure on cardiovascular pressure [1 mmHg = 1.36 cm H_2O].

Systemic Venous Return

In the mid-19th century Weber provided one of the earliest models of the circulatory system upon which current understanding is based [10, 11]. He took a loop of intestine which was made into a circle and filled with water. Within one end of the loop he placed a sponge to mimic the micro-vasculature; at the other end he placed two, one-way valves to act as the heart. The pressure within the intestine at standstill was termed the 'hydrostatic mean pressure' [i.e. 'statischer fullungs-druck']. He then squeezed the portion of the intestine located between the two, one-way valves to generate unidirectional flow. This action increased pressure on the 'arterial' side of the model and decreased pressure on the 'venous' side. Importantly, Weber took detailed pressure measurements of each segment of the model during flow and found that the average pressure through the system was unchanged from the mean hydrostatic pressure [i.e. when there was no flow]! In other words, the 'heart' did not generate pressure, but instead redistributed fluid, increasing pressure in one portion of the distensible model at the expensive of another. From this analysis it was deduced that edema formation occurs not by failure of the heart's pumping function [i.e. increasingly low flow] but rather by increased mean hydrostatic pressure, [e.g. by the addition of fluid to the model, or renal fluid retention in the patient] [12]. Significantly, this model underscores the determinants of hydrostatic mean pressure [later remained the mean circulatory filling pressure - Pmcf] in cardiovascular function. Nearly 100 years after Weber, Guyton expanded the analysis of mean systemic pressure and its relation to blood flow [venous return] which underpins much of our current understanding of cardiovascular function [13-17].

The Venous Return Curve

Because the veins are 30 times more compliant than the arteries and upwards of 70% of the blood volume is within the venous system [18, 19], the body's blood reservoir is located within the veins and the pressure within this reservoir is the 'upstream pressure' for venous return to the heart.[2] Additionally, the venous reservoir is the pressure point in the circulatory system that is closest to the mean circulatory filling pressure. Based on Weber's model described above, the pressure in the arterial tree during cardiac activity is higher than mean circulatory filling pressure, while the pressure in the great veins is less than mean circulatory pressure. The inflection point – where the vascular pressure is equal to the mean circulatory filling pressure – lies within the venous reservoir; for this reason, it is sometimes referred to as the 'pivoting pressure' of the cardiovascular system [19]. Consequently, the 'driving pressure' for venous return to the right heart is the mean circulatory filling pressure less the right atrial pressure. Venous return [or flow], in turn, is directly proportional to the 'driving pressure' and inversely related to the resistance to venous return [Rvr] [see equation 3 below].

The terms mean systemic filling pressure [Pmsf] and mean circulatory filling pressure [Pmcf] are used interchangeably in this volume. Importantly, their values are nearly identical, however, mean systemic filling pressure refers to the elastic recoil pressure of the systemic circulation during no flow. The value of the mean systemic pressure can be affected by blood flow distribution prior to cessation of cardiac activity. By contrast, the mean circulatory filling pressure refers to the elastic recoil generated by blood volume in all vascular beds and when pressure within the cardiovascular system equilibrates, the resultant pressure is the mean circulatory filling pressure [20].

$$(3) \quad venous\ return = \frac{Pmcf - Pra}{Rvr}$$

Equation 3: The equation describing venous return. Pmcf is mean circulatory filling pressure; Pra is right atrial pressure and Rvr is the resistance to venous return. This book will often use the mean systemic pressure [Pmsf] as interchangeable with Pmcf and the central venous pressure [CVP] as interchangeable with the Pra.

A graphical representation of venous return is made from the aforementioned equation [figure 2]. Mathematically and experimentally, this relationship is linear. With blood flow on the y-axis and right atrial pressure on the x-axis, it is clear that as the right atrial [downstream] pressure is reduced, venous return increases.

There are three fundamental attributes of this venous return curve which will be discussed in turn: 1. the slope of the curve 2. the x-intercept and 3. the plateau in venous return as atrial pressure approaches sub-atmospheric pressure [20].

[2] As noted at the outset of chapter 1, liquid [e.g. air, blood] flows down an energy gradient; however, pressure is often used as a clinical surrogate for this energy gradient. Thus, it appears that blood flows as a function of pressure within the vascular system.

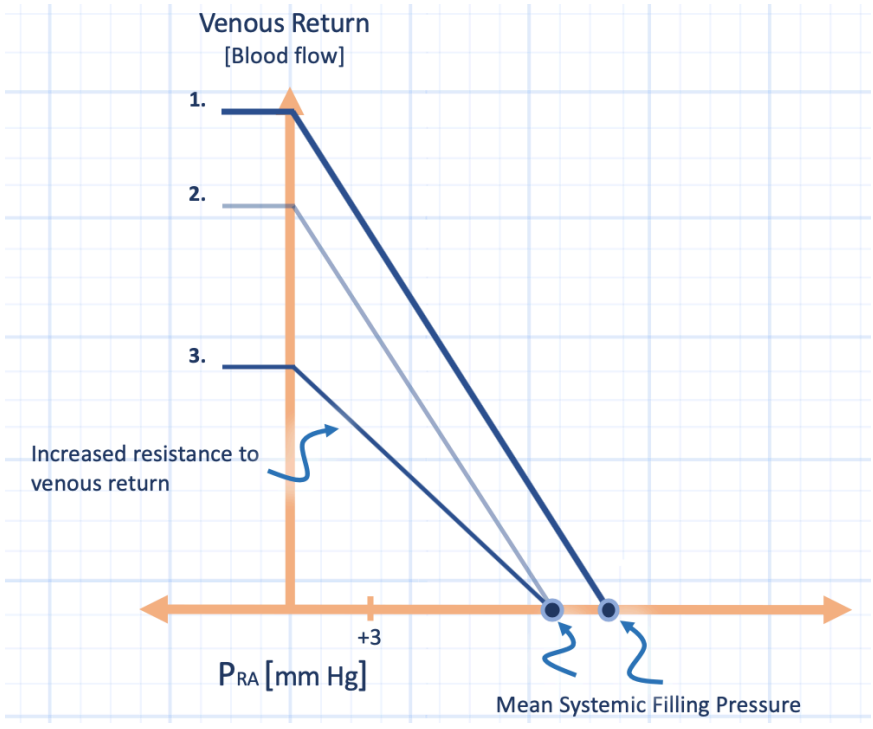

Figure 2: The venous return curve. The x-intercept is the mean systemic filling pressure [the equilibrium pressure when blood flow – the y-axis – is zero]. As right atrial pressure decreases, venous return to the thorax increases linearly with the pressure gradient defined by the mean systemic pressure and the right atrial pressure as seen on curve 2. An increase in mean systemic filling pressure [curve 1.] increases venous return for any given downstream [right atrial] pressure. An increase in the resistance to venous return [curve 3.] lowers venous return for any given downstream pressure. Pra is right atrial pressure in millimetres of mercury [mmHg].

Resistance to Venous Return

The slope of the venous return curve is equal to the resistance to venous return [Rvr]; as the resistance increases, the slope of the line is less steep [figure 2] [21]. The resistance to venous return may rise, consequent to diaphragm descent and impingement of the IVC, for example in COPD [22, 23]. It may occur as a result of an occlusive thrombus within the great veins or when abdominal pressure supersedes vascular pressure and collapses the IVC, as in states of intra-abdominal hypertension [24, 25]. Rvr may also change in response to adrenergic stimulation. Interestingly, Rvr tends to rise in response to pure alpha-agonism [26] while Rvr tends to fall in response to pure-beta agonism [27-29]. It is thought that this has to do with differential adrenergic receptor expression on various venous beds, especially within the hepatic veins [30]. The resistance to venous return may also effectively decrease as blood is diverted from a more compliant vascular bed [e.g. the splanchnic circulation] into a less compliant bed [e.g. the skeletal muscles]. While this effect may not be intuitive, it will become clearer following the discussion of mean systemic pressure below.

The Mean Circulatory and Systemic Pressure

In addition to the slope of the venous return curve, another essential aspect of the venous return curve is the x-intercept [figure 2]. When the heart is stopped, venous

return [and cardiac output] become zero. The right atrial pressure then increases to the mean circulatory filling pressure [Pmcf] or mean systemic filling pressure [Pmsf] as described above; therefore, at zero venous return, the x-intercept is the Pmsf [19].

The determinants of the Pmsf within the venous reservoir are understood in terms of vascular compliance. Importantly, however, the volume that determines pressure within the reservoir is not the total volume, but the 'stressed volume' of blood. The stressed volume is a dynamic variable that can change based on adrenergic tone and external compression of the vascular bed. Stressed volume may be modelled after an inflating balloon. A certain amount of air volume is added before pressure rises within the balloon. The amount of volume that is added without a significant rise in pressure is known as the 'unstressed volume,' whereas the volume added that increases the elastic recoil pressure of the balloon is known as the 'stressed volume.' The unstressed and stressed volumes sum to the total volume within the system. The mean systemic pressure is, accordingly, related to the stressed volume of the vascular bed and its compliance [10].

$$(4)\quad Pms(c)f = \frac{stressed\ volume}{venous\ compliance}$$

or

$$(5)\quad Pms(c)f = \frac{Total\ venous\ volume - unstressed\ venous\ volume}{venous\ compliance}$$

Equations 4 & 5: The value of the mean systemic or mean circulatory filling pressures.

From these equations, it can be seen that either increased stressed volume [e.g. increasing the total volume or decreasing the unstressed volume] or decreased venous vascular compliance both augment mean systemic pressure and shift the x-intercept of the venous return curve to the right. Clinically, this is seen in response to volume infusion or increased adrenergic tone, as adrenergic stimulation of the venous reservoir recruits unstressed volume into stressed volume. One very potent stimulus for adrenergic excitation – and consequent rightward shift of the venous return curve – is hypoxemia [31].

While stressed volume may be recruited from unstressed volume by the action of adrenergic receptors, stressed volume may also increase by elevation of ambient vascular pressure. An example of this occurs within the abdominal venous reservoir with increased intra-abdominal pressure. Abdominal pressure roughly approximates atmospheric pressure and, during normal inspiration, there is a small phasic increase in the pressure within the abdomen [Pab]. It is thought that increased pressure surrounding a vascular bed decreases the capacitance of the vessels [32]. Capacitance relates the total volume of a vascular bed to its pressure. While this is similar to compliance, it is not entirely the same as compliance refers to the change in volume in response to a change in pressure [figure 3] [33]. Physiologically, capacitance incorporates the stressed volume, unstressed volume

and compliance of a vascular bed. Therefore, as the capacitance of a blood vessel decreases, pressure rises for any given volume. Decreased capacitance is equivalent to increased mean systemic pressure or a rightward shift of the venous return curve. Hence, as abdominal pressure increases, the decrease in venous capacitance elevates venous return by augmenting the driving pressure to the right heart. In addition to changes in vascular capacitance, it is also likely that adrenergic tone [34] and shifts of blood volume from the central to the peripheral circulation [35] also mediate mean systemic filling pressure with respiration.

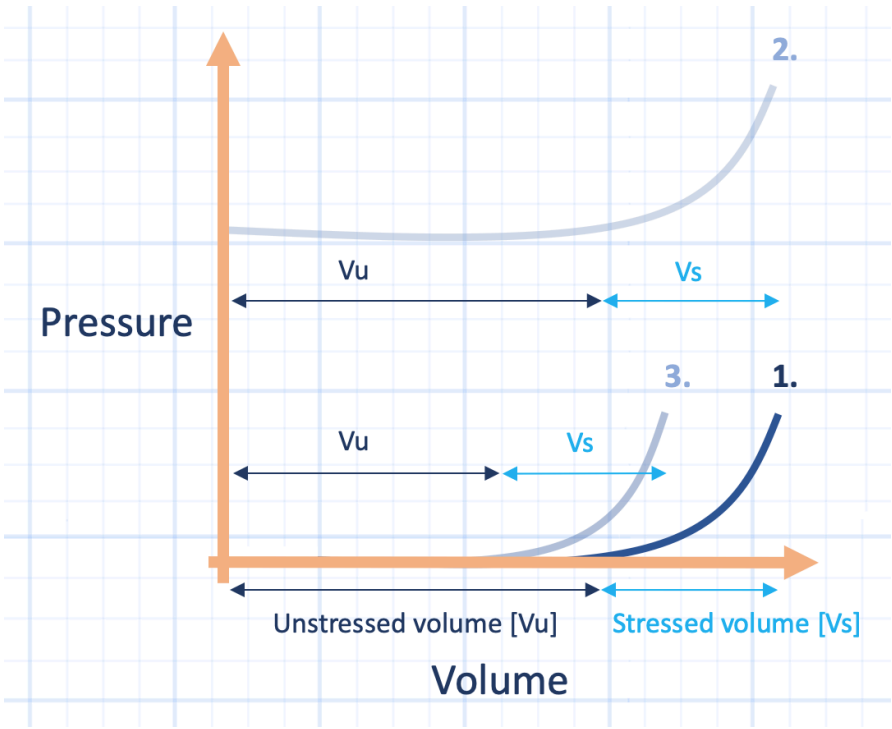

Figure 3: Three hypothetical venous capacitance curves. Note that curve 2. has a lower capacitance [higher pressure at any given volume] than curve 1. However, the slope [compliance] of the two curves is the same. A physiological example here is a change in external venous pressure [e.g. abdominal pressurization]. Curve 3. suggests the effect of alpha-agonists - a shift of the stressed portion of the curve to a lower volume. Such an effect may or may not be associated with a change in the slope [i.e. compliance] of the curve. Vu is unstressed volume [dark blue], Vs is stressed volume [light blue].

Maximal Venous Return

The final component of the venous return curve to be discussed is the plateau of the curve as it approaches atmospheric pressure. This is the pictorial representation of maximal venous return and results by the formation of a Starling resistor – when the pressure within a distensible vessel falls below its ambient pressure. As pleural pressure is integrally transmitted to the pericardial space, right atrium [36] and down the IVC, there is tendency for pressure within the IVC to fall below ambient intra-abdominal pressure. This is especially true during a spontaneous, unassisted inspiration as pressure in the right atrium, and down the IVC, tends to fall while intra-abdominal pressure tends to rise. When the ambient abdominal pressure supersedes intravascular pressure, the vessel collapses. The instant this happens, however, the intraluminal pressure rises to the Pmsf [the pressure head for venous return] and the vessel reopens. This cyclical phenomenon leads to an unmistakable fluttering effect of the blood vessel and this is the essence of a Starling resistor [37-39]. Crucially, a Starling resistor does not lead to a cessation of flow, instead it

creates maximal flow. Note that in a spontaneously breathing patient, with normal intra-abdominal pressure, the maximal venous flow will shift depending on the mean systemic pressure [figure 4].

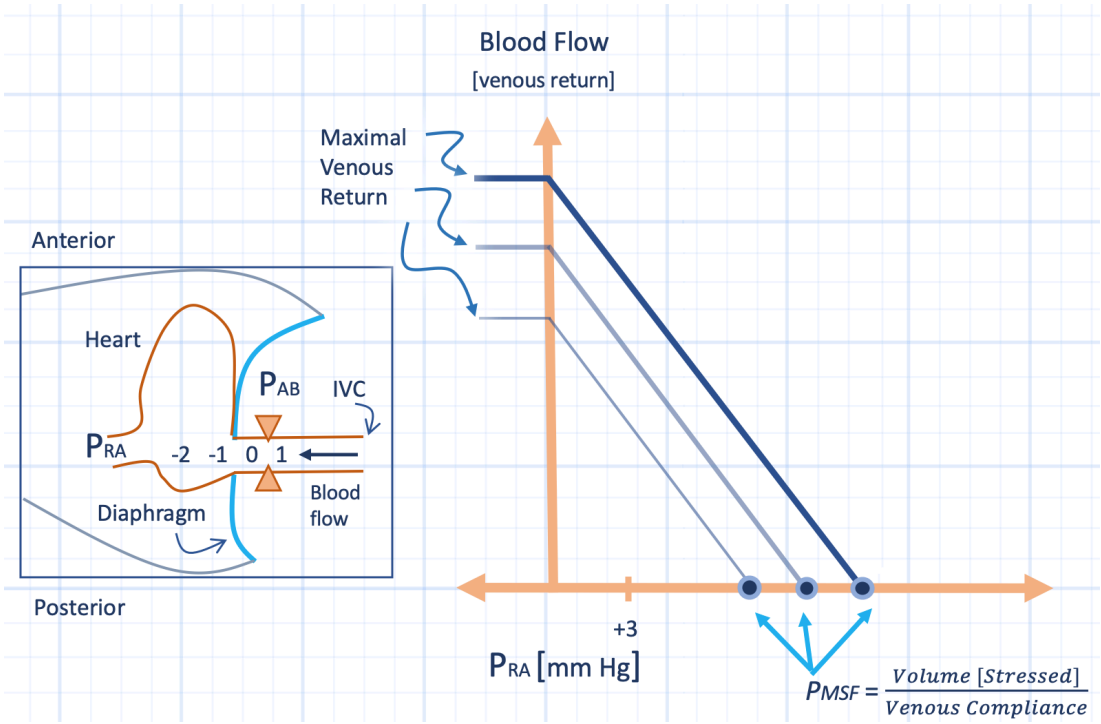

Figure 4: Maximal venous return occurs when the right atrial pressure [Pra] and, consequently, inferior vena cava [IVC] pressure drops below its surrounding abdominal pressure [Pab] – which is normally about atmospheric pressure [zero mmHg]. The result is a Starling resistor [left inset – triangles]. Note that the absolute value of maximal venous return increases with higher mean systemic filling pressure [Pmsf] – rightmost curve compared to leftmost.

For example, if the Pmsf increases and the venous return curve shifts to the right, maximal venous return also rises because augmented Pmsf elevates intravascular pressure and buffers the effects of the Starling resistor. Conversely, a shift in the venous return curve to the left decreases maximal venous flow. This reasoning can explain the somewhat paradoxical effects of abdominal pressure on venous return. As described above, elevated abdominal pressure decreases abdominal venous capacitance and favours venous return; simultaneously, increased abdominal pressure tends to collapse the IVC and depress maximal venous return. The predominant effect depends upon baseline mean systemic pressure [40, 41]. If the baseline Pmsf is high [e.g. in a state of volume overload] then the effect of collapse on the IVC is minimized and venous return is facilitated by increased Pab. Conversely, if the mean systemic pressure is low, then increased abdominal pressure promotes IVC collapse and retards maximal venous return.

Lastly, changes in the resistance to venous return may also change the magnitude of maximal venous flow. As above, Rvr is depicted by the slope of the venous return curve [figure 2]. Therefore, decreased Rvr increases maximal venous flow via an upshift in the slope of the curve. As above, an effective increase in venous return may occur when blood is redistributed into vascular beds with a low compliance. The venous return curve can be thought of as an average of return curves from various vascular beds. The non-splanchnic circulation [e.g. muscle beds] has a lower compliance than the splanchnic bed and therefore has a higher driving

pressure and a higher maximal venous return. When there is no overall change in mean systemic pressure [i.e. no change in the x-intercept], but blood is preferentially shifted into low compliant venous reservoirs, the result is an effective increase in the slope of the average venous return curve [42].

Circuit Function

As described, the venous return curve can shift based on changes in mean systemic pressure as well as by changes in the resistance to venous return. From this point forward, the term 'increased circuit function' is used to generically refer to any physiological change that augments venous return for a given right atrial pressure [27, 42-44]. Thus, increased circuit function follows a rightward shift in the return curve and/or an increase in its slope. As we have learned, multiple variables can increase circuit function. Conversely, 'decreased circuit function' may be secondary to leftward shift of the entire venous return curve [i.e. falling mean systemic pressure] and/or from increased resistance to venous return [i.e. a decrease in its slope]. A decrease in circuit function means that there is less venous return for any right atrial pressure [figures 2 & 4]. Circuit function is used to distinguish the modulation of right atrial pressure by changes in venous return, in distinction to cardiac function, elaborated below.

Pulmonary Venous Return

The discussion of venous return has, so far, focused on the return of blood from the systemic circulation to the right heart. An identical venous return curve could be constructed to depict blood flow from the pulmonary veins to the left atrium. The magnitude of the venous return [i.e. blood flow] is identical to that of the return from the systemic circulation as well as cardiac output because, averaged over time, the cardiac output from the left heart must equal that of the right heart. One important consideration within the pulmonary vasculature is the effect of increasing lung volume on pulmonary venous capacitance. In an analogous manner to increasing the ambient abdominal pressure [Pab], an increase in alveolar pressure relative to pleural pressure [i.e. the transpulmonary pressure - see chapter 1] decreases pulmonary vascular capacitance and favours blood flow towards to the left atrium. However, this only occurs in pulmonary zone III conditions [45]. Zone III conditions occur when the pulmonary arterial, capillary and venous pressure are all greater than alveolar pressure [46]. Under zone I or II conditions, the increase in trans-pulmonary pressure retards venous return to the left heart because the capillaries do not expel blood; instead, the effect of extra-alveolar vessels predominant and the lung tends to retain blood volume [45]. Thus, the effect of increasing transpulmonary pressure, like that of the abdominal pressure, depends upon the baseline mean systemic pressure [e.g. volume status]. If vascular volume is

high [e.g. zone III conditions], then increasing transpulmonary pressure augments venous return to the left heart, while under conditions of low vascular pressures [e.g. zone I and II conditions], enhancing transpulmonary pressure impairs venous return to the left heart [figure 5].

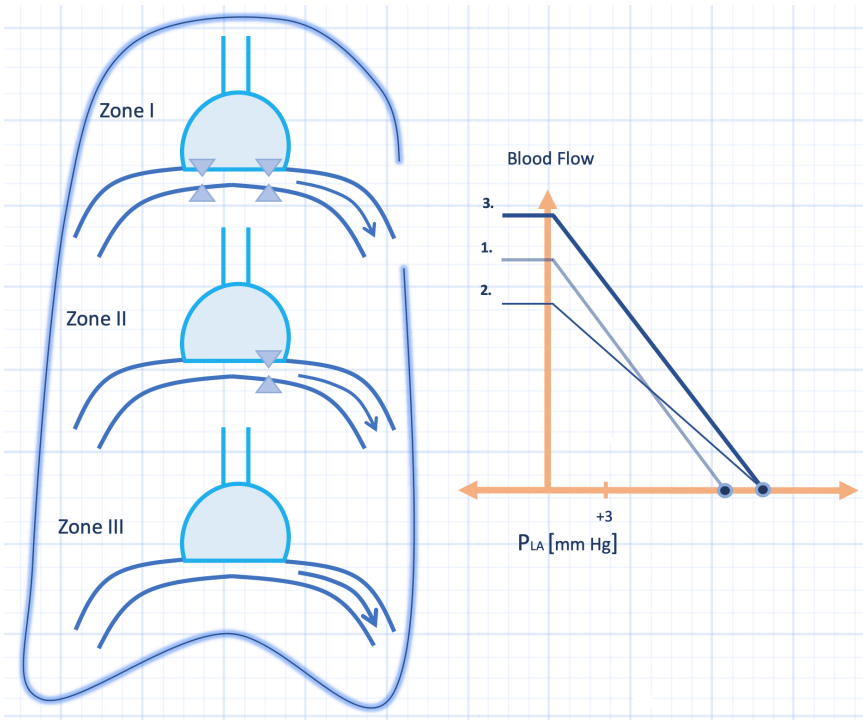

Figure 5: Pulmonary venous return is dependent upon the lumped zonal characteristics of the lung [left panel]. An increase in transpulmonary pressure decreases pulmonary venous capacitance and increases the pressure head for blood flow to the left heart [curve 1. compared to 2. & 3.]. However, there is only an increase in pulmonary venous return from zone III lung units [curve 2. compared to 3.]. Venous curve numbers do not necessarily correspond to lung zone. Pla is left atrial pressure.

Cardiac Function

Having spent the first half of this chapter reviewing the determinants of venous return and the physiological phenomena that alter circuit function, this portion examines the elements of cardiac function and its descriptive curve. Like the venous return curve, the cardiac function curve relates right atrial pressure to blood flow but in an inverse manner. Note that cardiac function has a direct relationship between right atrial pressure and blood flow; this is in complete contradistinction to circuit function and venous return [figure 6]. The direct relationship between right atrial pressure and cardiac output is a consequence of the Frank-Starling mechanism; that is, myocyte stretch augments troponin calcium sensitivity, actin-myosin relation and contraction [47].

Like circuit function, cardiac function can be enhanced or impaired and these changes are illustrated by shifts in the cardiac function curve. A shift of its slope, up and leftwards, depicts improved cardiac function because there is higher cardiac output for any given right atrial pressure [48]. On the other hand, impaired function is marked by a down and right shift of the cardiac function curve – revealing diminished cardiac output for any given atrial pressure. Crucially, a shift

in the cardiac function curve is not solely a consequence of changed cardiac contractility. While contractile state certainly alters the slope of the cardiac function curve, changes in diastolic properties, afterload, valve function and heart rhythm all modify the curve as well [18, 21]. Therefore, like the circuit function curve, the cardiac function curve is a relatively gross representation of multiple physiological variables [see also chapter 10].

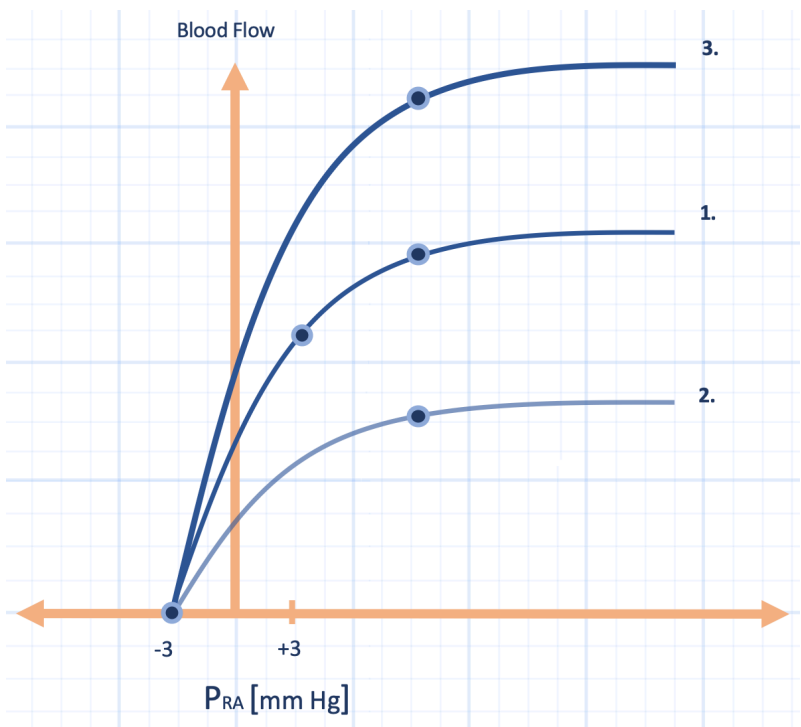

Figure 6: The cardiac function curve illustrates a direct relationship between right atrial pressure [Pra] on the x-axis and cardiac output [blood flow] on the y-axis – note the two points on curve 1. An increase in cardiac function is depicted by curve 3.,while a decrease in cardiac function by curve 2. Note that for the same Pra – between the curves – there is differing cardiac output [y-axis].

A more detailed analysis of cardiac output is undertaken by considering the relationship between volume and pressure within the ventricle during a cardiac cycle. This investigation was first proposed by Sagawa in the 1970s and is a valuable tool to scrutinize various pathological states [2, 3]. Ultimately, however, the detrimental effects of afterload, diastolic function, valvulopathy and heart rate that are visualized on the Sagawa pressure-volume relation are distilled into a depressed cardiac output for any given cardiac filling pressure.

Sagawa Pressure-Volume Relationship

The Sagawa pressure-volume relationship depicts changing pressure and volume within the ventricle during a single cardiac cycle [figure 7]. Accordingly, it is – as compared to the Frank-Starling cardiac function curve – a more detailed investigation of stroke volume and, ultimately, cardiac output. The x-axis is the ventricular volume, typically in millilitres while the y-axis is ventricular pressure in mmHg. The relationship portrays the pressure-volume curves of the ventricle in diastole [i.e. end diastolic pressure-volume relationship or EDPVR] and in systole

[i.e. end systolic pressure-volume relationship or ESPVR] [2, 3]. Bounded by these relationships is the change in volume and pressure during a cardiac cycle. Ventricular filling occurs along the EDPVR. The EDPVR relates the end diastolic volume to the end diastolic pressure; at this point, the second phase begins as the ventricle contracts. This phase is known as isovolumic contraction because the volume within the ventricular cavity remains constant while the pressure increases. Once the cavity pressure surpasses arterial diastolic pressure, the semilunar valve [pulmonic or aortic] opens and ejection begins. Note that during this third phase, ventricular volume decreases and the pressure tracing closely mirrors the pressure within the artery [pulmonary or aorta] into which the corresponding ventricle ejects. Once the pressure and volume of the ventricle reach a unique point on the ESPVR, the semilunar valves close as the arterial pressure eclipses ventricular pressure; thus, the ventricle returns to diastole and the pressure within the ventricle falls at a nearly constant volume [i.e. isovolumic relaxation] until the EDPVR is reached and filling resumes for the ensuing cardiac cycle [49].

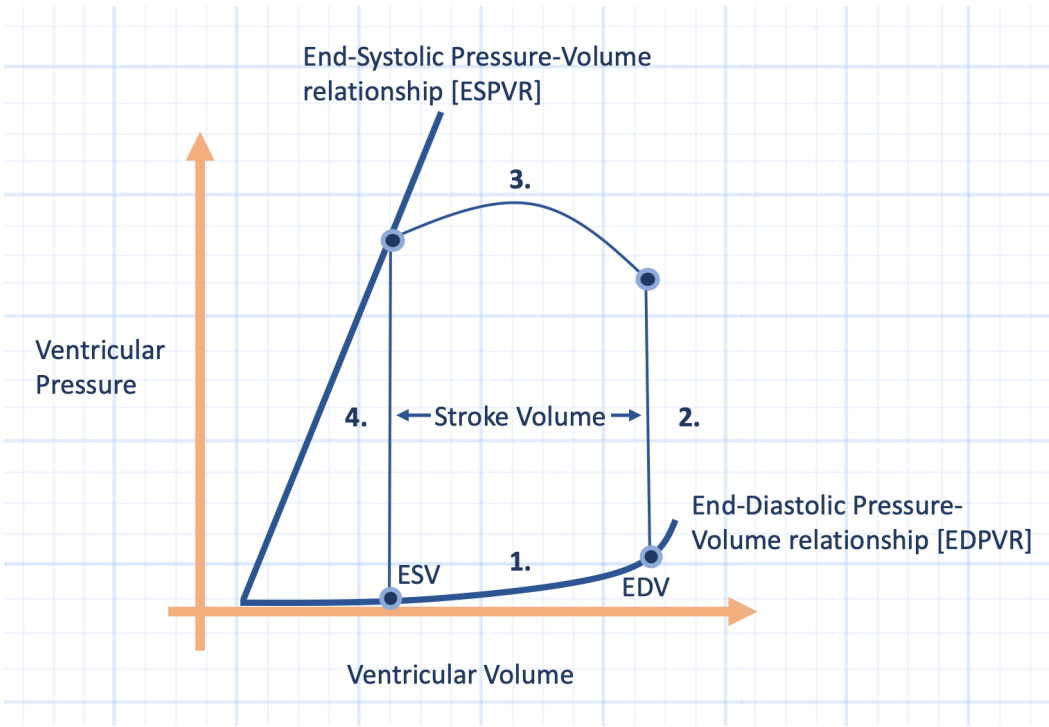

Figure 7: The Sagawa pressure-volume relationship of the heart. This diagram details cardiac function on a beat-by-beat basis in terms of the ventricle's end-diastolic pressure-volume relationship [EDPVR] and end-systolic pressure-volume relationship [ESPVR]. Ventricular filling occurs during portion [1.] of the diagram. When ventricular systole begins at the end-diastolic volume [EDV], there is isovolumic contraction [2.] until the diastolic pressure is reached. The semilunar valves open and ejection occurs during phase [3.]. When the ventricle meets its ESPVR, the semi-lunar valves close and there is isovolumic relaxation [4.] at ventricular end-systolic volume [ESV]. The difference between the EDV and ESV is the stroke volume.

While these phases are followed by both the right and left ventricle, there are qualitative and quantitative differences between the two sides of the heart. The right ventricle has a diminished isovolumic contraction phase as ejection begins at a lower pressure. Additionally, ejection in the right ventricle continues beyond that of the ESPVR, most likely secondary to the low impedance arterial tree into which it ejects. These qualitative differences give the right ventricular pressure-volume relationship a more triangular appearance, compared to the left ventricle [5, 50-53].

The End-Diastolic Pressure-Volume Relationship [EDPVR]

The end-diastolic pressure volume relationship is the curve that describes all possible pressure-volume combinations of the ventricle in its most relaxed state [54]. Because this graphical representation plots the change in pressure with respect to change in volume, the slope of this curve is elastance, which is the inverse of compliance. Therefore, the EDPVR demonstrates a much lower elastance [i.e. higher compliance] than the ESPVR. As can be gleaned from this relationship, for any given change in volume, there is trivial change in pressure until relatively large ventricular volumes are achieved in diastole. The increased elastance [i.e. decreased compliance] at high ventricular volume reflects pericardial constraint in normal hearts [54, 55].

The EDPVR illustrates preload. Preload is not a pressure but a volume as volume best approximates the degree of mycocyte stretch preceding contraction. Hence, the pressure located on the y-axis just prior to the onset of isovolumic contraction represents the end-diastolic filling pressure; this corresponds to the atrial pressure on the x-axis of the cardiac function [Frank-Starling] curve. Note that in states of impaired diastolic relaxation [e.g. infiltrative disease, ventricular hypertrophy, acute ischemia, pericardial disease, etc.] the EDPVR shifts up and to the left [figure 8] [56, 57]. In this situation, a given end-diastolic volume generates greater end-diastolic filling pressure. This is the primary reason why using pressure as a surrogate for volume can be problematic. Changes in the slope of the EDPVR may exhibit inter-patient variability and intra-patient variability during the trajectory of any given disease course [58].

An often, under-recognized cause of diastolic dysfunction is ventricular interdependence. Ventricular interdependence is the transmission of forces from one cardiac chamber to another that is separate from neural, humoural or circulatory effects [59]. It has been known for well over 100 years that volume loading one ventricle immediately decreases compliance in the opposite ventricle [60]. Interestingly, it has been shown that volume loading any of the four cardiac chambers causes leftward shift in the diastolic filling relationship of the other three chambers [61]. This effect is mediated by common muscle fibres, the septal wall and the pericardium; while ventricular interdependence does occur in the absence of the pericardium, it is attenuated [62]. The degree of diastolic interaction between the ventricles is mediated by the relative elastances of the septum and ventricular free walls [63, 64]. For example, a septum with high elastance [e.g. hypertrophic obstructive cardiomyopathy] coupled with low elastance ventricular free walls will diminish diastolic interaction [65]. Conversely, a stiff pericardium or ventricular free wall in addition to a low elastance septum, augments diastolic interaction [66].

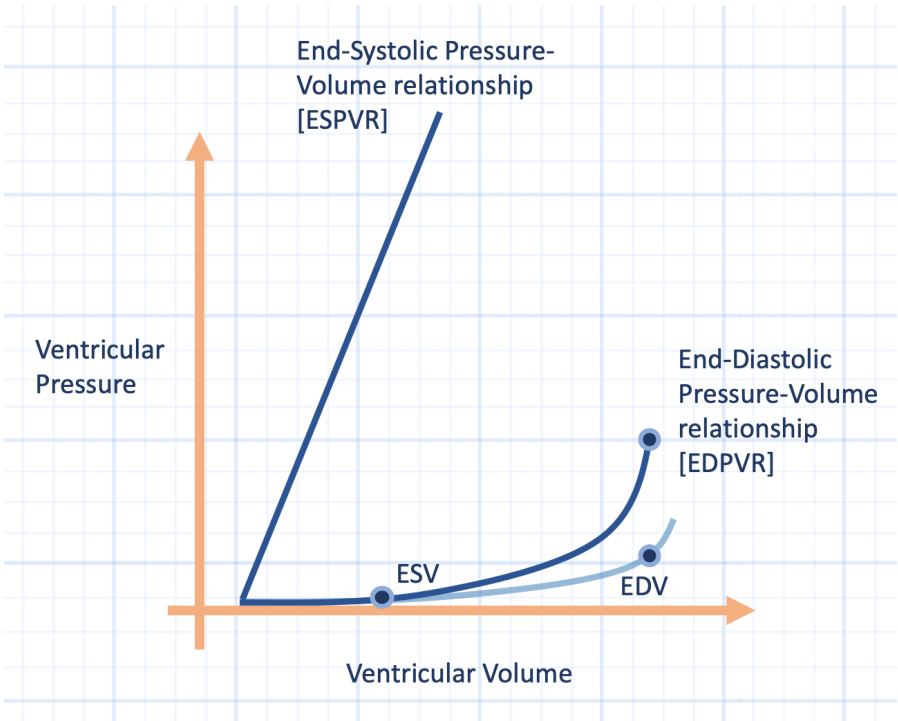

Figure 8: Impaired diastolic function as demonstrated by an up-leftwards shift of the EDPVR. Note at the same end-diastolic volume [EDV], there is a higher ventricular pressure [y-axis]. ESV is end-systolic volume – see also figure 7.

Table 1: Select Causes of Impaired Diastolic Function

Acute Causes	Chronic Causes
Regional or global schema [e.g. shock]	Hypertensive heart disease
Pericardial constraint [e.g. effusion]	Left ventricular hypertrophy
Cardiac fossa constraint [e.g. hyperinflation]	Restrictive myocardial disease [e.g. amyloidosis]
Intra-abdominal hypertension	Pericardial constraint [e.g. effusion]
Ventricular interdependence	
Hypothermia [core temp < 35.8 C]	

The End-Systolic Pressure-Volume Relationship [ESPVR]

Like the EDPVR, the ESPVR relates a unique set of pressure-volume relationships for the ventricle at the end of systole. Comparing the slope of this curve to the diastolic curve reveals greatly increased elastance, which is expected of the ventricle during maximal contraction. The ESPVR remains linear under many loading states and, importantly, is resistant to both changes in preload and afterload [2, 3]. The ESPVR is, therefore, a good marker of ventricular contractility [67]. A shift down and to the right represents reduced ventricular contractility as expected with either acute or chronic systolic dysfunction [figure 9]. On the contrary, an up and leftward shift of the ESPVR denotes increased ventricular contractility. This may occur in response to either endogenous or exogenous catecholamines or resolution of a disease process that impaired ventricular

Reduced systolic function invariably increases end-systolic volume and then end-diastolic volume as the ventricle attempts to maintain stroke volume. Impaired contractility, therefore, responds to afterload reduction more substantially than pure diastolic dysfunction [2, 69]. Regardless, pure systolic dysfunction creates higher end-diastolic filling pressure for any given stroke volume. Yet, systolic and diastolic dysfunction - whether acute or chronic - frequently co-exist and this exacerbates elevated filling pressure for any given stroke volume [70].

In addition to the diastolic ventricular interdependence described above, there is functional linkage between the ventricles during systole. While there are varying estimates, upwards of 50% of right ventricular pressure is generated by the left ventricle during systole. On the other hand, less than 10% of left ventricular systolic pressure is engendered by the right ventricle [71-73]. The mechanism by which the ventricles augment each other during systole is echoed in diastole, however, the role of the pericardium is minimal during systolic interaction [66, 74].

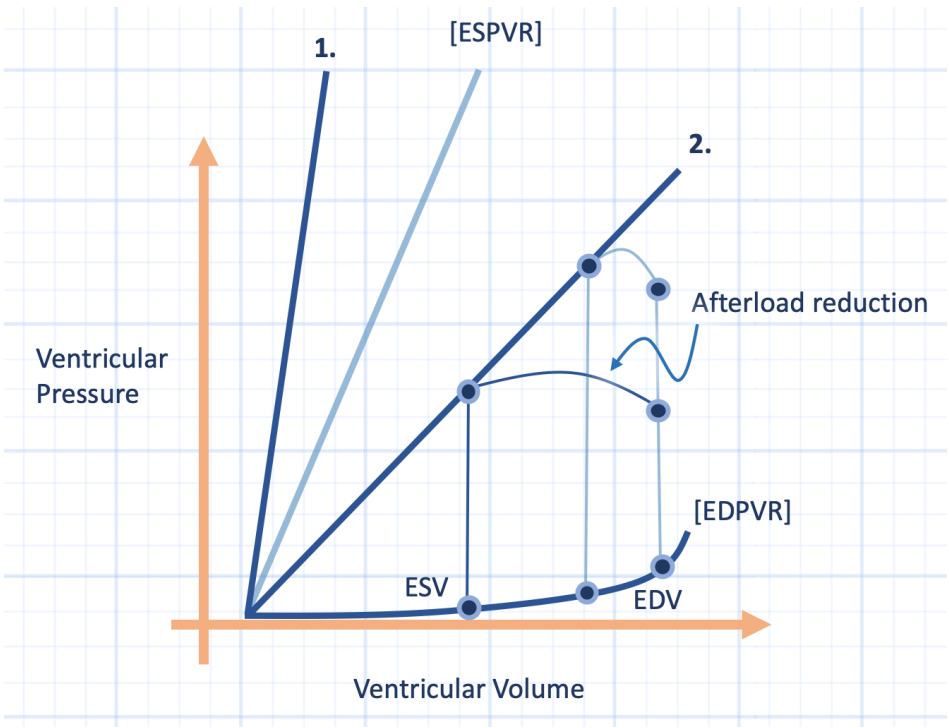

Figure 9: Changes in end-systolic pressure volume relationship [ESPVR] depict an increase [curve 1.] or a decrease [curve 2.] in ventricular function or contractile state. Not pictured here is increased end-diastolic volume [EDV] in response to diminished contractile state. Note how afterload reduction increases stroke volume in the setting of impaired contractility [curve 2.]. When contractile state is normal or increased, afterload reduction provides minimal augmentation of stroke volume [see also figures 7 and 8].

Table 2: Select Causes of Impaired Systolic Function

Acute Causes	Chronic Causes
Regional or global schema [e.g. shock] with or without hypoxemia	Chronic ischemia
Electrolyte abnormalities [e.g. hypocalcemia, hypophosphatemia]	Dilated 'cardiomyopathies' [e.g. viral, septic, uremic, post-partum, ethanol, etc.]
Acidemia	
Medications [e.g. beta-blockers, calcium channel blockers]	
Severe sepsis	
Extremes of body temperature	

Regurgitation

Incompetence of the atrio-ventricular valves is commonly encountered in the ICU. This pathology may be modelled via the Sagawa pressure-volume relationship. Fundamentally, regurgitation mirrors impaired systolic function [figure 9], even if there is no inherent abnormality in ventricular contractility [75, 76]. The reason for this similarity is that during regurgitation, stroke volume is diminished and proportional to the regurgitation volume backwards into the atrium; consequently, ejection fraction is effectively decreased. Similarly, afterload reduction enhances forward ejection into the great arteries in the setting of impaired systolic function and improves the hemodynamics of atrio-ventricular valve incompetence. As well, inotropic agents, which shift the ESPVR up and to the left, improve atrioventricular regurgitation; in other words, better forward flow lowers end-systolic and end-diastolic volume, decreases atrio-ventricular orifice area and mitigates regurgitant volume [77].

Impedance

The true afterload experienced by the ventricle is a complex and contentious subject. It is certainly not simply the pressure within the great artery into which the ventricle ejects! Nor is it adequately expressed by 'vascular resistance' as calculated by dividing mean arterial pressure by cardiac output! The calculated vascular resistance is a nebulous variable that is not directly measured; rather, it is derived by relating two objectively measured quantities. Further, calculated vascular resistance assumes that blood vessels are stable, non-branching, non-distensible entities, which they are not [78, 79]. These motifs are also considered in chapters 9

and 10 within the context of airway pressure and its specious relationship to right ventricular afterload.

A means to better model the complex concept of afterload is through arterial input impedance [80]. Impedance has been represented as the geometrical summation of both classical resistance [e.g. as described by Poiseulle's law] and compliance. The latter measure takes into consideration the pulsatile qualities of the vascular tree. This early approach to impedance is also known as the two-element Windkessel model first described by Frank in 1899 [81]; it is sometimes described by an 'impedance triangle' [82]. However, this model was deemed insufficient as better approximations of impedance took hold in the mid twentieth-century. Thus the three-element Windkessel model was proposed adding 'characteristic impedance' as the third element [83]. In the three-element model, characteristic impedance contributes to the ventricular load proximally and in series, while resistance and compliance act in parallel [figure 10]. The characteristic impedance [Zc] is the ratio of blood mass inertia to proximal arterial compliance. Zc takes into consideration the acceleration of blood mass at the onset of systole [84]. While the three-element Windkessel model appraises arterial input impedance fairly well [85], more complicated models have been proposed [e.g. the four-element Windkessel model] [86].

Vascular impedance may be approached graphically upon the cardiac pressure-volume relationship. The superposition of a line, known as arterial elastance [Ea], which stretches from the end-diastolic volume and intercepts the ESPVR, provides a composite measure of the impedance of the vascular bed into which the ventricle ejects [figure 10] [87]. Note that increased slope of this line represents greater arterial elastance [i.e. a lower compliance or higher resistance] and, therefore, a greater afterload. The opposite is true for a decreased slope and therefore a decreased elastance. During a single cardiac cycle, both the artery and the ventricle obey the principle of time-varying elastance [4, 88]. That is, the elastance of the ventricle changes as a function of time from very low elastance during diastole to relatively high elastance at end-systole or peak contractility. Contemporaneously, the great artery changes from a position of lower to higher elastance during ejection as the artery fills with blood and experiences blood runoff from the distal vascular bed.

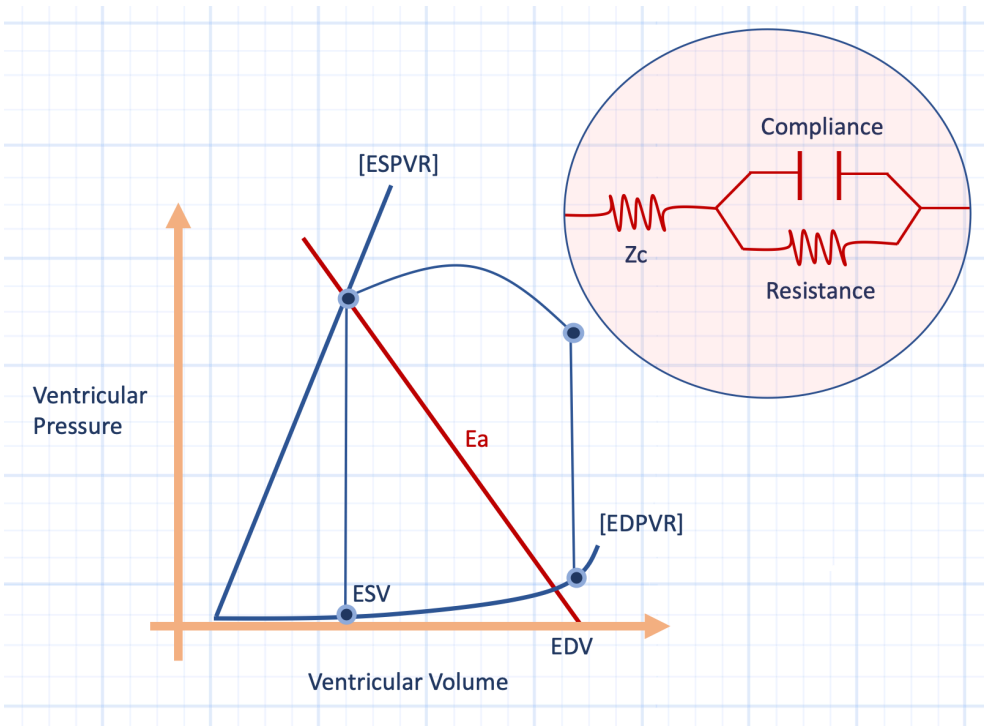

Figure 10: The graphical illustration of arterial input impedance. The inset demonstrates an electrical analogy for the 3-element Windkessel model [see text for detail] with Zc representing characteristic impedance. On the pressure-volume diagram, Ea or arterial elastance is a lumped descriptor for arterial input impedance [in red]. This line stretches from end-diastolic volume [EDV] to the pressure at which the aortic valve closes [i.e. the dicrotic notch]. The ratio of the slope of Ea to the end-systolic pressure-volume relationship [ESPVR] defines ventricular-vascular coupling.

While time-varying arterial elastance does not have perfect explanatory power, it does help model many of the effects of increased afterload on the ventricle and also explains why non-compliant arteries that occur with age predispose to impaired cardiac performance [6]. Arterial elastance also helps define an optimal relation between ventricle and artery. In fact, a ratio of the slope of the Ea to the ESPVR defines ventricular-vascular coupling in terms of myocardial work and oxygen consumption [89]. Ventricular-vascular or ventriculo-arterial coupling is readdressed in chapter 10 and extended upon to suppose an energetic efficiency between the veins, heart and even the lungs and ventilator!

Lastly, the concept of time-varying elastance and ventricular-vascular coupling can partially explain the effect of pathologically-low pleural pressure on left ventricular performance. Note that the y-axis of the pressure-volume curve is intra-cavitary or intra-luminal pressure. However, when perivascular or juxta-cardiac pressure is abruptly reduced, the pressure across the ventricular or vascular wall is increased [i.e. the transmural pressure is increased]. This effect augments transmural wall tension of both the ventricle and great artery. As ejection proceeds, the ventricle shrinks in volume while the artery expands. Further, because pleural pressure and thoracic aortic blood volume are inversely proportional [90], increased thoracic aortic blood volume renders the artery less compliant [91]; in other words, aortic elastance rises [i.e. the slope of Ea]. This effect is most pronounced in the setting of poor ventricular contractility as there is increased Ea/ESPVR ratio [i.e. poor ventricular-vascular coupling] [6].

Aortic Stenosis

A commonly encountered cause of increased impedance to ventricular outflow is aortic stenosis. In this example, the effective 'arterial' elastance is quite high, and it is fixed. The slope of the Ea in aortic stenosis obviously depends on the severity of the aortic valve area narrowing, but also on compensatory changes in arterial compliance and resistance which are known to occur in the setting of aortic stenosis [92]. Indeed, one group published a ventricular-vascular coupling model taking into account the effect of a stenotic valve as well as changes in the three-element Windkessel model [93]. Simply, aortic stenosis increases the effective elastance of the aorta into which the ventricle ejects. The fixed, steep Ea causes elevated end-systolic volume and, therefore, the stroke volume is essentially entirely dependent upon the end-diastolic volume [i.e. preload] [94]. In order to maintain an adequate stroke volume, the left ventricle must fill at a higher volume and therefore pressure. With time the left ventricle becomes hypertrophic, increasing its elastance; this results in diastolic dysfunction and even higher end-diastolic filling pressure [95].

While aortic stenosis chronically increases impedance to flow, the above reasoning may be applied to acute elevations in systemic resistance as well [e.g. hypertensive emergency]; the core principle being that elevated afterload diminishes stroke volume and elevates cardiac filling pressure [96, 97].

Pulmonary Vascular Resistance

As discussed above, models of pulmonary arterial input impedance contain a number of variables; resistance – commonly calculated as the pulmonary vascular resistance [PVR] – is one of them. PVR is a complex physiological consideration [98, 99] and relating pressure to flow is an oversimplification - be it systemic or pulmonary - for two key reasons [78, 79]. First, calculated vascular resistance assumes that the slope of the pressure-flow relationship is linear; that is, if pressure is plotted on the x-axis and flow on the y-axis, then a greater slope indicates decreased vascular resistance and vice versa. The slope of this relationship would be linear if blood vessels were non-distensible, infinitely rigid conduits, or so-called Poiseuille resistors [78]. Second, calculation of vascular resistance assumes that the pressure-flow relationship passes through the origin of the pressure-flow graphic; however, as discussed below, because of Starling resistors, the pressure-flow relationship does not pass through the origin. Thus, the vascular system – particularly the pulmonary vascular system – behaves in a complex manner which involves vascular distensibility and parallel vascular recruitment. Both of these phenomena generate a vascular pressure-flow relationship that is neither linear, nor passes through the origin; instead these phenomena create a pressure-flow relationship that is curvilinear that shifts along the pressure axis [99]. These are not

trivial points as assumption of linearity can lead to an erroneous interpretation of changes in vascular resistance when pressure and flow co-vary.

If one were to consider a single pulmonary vessel with an inflow pressure and outflow pressure, the generated flow follows the vessel's inherent resistance which is mostly dependent upon the radius of the vessel [100]. As above, this is the classical Poiseuille resistance. However, as the inflow pressure rises, the elasticity of the vessel causes it to distend as a function of vascular compliance. As the vessel distends, its radius increases and therefore its Poiseuille resistance decreases; accordingly, as driving pressure rises, flow increases exponentially. The curvilinear relationship means that the ratio of pressure to flow can change [i.e. a calculated change in resistance] without a true change in vasomotor tone [figure 11] [99]. Fortunately, unless under extremely low-flow conditions, the pressure-flow relationship is fairly linear meaning that Poiseuille resistance is a valid physiological assumption [79, 101]. Nevertheless, because the pressure-flow relationship is curvilinear at low flow, the entire curve is shifted away from a linear approximation; this shift, as discussed below, reduces the sensitivity and specificity of the calculated pulmonary vascular resistance [102]. If there is either a true increase is Poiseuille resistance or a decrease in vascular compliance, the pressure-flow relationship of a single blood vessel becomes less curvilinear and shifts down and to the right [79, 99, 100].

Another problem with the pressure-flow relationship of a pulmonary blood vessel occurs at the opposite extreme. When a vessel dilates to its elastic limit, it actually becomes stiff such that pressure rises disproportionately to flow. This is similar to ventilating a patient with auto-PEEP; the pressure in the airway rises despite the same tidal volume/flow because the lungs and the thorax have reached stiff portions of their compliance curves. In a blood vessel, the result is that pressure rises relative to flow/volume and the calculated resistance intimates that the vessel has constricted – because the calculated resistance rises – which is quite incorrect; the vessel is dilated to its limit! This is particularly important in left heart failure, as discussed below and in chapter 10.

Additionally, the pulmonary vasculature is many vessels in parallel. In fact, there are 10-times more arterioles in the pulmonary circulation as compared to the systemic circulation [103]. When the pulmonary interstitial pressure or vascular elastic recoil pressure supersedes the pulmonary capillary pressure, the vessel collapses and West zone I and II are created [46, 78]. When flow through a distensible tube is mediated by its external pressure it is known as a Starling resistor. The pressure at which the vessel collapses is sometimes referred to as the critical closing pressure; elevated closing pressure shifts the pressure-flow curve away from the origin along the pressure axis [figure 11] [104]. An example of this physiology is an increase in lung volume – be it spontaneous or mechanical. Indeed, increasing lung volume above functional residual capacity increases 'pulmonary vascular resistance' [105], but as Permutt pointed out 50 years ago, this is not due to an increase in Poiseuille resistance, but rather Starling resistance [106-108]. He termed this effect 'vascular waterfall' because the downstream left atrial pressure, like the height of a waterfall, no longer determines flow. While an increase in Starling resistance in the

pulmonary vascular bed does increase the actual load on the right ventricle [by increasing the closing pressure], the calculated pulmonary vascular resistance does not accurately detect this change. First, if the calculated pulmonary vascular resistance does increase with elevated Starling resistance, the calculation overestimates the true resistance imposed. Second, if the calculated PVR and Starling resistance rise in tandem, it can introduce false mechanistic reasoning [109]. A clinical example of this is elaborated in chapter 10 – a pulmonary embolism primarily increases the load on the right ventricle by increased Starling resistance. Thus, therapeutics that reduce Poiseuille resistance [i.e. pulmonary vasodilators] are likely to be less effective than treating the vascular obstruction. Finally, an increase in Starling resistance with perfectly proportional rise in both pressure and flow will yield no change in the calculated PVR, leading the clinician to think that the pulmonary vascular tree has not been altered.

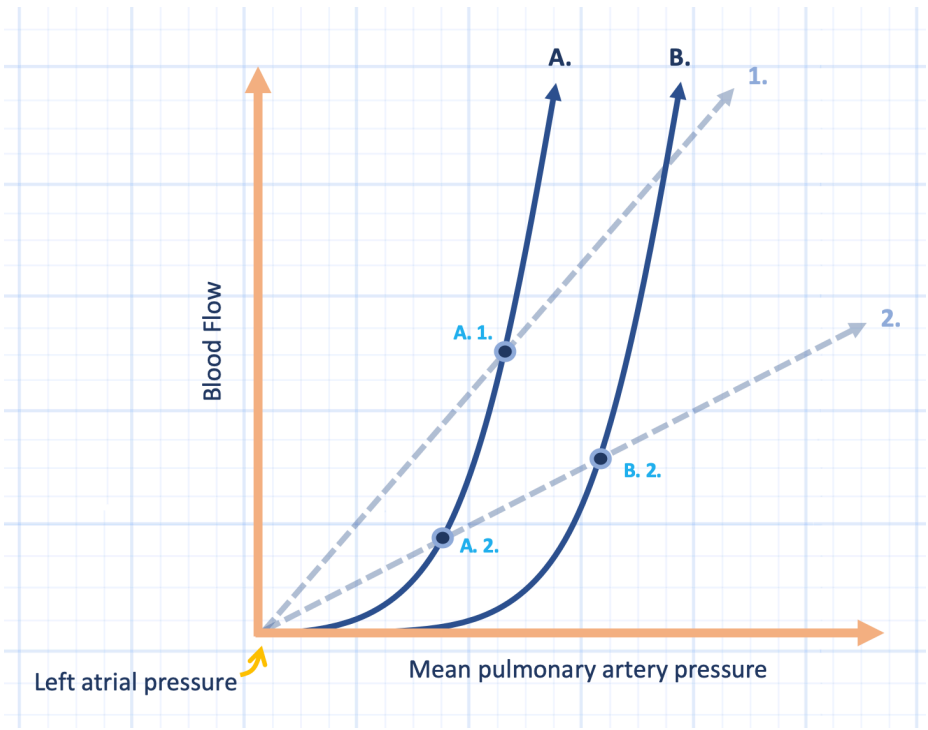

Figure 11: Pulmonary vascular resistance assumes linear relationship between blood pressure and flow with the origin being the left atrial pressure [dashed curves 1. & 2.]. However, as the true pressure-flow relationship is curvilinear [curves A., B. – see text for description], the calculated resistance may increase [curve 1. to curve 2.] without a true change in the lumped vascular properties [point A1 to A2]. Further, if there is an increase in Starling resistance [e.g. an increase in the critical closing pressure] as depicted by shifting curve A. to B., the use of a calculated resistance from dashed curve 2. overestimates the true vascular resistance faced by the right ventricle [compare point A1 to B2]. Not pictured is a concomitant rise in Starling [rightward shift] and Poiseuille [downward shift] resistance.

And the converse of the above is also true. If Starling resistance and calculated PVR concurrently fall, PVR overestimates the true effect of the former. Consider an intervention that reduces the calculated pulmonary vascular resistance but does so by reducing Starling resistance [e.g. a vasoactive substance that increases blood flow which recruits collapsed pulmonary vasculature]. If a clinician infers that the reduced, calculated PVR is from active dilation of pulmonary vascular smooth muscle [i.e. diminished Poiseuille resistance], he or she is led astray. If this same vasoactive substance – speciously thought to cause vasodilation – is administered to a patient with a maximally recruited pulmonary vascular bed [i.e. a very low Starling resistance], but a high calculated PVR, there will be no reduction in

pulmonary vascular resistance and the patient will have received a needless, and potentially harmful, intervention. How can the circulation have a maximally dilated vascular bed, but high calculated PVR? This is discussed more specifically in chapter 10 under left-heart pulmonary hypertension. And finally, a fall in Starling resistance in conjunction with an equal decrease in both pressure and flow yields and unchanged calculated pulmonary vascular resistance, despite there being a real change in the pulmonary vascular circulation.

In totality, the dynamic and curvilinear nature of the pulmonary vascular pressure-flow relationship means that a simple ratio of pressure to flow is a troublesome measure of true pulmonary vascular impedance. It follows that the calculated PVR has diminished sensitivity and specificity as a measure of pulmonary vascular physiology. As above, the problem is particularly prominent when both pressure and flow change in the same direction. Therefore, only when pressure and flow change in opposite directions, or if either pressure or flow remains constant, while the other changes, is more certainty achieved [79]. However, even in the latter situation, when pressure and flow diverge following an intervention, it must be remembered that this cannot definitively distinguish between changes in Starling [e.g. recruitment-mediated] and Poiseuille [i.e. distension-mediated] resistance.

The complexities of the pulmonary vasculature become more apparent if one considers physiological overlap between Starling and Poiseuille resistance. Consider hypoxemia, which causes both hypoxic vasoconstriction and increased critical closing pressure of the pulmonary blood vessels [110, 111]. Therefore, hypoxemia increases vascular resistance from reduced vascular radius [i.e. increasing Poiseuille resistance] which decreases the slope of the pressure-flow relationship; hypoxemia also shifts the pressure-flow curve to the right [i.e. increasing Starling resistance] consequent to elevated closing pressure. The effect of increasing alveolar pressure [e.g. by positive pressure ventilation and PEEP] has an additive effect on hypoxemia in terms of pressure-flow curve shift [111].

Cardiac Pressure-Volume Relationship and Cardiac Pressure-Flow Relationship

The pressure-volume relationship of the ventricle offers a detailed description of cardiac function and dysfunction; one can model abnormalities of diastolic and systolic function, pathological valves as well as impedance. Yet, there is connection between the Sagawa pressure-volume analysis and the Frank-Starling cardiac function curve [figure 12]. Whether the abnormality in cardiac function arises from anomalous impedance [i.e. afterload], contractility, diastolic function, valve activity and even heart rhythm, the net effect is diminished stroke volume – and therefore cardiac output – despite increased cardiac filling pressure [21]. Attenuated cardiac output with increased end-diastolic pressure defines embarrassed cardiac function and is represented by flattening of the cardiac function curve on the pressure-flow relation [112, 113].

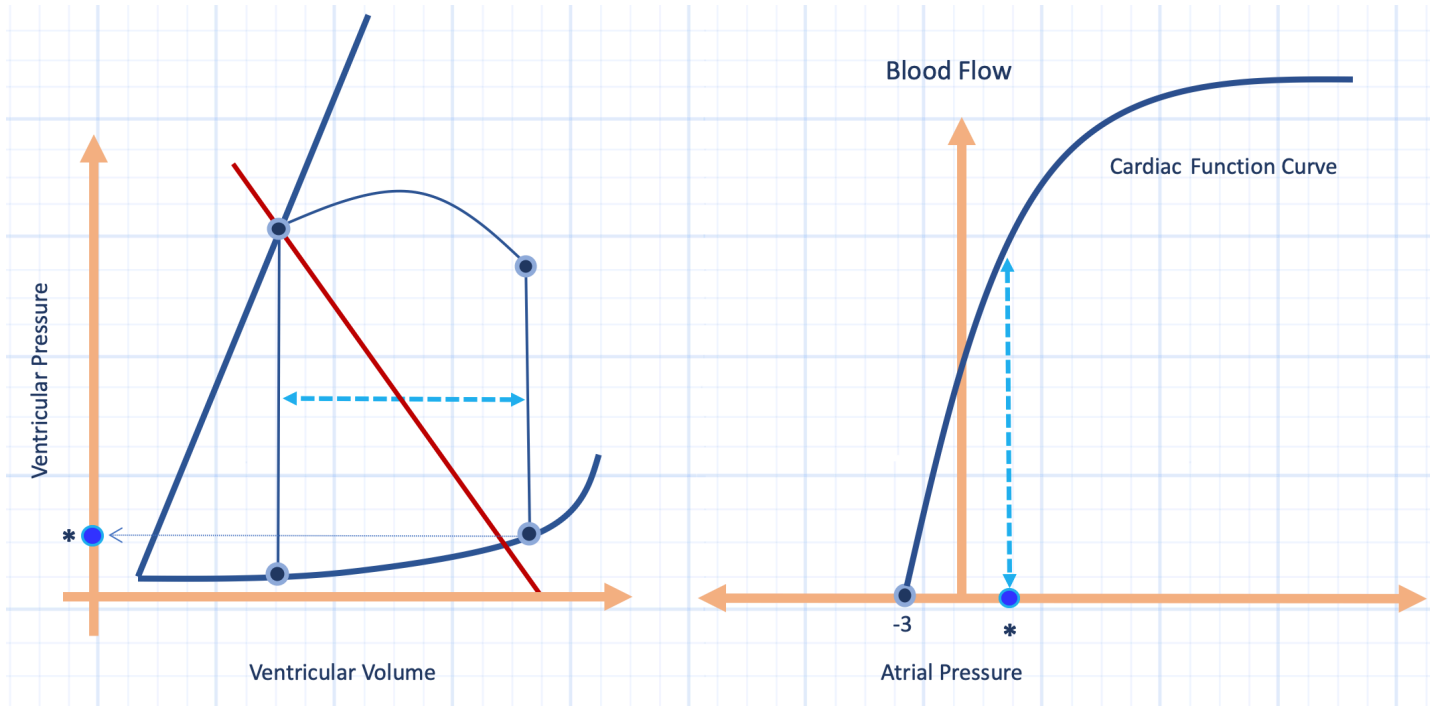

Figure 12: The relationship between the pressure-volume curve [left] and pressure-flow curve [right]. The horizontal, dashed, light blue, double-arrow of the pressure-volume curve represents stroke volume which is related to blood flow by heart rate. Thus, the vertical, dashed, light blue, double-arrow of the pressure-flow diagram is related to stroke volume on the right. The filling pressure is demarcated by the asterisk. A drop in the stroke volume [by any mechanism] flattens the pressure-flow curve.

The Cardiac Function Curve

The cardiac function curve defines the pressure-flow relationship for the heart [figure 6]. As above, increased atrial pressure – a surrogate for cardiac end-diastolic volume – augments cardiac output [48]. Like the venous return curve, the x-intercept of the cardiac function curve is also significant. When cardiac output is zero – cardiac function has ceased – and if venous egress to the heart is impeded, then pressure within the right atrium is slightly sub-atmospheric [figure 6 & 13]. This is because the resting pressure within the thorax is the pleural pressure, which is sub-atmospheric and this pressure is transmitted to the pericardial space [18]. In other words, the x-intercept of the cardiac pressure-flow relationship represents the juxta-cardiac pressure or the pressure surrounding the heart. This x-intercept explains why the cardiac function curve shifts during respiration and is why, by convention, atrial pressures are obtained at end-expiration. Because the pressure within the thorax – and therefore the position of the cardiac function curve – changes during respiration, a standardized approach is to record atrial pressure at the end of the respiratory cycle. This attempts to measure intra-cardiac pressure when the pleural pressure is near atmospheric pressure, i.e. when the ambient cardiac pressure approaches zero. When the surrounding pressure is zero, then the transmural, or distending, pressure is reduced to the intra-cardiac pressure.

Accordingly, while the pressure within the right atrium is an important variable for venous return – a dynamic pressure – it is also an important determinant of ventricular filling volume – a static pressure [see chapter 1]. Because the transmural

pressure is the pressure within the right atrium less the x-intercept, the distance between these two points is a graphical representation of the transmural pressure [18]. Importantly, the volume of a distensible structure depends on its compliance in addition to its transmural pressure. Nonetheless, as discussed in chapter 3, there are limitations to right atrial transmural pressure as a surrogate for right ventricular filling [114-116].

The slope of the cardiac function curve is an illustration of lumped cardiac function as detailed above in terms of the Sagawa pressure-volume relationship. A general improvement in pump function shifts the slope of the curve up and leftwards, revealing greater cardiac output for any given right atrial pressure. Conversely, diminished pump function is depicted by diminished slope of the cardiac function curve and a reduced cardiac output for any given right atrial pressure [11].

The flat portion of the cardiac function curve is determined largely by pericardial constraint and, to some extent, by the lungs under certain pathological conditions, though this is subsequently discussed in more detail [117, 118]. Note, however, that there is no descending portion of this curve [119]. Patients do not 'fall off' the Frank-Starling curve – it is not physiologically possible. If a single myocyte is stretched excessively, its contractile force falls, however, this degree of stretch cannot be achieved in vivo by an intact ventricle. At excessive cardiac filling volumes, the cardiac function curve is flattened, but this is because of worsening wall stress at constant myocyte stretch; that is, accentuated afterload [120, 121]. The plateau of the cardiac function curve indicates that there is a limit to the Frank-Starling mechanism and that at some point, ventricular pressure rises without improved pump function.

Superposition of Cardiac Function and Circuit Function

Having spent the first half of this chapter detailing the mechanisms of improved and impaired circuit function, and having spent the second half of the chapter doing the same for cardiac function, it is now appropriate to explore the physiologies of the heart and blood vessels simultaneously. Juxtaposition of the circuit function and cardiac function onto the same graph is known as the Guyton diagram [figure13] [16].

Importantly, circuit function and cardiac function have opposing responses to right atrial pressure in that increased right atrial pressure diminishes venous return, but augments cardiac output. Accordingly, there is one unique right atrial pressure that arises at the intersection of the two curves and determines cardiac output. Imperatively, from these curves we see that right atrial pressure is not determined by cardiac function alone, nor by circuit function alone, but by both physiologies in tandem [16].

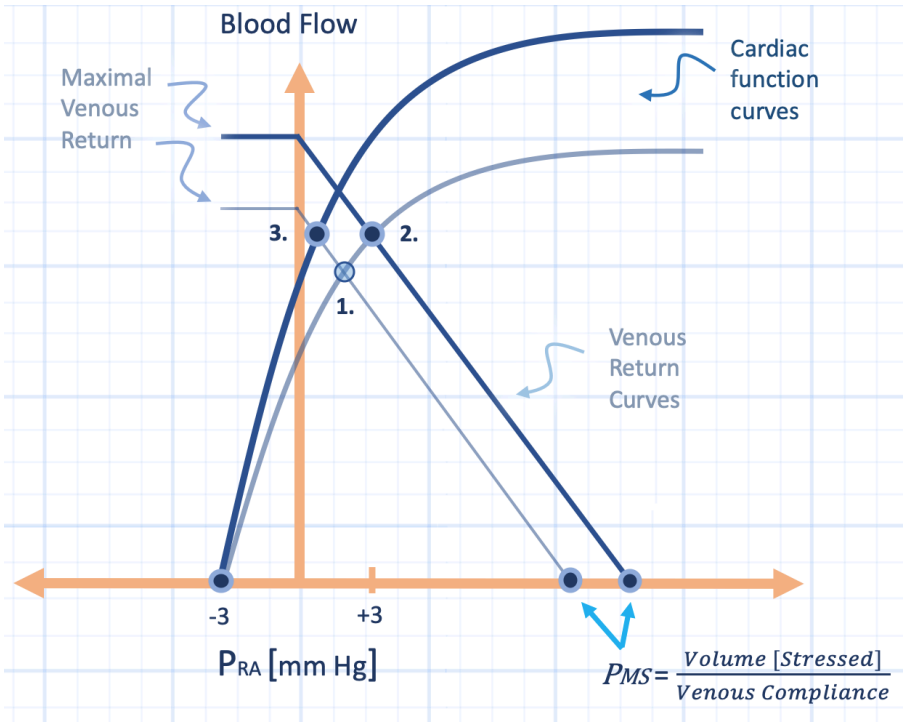

Figure 13: The Guyton diagram illustrates that both right atrial pressure [Pra] on the x-axis and the cardiac output on the y-axis arise from both cardiac function and circuit function working in tandem. Point 1. to point 2. reveals an increase in both right atrial pressure and cardiac output as a result of increased circuit function [right shift of the venous return curve]. However, point 3. has the same cardiac output as 2., but at a lower right atrial pressure; this is because of increased cardiac function. In a critically-ill patient, both the cardiac and circuit function curves may be rapidly dynamic.

Increased circuit function raises cardiac output and right atrial pressure while increased cardiac function raises cardiac output but lowers right atrial pressure. Conversely, diminished circuit function decreases cardiac output and filling pressure while impaired cardiac function lowers cardiac output but raises filling pressure. Clearly, the absolute value of the right atrial pressure should never be interpreted in isolation but instead with respect to both the circuit function and cardiac function [1].

As above, the position of the cardiac function curve is dynamic because the heart lies within the thorax. In other words, because, the x-intercept of the cardiac function curve corresponds to the intra-thoracic pressure, a drop in pleural pressure shifts the cardiac curve leftwards along the x-axis [figure 14] [122]. A shift in this direction, relative to circuit function, is analogous to an increase in circuit function [e.g. volume expansion]. Further, when the cardiac function curve shifts leftwards, the distance between its x-intercept and the right atrial pressure [i.e. the transmural pressure] increases, encouraging increased cardiac volume. Conversely, a rise in intra-thoracic pressure shifts the cardiac function curve rightwards which, effectively, decreases circuit function [e.g. volume loss]. In this situation, the transmural filling pressure, and therefore filling volume, tends to diminish [122].

There is a notable caveat to the aforementioned. The x-intercept of the cardiac function curve represents intra-thoracic pressure only in the absence of a pericardium. In actuality the ambient pressure for the cardiac transmural pressure is the pericardial pressure [Ppc] [114]. While intra-thoracic pressure is integrally transmitted to the pericardial space [123], the pericardial recoil pressure is added to the intra-thoracic pressure. The recoil pressure of the pericardium is a function of both pericardial volume and compliance [124]. At low pericardial volume, the recoil

pressure is small, however, at high cardiac – and therefore pericardial – volume, the pericardial recoil pressure can be significant. Therefore, as cardiac and pericardial volume increase, as in response to a fluid bolus, the pressure within the pericardial space may also rise along the pericardial compliance curve. Thus, the pericardium buffers cardiac transmural pressure [125]. As a result of the interdependence between right atrial intra-luminal and pericardial pressure, the right ventricle likely operates below its stressed volume in healthy hearts. Thus, right ventricular volume may change with little [124, 126] to no [114, 116] change in its transmural pressure.

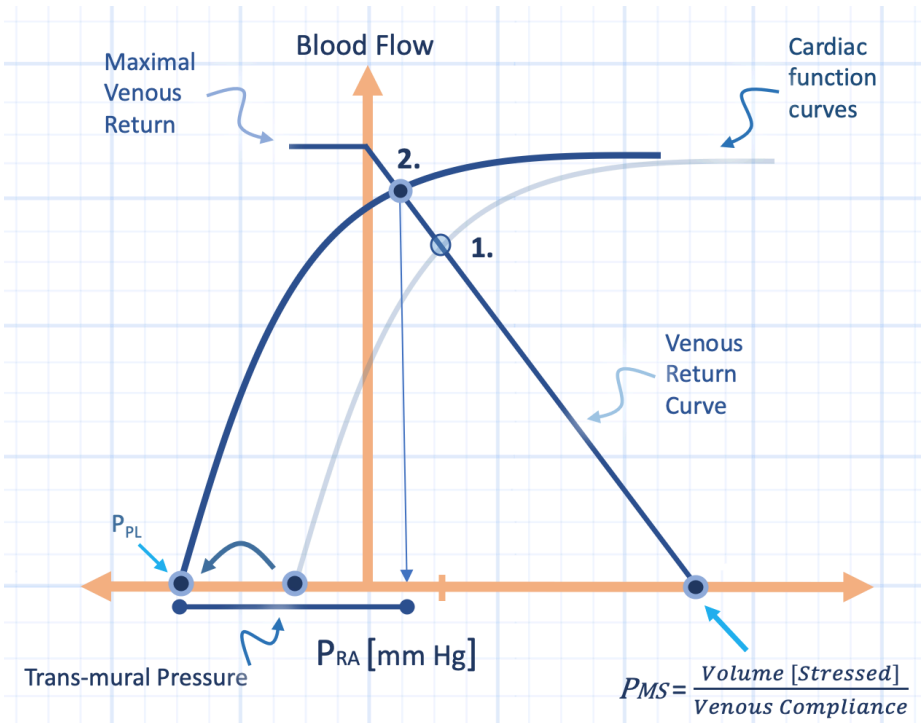

Figure 14: Effect of decreased intra-thoracic pressure on the Guyton diagram. Point 1. represents the right atrial pressure [Pra] on the x-axis and cardiac output on the y-axis, pre-inspiration. With a spontaneous breath, pleural pressure [Ppl] [x-intercept of the cardiac function curve] decreases [curved arrow] to its end-inspiratory value. Point 2., then represents the end-inspiratory right atrial pressure and cardiac output which have decreased and increased, respectively. The end-inspiratory distending pressure of the right atrium is the Ppl [x-intercept of the cardiac function curve] less the pressure within the right atrium and is represented by the 'dumbbell' below the x-axis. This figure assumes no change in circuit function during inspiration for simplicity. Pms is mean systemic pressure.

Table 3: Summary of Right Atrial Pressure Change

Increased right atrial pressure			**Decreased right atrial pressure**		
Cardiac	**Circuit**	**Thoracic**	**Cardiac**	**Circuit**	**Thoracic**
↓ function	↑ function	↑ pressure	↑ function	↓ function	↓ pressure
arrhythmia valve pathology ↑ afterload ↓ contractility	↑ Vs ↓venous capacitance ↓ venous resistance	mechanical inspiration ↑[auto]-PEEP ↑ thorax height relative to transducer	sinus rhythm ↓ afterload ↑ contractility	↓ Vs ↑venous capacitance ↑ venous resistance	spontaneous inspiration ↓[auto]-PEEP ↓ thorax height relative to transducer

Vs is stressed volume

Having presented a graphical representation of pleural pressure or intra-thoracic pressure and lung volume in chapter 1 – the Campbell diagram – and an illustration of cardiac filling pressure and flow in chapter 2 – the Guyton analysis – a new perspective on mechanical heart-lung interaction is introduced here [figure 15].

If pressure is maintained on the abscissa [note in mmHg and not cm H_2O], cardiac output on the y-axis and thoracic volume on the z-axis, then a relationship between the Campbell diagram and Guyton analysis is realized. As mentioned above, the cardiac function shifts along the abscissa with pleural pressure and pleural pressure is determined by the thoracic volume on the z-axis and the static and dynamic characteristics of the lung and chest wall.

This graphic illustrates atrial pressure, transmural pressure and cardiac output with respect to venous return and cardiac function whilst simultaneously depicting how the aforementioned cardiovascular variables are modified by lung and chest wall physiologies. While these effects are expanded upon in subsequent chapters, a relatively broad understanding of mechanical heart-lung interaction can be gleaned from this single diagram.

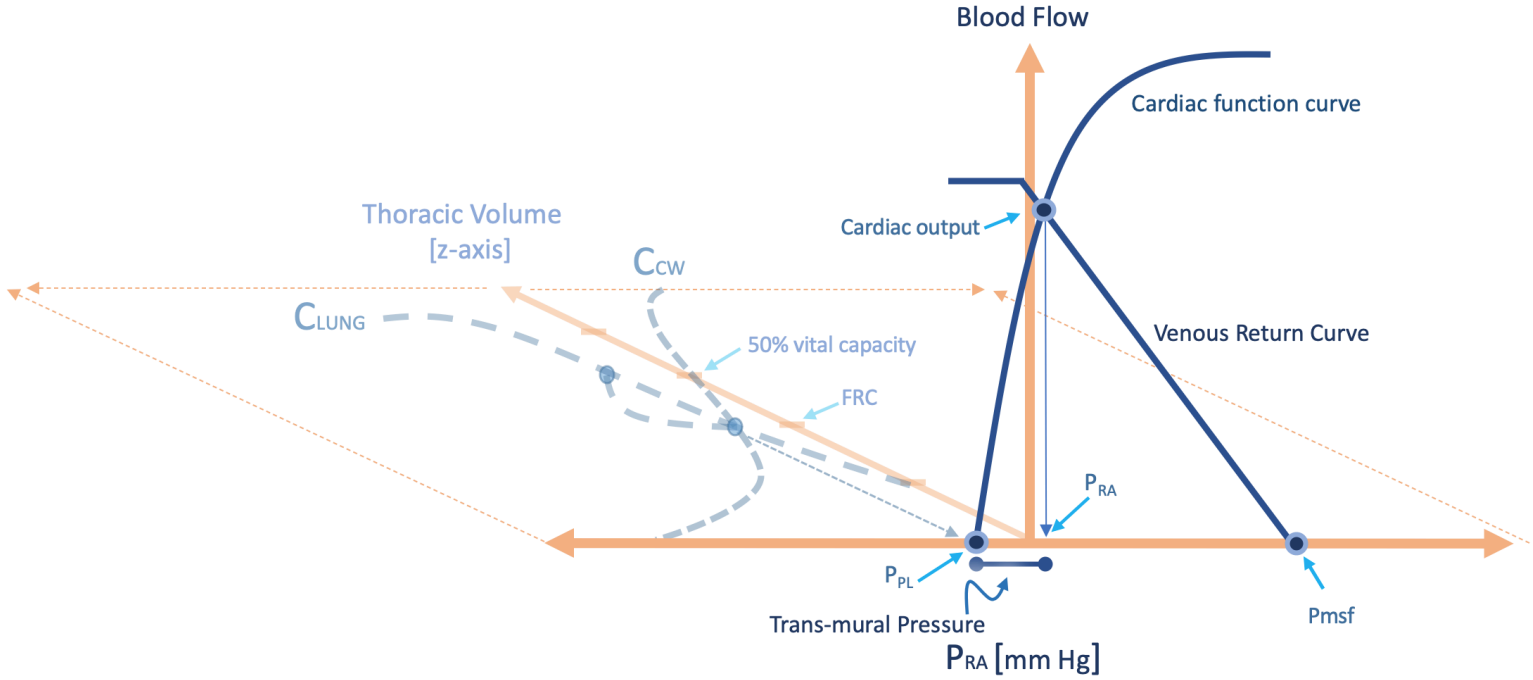

Figure 15: An approach to mechanical heart-lung interaction. The Campbell diagram – see chapter 1 – now occupies the x,z axes [into the page] with the Guyton diagram remaining on the x,y axes. Note that thoracic volume is on the z-axis and pressure remains on the x-axis which is the shared variable. Because the x-intercept of the cardiac function curve tracks changes in intra-thoracic pressure [e.g. pleural pressure, Ppl], the cardiac function curve shifts along the pressure axis in response. Pictured here is the beginning of inspiration [intra-thoracic pressure is at functional residual capacity, FRC]. Pra is right atrial pressure in millimetres of mercury [mmHg], Pmsf is mean systemic filling pressure. Ccw is chest wall compliance, Clung is lung compliance, see chapter 1.

References

1. Magder S: Bench-to-bedside review: An approach to hemodynamic monitoring - Guyton at the bedside. Crit Care 2012, 16(5):236.
2. Sagawa K: The ventricular pressure-volume diagram revisited. Circulation research 1978, 43(5): 677-687.
3. Sagawa K: The end-systolic pressure-volume relation of the ventricle: definition, modifications and clinical use. Circulation 1981, 63(6):1223-1227.
4. Sunagawa K, Sagawa K: Models of ventricular contraction based on time-varying elastance. Critical reviews in biomedical engineering 1982, 7(3):193-228.
5. Dell'Italia LJ, Walsh RA: Application of a time varying elastance model to right ventricular performance in man. Cardiovascular research 1988, 22(12):864-874.
6. Fox JM, Maurer MS: Ventriculovascular coupling in systolic and diastolic heart failure. Current heart failure reports 2005, 2(4):204-211.
7. Kassab GS: Biomechanics of the cardiovascular system: the aorta as an illustratory example. Journal of the Royal Society, Interface / the Royal Society 2006, 3(11):719-740.
8. Pfitzner J: Poiseuille and his law. Anaesthesia 1976, 31(2):273-275.
9. Watenpaugh DE, Hargens AR: The cardiovascular system in microgravity. Comprehensive Physiology 1996.
10. Sylvester JT, Goldberg HS, Permutt S: The Role of the Vasculature in the Regulation of Cardiac-Output. Clin Chest Med 1983, 4(2):111-126.
11. Jacobsohn E, Chorn R, OConnor M: The role of the vasculature in regulating venous return and cardiac output: historical and graphical approach. Can J Anaesth 1997, 44(8):849-867.
12. Starr I: Role of the" static blood pressure" in abnormal increments of venous pressure, especially in heart failure. ii. clinical and experimental studies. The American Journal of the Medical Sciences 1940, 199(1):40-54.
13. Guyton AC, Polizo D, Armstrong GG: Mean circulatory filling pressure measured immediately after cessation of heart pumping. The American journal of physiology 1954, 179(2):261-267.
14. Guyton AC, Adkins LH: Quantitative aspects of the collapse factor in relation to venous return. The American journal of physiology 1954, 177(3):523-527.
15. Guyton AC, Lindsey AW, Kaufmann BN: Effect of mean circulatory filling pressure and other peripheral circulatory factors on cardiac output. The American journal of physiology 1955, 180(3): 463-468.
16. Guyton AC: Determination of cardiac output by equating venous return curves with cardiac response curves. Physiological reviews 1955, 35(1):123-129.
17. Guyton AC, Lindsey AW, Abernathy B et al: Venous return at various right atrial pressures and the normal venous return curve. The American journal of physiology 1957, 189(3):609-615.
18. Magder S: Fluid status and fluid responsiveness. Curr Opin Crit Care 2010, 16(4):289-296.
19. Gelman S: Venous function and central venous pressure: a physiologic story. Anesthesiology 2008, 108(4):735-748.
20. Henderson WR, Griesdale DE, Walley KR et al: Clinical review: Guyton–the role of mean circulatory filling pressure and right atrial pressure in controlling cardiac output. Crit Care 2010, 14(6):243.
21. Feihl F, Broccard AF: Interactions between respiration and systemic hemodynamics. Part I: basic concepts. Intensive care medicine 2009, 35(1):45-54.
22. Natori H, Tamaki S, Kira S: Ultrasonographic evaluation of ventilatory effect on inferior vena caval configuration. The American review of respiratory disease 1979, 120(2):421-427.
23. Nakhjavan FK, Palmer WH, McGregor M: Influence of respiration on venous return in pulmonary emphysema. Circulation 1966, 33(1):8-16.
24. Lloyd TC, Jr.: Effect of inspiration on inferior vena caval blood flow in dogs. Journal of applied physiology: respiratory, environmental and exercise physiology 1983, 55(6):1701-1708.
25. Rubinson RM, Vasko JS, Doppman JL et al: Inferior Vena Caval Obstruction from Increased Intra-Abdominal Pressure - Experimental Hemodynamic and Angiographic Observations. Arch Surg-Chicago 1967, 94(6):766-&.
26. Appleton C, Olajos M, Morkin E et al: Alpha-1 adrenergic control of the venous circulation in intact dogs. The Journal of pharmacology and experimental therapeutics 1985, 233(3):729-734.
27. Datta P, Magder S: Hemodynamic response to norepinephrine with and without inhibition of nitric oxide synthase in porcine endotoxemia. American journal of respiratory and critical care medicine 1999, 160(6):1987-1993.
28. Maas JJ, Pinsky MR, de Wilde RB et al: Cardiac output response to norepinephrine in postoperative cardiac surgery patients: interpretation with venous return and cardiac function curves. Critical care medicine 2013, 41(1):143-150.
29. Persichini R, Silva S, Teboul JL et al: Effects of norepinephrine on mean systemic pressure and venous return in human septic shock. Critical care medicine 2012, 40(12):3146-3153.
30. Green JF: Mechanism of action of isoproterenol on venous return. The American journal of physiology 1977, 232(2):H152-156.

31. Tarasiuk A, Scharf SM: Effects of periodic obstructive apneas on venous return in closed-chest dogs. The American review of respiratory disease 1993, 148(2):323-329.
32. Nanas S, Magder S: Adaptations of the peripheral circulation to PEEP. The American review of respiratory disease 1992, 146(3):688-693.
33. Rothe CF: Physiology of venous return. An unappreciated boost to the heart. Archives of internal medicine 1986, 146(5):977-982.
34. Scharf SM, Ingram RH, Jr.: Influence of abdominal pressure and sympathetic vasoconstriction on the cardiovascular response to positive end-expiratory pressure. The American review of respiratory disease 1977, 116(4):661-670.
35. Peters J, Hecker B, Neuser D et al: Regional blood volume distribution during positive and negative airway pressure breathing in supine humans. J Appl Physiol (1985) 1993, 75(4):1740-1747.
36. Morgan BC, Guntheroth WG, Dillard DH: Relationship of Pericardial to Pleural Pressure during Quiet Respiration and Cardiac Tamponade. Circulation research 1965, 16:493-498.
37. Bodson L, Vieillard-Baron A: Respiratory variation in inferior vena cava diameter: surrogate of central venous pressure or parameter of fluid responsiveness? Let the physiology reply. Crit Care 2012, 16(6):181.
38. Jardin F, Vieillard-Baron A: Ultrasonographic examination of the venae cavae. Intensive care medicine 2006, 32(2):203-206.
39. Funk DJ, Jacobsohn E, Kumar A: The role of venous return in critical illness and shock-part I: physiology. Critical care medicine 2013, 41(1):255-262.
40. Takata M, Robotham JL: Effects of inspiratory diaphragmatic descent on inferior vena caval venous return. J Appl Physiol (1985) 1992, 72(2):597-607.
41. Takata M, Wise RA, Robotham JL: Effects of abdominal pressure on venous return: abdominal vascular zone conditions. J Appl Physiol (1985) 1990, 69(6):1961-1972.
42. Magder S, Vanelli G: Circuit factors in the high cardiac output of sepsis. Journal of critical care 1996, 11(4):155-166.
43. Magder S, Bafaqeeh F: The clinical role of central venous pressure measurements. Journal of intensive care medicine 2007, 22(1):44-51.
44. Magder S, De Varennes B: Clinical death and the measurement of stressed vascular volume. Critical care medicine 1998, 26(6):1061-1064.
45. Brower R, Wise RA, Hassapoyannes C et al: Effect of lung inflation on lung blood volume and pulmonary venous flow. J Appl Physiol (1985) 1985, 58(3):954-963.
46. West JB, Dollery CT, Naimark A: Distribution of Blood Flow in Isolated Lung; Relation to Vascular and Alveolar Pressures. Journal of applied physiology 1964, 19:713-724.
47. Allen DG, Kentish JC: The cellular basis of the length-tension relation in cardiac muscle. Journal of molecular and cellular cardiology 1985, 17(9):821-840.
48. Sarnoff SJ: Myocardial contractility as described by ventricular function curves; observations on Starling's law of the heart. Physiological reviews 1955, 35(1):107-122.
49. Burkhoff D, Mirsky I, Suga H: Assessment of systolic and diastolic ventricular properties via pressure-volume analysis: a guide for clinical, translational, and basic researchers. American journal of physiology Heart and circulatory physiology 2005, 289(2):H501-512.
50. Maughan WL, Shoukas AA, Sagawa K et al: Instantaneous pressure-volume relationship of the canine right ventricle. Circulation research 1979, 44(3):309-315.
51. Brown KA, Ditchey RV: Human right ventricular end-systolic pressure-volume relation defined by maximal elastance. Circulation 1988, 78(1):81-91.
52. Dell'Italia LJ, Walsh RA: Right ventricular diastolic pressure-volume relations and regional dimensions during acute alterations in loading conditions. Circulation 1988, 77(6):1276-1282.
53. Starling MR, Walsh RA, Dell'Italia LJ et al: The relationship of various measures of end-systole to left ventricular maximum time-varying elastance in man. Circulation 1987, 76(1):32-43.
54. Gilbert JC, Glantz SA: Determinants of left ventricular filling and of the diastolic pressure-volume relation. Circulation research 1989, 64(5):827-852.
55. Maniar HS, Prasad SM, Gaynor SL et al: Impact of pericardial restraint on right atrial mechanics during acute right ventricular pressure load. American journal of physiology Heart and circulatory physiology 2003, 284(1):H350-357.
56. Aurigemma GP, Gaasch WH: Clinical practice. Diastolic heart failure. The New England journal of medicine 2004, 351(11):1097-1105.
57. Zile MR, Baicu CF, Gaasch WH: Diastolic heart failure--abnormalities in active relaxation and passive stiffness of the left ventricle. The New England journal of medicine 2004, 350(19): 1953-1959.
58. Pinsky MR: Clinical significance of pulmonary artery occlusion pressure. Intensive care medicine 2003, 29(2):175-178.
59. Bove AA, Santamore WP: Ventricular interdependence. Progress in cardiovascular diseases 1981, 23(5):365-388.
60. Henderson Y, Prince AL: The relative systolic discharges of the right and left ventricles and their bearing on pulmonary congestion and depletion. Heart 1914, 5(217):1913-1914.
61. Maruyama Y, Ashikawa K, Isoyama S et al: Mechanical interactions between four heart chambers with and without the pericardium in canine hearts. Circulation research 1982, 50(1): 86-100.
62. Spadaro J, Bing OH, Gaasch WH et al: Pericardial modulation of right and left ventricular diastolic interaction. Circulation research 1981, 48(2):233-238.

63. Maughan WL, Sunagawa K, Sagawa K: Ventricular systolic interdependence: volume elastance model in isolated canine hearts. The American journal of physiology 1987, 253(6 Pt 2):H1381-1390.
64. Chung DC, Niranjan SC, Clark JW, Jr. et al: A dynamic model of ventricular interaction and pericardial influence. The American journal of physiology 1997, 272(6 Pt 2):H2942-2962.
65. Little WC, Badke FR, O'Rourke RA: Effect of right ventricular pressure on the end-diastolic left ventricular pressure-volume relationship before and after chronic right ventricular pressure overload in dogs without pericardia. Circulation research 1984, 54(6):719-730.
66. Farrar DJ, Woodard JC, Chow E: Pacing-induced dilated cardiomyopathy increases left-to-right ventricular systolic interaction. Circulation 1993, 88(2):720-725.
67. Mehmel HC, Stockins B, Ruffmann K et al: The linearity of the end-systolic pressure-volume relationship in man and its sensitivity for assessment of left ventricular function. Circulation 1981, 63(6):1216-1222.
68. Borow KM, Neumann A, Wynne J: Sensitivity of end-systolic pressure-dimension and pressure-volume relations to the inotropic state in humans. Circulation 1982, 65(5):988-997.
69. Khot UN, Novaro GM, Popovic ZB et al: Nitroprusside in critically ill patients with left ventricular dysfunction and aortic stenosis. The New England journal of medicine 2003, 348(18): 1756-1763.
70. De Keulenaer GW, Brutsaert DL: Systolic and diastolic heart failure are overlapping phenotypes within the heart failure spectrum. Circulation 2011, 123(18):1996-2004; discussion 2005.
71. Yaku H, Slinker BK, Bell SP et al: Effects of free wall ischemia and bundle branch block on systolic ventricular interaction in dog hearts. The American journal of physiology 1994, 266(3 Pt 2):H1087-1094.
72. Damiano RJ, Jr., La Follette P, Jr., Cox JL et al: Significant left ventricular contribution to right ventricular systolic function. The American journal of physiology 1991, 261(5 Pt 2):H1514-1524.
73. Yamaguchi S, Harasawa H, Li KS et al: Comparative significance in systolic ventricular interaction. Cardiovascular research 1991, 25(9):774-783.
74. Schertz C, Pinsky MR: Effect of the pericardium on systolic ventricular interdependence in the dog. Journal of critical care 1993, 8(1):17-23.
75. Berko B, Gaasch WH, Tanigawa N et al: Disparity between ejection and end-systolic indexes of left ventricular contractility in mitral regurgitation. Circulation 1987, 75(6):1310-1319.
76. Gaemperli O, Biaggi P, Gugelmann R et al: Real-time left ventricular pressure-volume loops during percutaneous mitral valve repair with the MitraClip system. Circulation 2013, 127(9): 1018-1027.
77. Keren G, Katz S, Strom J et al: Dynamic mitral regurgitation. An important determinant of the hemodynamic response to load alterations and inotropic therapy in severe heart failure. Circulation 1989, 80(2):306-313.
78. Versprille A: Pulmonary vascular resistance. A meaningless variable. Intensive care medicine 1984, 10(2):51-53.
79. Naeije R: Pulmonary vascular resistance. A meaningless variable? Intensive care medicine 2003, 29(4):526-529.
80. Milnor WR: Arterial impedance as ventricular afterload. Circulation research 1975, 36(5):565-570.
81. Sagawa K, Lie RK, Schaefer J: Translation of Otto frank's paper "Die Grundform des arteriellen Pulses" zeitschrift für biologie 37: 483–526 (1899). Journal of molecular and cellular cardiology 1990, 22(3):253-254.
82. Yanof HM: Biomedical electronics: Davis; 1972.
83. Westerhof N, Elzinga G, Sipkema P: An artificial arterial system for pumping hearts. Journal of applied physiology 1971, 31(5):776-781.
84. Tedford RJ: Determinants of right ventricular afterload (2013 Grover Conference series). Pulmonary circulation 2014, 4(2):211-219.
85. Grant BJ, Paradowski LJ: Characterization of pulmonary arterial input impedance with lumped parameter models. The American journal of physiology 1987, 252(3 Pt 2):H585-593.
86. Stergiopulos N, Westerhof BE, Westerhof N: Total arterial inertance as the fourth element of the windkessel model. The American journal of physiology 1999, 276(1 Pt 2):H81-88.
87. Kelly RP, Ting CT, Yang TM et al: Effective arterial elastance as index of arterial vascular load in humans. Circulation 1992, 86(2):513-521.
88. Segers P, Stergiopulos N, Westerhof N: Relation of effective arterial elastance to arterial system properties. American journal of physiology Heart and circulatory physiology 2002, 282(3):H1041-1046.
89. Asanoi H, Sasayama S, Kameyama T: Ventriculoarterial coupling in normal and failing heart in humans. Circulation research 1989, 65(2):483-493.
90. Fessler HE, Brower RG, Wise RA et al: Mechanism of reduced LV afterload by systolic and diastolic positive pleural pressure. J Appl Physiol (1985) 1988, 65(3):1244-1250.
91. Ferguson JJ, 3rd, Miller MJ, Sahagian P et al: Assessment of aortic pressure-volume relationships with an impedance catheter. Catheterization and cardiovascular diagnosis 1988, 15(1):27-36.
92. Briand M, Dumesnil JG, Kadem L et al: Reduced systemic arterial compliance impacts significantly on left ventricular afterload and function in aortic stenosis: implications for diagnosis and treatment. Journal of the American College of Cardiology 2005, 46(2):291-298.
93. Garcia D, Barenbrug PJ, Pibarot P et al: A ventricular-vascular coupling model in presence of aortic stenosis. American journal of physiology Heart and circulatory physiology 2005, 288(4):H1874-1884.

94. Dekker AL, Barenbrug PJ, van der Veen FH et al: Pressure-volume loops in patients with aortic stenosis. The Journal of heart valve disease 2003, 12(3):325-332.
95. Peterson KL, Tsuji J, Johnson A et al: Diastolic left ventricular pressure-volume and stress-strain relations in patients with valvular aortic stenosis and left ventricular hypertrophy. Circulation 1978, 58(1):77-89.
96. Margulescu AD, Rimbas RC, Florescu M et al: Cardiac adaptation in acute hypertensive pulmonary edema. The American journal of cardiology 2012, 109(10):1472-1481.
97. Starling MR: Left ventricular-arterial coupling relations in the normal human heart. American heart journal 1993, 125(6):1659-1666.
98. Naeije R: Physiology of the pulmonary circulation and the right heart. Current hypertension reports 2013, 15(6):623-631.
99. Mitzner W: Resistance of the pulmonary circulation. Clin Chest Med 1983, 4(2):127-137.
100. Zhuang FY, Fung YC, Yen RT: Analysis of blood flow in cat's lung with detailed anatomical and elasticity data. Journal of applied physiology: respiratory, environmental and exercise physiology 1983, 55(4):1341-1348.
101. McGregor M, Sniderman A: On pulmonary vascular resistance: the need for more precise definition. The American journal of cardiology 1985, 55(1):217-221.
102. Graham R, Skoog C, Macedo W et al: Dopamine, dobutamine, and phentolamine effects on pulmonary vascular mechanics. Journal of applied physiology: respiratory, environmental and exercise physiology 1983, 54(5):1277-1283.
103. Saouti N, Westerhof N, Postmus PE et al: The arterial load in pulmonary hypertension. European respiratory review : an official journal of the European Respiratory Society 2010, 19(117):197-203.
104. Graham R, Skoog C, Oppenheimer L et al: Critical closure in the canine pulmonary vasculature. Circulation research 1982, 50(4):566-572.
105. Whittenberger JL, Mc GM, Berglund E et al: Influence of state of inflation of the lung on pulmonary vascular resistance. Journal of applied physiology 1960, 15:878-882.
106. Permutt S, Bromberger-Barnea B, Bane HN: Alveolar pressure, pulmonary venous pressure, and the vascular waterfall. Medicina thoracalis 1962, 19:239-260.
107. Permutt S, Riley RL: Hemodynamics of Collapsible Vessels with Tone: The Vascular Waterfall. Journal of applied physiology 1963, 18:924-932.
108. Lopez-Muniz R, Stephens NL, Bromberger-Barnea B et al: Critical closure of pulmonary vessels analyzed in terms of Starling resistor model. Journal of applied physiology 1968, 24(5):625-635.
109. Magder S, Guerard B: Heart-lung interactions and pulmonary buffering: lessons from a computational modeling study. Respiratory physiology & neurobiology 2012, 182(2-3):60-70.
110. Mitzner W, Sylvester JT: Hypoxic vasoconstriction and fluid filtration in pig lungs. Journal of applied physiology: respiratory, environmental and exercise physiology 1981, 51(5):1065-1071.
111. Sylvester JT, Mitzner W, Ngeow Y et al: Hypoxic constriction of alveolar and extra-alveolar vessels in isolated pig lungs. Journal of applied physiology: respiratory, environmental and exercise physiology 1983, 54(6):1660-1666.
112. Glower DD, Spratt JA, Snow ND et al: Linearity of the Frank-Starling relationship in the intact heart: the concept of preload recruitable stroke work. Circulation 1985, 71(5):994-1009.
113. Linderer T, Chatterjee K, Parmley WW et al: Influence of atrial systole on the Frank-Starling relation and the end-diastolic pressure-diameter relation of the left ventricle. Circulation 1983, 67(5):1045-1053.
114. Tyberg JV, Taichman GC, Smith ER et al: The relationship between pericardial pressure and right atrial pressure: an intraoperative study. Circulation 1986, 73(3):428-432.
115. Hamilton DR, Dani RS, Semlacher RA et al: Right atrial and right ventricular transmural pressures in dogs and humans. Effects of the pericardium. Circulation 1994, 90(5):2492-2500.
116. Pinsky MR: My paper 20 years later: Effect of positive end-expiratory pressure on right ventricular function in humans. Intensive care medicine 2014, 40(7):935-941.
117. Magder S: How to use central venous pressure measurements. Curr Opin Crit Care 2005, 11(3): 264-270.
118. Butler J: The heart is in good hands. Circulation 1983, 67(6):1163-1168.
119. Sarnoff SJ, Berglund E: Ventricular function. I. Starling's law of the heart studied by means of simultaneous right and left ventricular function curves in the dog. Circulation 1954, 9(5):706-718.
120. MacGregor DC, Covell JW, Mahler F et al: Relations between afterload, stroke volume, and descending limb of Starling's curve. The American journal of physiology 1974, 227(4):884-890.
121. Ross J, Jr.: Mechanisms of cardiac contraction. What roles for preload, afterload and inotropic state in heart failure? European heart journal 1983, 4 Suppl A:19-28.
122. Magder S: Clinical usefulness of respiratory variations in arterial pressure. American journal of respiratory and critical care medicine 2004, 169(2):151-155.
123. Morgan BC, Martin WE, Hornbein TF et al: Hemodynamic effects of intermittent positive pressure respiration. Anesthesiology 1966, 27(5):584-590.
124. Takata M, Mitzner W, Robotham JL: Influence of the pericardium on ventricular loading during respiration. J Appl Physiol (1985) 1990, 68(4):1640-1650.
125. Takata M, Harasawa Y, Beloucif S et al: Coupled vs. uncoupled pericardial constraint: effects on cardiac chamber interactions. J Appl Physiol (1985) 1997, 83(6):1799-1813.
126. Scharf SM, Brown R, Warner KG et al: Intrathoracic pressures and left ventricular configuration with respiratory maneuvers. J Appl Physiol (1985) 1989, 66(1):481-491.

Chapter Three

Mechanical Interactions Between the Respiratory & Cardiovascular Systems in Health: integration of the Campbell and Guyton diagrams

Abstract

Appreciation for mechanical interaction between the cardiovascular system and the lung and chest wall flows from both the Campbell and Guyton diagrams. Intra-thoracic pressure and lung volume are the two variables graphically represented by the Campbell diagram and the key elements mechanically influencing cardio-circulatory behaviour. Changing intra-thoracic pressure shifts the right ventricular cardiac function curve on the Guyton diagram relative to systemic venous return curve which alters right ventricular preload; left ventricular preload is then affected via parallel and series effects. Additionally, lung and abdominal volume may alter systemic and pulmonary vascular capacitance, further regulating biventricular loading. Awareness of these complex and sometimes conflicting events in the healthy patient facilitates discussion in the diseased patient.

Keywords: Guyton diagram, Campbell diagram, heart-lung interaction, preload, afterload, systemic venous return, pulmonary venous return, intermittent positive pressure ventilation, positive end-expiratory pressure.

Introduction

As the Campbell diagram illustrates the relationship between pleural pressure and thoracic volume [1], this diagram is well-suited to explore the mechanical effects of the respiratory system upon the cardiovascular system [figure 1]. Indeed, changes in lung volume and intra-thoracic pressure are the two main mechanical mediators of heart-lung interactions [2-5]. Consequently, this chapter parses out the effects of lung volume and intra-thoracic pressure upon the cardio-circulatory system. Subsequently, the combination of changes in thoracic volume and pressure are considered as the integrated acts of spontaneous ventilation and intermittent positive pressure ventilation. It may seem obvious, but increased thoracic volume is shared by both spontaneous and intermittent positive-pressure ventilation; therefore, the key difference between the two acts – in terms of mechanical coupling between the respiratory and cardiovascular systems – is the change in intra-thoracic pressure [figure 2].

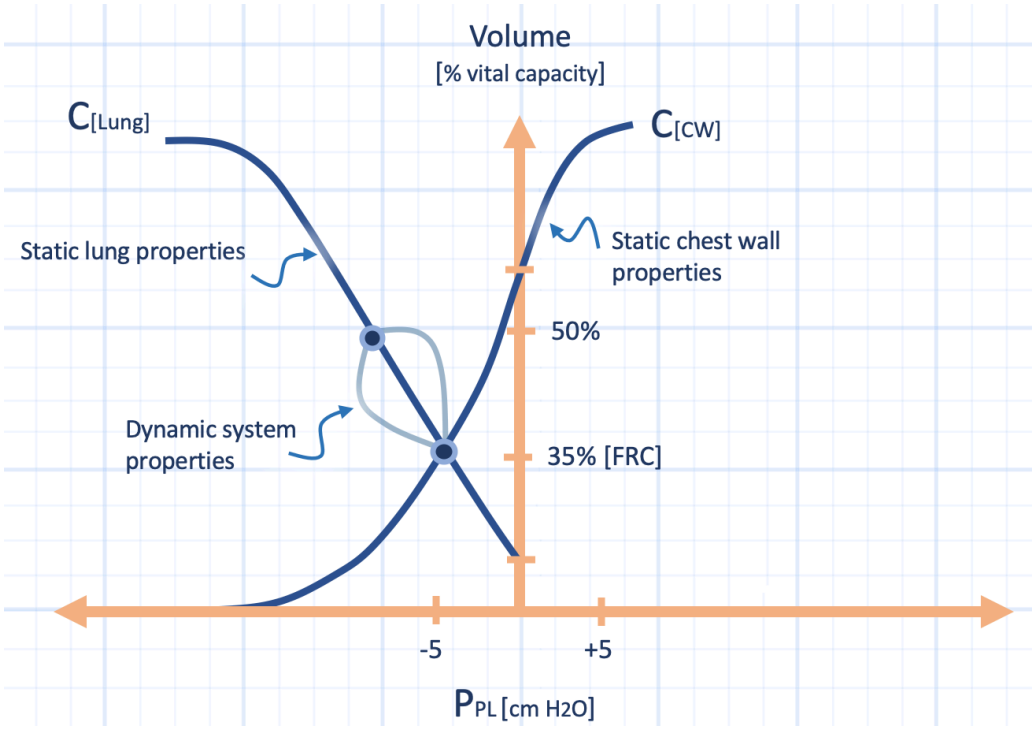

Figure 1: The Campbell diagram; see also chapter 1. The relationship between thoracic volume in percent vital capacity [ordinate] and pleural or intra-thoracic pressure [abscissa]. Static properties refer to compliance or elastance while dynamic properties are primarily airflow resistance. Ppl is pleural pressure; FRC is functional residual capacity; cm H2O is centimetres of water; Clung is lung compliance and Ccw is chest wall compliance.

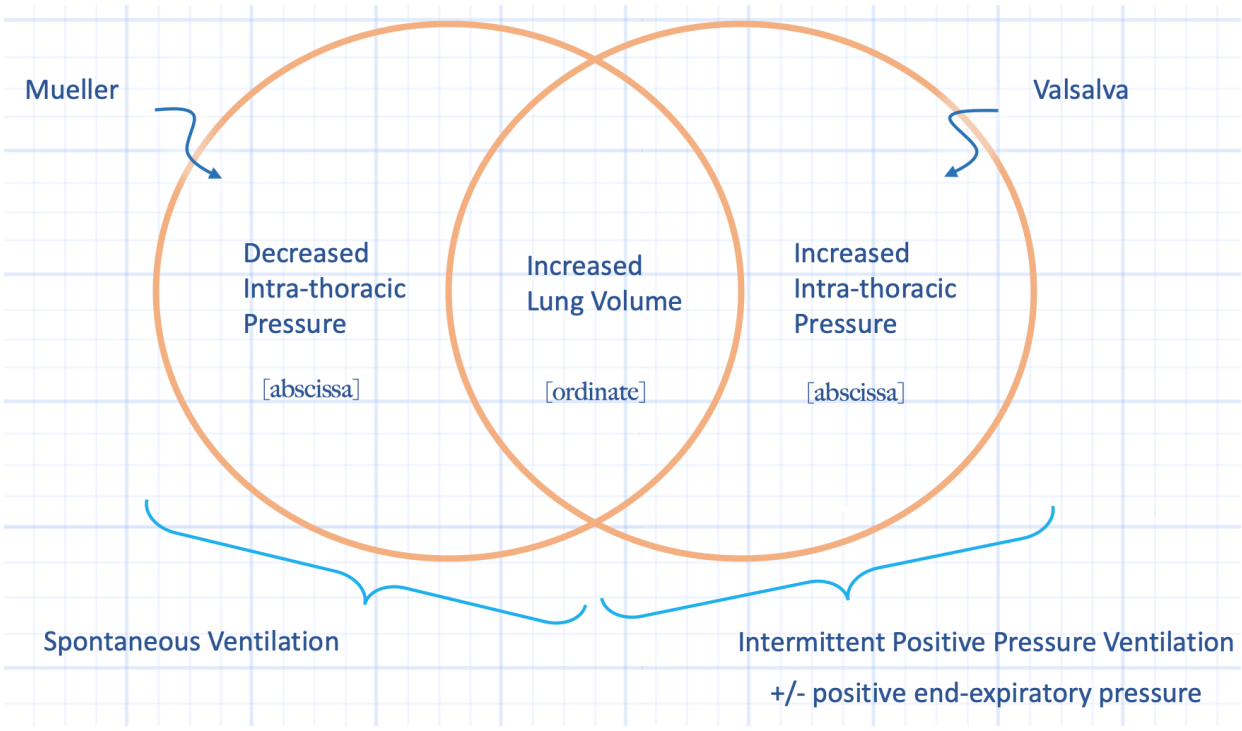

Figure 2: An approach to chapter 3. Each of these respiratory effects will be discussed in terms of stresses placed upon the cardiovascular system. Abscissa and ordinate refer to the Campbell diagram - see figure 1. A decrease in intra-thoracic pressure [or pleural pressure] without a change in lung volume is a 'Mueller maneuver' while an increase in intra-thoracic pressure without a change in lung volume is a 'Valsalva maneuver.'

It must be stressed, however, that this chapter focuses on heart-lung interactions in the healthy individual; this assists interpretation of these complicated, parallel influences in various disease states in subsequent discussions. Review of the biochemical and neurohumoural communication within the cardiorespiratory system is beyond the scope of this volume [6].

Change in Lung and Thoracic Volume

It is somewhat artificial to consider the cardiovascular effects of changing lung and thoracic volume in isolation from intra-thoracic pressure; the volume of the thorax is altered in conjunction with changing transpulmonary pressure. As discussed in chapter 1, the transpulmonary pressure is the difference between the alveolar and pleural pressure. Lung volume increases during spontaneous ventilation with pleural pressure falling relative to alveolar pressure. On the other hand, lung volume increases during intermittent positive pressure ventilation with alveolar pressure rising relative to pleural pressure. Despite these opposing methods of increasing transpulmonary pressure and lung volume, unique stresses are placed upon the cardiovascular system regardless of the method by which transpulmonary pressure changes.

Generally, increased lung volume stresses the heart, pulmonary and abdominal vessels. The outcome of this stress is unique to the underlying vascular bed or structure upon which the distending force is acted, as well as the pre-existing volume status of the vasculature.

Systemic and Pulmonary Venous Return

The bulk of research on venous return to the right heart has focused on flow through the inferior vena cava [IVC] from the abdominal blood vessels. Diaphragm descent – which occurs with rising lung volume – pressurizes the abdominal cavity. The extent to which the intra-abdominal pressure increases depends upon a number of factors including the relative compliances of the chest wall and the abdominal wall, the use of diaphragmatic versus thoracic cage versus abdominal muscles of respiration and the total change in volume between the two compartments [3, 7-11]. Consequently, the greater the ordinate changes on the Campbell diagram [i.e. the greater the volume change], the greater the vascular system is stressed.

Within the abdominal cavity, the stress on the splanchnic vascular bed augments the mean systemic pressure [12-15]; ostensibly, this occurs because of diminished venous capacitance as well as sympathetic activity acting upon the venous capacitance beds [16]. The Guytonian analysis depicts this effect as a rightward shift of the venous return curve and a tendency to increase both right atrial pressure and cardiac output.

However, the result is not simply a shift of the venous return curve to the right in parallel. When the patient has underlying volume depletion, complete obliteration of venous capacitance beds may occur and this raises resistance to venous return [9, 10, 17]. Increased resistance to venous return shifts the slope of the venous return

curve downwards. Therefore, while the mean systemic pressure [i.e. x-intercept of the circuit function curve - see chapter 2] may shift to the right in response to diaphragmatic descent, venous return may be depressed [Figure 3]. It is suggested that the venous bed of the liver plays an important role in venous return resistance when the abdominal compartment is pressurized [14, 18-21]. Additionally, collapse of the IVC impairs maximal venous return, and therefore cardiac output. Again, these effects take precedence when either the intra-luminal pressure of the vascular bed is low [e.g. hypovolemia] or if the intra-abdominal pressure is excessively high. Collapse of the IVC occurs when the intra-abdominal pressure supersedes intra-luminal IVC pressure by about 5 cm H2O [11].

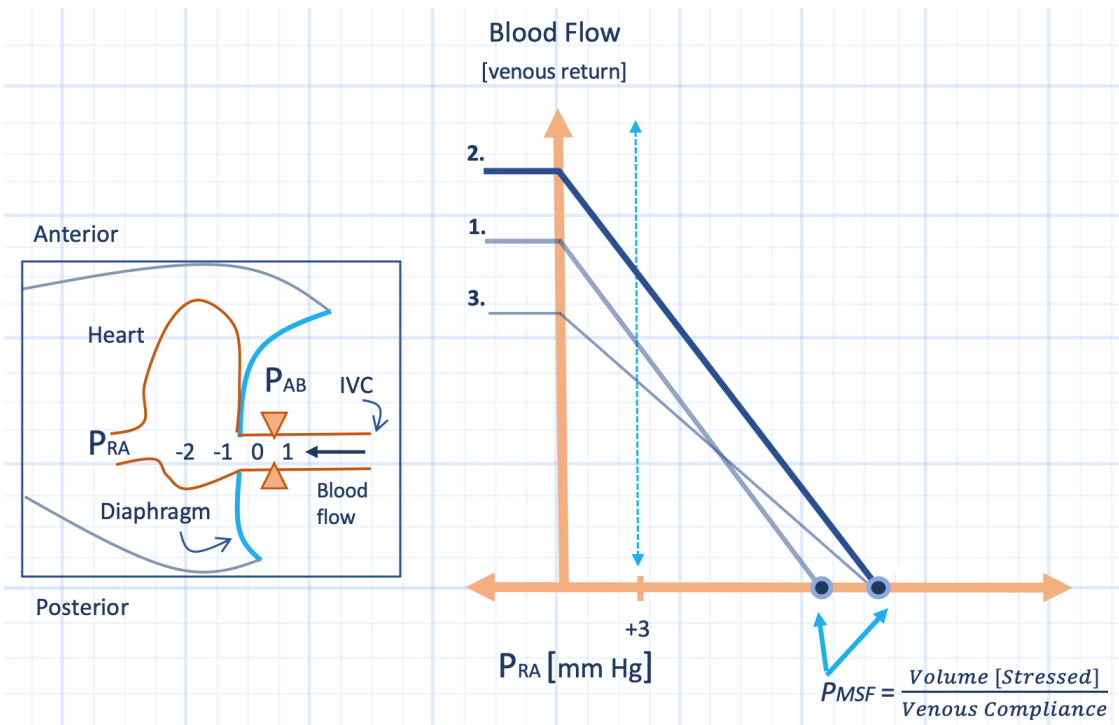

Figure 3: Lung volume and the systemic venous return, or circuit function curve. Pra is right atrial pressure on the x-axis and blood flow, or venous return, is on y-axis. Pmsf is mean systemic filling pressure [see also mean circulatory filling pressure in chapter 2]. Ostensibly, abdominal pressurization by diaphragm descent decreases venous capacitance, effectively raising stressed venous volume and, therefore, Pmsf [curve 2. & 3.]. However, zonal characteristics of the venous beds may change [e.g. increase] resistance [curve 3.] The inset depicts inferior vena cava [IVC] collapse from rising abdominal pressure [Pab] which diminishes maximal venous return [see chapter 2]. The vertical line at Pra [3 mmHg] shows the effect on blood flow [y-axis] with abdominal pressurization; see text for details.

Conversely, when a patient has underlying high total body blood volume, the effect of venous bed collapse and IVC collapse is attenuated. In such patients, increased lung volume and pressurization of the abdominal compartment favours IVC flow [9, 11, 14]. This is illustrated by a nearly complete, parallel, rightward shift of the venous return curve on the Guyton diagram.

Pulmonary venous return to the left heart follows somewhat similar physiology. As elaborated below, lung volume modifies pulmonary vascular resistance and also pulmonary vascular capacitance [22-25]. As lung volume increases above functional residual capacity, the pulmonary vascular capacitance decreases and blood is extruded into the pulmonary veins – augmenting venous return [24]. However, this effect is highly dependent upon the zonal characteristics of the lungs which, in turn, depends upon total body blood volume. In states of hypovolemia or poor perfusion to the pulmonary vascular bed, zone I and zone II states may predominate. In these

situations, the pulmonary capillary tends to 'collapse' when the transpulmonary pressure supersedes the pulmonary capillary trans-mural pressure. These zonal conditions do not facilitate pulmonary venous return to the left heart and, effectively, raise the resistance to venous return. By contrast, zone III conditions occur when the transpulmonary pressure at end-inspiration does not exceed pulmonary capillary trans-mural pressure. In these conditions, blood is extruded from the lungs and pulmonary venous return is facilitated [22, 24].

On the Guyton diagram, increased lung volume – which decreases pulmonary vascular capacitance – is analogous to shifting the venous return curve to the right, however, the effective resistance to pulmonary venous return may be increased if excessive collapse of the pulmonary venous system occurs under zone I and zone II conditions [figure 3].

While increased lung volume affects the vasculature and therefore the systemic and pulmonary venous return curves, lung inflation also stresses biventricular loading and, accordingly, the cardiac function curves.

Right Ventricular Loading

There is evidence that at very high lung volumes the right ventricle becomes less compliant and that the diaphragm acts as a sphincter to impinge IVC blood flow; in health, these effects are minimal [26, 27]. Right ventricular diastolic properties are not altered with normal tidal volumes. Potentially, this is a function of right ventricular geometry and orientation relative to the expanding lung. Further, the suggestion of impaired right ventricular compliance at high lung volume may reflect abnormally large right ventricular afterload; retention of blood in the right ventricle would impair its compliance [28, 29].

A key effect lung distention exerts upon the right ventricle is altering pulmonary arterial impedance. Recall from chapter 2 that the impedance of a vascular bed is sometimes modelled as the geometric summation of both the resistance and reactance of the system via the 'impedance triangle;' though this analogy is more truly a model of electrical impedance. Reactance quantifies the distensible nature of blood vessels while resistance is the traditional relationship between pressure and flow and highly dependent upon cross-sectional vascular diameter. Modelling the pulmonary arterial load using both resistance and reactance is also known as the '2-element Windkessel' model [30] and is, admittedly, an oversimplification as it neglects characteristic impedance [31]. Nevertheless, evidence suggests that while both reactance and resistance affect impedance, vascular resistance may play a more important quantitative role [32].

The effect of lung volume on calculated pulmonary vascular resistance is biphasic [25]. At low lung volume, below functional residual capacity, raising lung volume lowers the calculated pulmonary vascular resistance. There are a few mechanisms behind this. First, the extra-alveolar vessels are tethered open and made less

tortuous which increases their cross-sectional area, improving resistance to blood flow [33, 34]. Further, in vivo, low lung volume favours alveolar collapse, V/Q mismatching [34-36], local hypoxemia and hypoxic vasoconstriction [37]. Increased lung volume opens alveolar units, mitigates hypoxemia and vascular resistance is improved. Finally, the oft-quoted relationship between lung volume and vascular resistance may arise by assuming that left atrial pressure is always the downstream pressure in the vascular resistance equation. Increasing lung volume actually changes the Starling resistance of the pulmonary vascular bed [see chapter 2] and the rise in calculated pulmonary vascular resistance may be driven largely by incorrect physiological assumptions [figure 4].

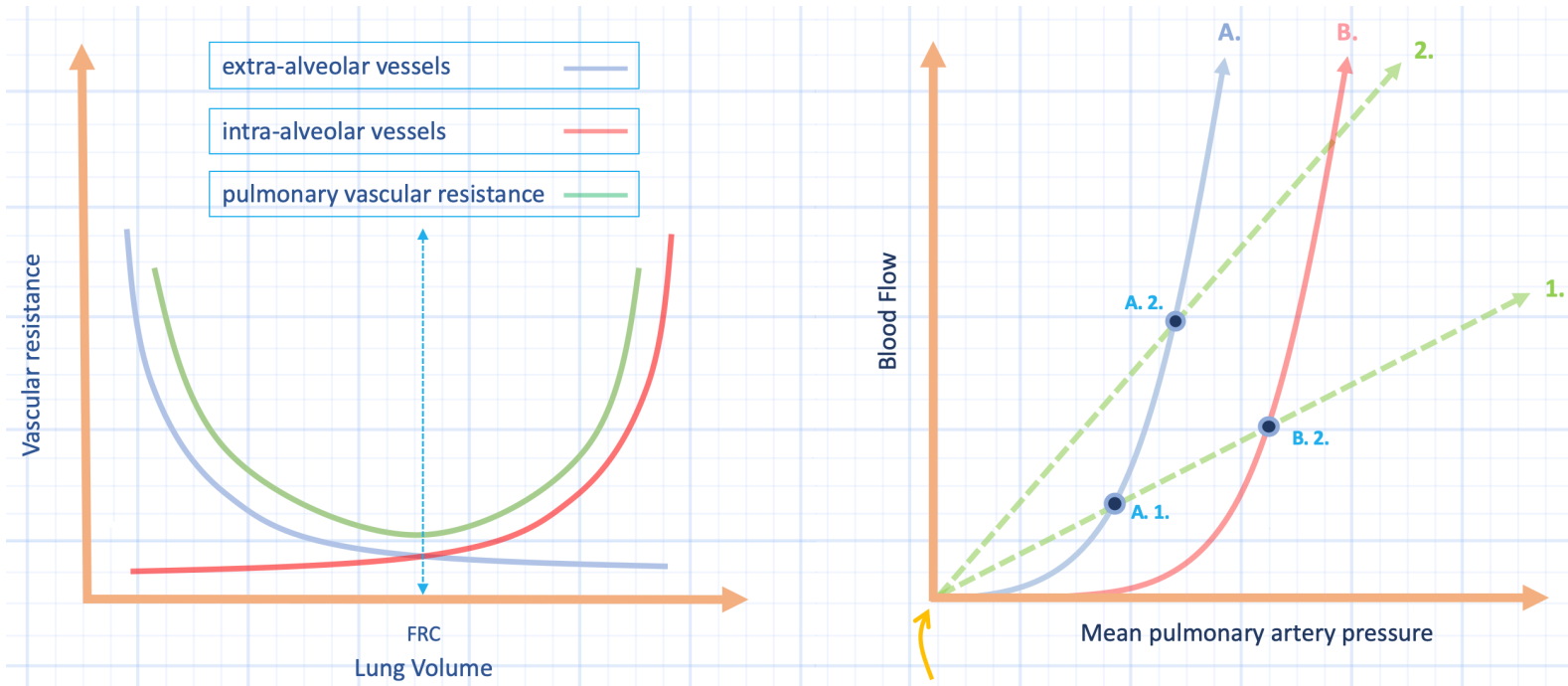

Figure 4: Lung volume and the calculated pulmonary vascular resistance. Left panel shows traditional explanation for relationship between lung volume [x-axis] and calculated pulmonary vascular resistance [y-axis]. FRC is functional residual capacity. The calculated resistance of the extra-alveolar [blue] and alveolar [red] vessels are shown with total calculated resistance in green. Right panel shows Starling resistor explanation. Point A1 is baseline. Point A2 is increasing lung volume below FRC - conductance rises, or calculated resistance falls [dotted line slopes 1 to 2]. Point A2 to B2 represents lung volume rise above FRC - calculated vascular resistance rises [slope of green dotted line 2 compared to line 1] but the true difference is increased critical closing pressure [see chapter 2] or curve A moving to B.

Once lung volume rises above functional residual capacity, the effect of recruiting the extra-alveolar vessels is exhausted and the intra-alveolar vessels play a greater role in the calculated pulmonary vascular resistance [25]. The intra-alveolar vessels are exposed primarily to the alveolar pressure. With increased lung volume, the alveolar pressure rises above the pressure surrounding the right ventricle [i.e. the pleural and pericardial pressure]. Accordingly, the alveolar pressure becomes the effective pressure against which the right ventricular ejects [23]. Consequently, calculated pulmonary vascular resistance rises beyond functional residual capacity not because of vessel 'collapse' – as is often taught – but because the closing pressure of the pulmonary vascular tree rises [38]. Nevertheless, the consequence is that total pulmonary vascular resistance has a biphasic curve with respect to lung volume.

Recall that the cardiac function curve on the Guyton diagram is a summation of all of the determinants of cardiac output between the right atrium and the aorta. Therefore, an increase in pulmonary arterial impedance [i.e. right ventricular afterload] bends the cardiac function curve down and to the right. In health, under conditions of normal tidal volume, this effect is trivial [2, 39].

Left Ventricular Loading

Because of the position of the left ventricle [LV] relative to the left lung, it may be affected more by lung inflation than the right ventricle [40, 41]. Indeed, expansion of the lung compresses the lateral wall of the left ventricle and shrinks the ventricular cavity in the septo-lateral dimension [42]. This effect will increase the left ventricular cavity pressure and diminish LV volume, that is, decrease LV compliance [2, 43]. However, this is probably only an apparent decrement in compliance. When the ventricle is compressed by the lungs and the left ventricular transmural pressure measured, there is no change in the cardiac function curve slope [stroke volume versus transmural filling pressure] [26]. Nevertheless, because these studies employed PEEP to increase lung volume, it is possible that stroke volume may remain unchanged if both LV diastolic compliance is decreased [i.e. lower LV end-diastolic volume] and LV ejection improved [i.e. lower LV end-systolic volume] [44]. Regardless, the apposition of the lung and the pericardium during inspiration is one potential reason why the juxta-cardiac pleural pressure typically increases more than the lateral pleural pressure when the lung is allowed to expand [45].

A change in lung volume, per se, does not alter the left ventricular afterload. There is, however, some evidence to suggest that LV afterload is increased by pressurization of the abdominal compartment [46]. This effect is less important than the effect of augmented abdominal pressure on venous return. The reasoning is likely that the transmission of abdominal pressure occurs more readily into the thin-walled veins. Further, the great veins have a lower intra-luminal pressure than arteries and are therefore more collapsible.

Decreased Intra-thoracic Pressure

Changes in intra-thoracic pressure without a change in lung volume can also affect the cardiovascular system. Diminished intra-thoracic pressure without a change in lung volume is undertaken clinically by having a patient activate the muscles of inspiration against a closed glottis, that is, perform a Mueller maneuver [figure 2]. On the Campbell diagram, this exercise is depicted by a change in the pleural pressure [i.e. a left shift along the y-axis] without a change in lung volume on the ordinate.

Because the x-intercept of the cardiac function curve on the Guyton diagram corresponds to the intra-thoracic pressure, changes in the intra-thoracic pressure can be illustrated by corresponding parallel shifts in the cardiac function curve on the Guyton diagram.

Right Ventricular Loading

Because the right atrium is a thin-walled, pliable structure, its intra-luminal pressure tends to track the intra-thoracic pressure [47]. In health, a normal right atrial pressure is nearly atmospheric, so the drop in intra-thoracic pressure during normal inspiration generates sub-atmospheric atrial pressure [48-50]. Yet despite decreased intra-luminal pressure, venous return rises, right heart volume increases and pulmonary artery outflow also increases [51-55]. This seeming paradox is reconciled by the fact that while the intra-luminal pressure is lowered by decreased intra-thoracic pressure, the trans-mural pressure [i.e. the intra-luminal pressure less the intra-thoracic pressure] rises [48, 56-58]. Increased transmural pressure is illustrated by a shift in the cardiac function curve leftwards relative to the venous return curve [59, 60]. The transmural pressure is equal to the pressure at the x-intercept of the cardiac function curve less the right atrial pressure [61]. Note that the more intra-thoracic pressure falls, the greater is the leftwards shift of the cardiac function curve relative to the venous return curve [figure 5].

The decline in right atrial pressure that occurs consequent to falling intra-thoracic pressure is the greatest hemodynamic stress placed upon the cardiovascular system in health. The reason is the small gradient between the mean circulatory pressure and the right atrial pressure [see chapter 2 for the difference between mean systemic and circulatory pressure]. A typical gradient is roughly 5 mmHg and this is the driving pressure for the entirety of venous return [48, 62]. If the right atrial pressure were to fall by 3 mmHg, there is an increase in venous return by 60% [i.e. if the right atrial pressure were 0 mmHg, a drop in 3 mmHg increases the pressure gradient from 5 mmHg to 8 mmHg]. The reason that the right heart tolerates great swings in venous return is that it is able to eject the blood into a highly compliant pulmonary vascular tree that has a great capacity to recruit and dilate blood vessels; in other words, pulmonary impedance falls as cardiac output rises [see chapter 2] [52, 63, 64].

As described in chapter 2, the afterload experienced by a ventricle is approximated by the modified LaPlace law [65]. This is an expression of the wall tension experienced by the ventricle during ejection. The radius of curvature is directly related to the wall tension as is the transmural wall pressure. The transmural wall pressure experienced by the right [or left] ventricle during ejection is a dynamic parameter – itself dependent upon the right ventricular outflow tract ejection pressure and pulmonary arterial impedance [66]. Decreased intra-thoracic pressure without increased lung volume favours expansion of the right ventricular radius of curvature and, therefore, the wall tension. Yet, because impedance of the normal pulmonary arterial bed is so low and accommodating [64] and also because the

right ventricle behaves as an unstressed chamber in healthy patients [67, 68], the right ventricular wall experiences minimal tension in normal individuals. Note that because the right ventricle and pulmonary artery share the intra-thoracic cavity, diminished intra-thoracic pressure without changing lung volume does not alter the transmural pressure between these two structures [this is also explored in chapters 9 and 10 with a discussion on fighter pilot physiology]. Nevertheless, and somewhat curiously, decreased intra-thoracic pressure without lung volume change may still afterload the right ventricle [69] via parallel ventricular interaction. Ventricular interdependence, as described next, is typically thought to be a diastolic event. However, it also occurs during systole [70]. In fact, as much as 60% of the systolic pressure generated by the right ventricle is actually due to the contracting left ventricular muscle mass [71, 72]. Because falling intra-thoracic pressure afterloads the left ventricle, right ventricular ejection may also experience heightened afterload. Additionally, to the extent that right ventricular volume rises and impairs left ventricular compliance via diastolic ventricular interdependence, left ventricular filling pressure also rises; thus, right ventricular preload becomes its own afterload [73]!

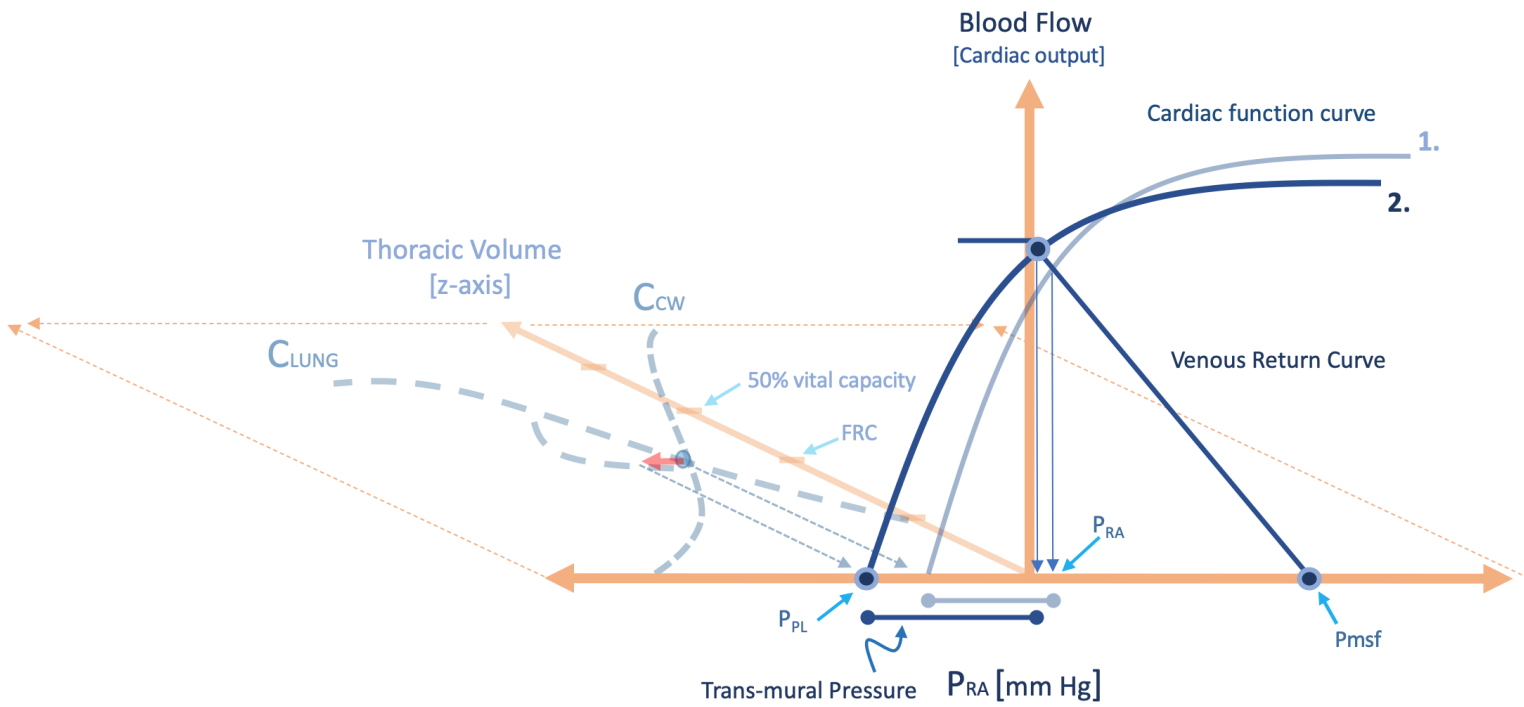

Figure 5: Illustration of decreased intra-thoracic pressure without lung volume change. The fall in intra-thoracic pressure or pleural pressure [Ppl] is seen as the red arrow on the Campbell diagram [x,z plane]; there is no change in lung volume [z-axis]. The cardiac function curve 1 shifts leftwards to curve 2. Right atrial pressure [Pra] falls, but cardiac output [y-axis] and right atrial trans-mural pressure [blue dumbbell] rise. The cardiac function curve flattens slightly with no significant change in the circuit function curve or mean systemic filling pressure [Pmsf]. Clung is lung compliance; Ccw is chest wall compliance; FRC is functional residual capacity.

Given the above, left shift of the right ventricular cardiac function curve in response to falling intra-thoracic pressure may be associated with minor flattening of its slope – from augmented afterload [figure 5]. Further, as the x-intercept of the cardiac function curve left-shifts with respect to the systemic venous return curve, there is a tendency for central venous pressure to fall and right heart output to rise. As well, the transmural pressure of the right heart increases which favours right heart enlargement.

Ventricular Interdependence

As augmented inflow of blood to the right heart affects the left ventricle in series by increasing preload to the left heart, it also affects the left ventricle in parallel as the two chambers share a septum, myofibres and the pericardium. Even in healthy hearts, increased volume of one ventricle tends to diminish the compliance and volume of the opposite ventricle [55, 74-78]. Hence when the right ventricle is engorged with blood, the left ventricle suffers from acute diastolic incompetence. Accordingly, decreased intra-thoracic pressure augments right heart venous return which leads to an acute and transient flattening of the left ventricular cardiac function curve. Notably, this supports elevation of left atrial filling pressure and decreased cardiac output. In other words, there is diminished left ventricular compliance because filling pressure rises with attenuated cardiac output. This effect tends to be minor in health, but is likely the primary mechanism of the normal inspiratory decrease in left ventricular stroke volume [51].

The degree to which right ventricular volume and filling pressure modify left ventricular filling properties is largely dependent upon the compliances of the respective ventricular free walls [and this includes the pericardium] as well as the compliance of the septum. Poorly compliant [i.e. stiff] ventricular free walls augment ventricular interdependence while a poorly compliant septum diminishes this effect [78-81].

Left Ventricular Loading

In a handful of previous investigations, decreased intra-thoracic pressure without lung volume change inconsistently altered left ventricular volume, but consistently impaired its output [7, 82-85]. The reason for the conflicting results, in terms of left ventricular volume, may have to do with when the fall in intra-thoracic pressure occurs within the cardiac cycle. As elegantly detailed by Robotham's group in the late 1980s, decreased intra-thoracic pressure timed to ventricular diastole impaired left ventricular output by reducing its preload; presumably via shift of the septum and ventricular interdependence [86, 87]. By contrast, a fall in intra-thoracic pressure timed to systole reduced LV output, but increased left ventricular volume; presumably via increased LV afterload [87-89]. Because there are multiple cardiac cycles during a fall in intra-thoracic pressure, these mechanisms co-conspire to diminish left ventricular output. It is interesting to note that in Robotham's work, decreased intra-thoracic pressure timed to diastole reduced LV stroke volume by about 31%, whereas when timed to systole, LV stroke volume fell by only 13% [87]. What may account for these quantitative differences? Robotham's group also observed that when timed to diastole, falling intra-thoracic pressure also prevented egress of blood from the thoracic aorta – such that during the following systole, the

greater blood volume in the thoracic aorta increased afterload [87, 89-91]. Thus, decreased intra-thoracic pressure timed to diastole may have multiplicative effects on the left ventricle. Additionally, as noted by Scharf [54], the relative effects of diastolic events and systolic events may play different roles at different times during a drop in intra-thoracic pressure; that is, falling intra-thoracic pressure imparts a biphasic response upon the left ventricle. As above, the initial parallel interaction between the right and left ventricles briefly decreases left ventricular compliance, cardiac output and raises left atrial filling pressure via ventricular interdependence. This is corroborated by a decrease in the LV septo-lateral dimension – similar to the effect of the lung pressing against the left ventricle as lung volume increases [3]. Then, after one-to-two cardiac cycles, the augmented right ventricular output reaches the left heart and preload returns to baseline. The increase in pulmonary venous return from the right ventricle is illustrated by a transient right shift of the pulmonary venous return curve. These mechanisms play pivotal roles in stroke volume and pulse pressure variation, as discussed in subsequent chapters.

As low intra-thoracic pressure increases the left ventricular transmural pressure, left ventricular afterload is intensified. During a typical ejection, the LV radius of curvature decreases more than the rise in systolic transmural pressure. Therefore, during a normal inspiratory decrease in intra-thoracic pressure and in a patient with a normal left ventricle, the effect of intra-thoracic pressure on afterload is slight [92]. As considered in chapter 4, increased transmural pressure features more prominently in LV afterload when the intra-thoracic pressure is very low or when the LV radius of curvature does not shrink as readily during ejection [e.g. a dilated cardiomyopathy].

There is an important distinction between the graphical analysis of the right and left heart that should be mentioned here. Decreased intra-thoracic pressure left shifts the right heart function curve relative to the systemic venous return curve because the abdominal venous capacitance beds are exposed to abdominal pressure [i.e. roughly atmospheric] while the right heart is exposed to intra-thoracic pressure. By contrast, both the left heart and the pulmonary veins are exposed to intra-thoracic pressure. Therefore, reduced intra-thoracic pressure without increased lung volume shifts both the left heart function curve and the pulmonary venous return curve simultaneously. For simplicity, this left shift is not illustrated in the supplemental material.

The Mueller Maneuver

Much of the physiology germane to the Mueller maneuver was described in the previous section on left ventricular loading in response to decreased intra-thoracic pressure. This section discusses the Mueller maneuver in more detail; importantly, it is not simply the physiological converse of Valsalva. The Mueller maneuver is a sustained, pronounced drop in intra-thoracic pressure against a closed glottis such that lung volume does not change. It is logical that the Mueller maneuver would invariably increase right heart volume, though this is not consistently observed. [7,

54, 55, 77, 93, 94]. Because of the abrupt, large decrease in intra-thoracic pressure, great vessel collapse may limit venous return to the right heart; consequently, right heart volume and pulmonary arterial flow may actually shrink [63, 95, 96]. Great vein collapse physiology is also favoured when abdominal pressure exceeds IVC pressure [9, 11, 95, 97] or when the diaphragm is used preferentially to the accessory muscles of respiration [98]. Therefore, if there is preload limitation during the Mueller maneuver, the immediate effect upon the left ventricle is minimization of ventricular interdependence. As a result, afterload effects predominant as the cause of diminished left ventricular stroke volume. Sustained Mueller maneuver, in the setting of great vessel collapse, gradually impairs left ventricular preload because the reduced right heart output eventually affects the left. Additionally, diminished preload is accentuated by the increased left ventricular afterload [3, 54]. Note that if increased afterload reduces LV stroke volume, both left ventricular end-diastolic and end-systolic volumes rise [85]. Conversely, if right ventricular volume were to increase during a Mueller maneuver, ventricular interdependence would be minimized if pericardial constraint is attenuated [e.g. post-surgical pericardiotomy] or if septal hypertrophy is present [80, 83, 85, 99-101].

On the other hand, a slow, consistent drop in intra-thoracic pressure combined with hypervolemia enhances venous return and, therefore, right heart volume. This is because high baseline right atrial pressure permits greater change in venous return driving pressure with inspiration [9, 10, 13, 95]; this physiology shrinks left heart volume during a Mueller maneuver via ventricular interdependence. Given these conflicting and co-varying aspects of venous return, it is not surprising that when performing the Mueller maneuver, some patients increase in left ventricular end-diastolic volume [i.e. afterload effect] while others sustain a decrease [i.e. preload effect via ventricular interdependence]. It has been postulated that the former is more likely to occur during pronounced drops in intra-thoracic pressure [i.e. when great vessel collapse limits RV distention] while the latter is the predominant mechanism during normal decrement in pleural pressure [i.e. when right heart volume expands to a greater extent] [102]. It is therefore imperative, when interpreting studies of cardiopulmonary interaction, that the reader be aware of the subjects' baseline characteristics and methods of the study. Interestingly, changing intra-thoracic pressure has also been observed to directly alter thoracic aortic compliance [90, 91, 103]. One may therefore speculate that reduced intra-thoracic pressure increases LV afterload not just by increasing the left ventricular and thoracic aortic transmural wall stress during ejection, but also by acting upon the biophysical properties of the aorta itself.

With release of Mueller, the abrupt increase in intra-thoracic pressure facilitates cardiac output by both systolic and diastolic effects. If the intra-thoracic pressure rise occurs, by chance, with diastole then left ventricular preload is augmented. Conversely, if the abrupt increase in intra-thoracic pressure occurs, by chance, with systole then left ventricular afterload is reduced [86, 87, 89]. In both circumstances, left ventricular output is facilitated upon release of Mueller maneuver.

Having considered the separate effects of both increased lung volume and decreased intra-thoracic pressure on the cardiovascular system, we now turn to the combination of these two phenomena, that is, spontaneous ventilation [figure 2].

For simplicity, the following sections focus on the effects of a single inspiration. Because respiration is phasic, the perturbations that occur during inspiration are reversed during expiration; this mitigates the hemodynamic consequences of ventilation.

Right Ventricular Loading

With decreased intra-thoracic pressure and increased lung volume, the right ventricle experiences augmented venous return [52, 55, 104, 105]. This occurs not only because of decreased right atrial pressure relative to atmosphere, but also from increased mean systemic pressure as the abdominal venous capacitance beds are compressed by diaphragm descent [9, 10, 12, 15, 17]. Hence, on the Guyton diagram, the cardiac function curve shifts leftwards and the venous return shifts rightwards which tend to increase all of: right heart transmural pressure, right heart volume and cardiac output. However, as elaborated above, the venous return curve may, in response to diaphragm descent, increase or decrease its function depending upon the patient's pre-existing volume status. In hypervolemic patients [i.e. in abdominal zone III], rising abdominal pressure enhances circuit function which promotes venous return to the right ventricle [10, 13]. At the end of inspiration, the transmural right atrial pressure is increased and so too is cardiac output [figure 6].

This preload-mediated rise in right ventricular output is slightly tempered by heightened right ventricular afterload when lung volume exceeds functional residual capacity [22-25, 38, 106, 107]. As the right ventricular volume rises so too does its afterload by intensified transmural wall stress [73]. Further, the fall in intra-thoracic pressure itself seems to impede RV output [7, 69]. These afterload effects flatten the right ventricular cardiac function curve which elevates right atrial pressure and decreases cardiac output. Notably, both preload and afterload effects on the right ventricle during spontaneous ventilation augment right ventricular volume. This could diminish LV compliance via ventricular interdependence which, in turn, affects left ventricular loading on inspiration [75, 78, 104, 108].

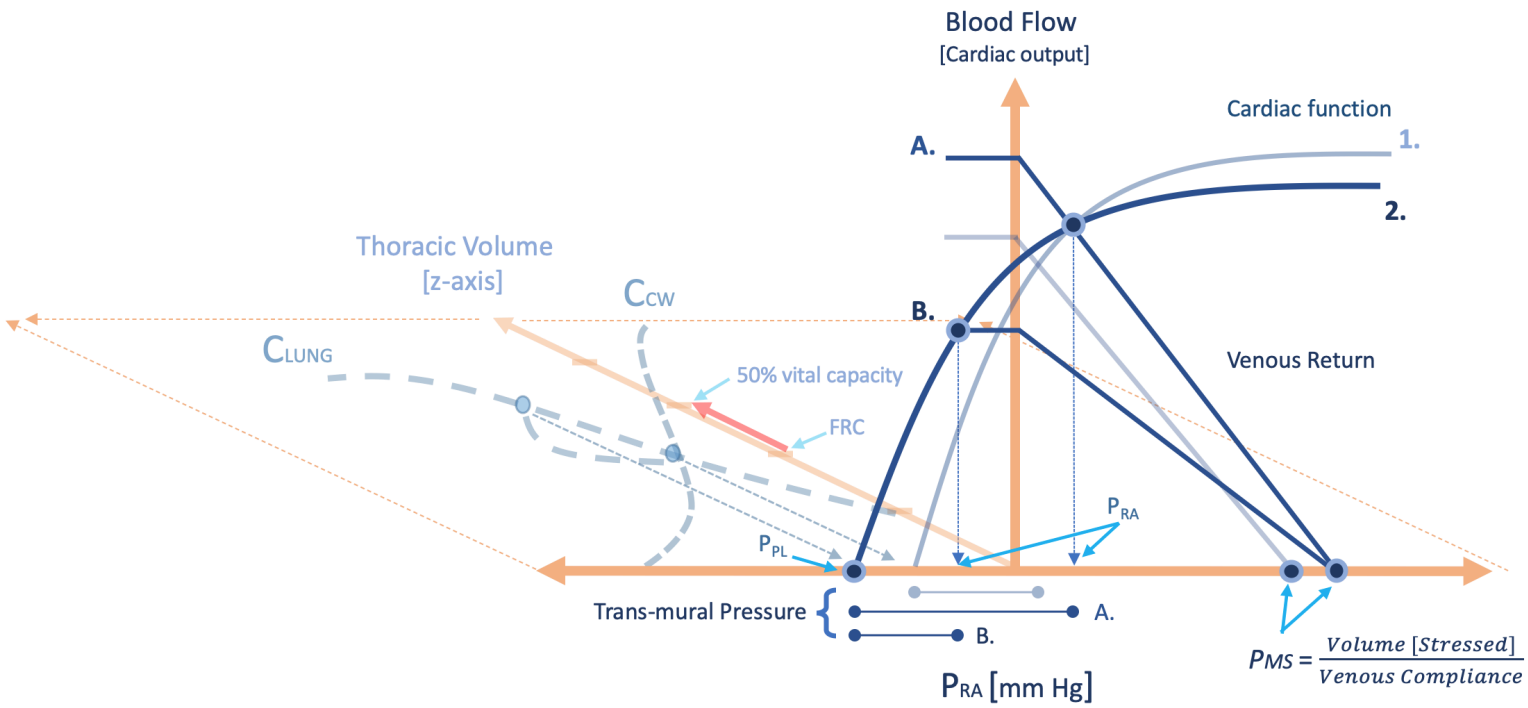

Figure 6: Illustration of spontaneous inspiration. The rise in lung volume is seen as the red arrow on the z-axis of the Campbell diagram. The cardiac function curve 1 shifts leftwards to curve 2. With compression of the abdominal compartment, mean systemic pressure [Pms] increases slightly, depending on volume status, the resistance to venous return may change. A. represents abdominal zone III conditions while B. represents abdominal zone I conditions. Note the difference in trans-mural pressure despite the same lung volume change. Pra is right atrial pressure; FRC is functional residual capacity. For these diagrams, assume normal vital capacity of 4.5 L and that FRC is about 1/3 of the vital capacity. Thus, an 11% change in vital capacity is nearly 500 mL. FRC to 50% vital capacity is a 700-800 mL breath.

Left Ventricular Loading

With a concomitant drop in intra-thoracic pressure and rise in lung volume, the left ventricle has multiple, simultaneous forces acting upon it. Each of these variables, in turn, are modulated by physiological elements such as intra-vascular volume state, pressure change and compliance. As a spontaneous breath proceeds, the left ventricle has three general phenomena mediating its preload during diastole: 1. ventricular interdependence, 2. compression of the left ventricular free wall by the expanding lung and 3. pulmonary venous return. All of these effects have already been discussed in this chapter, but in the healthy patient with a normal inspiratory effort, ventricular interdependence effects predominate and contribute to inspiratory diminution in left ventricular stroke volume [55, 104, 109]. This fall in LV stroke volume is compounded by compression of the left ventricular lateral wall by the expanding lung [108, 110]. Though, as above, it is unclear if mechanical interaction between the lung and heart imparts left ventricular diastolic dysfunction [92]. Experimentally, it has been observed that with normal, spontaneous tidal volumes, compression of the left ventricle does not have significant hemodynamic consequences [3, 111]. Thus, to the extent that right ventricular volume rises during spontaneous ventilation, septal shift temporarily impairs left ventricular diastolic function. Graphically, the LV cardiac function curve slightly flattens. Consequently, left atrial filling pressure rises and this is accompanied by a momentary decrease in cardiac output.

While left ventricular preload is mechanically impinged upon by both the intra-ventricular septum and, potentially, the expanding lung, its filling is also altered during spontaneous inspiration via changes in pulmonary venous return. Like the compression of the abdominal venous capacitance bed with increased lung volume [9], the pulmonary veins similarly diminish their capacitance above functional residual capacity [22, 107]. Depending on the zonal characteristics of the lung, this may or may not facilitate pulmonary venous return [24] by shifting the pulmonary venous return curve rightwards relative to the left ventricular cardiac function curve; the shift in the pulmonary venous return curve relative to the cardiac function curve preserves cardiac output.

In addition to left ventricular diastolic perturbations with spontaneous ventilation, falling intra-thoracic pressure raises afterload, which also impairs left ventricular cardiac function. As above, increased lung volume, per se, does not affect left ventricular afterload to the extent that intra-abdominal pressure is normal [46]. The effect of intra-thoracic pressure on left ventricular loading conditions depends upon which phase of the cardiac cycle the fall in pleural pressure is greatest. When the drop in intra-thoracic pressure corresponds mostly with diastole, then increased right heart volume and ventricular interdependence effects predominate [86]. Conversely, if decreased intra-thoracic pressure occurs principally with systole [89], then the afterload effect predominates. Clearly, the superposition of the cardiac cycle and change in pleural pressure varies depending on both respiratory and heart rates.

Increased Intra-thoracic Pressure

Having examined the role of diminished intra-thoracic pressure on cardiovascular function – first without a change in lung volume and then with a change in lung volume – this section turns to the impact of increased intra-thoracic pressure on the cardiac function curve. As discussed above, intra-thoracic pressure change without altering lung volume alters the position and shape of the cardiac function curve rather than the venous return curve. Variation of intra-thoracic pressure shifts the right ventricular cardiac function curve along the pressure axis of the Guyton diagram with respect to the systemic venous return curve. These curve shifts may also be associated with changes slope. By contrast, the left ventricular cardiac function curve shifts in unison with the pulmonary venous return curve when lung volume does not change as both the pulmonary venous capacitance beds and the left heart are affected equally by the change in pressure.

Right Ventricular Loading

Increased intra-thoracic pressure moves the right ventricular cardiac function curve rightwards with respect to the venous return curve [figure 7]. Consequently, the

right atrial pressure rises but pulmonary arterial flow and cardiac output fall [52, 63, 112-115]. Again, this seemingly paradoxical finding [i.e. an increase in right atrial pressure with a decrease in cardiac output] is clarified by inspection of the right atrial transmural pressure, which decreases in response to isolated intra-thoracic pressure augmentation. Indeed, for every 1 mmHg decrease in right atrial transmural pressure, there is an 8% decrease in pulmonary arterial flow [116]. Again, the decrease in right ventricular volume, and therefore right heart output, is most pronounced when the increased intra-thoracic pressure coincides with diastole [91].

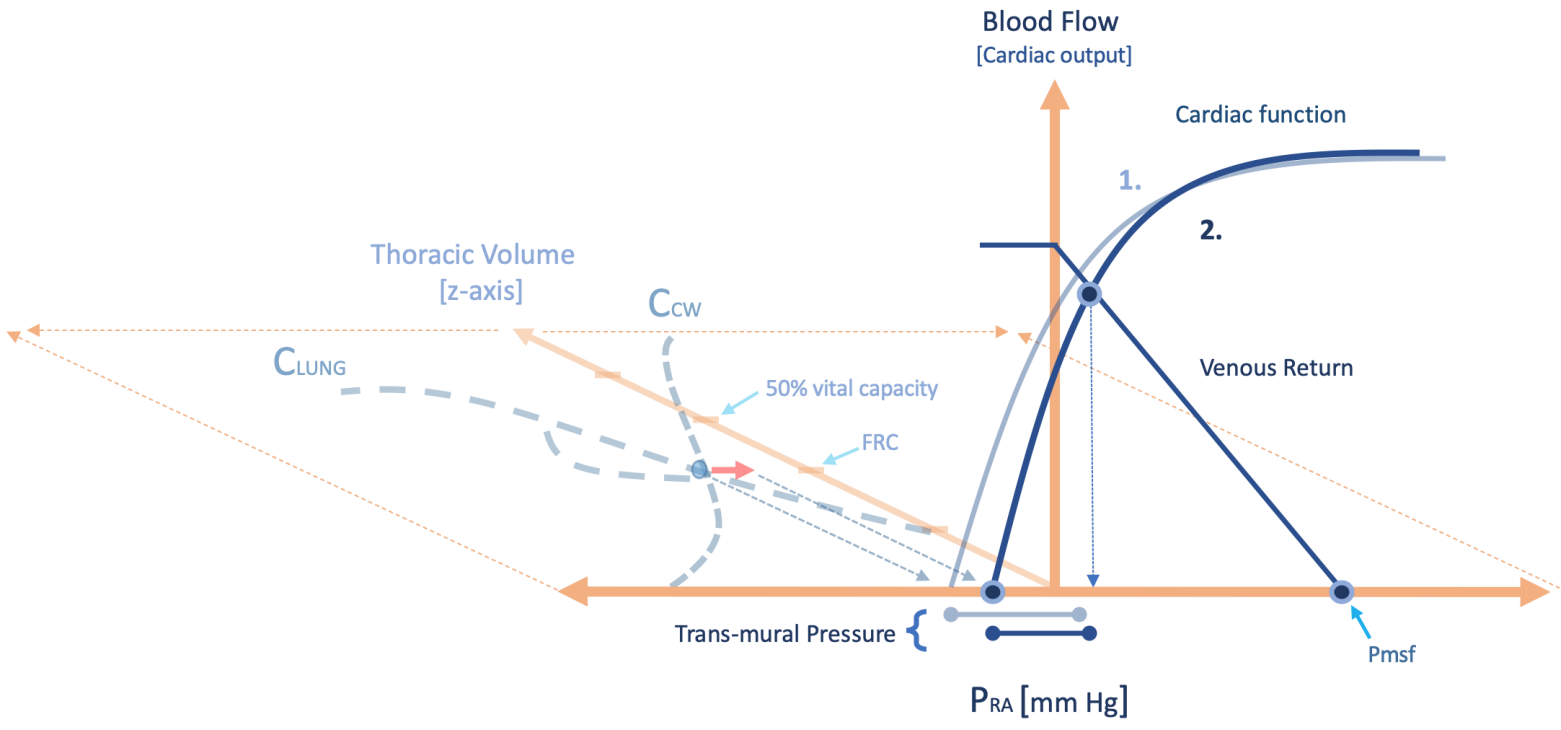

Figure 7: Illustration of isolated increase in intra-thoracic pressure. There is no change in lung volume on the z-axis of the Campbell diagram. The cardiac function curve 1 shifts rightwards to curve 2. Without change in abdominal capacitance, there is no significant change in Pmsf [mean systemic filling pressure]. While right atrial pressure [Pra] rises, trans-mural pressure and cardiac output [y-axis] fall. FRC is functional residual capacity; Clung in lung compliance, Ccw is chest wall compliance.

In the absence of changing lung volume, right ventricular afterload is minimally affected by elevating intra-thoracic pressure and this is because the right ventricle and pulmonary arterial tree are exposed to, essentially, the same increment in ambient pressure [92, 117, 118]. In fact, and perhaps counterintuitively, to the extent that the increase in thoracic pressure augments left ventricular ejection, systolic ventricular interdependence may slightly increase RV ejection during the initial phase of a Valsalva; admittedly, this is conjecture. Yet, in agreement with this physiology are data from stressed respiratory maneuvers. First, Valsalva shrinks right ventricular end-systolic volume which suggests – but does not prove – reduced impedance to RV ejection [55]; conversely, during the opposite of a Valsalva [i.e. Mueller maneuver] the right ventricular end-systolic volume rises, suggesting increased impedance to RV ejection [3, 7]. Even more convincing data lies in the response of the pulmonary artery transmural pressure to an isolated increase in intra-thoracic pressure. Increased right ventricular afterload is evidenced by higher pulmonary arterial transmural pressure [i.e. the pressure within the pulmonary artery relative to the intra-thoracic pressure] which is seen in patients with dynamic hyperinflation [119], those with electrocardiographic

evidence of right heart strain [120] and pulmonary emboli [118]. By contrast, transmural pulmonary arterial pressure falls in response to reduced afterload – as observed with pulmonary vasodilation [121]. Notably, many studies have documented reduced transmural pulmonary artery pressure as a consequence of Valsalva [52, 63, 114], which argues strongly against amplified RV afterload in the setting of increased intra-thoracic pressure without change in lung volume [this physiology is also discussed with respect to fighter pilots in chapter 9 and the right ventricular afterload in chapter 10]. Notably, Charlier's group erroneously concluded that Valsalva increased pulmonary arterial 'impedance' because calculated pulmonary vascular resistance increased with Valsalva; this illustrates a physiological inaccuracy of the calculated pulmonary vascular resistance [122, 123]. In the case of augmented intra-thoracic pressure without change in lunge volume, there is reduced systemic venous return to the right heart as described above. Accordingly, there is less RV output ejected into the pulmonary arterial tree. The reduced cardiac output is not in response to elevated RV afterload nor any true change in the characteristics of the pulmonary vascular bed, but instead a result of reduced RV preload. Nevertheless, calculated PVR rises because its denominator [i.e. cardiac output] falls. It is not physiologically consistent for increased pulmonary arterial impedance to be accompanied by reduced transmural pulmonary arterial pressure!

Left Ventricular Loading

The hemodynamic perturbation felt by the left ventricle following isolated increase in intra-thoracic pressure depends largely upon the duration of the change in pressure [e.g. a prolonged increase in pressure as in Valsalva]. Additionally, the effect is mediated by when the largest increase in intra-thoracic pressure occurs with respect to the cardiac cycle [i.e. diastole versus systole] and the patient's underlying volume status and cardiac function [91]. In the healthy patient, with normal cardiac function [i.e. not afterload sensitive], increased intra-thoracic pressure immediately boosts left ventricular stroke volume by increasing left ventricular end-diastolic volume [124]. Mechanistically, this is via reduced systemic venous return and RV volume, rightward shift of the intra-ventricular septum and improved left ventricular compliance [78, 125-127]. Importantly, in Natarajan's study, the left ventricular end-systolic volume immediately increased, intimating minimal afterload reduction in healthy subjects [124] such that neither diminished left ventricular wall tension during systole [91] nor thoracic aortic blood depletion during diastole [90, 91, 103] were prominent mechanisms. After a couple of cardiac cycles, however, the preload of the left ventricle lessens as reduced RV output reaches the left heart. The reduction in venous return by series effect is represented by a parallel, leftward shift of the pulmonary venous return curve relative to the left ventricular cardiac function curve.

Decreased left ventricular transmural pressure as a consequence of increased intra-thoracic pressure should facilitate left ventricular unloading. Therefore, augmented

intra-thoracic pressure timed to ventricular systole may demonstrate decreased left ventricular volume. Yet, as above, the effect of intra-thoracic pressure on afterload in the setting of normal cardiac contractility tends to be minimal because the radius of curvature during ejection is readily reduced [92, 128]. Importantly, all means of afterload reduction are limited by the extent to which the end-systolic volume is reduced relative to the end-diastolic volume. In other words, if the end-diastolic volume is reduced [i.e. preload effect] more than the end-systolic volume [i.e. afterload effect], then stroke volume will not rise, but fall.

Valsalva

The physiology of the Valsalva maneuver has been described in some detail above. The maneuver requires an abrupt increase in intra-thoracic pressure against a closed glottis; because the glottis is closed, there is no change in lung volume and therefore only the effects of intra-thoracic pressure modulate the hemodynamic response. The Valsalva maneuver is typically prolonged – for 10 seconds – which renders it somewhat different from ventilator breaths which are phasic. However, it is somewhat similar to positive end-expiratory pressure as PEEP imparts a steady-state increase in intra-thoracic pressure. Nevertheless, both PEEP and intermittent positive pressure ventilation also change lung volume, while Valsalva does not.

The Valsalva maneuver is typically analyzed in four phases [113]. The first phase is marked by the first few cardiac cycles following the onset of increased intra-thoracic pressure. Notably, during these initial beats arterial blood pressure rises while there is stable, or increased, stroke volume [113, 124, 129]. There are a number of explanations for phase one, but it is most likely driven by transmission of the intra-thoracic pressure to the lumen of the aorta and/or increased left ventricular stroke volume [130]. In healthy individuals, the initial augmentation of left ventricular stroke volume is more a function of increased left ventricular end-diastolic volume [i.e. improved LV preload due to decreased RV preload] rather than reduced end-systolic left ventricular volume [i.e. improved afterload], as elaborated in the previous section [124]. The second phase of Valsalva is marked by a progressive reduction in arterial pressure and stroke volume from the left ventricle which is in response to diminished right ventricular preload. This is referred to as a ventricular 'series' effect rather than a 'parallel' effect because the left ventricle ultimately receives output from the right. Phase three of Valsalva begins upon release of the maneuver, marked by a rapid decrease in intra-thoracic pressure. Like phase one, phase three is typified by only a few cardiac cycles, but unlike the first phase, the third phase is distinguished by further stroke volume reduction. As intra-thoracic pressure rapidly falls during phase three, the left ventricular preload is also reduced as a function of increased right heart venous return and heightened LV afterload. As an extension of Robotham's cycle-specific analysis of intra-thoracic pressure [86, 87, 89], should the rapid drop in intra-thoracic pressure of Valsalva's third phase randomly occur during diastole, one would expect LV preload reduction secondary

to ventricular interdependence. By contrast, if reduced intra-thoracic pressure occurred, by chance, upon ventricular systole, then increased afterload is the presumed culprit. Finally phase four, in a healthy patient, is distinguished by increased cardiac output as the increased venous return reaches the left heart and autonomic reflexes activated during the maneuver facilitate cardiac output [131].

Intermittent Positive Pressure Ventilation

Intermittent positive pressure ventilation can now be examined as the combination of both increased intra-thoracic pressure and lung volume, as described above [figure 2]. The following section explores this physiology in the absence of positive end-expiratory pressure [PEEP]; this condition is sometimes referred to as zero end-expiratory pressure, or ZEEP.

Airway Pressure Versus Pleural Pressure

Before discussing the role of intermittent positive pressure ventilation as a modulator cardiovascular function, a review of airway pressure and pleural pressure is in order. There can be considerable clinical confusion about the relationship between proximal tracheal pressure – the airway pressure measured by the ventilator – and the intra-thoracic pressure. It is the latter that is experienced by the heart and great vessels. This topic was also explored in chapter 1. During a fully passive breath, the proximal tracheal pressure is a function of both the dynamic [e.g. airway resistance] and static [e.g. lung and chest wall stiffness] properties of the lung and thorax. However, the pleural pressure – for simplicity also referred to as intra-thoracic pressure – follows the static compliance curve of the chest wall. In the patient fully-passive, or adapted, with the ventilator [i.e. not generating any respiratory efforts] the inspiratory rise in intra-thoracic pressure is directly related to tidal volume and indirectly related to chest wall compliance as the lung expands against the thoracic cage and abdominal contents [4, 132, 133] [figure 8].

Of utmost importance is that the aforementioned relationship breaks down when the patient generates spontaneous respiratory efforts – either inspiratory or expiratory. In other words, when the patient is not fully passive or adapted with the ventilator. When this occurs, it is impossible to predict the pleural pressure, though its direction and magnitude may be estimated by the deflection of the pulmonary artery diastolic pressure or pulmonary artery occlusion pressure if a pulmonary artery catheter is in situ [134, 135]. Further, esophageal manometry may be used to estimate pleural pressure [136, 137]. Regardless, it must be emphasized that not all patients receiving mechanical ventilation experience an inspiratory increase in intra-thoracic pressure throughout a breath. When a patient is awake and breathing [e.g. on pressure support], the intra-thoracic pressure may actually be decreasing during a portion, or the entirety, of a ventilator-delivered breath!

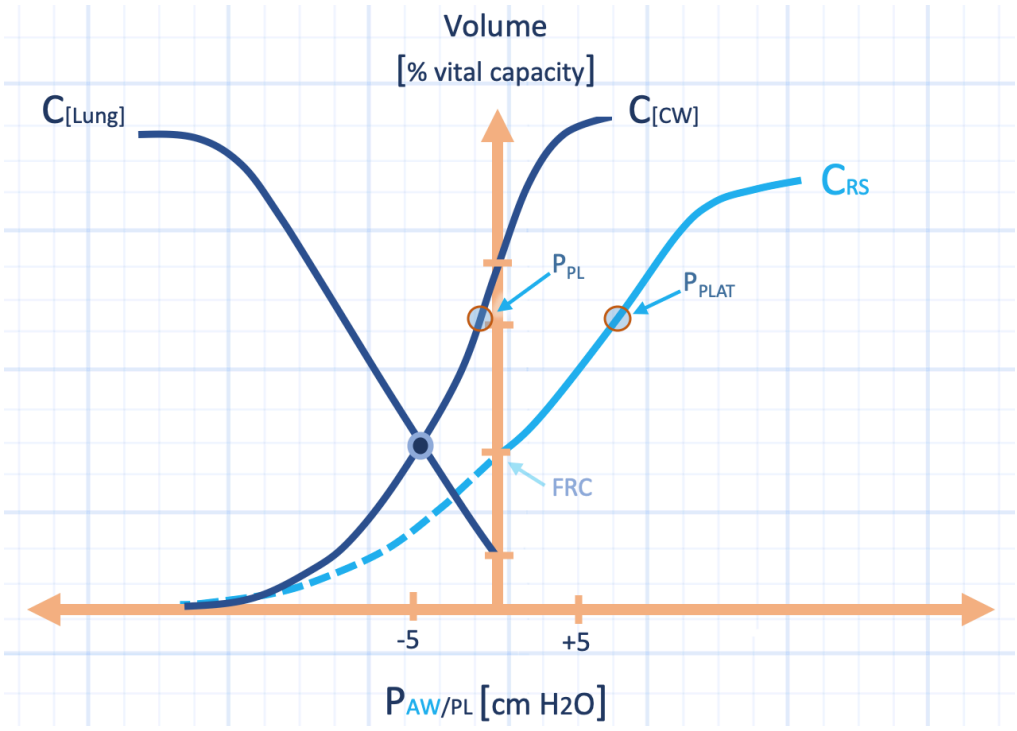

Figure 8: The Campbell diagram with respiratory system mechanics [see also chapter 1]. The y-axis is lung volume and x-axis is pressure - either airway [Paw] or pleural [Ppl]. The pleural pressure follows the chest wall compliance curve [Ccw] while the plateau pressure [Pplat] follows the static respiratory system compliance curve [Crs]. The dashed portion of the Crs may be omitted for clarity when combined with the Guyton diagram; i.e. when the y-axis of the Campbell diagram becomes the z-axis. The Clung and Ccw meet at functional residual capacity [FRC]. This figure becomes the z-axis in figure 9.

Right Ventricular Loading

With the delivery of a positive pressure breath, the transpulmonary pressure rises and this pressure gradient changes lung volume. As before, the right ventricular cardiac function curve shifts rightwards with the pleural pressure; this increases right atrial pressure, but decreases the transmural pressure, and therefore right heart volume or preload [52, 63]. Diminished venous return, however, may be blunted during a mechanical breath as the diaphragm descends, pressurizes the abdominal cavity and augments the pressure head for venous return, the mean circulatory filling pressure [Pmcf or Pmsf– see chapter 2] [9, 10, 17, 20, 138, 139] [figure 8]. Again, the overall effect of abdominal pressurization on the venous return curve is dependent upon the baseline volume status of the patient [figure 3]. With relative hypervolemia [or abdominal 'zone III' conditions], compression of the abdominal venous capacitance vessels augments IVC blood flow [9, 11].

The extent to which the lung expands beyond functional residual capacity is a key determinant of right ventricular afterload. In a healthy subject, the decrease in right ventricular volume with intermittent positive pressure ventilation minimally reduces right ventricular afterload mostly because the right ventricle operates as an unstressed structure. In other words, reduced RV volume insignificantly affects the transmural wall stress [67, 68, 140]. However, increased lung volume does raise pulmonary vascular impedance. Accordingly, lung volume above functional residual capacity nominally impedes right ventricular ejection when there is normal baseline physiology [52]. Therefore, the right ventricular function curve slightly

flattens and this minimally increases right atrial pressure and diminishes cardiac output.

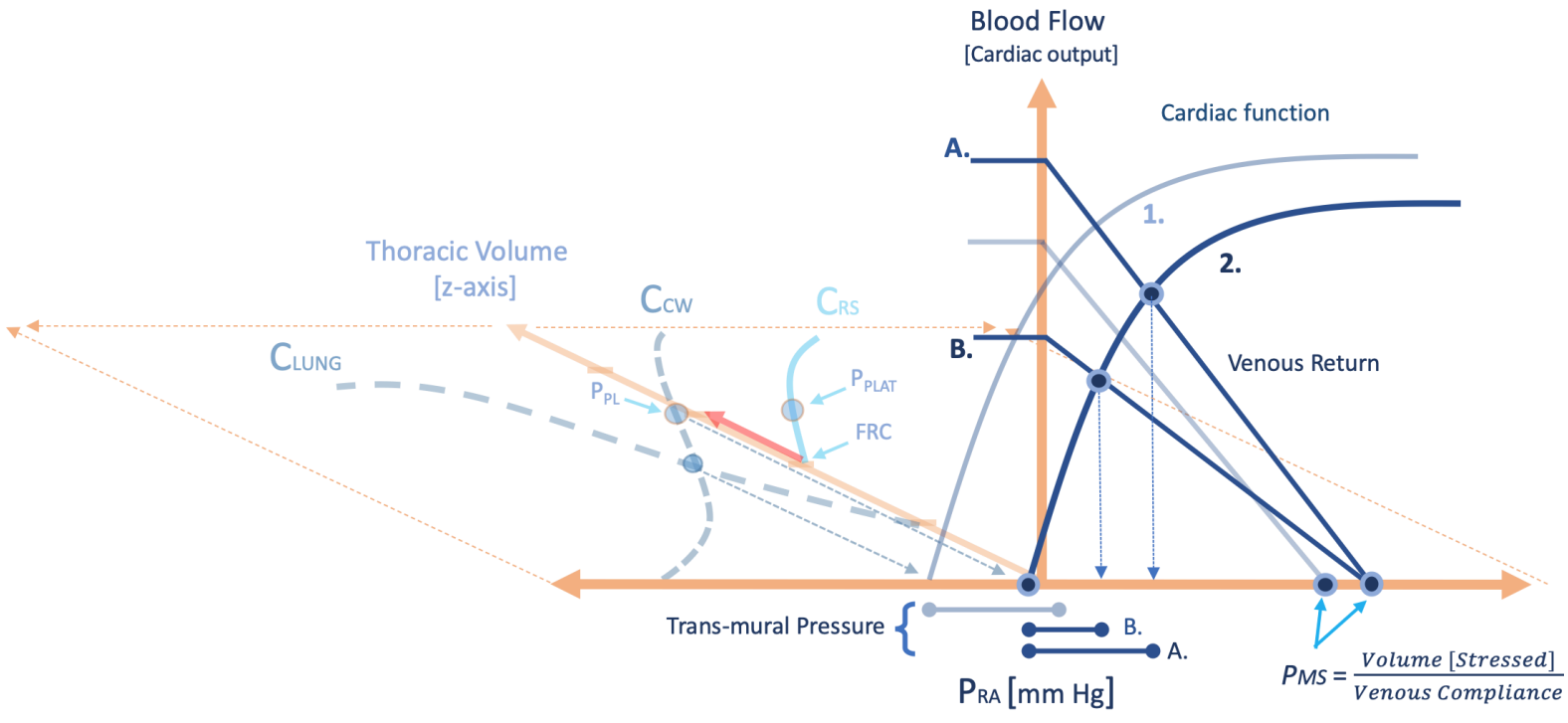

Figure 9: Illustration of a passive mechanical breath at zero end-expiratory pressure. The change in lung volume on the z-axis of the Campbell diagram is the same as figure 6 and 8; i.e. from functional residual capacity [FRC] to 50% vital capacity [red arrow, z-axis]. The cardiac function curve 1. shifts rightwards to curve 2. With change in abdominal capacitance, the Pms [mean systemic filling pressure] rises slightly; volume status determines circuit function curve A versus B. Right atrial pressure [Pra] rises but trans-mural pressure [blue dumbbells] and cardiac output [y-axis] fall. Ppl is pleural pressure; Pplat is plateau pressure; Crs is respiratory system compliance; Clung in lung compliance and Ccw is chest wall compliance.

Remarkable data has confirmed the conflicting influences upon the right atrium and ventricle during positive pressure ventilation following elective coronary bypass surgery [141, 142]. These data demonstrate that in response to mechanical insufflation of the lungs, some patients experience an increase in right heart trans-mural pressure, while in others, the right heart distending pressure falls. These data are not contradictory, but readily explained by the Guyton diagram [figure 9]. For instance, large inspiratory-associated augmentation of intra-thoracic, or pleural pressure [e.g. high tidal volume, low chest wall compliance] without heightening transpulmonary pressure [and therefore right ventricular afterload] diminishes right atrial distending pressure. A subtle, however important point is raised here; for a given tidal volume applied by a ventilator, the effect upon transpulmonary pressure [and therefore right ventricular afterload] is determined by the relative compliances of the lungs and thorax. When chest wall compliance is reduced relative to the pulmonary compliance, a greater fraction of the airway pressure is felt by the pleural space [133, 143, 144]. In such a clinical scenario [e.g. stiff chest wall relative to the lung], the transpulmonary pressure and right ventricular afterload is reduced for the applied ventilator volume. Lastly, attenuated right atrial distending pressure is favoured by diminished systemic venous return as would occur in a patient with abdominal vessels in zone II conditions. Thus, a clinical example where right atrial distending pressure might shrink with passive, mechanical

inspiration would be an obese patient with normal pulmonary compliance and with relative hypovolemia. Conversely, a thin patient with acute respiratory distress syndrome and hypervolemia might increase right atrial distending pressure with the same tidal volume delivered. This is discussed in more detail in chapter 4.

Left Ventricular Loading

Understanding left ventricular loading conditions during intermittent positive pressure ventilation with ZEEP is important when analyzing dynamic changes in left ventricular output. This is further elaborated in chapter 8. In a manner analogous to spontaneous ventilation – discussed above – left ventricular preload during intermittent positive pressure ventilation is variably affected depending upon both diastolic [e.g. ventricular interdependence, physical heart-lung interaction, pulmonary venous return] and systolic [i.e. afterload] factors.

When an abrupt increase in intra-thoracic pressure is timed with diastole, the right ventricle loses venous return and preload while the left ventricle sustains a small rise in end-diastolic volume [78, 91, 124, 126, 127]. As the lung expands, however, compression of the lateral left ventricular wall may retard pulmonary venous return but this seems to occur only at fairly large tidal volumes [3, 111]. Individual analysis of the left ventricular end-diastolic and end-systolic pressure volume relationships during mechanical ventilation suggests that increased lung volume momentarily imparts diastolic incompetence upon the left ventricle [44]. The mechanisms involved may be due to either lung compression of the LV free wall [42, 145], or via ventricular interdependence as RV ejection is retarded when lung volume rises [74, 146, 147]. Scharf's group used a unique approach for solving the aforementioned mechanistic conundrum [3, 111]. By measuring LV surface pressure during various respiratory maneuvers and while fibrillating the heart [to abolish preload and afterload effects], they found that LV geometry is only affected during intermittent positive pressure ventilation and at relatively high lung volumes; this agrees with previously discussed work with PEEP [26]. By contrast, spontaneous ventilation did not impart significant LV compressive effects [111]. It is not entirely clear why lung compression seems to be more dominant during passive, positive pressure ventilation as compared to spontaneous ventilation, but it may be secondary to differential effects of inspiratory muscle activation upon pressure around the cardiac fossa. This is suggested as lateral pleural pressure differs as a function of inspiratory muscle activation [148-150]. Thus, the particular clinical scenario may determine left ventricular inspiratory compression; dynamic hyperinflation of the lower lobes in COPD may affect the LV free wall [151] whereas poor lower lobe compliance and large right ventricular afterload in pulmonary ARDS may cause leftward septal shift secondary to right ventricular enlargement [147, 152, 153]. Nevertheless, these conflicting left ventricular preload effects tend to be minimal in the healthy heart and lungs.

The most important hemodynamic effect placed upon the left ventricle during intermittent positive pressure ventilation is that of pulmonary venous return. As

with spontaneous ventilation, increased lung volume can express blood into the pulmonary veins and facilitate pulmonary venous return, though this response is influenced heavily by the proportion of zone III pulmonary physiology [24]. As elaborated above, rising lung volume shifts the pulmonary venous return curve rightwards relative to the left ventricular cardiac function curve. The effect of lung volume on pulmonary venous return during intermittent positive pressure ventilation has been likened to a piston, as the pulmonary vascular capacitance decreases during expiration and then increases with inspiration [2, 154, 155]. Thus, blood is received by the pulmonary vascular bed during expiration from the filled right ventricle and then discharged to the LV during inspiration; this is the predominant mechanism of left ventricular stroke volume variation during mechanical ventilation. This is somewhat intuitive as the ventilator immediately raises transpulmonary pressure. Recall that the transpulmonary pressure and lung volume drive pulmonary venous inflow to the left atrium. By contrast, the rise in pleural and, therefore, juxta-cardiac pressure caused by the ventilator may be much less. As a result, preload and afterload effects driven by direct changes in juxta-cardiac pressure are of secondary importance.

One might expect that the attenuated left ventricular transmural pressure caused by positive pressure inspiration would reduce afterload and improve ventricular ejection. This effect is particularly pronounced when the upswing in pleural pressure is timed with ventricular systole [91]. Nevertheless, because the left ventricular radius readily shrinks during ejection in healthy hearts, diminished transmural wall pressure by positive pressure ventilation does not significantly decrease afterload, per the LaPlace approximation. Indeed, with positive pressure ventilation, the left ventricular end-diastolic volume may fall more than the end-systolic volume – diminishing stroke volume [4, 92].

Positive End-Expiratory Pressure

The application of positive end-expiratory pressure to the upper airway creates a steady-state augmentation of both lung volume and intra-thoracic pressure. This is in distinction to the phasic effects of intermittent positive pressure ventilation discussed in the previous section. Somewhat similar to the physiology in the passive patient detailed above, the extent to which the thoracic volume increases in response to PEEP is dependent upon the compliance of the lungs and the chest wall together, but the degree to which pleural pressure increases depends upon the compliance of the chest wall [143, 156, 157] [figure 10].

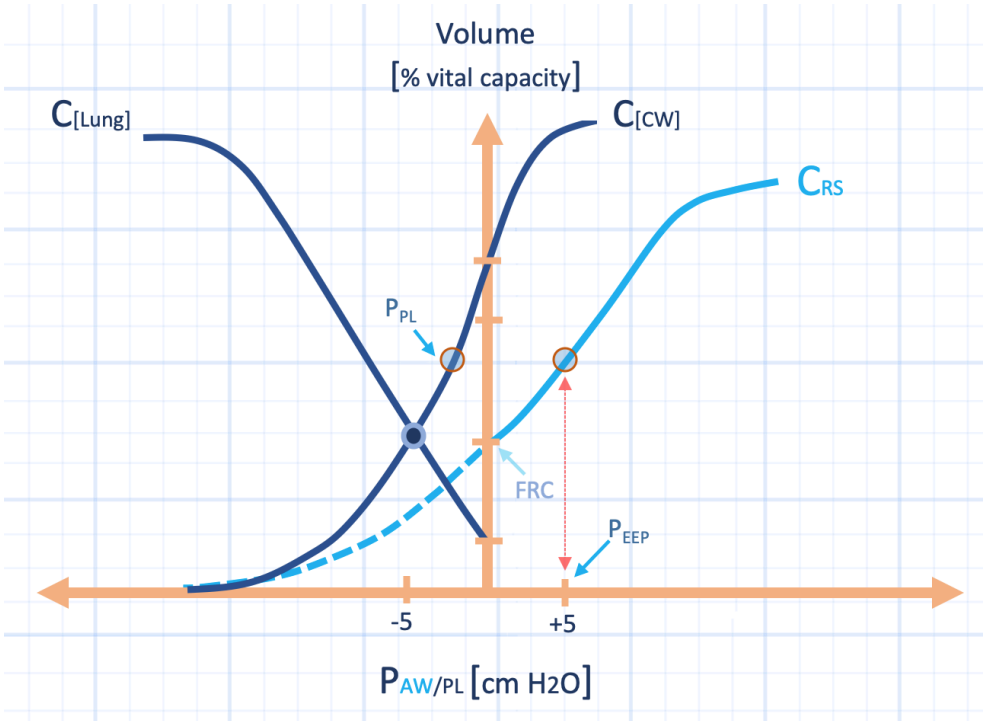

Figure 10: The Campbell diagram plus respiratory system mechanics [see also figure 8] with the application of 5 cm H2O of positive end-expiratory pressure [PEEP]. The y-axis is lung volume and x-axis is pressure - either airway [Paw] or pleural [Ppl]. The pleural pressure follows the chest wall compliance curve [Ccw]. With PEEP application, the airway pressure [Paw] rises to 5 and the pleural pressure [Ppl] rises from -5 cm H2O at functional residual capacity [FRC] to roughly -1 cm H2O. The light blue, dashed line of the respiratory system compliance curve [Crs] may be omitted for clarity when combined with the Guyton diagram.The Clung and Ccw meet at functional residual capacity [FRC]. This figure becomes the z-axis in figure 12.

Venous Return

Applying positive end-expiratory pressure was long thought to decrease venous return simply by raising the right atrial pressure. By increasing the back pressure to blood flow, it was reasoned that the gradient for venous return is reduced. However, many investigators have found that applying end-expiratory pressure does not diminish the gradient for venous return [12-15]. As end-expiratory pressure raises thoracic volume and pressurizes the abdomen, the mean systemic pressure also increases which offsets right atrial pressure elevation. Further, positive end-expiratory pressure leads to an acute release of catecholamines and a chronic release of anti-diuretic hormone [16, 158-161]. The ultimate result of each of these physiological responses is elevated mean systemic pressure and maintenance of the venous return pressure gradient [5, 162].

Nevertheless, end-expiratory pressure can reduce venous return. First, positive end-expiratory pressure may raise the resistance to venous return. The mechanism for this is not entirely known, but may be compression of the hepatic venous bed as well as the inferior vena cava [14, 18, 20, 21]. The effect of increased resistance to venous return is illustrated by a diminished slope of the venous return curve. Second, because the abdomen is pressurized, the IVC is more collapsible and maximal venous return is reduced. Maximal venous return is represented by the plateau of the venous return curve and it forms at the critical collapsing pressure or Pcrit. When right atrial pressure is reduced, for example by hypovolemia or by the

generation of low intra-thoracic pressure [9-11, 17, 98], then maximal venous return diminishes cardiac output [163]. The effect of PEEP is visualized on the Guyton diagram by reduced maximal venous return [figure 11] and elevated critical collapse pressure [Pcrit]. Presumably, if right atrial pressure is maintained above the pressure at which IVC collapse occurs, i.e. Pcrit, then PEEP will not reduce venous return [163].

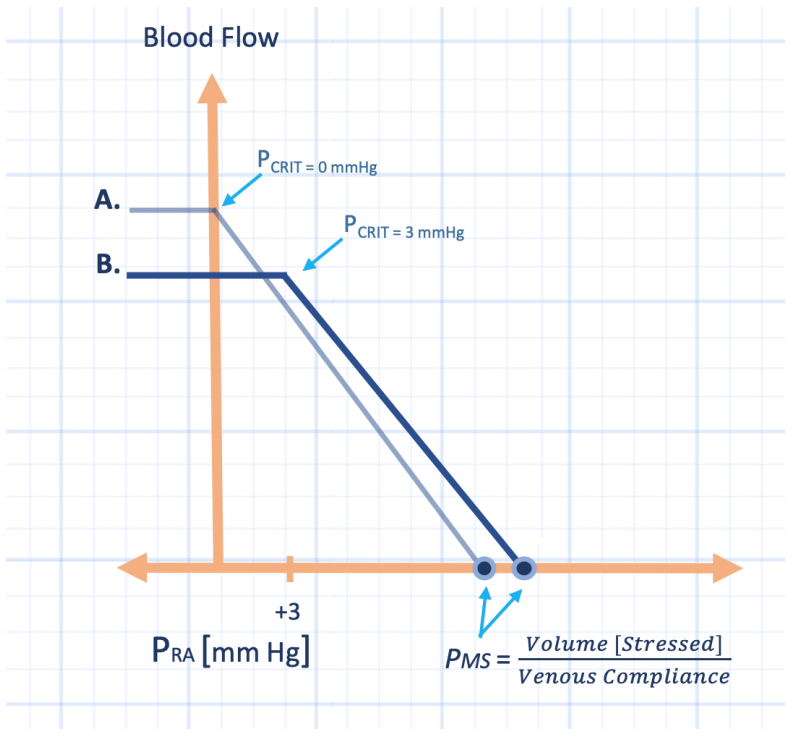

Figure 11: The effect of positive end-expiratory pressure [PEEP] on venous return. The application of 5 cm H_2O of PEEP increases the mean systemic filling pressure [Pms] and the critical collapse pressure [Pcrit - from curve A to curve B]. The Pcrit will rise by roughly the same degree as the pleural pressure under normal conditions. Pra is right atrial pressure; blood flow or venous return is the y-axis.

Right Ventricular Loading

In a manner similar to intermittent positive pressure ventilation, the application of end-expiratory pressure increases pleural pressure, provided that the patient is making minimal respiratory efforts. However, PEEP is a steady-state change in the intra-thoracic pressure. If the patient is receiving biphasic positive airway pressure [BiPAP] or mechanical ventilation, then intermittent breaths are delivered above that of the end-expiratory pressure. PEEP, therefore, creates a greater, baseline intra-thoracic pressure.

The right ventricular cardiac function curve is shifted rightwards in response to PEEP which increases right atrial pressure and favours a fall in right atrial transmural pressure [52, 63] [figure 12]. However, as previously mentioned in relatively healthy human hearts, the right ventricle behaves as an unstressed structure [67, 68]. As applied to the Guyton diagram, this means that within the constraints of normal physiology, the right ventricular cardiac function curve approximates a vertical line; that is, as the cardiac function curve shifts relative to the venous return curve, pulmonary artery flow [on the y-axis] changes with minimal effective change in the distending pressure. This physiology is consistent with the preload reserve

found in healthy subjects [164, 165]. Further, as elaborated in the previous section, PEEP also modifies the venous return function. Because the venous return curve is shifted rightwards as well, the increase in mean systemic pressure maintains the gradient for blood flow to the right heart. Consequently, neither the right atrial transmural pressure nor the cardiac output are dramatically reduced – provided that there is not a large, contemporaneous increase in the resistance to venous return [9-14, 20, 21, 163]. In a hypovolemic patient, or in patients who receive adrenergic blockade or sedation, the rightward shift in the venous return curve is mitigated and cardiac output may drop precipitously [16, 160]. Again, only at very high PEEP levels – which greatly increase lung volume – could the lung impinge upon the right ventricle and induce diastolic dysfunction [26, 40].

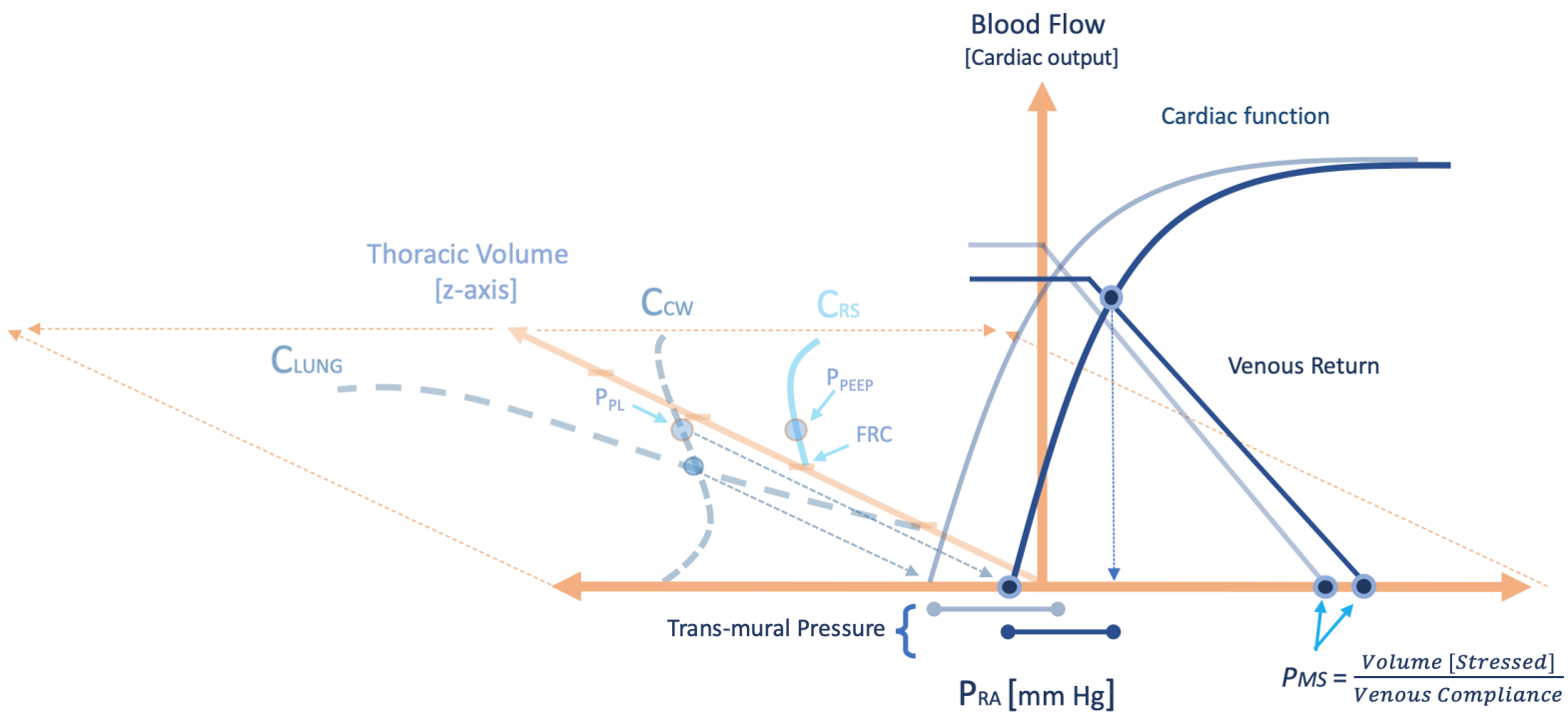

Figure 12: Positive end-expiratory pressure [PEEP] and heart-lung interaction. Figure 10 is in the x-z-plane and figure 11 is on the x-y plane. The application of PEEP to the respiratory system compliance curve [Crs] raises lung volume along the z-axis and pleural pressure [Ppl] along the chest wall compliance curve [Ccw]. The cardiac function curve shifts right and so too does the venous return curve. Trans-mural pressure is minimally-affected [blue dumbbells]. Right atrial pressure [Pra] rises and cardiac output [y-axis] is minimally affected. Clung in lung compliance; FRC is functional residual capacity; Pms is mean systemic pressure.

As PEEP increases lung volume, it also raises pulmonary vascular impedance. In healthy canine lungs, this effect is usually small at PEEP levels below 15 cm H2O to 20 cm H2O [166, 167], but difficult to predict in humans [67, 68, 168]. Nevertheless, increased right ventricular afterload flattens the slope of the right ventricular cardiac function curve and this favours right atrial pressure elevation with diminished cardiac output [52].

Left Ventricular Loading

Left ventricular preload is an aggregate of inter-ventricular, lung-heart mechanical effects as well as changing pulmonary venous return; the latter mechanism being the most prominent. There are decades of conflicting research addressing the influence of PEEP upon left ventricular compliance [2, 5, 162, 169]. Much of the disagreement arises from the assessment of the true left heart transmural pressure. The pericardial pressure is the true constraining pressure of the left ventricle, but this pressure is exceptionally difficult to measure accurately in vivo [170]. Additionally, if LV compliance is diminished, the means by which this occurs is also contentious with some positing LV compression by the expanding lungs [76, 171] and others suggesting RV distension and interdependence effects [28, 146]. Despite being mechanistically interesting, the effect of PEEP on left ventricular compliance is likely of minor hemodynamic significance save for states of prominent hyperinflation [5, 172]. In Veddeng's study, the selective application of 20 cm H2O to the canine left lung resulted in the greatest compressive deformation of the left ventricle, but no change in cardiac output!

As above, the most important hemodynamic effect of PEEP is its modification of pulmonary venous return [5, 162]. Because the pulmonary veins and left ventricle are exposed to roughly the same intra-thoracic pressure, both the pulmonary venous return curve and left ventricular function curve shift rightwards in unison in direct response to PEEP. However, the pulmonary venous return curve still may change relative to the left ventricular function curve for a multitude of reasons. First, the pulmonary venous return curve moves leftwards given diminished systemic venous return to the right heart, right ventricular output and, therefore, reduced pulmonary venous return. However, the pulmonary venous return curve could also right-shift relative to the left ventricular cardiac function curve due to decreased pulmonary venous capacitance induced by lung volume above functional residual capacity [22-25, 107, 173]. Again, which effect predominates is likely determined by the patient's underlying volume status; hypovolemia supports leftwards movement of the pulmonary venous return curve, while hypervolemia promotes right shift. Thus, by decreasing pulmonary venous capacitance, PEEP reduces the pulmonary vascular time-constant. Consequently, the effect of PEEP on pulmonary venous capacitance may have some role in mechanical-ventilation induced LV stroke volume variation. Consider that PEEP application raises inspiratory aortic flow and that the elevated flow occurs later in the respiratory cycle as compared to intermittent positive pressure ventilation without PEEP [174]. As described below, given the minimal effect of PEEP on left ventricular afterload in the normal heart, it may be that increasing PEEP shifts blood from the pulmonary vascular bed to the left heart due to diminished pulmonary vascular capacitance.

The role PEEP plays on afterload follows the physiology described above [5, 162, 175]; PEEP can reduce left ventricular afterload and improve stroke volume in states of high left-ventricular end-diastolic volume and when there are large, negative intra-thoracic pressure swings [176, 177]. However, in the healthy patient, these effects are trivial because the change in transmural pressure across the left ventricle is small and the LV cavity radius shrinks during ejection [92]. Overall, the reduced LV end-diastolic volume consequent to PEEP is typically greater than the

fall in end-systolic volume when there is normal contractility. Lastly, there is some evidence suggesting that PEEP lowers aortic impedance as well, potentially by emptying the thoracic portion of the aorta [90, 91].

Conclusion

While the summative effects of varying intra-thoracic pressure and lung volume can be complicated and at times contrary, basic tenants are surmised when one realizes the interactions between venous return, biventricular function and the intra-thoracic milieu. Falling intra-thoracic pressure supports blood retention within the thorax, either by promoting systemic venous return or retarding left ventricular output; increased intra-thoracic pressure favours just the opposite. Rising lung volume, on the other hand, impairs right ventricular ejection and enhances pulmonary venous return. In any case, underlying volume status, cardiac function and the degree to which lung volume and intra-thoracic pressure change each modulate these responses and explain conflicting experimental results. In health, that is, in a patient with normal physiology and without exaggerated changes in intra-thoracic physiology, mechanical heart-lung interactions are typically of small consequence. In sickness, by contrast, there are often profound anomalies of venous return, cardiac function, intra-thoracic pressure, lung volume or any combination thereof. As detailed in the following chapter, awareness of mechanical cardiopulmonary influence serves the clinician well. Interpreting both invasive and non-invasive hemodynamic data, approaching patients with abnormalities of respiratory and cardiac load and formulating rational treatment plans in the intensive care unit all depend, to some extent, upon mechanical heart-lung interaction.

References

1. Banner, M.J., M.J. Jaeger, and R.R. Kirby, Components of the work of breathing and implications for monitoring ventilator-dependent patients. Crit Care Med, 1994. 22(3): p. 515-23.
2. Robotham, J.L. and S.M. Scharf, Effects of positive and negative pressure ventilation on cardiac performance. Clin Chest Med, 1983. 4(2): p. 161-87.
3. Scharf, S.M., Cardiovascular effects of airways obstruction. Lung, 1991. 169(1): p. 1-23.
4. Pinsky, M.R., Recent advances in the clinical application of heart-lung interactions. Curr Opin Crit Care, 2002. 8(1): p. 26-31.
5. Luecke, T. and P. Pelosi, Clinical review: Positive end-expiratory pressure and cardiac output. Crit Care, 2005. 9(6): p. 607-21.
6. Frazier, S.K., Neurohormonal responses during positive pressure mechanical ventilation. Heart Lung, 1999. 28(3): p. 149-65; quiz 166-7.
7. Scharf, S.M., et al., Cardiac effects of increased lung volume and decreased pleural pressure in man. J Appl Physiol Respir Environ Exerc Physiol, 1979. 47(2): p. 257-62.
8. Scharf, S.M., et al., The effects of large negative intrathoracic pressure on left ventricular function in patients with coronary artery disease. Circulation, 1981. 63(4): p. 871-5.
9. Takata, M., R.A. Wise, and J.L. Robotham, Effects of abdominal pressure on venous return: abdominal vascular zone conditions. J Appl Physiol (1985), 1990. 69(6): p. 1961-72.
10. Robotham, J.L. and M. Takata, Mechanical abdomino/heart/lung interaction. J Sleep Res, 1995. 4(S1): p. 50-52.
11. Lloyd, T.C., Jr., Effect of inspiration on inferior vena caval blood flow in dogs. J Appl Physiol Respir Environ Exerc Physiol, 1983. 55(6): p. 1701-8.
12. Fessler, H.E., et al., Effects of Positive End-Expiratory Pressure on the Gradient for Venous Return. American Review of Respiratory Disease, 1991. 143(1): p. 19-24.
13. Fessler, H.E., Heart-lung interactions: applications in the critically ill. Eur Respir J, 1997. 10(1): p. 226-37.
14. Jellinek, H., et al., Influence of positive airway pressure on the pressure gradient for venous return in humans. J Appl Physiol (1985), 2000. 88(3): p. 926-32.
15. van den Berg, P.C., J.R. Jansen, and M.R. Pinsky, Effect of positive pressure on venous return in volume-loaded cardiac surgical patients. J Appl Physiol (1985), 2002. 92(3): p. 1223-31.
16. Scharf, S.M. and R.H. Ingram, Jr., Influence of abdominal pressure and sympathetic vasoconstriction on the cardiovascular response to positive end-expiratory pressure. Am Rev Respir Dis, 1977. 116(4): p. 661-70.
17. Takata, M. and J.L. Robotham, Effects of inspiratory diaphragmatic descent on inferior vena caval venous return. J Appl Physiol (1985), 1992. 72(2): p. 597-607.
18. Dorinsky, P.M., R.L. Hamlin, and J.E. Gadek, Alterations in regional blood flow during positive end-expiratory pressure ventilation. Crit Care Med, 1987. 15(2): p. 106-13.
19. Sha, M., et al., Effects of continuous positive-pressure ventilation on hepatic blood flow and intrahepatic oxygen delivery in dogs. Crit Care Med, 1987. 15(11): p. 1040-3.
20. Brienza, N., et al., Regional control of venous return: liver blood flow. Am J Respir Crit Care Med, 1995. 152(2): p. 511-8.
21. Brienza, N., et al., Effects of PEEP on liver arterial and venous blood flows. Am J Respir Crit Care Med, 1995. 152(2): p. 504-10.
22. Permutt, S., et al., Effect of lung inflation on static pressure-volume characteristics of pulmonary vessels. J Appl Physiol, 1961. 16: p. 64-70.
23. Permutt, S. and R.L. Riley, Hemodynamics of Collapsible Vessels with Tone: The Vascular Waterfall. J Appl Physiol, 1963. 18: p. 924-32.
24. Brower, R., et al., Effect of lung inflation on lung blood volume and pulmonary venous flow. J Appl Physiol (1985), 1985. 58(3): p. 954-63.
25. Whittenberger, J.L., et al., Influence of state of inflation of the lung on pulmonary vascular resistance. J Appl Physiol, 1960. 15: p. 878-82.
26. Marini, J.J., B.H. Culver, and J. Butler, Effect of positive end-expiratory pressure on canine ventricular function curves. J Appl Physiol Respir Environ Exerc Physiol, 1981. 51(6): p. 1367-74.
27. Nakhjavan, F.K., W.H. Palmer, and M. McGregor, Influence of respiration on venous return in pulmonary emphysema. Circulation, 1966. 33(1): p. 8-16.
28. Schulman, D.S., et al., Effect of positive end-expiratory pressure on right ventricular performance. Importance of baseline right ventricular function. Am J Med, 1988. 84(1): p. 57-67.
29. Biondi, J.W., et al., The effect of incremental positive end-expiratory pressure on right ventricular hemodynamics and ejection fraction. Anesth Analg, 1988. 67(2): p. 144-51.
30. Saouti, N., et al., The arterial load in pulmonary hypertension. Eur Respir Rev, 2010. 19(117): p. 197-203.

31. Tedford, R.J., Determinants of right ventricular afterload (2013 Grover Conference series). Pulm Circ, 2014. 4(2): p. 211-9.
32. Saouti, N., et al., Right ventricular oscillatory power is a constant fraction of total power irrespective of pulmonary artery pressure. Am J Respir Crit Care Med, 2010. 182(10): p. 1315-20.
33. Lai-Fook, S.J., A continuum mechanics analysis of pulmonary vascular interdependence in isolated dog lobes. J Appl Physiol Respir Environ Exerc Physiol, 1979. 46(3): p. 419-29.
34. West, J.B., C.T. Dollery, and B.E. Heard, Increased Pulmonary Vascular Resistance in the Dependent Zone of the Isolated Dog Lung Caused by Perivascular Edema. Circ Res, 1965. 17: p. 191-206.
35. West, J.B., C.T. Dollery, and A. Naimark, Distribution of Blood Flow in Isolated Lung; Relation to Vascular and Alveolar Pressures. J Appl Physiol, 1964. 19: p. 713-24.
36. West, J.B., Perivascular edema, a factor in pulmonary vascular resistance. Am Heart J, 1965. 70(4): p. 570-2.
37. Orchard, C.H., R. Sanchez de Leon, and M.K. Sykes, The relationship between hypoxic pulmonary vasoconstriction and arterial oxygen tension in the intact dog. J Physiol, 1983. 338: p. 61-74.
38. Magder, S. and B. Guerard, Heart-lung interactions and pulmonary buffering: lessons from a computational modeling study. Respir Physiol Neurobiol, 2012. 182(2-3): p. 60-70.
39. Shuler, R.H., et al., The differential effects of respiration on the left and right ventricles. Vol. 137. 1942. 620-627.
40. Wallis, T.W., et al., Mechanical heart-lung interaction with positive end-expiratory pressure. J Appl Physiol Respir Environ Exerc Physiol, 1983. 54(4): p. 1039-47.
41. Lloyd, T.C., Jr., Respiratory system compliance as seen from the cardiac fossa. J Appl Physiol Respir Environ Exerc Physiol, 1982. 53(1): p. 57-62.
42. Cassidy, S.S. and M. Ramanathan, Dimensional analysis of the left ventricle during PEEP: relative septal and lateral wall displacements. Am J Physiol, 1984. 246(6 Pt 2): p. H792-805.
43. Haynes, J.B., et al., Positive end-expiratory pressure shifts left ventricular diastolic pressure-area curves. J Appl Physiol Respir Environ Exerc Physiol, 1980. 48(4): p. 670-6.
44. Denault, A.Y., J. Gorcsan, 3rd, and M.R. Pinsky, Dynamic effects of positive-pressure ventilation on canine left ventricular pressure-volume relations. J Appl Physiol (1985), 2001. 91(1): p. 298-308.
45. Novak, R., G.M. Matuschak, and M.R. Pinsky, Effect of positive-pressure ventilatory frequency on regional pleural pressure. J Appl Physiol (1985), 1988. 65(3): p. 1314-23.
46. Robotham, J.L., R.A. Wise, and B. Bromberger-Barnea, Effects of changes in abdominal pressure on left ventricular performance and regional blood flow. Crit Care Med, 1985. 13(10): p. 803-9.
47. Morgan, B.C., W.G. Guntheroth, and D.H. Dillard, Relationship of Pericardial to Pleural Pressure during Quiet Respiration and Cardiac Tamponade. Circ Res, 1965. 16: p. 493-8.
48. Guyton, A.C., Determination of cardiac output by equating venous return curves with cardiac response curves. Physiol Rev, 1955. 35(1): p. 123-9.
49. Jacobsohn, E., R. Chorn, and M. OConnor, The role of the vasculature in regulating venous return and cardiac output: historical and graphical approach. Canadian Journal of Anaesthesia-Journal Canadien D Anesthesie, 1997. 44(8): p. 849-867.
50. Sylvester, J.T., H.S. Goldberg, and S. Permutt, The Role of the Vasculature in the Regulation of Cardiac-Output. Clinics in Chest Medicine, 1983. 4(2): p. 111-126.
51. Wise, R.A., J.L. Robotham, and W.R. Summer, Effects of spontaneous ventilation on the circulation. Lung, 1981. 159(4): p. 175-86.
52. Pinsky, M.R., Determinants of pulmonary arterial flow variation during respiration. J Appl Physiol Respir Environ Exerc Physiol, 1984. 56(5): p. 1237-45.
53. Guntheroth, W.G., B.C. Morgan, and G.L. Mullins, Effect of respiration on venous return and stroke volume in cardiac tamponade. Mechanism of pulsus parodoxus. Circ Res, 1967. 20(4): p. 381-90.
54. Scharf, S.M., et al., Effects of normal and loaded spontaneous inspiration on cardiovascular function. J Appl Physiol Respir Environ Exerc Physiol, 1979. 47(3): p. 582-90.
55. Claessen, G., et al., Interaction between respiration and right versus left ventricular volumes at rest and during exercise: a real-time cardiac magnetic resonance study. Am J Physiol Heart Circ Physiol, 2014. 306(6): p. H816-24.
56. Guyton, A.C., D. Polizo, and G.G. Armstrong, Mean circulatory filling pressure measured immediately after cessation of heart pumping. Am J Physiol, 1954. 179(2): p. 261-7.
57. Feihl, F. and A.F. Broccard, Interactions between respiration and systemic hemodynamics. Part I: basic concepts. Intensive Care Med, 2009. 35(1): p. 45-54.
58. Broccard, A.F., Cardiopulmonary interactions and volume status assessment. J Clin Monit Comput, 2012. 26(5): p. 383-91.
59. Magder, S., Clinical usefulness of respiratory variations in arterial pressure. Am J Respir Crit Care Med, 2004. 169(2): p. 151-5.
60. Magder, S., Bench-to-bedside review: An approach to hemodynamic monitoring - Guyton at the bedside. Crit Care, 2012. 16(5): p. 236.
61. Magder, S., Fluid status and fluid responsiveness. Current Opinion in Critical Care, 2010. 16(4): p. 289-96.
62. Guyton, A.C., A.W. Lindsey, and B.N. Kaufmann, Effect of mean circulatory filling pressure and other peripheral circulatory factors on cardiac output. Am J Physiol, 1955. 180(3): p. 463-8.

63. Pinsky, M.R., Instantaneous venous return curves in an intact canine preparation. J Appl Physiol Respir Environ Exerc Physiol, 1984. 56(3): p. 765-71.
64. Grant, B.J. and B.B. Lieber, Compliance of the main pulmonary artery during the ventilatory cycle. J Appl Physiol (1985), 1992. 72(2): p. 535-42.
65. McHale, P.A. and J.C. Greenfield, Jr., Evaluation of several geometric models for estimation of left ventricular circumferential wall stress. Circ Res, 1973. 33(3): p. 303-12.
66. Maughan, W.L., et al., Instantaneous pressure-volume relationship of the canine right ventricle. Circ Res, 1979. 44(3): p. 309-15.
67. Pinsky, M.R., J.M. Desmet, and J.L. Vincent, Effect of positive end-expiratory pressure on right ventricular function in humans. Am Rev Respir Dis, 1992. 146(3): p. 681-7.
68. Pinsky, M.R., My paper 20 years later: Effect of positive end-expiratory pressure on right ventricular function in humans. Intensive Care Med, 2014. 40(7): p. 935-41.
69. Koshino, Y., et al., Changes in left and right ventricular mechanics during the Mueller maneuver in healthy adults: a possible mechanism for abnormal cardiac function in patients with obstructive sleep apnea. Circ Cardiovasc Imaging, 2010. 3(3): p. 282-9.
70. Slinker, B.K. and S.A. Glantz, End-systolic and end-diastolic ventricular interaction. Am J Physiol, 1986. 251(5 Pt 2): p. H1062-75.
71. Damiano, R.J., Jr., et al., Significant left ventricular contribution to right ventricular systolic function. Am J Physiol, 1991. 261(5 Pt 2): p. H1514-24.
72. Yamaguchi, S., et al., The left ventricle affects the duration of right ventricular ejection. Cardiovasc Res, 1993. 27(2): p. 211-5.
73. Lockhart, A., et al., Elevated pulmonary artery wedge pressure at rest and during exercise in chronic bronchitis: fact or fancy. Clin Sci, 1969. 37(2): p. 503-17.
74. Bove, A.A. and W.P. Santamore, Ventricular interdependence. Prog Cardiovasc Dis, 1981. 23(5): p. 365-88.
75. Weber, K.T., et al., Contractile mechanics and interaction of the right and left ventricles. Am J Cardiol, 1981. 47(3): p. 686-95.
76. Santamore, W.P., J.L. Heckman, and A.A. Bove, Right and left ventricular pressure-volume response to respiratory maneuvers. J Appl Physiol Respir Environ Exerc Physiol, 1984. 57(5): p. 1520-7.
77. Guzman, P.A., et al., Transseptal pressure gradient with leftward septal displacement during the Mueller manoeuvre in man. Br Heart J, 1981. 46(6): p. 657-62.
78. Little, W.C., F.R. Badke, and R.A. O'Rourke, Effect of right ventricular pressure on the end-diastolic left ventricular pressure-volume relationship before and after chronic right ventricular pressure overload in dogs without pericardia. Circ Res, 1984. 54(6): p. 719-30.
79. Maughan, W.L., K. Sunagawa, and K. Sagawa, Ventricular systolic interdependence: volume elastance model in isolated canine hearts. Am J Physiol, 1987. 253(6 Pt 2): p. H1381-90.
80. Farrar, D.J., J.C. Woodard, and E. Chow, Pacing-induced dilated cardiomyopathy increases left-to-right ventricular systolic interaction. Circulation, 1993. 88(2): p. 720-5.
81. Takata, M., W. Mitzner, and J.L. Robotham, Influence of the pericardium on ventricular loading during respiration. J Appl Physiol (1985), 1990. 68(4): p. 1640-50.
82. Robotham, J.L., et al., Left ventricular hemodynamics during respiration. J Appl Physiol Respir Environ Exerc Physiol, 1979. 47(6): p. 1295-1303.
83. Robotham, J.L. and W. Mintzner, A model of the effects of respiration on left ventricular performance. J Appl Physiol Respir Environ Exerc Physiol, 1979. 46(3): p. 411-8.
84. Karam, M., et al., Mechanism of decreased left ventricular stroke volume during inspiration in man. Circulation, 1984. 69(5): p. 866-73.
85. Buda, A.J., et al., Effect of intrathoracic pressure on left ventricular performance. N Engl J Med, 1979. 301(9): p. 453-9.
86. Peters, J., M.K. Kindred, and J.L. Robotham, Transient analysis of cardiopulmonary interactions. I. Diastolic events. J Appl Physiol (1985), 1988. 64(4): p. 1506-17.
87. Peters, J., et al., Negative intrathoracic pressure decreases independently left ventricular filling and emptying. Am J Physiol, 1989. 257(1 Pt 2): p. H120-31.
88. Robotham, J.L., et al., Effects of changes in left ventricular loading and pleural pressure on mitral flow. J Appl Physiol (1985), 1988. 65(4): p. 1662-75.
89. Peters, J., M.K. Kindred, and J.L. Robotham, Transient analysis of cardiopulmonary interactions. II. Systolic events. J Appl Physiol (1985), 1988. 64(4): p. 1518-26.
90. Fessler, H.E., et al., Mechanism of reduced LV afterload by systolic and diastolic positive pleural pressure. J Appl Physiol (1985), 1988. 65(3): p. 1244-50.
91. Pinsky, M.R., et al., Hemodynamic effects of cardiac cycle-specific increases in intrathoracic pressure. J Appl Physiol (1985), 1986. 60(2): p. 604-12.
92. Pinsky, M.R., Cardiovascular issues in respiratory care. Chest, 2005. 128(5 Suppl 2): p. 592S-597S.
93. Condos, W.R., Jr., et al., Hemodynamics of the Mueller maneuver in man: right and left heart micromanometry and Doppler echocardiography. Circulation, 1987. 76(5): p. 1020-8.
94. Brinker, J.A., et al., Leftward septal displacement during right ventricular loading in man. Circulation, 1980. 61(3): p. 626-33.
95. Guyton, A.C. and L.H. Adkins, Quantitative aspects of the collapse factor in relation to venous return. Am J Physiol, 1954. 177(3): p. 523-7.
96. Guyton, A.C., et al., Venous return at various right atrial pressures and the normal venous return curve. Am J Physiol, 1957. 189(3): p. 609-15.

97. Rubinson, R.M., et al., Inferior Vena Caval Obstruction from Increased Intra-Abdominal Pressure - Experimental Hemodynamic and Angiographic Observations. Archives of Surgery, 1967. 94(6): p. 766-&.
98. Kimura, B.J., et al., The effect of breathing manner on inferior vena caval diameter. European Journal of Echocardiography, 2011. 12(2).
99. Janicki, J.S., Influence of the pericardium and ventricular interdependence on left ventricular diastolic and systolic function in patients with heart failure. Circulation, 1990. 81(2 Suppl): p. III15-20.
100. Janicki, J.S. and K.T. Weber, The pericardium and ventricular interaction, distensibility, and function. Am J Physiol, 1980. 238(4): p. H494-503.
101. Takata, M., et al., Coupled vs. uncoupled pericardial constraint: effects on cardiac chamber interactions. J Appl Physiol (1985), 1997. 83(6): p. 1799-813.
102. Wead, W.B. and J.F. Norton, Effects of intrapleural pressure changes on canine left ventricular function. J Appl Physiol Respir Environ Exerc Physiol, 1981. 50(5): p. 1027-35.
103. Pinsky, M.R., G.M. Matuschak, and M. Klain, Determinants of cardiac augmentation by elevations in intrathoracic pressure. J Appl Physiol (1985), 1985. 58(4): p. 1189-98.
104. Kim, B.H., et al., Effects of spontaneous respiration on right and left ventricular function: evaluation by respiratory and ECG gated radionuclide ventriculography. J Nucl Med, 1987. 28(2): p. 173-7.
105. Hoffman, J.I., et al., Stroke volume in conscious dogs; effect of respiration, posture, and vascular occlusion. J Appl Physiol, 1965. 20(5): p. 865-77.
106. Hakim, T.S., R.P. Michel, and H.K. Chang, Effect of lung inflation on pulmonary vascular resistance by arterial and venous occlusion. J Appl Physiol Respir Environ Exerc Physiol, 1982. 53(5): p. 1110-5.
107. Howell, J.B., et al., Effect of inflation of the lung on different parts of pulmonary vascular bed. J Appl Physiol, 1961. 16: p. 71-6.
108. Robotham, J.L., et al., Regional left ventricular performance during normal and obstructed spontaneous respiration. J Appl Physiol Respir Environ Exerc Physiol, 1983. 55(2): p. 569-77.
109. Scharf, S.M., et al., Respiratory phasic effects of inspiratory loading on left ventricular hemodynamics in vagotomized dogs. J Appl Physiol (1985), 1992. 73(3): p. 995-1003.
110. Cassidy, S.S., et al., Changes in left ventricular geometry during spontaneous breathing. J Appl Physiol (1985), 1987. 63(2): p. 803-11.
111. Scharf, S.M., et al., Intrathoracic pressures and left ventricular configuration with respiratory maneuvers. J Appl Physiol (1985), 1989. 66(1): p. 481-91.
112. Mastenbrook, S.M., Jr., J.G. Webster, and S.J. Updike, Venous return curves obtained from graded series of Valsalva maneuvers. Med Res Eng, 1977. 12(6): p. 20-9.
113. Porth, C.J., et al., The Valsalva maneuver: mechanisms and clinical implications. Heart Lung, 1984. 13(5): p. 507-18.
114. Charlier, A.A., P.M. Jaumin, and H. Pouleur, Circulatory effects of deep inspirations, blocked expirations and positive pressure inflations at equal transpulmonary pressures in conscious dogs. J Physiol, 1974. 241(3): p. 589-605.
115. Holt, J.P., the effect of positive and negative intrathoracic pressure on cardiac output and venous pressure in the dog. Vol. 142. 1944. 594-603.
116. Wilkinson, P.L., et al., Pressure and flow changes during Valsalva-like maneuvers in dogs following volume infusion. Am J Physiol, 1977. 233(1): p. H93-9.
117. Robotham, J.L., et al., Cardiorespiratory interactions in patients with an artificial heart. Anesthesiology, 1990. 73(4): p. 599-609.
118. Naeije, R., J.M. Maarek, and H.K. Chang, Pulmonary vascular impedance in microembolic pulmonary hypertension: effects of synchronous high-frequency jet ventilation. Respir Physiol, 1990. 79(3): p. 205-17.
119. Jardin, F., et al., Mechanism of paradoxic pulse in bronchial asthma. Circulation, 1982. 66(4): p. 887-94.
120. Gelb, A.F., et al., P pulmonale in status asthmaticus. J Allergy Clin Immunol, 1979. 64(1): p. 18-22.
121. Muramoto, A., et al., Nifedipine dilates the pulmonary vasculature without producing symptomatic systemic hypotension in upright resting and exercising patients with pulmonary hypertension secondary to chronic obstructive pulmonary disease. Am Rev Respir Dis, 1985. 132(5): p. 963-6.
122. Versprille, A., Pulmonary vascular resistance. A meaningless variable. Intensive Care Med, 1984. 10(2): p. 51-3.
123. Naeije, R., Pulmonary vascular resistance. A meaningless variable? Intensive Care Med, 2003. 29(4): p. 526-9.
124. Natarajan, T.K., et al., Immediate effect of expiratory loading on left ventricular stroke volume. Circulation, 1987. 75(1): p. 139-45.
125. Smith, P.K., et al., Cardiovascular effects of ventilation with positive expiratory airway pressure. Ann Surg, 1982. 195(2): p. 121-30.
126. Mitchell, J.R., et al., RV filling modulates LV function by direct ventricular interaction during mechanical ventilation. Am J Physiol Heart Circ Physiol, 2005. 289(2): p. H549-57.
127. Santamore, W.P., J.L. Heckman, and A.A. Bove, Cardiovascular changes from expiration to inspiration during IPPV. Am J Physiol, 1983. 245(2): p. H307-12.

128. Romand, J.A., et al., Hemodynamic effects of synchronized high-frequency jet ventilation compared with low-frequency intermittent positive-pressure ventilation after myocardial revascularization. Anesthesiology, 2000. 92(1): p. 24-30.
129. Wang, Z., et al., Simultaneous beat-by-beat investigation of the effects of the Valsalva maneuver on left and right ventricular filling and the possible mechanism. PLoS One, 2013. 8(1): p. e53917.
130. Looga, R., The Valsalva manoeuvre--cardiovascular effects and performance technique: a critical review. Respir Physiol Neurobiol, 2005. 147(1): p. 39-49.
131. Felker, G.M., P.S. Cuculich, and M. Gheorghiade, The Valsalva maneuver: a bedside "biomarker" for heart failure. Am J Med, 2006. 119(2): p. 117-22.
132. Mesquida, J., H.K. Kim, and M.R. Pinsky, Effect of tidal volume, intrathoracic pressure, and cardiac contractility on variations in pulse pressure, stroke volume, and intrathoracic blood volume. Intensive Care Med, 2011. 37(10): p. 1672-9.
133. Jardin, F., et al., Influence of lung and chest wall compliances on transmission of airway pressure to the pleural space in critically ill patients. Chest, 1985. 88(5): p. 653-8.
134. Magder, S., G. Georgiadis, and T. Cheong, Respiratory Variations in Right Atrial Pressure Predict the Response to Fluid Challenge. Journal of Critical Care, 1992. 7(2): p. 76-85.
135. Magder, S., Predicting volume responsiveness in spontaneously breathing patients: still a challenging problem. Crit Care, 2006. 10(5): p. 165.
136. Akoumianaki, E., et al., The application of esophageal pressure measurement in patients with respiratory failure. Am J Respir Crit Care Med, 2014. 189(5): p. 520-31.
137. Brochard, L., Measurement of esophageal pressure at bedside: pros and cons. Curr Opin Crit Care, 2014. 20(1): p. 39-46.
138. Chihara, E., et al., Elevated mean systemic filling pressure due to intermittent positive-pressure ventilation. Am J Physiol, 1992. 262(4 Pt 2): p. H1116-21.
139. Barnes, G.E., et al., Cardiovascular responses to elevation of intra-abdominal hydrostatic pressure. Am J Physiol, 1985. 248(2 Pt 2): p. R208-13.
140. Tyberg, J.V., et al., The relationship between pericardial pressure and right atrial pressure: an intraoperative study. Circulation, 1986. 73(3): p. 428-32.
141. Lansdorp, B., et al., Mechanical ventilation-induced intrathoracic pressure distribution and heart-lung interactions*. Crit Care Med, 2014. 42(9): p. 1983-90.
142. Pinsky, M.R., Why knowing the effects of positive-pressure ventilation on venous, pleural, and pericardial pressures is important to the bedside clinician?*. Crit Care Med, 2014. 42(9): p. 2129-31.
143. O'Quin, R.J., et al., Transmission of airway pressure to pleural space during lung edema and chest wall restriction. J Appl Physiol (1985), 1985. 59(4): p. 1171-7.
144. Venus, B., L.E. Cohen, and R.A. Smith, Hemodynamics and intrathoracic pressure transmission during controlled mechanical ventilation and positive end-expiratory pressure in normal and low compliant lungs. Crit Care Med, 1988. 16(7): p. 686-90.
145. Robotham, J.L., et al., Left ventricular geometry during positive end-expiratory pressure in dogs. Crit Care Med, 1985. 13(8): p. 617-24.
146. Scharf, S.M. and R. Brown, Influence of the right ventricle on canine left ventricular function with PEEP. J Appl Physiol Respir Environ Exerc Physiol, 1982. 52(1): p. 254-9.
147. Jardin, F., et al., Influence of positive end-expiratory pressure on left ventricular performance. N Engl J Med, 1981. 304(7): p. 387-92.
148. Brown, R., S.M. Scharf, and R. Ingram, Jr., Nonhomogeneous alveolar pressure swings: effect of different respiratory muscles. J Appl Physiol Respir Environ Exerc Physiol, 1982. 52(3): p. 638-41.
149. D'Angelo, E., et al., Local transpulmonary pressure after lobar occlusion. Respir Physiol, 1973. 18(3): p. 328-37.
150. Minh, V.D., et al., Ipsilateral transpulmonary pressures during unilateral electrophrenic respiration. J Appl Physiol, 1974. 37(4): p. 505-9.
151. Butler, J., et al., Cause of the raised wedge pressure on exercise in chronic obstructive pulmonary disease. Am Rev Respir Dis, 1988. 138(2): p. 350-4.
152. Vieillard-Baron, A., et al., Cyclic changes in right ventricular output impedance during mechanical ventilation. J Appl Physiol (1985), 1999. 87(5): p. 1644-50.
153. Jardin, F. and A. Vieillard-Baron, Right ventricular function and positive pressure ventilation in clinical practice: from hemodynamic subsets to respirator settings. Intensive Care Med, 2003. 29(9): p. 1426-34.
154. Robotham, J.L., et al., A re-evaluation of the hemodynamic consequences of intermittent positive pressure ventilation. Crit Care Med, 1983. 11(10): p. 783-93.
155. Scharf, S.M., et al., Hemodynamic effects of positive-pressure inflation. J Appl Physiol Respir Environ Exerc Physiol, 1980. 49(1): p. 124-31.
156. Chapin, J.C., et al., Lung expansion, airway pressure transmission, and positive end-expiratory pressure. Arch Surg, 1979. 114(10): p. 1193-7.
157. Hess, D.R. and L.M. Bigatello, The chest wall in acute lung injury/acute respiratory distress syndrome. Curr Opin Crit Care, 2008. 14(1): p. 94-102.
158. Tang, P.C., F.W. Maire, and V.E. Amassian, Respiratory influence on the vasomotor center. Am J Physiol, 1957. 191(2): p. 218-24.
159. Glick, G., et al., Cardiac dimensions in intact unanesthetized man. VI. Effects of changes in heart rate. J Appl Physiol, 1966. 21(3): p. 947-52.

160. Nanas, S. and S. Magder, Adaptations of the peripheral circulation to PEEP. Am Rev Respir Dis, 1992. 146(3): p. 688-93.
161. Bark, H., et al., Elevations in plasma ADH levels during PEEP ventilation in the dog: mechanisms involved. Am J Physiol, 1980. 239(6): p. E474-81.
162. Vargas, M., et al., PEEP role in ICU and operating room: from pathophysiology to clinical practice. ScientificWorldJournal, 2014. 2014: p. 852356.
163. Fessler, H.E., Effects of CPAP on venous return. J Sleep Res, 1995. 4(S1): p. 44-49.
164. Nixon, J.V., et al., Effect of large variations in preload on left ventricular performance characteristics in normal subjects. Circulation, 1982. 65(4): p. 698-703.
165. Michard, F. and J.L. Teboul, Using heart-lung interactions to assess fluid responsiveness during mechanical ventilation. Crit Care, 2000. 4(5): p. 282-9.
166. Schulman, D.S., et al., Left ventricular diastolic function during positive end-expiratory pressure. Impact of right ventricular ischemia and ventricular interaction. Am Rev Respir Dis, 1992. 145(3): p. 515-21.
167. Luecke, T., et al., Assessment of cardiac preload and left ventricular function under increasing levels of positive end-expiratory pressure. Intensive Care Med, 2004. 30(1): p. 119-26.
168. Neidhart, P.P. and P.M. Suter, Changes of right ventricular function with positive end-expiratory pressure (PEEP) in man. Intensive Care Med, 1988. 14 Suppl 2: p. 471-3.
169. Biondi, J.W., D.S. Schulman, and R.A. Matthay, Effects of mechanical ventilation on right and left ventricular function. Clin Chest Med, 1988. 9(1): p. 55-71.
170. Smiseth, O.A., et al., Nonuniformity of pericardial surface pressure in dogs. Circulation, 1987. 75(6): p. 1229-36.
171. Takata, M. and J.L. Robotham, Ventricular external constraint by the lung and pericardium during positive end-expiratory pressure. Am Rev Respir Dis, 1991. 143(4 Pt 1): p. 872-5.
172. Veddeng, O.J., et al., Selective positive end-expiratory pressure and intracardiac dimensions in dogs. J Appl Physiol (1985), 1992. 73(5): p. 2016-20.
173. Roos, A., et al., Pulmonary vascular resistance as determined by lung inflation and vascular pressures. J Appl Physiol, 1961. 16: p. 77-84.
174. Bell, R.C., et al., Left ventricular geometry during intermittent positive pressure ventilation in dogs. J Crit Care, 1987. 2(4): p. 230-244.
175. Klinger, J.R., Hemodynamics and positive end-expiratory pressure in critically ill patients. Crit Care Clin, 1996. 12(4): p. 841-64.
176. Pinsky, M.R. and W.R. Summer, Cardiac augmentation by phasic high intrathoracic pressure support in man. Chest, 1983. 84(4): p. 370-5.
177. Pinsky, M.R., et al., Augmentation of cardiac function by elevation of intrathoracic pressure. J Appl Physiol Respir Environ Exerc Physiol, 1983. 54(4): p. 950-5.

Chapter Four

Mechanical Interactions between the Respiratory and Cardiovascular Systems in Sickness: integration of the Campbell and Guyton diagrams

Abstract

Aberrant compliance and resistance of the lungs and chest wall typify many diseases encountered in the intensive care unit. These anomalies are represented on the Campbell diagram as shifts in the pulmonary, chest wall and respiratory system static and dynamic compliance curves. Similarly, abnormal venous return and cardiac function are commonly encountered in critically-ill patients. Cardiovascular pathophysiology is summarized on the Guyton diagram as deviations of the cardiac and venous return function curves. When the Guyton and Campbell diagrams are superimposed, interaction between the diseased respiratory and cardiovascular systems is illustrated. Awareness of heart-lung interrelation is imperative when anticipating a patient's response to the initiation or subtraction of mechanical ventilation as well as recognizing and interpreting hemodynamic data.

Keywords: Guyton diagram, Campbell diagram, heart-lung interaction, preload, afterload, systemic venous return, positive end-expiratory pressure, ARDS, COPD, asthma, heart failure

Introduction

In the previous chapter, the effects of the respiratory system upon the cardiovascular system were delineated in the patient without significant cardiopulmonary duress. The Campbell diagram depicted changes in thoracic volume as a function of intra-thoracic pressure; notably, thoracic pressure and volume are the two key variables that mechanically influence the cardiovascular system. Ultimately, pressure and volume effects of the thorax alter biventricular loading conditions as well as venous return. The cardiac function and venous return curves are thus reshaped and illustrate the cardiovascular response.

This chapter focuses on four clinical scenarios to demonstrate the pathomechanics of cardio-respiratory interaction. First, broncho-obstructive disease reveals how excessively elevated airway resistance and loss of pulmonary elastic recoil

contribute to large swings in intra-thoracic pressure and hyperinflation of the lungs. Second, systolic heart failure illustrates how poor pulmonary compliance affects the cardiovascular system and highlights how cardiac pathology can alter respiratory physiology. Third, pulmonary and extra-pulmonary ARDS, as proposed by Gattinoni and colleagues, afford a physiological model to demonstrate how changes in pulmonary compliance versus chest wall compliance modify cardiac function and venous return during mechanical ventilation. Lastly, the septic cirrhotic patient encompasses a host of cardiovascular and respiratory disturbances which reemphasize and solidify many of the concepts introduced.

Before turning to these scenarios, however, a brief discussion of ventilation, work-of-breathing and oxygen utilization is in order. While this is not a strict mechanical dynamic shared between the respiratory and cardiovascular systems, it certainly modifies the cardiovascular response to high work of breathing.

Ventilation as Exercise

While the focus of this volume is the mechanical interactions between the heart and lungs, that ventilation taxes the cardiovascular system via oxygen supply and demand matching cannot be ignored [1]. Work of breathing was discussed in the first chapter and is increased in states of both high airways resistance and altered lung and chest wall compliance [2]. When increased airways resistance is the primary cause of high work of breathing, the dominant mechanical means of compensation is by breathing at higher lung volume. High lung volume breathing lowers expiratory airway resistance [3] which helps maintain gas exchange despite higher elastic and inspiratory work of breathing [4, 5]. In acute broncho-obstruction, work of breathing may be many times normal. By contrast, when the elastic load is the root of high breathing work, the body tends to compensate by rapid-shallow-breathing [6, 7]. This offsets the elastic work required to move the thorax and maintain gas-exchange, but impairs alveolar ventilation as relative dead-space rises [8]. Breathing work and effort is further discussed in chapter 9 within the contexts of high flow oxygen therapy and mechanical power.

Tissue oxygen utilization [VO_2] is a surrogate for work of breathing when plotted against minute ventilation. There is normally an exponential relationship between minute ventilation and VO_2. In diseased states such as emphysema, the curve is shifted to the left and steeper [9, 10] [figure 1]. The augmented VO_2 is the result of recruited muscles of respiration [11]. This increases blood flow to these muscle units by 5-6 fold [12-14]. If the cardiovascular response is not capable of maintaining minimum oxygen delivery [DO_2] to these muscles, then cardiovascular collapse may occur [1]. Additionally, oxygen demand-supply inequality may cause low mixed venous oxygen saturation which enhances hypoxemic pulmonary vasoconstriction and, consequently, increases pulmonary artery impedance [15, 16].

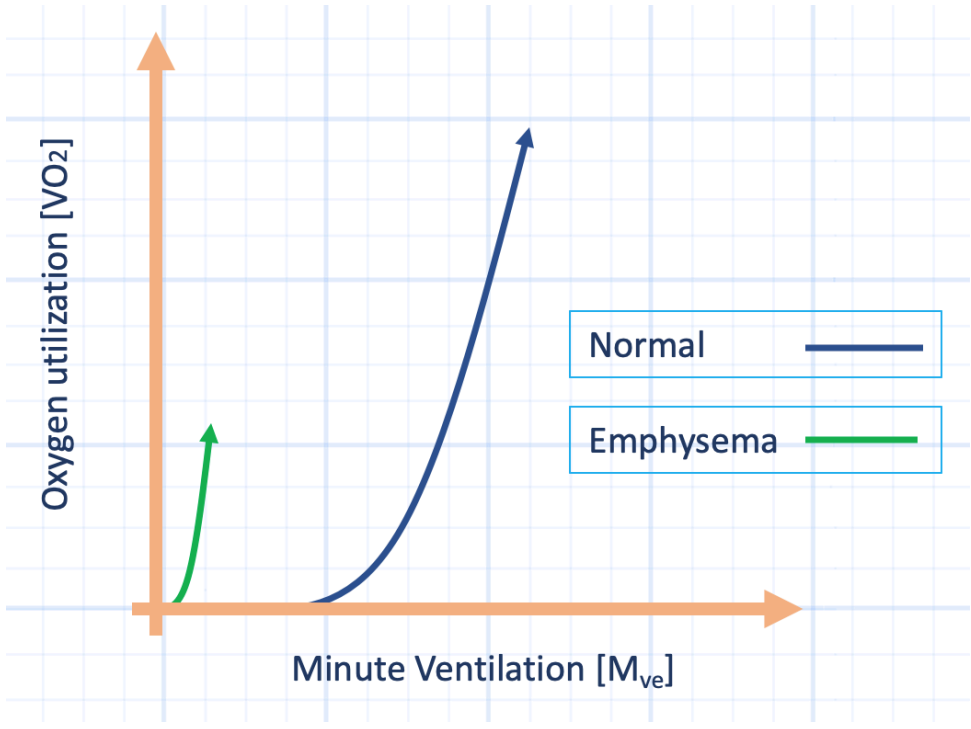

Figure 1: Minute ventilation versus oxygen utilization in normals and patients with emphysema. Note the steep rise in oxygen utilization at a much lower minute ventilation in those with emphysema.

Acute Broncho-obstruction

Excessive swings of thoracic volume and intra-thoracic pressure drive heart-lung pathomechanics. During acute broncho-obstruction [e.g. status asthmaticus, acute exacerbation of COPD] there can be severe departures from normal of both thoracic volume and intra-thoracic pressure, as described below.

Changes in Thoracic Volume

Dynamic Hyperinflation

Dynamic hyperinflation occurs when the lungs cannot empty. The phenomenon is most likely to occur when the lung, or portions of the lung have prolonged time-constants, the expiratory time is short or, as is often the case, a combination of the two [17-20]. A time constant is the time it takes a viscoelastic structure to return to its pre-deformation state. In the lung, the time constant is directly proportional to both resistance and compliance. Therefore, as the resistance and/or the compliance increase, the lung takes longer to empty. High resistance and compliance typify emphysema, however, at high volumes both the resistance and compliance of the lung decrease which diminishes the time-constant and protects expiratory flow. Additionally, as the respiratory rate increases, expiratory time decreases. If tachypnea is coupled with prolonged time-constants, then dynamic hyperinflation of the lungs occurs [4, 5, 21, 22] [figure 2]. As discussed in the previous chapter, when lung volume increases, the heart, as well as the pulmonary and abdominal

vascular beds, can be compressed. These effects contribute to many of the heart-lung interactions encountered in patients with emphysema.

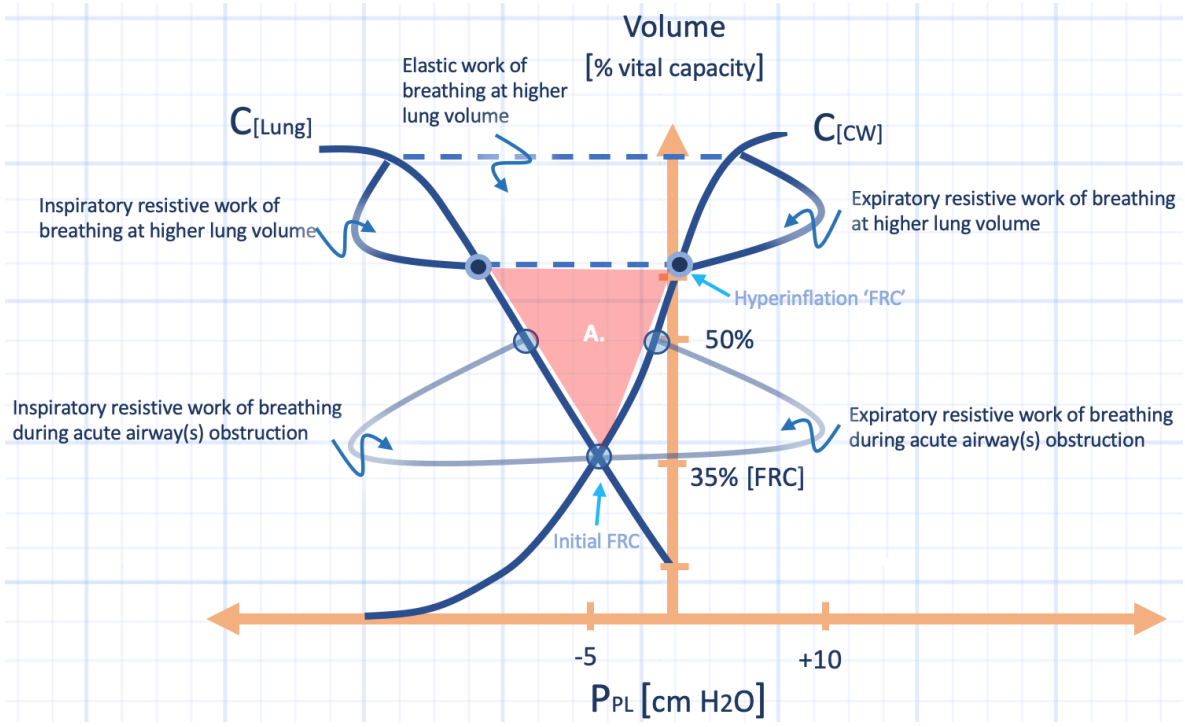

Figure 2: Illustration of dynamic hyperinflation on Campbell diagram. Note increased inspiratory and expiratory resistance at normal lung volumes. Higher lung volume breathing is marked by lower resistive work, but higher elastic work. Shaded area A. is the work done on the respiratory system by Auto-PEEP and poses an inspiratory threshold load on the patient; this may be offset by extrinsic PEEP [see chapter 1]. The x-axis is pleural pressure in centimetres of water [cm H_2O] and the y-axis is thoracic volume in percent vital capacity. Clung is lung compliance; Ccw is chest wall compliance; FRC is functional residual capacity; Ppl is pleural pressure. This figure will be the x-z plane in figure 4.

Systemic Venous Return

Similar to applied positive end-expiratory pressure, dynamic hyperinflation results in alveolar pressure that is above atmospheric pressure at end-expiration; that is, the positive pressure at end-expiration reflects the gas trapped within the alveolus [23]. The increased lung volume shifts the diaphragm downwards and pressurizes the abdomen. Further, released catecholamines act upon the peripheral vasculature and recruit unstressed volume [24, 25]. The consequence is augmented mean systemic pressure or a rightward shift of the venous return curve on the Guyton diagram [26-29], as discussed in chapter 3. However, it does not shift the venous return curve in a completely parallel manner. The combination of the pressurized abdomen and, potentially, constriction of the IVC [30-32] increases the resistance to venous return and decreases maximal venous return [i.e. the quantity of blood flow at the plateau of the venous return curve]. By these mechanisms, cardiac output is limited by venous return. The extent to which maximal venous return is reduced depends upon the patient's pre-existing volume status, compliance of the splanchnic circulation, compliance of the abdomen [e.g. expiratory muscle recruitment] and distribution of blood between the extremities and abdominal compartment [33]. The pressure at which maximal venous return occurs is labeled Pcrit [or critical pressure] and is, in the healthy patient, typically close to or slightly

below atmospheric pressure [34, 35]. Notably, extrinsic PEEP and/or auto-PEEP enhances both the mean systemic pressure and Pcrit to roughly the same degree; this maintains the pressure gradient for venous return [36]. Therefore, venous return limitation is driven primarily by increased resistance to venous return and reduced maximal venous return; not a reduced pressure gradient.

As cardiac output is defined by the operating point of the Guyton diagram – the point at which the venous return and cardiac function curves intersect – reduced maximal venous return and increased resistance to venous return diminish the operating point and, consequently, cardiac output [figure 3].

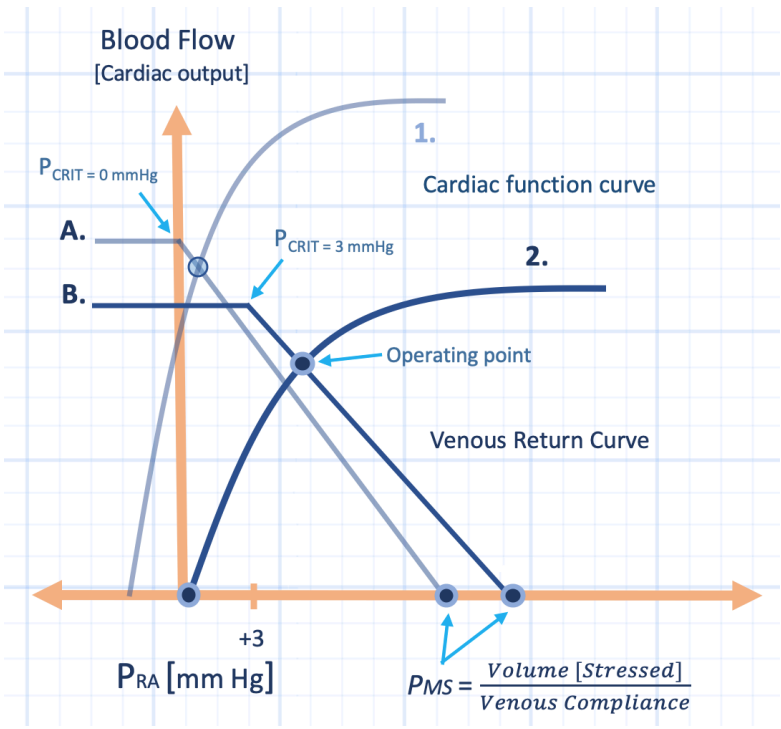

Figure 3: The effect of PEEP or auto-PEEP on venous return and cardiac function. The emboldened venous return [B] and cardiac function [2] curves represent the effect of PEEP [or auto-PEEP]. The mean systemic pressure [Pms] and the critical collapse pressure [Pcrit] rise in response to auto-PEEP. The afterload increases, so the cardiac function curve bends. Baseline venous return [A] and cardiac function [1] are shown for comparison. Elevated pleural pressure shifts the cardiac function curve rightwards [2]. Pra is right atrial pressure. This will be the x-y plane in figure 4. The x-axis is right atrial pressure [Pra] in millimetres of mercury [mmHg] and the y-axis is cardiac output and/or venous return.

Right Ventricular Loading

In emphysema, gas-trapping usually affects the lower lobes and, when severe, can compress the heart within the cardiac fossa [37]. On the Guyton diagram, this is illustrated by a parallel, rightward shift of the cardiac function curve with respect to the systemic venous return curve. The lower-lobe gas-trapping explains why juxta-cardiac pleural pressure is usually higher than other parts of the thorax [38, 39] as the heart is compressed by the expanding lung. Lower-lobe gas-trapping increases both the wedge pressure and right atrial pressure, but shrinks cardiac size [37, 40, 41]. This is compatible with decreased cardiac transmural pressure despite elevated intra-vascular pressure; as before, it is the right atrial transmural pressure that best approximates true end-diastolic volume or preload, not simply the right atrial pressure [i.e. the central venous pressure] [42]. Hence, dynamic hyperinflation

reduces cardiac preload by external compression. Whether cardiac constriction by the lungs within the cardiac fossa impairs diastolic function has been debated, as discussed in chapter 3. In animal models – with the elimination of venous return – compression of the heart induced by PEEP produced only a parallel shift in the relationship between transmural filling pressure and stroke volume. Thus, at lung volumes created by PEEP up to 15-20 cmH_2O, there is likely minimal, if any, effect on the diastolic properties of the heart [43, 44].

In addition, lung volume beyond functional residual capacity [FRC] increases the calculated pulmonary vascular resistance [45-49] as covered in chapters 2 and 3. This effect is amplified in patients with underlying destruction and reduction of pulmonary vasculature cross-sectional area [50]. Recall that the normal pulmonary circulation can adapt to large changes in cardiac output by recruitment and dilatation of the pulmonary vascular bed [51]. Accordingly, there is evidence that lung volume reduction surgery improves right ventricular function, putatively, because removing emphysematous lung decreases the impedance of the pulmonary arterial tree [52-55]. On the Guyton Diagram, dynamic hyperinflation is modelled by flattening of the right ventricular cardiac function curve slope; functional tricuspid regurgitation imitates this effect as well. Bending the cardiac function curve downwards elevates right atrial pressure and reduces the operating point of the Guyton diagram [figure 3].

Ventricular Interdependence and Left Ventricular Loading

As the right and left ventricles share a septum, muscular free wall fibres and the pericardium, the volume of one chamber is inexorably and inversely related to the other [56-58]. Importantly, septal hypertrophy – often observed in chronic lung disease patients – diminishes diastolic ventricular interdependence as discussed in chapter 3 [59-61]. While some studies of left ventricular [LV] ejection fraction do not reveal impaired LV function during exercise in COPD patients [62-65], early studies of the ejection fraction were not reliable indicators of LV diastolic function. In patients with even mild pulmonary hypertension, there is clear impairment of LV diastolic function when pressure-volume curves are generated [66, 67]. Interestingly, in patients with no evidence of air-trapping, exercise increased the pulmonary artery occlusion pressure [Ppao], but the rise of the Ppao was directly related to right ventricular pressure and unrelated to esophageal pressure [i.e. intra-thoracic pressure]. The authors concluded that ventricular interdependence has significant clinical implications – upwards of 5 mmHg of the left ventricular filling pressure was secondary to right ventricular impingement [68]. Therefore, increased lung volume does impair LV diastolic function, if not by direct compression of the LV, then by parallel effects of the enlarging right ventricle [RV] [69-71].

The capacitance of the pulmonary vascular bed is greatest when calculated resistance is at its nadir, that is, at FRC [72, 73]. Above FRC, capacitance of the vascular bed falls, so each tidal volume shifts the pulmonary venous return curve

rightwards – transiently – much as the systemic venous return curve is shifted when the abdomen is pressurized [26, 27].

To the extent that pulmonary hyperinflation decreases ventricular transmural pressure and shrinks the ventricular cavity, LV afterload is reduced. However, in patients who are euvolemic or hypovolemic – as are many patients with obstructive airways disease exacerbation – reduced preload may predominate [1, 74].

Changes in Intra-thoracic Pressure

Mechanism and Values

During an exacerbation of obstructive airways disease, dynamic hyperinflation may cause high lung volume. While this tends to lower airway resistance, pulmonary and chest wall compliances are diminished at high volume. This is illustrated by greater separation between the lung and chest wall compliance curves on the Campbell diagram [2, 75]. Consequently, both work of breathing and pleural pressure change is greater [76, 77]. In status asthmaticus, pleural pressures have been documented between -20 to -40 cm H_2O on inspiration to +7 to +10 cm H_2O during expiration [78-80]. During an emphysema exacerbation, these values typically fall between - 20 and + 20 cm H_2O [17], but can vary greatly [81, 82]. These abnormalities are easily gleaned from the Campbell diagram [83]; both resistive and elastic work of breathing are elevated [figure 2 - see also chapter 1]. If the Campbell and Guyton diagrams are analyzed on the same graph, with the x-axis representing pressure, the effects of altered lung volume and intra-thoracic pressure upon the cardiovascular system are considered in greater detail.

Systemic Venous Return

The right atrium is a compliant structure exposed to the intra-thoracic pressure or pleural pressure [84]. Changes in pleural pressure, therefore, have acute effects on systemic venous return. Because the gradient for venous return to the right heart is typically less than 5 mmHg and, over time, venous return is equivalent to cardiac output, then very small changes in the downstream pressure [i.e. right atrial pressure] significantly influence the circulation [85]. Consequent to inspiration, a leftwards, parallel shift of the cardiac function curve along the venous return curve demonstrates how the operating point of the system and, therefore, cardiac output rises [86, 87]. However, because of collapsing great vessels at Pcrit, the rise of the system's operating point is finite – the plateau of the venous return is reached. Collapse of the great vessels normally occurs between -4 and -8 cm H_2O which are typical values during quiet, tidal breathing [88-91]. In patients with COPD exacerbation, IVC collapse can limit cardiac output [30]. Further, activation of

abdominal muscles during expiration pressurize the abdomen and increase the resistance to venous return. This diminishes the slope of the venous return curve and is dependent upon pre-existing volume status [92-94], as described in chapter 3.

Notably, the right ventricular preload, or right ventricular end-diastolic volume, may be estimated by the ventricular transmural pressure. On the Guyton diagram, the x-intercept of the cardiac function curve approximates the intra-thoracic or pleural pressure as this is the pressure within the right atrium when both cardiac output is zero and systemic venous return is prevented from entering the thorax. Therefore, the distance between the x-intercept of the cardiac function curve and the intra-luminal right atrial pressure graphically represents the transmural filling pressure [86]; this has been discussed in both chapter 2 and 3. In patients with an exacerbation of COPD, it is the transmural pressure of the right heart which best approximates right ventricular volume or preload [42]. Graphically, increased right ventricular transmural pressure can only raise the operating point – and therefore cardiac output – when both the venous return curve and cardiac function curves intersect at their steep sections.

Right Ventricular Loading

As described above with respect to venous return, lower intra-thoracic pressure favours right ventricular preload augmentation [42]. The normal respiratory variation in right ventricular output is greater than that of the left ventricle and this is due to the changes in intra-thoracic pressure with respect to the systemic venous return curve [95, 96]. During forced expiration with positive pleural pressure, the opposite occurs. As the cardiac function curve shifts rightwards relative to venous return, the transmural pressure falls despite rising right atrial pressure. As well, the operating point of the Guyton diagram falls and so too does cardiac output [97, 98]. Fluctuating pleural pressure during inspiration and expiration, therefore, has conflicting effects on cardiac output. While expiration is prolonged with acute broncho-obstruction, cardiac output is generally increased in status asthmaticus [99]. In patients with emphysema and forced hyperventilation, cardiac output typically remains stable, though there can be extremely variable cardiovascular responses depending on underlying ventricular function [37, 100, 101].

As detailed in the previous section describing the hemodynamic effects of lung volume, with acute broncho-obstruction, the right ventricular afterload rises secondary to heightened transpulmonary pressure [49]. Yet, there is evidence suggesting that RV afterload is increased with Mueller maneuver [102, 103]. As described in chapter 3, Mueller's maneuver is diminished pleural pressure with stable lung volume. Yet the mechanism by which this augments RV outflow impedance is not entirely clear. Ostensibly, systolic ventricular interdependence [104], reflection of elevated left ventricular end-diastolic pressure across the pulmonary vasculature [68] or an increase in the RV radius of curvature [105, 106] are all causes [figure 4]. The effect of amplified RV afterload is accentuated by RV

ischemia [70, 71]. This is further discussed in chapter 10 with respect to pulmonary embolism physiology.

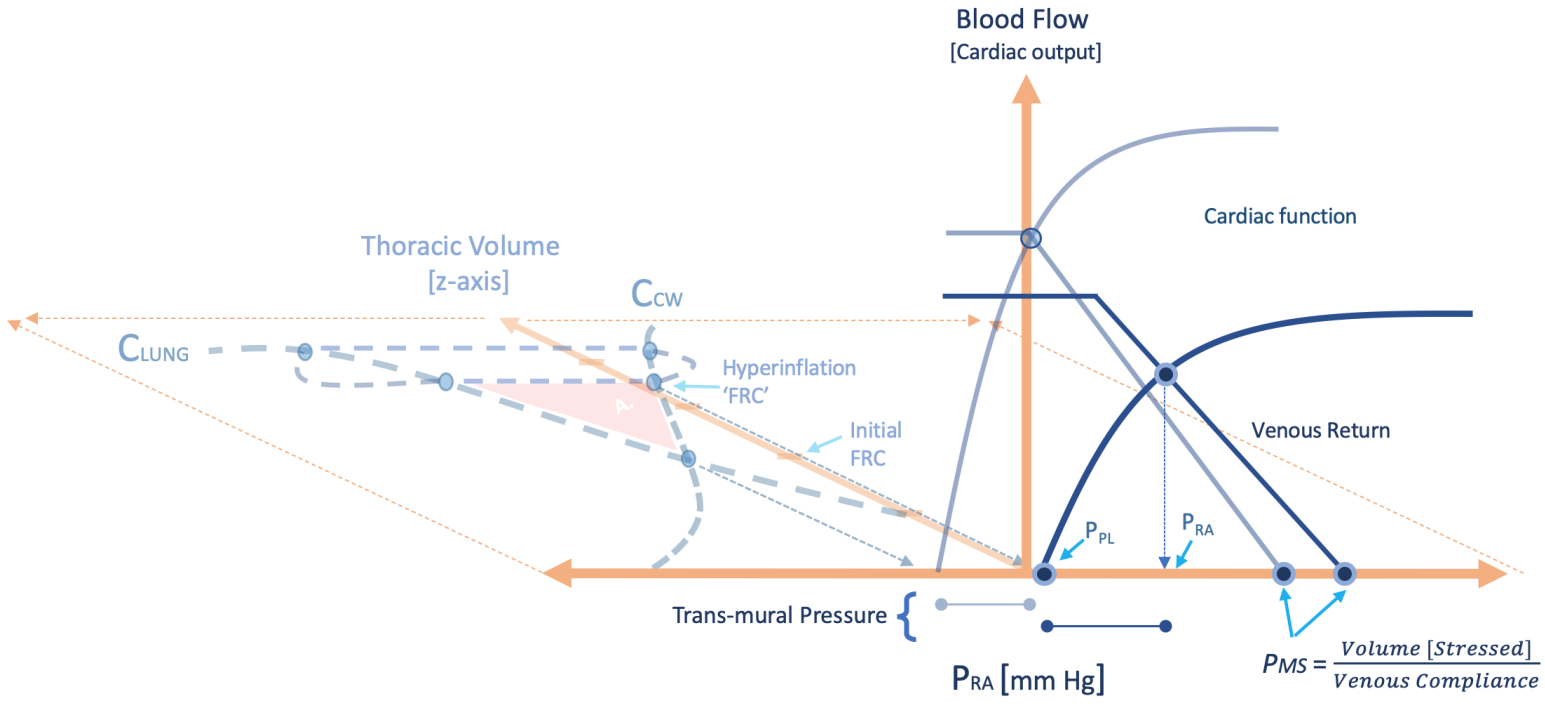

Figure 4: Auto-PEEP & the heart-lung interaction diagram. As in figure 3, the translucent venous return and cardiac function curves represent baseline state at a normal functional residual capacity [FRC on z-axis]. With hyperinflation, lung volume rises on the z-axis which raises pleural pressure along the chest wall compliance curve [Ccw] to the elevated FRC. This shifts and bends the cardiac function curve as described. It also changes the venous return curve as described in the text. The intersection of the venous return and cardiac function curve marks the operating point - defining the right atrial pressure [x-axis] and cardiac output [y-axis]. Note the fall in cardiac output and rise in right atrial transmural pressure [dumbbells below x-axis]. Pms is mean systemic pressure; Ppl is pleural pressure; Pra is right atrial pressure. Clung is lung compliance. See also figures 2 & 3.

Ventricular Interdependence and Left Ventricular Loading

Changes in intra-thoracic pressure may have conflicting effects upon left ventricular preload. As discussed in chapter 3, in the absence of changing lung volume [e.g. during Mueller or Valsalva] the left ventricle is affected independently by both diastolic and systolic events [107-109]. There is evidence that these phenomena play a role in exacerbations of obstructive airways disease. A large decrement in pleural pressure on inspiration tends to raise right ventricular volume and, therefore, impair left ventricular compliance [68]. The opposite is favoured during expiration. Again, these effects are modulated by the relative compliances of the ventricular free walls to the inter-ventricular septum [60]. Because any change in intra-thoracic pressure affects the pulmonary vasculature and left atrium equally, there is no change in the gradient for pulmonary venous flow when there is no change in lung volume. Graphically, therefore, the relationship between the pulmonary venous return curve and the left ventricular function curve is stable. Consequently, if there is change in intra-thoracic pressure relative to atmosphere with stable lung volume, then the observed variation of intra-vascular pressure [e.g. when reading a typical ICU pressure monitor] does not indicate a true difference in the venous driving pressure to the left heart. This is discussed in more detail in chapter 7.

Nevertheless, during acute broncho-obstruction, lung volume does increase, as explained above. In this situation, the left ventricle is rendered less compliant by both expansion of the right ventricle and the left lower lobe [37, 102, 110]. Thus, pulmonary venous return is retarded by compression of the left ventricle between its septum and free wall. As well, this augments wall stress upon both the anterior and posterior left ventricular walls which could exacerbate local ischemia – especially if there is focal coronary flow limitation [106]. Indeed, changes in intra-thoracic pressure have been used to induce focal wall motion abnormalities and diagnose coronary disease [111-113]. To model this on the Guyton diagram, diminished intra-thoracic pressure flattens the left ventricular cardiac function curve secondary to acute diastolic dysfunction; the result is smaller cardiac output at greater left atrial pressure. Again, without changing lung volume, there is no deviation of left atrial transmural pressure as a consequence of altered pulmonary venous return. This is because the pulmonary venous return and cardiac function curves do not shift relative to each other; they do, however, change in tandem with respect to atmospheric pressure.

The change in pulmonary venous return as a function of intra-thoracic pressure is mediated primarily by right ventricular output. Because of phase lag between right ventricular filling and pulmonary venous flow, tracking these changes is clinically challenging [114]. Specifically, during acute brocho-obstruction, these changes are large and reciprocal such that during increased intra-thoracic pressure [e.g. during expiration], right ventricular output can fall substantially. As these changes are cyclical – which tends to minimize the hemodynamic impact over time – they do induce notable shifts in beat-to-beat stroke volume variation. This latter point is discussed in more detail in chapter 8 with respect to functional hemodynamics [115]. Thus, the pulmonary venous return curve shifts rightwards relative to the left ventricular cardiac function curve a few cardiac cycles following a large drop in intra-thoracic pressure, but only if the operating point of the right ventricle is on the steep portion of its function curve and/or not limited by great vein collapse. This is because inspiration augments right ventricular output by the Frank-Starling mechanism which then charges the pulmonary vasculature with blood. Conversely, the pulmonary venous return curve shifts leftwards relative to the left heart function curve a few cardiac cycles following increased intra-thoracic pressure – as the pulmonary vasculature is under-filled by the right ventricle.

Large intra-thoracic pressure variation during broncho-obstruction also mediates left ventricular afterload. Indeed, both Wead and Norton, in addition to Scharf and colleagues, concluded that an exaggerated fall in intra-thoracic pressure augments left ventricular afterload and likely plays the predominant role reducing LV output – beyond that of ventricular interdependence [110, 116]. The mechanism of the aforementioned was covered in chapter 3. Briefly, because the great veins collapse when the intra-thoracic pressure falls lower than - 8 mmHg [91], the tendency to enlarge the right ventricle is minimized secondary to venous return limitation; consequently, LV afterload effects predominate [33]. Nevertheless, in patients with cor pulmonale and high baseline right atrial pressure, a greater fall in intra-thoracic pressure can occur before the distended great veins collapse [27]; in such patients, ventricular interdependence may still play a prominent role in reducing LV output

[117, 118]. With respect to LV afterload, as the pleural pressure drops, LV ejection is impeded secondary to increased left ventricular transmural pressure [119]. To the extent that the left ventricular cavity is diminished by lung expansion and auto-PEEP, this afterload effect is minimized as the left ventricle's radius of curvature shrinks during systole despite the large transmural pressure gradient [1]. In states of super-imposed systolic heart failure – when the left ventricle has a distended radius of curvature – the effect of pleural pressure on afterload is more pronounced during both inspiration and expiration. In line with this physiology, lung volume reduction surgery has been observed to ablate swings in intra-thoracic pressure [52, 54] and improve left ventricular performance [120]. On the Guyton diagram, inspiratory fall in intra-thoracic pressure flattens the slope of the left ventricular function curve, while an expiratory rise in intra-thoracic pressure causes the opposite.

Spontaneous Ventilation

The previous sections artificially separated intra-thoracic pressure from lung volume changes to refine the underlying mechanisms of respiratory-circulatory interaction. During an acute attack of broncho-obstruction, however, lung volume expands as intra-thoracic drops during inspiration while expiration is the converse. Putting this together graphically, one sees that inspiration left-shifts the right ventricular cardiac function curve while simultaneously flattening its slope. These changes occur because the right atrium is exposed to the intra-thoracic pressure and elevated lung volume impairs right ventricular afterload, respectively. If auto-PEEP is generated, the end-expiratory intra-thoracic pressure shifts rightwards along the chest wall compliance curve on the Campbell diagram [83]. This tends to shrink right atrial transmural pressure, preload and cardiac output [115]. To some extent this is overcome by large inspiratory decreases in intra-thoracic pressure. Yet auto-PEEP, like extrinsic PEEP, alters the systemic venous return curve by lowering its maximal value; the venous return curve plateau is the result of collapse of the great veins at the entrance of the thorax [121]. If maximal venous return is hindered, no inspiratory decrease in intra-thoracic pressure will compensate for impaired venous return and hemodynamic collapse may occur [122]. During forced expiration, enhanced intra-thoracic pressure pushes the right ventricular function curve rightwards with respect to the systemic venous return curve; accordingly, right atrial transmural pressure, preload and the operating point on the Guyton diagram fall. The expiratory decrease in right ventricular afterload mitigates this effect somewhat [figure 5].

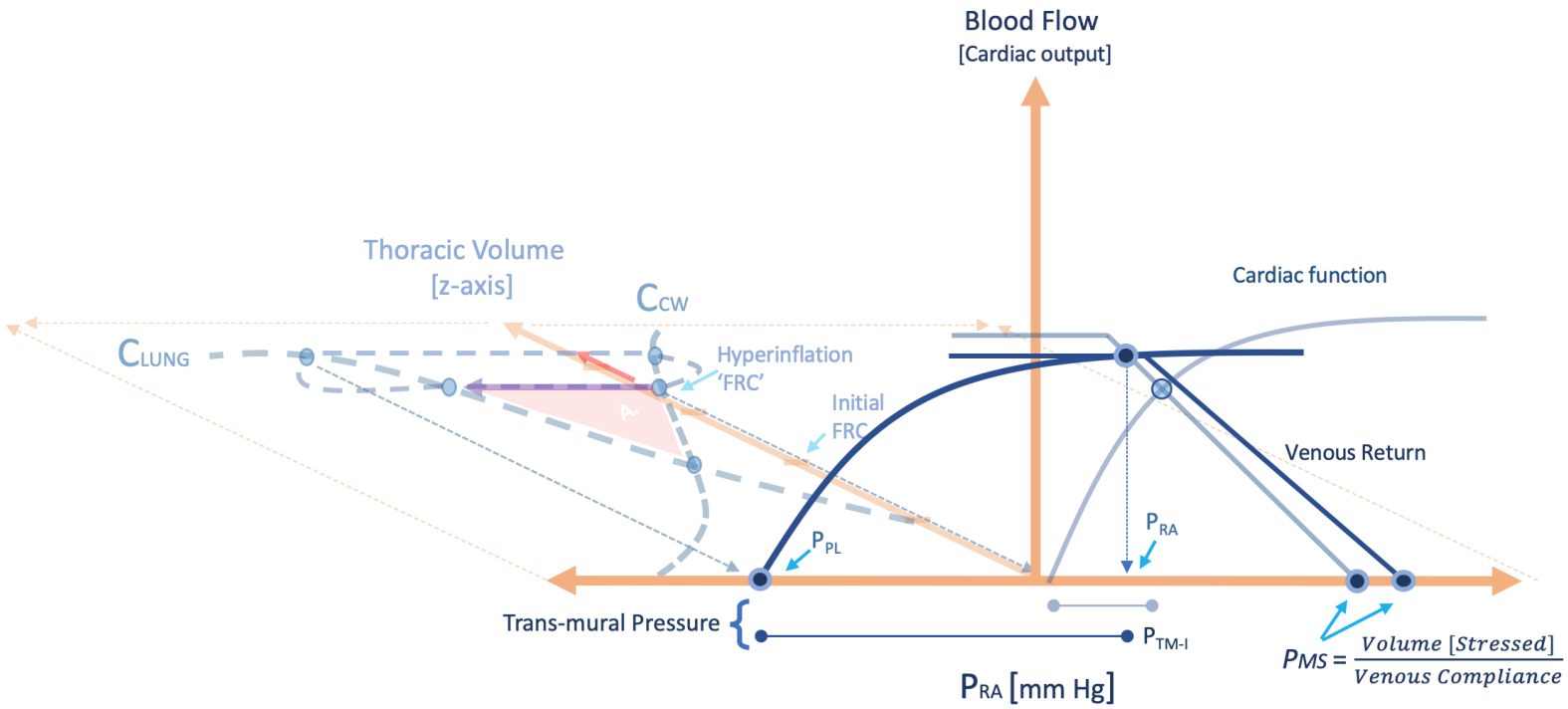

Figure 5: The effect of spontaneous inspiration during dynamic hyperinflation. The tidal volume is marked by the red arrow on the z-axis and intrathoracic pressure falls along the lung compliance [Clung] curve. Note the inspiratory pressure threshold that must be generated before the rise in lung volume [the purple arrow atop the triangle A]. The decrease in intra-thoracic pressure pulls the cardiac function curve leftwards and bends its slope; the inspiratory trans-mural pressure [Ptm-I] rises; cardiac output on y-axis rises minimally given increased afterload and resistance to venous return. Baseline characteristics are translucent and begin from 'hyperinflation FRC'. Pra is right atrial pressure; Pms is mean systemic pressure; Ppl is pleural pressure; FRC is functional residual capacity; Ccw is chest wall compliance. See also figure 4.

Like the right ventricle, the left ventricular cardiac function curve shifts downwards during spontaneous inspiration, but for different reasons. As above, this may result from impaired diastolic properties. During inspiration the left ventricle is affected by both right ventricular filling and left lower lobe expansion [37, 40, 41, 58, 123, 124]. These effects are pronounced to the extent that lower lobe gas-trapping occurs. Further, increased afterload during left ventricular systole bends its function curve downwards during inspiration [107, 119]. The relationship between pulmonary venous return and the left ventricular function curve during inspiration is complicated. Increased lung volume favours right shift of the pulmonary venous return curve relative to the left ventricular function curve, but this may be tempered by the preceding expiration if right ventricular output was significantly impaired by the elevated intra-thoracic pressure. The aforementioned effects tend to be reversed during expiration. Regardless, pulmonary venous return is facilitated when the lungs are in zone III physiology [72, 125].

As above, the cyclical effects of inspiration and expiration are transient and tend to cancel each other out during an acute exacerbation of broncho-obstruction. However, the mechanisms are important to understand when considering beat-to-beat variation in cardiac output during the respiratory cycle. As gleaned from the Guyton diagram, the most powerful mediator of cardiac output is the generation of auto-PEEP; this induces steady-state change in the systemic venous return curve and, therefore, cardiac output regardless of inspiratory cycle phase [27].

Mechanical ventilation is not simply the reverse of spontaneous ventilation [106, 126]. In both states, lung volume rises with inspiration, so the effects of high lung volume are similar for both. By contrast, passive mechanical ventilation [i.e. no spontaneous efforts are made] raises intra-thoracic pressure during inspiration [74]. As discussed in chapter 1, the increase in proximal airway pressure – as measured on the ventilator – does not equate with intra-thoracic pressure; the latter is attenuated by both airway resistance and pulmonary compliance. The intra-thoracic pressure follows the chest wall compliance curve such that for similar pulmonary characteristics, a given proximal airway pressure is associated with larger intra-thoracic pressure if the chest wall is less compliant [127-133].

If the Campbell diagram is simultaneously analyzed with the compliance curve of the respiratory system [the lung and chest wall together] then the transpulmonary pressure during mechanical ventilation of the completely passive patient is qualitatively obtained [figure 6]. The transpulmonary pressure is the lateral distance between the static compliance curve of the respiratory system [which estimates end-expiratory alveolar pressure] and the chest wall compliance curve [which estimates end-expiratory pleural pressure]. The transpulmonary pressure is the pressure gradient that determines lung volume at any given pulmonary compliance.

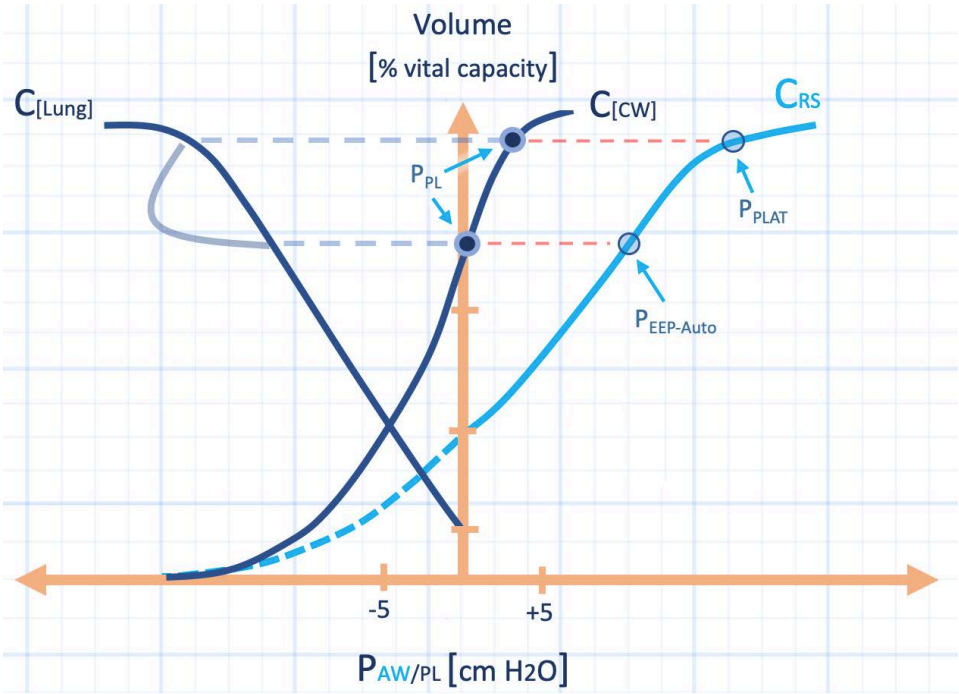

Figure 6: Simultaneous analysis of respiratory system compliance curve [Crs] on Campbell diagram [see chapter 1] during passive mechanical inspiration. Dynamic hyperinflation moves lung volume higher along y-axis [see figure 2]. This generates auto-PEEP on the respiratory system compliance curve. The red dotted line is the trans-pulmonary pressure. A delivered tidal volume increases the pleural pressure along the passive chest wall compliance curve [Ccw] which increases the airway pressure to the plateau pressure [Pplat]. Clung is lung compliance curve. The dashed portion of the Crs is left out in many figures for clarity. Paw is airway pressure; Ppl is pleural pressure. This figure becomes the x-z plane of figure 7.

This analysis falls apart when the patient is lightly sedated and generating inspiratory efforts [i.e. non-passive or non-adapted with the ventilator]. In this situation, the pleural pressure will not follow the chest wall compliance curve because respiratory muscle activity alters the pleural pressure. The magnitude of this effect is very difficult to estimate clinically even with the presence of an esophageal balloon. The direction of change of pleural pressure may be judged by watching the direction of pressure change on a pulmonary artery catheter during inspiration and expiration [134].

Systemic Venous Return

Typically, an average adult tolerates large minute ventilation without generating significant air-trapping [135]. Because of prolonged time-constants in obstructive airways disease, air-trapping and auto-PEEP are much more likely to occur [23]. Auto-PEEP reduces maximal venous return and impairs cardiac output by diminishing the operating point of the cardiovascular system [34, 35]. While increased intra-thoracic pressure and lung volume augment Pmsf – which shifts the systemic venous return curve rightwards – they also raise both the resistance to flow and the Pcrit; auto-PEEP and extrinsic PEEP from the ventilator will have identical hemodynamic consequences [1]. The degree to which the mean systemic pressure and Pcrit rise is determined by multiple factors. Abdominal pressurization, activation of the sympathetic nervous system and shifting blood volume from the thoracic to systemic vascular compartments all mediate the rise in Pmsf [24-27, 36, 121, 136]; whereas the relative increase in abdominal pressure to intra-thoracic pressure determines IVC collapse [32] and therefore Pcrit and maximal venous return. This physiology, however, is probably more complicated in humans than in the canine model [28, 137, 138] because unlike dogs, humans lack a true intra-thoracic IVC. During passive, mechanical inspiration, the systemic venous return curve is transiently shifted rightwards, but the resistance to venous return is altered based on pre-existing volume status [92-94]. As previously mentioned, at very high lung volumes, the diaphragm can act as a sphincter upon the IVC which increases resistance to venous return [30].

Right Ventricular Loading

During mechanical insufflation of the lungs in a fully adapted patient, the increase in intra-thoracic pressure shifts the right ventricular cardiac function curve rightwards as discussed in previous sections. The extent to which the slope of the curve flattens largely depends upon the afterload imparted by lung volume [98]. This is accentuated in emphysema from obliteration of the pulmonary vascular bed [118, 139]. Additionally, if chronic cor pulmonale is present [122, 140, 141], right ventricular function is impaired [142-144]. The ultimate effect of a mechanical

breath, therefore, is to diminish right ventricular preload and cardiac output at a higher right atrial pressure. Because of the contemporaneous right shift of the venous return curve, diminished cardiac output may be offset to some extent as long as right atrial pressure remains above Pcrit. There is no good evidence to suggest that positive intra-thoracic pressure, per se, reduces right ventricular afterload, though to the degree that it improves oxygenation [145-147] and mitigates large negative swings in intra-thoracic pressure [103], pulmonary arterial input impedance can improve [figure 7].

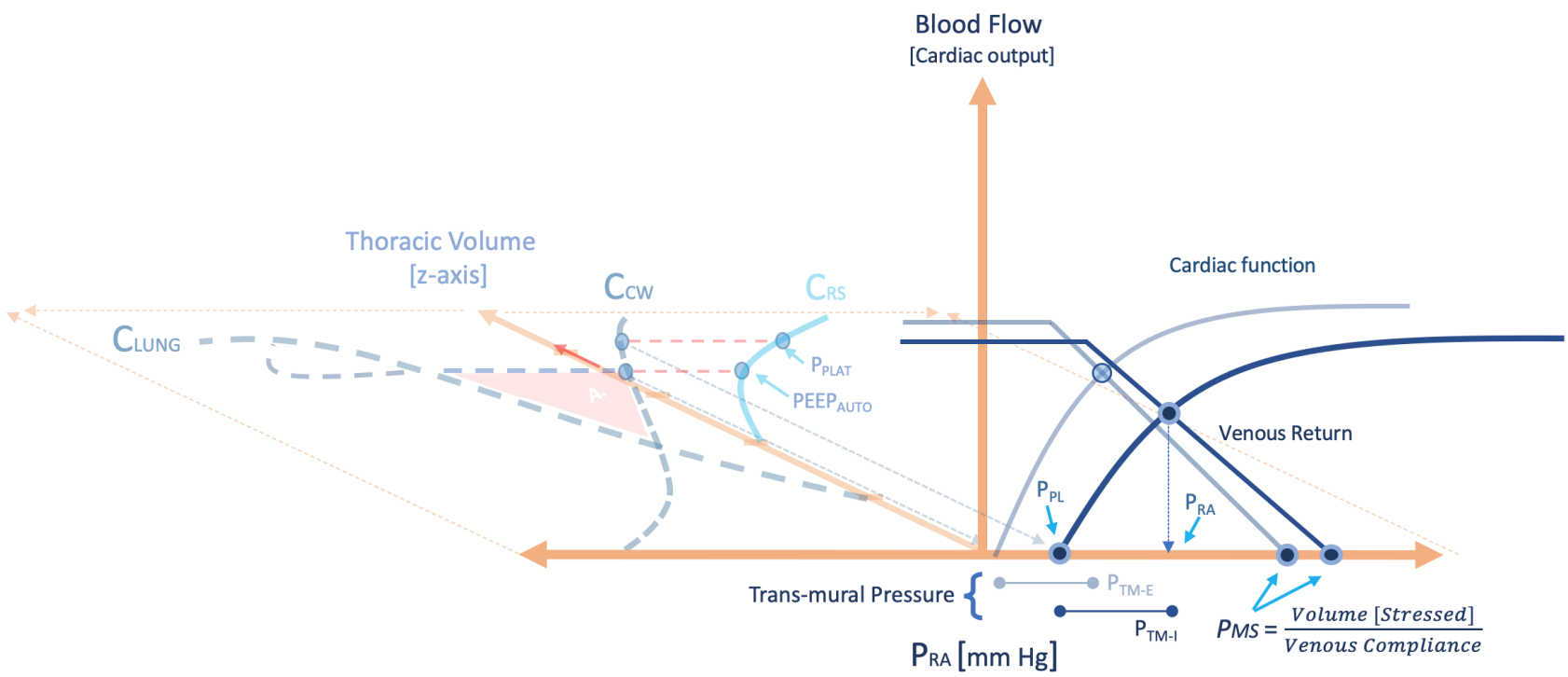

Figure 7: A tidal breath delivered to a patient with dynamic hyperinflation. The tidal volume is the red arrow on the z-axis. Airway pressure rises along the respiratory system compliance curve [Crs] to the Pplat and pleural pressure rises along the chest wall compliance curve [Ccw] which shifts the cardiac function curve rightwards. The inspiratory trans-mural pressure [Ptm-I] rises slightly above the expiratory value [Ptm-E]. Pms is mean systemic pressure; Pra is right atrial pressure; Ppl is pleural pressure; Clung is lung compliance. Note the cardiac output falls slightly on inspiration [y-axis] despite the rise in the trans-mural pressure.

Ventricular Interdependence and Left Ventricular Loading

The effect of mechanical ventilation on the left ventricle, in broncho-obstructive states, is complicated. There are conflicting factors which both transiently augment and restrict left ventricular filling and output. The cyclical changes induced by positive pressure breathing may include inspiratory improvement in left ventricular diastolic filling via ventricular interdependence if the RV shrinks in size. By contrast, there could be impaired inspiratory diastolic filling due to lower lobe lung expansion or right ventricular distention if RV afterload enlarges. While there is no study demonstrating which effect predominates, ventricular interdependence can account for changes in LVEDP up to 5 mmHg [68] as previously mentioned. Inspiratory RV distention is probably favoured when there is poor baseline RV function [70, 71]. In volume-overloaded patients, for example with chronic cor pulmonale and RV congestion, application of positive pressure might transiently

augment LV performance. By contrast, gas trapping of the lower lobes with the initiation of mechanical ventilation may impair left ventricular output by inducing diastolic incompetence of the left ventricle; it is difficult to predict whether an inspiratory mechanical breath will augment or impair LV stroke volume. Additionally, rising lung volume enhances pulmonary venous flow [125], especially if the preceding expiration improved right ventricular filling. To the extent that the LV is sensitive to reduced afterload, mechanical ventilation also improves left ventricular output during an inspiratory breath. However, in severe obstructive airways disease, patients often have small, hypertrophied left ventricles [148-150]; this makes inspiratory afterload reduction less significant.

Steady-state effects on the left ventricle depend largely on the amount of generated auto-PEEP or applied PEEP desired by the clinician. It is important to recognize that PEEP exerts significant hemodynamic effects [43, 44, 46, 69-71, 151-153] because, in contrast to the transient effects of tidal respiration, the consequence of PEEP is steady-state [27]. By series-effects, reduced right ventricular output – from either diminished venous return or heightened pulmonary arterial impedance – translates to leftward movement of the pulmonary venous return curve relative to the left ventricular function curve. In these patients, bedside echocardiography can help delineate the hemodynamic impact of PEEP on biventricular function [133, 154, 155] and therefore guide management. Note that treating auto-PEEP requires a decrease in the ventilator-set minute ventilation to allow lung units with high time-constants to empty [23, 122]. The application of extrinsic PEEP to treat auto-PEEP is beneficial only when patients initiate inspiration as the extrinsic PEEP improves trigger sensitivity; this was discussed in chapter 1.

Asthma versus COPD

It is generally accepted that the asthmatic lung pressure-volume curve is shifted upwards in parallel compared to the normal pulmonary pressure-volume relationship. Because of hyperinflation, the change in pleural pressure during spontaneous inspiration is typically greater than expiration. This is also due to increased pulmonary elastic recoil that occurs at high lung volume in asthmatic lungs; this facilitates expiratory flow [79, 156]. Emphysema, by contrast, typically has equally abnormal spontaneous inspiratory and expiratory changes in pleural pressure. This is because high volume breathing coupled with loss of elastic recoil demands greater expiratory pleural pressure [157] as compared to asthma. This physiology is explained by the equal pressure point theory which predicts that 'waterfall-like' physiology plays a role in emphysema during expiration [158, 159]. In other words, collapse of compliant airways under positive pleural pressure renders expiratory flow independent of aboral airway pressure during expiration. Despite these differences between classical asthma and emphysema, there is considerable anatomic, radiographic and physiologic overlap between the two [160-162]. It is reasonable to assume that, during acute exacerbation, the cardiopulmonary

interaction between the two disease states may be similar aside from the smoking-related co-morbidities found in those with underlying COPD.

Systolic Heart Failure

Systolic dysfunction of the left ventricle can be described by flattening of its function curve. On the Guyton diagram, the operating point is therefore decreased [i.e. lower cardiac output] at higher left atrial filling pressure [163]. On the Sagawa diagram, the end-systolic pressure volume relationship is shifted down and to the right which reduces stroke volume at higher end-diastolic pressure [164] [see chapter 2]. The high left ventricular filling pressure impairs pulmonary venous return and favours excess pulmonary lung water. Before discussing the effects of pulmonary congestion upon cardiac function, an examination of systemic venous return in the setting of heart failure is presented.

Systemic Venous Return

In states of salt and water excess, the venous return curve is shifted rightwards in a parallel fashion. As the mean systemic or circulatory filling pressure [Pmsf – see chapter 2 for distinction] is directly related to the total blood volume of the venous capacitance beds, excess blood volume increases the Pmsf [figure 8].

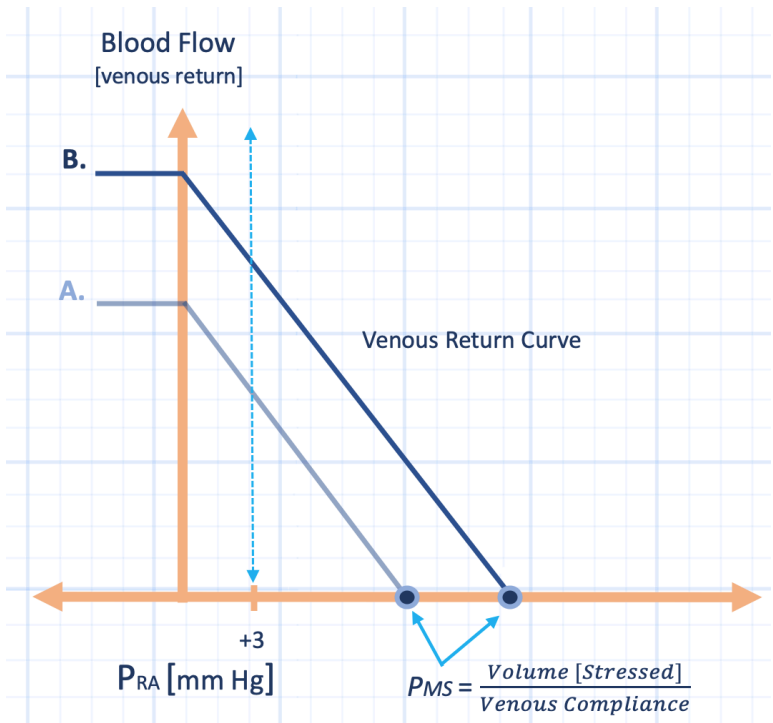

Figure 8: Effect of increased blood volume on venous return curve. The mean systemic pressure [Pms] rises [curve A to B]. For the same right atrial pressure [Pra] venous return [y-axis] is greater - vertical blue dotted line.

Accordingly, the x-intercept of the venous return curve moves rightwards leading to increased venous return, maximal venous flow and the venous return curve withstands increased resistance because the diaphragm shifts caudad [92, 94]. Importantly, the elevated right heart filling pressure in severe heart failure is determined not simply by poor cardiac function, but also because of excess blood volume The right atrial pressure is determined by the intersection of cardiac and circuit function! This principle was demonstrated decades ago in moribund patients who were catheterized shortly before and following death [i.e. zero blood flow]. The right atrial pressure changed little after the heart stopped beating illustrating that mean systemic filling pressure and right atrial pressure were nearly equal while the heart was still beating [165-167]. The mean systemic filling pressure is discussed in additional detail in chapter 10.

Pulmonary Congestion

Pulmonary edema formation has been studied by gradually elevating the left atrial pressure followed by freeze-fracture microscopy. While degrees of excess lung water are described, these histologies do not necessarily imply a temporal sequence in vivo [168, 169].

Mechanism and Effects

With increased left atrial pressure, blood volume is redistributed into the pulmonary vasculature. While this increases overall pulmonary blood volume, decreased pulmonary vascular compliance – which may be present in the face of chronic heart failure – tempers this effect [170]. This early state is typically referred to as 'pulmonary congestion' as pulmonary blood volume is increased without extravasation of fluid into the interstitial space. Radiographically, pulmonary congestion is described as vascular 'cephalization;' blood is distributed against gravity to the upper lobes [171-173]. If pulmonary venous pressure remains elevated, water and small solutes leak into the alveolar interstitium. However, fluid does not remain within the alveolar interstitium because there is a flow gradient towards the hilum [174]. The bronchovascular interstitium is composed of a highly compliant matrix that curbs pressure elevation. Additionally, the bronchovascular interstitium is exposed to pleural pressure which is lower than alveolar interstitial pressure. As a consequence, the bronchovascular interstitium acts as a fluid sump that may contain upwards of 500 mL of fluid before alveolar interstitial edema develops [175]. Once the aforementioned reservoir is eclipsed, alveolar interstitial edema forms. Fluid typically leaks first into the interstitial space between the pulmonary capillary endothelial and alveolar epithelial cells [176, 177].

There is normally a tight junction – impermeable to water and solutes – between alveolar epithelial cells [178]. As a result, even in the presence of alveolar interstitial

edema, fluid does not readily penetrate the alveolar space and impair gas exchange. However, with increasing alveolar interstitial pressure, these junctions can become porous and the reflection coefficient of the Starling equation [σ] changes from nearly 1 [impermeable] to zero [176]. Recall the Starling equation predicts the net filtration of fluid and proteins across a semi-permeable membrane.

$$(1)\quad Net\ filtration\ =\ k\ x\ [(Pmv\ -\ Ppmv)\ -\ \sigma(umv\ -\ upmv)]$$

Equation 1: The traditional Starling equation. K is the filtration coefficient of the membrane, Pmv is microvascular pressure, Ppmv is the perivascular microvascular pressure, σ is the reflection coefficient of the membrane to proteins, μmv is the microvascular osmotic pressure and μpmv is the perivascular osmotic microvascular pressure. Note, that the revised Starling principle posits that the oncotic gradient is not trans-endothelial, but rather intra-endothelial with the glycocalyx. This is discussed further in chapter 10.

As fluid invades the alveolar spaces, it occurs in an 'all-or-none' manner, also termed 'quantal filling' in that alveoli are either completely flooded or not at all [169, 176]. This 'stage' of lung water is 'alveolar edema' and causes the greatest physiological derangements.

In all phases of excess pulmonary lung water, compliance is decreased and airway resistance increased [170, 179-184]. These abnormalities occur via a variety of mechanisms, however, the greatest aberration of both pulmonary compliance and resistance occurs with frank alveolar edema [180]. Ostensibly, loss of surfactant activity, alveolar volume and plugging of the airways from bubble froth are the primary mechanisms [figure 9].

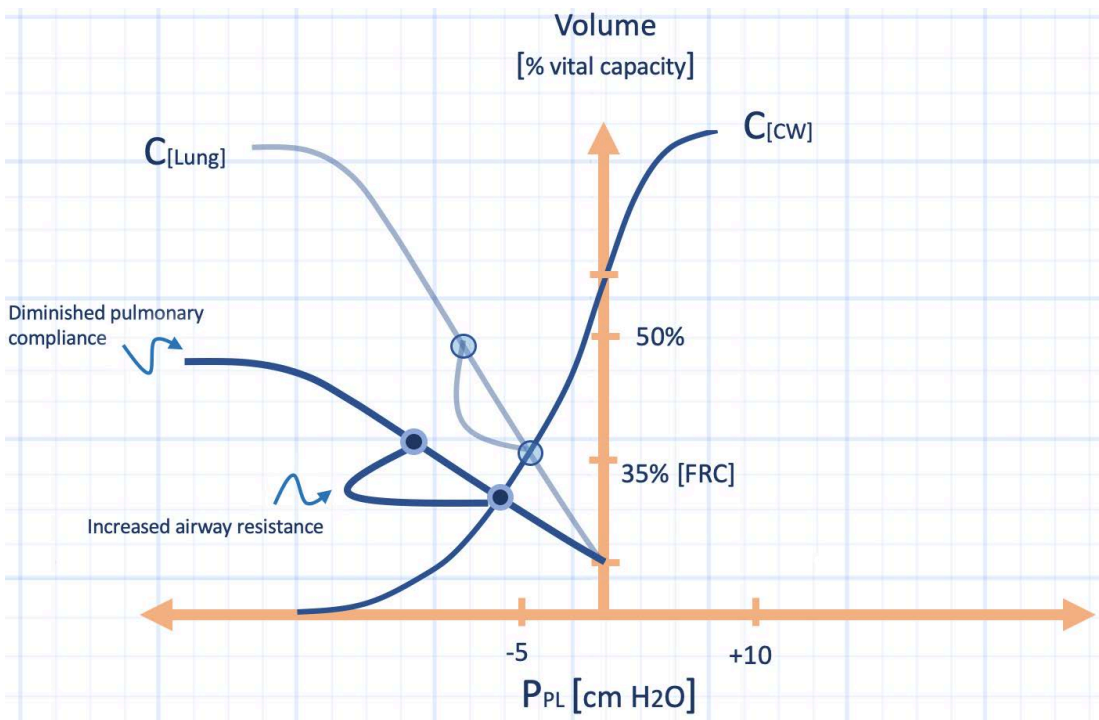

Figure 9: The effect of pulmonary edema on the Campbell diagram. Lung compliance [Clung] falls and resistance rises. Ppl is pleural pressure in centimetres of water [cm H_2O]. FRC is functional residual capacity; Ccw is chest wall compliance. This becomes the x-z axis in figure 10.

Increased Thoracic Volume

Excess pulmonary lung water increases intra-thoracic volume, but not to the same extent as dynamic hyperinflation in obstructive airways disease. The excess lung water does, however, tend to 'compress' the pulmonary vasculature in a manner mechanistically similar to dynamic hyperinflation. As described below, the two means by which vascular caliber is reduced are via interstitial edema and pleural effusion [185-187]. The extent to which pulmonary congestion and edema affect abdominal pressure is not known; furthermore it is unknown if edematous lung can directly compress the heart as with gas-trapping [37, 40, 41].

Pulmonary Congestion and Right Ventricular Loading

There is a close correlation between the ratio of upper lobe-to-lower lobe blood flow and pulmonary venous pressure [188, 189]. As above, this is commonly called 'cephalization' of blood flow which is seen in early interstitial edema. Normally, the lower lobes receive the bulk of pulmonary blood flow and this is gravity-dependent [190]. However, with interstitial edema, the lower lobe blood vessels are narrowed while the upper lobe vessels become engorged [185, 186]. The mechanism for this effect is compression of extra-alveolar vessels by interstitial edema or so-called West zone IV physiology. It is thought that the interstitial edema impairs the tethering effect lung volume imparts upon the extra-alveolar vessels. To this end, increasing lung volume can reverse West zone IV physiology to some degree [191, 192]. If interstitial edema and alveolar edema co-exist, hypoxemia from Va/Q mismatching is accentuated as is hypoxemic pulmonary vasoconstriction which also impairs pulmonary vascular blood flow [193, 194].

In addition to West zone IV physiology, the appearance of pleural effusion in cardiogenic pulmonary edema may also affect pulmonary arterial impedance. Pleural effusion is classically thought to inflict restrictive defects on the lungs and chest wall, however, it is not this simple [195]. A pleural effusion may be considered as a space-occupying lesion within the thorax. The extent to which it increases intra-thoracic pressure, alters cardiac loading conditions and results in compressive atelectasis is largely dependent upon the compliance of the chest wall. A poorly compliant chest wall magnifies the compressive effects of the pleural effusion; that is, amplified atelectasis, hypoxemia and cardiovascular embarrassment [196, 197].

Most of the abnormalities described above augment right ventricular afterload. On the Guyton diagram this flattens the right ventricular cardiac function curve [98]; right atrial pressure is elevated for any given pulmonary arterial flow. The increase in intra-thoracic blood volume does not affect right ventricular preload save for the changes in the systemic venous return curve described at the outset of this section. In theory, however, a large pleural effusion confined within a poorly compliant thorax could increase intra-thoracic pressure and shift the right ventricular cardiac

function curve rightwards in a parallel manner, similar to auto-PEEP [198]. The effect of diminished preload is typically blunted by slow progression of the effusions and increased systemic venous return.

Pulmonary Congestion and Left Ventricular Loading

In a manner similar to the systemic venous return curve, the pulmonary venous return curve shifts rightwards as pulmonary blood volume increases. At lung volume beyond FRC, pulmonary venous capacitance decreases and blood is discharged towards the pulmonary veins [125]. This physiology augments left ventricular preload. Note that depending on where the pulmonary venous return curve intersects the LV function curve, increased preload could cyclically augment stroke volume.

The slope of the left ventricular cardiac function curve is flattened via multiple mechanisms and this is often the initiating insult in systolic heart failure. However, this abnormal physiology is exacerbated by volume overload via multiple mechanisms. If right ventricular volume increases by elevated right ventricular preload and afterload, left ventricular compliance can be impaired via ventricular interdependence [58, 123, 199]. Interdependence effects are particularly prominent if the heart is large and expanded against the pericardium and if the inter-ventricular septum is thin and compliant [60, 200]. Acute diastolic dysfunction from excessive interdependence may flatten the left ventricular function curve; that is, any given LV output occurs at higher left ventricular filling pressure [201]. Further, as left ventricular preload becomes excessive, end-diastolic filling pressure increases exponentially without enhanced stroke volume. The reason for this is best gleaned from the Sagawa pressure-volume diagram [164]. With impaired LV inotropy, the end-diastolic pressure volume relationship is much steeper at high filling volume than the end-systolic pressure volume relationship. If this physiology is transposed to the Guyton diagram, the left ventricular cardiac function curve flattens [see also chapter 2] [201, 202].

Changes in Intra-thoracic Pressure

In addition to increased thoracic volume as a result of excessive lung water, cardiogenic pulmonary edema also induces significant changes in intra-thoracic pressure.

Mechanism

The reason for the changes in intra-thoracic pressure can be best visualized via the Campbell diagram [figure 9]. As above, all phases of excess lung water reduce pulmonary compliance, but the most abrupt drop occurs with frank alveolar edema [180, 203]. Diminished pulmonary compliance is illustrated by a down-and-left shift of the pulmonary compliance curve [2, 204]. Additionally, airways resistance also rises, so the dynamic limb of the Campbell diagram is pronounced [179, 205]. The result is that inspiration necessitates a large decrease in intra-thoracic pressure during spontaneous inspiration. These mechanisms were elaborated more fully in chapter 1. For illustrative purposes, cardiogenic pulmonary edema is represented by reduced pulmonary compliance and increased airways resistance with spared chest wall compliance. However, in clinical practice, ascites, obesity and chest wall edema frequently complicate cardiogenic pulmonary edema. The physiology of impaired chest wall compliance is discussed in the context of ARDS below.

Systemic Venous Return

As previously discussed, spontaneous inspiration occurs by generation of a sub-atmospheric intra-thoracic pressure. Because the right atrium is compliant and exposed to the pleural pressure, the inspiratory pleural pressure drop is transmitted to the right atrium. Diminished right atrial pressure facilitates venous return. Further, as the abdomen is pressurized by diaphragm descent, the venous return curve shifts rightwards in a phasic manner. In cardiogenic pulmonary edema, the entire systemic venous return curve moves rightwards on account of increased stressed venous blood volume and adrenergic tone [166, 167]. Thus, inspiration boluses the right heart by increasing the upstream pressure and decreasing the downstream pressure [figure 10].

Right Ventricular Loading

With spontaneous inspiration, the inspiratory drop in intra-thoracic pressure is exaggerated; this left shifts the the right ventricular cardiac function curve relative to the right-shifted venous return curve. Simultaneous analysis with the Campbell diagram reveals that this inspiratory effort is in response to both low pulmonary compliance and increased airways resistance. As the right ventricular cardiac function curve shifts leftwards, the right atrial and right ventricular transmural filling pressures rise; so too does right heart filling volume [95, 97, 98]. Because the systemic venous return curve is right-shifted in states of volume overload, the transmural filling pressure may be pronounced.

For reasons discussed above, pulmonary arterial impedance is high in cardiogenic pulmonary edema. While the act of generating low intra-thoracic pressure, per se, may also increase right ventricular afterload [33, 102, 103], the predominant effect upon right ventricular afterload is likely pulmonary vascular edema. Accordingly,

while the right ventricular function curve moves leftwards, its slope flattens [figure 10]. If the flat portion of the cardiac function curve intersects the venous return curve, there may be little change in the operating point of the Guyton diagram. In this situation, transmural filling pressure rises, but there is no significant change in right ventricular output [206].

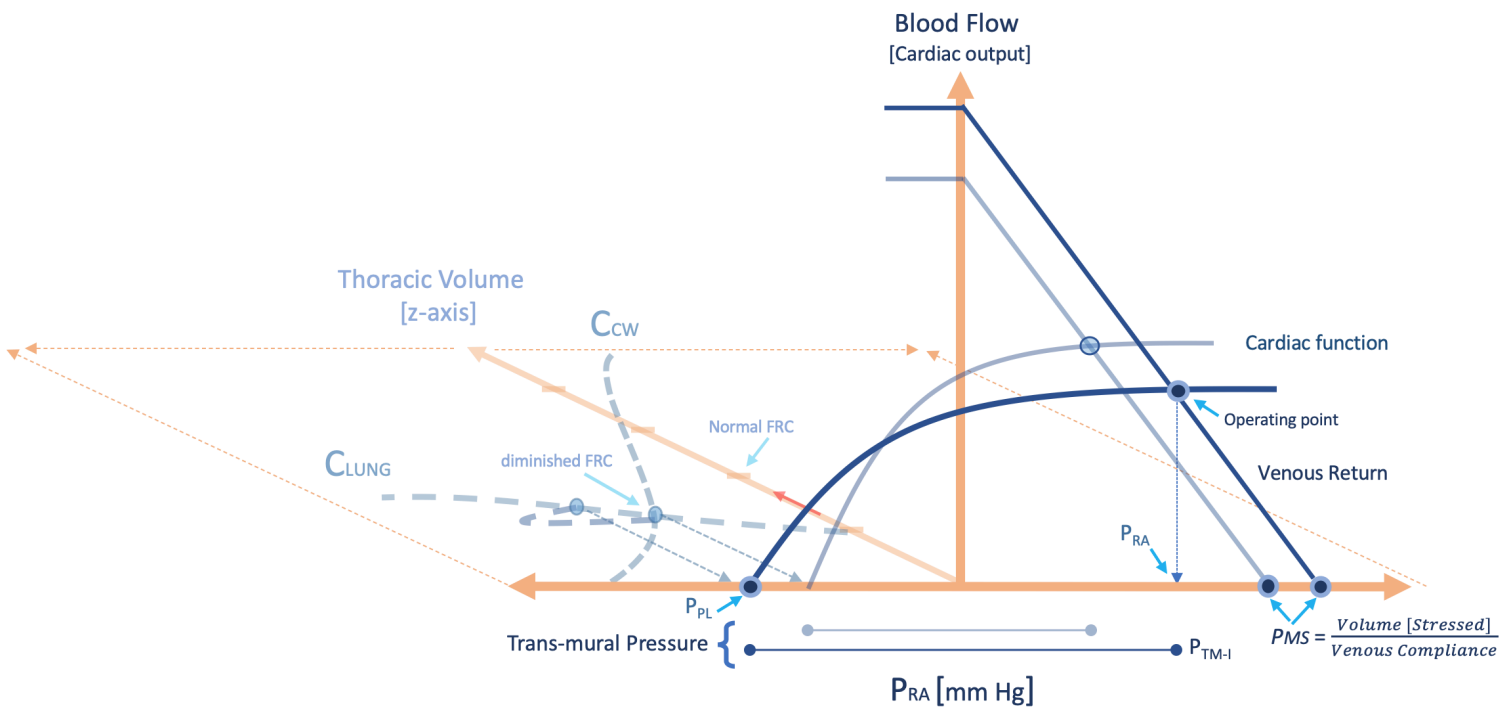

Figure 10: Spontaneous inspiration during cardiogenic pulmonary edema. Tidal volume is the red arrow on z-axis into page. The decrease in lung compliance [Clung] and increase in airway resistance [see figure 9] lower inspiratory intra-thoracic pressure on x-z plane. This pulls the cardiac function curve leftwards and flattens its slope from high afterload. Inspiratory trans-mural pressure [Ptm-I] rises compared to baseline at functional residual capacity [FRC]. The operating point falls - cardiac output falls on y-axis. Pms is mean systemic pressure; Pra is right atrial pressure; Ppl is pleural pressure; Ccw is chest wall compliance; FRC is functional residual capacity.

Ventricular Interdependence and Left Ventricular Loading

A change in intra-thoracic pressure does not, by itself, alter the upstream pressure for pulmonary venous return to the left heart. Without a change in lung volume, the left ventricular cardiac function curve and pulmonary venous return curve shift in unison such that there is no effective change in the pressure gradient between the two. However, in overload states, left ventricular function may be significantly altered by inspiratory increase in right heart volume [105, 199, 207, 208]. Even transient diastolic incompetence diminishes the slope of the LV cardiac function curve. Recall that ventricular interdependence is mitigated when septal compliance is poor, but augmented when ventricular free wall compliances are impaired [200]. The latter tends to occur when the heart is large and dilated as the pericardium approaches its elastic limit.

There is robust evidence demonstrating that decreased intra-thoracic pressure heightens left ventricular afterload both during systole [107, 109] and, potentially, during diastole to the extent that low intra-thoracic pressure retains blood within

the thoracic aorta [108, 209]. As the pressure surrounding the left ventricle and thoracic aorta fall relative to the extra-thoracic compartment, the transmural pressure increases which augments the stress experienced by the left ventricle during systole. The dilated LV is particularly susceptible to increased systolic wall stress [1]; indeed, this has been demonstrated empirically [210, 211] Therefore, in the heart failure patient, falling intra-thoracic pressure – even in the absence of lung volume change [e.g. a Mueller maneuver] – flattens the left ventricular cardiac function curve by both diastolic and systolic mechanisms. Intuitively, these actions tend to reverse during expiration.

Mechanical Ventilation

Again, the model of mechanical ventilation herein assumes that the patient is completely passive, or adapted with the ventilator such that there are no patient-mediated changes in intra-thoracic pressure during inspiration or expiration. The reason this paradigm is assumed is because patient effort significantly complicates analysis of heart-lung interaction. Unfortunately, this is frequently encountered in clinical medicine, for example, in the patient receiving non-invasive positive pressure ventilation [e.g. BiPAP].

Systemic Venous Return

As previously discussed, the systemic venous return curve changes with increased lung volume and abdominal pressurization. In states of volume overload, the right shift of the venous return curve can be marked. Further, increased resistance to venous return is less pronounced given intransigence to vascular collapse when vascular volume is high [92, 94].

With applied PEEP, maximal venous return falls but the value of maximal venous return is nevertheless high relative to the euvolemic or hypovolemic patient [29]. Also, sympathetic activity mediates the cardiovascular response to elevated intra-thoracic pressure [24, 25, 212]. Importantly, as discussed previously, if mechanical ventilation and/or PEEP maintains the right atrial pressure above Pcrit [i.e. the pressure at which the great veins collapse entering the thorax] in the volume-overloaded patient, then systemic venous return may, paradoxically, increase because the pressure head for venous return [i.e. the mean systemic filling pressure] also rises [27, 121]!

Right Ventricular Loading

Except at relatively high levels of positive pressure [more than 15 -20 cm H_2O of PEEP], the slope of the right ventricular cardiac function curve is not altered [213]. In the normal heart, the right atrial transmural pressure does not change in response to increased venous return [214]. As mentioned, this may be modelled on the Guyton diagram as a near vertical line for the right ventricular cardiac function curve. Indeed, this is observed empirically [201]. However, this illustration is, admittedly, an oversimplification. Mechanistically, it is argued, the absence of right atrial transmural pressure change occurs by the following: as the right atrial pressure increases in response to volume, it expands against the pericardium such that both intra-atrial and pericardial pressures rise in concert [214]. Therefore, on the Guyton diagram, the act of increasing venous return – and therefore cardiac volume – simultaneously shifts the cardiac function curve rightwards as the true surrounding pressure of the heart – the pericardial pressure – rises by pericardial restraint. Consequently, the pericardium retards [215], if not abolishes [214] increased right heart transmural pressure in response to changes in heart volume. That the pericardium restrains right heart filling and cardiac volume is not without its critics [216]. Nevertheless, appreciation for the role of the pericardium in cardiac loading is particularly prominent in congestive heart failure states, when cardiac volume is high. This is because the pericardial elastance [i.e. the inverse of compliance] curve is exponential. At high cardiac volume, the change in pericardial pressure is great. By contrast, at small cardiac volumes, pericardial pressure change is minimal. This physiology explains why some investigators have found a seemingly paradoxical reduction in pericardial pressure in response to positive intra-thoracic pressure [217, 218]. The reason being that increased intra-thoracic pressure reduces venous return and shrinks the enlarged heart; as a consequence, there is a large drop in pericardial pressure because it is pulled away from its elastic limit. Therefore, while increased intra-thoracic pressure occurring with PEEP – or with intermittent breaths – right shifts the cardiac function curve along the systemic venous return curve, the shift is tempered if the pericardium is at its elastic limit. In other words, the surface pressure of the heart [i.e. the 'epicardial pressure' or the true external pressure determining myocyte stretch] is the arithmetic sum of the intra-thoracic pressure and the pericardial elastic pressure [218]; the latter pressure being greater at high cardiac volume [219, 220].

Despite these subtleties of ventricular filling, in the patient with cardiogenic pulmonary edema, positive pressure usually has salubrious effects on impaired right ventricular cardiac function. During an acute exacerbation of heart failure, the right heart may be insulted by new or worsening tricuspid regurgitation, elevated pulmonary arterial impedance, and poor contractility. Accordingly, the application of positive pressure may simultaneously mitigate or reverse the aforementioned hemodynamic insults and increase the slope of the curve. This may occur by improving oxygenation, recruiting atelectatic lung, preventing RV distention and, therefore, enhancing right ventricular forward flow [185, 186, 221]. This is visualized as an increased operating point on the Guyton diagram [figure 11]. Nevertheless, as considered in the following section, initiation of mechanical ventilation and PEEP may have conflicting effects on the right ventricle.

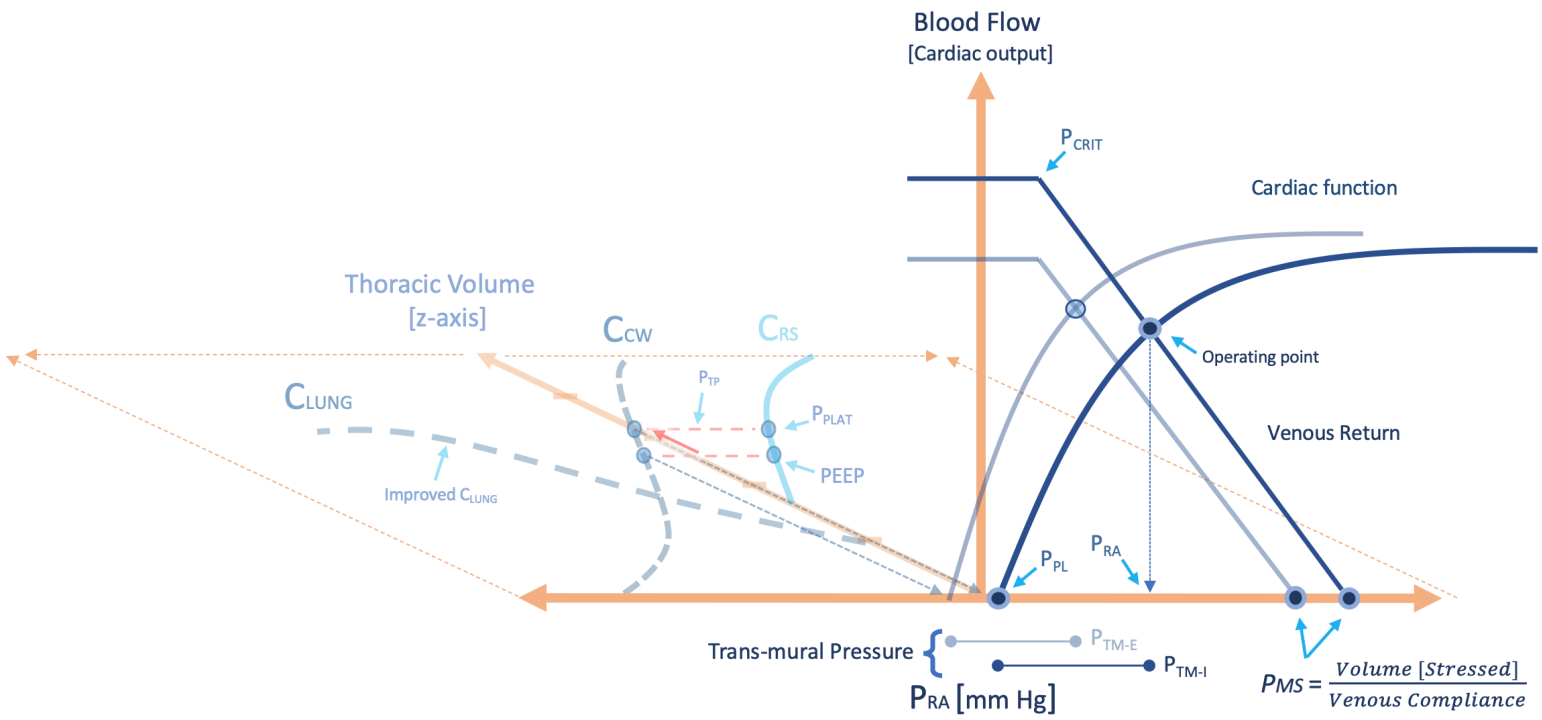

Figure 11: Mechanical ventilation in cardiogenic pulmonary edema. Lung compliance [Clung] is improved on the x-z plane. Positive end-expiratory pressure [PEEP] is applied to the respiratory system compliance curve [Crs] and this generates a pleural pressure on the chest wall compliance curve [Ccw]. The tidal volume delivered on the z-axis is the red arrow - raising pleural pressure along the Ccw and creating the plateau pressure [Pplat] on the Crs. The trans-pulmonary pressure [Ptp] is the red dotted line. The cardiac function curve moves rightwards in-step with the rise in pleural pressure [Ppl]; the slope rises as afterload is reduced. Inspiratory trans-mural pressure [Ptm-I] increases slightly with inspiration as does the mean systemic pressure [Pms]. Cardiac output on the y-axis is improved compared to figure 10. Pcrit is the critical collapse pressure and is elevated by PEEP application. Pra is right atrial pressure; Ptm-E is expiratory trans-mural pressure of the right atrium.

Much clinical investigation has focused on the effects of positive pressure upon left ventricular filling. Conflicting data likely reflects disparities in ventricular function, volume status and thoracic mechanics. In healthy patients, at high levels of PEEP [typically defined as above 15 cm H2O], RV enlargement is noted [153] and thought to decrease left ventricular compliance via interdependence of the ventricles [46, 222-224]. Supporting this hypothesis, interdependence effects were particularly profound in the setting of poor RV systolic function and RV ischemia – reflecting afterload sensitivity [70]. If PEEP reduces cardiac output by increasing impedance to RV ejection, this could induce hypotension and aggravate LV ischemia in patients with underlying coronary disease [71, 225]. By contrast, if positive pressure diminishes RV volume by preload reduction, left ventricular compliance may improve [226]. Predicting whether a ventilator breath and PEEP will enlarge or shrink the RV is difficult and this physiology is considered in more detail within the discussion of ARDS. Nevertheless, if initiating mechanical ventilation enhances systemic venous return, pulmonary West zone II physiology [i.e. increased RV afterload] or RV ischemia, then the RV tends to enlarge. By contrast, if mechanical ventilation reduces systemic venous return or improves RV afterload, then the RV tends to shrink.

Increased lung volume during positive pressure ventilation shifts the pulmonary venous return curve rightwards relative to the left ventricular cardiac function curve. This is especially important in overload states because pulmonary venous return is facilitated by the fraction of West zone III [125].

Additionally, PEEP and intermittent positive pressure ventilation can compress the left ventricular free wall and impair its compliance, but this effect is probably blunted when the lower lobes are edematous. Poor lower lobe compliance from edema hinders expansion towards the left ventricle. Nevertheless, as mentioned in chapter 3, even in the healthy state, this mechanism is likely of minor significance [227].

Left ventricular performance is improved by elevated intra-thoracic pressure when baseline cardiac function is poor [128, 228-232]. Indeed, multiple investigations have shown that invasive or non-invasive ventilation increases stroke volume and cardiac output, but this is typically only seen when cardiac filling pressures are high [233-236]. The mechanism of this effect is best understood by inspection of the Sagawa pressure-volume relationship as described above. When cardiac systolic function is poor, the end-systolic pressure volume relationship is shifted down and to the right. Consequently, elevated cardiac volume raises filling pressure with progressively smaller stroke volume. By limiting venous return, positive pressure ventilation shrinks left ventricular end-diastolic transmural pressure and augments stroke volume simply due to the physical principles governing diastolic and systolic properties of the heart and pericardium [237]. Second, increased intra-pleural pressure diminishes left ventricular transmural pressure which augments stroke volume for any given filling pressure [229, 232]; however, reduced LV transmural pressure has not been universally observed in response to positive intra-thoracic pressure in heart failure [217]. Lastly, there is some evidence to suggest that intra-thoracic pressure elevation reduces thoracic aortic impedance as well, potentially by diastolic emptying of the thoracic aorta. In other words, with the application of positive pressure, the left ventricle ejects into a relatively empty aorta [209, 232]. Each of these factors steepen the slope of the left ventricular cardiac function curve; the operating point of the Guyton diagram and, therefore, cardiac output rises at lower filling pressure.

Physiology of Diuresis

The administration of furosemide results in an immediate, abrupt increase in venous capacitance [238]. Notably, this effect is faster and more pronounced than nitroglycerine [239], though this finding is not universal [240]. Increased venous capacitance effectively left shifts the systemic venous return curve. This physiology is equivalent to volume loss – reducing atrial filling pressure and cardiac output [241]. The effect on cardiac output depends on the shape and slope of the cardiac function curve. If, prior to administration of a venodilator, the operating point of

the cardiovascular system lies upon the flat portion of the cardiac function curve, then cardiac output will not fall and there is only reduced filling pressure.

In the context of the aforementioned discussion on cardiac function at high ventricular volumes, preload reduction [e.g. with furosemide or mechanical ventilation] also improves the cardiac function curve, that is, shift its slope up and leftwards. This physiology is prominent when left ventricular systolic function is relatively poor. When the ventricle is excessively distended, preload reduction reduces ventricular wall stress and enhances stroke volume by lowering end-systolic volume more than end-diastolic volume [220, 230, 242, 243]. Preload reduction may also mitigate functional mitral regurgitation [244].

Only after many minutes does the diuretic effect take precedence; thus, with time, fluid is drawn away from the alveoli and pulmonary interstitium [238].

Acute Respiratory Distress Syndrome

The acute onset of bilateral pulmonary infiltrates that is not secondary to volume overload and associated with impaired oxygenation typifies the acute respiratory distress syndrome [ARDS] [245]. This syndrome is almost invariably associated with impaired calculated compliance of the respiratory system, elevating static airway pressures during mechanical ventilation [127, 246]. Application of more physiological tidal volumes in ARDS management has reduced mortality [247]. Additional importance is placed on maintaining static airway pressure below 30 cm H_2O; however, this assumes that reduced thoracic compliance is entirely due to poor pulmonary compliance. Under this assumption, decreasing the plateau pressure maintains the transpulmonary pressure below a level that traumatizes the lungs [248].

However, the compliance of the respiratory system – which is measured during a plateau pressure – is composed not only of the lungs, but also the chest wall [249, 250]. If either the lungs or the chest wall have reduced compliance, then the total respiratory system compliance is reduced; yet, as discussed below, specific abnormalities of the lungs versus the chest wall can have opposing cardiovascular responses [251].

Pulmonary and Extra-pulmonary ARDS

Clinically, ARDS has been parsed into 'pulmonary' and 'extra-pulmonary' sources as these different entities have distinct effects on respiratory system mechanics [127, 246]. Pulmonary ARDS is associated with direct injury [e.g. pneumonia] and reveals consolidation as the primary insult early in ARDS. By contrast, intra-abdominal sepsis, trauma and hemorrhage were commonly associated with extra-

pulmonary ARDS. In these cases, the primary pulmonary insults were atelectasis and interstitial edema of the lung. While both types of ARDS similarly decreased the respiratory system compliance, pulmonary ARDS predominantly impaired the calculated pulmonary compliance, while extra-pulmonary ARDS showed impaired chest wall compliance [246]. Notably, chest wall compliance in extra-pulmonary ARDS was highly correlated with intra-abdominal pressure. These distinctions are important; while plateau pressure in both conditions is high, the hemodynamic consequences may be contradictory. Finally, the issues of compliance, specific elastance, barotrauma, volutrauma and ergotrauma are developed more fully in chapter 9.

Changes in Intra-thoracic Pressure on Mechanical Ventilation

If plotted simultaneously on the Campbell diagram, the compliance curves of the lung and chest wall may be combined to form the compliance curve of the respiratory system. As discussed in both chapter 1 and 3, the respiratory system curve illustrates the proximal airway pressure in a passive, mechanically-ventilated patient [2, 75]. At a given lung volume [the y-axis on the Campbell diagram] the horizontal distance between the chest wall compliance curve and the pulmonary compliance curve depicts the pressure that must be generated by either the muscles of respiration to achieve said volume, or the proximal airway pressure applied by the ventilator. Importantly, reduced compliance of the respiratory system does not distinguish between a primary insult to the lungs, chest wall or both [figure 12].

In the completely passive patient receiving mechanical ventilation, change in intra-thoracic [or pleural] pressure is directly related to the tidal volume delivered, and indirectly related to the compliance of the chest wall [252]. On the Campbell diagram, this means that the pleural pressure follows the chest wall compliance curve during passive mechanical ventilation. Because the alveolar pressure tracks the static compliance curve of the respiratory system, the horizontal distance between the compliance curve of the respiratory system and the chest wall represents the transpulmonary pressure [i.e. the pressure in the alveolus less the pleural pressure]. Careful inspection of these curves reveals that when the compliance of the chest wall falls [as in extra-pulmonary ARDS], so too does the transpulmonary pressure because the pleural pressure rises at any lung volume. In other words, the pleural pressure gets 'closer' to the airway or alveolar pressure [figure 13]. Increased pleural pressure in extra-pulmonary ARDS means that when simultaneously analyzing the Guyton and Campbell diagrams, there is larger rightward shift of the right ventricular cardiac function curve.

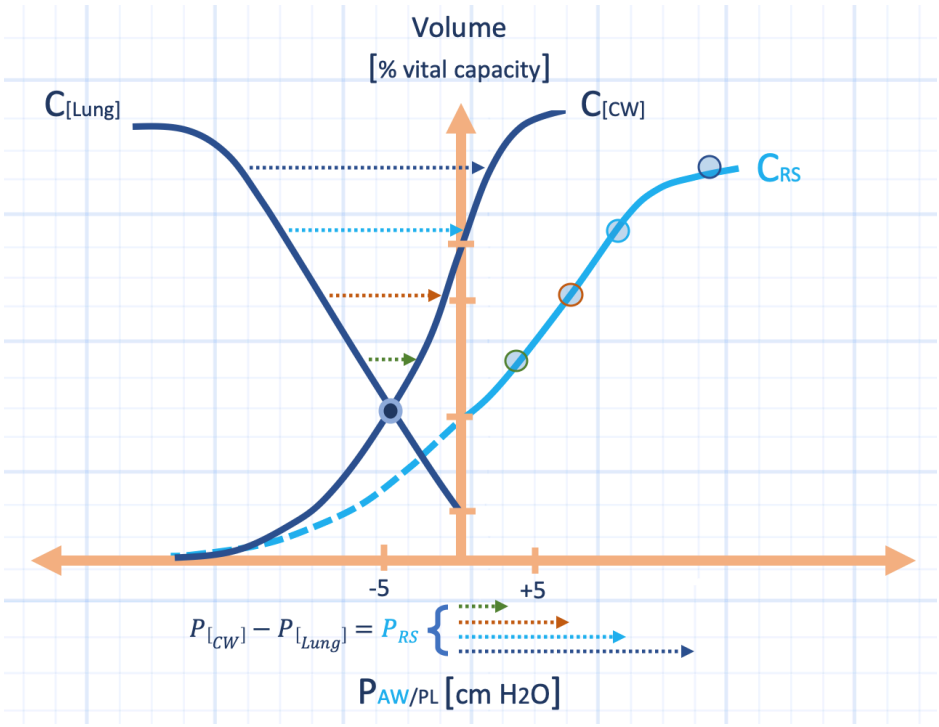

Figure 12: The derivation of the respiratory system compliance curve [Crs] from the Campbell diagram [see also chapter 1]. The distance between the lung compliance curve [Clung] and chest wall compliance curve [Ccw] is the pressure generated by the muscles of inspiration to generate a particular volume [different colours] or the pressure applied at the airway by the ventilator [the circles along Crs]. Paw is airway pressure; Ppl is pleural pressure. The dashed portion of Crs is omitted for clarity in subsequent figures.

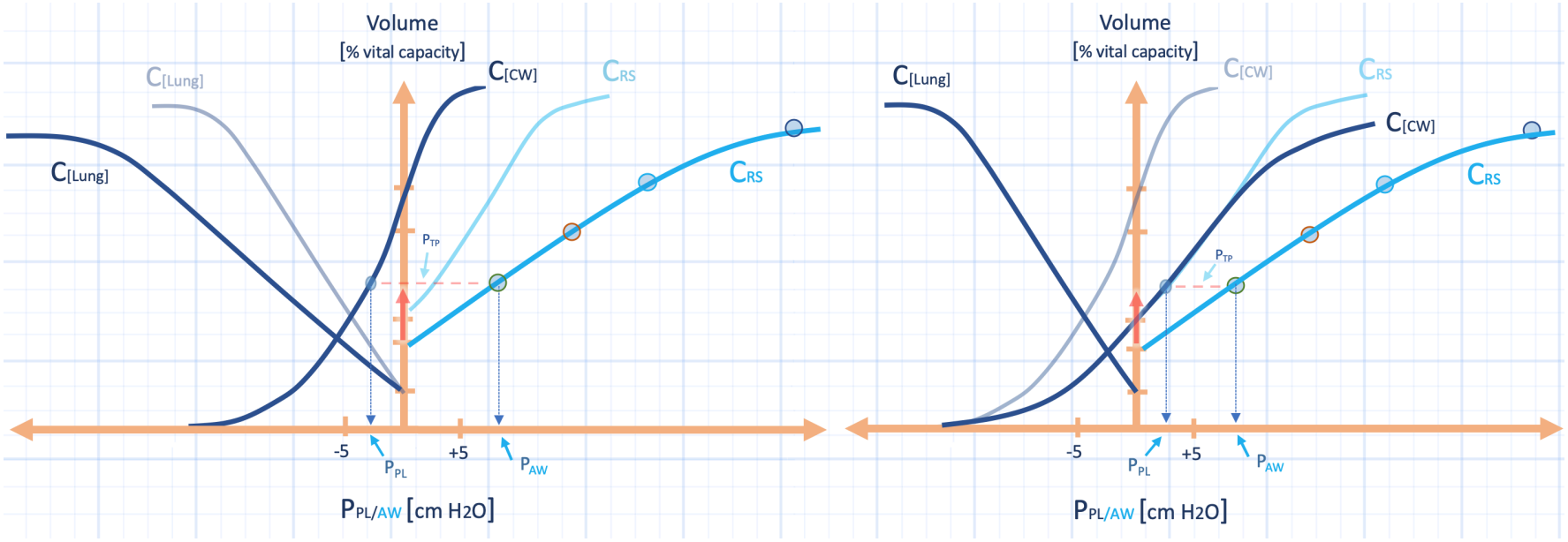

Figure 13: Pulmonary versus extra-pulmonary ARDS on the Campbell diagram. The left panel shows the effect of reduced lung compliance [Clung] on the respiratory system compliance curve [Crs]. The greater distance between Clung and the chest wall compliance curve [Ccw], the greater the airway pressure [Paw] applied to achieve said volume [see figure 12]. The lateral distance between the Crs and Ccw at any given volume is the trans-pulmonary pressure [Ptp] because it is the Paw less the pleural pressure [Ppl]. Right panel shows pure extra-pulmonary ARDS. The Crs is reduced to exactly the same degree as the left panel but entirely by reduced Ccw. The Paw is the same for each volume, but the Ppl is greater, so the Ptp is reduced. These become the x-z planes in figures 14 & 15.

In distinction, a primary reduction in pulmonary compliance yields greater transpulmonary pressure because the lateral distance between the chest wall compliance curve and respiratory system curve remains large. Accordingly, on the simultaneous analysis, the right ventricle moves less [i.e. diminished preload effect]

but its slope is flattened [i.e. a greater afterload effect]. In other words, the pleural pressure changes less than the transpulmonary pressure [251] and the transpulmonary pressure is an arbiter of pulmonary arterial impedance.

Systemic Venous Return

ARDS, per se, does not alter the venous return curve save for the underlying disease mechanism which precipitates the lung injury [e.g. sepsis]. It is fair to assume that, with the increased intra-abdominal pressure observed in extra-pulmonary ARDS, there is diminished venous capacitance and increased resistance to venous return. This is almost certainly mediated by volume status as discussed in chapters 2 and 3. The volume status of the patient with ARDS may vary depending upon degree of resuscitation, insensible loses and third-spacing [253]. The effects of sepsis on the venous return curve are explored in more depth below.

Right Ventricular Loading

As alluded to above, one way to model pure pulmonary ARDS on the Campbell diagram is a downward and left shift of the pulmonary compliance curve [see also chapter 1 and 9] [246]. This increases the distance between the pulmonary and chest wall curves, illustrating that the compliance of the system is reduced. If chest wall compliance is unaffected, then there will be little effect on pleural pressure during mechanical ventilation. The application of PEEP or an intermittent breath shifts the right ventricular cardiac function curve rightwards with respect to the venous return curve. Additionally, as the transpulmonary pressure rises, so too does the right ventricular afterload. Thus, the slope of the RV function curve flattens, elevates right atrial filling pressure and impairs cardiac output [figure 14]. This has been quantified in ARDS patients in terms of the velocity-time integral across the pulmonic valve [254, 255] and may also explain the common co-occurrence of tricuspid regurgitation during mechanical ventilation [256]. In patients with pulmonary ARDS, chest wall binding – which diminishes chest wall compliance and therefore increases pleural pressure – reduces the transpulmonary pressure and unloads the right ventricle [255].

In extra-pulmonary ARDS, reduced chest wall compliance exaggerates the increase in pleural pressure [249, 250]. Pleural pressure elevation with a positive pressure breath, or the application of PEEP, affects the right ventricular preload more prominently. On the combined diagram, the cardiac function curve shifts rightwards along the systemic venous return curve to a larger extent. Accordingly, the right atrial transmural pressure is reduced and, because the transpulmonary pressure is not as great, the right ventricular afterload is less than that in extra-

pulmonary ARDS. The net result is that right ventricular cavity size may shrink [figure 15].

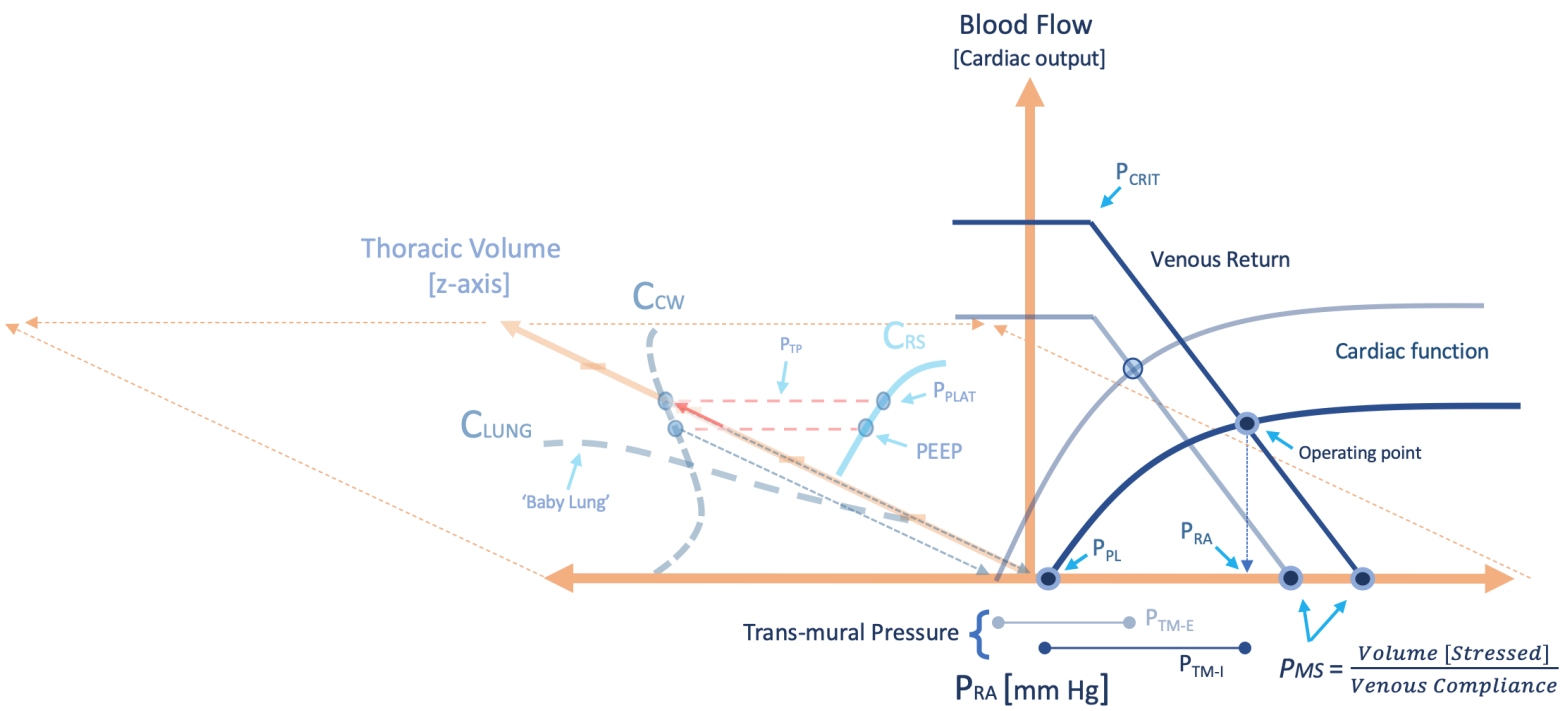

Figure 14: Heart-lung interaction in pulmonary ARDS. The z-axis is thoracic volume, the red arrow is the tidal volume delivered. The lung compliance [Clung] is improved with mechanical ventilation. Positive end-expiratory pressure [PEEP] applied to the respiratory system compliance [Crs] generates a pleural pressure on the chest wall compliance curve [Ccw]. Pleural pressure [Ppl] rises with the breath along the Ccw and the plateau pressure is generated [Pplat]. This pushes the cardiac function curve rightwards and bends its slope as the trans-pulmonary pressure [Ptp] rises [RV afterload]. The inspiratory trans-mural pressure of the right atrium [Ptm-I] rises and cardiac output [y-axis, operating point] falls. Pcrit is critical collapse pressure generated by PEEP on venous return curve. Ptm-E is expiratory trans-mural pressure of right atrium. Pms is mean systemic pressure. Pra is right atrial pressure.

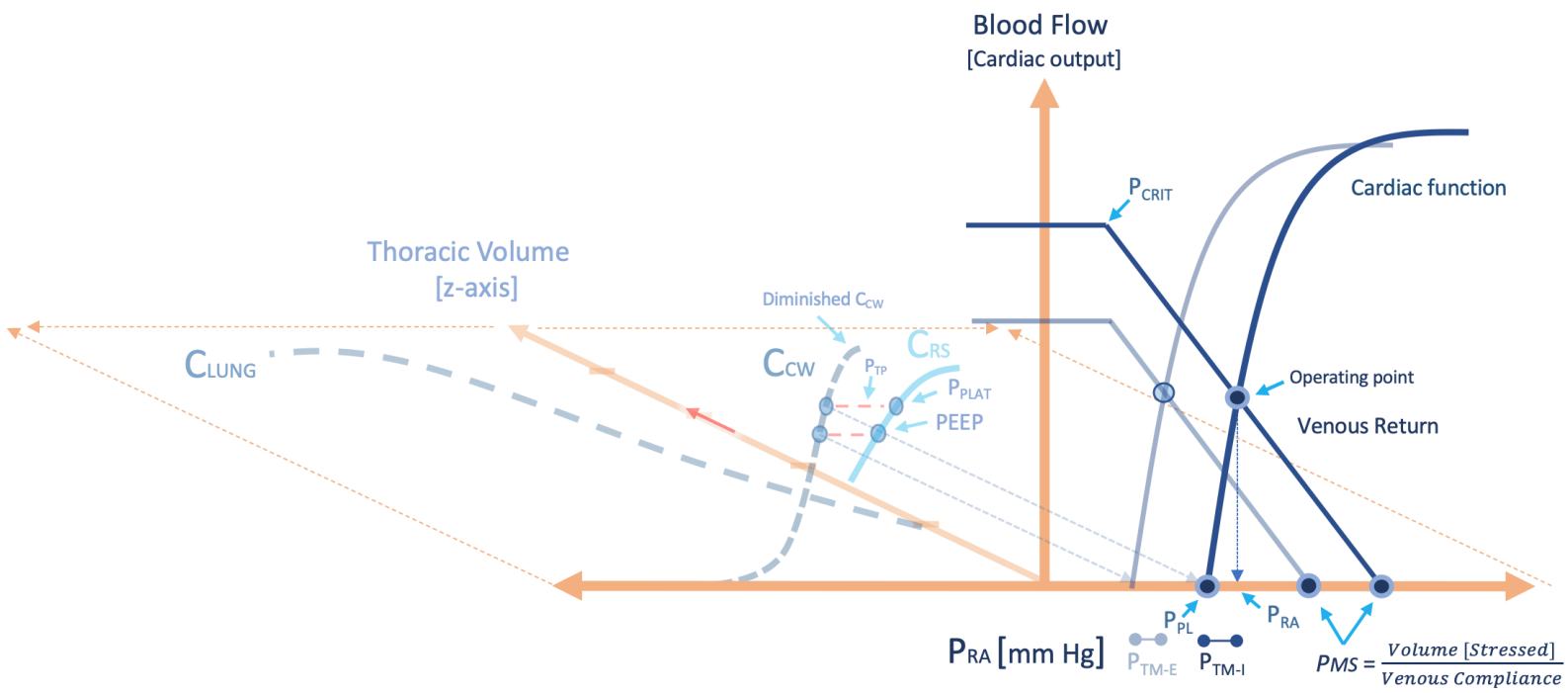

Figure 15: Heart-lung interaction in extra-pulmonary ARDS. Compare to figure 14; the reduced Crs is driven by the diminished Ccw. The cardiac function curve is pushed rightwards during inspiration to a greater degree. Trans-mural pressure [Ptm-I and Ptm-E] shrink and the operating point rises with reduced RV afterload. See figure 14 for abbreviations; see also figure 13.

Considering the aforementioned clinical subtypes of ARDS, one may reconcile the seemingly disparate findings of right ventricular enlargement versus contraction in echocardiographic studies of ARDS. Importantly, a patient may initially have improved right ventricular afterload as positive pressure enhances oxygenation and recruits collapsed alveoli in extra-pulmonary ARDS. As well, with increased pleural pressure, the right ventricular preload is minimized. The combination of diminished afterload and preload co-conspire to reduce right ventricular cavity size. By contrast, applying positive pressure and/or PEEP to pulmonary ARDS may cause alveolar over-distension and worsened pulmonary compliance. Here, transpulmonary pressure rises, right ventricular loading is impaired and enlarged end-diastolic volume is the consequence [222, 251] [compare figures 14 & 15].

Ventricular Interdependence and Left Ventricular Loading

Flowing from the discussion above, the left ventricular preload is affected by both parallel and series effects from the right ventricle. If the lungs are predominantly in zone III, increased transpulmonary pressure [i.e. lung volume] lowers vascular capacitance of the alveolar vessels and blood propels from the pulmonary capillaries to the pulmonary veins [125]. Subsequently, increased pulmonary venous return preloads the left ventricle and on the Guyton diagram this is illustrated as a right shift of the pulmonary venous return curve relative to the LV function curve.

To the extent that the right ventricle dilates [e.g. in pulmonary ARDS] with inspiration, left ventricular compliance falls and preload is diminished [70, 71, 153]. This was discussed in more detail in the section on mechanical ventilation and left ventricular loading in systolic heart failure. Note that on subsequent expiration, left ventricular stroke volume might not recover because the inspiratory rise in right ventricular afterload impairs charging of the pulmonary vasculature with blood [257-259].

By contrast, if the right ventricle shrinks in volume during inspiration [e.g. in extra-pulmonary ARDS], left ventricular compliance may improve and left ventricular end-diastolic volume transiently rise [226, 260, 261]. Following this inspiratory rise in stroke volume, an expiratory decrease in left ventricular stroke volume may be observed as the diminished right ventricular preload reaches the left ventricle 2-3 cardiac cycles later, on expiration. While these aforementioned effects are driven by cyclical changes in airway pressure, the application of PEEP results in steady-state change based on the patient's underlying physiological predisposition towards RV enlargement or depletion [27, 43, 262].

The LV afterload effects of positive pressure could be more pronounced in those with extra-pulmonary ARDS as the reduced chest wall compliance 'delivers' more of the airway pressure to the pleural space [127-129, 132, 133, 228, 230-232]. As discussed in systolic heart failure, elevated cardiac surface pressure facilitates systolic unloading of the left ventricle when left ventricular end-diastolic volume is high.

Septic Shock in Cirrhosis

Many of the aforementioned principles are encountered in the septic patient with decompensated cirrhosis; for example, endotoxemia from spontaneous bacterial peritonitis. These perplexing patients can have complex and conflicting alterations in both pulmonary and cardiovascular physiologies.

Changes in Pulmonary Mechanics

The changes in pulmonary mechanics that occur as a result of slowly decompensated cirrhosis are physiologically akin to that of cardiogenic pulmonary edema [169, 176]. That is, there should be both reduced pulmonary compliance and increased airways resistance from fluid accumulation in the bronchovascular interstitium. Indeed, restrictive pulmonary physiology is common in cirrhosis [263], but the difference in forced vital capacity between those with ascites and those without has been documented in one study to be minimal [264]. Furthermore, lung volume and pulmonary compliance improve following diuresis and large volume paracentesis [265-267]. As well, there is evidence that cirrhosis increases airways resistance and lower lobe gas-trapping, even without underlying obstructive lung disease or ascites [268]. Presumably, increased closing volume in cirrhotic patients is secondary to mechanical airway compression by airway edema [268]. Notably, edema in the perivascular space can impair pulmonary compliance [203]. As alluded to above, with the development of frank ascites, the thorax is loaded and chest wall compliance changes in a manner similar to obesity [269, 270]. On the Campbell diagram, these changes are represented by a down and leftwards shift of the pulmonary compliance curve and rightwards shift of the chest wall compliance curve. The distance between the lung and chest wall compliance curves indicates that at any given lung volume, the muscles of respiration must generate greater pressure [figure 16]. To compensate for this increased muscle work, these patients typically breathe in a rapid-shallow manner [2].

The onset of sepsis from endotoxemia accentuates the above physiology [271]. Capillary leak worsens pulmonary interstitial edema and lung mechanics [272]. Should ARDS ensue from the intra-abdominal pathology, there may be increased intra-abdominal pressure and worsened chest wall compliance as described above in extra-pulmonary ARDS [127].

In the spontaneously breathing patient, these altered pulmonary mechanics may lead to great variation in pleural pressure during inspiration and expiration. Oftentimes, expiratory abdominal muscles are recruited which amplify expiratory intra-thoracic pressure [87, 271]. Pleural effusions can accentuate cardiac filling

abnormalities as well as atelectasis as the poorly compliant thoracic wall is unable to accommodate the space-occupying effusion [197].

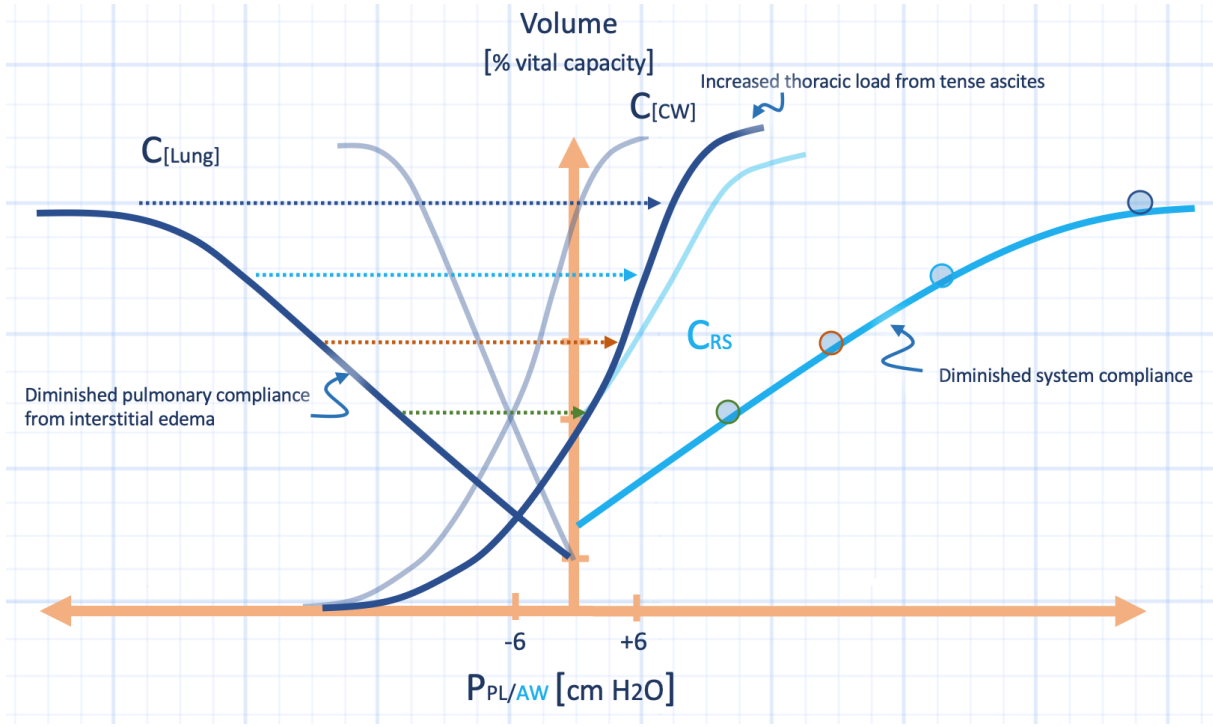

Figure 16: Hypothetical effects of decompensated cirrhosis on the Campbell diagram. Lung compliance [Clung] is reduced and the load placed on the chest wall [Ccw] is increased. This may shift the slope downwards and/or right shift the curve. See also figures 12 and 13. The respiratory system compliance curve [Crs] is reduced such that airway pressure [Paw] is elevated at each lung volume on the y-axis.

Increased pulmonary lung water with or without pleural effusion favours high right ventricular afterload. As before, this flattens the slope of the right ventricular cardiac function curve, moving the operating point downwards. Indeed, in stable cirrhotic patients, this hemodynamic profile is seen, however mild [273]. Because of shifting intra-thoracic pressure during inspiration and expiration, cardiac output varies. Yet, fluctuation in biventricular output depends on the shapes of the venous return and ventricular function curves. Generally, with spontaneous inspiration, cardiac output and right atrial transmural pressure rise, while on expiration they fall [97, 98]. As elaborated below, when cardiac function and venous return both increase [e.g. elevated contractility and diminished resistance to venous return], cardiac output change is more pronounced with respiratory variation.

Depending upon the relative compliances of the ventricular septum and free walls, inspiration may have conflicting effects on the left ventricle. Further, high zone III conditions of the pulmonary capillaries augments LV filling during inspiration [125], but ventricular interdependence would hinder it. These phasic changes may have less effect on cardiac output with time, but are important to understand in the setting of pulse pressure variation interpretation.

The vascular blood volume is enlarged in patients with cirrhosis, as determined by radio-labeled erythrocytes [274]. While this should raise mean systemic pressure and venous return, increased vascular capacitance – especially in the splanchnic bed – tempers the effect of elevated blood volume [275]. Further, increased resistance to venous return in the portal circulation [276] impairs the venous return function. There is a paucity of data regarding venous return in patients with cirrhosis, so it is difficult to know which effect predominates. Most likely the effect that prevails in any particular patient is a function of disease severity. Ostensibly, in early disease, increased vascular volume maintains venous return and cardiac output. Then, as cirrhosis progresses, the reduced vascular capacitance and high resistance to venous return spoil hemodynamics and cardiac reserve is limited [277]. In general, the abdomen is in zone III physiology, so the inspiratory rise in thoracic volume may have less effect on venous resistance [92-94, 137, 138] – unless complicated by massive ascites and intra-abdominal hypertension [278, 279] [figure 17].

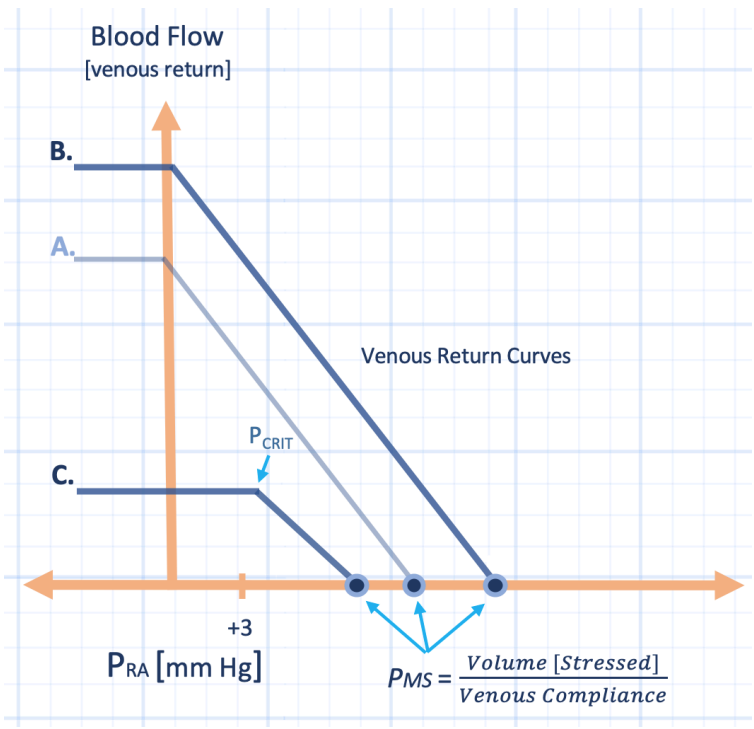

Figure 17: Hypothetical effect of decompensated cirrhosis on venous return. From baseline [A] blood volume is increased which would increase circuit function to curve [B] as in heart failure. However, increased venous capacitance might shift the curve leftwards to C. Increased intra-abdominal pressure from ascites may create a PEEP-like effect, increase venous return resistance and the critical collapse pressure [Pcrit]. Pra is right atrial pressure; Pms is mean systemic pressure.

By contrast, sepsis alters the venous return curve by reducing its resistance [280-282]. The decrease in resistance to venous return helps explain high cardiac output at a relatively high cardiac filling pressure. Additionally, the loss of venous capacitance in the septic state tends to de-recruit stressed volume into unstressed volume and shift the x-intercept of the venous return curve leftwards [280]. Notably, there is renewed interest in the role of venous return in sepsis. Maas and colleagues have published elegant work by extrapolating venous return curves at the bedside [283-285]. They employed instantaneous and simultaneous central

venous pressure and cardiac output monitoring to generate bedside venous return curves [89, 90, 286]. Importantly, their work confirmed that adrenergic tone has complicated and sometimes conflicting effects upon venous return [287]. For example, stimulation of alpha receptors lessens venous capacitance which raises Pmsf. But alpha stimulation also elevates the resistance to venous return [288]. Conversely, beta receptor stimulation diminishes resistance to venous return [282]. Indeed, this was shown by Monnet's group using the methods of Maas and colleagues – studying the effect of norepinephrine on patients in septic shock [289].

Cardiac Function in Cirrhosis and Sepsis

In stable, compensated cirrhosis, a sub-population of patients may develop porto-pulmonary hypertension - a particularly morbid form of pulmonary hypertension [273, 290]. This complication specifically alters the right ventricular cardiac function curve as the pulmonary vascular impedance is increased. Conversely, other cirrhotic patients can develop arteriovenous shunting in the lower lung lobes, leading to hypoxemia, especially when the patient sits upright given gravity-dependent blood flow [291]. By contrast, the left ventricle is typically exposed to lower afterload in the cirrhotic state as a consequence of vasodilation [292].

Septic physiology exacerbates the aforementioned cardiac insults. Commonly, there is biventricular dysfunction in sepsis [293-296]. Again, a flattened right ventricular cardiac function curve favours diminished cardiac output at higher filling pressure. As discussed in later chapters, when the flat aspect of the cardiac function curve intersects the venous return curve, respiratory variation in cardiac output is minimized, even if the resistance to venous return is low.

Heart-Lung Interaction in Cirrhotic Endotoxemia

In the spontaneously breathing cirrhotic patient with large ascites and sepsis, rapid-shallow breathing minimizes the load placed upon the thorax [297]. Rapid-shallow breathing can cause hypercapnia given the increase in dead space fraction as a consequence of diminished tidal volume [298] [see chapter 9].

However, large deflections of pleural pressure cause large changes in ventricular loading conditions. While the steep venous return curve in cirrhotic endotoxemia enhances respiratory fluctuation in cardiac output and while right-ventricular trans-mural pressure increases with exaggerated inspiratory effort, the degree to which cardiac output rises depends on the slope of the cardiac function curve. If the cardiac function curve is flattened by underlying pulmonary hypertension, acquired pulmonary hypertension [e.g. from hypoxemia, hypercapnia and/or compressive atelectasis], or sepsis-induced myocardial depression, then neither right atrial pressure nor right heart output will vary much with inspiration [86]. Similarly, for

the left ventricle, inspiratory pulmonary venous return rises, but this is tempered by flattening of the left ventricular cardiac function curve [115]. Sepsis-induced depression of the left ventricle may impose a steady-state decrement in LV function. Further, transient LV abnormalities may arise due to diastolic dysfunction from ventricular interdependence and/or augmented left ventricular afterload secondary to elevated inspiratory trans-mural pressure [199, 208, 210, 211].

By contrast, during expiration, the right ventricular cardiac function curve shifts rightwards with respect to systemic venous return. Abdominal muscle recruitment during expiration may increase the resistance to venous return from the high capacitance abdominal vessels; this will be pronounced in the setting of tense ascites [32, 278]. The right shift in the cardiac function curve decreases right atrial transmural pressure and right ventricular cardiac output. If the intersection of the systemic venous return curve and right ventricular cardiac function curve meet upon the latter's steep or ascending portion, the drop in cardiac output will be marked [figure 18]. Simultaneously, the pulmonary venous return curve shifts leftwards on expiration as lung volume decreases. The left shift of the pulmonary venous return curve is accentuated if there is steady-state reduction in right ventricular function. Furthermore, the slope of the left ventricular cardiac function curve will improve during forced expiration as ventricular interdependence is minimized during diastole and afterload is reduced during systole. It is therefore possible that, during forced expiration, there is transitory left ventricular output augmentation and, consequently, respiratory variation noted in an arterial line tracing [299].

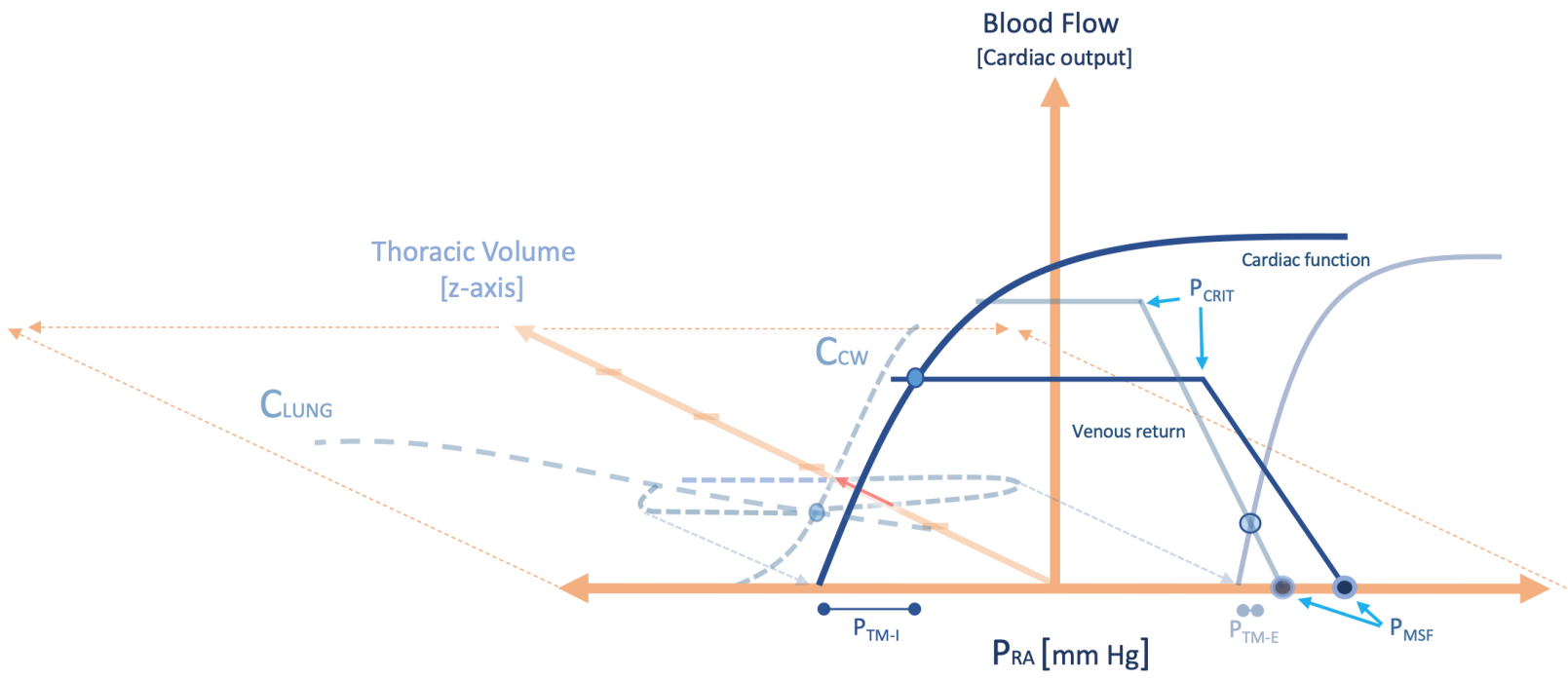

Figure 18: Example of spontaneous inspiratory and expiratory variation in cirrhosis. Red arrow on z-axis is tidal volume. Reduced lung compliance [Clung] and increased airways resistance leads to reduced inspiratory intra-thoracic pressure. Inspiratory trans-mural pressure [Ptm-I] is greater than expiratory transmural pressure [Ptm-E]; inspiration is limited by great vein collapse [maximal venous return - see chapter 3]. Forced expiration pushes the cardiac function curve rightwards, diminishing cardiac output on the y-axis. On expiration right atrial pressure [Pra] is greater than critical collapse pressure [Pcrit] which means that the IVC distends while diminished Ptm-E means that the right heart [and SVC] shrinks. Pmsf is mean systemic pressure. Ccw is chest wall compliance. Perit is critical collapse pressure. See also figures 16 & 17.

While discussion of heart-lung interactions and beat-to-beat pulse pressure variation is discussed in more detail later, note that the critically-ill patient with significant aberrations in pulmonary mechanics may have conflicting effects on left ventricular loading while spontaneously breathing. These confounding variables include large and disparate pleural pressure swings during respiration, in addition to variable effects of pulmonary venous return and ventricular interdependence.

Implications for Mechanical Ventilation

The application of PEEP reduces maximal venous return and increases mean systemic filling pressure typically to the same extent as it raises Pcrit [i.e. the gradient for venous return is not changed]. As long as right atrial pressure remains at-or-above Pcrit, cardiac output will not fall in response to PEEP application [121]. Because of abdominal pressurization and catecholamine release, the resistance to venous return may rise, as demonstrated by diminished slope of the venous return curve. Again, excess total body volume places the abdominal vasculature in zone III conditions and blunts the effect of PEEP on venous return [92].

Institution of mechanical ventilation in the septic, decompensated cirrhotic typically causes high plateau pressure due to reduced compliance of the respiratory system [300]. Part of the reason for the high static, proximal airway pressure measured by the ventilator is the low chest wall compliance, which raises the pleural pressure [267]. A shifted chest wall compliance curve on the Campbell diagram reveals that the transpulmonary pressure [i.e. right ventricular afterload] is not as elevated as compared to the same plateau pressure secondary to a pure pulmonary insult. This is illustrated by simultaneously graphing the pulmonary, chest wall and respiratory system compliances upon the Campbell diagram [figures 12 & 13]. Again, it is the lateral distance between the chest wall compliance curve and the static respiratory system compliance curve that depicts the transpulmonary pressure at end-inspiration.

Nevertheless, to the extent that mechanical ventilation improves oxygenation, recruits atelectatic lung and reduces work of breathing, there can be significant biventricular function augmentation [301]. Steepening the slope of the right ventricular cardiac function curve helps place the operating point on the ascending portion of the cardiac function curve. Accordingly, right shift of the RV cardiac function curve relative to the venous return curve transiently diminishes cardiac output [302]. As the chest wall compliance curve in massive ascites accentuates pleural pressure, the right ventricular cardiac function curve may predominantly experience preload effects rather than afterload effects [akin to extra-pulmonary ARDS above]. Again, because the inspiratory increase in intra-thoracic pressure is transmitted to the cardiac surface, pleural pressure elevation from abnormal chest wall mechanics preferentially diminishes preload [128, 132] [figure 19].

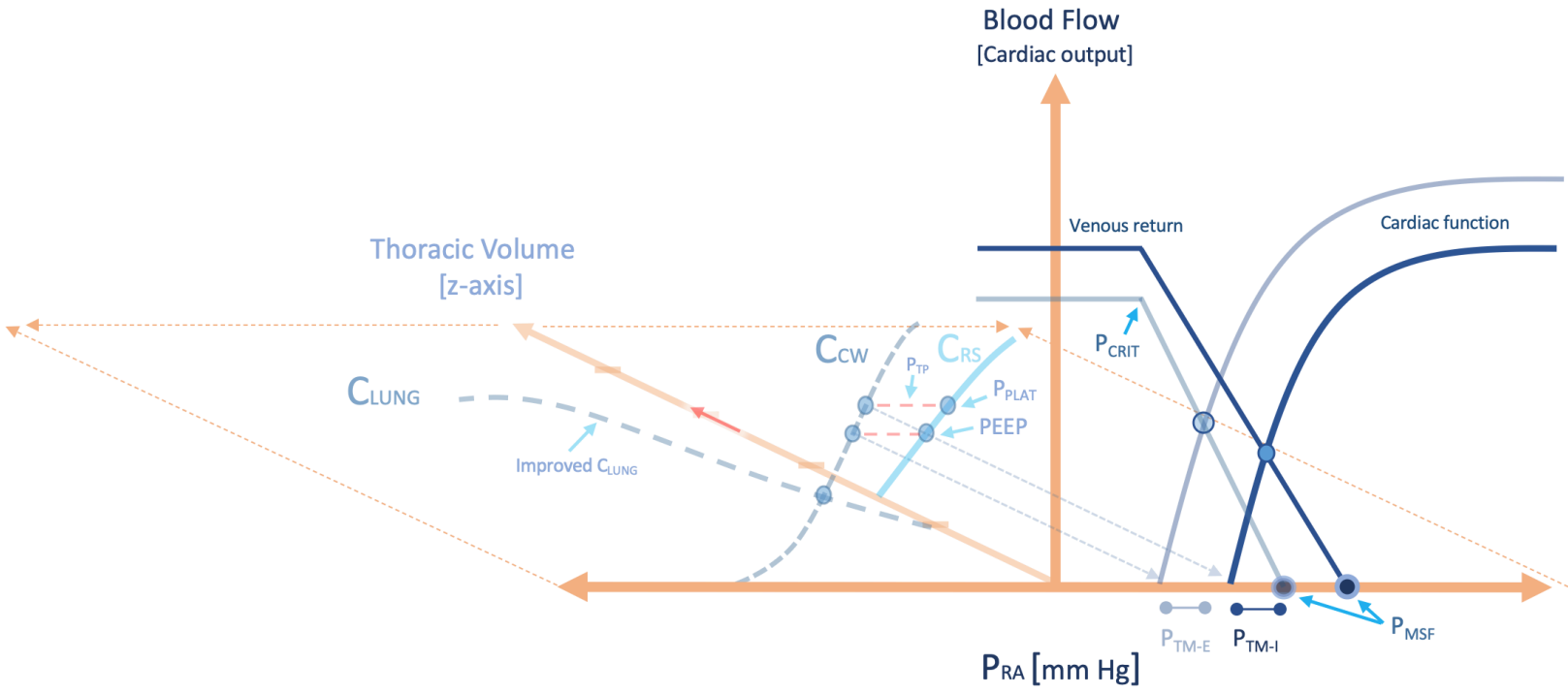

Figure 19: Hypothetical heart-lung interaction during ventilated cirrhosis. Lung compliance [Clung] improves with PEEP and ventilation. Without large volume paracentesis, the chest wall load is still high [right-shifted Ccw]. This increases the pleural pressure [Ppl] for any tidal volume on the z-axis. Ppl rises along the Ccw and shifts the cardiac function curve rightwards with inspiration. The red arrow is the tidal volume delivered by the ventilator. The lower trans-pulmonary pressure [Ptp] reduces RV afterload. There is less variation in cardiac output [y-axis] compared to spontaneous ventilation despite improved cardiac function. The inspiratory and expiratory right atrial transmural pressures [Ptm-I and E] shrink compared to figure 18 but the right atrial pressure [Pra] is above the critical collapse pressure [Pcrit] on inspiration & expiration meaning IVC distension throughout. Crs is respiratory system compliance; Pmsf is mean systemic pressure.

As well, the slope of the left ventricular cardiac function curve rises during a passive mechanical breath as the increased cardiac surface pressure reduces afterload; diminished right ventricular volume also improves LV diastolic compliance [228-230, 232]. Additionally, increased lung volume decreases pulmonary vascular capacitance – shifting the pulmonary venous return curve rightwards with respect to the left ventricular cardiac function curve [125]. If the left ventricular cardiac function curve intersects the pulmonary venous return curve upon its ascending region, then left ventricular stroke volume rises during the mechanical breath. In the passive patient receiving mechanical ventilation, the aforementioned changes during inspiration are essentially reversed during expiration.

However, none of these cyclical changes in biventricular function are observed if the venous return curve is shifted so far rightwards that the cardiac function curve is intersected at its flat region, regardless of its slope [115].

Implications for the General Management of Cirrhotic Endotoxemia

Non-ventilatory management of cirrhotic patients with endotoxemia is highlighted given the cardiovascular and pulmonary effects described above. Treatment may include inotropes to augment biventricular function [303]. As well, attempts should

be made to decrease the work of breathing and improve lung and chest wall mechanics via large volume paracentesis [265-267, 276, 290]. The administration of albumin to maintain intra-vascular volume is also favoured, especially if paracentesis is undertaken [304]. Judicious use of diuretics may also improve heart-lung interaction and renal perfusion, though this should be done with exquisitely close monitoring in the setting of septic shock. Great vein Doppler pulsatility, described in chapter 10, is one potential monitoring approach.

Conclusions

The transient and steady state effects of lung volume and intra-thoracic pressure on the cardiovascular system can be discordant and seemingly inexplicable at times. Thoracic mechanics alter right and left ventricular loading simultaneously via multiple mechanisms. The generalities are as follows: both spontaneous and mechanical inspiration increase lung volume and this reduces venous capacitance in the abdomen and lungs. Reduced vascular capacitance increases the upstream pressure for venous return and enhances diastolic filling of the ventricles. When intra-thoracic pressure falls in conjunction with increased lung volume, right heart diastolic filling is enhanced if not limited by great vein collapse. To the extent that right heart volume increases, left heart filling is impaired through the septum. During systole, right heart ejection is typically hindered by lung volume above functional residual capacity; egress of blood to the left ventricle is also diminished.

Passive, mechanical ventilation is not the exact converse of spontaneous breathing as it too increases lung volume, but intra-thoracic pressure change is different. With mechanical inspiration, the right ventricle experiences competing interests – the pressure head for venous return increases, but the downstream pressure does as well; the afterload of the RV still rises. Regarding the LV, the pressure head for pulmonary venous return grows as the lung expands, but the effects of ventricular interdependence are variable; the afterload of the LV is reduced during systole.

The intermediaries of these responses are volume status, cardiac function, intra-thoracic pressure and volume. In the disease states discussed above, any or all of these effectors of cardiorespiratory interaction are altered. Certainly, spontaneous inspiratory pressures are more negative and expiration more positive as a function of the dynamic and elastic respiratory loads. Lung volume may be pathologically high or low and the ratio of pulmonary to chest wall compliance determine biventricular loading during passive mechanical ventilation.

Simultaneous analysis of the Guyton and Campbell diagrams leads the clinician down a systematic path, considering each abnormality in turn. Mentally constructing the venous return curve, cardiac function curve and their reactions to static and elastic respiratory loads rationalizes therapy, predicts hemodynamic embarrassment [e.g. when liberating a patient from mechanical ventilation] and explains hemodynamic measurements such the central venous pressure, pulmonary artery occlusion pressure and variation of left ventricular stroke volume.

Importantly, the physiology reviewed in this chapter cannot be applied to every patient under all circumstances because the physiology cannot always be known in contemporary medicine. Nevertheless, a methodical approach to heart-lung physiology helps clarify hemodynamic evaluation and management of the critically-ill.

References

1. Pinsky, M.R., Cardiovascular issues in respiratory care. Chest, 2005. 128(5 Suppl 2): p. 592S-597S.
2. Banner, M.J., M.J. Jaeger, and R.R. Kirby, Components of the work of breathing and implications for monitoring ventilator-dependent patients. Crit Care Med, 1994. 22(3): p. 515-23.
3. Fredberg, J.J., et al., Airway smooth muscle, tidal stretches, and dynamically determined contractile states. Am J Respir Crit Care Med, 1997. 156(6): p. 1752-9.
4. O'Donnell, D.E. and P. Laveneziana, The clinical importance of dynamic lung hyperinflation in COPD. COPD, 2006. 3(4): p. 219-32.
5. O'Donnell, D.E., Hyperinflation, dyspnea, and exercise intolerance in chronic obstructive pulmonary disease. Proc Am Thorac Soc, 2006. 3(2): p. 180-4.
6. Axen, K., et al., Ventilatory adjustments during sustained mechanical loading in conscious humans. J Appl Physiol Respir Environ Exerc Physiol, 1983. 55(4): p. 1211-8.
7. Axen, K., et al., Effect of mechanical loading on breathing patterns in women. J Appl Physiol Respir Environ Exerc Physiol, 1984. 56(1): p. 175-81.
8. Rochester, D.F., Respiratory muscles and ventilatory failure: 1993 perspective. Am J Med Sci, 1993. 305(6): p. 394-402.
9. O'Donnell, D.E., et al., Qualitative aspects of exertional breathlessness in chronic airflow limitation: pathophysiologic mechanisms. Am J Respir Crit Care Med, 1997. 155(1): p. 109-15.
10. Levison, H. and R.M. Cherniack, Ventilatory cost of exercise in chronic obstructive pulmonary disease. J Appl Physiol, 1968. 25(1): p. 21-7.
11. Roussos, C. and P.T. Macklem, The respiratory muscles. N Engl J Med, 1982. 307(13): p. 786-97.
12. Aubier, M., et al., Respiratory muscle contribution to lactic acidosis in low cardiac output. Am Rev Respir Dis, 1982. 126(4): p. 648-52.
13. Vogiatzis, I., et al., Intercostal muscle blood flow limitation during exercise in chronic obstructive pulmonary disease. Am J Respir Crit Care Med, 2010. 182(9): p. 1105-13.
14. Stock, M.C., et al., Lung mechanics and oxygen consumption during spontaneous ventilation and severe heart failure. Chest, 1992. 102(1): p. 279-83.
15. Young, I.H. and P.T. Bye, Gas exchange in disease: asthma, chronic obstructive pulmonary disease, cystic fibrosis, and interstitial lung disease. Compr Physiol, 2011. 1(2): p. 663-97.
16. Bishop, J.M. and K.W. Cross, Use of other physiological variables to predict pulmonary arterial pressure in patients with chronic respiratory disease. Multicentre study. Eur Heart J, 1981. 2(6): p. 509-17.
17. Potter, W.A., S. Olafsson, and R.E. Hyatt, Ventilatory mechanics and expiratory flow limitation during exercise in patients with obstructive lung disease. J Clin Invest, 1971. 50(4): p. 910-9.
18. Stubbing, D.G., et al., Pulmonary mechanics during exercise in subjects with chronic airflow obstruction. J Appl Physiol Respir Environ Exerc Physiol, 1980. 49(3): p. 511-5.
19. Stubbing, D.G., et al., Pulmonary mechanics during exercise in normal males. J Appl Physiol Respir Environ Exerc Physiol, 1980. 49(3): p. 506-10.
20. Celli, B.R., Pathophysiology of chronic obstructive pulmonary disease. Chest Surg Clin N Am, 1995. 5(4): p. 623-34.
21. O'Donnell, D.E., S.M. Revill, and K.A. Webb, Dynamic hyperinflation and exercise intolerance in chronic obstructive pulmonary disease. Am J Respir Crit Care Med, 2001. 164(5): p. 770-7.
22. O'Donnell, D.E. and K.A. Webb, The major limitation to exercise performance in COPD is dynamic hyperinflation. J Appl Physiol (1985), 2008. 105(2): p. 753-5; discussion 755-7.
23. Marini, J.J., Dynamic hyperinflation and auto-positive end-expiratory pressure: lessons learned over 30 years. Am J Respir Crit Care Med, 2011. 184(7): p. 756-62.
24. Nanas, S. and S. Magder, Adaptations of the peripheral circulation to PEEP. Am Rev Respir Dis, 1992. 146(3): p. 688-93.
25. Scharf, S.M. and R.H. Ingram, Jr., Influence of abdominal pressure and sympathetic vasoconstriction on the cardiovascular response to positive end-expiratory pressure. Am Rev Respir Dis, 1977. 116(4): p. 661-70.
26. Fessler, H.E., et al., Effects of Positive End-Expiratory Pressure on the Gradient for Venous Return. American Review of Respiratory Disease, 1991. 143(1): p. 19-24.
27. Fessler, H.E., Heart-lung interactions: applications in the critically ill. Eur Respir J, 1997. 10(1): p. 226-37.
28. Jellinek, H., et al., Influence of positive airway pressure on the pressure gradient for venous return in humans. J Appl Physiol (1985), 2000. 88(3): p. 926-32.
29. van den Berg, P.C., J.R. Jansen, and M.R. Pinsky, Effect of positive pressure on venous return in volume-loaded cardiac surgical patients. J Appl Physiol (1985), 2002. 92(3): p. 1223-31.
30. Nakhjavan, F.K., W.H. Palmer, and M. McGregor, Influence of respiration on venous return in pulmonary emphysema. Circulation, 1966. 33(1): p. 8-16.
31. Natori, H., S. Tamaki, and S. Kira, Ultrasonographic evaluation of ventilatory effect on inferior vena caval configuration. Am Rev Respir Dis, 1979. 120(2): p. 421-7.

32. Lloyd, T.C., Jr., Effect of inspiration on inferior vena caval blood flow in dogs. J Appl Physiol Respir Environ Exerc Physiol, 1983. 55(6): p. 1701-8.
33. Scharf, S.M., Cardiovascular effects of airways obstruction. Lung, 1991. 169(1): p. 1-23.
34. Feihl, F. and A.F. Broccard, Interactions between respiration and systemic hemodynamics. Part I: basic concepts. Intensive Care Med, 2009. 35(1): p. 45-54.
35. Broccard, A.F., Cardiopulmonary interactions and volume status assessment. J Clin Monit Comput, 2012. 26(5): p. 383-91.
36. Fessler, H.E., et al., Effects of positive end-expiratory pressure on the canine venous return curve. Am Rev Respir Dis, 1992. 146(1): p. 4-10.
37. Butler, J., et al., Cause of the raised wedge pressure on exercise in chronic obstructive pulmonary disease. Am Rev Respir Dis, 1988. 138(2): p. 350-4.
38. Novak, R., G.M. Matuschak, and M.R. Pinsky, Effect of positive-pressure ventilatory frequency on regional pleural pressure. J Appl Physiol (1985), 1988. 65(3): p. 1314-23.
39. Brookhart, J.M. and T.E. Boyd, Local differences in intrathoracic pressure and their relation to cardiac filling pressure in the dog. Am J Physiol, 1947. 148(2): p. 434-44.
40. Lloyd, T.C., Jr., Respiratory system compliance as seen from the cardiac fossa. J Appl Physiol Respir Environ Exerc Physiol, 1982. 53(1): p. 57-62.
41. Butler, J., The heart is in good hands. Circulation, 1983. 67(6): p. 1163-8.
42. Cobelli, F., N. Ambrosino, and C. Opasich, Pulmonary hemodynamics during resistive load breathing in chronic obstructive lung disease. Current topics in rehabilitation: Pathophysiology and treatment of pulmonary circulation. Londres: Springer-Verlag, 1988.
43. Luecke, T. and P. Pelosi, Clinical review: Positive end-expiratory pressure and cardiac output. Crit Care, 2005. 9(6): p. 607-21.
44. Vargas, M., et al., PEEP role in ICU and operating room: from pathophysiology to clinical practice. ScientificWorldJournal, 2014. 2014: p. 852356.
45. Whittenberger, J.L., et al., Influence of state of inflation of the lung on pulmonary vascular resistance. J Appl Physiol, 1960. 15: p. 878-82.
46. Scharf, S.M. and R. Brown, Influence of the right ventricle on canine left ventricular function with PEEP. J Appl Physiol Respir Environ Exerc Physiol, 1982. 52(1): p. 254-9.
47. Permutt, S., B. Bromberger-Barnea, and H.N. Bane, Alveolar pressure, pulmonary venous pressure, and the vascular waterfall. Med Thorac, 1962. 19: p. 239-60.
48. Lopez-Muniz, R., et al., Critical closure of pulmonary vessels analyzed in terms of Starling resistor model. J Appl Physiol, 1968. 24(5): p. 625-35.
49. Magder, S. and B. Guerard, Heart-lung interactions and pulmonary buffering: lessons from a computational modeling study. Respir Physiol Neurobiol, 2012. 182(2-3): p. 60-70.
50. Naeije, R. and J.A. Barbera, Pulmonary hypertension associated with COPD. Crit Care, 2001. 5(6): p. 286-9.
51. Naeije, R., Pulmonary vascular resistance. A meaningless variable? Intensive Care Med, 2003. 29(4): p. 526-9.
52. Gelb, A.F., et al., Mechanism of short-term improvement in lung function after emphysema resection. Am J Respir Crit Care Med, 1996. 154(4 Pt 1): p. 945-51.
53. Brenner, M., et al., Lung volume reduction surgery for emphysema. Chest, 1996. 110(1): p. 205-18.
54. Sciurba, F.C., et al., Improvement in pulmonary function and elastic recoil after lung-reduction surgery for diffuse emphysema. N Engl J Med, 1996. 334(17): p. 1095-9.
55. Oswald-Mammosser, M., et al., Effect of lung volume reduction surgery on gas exchange and pulmonary hemodynamics at rest and during exercise. Am J Respir Crit Care Med, 1998. 158(4): p. 1020-5.
56. Bove, A.A. and W.P. Santamore, Ventricular interdependence. Prog Cardiovasc Dis, 1981. 23(5): p. 365-88.
57. Santamore, W.P., J.L. Heckman, and A.A. Bove, Right and left ventricular pressure-volume response to respiratory maneuvers. J Appl Physiol Respir Environ Exerc Physiol, 1984. 57(5): p. 1520-7.
58. Weber, K.T., et al., Contractile mechanics and interaction of the right and left ventricles. Am J Cardiol, 1981. 47(3): p. 686-95.
59. Maughan, W.L., et al., Instantaneous pressure-volume relationship of the canine right ventricle. Circ Res, 1979. 44(3): p. 309-15.
60. Maughan, W.L., K. Sunagawa, and K. Sagawa, Ventricular systolic interdependence: volume elastance model in isolated canine hearts. Am J Physiol, 1987. 253(6 Pt 2): p. H1381-90.
61. Farrar, D.J., J.C. Woodard, and E. Chow, Pacing-induced dilated cardiomyopathy increases left-to-right ventricular systolic interaction. Circulation, 1993. 88(2): p. 720-5.
62. Khaja, F. and J.O. Parker, Right and left ventricular performance in chronic obstructive lung disease. Am Heart J, 1971. 82(3): p. 319-27.
63. Baum, G.L., et al., Left ventricular function in chronic obstructive lung disease. N Engl J Med, 1971. 285(7): p. 361-5.
64. Jezek, V. and F. Schrijen, Left ventricular function in chronic obstructive pulmonary disease with and without cardiac failure. Clin Sci Mol Med, 1973. 45(3): p. 267-79.
65. Jezek, V., F. Schrijen, and P. Sadoul, Right ventricular function and pulmonary hemodynamics during exercise in patients with chronic obstructive bronchopulmonary disease. Cardiology, 1973. 58(1): p. 20-31.

66. Kasner, M., et al., Left ventricular dysfunction induced by nonsevere idiopathic pulmonary arterial hypertension: a pressure-volume relationship study. Am J Respir Crit Care Med, 2012. 186(2): p. 181-9.
67. Granton, J., The right ventricle in pulmonary hypertension: when good neighbors go bad. Am J Respir Crit Care Med, 2012. 186(2): p. 121-3.
68. Lockhart, A., et al., Elevated pulmonary artery wedge pressure at rest and during exercise in chronic bronchitis: fact or fancy. Clin Sci, 1969. 37(2): p. 503-17.
69. Biondi, J.W., D.S. Schulman, and R.A. Matthay, Effects of mechanical ventilation on right and left ventricular function. Clin Chest Med, 1988. 9(1): p. 55-71.
70. Schulman, D.S., et al., Effect of positive end-expiratory pressure on right ventricular performance. Importance of baseline right ventricular function. Am J Med, 1988. 84(1): p. 57-67.
71. Schulman, D.S., et al., Left ventricular diastolic function during positive end-expiratory pressure. Impact of right ventricular ischemia and ventricular interaction. Am Rev Respir Dis, 1992. 145(3): p. 515-21.
72. Permutt, S., et al., Effect of lung inflation on static pressure-volume characteristics of pulmonary vessels. J Appl Physiol, 1961. 16: p. 64-70.
73. Howell, J.B., et al., Effect of inflation of the lung on different parts of pulmonary vascular bed. J Appl Physiol, 1961. 16: p. 71-6.
74. Pinsky, M.R., Recent advances in the clinical application of heart-lung interactions. Curr Opin Crit Care, 2002. 8(1): p. 26-31.
75. Gibson, G.J., Lung volumes and elasticity. Clin Chest Med, 2001. 22(4): p. 623-35, vii.
76. Byrd, R.B. and R.E. Hyatt, Maximal respiratory pressures in chronic obstructive lung disease. Am Rev Respir Dis, 1968. 98(5): p. 848-56.
77. Gibson, G.J., E. Clark, and N.B. Pride, Static transdiaphragmatic pressures in normal subjects and in patients with chronic hyperinflation. Am Rev Respir Dis, 1981. 124(6): p. 685-9.
78. Freedman, S., A.E. Tattersfield, and N.B. Pride, Changes in lung mechanics during asthma induced by exercise. J Appl Physiol, 1975. 38(6): p. 974-82.
79. Holmes, P.W., A.H. Campbell, and C.E. Barter, Acute changes of lung volumes and lung mechanics in asthma and in normal subjects. Thorax, 1978. 33(3): p. 394-400.
80. Stalcup, S.A. and R.B. Mellins, Mechanical forces producing pulmonary edema in acute asthma. N Engl J Med, 1977. 297(11): p. 592-6.
81. Fry, D.L. and R.E. Hyatt, Pulmonary mechanics. A unified analysis of the relationship between pressure, volume and gasflow in the lungs of normal and diseased human subjects. Am J Med, 1960. 29: p. 672-89.
82. Fry, D.L., et al., The mechanics of pulmonary ventilation in normal subjects and in patients with emphysema. Am J Med, 1954. 16(1): p. 80-97.
83. Vassilakopoulos, T., Understanding wasted/ineffective efforts in mechanically ventilated COPD patients using the Campbell diagram. Intensive Care Med, 2008. 34(7): p. 1336-9.
84. Morgan, B.C., W.G. Guntheroth, and D.H. Dillard, Relationship of Pericardial to Pleural Pressure during Quiet Respiration and Cardiac Tamponade. Circ Res, 1965. 16: p. 493-8.
85. Magder, S., Hemodynamic monitoring in the mechanically ventilated patient. Curr Opin Crit Care, 2011. 17(1): p. 36-42.
86. Magder, S., Fluid status and fluid responsiveness. Current Opinion in Critical Care, 2010. 16(4): p. 289-96.
87. Magder, S., Bench-to-bedside review: An approach to hemodynamic monitoring - Guyton at the bedside. Crit Care, 2012. 16(5): p. 236.
88. Guyton, A.C. and L.H. Adkins, Quantitative aspects of the collapse factor in relation to venous return. Am J Physiol, 1954. 177(3): p. 523-7.
89. Guyton, A.C., A.W. Lindsey, and B.N. Kaufmann, Effect of mean circulatory filling pressure and other peripheral circulatory factors on cardiac output. Am J Physiol, 1955. 180(3): p. 463-8.
90. Guyton, A.C., et al., Venous return at various right atrial pressures and the normal venous return curve. Am J Physiol, 1957. 189(3): p. 609-15.
91. Brecher, G.A., Mechanism of venous flow under different degrees of aspiration. Am J Physiol, 1952. 169(2): p. 423-33.
92. Takata, M., R.A. Wise, and J.L. Robotham, Effects of abdominal pressure on venous return: abdominal vascular zone conditions. J Appl Physiol (1985), 1990. 69(6): p. 1961-72.
93. Takata, M. and J.L. Robotham, Effects of inspiratory diaphragmatic descent on inferior vena caval venous return. J Appl Physiol (1985), 1992. 72(2): p. 597-607.
94. Robotham, J.L. and M. Takata, Mechanical abdomino/heart/lung interaction. J Sleep Res, 1995. 4(S1): p. 50-52.
95. Robotham, J.L., et al., Effects of respiration on cardiac performance. J Appl Physiol Respir Environ Exerc Physiol, 1978. 44(5): p. 703-9.
96. Scharf, S.M., et al., Hemodynamic effects of positive-pressure inflation. J Appl Physiol Respir Environ Exerc Physiol, 1980. 49(1): p. 124-31.
97. Pinsky, M.R., Instantaneous venous return curves in an intact canine preparation. J Appl Physiol Respir Environ Exerc Physiol, 1984. 56(3): p. 765-71.
98. Pinsky, M.R., Determinants of pulmonary arterial flow variation during respiration. J Appl Physiol Respir Environ Exerc Physiol, 1984. 56(5): p. 1237-45.
99. Jardin, F., et al., Mechanism of paradoxic pulse in bronchial asthma. Circulation, 1982. 66(4): p. 887-94.

100. Harris, P., N. Segel, and J.M. Bishop, The relation between pressure and flow in the pulmonary circulation in normal subjects and in patients with chronic bronchitis and mitral stenosis. Cardiovasc Res, 1968. 2(1): p. 73-83.
101. Burrows, B., et al., Patterns of cardiovascular dysfunction in chronic obstructive lung disease. N Engl J Med, 1972. 286(17): p. 912-8.
102. Scharf, S.M., et al., Cardiac effects of increased lung volume and decreased pleural pressure in man. J Appl Physiol Respir Environ Exerc Physiol, 1979. 47(2): p. 257-62.
103. Koshino, Y., et al., Changes in left and right ventricular mechanics during the Mueller maneuver in healthy adults: a possible mechanism for abnormal cardiac function in patients with obstructive sleep apnea. Circ Cardiovasc Imaging, 2010. 3(3): p. 282-9.
104. Damiano, R.J., Jr., et al., Significant left ventricular contribution to right ventricular systolic function. Am J Physiol, 1991. 261(5 Pt 2): p. H1514-24.
105. Sibbald, W.J. and A.A. Driedger, Right ventricular function in acute disease states: pathophysiologic considerations. Crit Care Med, 1983. 11(5): p. 339-45.
106. Robotham, J.L. and S.M. Scharf, Effects of positive and negative pressure ventilation on cardiac performance. Clin Chest Med, 1983. 4(2): p. 161-87.
107. Peters, J., M.K. Kindred, and J.L. Robotham, Transient analysis of cardiopulmonary interactions. II. Systolic events. J Appl Physiol (1985), 1988. 64(4): p. 1518-26.
108. Peters, J., M.K. Kindred, and J.L. Robotham, Transient analysis of cardiopulmonary interactions. I. Diastolic events. J Appl Physiol (1985), 1988. 64(4): p. 1506-17.
109. Peters, J., et al., Negative intrathoracic pressure decreases independently left ventricular filling and emptying. Am J Physiol, 1989. 257(1 Pt 2): p. H120-31.
110. Scharf, S.M., et al., Effects of normal and loaded spontaneous inspiration on cardiovascular function. J Appl Physiol Respir Environ Exerc Physiol, 1979. 47(3): p. 582-90.
111. Scharf, S.M., et al., The effects of large negative intrathoracic pressure on left ventricular function in patients with coronary artery disease. Circulation, 1981. 63(4): p. 871-5.
112. Scharf, S.M., et al., Effects of the Mueller maneuver on global and regional left ventricular function in angina pectoris with or without previous myocardial infarction. Am J Cardiol, 1987. 59(15): p. 1305-9.
113. Scharf, S.M., et al., Mueller maneuver and LV function in coronary artery disease. Ann Biomed Eng, 1987. 15(3-4): p. 297-310.
114. Rooke, G.A., H.A. Schwid, and Y. Shapira, The effect of graded hemorrhage and intravascular volume replacement on systolic pressure variation in humans during mechanical and spontaneous ventilation. Anesth Analg, 1995. 80(5): p. 925-32.
115. Magder, S., Clinical usefulness of respiratory variations in arterial pressure. Am J Respir Crit Care Med, 2004. 169(2): p. 151-5.
116. Wead, W.B. and J.F. Norton, Effects of intrapleural pressure changes on canine left ventricular function. J Appl Physiol Respir Environ Exerc Physiol, 1981. 50(5): p. 1027-35.
117. Robotham, J.L., Cardiovascular disturbances in chronic respiratory insufficiency. Am J Cardiol, 1981. 47(4): p. 941-9.
118. Matthay, R.A. and H.J. Berger, Cardiovascular function in cor pulmonale. Clin Chest Med, 1983. 4(2): p. 269-95.
119. Buda, A.J., et al., Effect of intrathoracic pressure on left ventricular performance. N Engl J Med, 1979. 301(9): p. 453-9.
120. Jorgensen, K., et al., Effects of lung volume reduction surgery on left ventricular diastolic filling and dimensions in patients with severe emphysema. Chest, 2003. 124(5): p. 1863-70.
121. Fessler, H.E., Effects of CPAP on venous return. J Sleep Res, 1995. 4(S1): p. 44-49.
122. Berlin, D., Hemodynamic consequences of auto-PEEP. J Intensive Care Med, 2014. 29(2): p. 81-6.
123. Janicki, J.S. and K.T. Weber, The pericardium and ventricular interaction, distensibility, and function. Am J Physiol, 1980. 238(4): p. H494-503.
124. Funk, G.C., et al., Left ventricular diastolic dysfunction in patients with COPD in the presence and absence of elevated pulmonary arterial pressure. Chest, 2008. 133(6): p. 1354-9.
125. Brower, R., et al., Effect of lung inflation on lung blood volume and pulmonary venous flow. J Appl Physiol (1985), 1985. 58(3): p. 954-63.
126. Robotham, J.L., et al., A re-evaluation of the hemodynamic consequences of intermittent positive pressure ventilation. Crit Care Med, 1983. 11(10): p. 783-93.
127. Gattinoni, L., et al., Bench-to-bedside review: chest wall elastance in acute lung injury/acute respiratory distress syndrome patients. Crit Care, 2004. 8(5): p. 350-5.
128. Mesquida, J., H.K. Kim, and M.R. Pinsky, Effect of tidal volume, intrathoracic pressure, and cardiac contractility on variations in pulse pressure, stroke volume, and intrathoracic blood volume. Intensive Care Med, 2011. 37(10): p. 1672-9.
129. O'Quin, R.J., et al., Transmission of airway pressure to pleural space during lung edema and chest wall restriction. J Appl Physiol (1985), 1985. 59(4): p. 1171-7.
130. Jardin, F., et al., Influence of lung and chest wall compliances on transmission of airway pressure to the pleural space in critically ill patients. Chest, 1985. 88(5): p. 653-8.
131. Venus, B., L.E. Cohen, and R.A. Smith, Hemodynamics and intrathoracic pressure transmission during controlled mechanical ventilation and positive end-expiratory pressure in normal and low compliant lungs. Crit Care Med, 1988. 16(7): p. 686-90.

132. Lansdorp, B., et al., Mechanical ventilation-induced intrathoracic pressure distribution and heart-lung interactions*. Crit Care Med, 2014. 42(9): p. 1983-90.
133. Pinsky, M.R., Why knowing the effects of positive-pressure ventilation on venous, pleural, and pericardial pressures is important to the bedside clinician?*. Crit Care Med, 2014. 42(9): p. 2129-31.
134. Magder, S., Predicting volume responsiveness in spontaneously breathing patients: still a challenging problem. Crit Care, 2006. 10(5): p. 165.
135. Harris, P., et al., The influence of the airways resistance and alveolar pressure on the pulmonary vascular resistance in chronic bronhcitis. Cardiovasc Res, 1968. 2(1): p. 84-92.
136. Chihara, E., et al., Elevated mean systemic filling pressure due to intermittent positive-pressure ventilation. Am J Physiol, 1992. 262(4 Pt 2): p. H1116-21.
137. Brienza, N., et al., Regional control of venous return: liver blood flow. Am J Respir Crit Care Med, 1995. 152(2): p. 511-8.
138. Brienza, N., et al., Effects of PEEP on liver arterial and venous blood flows. Am J Respir Crit Care Med, 1995. 152(2): p. 504-10.
139. Voelkel, N.F., J. Gomez-Arroyo, and S. Mizuno, COPD/emphysema: The vascular story. Pulm Circ, 2011. 1(3): p. 320-6.
140. Neidhart, P.P. and P.M. Suter, Changes of right ventricular function with positive end-expiratory pressure (PEEP) in man. Intensive Care Med, 1988. 14 Suppl 2: p. 471-3.
141. Pinsky, M.R., My paper 20 years later: Effect of positive end-expiratory pressure on right ventricular function in humans. Intensive Care Med, 2014. 40(7): p. 935-41.
142. Grau, M., et al., Percent emphysema and right ventricular structure and function: the Multi-Ethnic Study of Atherosclerosis-Lung and Multi-Ethnic Study of Atherosclerosis-Right Ventricle Studies. Chest, 2013. 144(1): p. 136-44.
143. Vonk-Noordegraaf, A., et al., Right heart adaptation to pulmonary arterial hypertension: physiology and pathobiology. J Am Coll Cardiol, 2013. 62(25 Suppl): p. D22-33.
144. Takao, M., et al., Noninvasive assessment of right heart function by 81mKr equilibrium radionuclide ventriculography in chronic pulmonary diseases. Chest, 1996. 109(1): p. 67-72.
145. Madden, J.A., C.A. Dawson, and D.R. Harder, Hypoxia-induced activation in small isolated pulmonary arteries from the cat. J Appl Physiol (1985), 1985. 59(1): p. 113-8.
146. Dawson, C.A., D.J. Grimm, and J.H. Linehan, Lung inflation and longitudinal distribution of pulmonary vascular resistance during hypoxia. J Appl Physiol Respir Environ Exerc Physiol, 1979. 47(3): p. 532-6.
147. Abraham, A.S., et al., Factors contributing to the reversible pulmonary hypertension of patients with acute respiratory failure studies by serial observations during recovery. Circ Res, 1969. 24(1): p. 51-60.
148. Edwards, C.W., Left ventricular hypertrophy in emphysema. Thorax, 1974. 29(1): p. 75-80.
149. Fluck, D.C., R.G. Chandrasekar, and F.V. Gardner, Left ventricular hypertrophy in chronic bronchitis. Br Heart J, 1966. 28(1): p. 92-7.
150. Murphy, M.L., J. Adamson, and F. Hutcheson, Left ventricular hypertrophy in patients with chronic bronchitis and emphysema. Ann Intern Med, 1974. 81(3): p. 307-13.
151. Luecke, T., et al., Assessment of cardiac preload and left ventricular function under increasing levels of positive end-expiratory pressure. Intensive Care Med, 2004. 30(1): p. 119-26.
152. Ranieri, V.M., M. Dambrosio, and N. Brienza, Intrinsic PEEP and cardiopulmonary interaction in patients with COPD and acute ventilatory failure. Eur Respir J, 1996. 9(6): p. 1283-92.
153. Biondi, J.W., et al., The effect of incremental positive end-expiratory pressure on right ventricular hemodynamics and ejection fraction. Anesth Analg, 1988. 67(2): p. 144-51.
154. Jardin, F. and A. Vieillard-Baron, Acute cor pulmonale. Curr Opin Crit Care, 2009. 15(1): p. 67-70.
155. Jardin, F., Ventricular interdependence: how does it impact on hemodynamic evaluation in clinical practice? Intensive Care Med, 2003. 29(3): p. 361-3.
156. Terplan, M. and G. Fruhmann, Significance of the Dynamic Pressure-Volume Curve in Subjects with and without Obstructive Respiratory Disease. Med Thorac, 1963. 20: p. 372-85.
157. Niewoehner, D.E., J. Kleinerman, and L. Liotta, Elastic behavior of postmortem human lungs: effects of aging and mild emphysema. J Appl Physiol, 1975. 39(6): p. 943-9.
158. Brusasco, V. and F. Martinez, Chronic obstructive pulmonary disease. Compr Physiol, 2014. 4(1): p. 1-31.
159. Zamel, N., J. Hogg, and A. Gelb, Mechanisms of maximal expiratory flow limitation in clinically unsuspected emphysema and obstruction of the peripheral airways. Am Rev Respir Dis, 1976. 113(3): p. 337-45.
160. Sciurba, F.C., Physiologic similarities and differences between COPD and asthma. Chest, 2004. 126(2 Suppl): p. 117S-124S; discussion 159S-161S.
161. Gelb, A.F., et al., Unsuspected mild emphysema in nonsmoking patients with chronic asthma with persistent airway obstruction. J Allergy Clin Immunol, 2014. 133(1): p. 263-5 e1-3.
162. Hardin, M., et al., The clinical features of the overlap between COPD and asthma. Respir Res, 2011. 12: p. 127.
163. Guyton, A.C., Determination of cardiac output by equating venous return curves with cardiac response curves. Physiol Rev, 1955. 35(1): p. 123-9.
164. Sagawa, K., The end-systolic pressure-volume relation of the ventricle: definition, modifications and clinical use. Circulation, 1981. 63(6): p. 1223-7.

165. Starr, I., Role of the" static blood pressure" in abnormal increments of venous pressure, especially in heart failure. ii. clinical and experimental studies. The American Journal of the Medical Sciences, 1940. 199(1): p. 40-54.
166. Sylvester, J.T., H.S. Goldberg, and S. Permutt, The Role of the Vasculature in the Regulation of Cardiac-Output. Clinics in Chest Medicine, 1983. 4(2): p. 111-126.
167. Jacobsohn, E., R. Chorn, and M. OConnor, The role of the vasculature in regulating venous return and cardiac output: historical and graphical approach. Canadian Journal of Anaesthesia-Journal Canadien D Anesthesie, 1997. 44(8): p. 849-867.
168. Staub, N.C., H. Nagano, and M.L. Pearce, The sequence of events during fluid accumulation in acute pulmonary edema. Jpn Heart J, 1967. 8(6): p. 683-9.
169. Staub, N.C., H. Nagano, and M.L. Pearce, Pulmonary edema in dogs, especially the sequence of fluid accumulation in lungs. J Appl Physiol, 1967. 22(2): p. 227-40.
170. Giuntini, C., A. Maseri, and R. Bianchi, Pulmonary vascular distensibility and lung compliance as modified by dextran infusion and subsequent atropine injection in normal subjects. J Clin Invest, 1966. 45(11): p. 1770-89.
171. SIMON, M., The Pulmonary Vessels in Incipient Left Ventricular Decompensation Radiologic Observations. Circulation, 1961. 24(2): p. 185-190.
172. Turner, A.F., F.Y. Lau, and G. Jacobson, A method for the estimation of pulmonary venous and arterial pressures from the routine chest roentgenogram. Am J Roentgenol Radium Ther Nucl Med, 1972. 116(1): p. 97-106.
173. Surette, G.D., et al., Roentgenographic study of blood flow redistribution in acute pulmonary edema in dogs. Invest Radiol, 1975. 10(2): p. 109-14.
174. Bhattacharya, J. and N.C. Staub, Direct measurement of microvascular pressures in the isolated perfused dog lung. Science, 1980. 210(4467): p. 327-8.
175. Gee, M.H. and D.O. Williams, Effect of lung inflation on perivascular cuff fluid volume in isolated dog lung lobes. Microvasc Res, 1979. 17(2): p. 192-201.
176. Staub, N.C., The pathogenesis of pulmonary edema. Prog Cardiovasc Dis, 1980. 23(1): p. 53-80.
177. Schneeberger, E.E. and M.J. Karnovsky, Substructure of intercellular junctions in freeze-fractured alveolar-capillary membranes of mouse lung. Circ Res, 1976. 38(5): p. 404-11.
178. Hastings, R.H., et al., Clearance of different-sized proteins from the alveolar space in humans and rabbits. J Appl Physiol (1985), 1992. 73(4): p. 1310-6.
179. Noble, W.H., J.C. Kay, and J. Obdrzalek, Lung mechanics in hypervolemic pulmonary edema. J Appl Physiol, 1975. 38(4): p. 681-7.
180. Sharp, J.T., et al., Ventilatory mechanics in pulmonary edema in man. J Clin Invest, 1958. 37(1): p. 111-7.
181. Ishii, M., et al., Effects of hemodynamic edema formation on peripheral vs. central airway mechanics. J Appl Physiol (1985), 1985. 59(5): p. 1578-84.
182. Hogg, J.C., et al., Distribution of airway resistance with developing pulmonary edema in dogs. J Appl Physiol, 1972. 32(1): p. 20-4.
183. Pepine, C.J. and L. Wiener, Relationship of anginal symptoms to lung mechanics during myocardial ischemia. Circulation, 1972. 46(5): p. 863-9.
184. Hales, C.A. and H. Kazemi, Small-airways function in myocardial infarction. N Engl J Med, 1974. 290(14): p. 761-5.
185. West, J.B., Perivascular edema, a factor in pulmonary vascular resistance. Am Heart J, 1965. 70(4): p. 570-2.
186. West, J.B., C.T. Dollery, and B.E. Heard, Increased Pulmonary Vascular Resistance in the Dependent Zone of the Isolated Dog Lung Caused by Perivascular Edema. Circ Res, 1965. 17: p. 191-206.
187. Mitrouska, I., M. Klimathianaki, and N.M. Siafakas, Effects of pleural effusion on respiratory function. Can Respir J, 2004. 11(7): p. 499-503.
188. Friedman, W.F. and E. Braunwald, Alterations in regional pulmonary blood flow in mitral valve disease studied by radioisotope scanning. A simple nontraumatic technique for estimation of left atrial pressure. Circulation, 1966. 34(3): p. 363-76.
189. Dollery, C.T. and J.B. West, Regional uptake of radioactive oxygen, carbon monoxide and carbon dioxide in the lungs of patients with mitral stenosis. Circ Res, 1960. 8: p. 765-71.
190. West, J.B., C.T. Dollery, and A. Naimark, Distribution of Blood Flow in Isolated Lung; Relation to Vascular and Alveolar Pressures. J Appl Physiol, 1964. 19: p. 713-24.
191. Hughes, J.M., et al., Effect of extra-alveolar vessels on distribution of blood flow in the dog lung. J Appl Physiol, 1968. 25(6): p. 701-12.
192. Hughes, J.M., et al., Effect of lung volume on the distribution of pulmonary blood flow in man. Respir Physiol, 1968. 4(1): p. 58-72.
193. Muir, A.L., et al., Distribution of blood flow in the lungs in acute pulmonary edema in dogs. J Appl Physiol, 1972. 33(6): p. 763-9.
194. Tsang, J.Y., E.M. Baile, and J.C. Hogg, Relationship between regional pulmonary edema and blood flow. J Appl Physiol (1985), 1986. 60(2): p. 449-57.
195. Graf, J., Pleural effusion in the mechanically ventilated patient. Curr Opin Crit Care, 2009. 15(1): p. 10-7.
196. Franklin, D.L., R.L. Van Citters, and R.F. Rushmer, Balance between right and left ventricular output. Circ Res, 1962. 10: p. 17-26.

197. Formenti, P., et al., Drainage of pleural effusion in mechanically ventilated patients: Time to measure chest wall compliance? J Crit Care, 2014. 29(5): p. 808-13.
198. Chattranukulchai, P., et al., A rare cause of pulsus paradoxus: acute tension hydrothorax. BMJ Case Rep, 2013. 2013.
199. Janicki, J.S., Influence of the pericardium and ventricular interdependence on left ventricular diastolic and systolic function in patients with heart failure. Circulation, 1990. 81(2 Suppl): p. III15-20.
200. Takata, M., et al., Coupled vs. uncoupled pericardial constraint: effects on cardiac chamber interactions. J Appl Physiol (1985), 1997. 83(6): p. 1799-813.
201. Sarnoff, S.J., Myocardial contractility as described by ventricular function curves; observations on Starling's law of the heart. Physiol Rev, 1955. 35(1): p. 107-22.
202. Case, R.B., E. Berglund, and S.J. Sarnoff, Ventricular function. II. Quantitative relationship between coronary flow and ventricular function with observations on unilateral failure. Circ Res, 1954. 2(4): p. 319-25.
203. Lowe, K., et al., Perivascular fluid cuffs decrease lung compliance by increasing tissue resistance. Crit Care Med, 2010. 38(6): p. 1458-66.
204. Cook, C.D., et al., Pulmonary mechanics during induced pulmonary edema in anesthetized dogs. J Appl Physiol, 1959. 14(2): p. 177-86.
205. Bernard, G.R., et al., Comparison of the pulmonary dysfunction caused by cardiogenic and noncardiogenic pulmonary edema. Chest, 1995. 108(3): p. 798-803.
206. Magder, S., G. Georgiadis, and T. Cheong, Respiratory Variations in Right Atrial Pressure Predict the Response to Fluid Challenge. Journal of Critical Care, 1992. 7(2): p. 76-85.
207. Pepi, M., et al., Diastolic ventricular interaction in normal and dilated heart during head-up tilting. Clin Cardiol, 2000. 23(9): p. 665-72.
208. Atherton, J.J., et al., Diastolic ventricular interaction in chronic heart failure. Lancet, 1997. 349(9067): p. 1720-4.
209. Fessler, H.E., et al., Mechanism of reduced LV afterload by systolic and diastolic positive pleural pressure. J Appl Physiol (1985), 1988. 65(3): p. 1244-50.
210. Hall, M.J., et al., Magnitude and time course of hemodynamic responses to Mueller maneuvers in patients with congestive heart failure. J Appl Physiol (1985), 1998. 85(4): p. 1476-84.
211. Bradley, T.D., et al., Hemodynamic effects of simulated obstructive apneas in humans with and without heart failure. Chest, 2001. 119(6): p. 1827-35.
212. Tang, P.C., F.W. Maire, and V.E. Amassian, Respiratory influence on the vasomotor center. Am J Physiol, 1957. 191(2): p. 218-24.
213. Marini, J.J., B.H. Culver, and J. Butler, Effect of positive end-expiratory pressure on canine ventricular function curves. J Appl Physiol Respir Environ Exerc Physiol, 1981. 51(6): p. 1367-74.
214. Tyberg, J.V., et al., The relationship between pericardial pressure and right atrial pressure: an intraoperative study. Circulation, 1986. 73(3): p. 428-32.
215. Takata, M., W. Mitzner, and J.L. Robotham, Influence of the pericardium on ventricular loading during respiration. J Appl Physiol (1985), 1990. 68(4): p. 1640-50.
216. Slinker, B.K., et al., Right heart pressure does not equal pericardial pressure in the potassium chloride-arrested canine heart in situ. Circulation, 1987. 76(2): p. 357-62.
217. Huberfeld, S.I., et al., Effect of CPAP on pericardial pressure and respiratory system mechanics in pigs. Am J Respir Crit Care Med, 1995. 152(1): p. 142-7.
218. Cabrera, M.R., et al., Effect of airway pressure on pericardial pressure. Am Rev Respir Dis, 1989. 140(3): p. 659-67.
219. Takata, M. and J.L. Robotham, Ventricular external constraint by the lung and pericardium during positive end-expiratory pressure. Am Rev Respir Dis, 1991. 143(4 Pt 1): p. 872-5.
220. Scharf, S.M., et al., Intrathoracic pressures and left ventricular configuration with respiratory maneuvers. J Appl Physiol (1985), 1989. 66(1): p. 481-91.
221. Orchard, C.H., R. Sanchez de Leon, and M.K. Sykes, The relationship between hypoxic pulmonary vasoconstriction and arterial oxygen tension in the intact dog. J Physiol, 1983. 338: p. 61-74.
222. Jardin, F., et al., Influence of positive end-expiratory pressure on left ventricular performance. N Engl J Med, 1981. 304(7): p. 387-92.
223. Haynes, J.B., et al., Positive end-expiratory pressure shifts left ventricular diastolic pressure-area curves. J Appl Physiol Respir Environ Exerc Physiol, 1980. 48(4): p. 670-6.
224. Santamore, W.P., A.A. Bove, and J.L. Heckman, Right and left ventricular pressure-volume response to positive end-expiratory pressure. Am J Physiol, 1984. 246(1 Pt 2): p. H114-9.
225. Schulman, D.S., et al., Differing responses in right and left ventricular filling, loading and volumes during positive end-expiratory pressure. Am J Cardiol, 1989. 64(12): p. 772-7.
226. Mitchell, J.R., et al., RV filling modulates LV function by direct ventricular interaction during mechanical ventilation. Am J Physiol Heart Circ Physiol, 2005. 289(2): p. H549-57.
227. Veddeng, O.J., et al., Selective positive end-expiratory pressure and intracardiac dimensions in dogs. J Appl Physiol (1985), 1992. 73(5): p. 2016-20.
228. Pinsky, M.R. and W.R. Summer, Cardiac augmentation by phasic high intrathoracic pressure support in man. Chest, 1983. 84(4): p. 370-5.
229. Pinsky, M.R., et al., Augmentation of cardiac function by elevation of intrathoracic pressure. J Appl Physiol Respir Environ Exerc Physiol, 1983. 54(4): p. 950-5.

230. Pinsky, M.R., G.M. Matuschak, and M. Klain, Determinants of cardiac augmentation by elevations in intrathoracic pressure. J Appl Physiol (1985), 1985. 58(4): p. 1189-98.
231. Matuschak, G.M., M.R. Pinsky, and M. Klain, Hemodynamic effects of synchronous high-frequency jet ventilation during acute hypovolemia. J Appl Physiol (1985), 1986. 61(1): p. 44-53.
232. Pinsky, M.R., et al., Hemodynamic effects of cardiac cycle-specific increases in intrathoracic pressure. J Appl Physiol (1985), 1986. 60(2): p. 604-12.
233. Bradley, T.D., et al., Cardiac output response to continuous positive airway pressure in congestive heart failure. Am Rev Respir Dis, 1992. 145(2 Pt 1): p. 377-82.
234. De Hoyos, A., et al., Haemodynamic effects of continuous positive airway pressure in humans with normal and impaired left ventricular function. Clin Sci (Lond), 1995. 88(2): p. 173-8.
235. Genovese, J., et al., Effects of continuous positive airway pressure on cardiac output in normal and hypervolemic unanesthetized pigs. Am J Respir Crit Care Med, 1994. 150(3): p. 752-8.
236. Genovese, J., et al., Effects of CPAP on cardiac output in pigs with pacing-induced congestive heart failure. Am J Respir Crit Care Med, 1995. 152(6 Pt 1): p. 1847-53.
237. Permutt, S. and R.A. Wise, The control of cardiac output through coupling of heart and blood vessels, in Ventricular/Vascular Coupling1987, Springer. p. 159-179.
238. Dikshit, K., et al., Renal and extrarenal hemodynamic effects of furosemide in congestive heart failure after acute myocardial infarction. N Engl J Med, 1973. 288(21): p. 1087-90.
239. Elkayam, U., et al., Comparison of effects on left ventricular filling pressure of intravenous nesiritide and high-dose nitroglycerin in patients with decompensated heart failure. Am J Cardiol, 2004. 93(2): p. 237-40.
240. Kraus, P.A., J. Lipman, and P.J. Becker, Acute preload effects of furosemide. Chest, 1990. 98(1): p. 124-8.
241. Ross, J., Jr., Mechanisms of cardiac contraction. What roles for preload, afterload and inotropic state in heart failure? Eur Heart J, 1983. 4 Suppl A: p. 19-28.
242. Cassidy, S.S., et al., Geometric left-ventricular responses to interactions between the lung and left ventricle: positive pressure breathing. Ann Biomed Eng, 1987. 15(3-4): p. 285-95.
243. Grace, M.P. and D.M. Greenbaum, Cardiac performance in response to PEEP in patients with cardiac dysfunction. Crit Care Med, 1982. 10(6): p. 358-60.
244. Rosario, L.B., et al., The mechanism of decrease in dynamic mitral regurgitation during heart failure treatment: importance of reduction in the regurgitant orifice size. J Am Coll Cardiol, 1998. 32(7): p. 1819-24.
245. Hess, D.R., B.T. Thompson, and A.S. Slutsky, Update in acute respiratory distress syndrome and mechanical ventilation 2012. Am J Respir Crit Care Med, 2013. 188(3): p. 285-92.
246. Gattinoni, L., et al., Acute respiratory distress syndrome caused by pulmonary and extrapulmonary disease. Different syndromes? Am J Respir Crit Care Med, 1998. 158(1): p. 3-11.
247. Ventilation with lower tidal volumes as compared with traditional tidal volumes for acute lung injury and the acute respiratory distress syndrome. The Acute Respiratory Distress Syndrome Network. N Engl J Med, 2000. 342(18): p. 1301-8.
248. Akoumianaki, E., et al., The application of esophageal pressure measurement in patients with respiratory failure. Am J Respir Crit Care Med, 2014. 189(5): p. 520-31.
249. Owens, R.L., et al., Effect of the chest wall on pressure-volume curve analysis of acute respiratory distress syndrome lungs. Crit Care Med, 2008. 36(11): p. 2980-5.
250. Talmor, D., et al., Mechanical ventilation guided by esophageal pressure in acute lung injury. N Engl J Med, 2008. 359(20): p. 2095-104.
251. Jardin, F. and A. Vieillard-Baron, Right ventricular function and positive pressure ventilation in clinical practice: from hemodynamic subsets to respirator settings. Intensive Care Med, 2003. 29(9): p. 1426-34.
252. Hess, D.R. and L.M. Bigatello, The chest wall in acute lung injury/acute respiratory distress syndrome. Curr Opin Crit Care, 2008. 14(1): p. 94-102.
253. Jozwiak, M., et al., Beneficial hemodynamic effects of prone positioning in patients with acute respiratory distress syndrome. Am J Respir Crit Care Med, 2013. 188(12): p. 1428-33.
254. Jardin, F., et al., Relation between transpulmonary pressure and right ventricular isovolumetric pressure change during respiratory support. Cathet Cardiovasc Diagn, 1989. 16(4): p. 215-20.
255. Vieillard-Baron, A., et al., Cyclic changes in right ventricular output impedance during mechanical ventilation. J Appl Physiol (1985), 1999. 87(5): p. 1644-50.
256. Jullien, T., et al., Incidence of tricuspid regurgitation and vena caval backward flow in mechanically ventilated patients. A color Doppler and contrast echocardiographic study. Chest, 1995. 107(2): p. 488-93.
257. Wyler von Ballmoos, M., et al., Pulse-pressure variation and hemodynamic response in patients with elevated pulmonary artery pressure: a clinical study. Crit Care, 2010. 14(3): p. R111.
258. Daudel, F., et al., Pulse pressure variation and volume responsiveness during acutely increased pulmonary artery pressure: an experimental study. Crit Care, 2010. 14(3): p. R122.
259. Magder, S., Further cautions for the use of ventilatory-induced changes in arterial pressures to predict volume responsiveness. Critical Care, 2010. 14(5).
260. Little, W.C., F.R. Badke, and R.A. O'Rourke, Effect of right ventricular pressure on the end-diastolic left ventricular pressure-volume relationship before and after chronic right ventricular pressure overload in dogs without pericardia. Circ Res, 1984. 54(6): p. 719-30.
261. Santamore, W.P., J.L. Heckman, and A.A. Bove, Cardiovascular changes from expiration to inspiration during IPPV. Am J Physiol, 1983. 245(2): p. H307-12.

262. Klinger, J.R., Hemodynamics and positive end-expiratory pressure in critically ill patients. Crit Care Clin, 1996. 12(4): p. 841-64.
263. Yao, E.H., et al., Pulmonary function changes in cirrhosis of the liver. Am J Gastroenterol, 1987. 82(4): p. 352-4.
264. Yigit, I.P., et al., The relationship between severity of liver cirrhosis and pulmonary function tests. Dig Dis Sci, 2008. 53(7): p. 1951-6.
265. Chao, Y., et al., Effect of large-volume paracentesis on pulmonary function in patients with cirrhosis and tense ascites. J Hepatol, 1994. 20(1): p. 101-5.
266. Chang, S.C., et al., Therapeutic effects of diuretics and paracentesis on lung function in patients with non-alcoholic cirrhosis and tense ascites. J Hepatol, 1997. 26(4): p. 833-8.
267. Duranti, R., et al., Respiratory mechanics in patients with tense cirrhotic ascites. Eur Respir J, 1997. 10(7): p. 1622-30.
268. Ruff, F., et al., Regional lung function in patients with hepatic cirrhosis. J Clin Invest, 1971. 50(11): p. 2403-13.
269. Selvi, E.C., K.V.R. K, and Malathi, Should the Functional Residual Capacity be Ignored? J Clin Diagn Res, 2013. 7(1): p. 43-5.
270. Naimark, A. and R.M. Cherniack, Compliance of the respiratory system and its components in health and obesity. J Appl Physiol, 1960. 15: p. 377-82.
271. Magder, S., Bench-to-bedside review: ventilatory abnormalities in sepsis. Crit Care, 2009. 13(1): p. 202.
272. Sessler, C.N., G.L. Bloomfield, and A.A. Fowler, 3rd, Current concepts of sepsis and acute lung injury. Clin Chest Med, 1996. 17(2): p. 213-35.
273. Moller, S. and J.H. Henriksen, Cirrhotic cardiomyopathy: a pathophysiological review of circulatory dysfunction in liver disease. Heart, 2002. 87(1): p. 9-15.
274. Lieberman, F.L. and T.B. Reynolds, Plasma volume in cirrhosis of the liver: its relation of portal hypertension, ascites, and renal failure. J Clin Invest, 1967. 46(8): p. 1297-308.
275. Gines, P. and R.W. Schrier, Renal failure in cirrhosis. N Engl J Med, 2009. 361(13): p. 1279-90.
276. Gines, P., et al., Management of cirrhosis and ascites. N Engl J Med, 2004. 350(16): p. 1646-54.
277. Schrier, R.W., et al., Peripheral arterial vasodilation hypothesis: a proposal for the initiation of renal sodium and water retention in cirrhosis. Hepatology, 1988. 8(5): p. 1151-7.
278. Rubinson, R.M., et al., Inferior Vena Caval Obstruction from Increased Intra-Abdominal Pressure - Experimental Hemodynamic and Angiographic Observations. Archives of Surgery, 1967. 94(6): p. 766-&.
279. Barnes, G.E., et al., Cardiovascular responses to elevation of intra-abdominal hydrostatic pressure. Am J Physiol, 1985. 248(2 Pt 2): p. R208-13.
280. Magder, S. and G. Vanelli, Circuit factors in the high cardiac output of sepsis. J Crit Care, 1996. 11(4): p. 155-66.
281. Rastegarpanah, M. and S. Magder, Role of sympathetic pathways in the vascular response to sepsis. J Crit Care, 1998. 13: p. 169-176.
282. Datta, P. and S. Magder, Hemodynamic response to norepinephrine with and without inhibition of nitric oxide synthase in porcine endotoxemia. Am J Respir Crit Care Med, 1999. 160(6): p. 1987-93.
283. Maas, J.J., et al., Assessment of venous return curve and mean systemic filling pressure in postoperative cardiac surgery patients. Crit Care Med, 2009. 37(3): p. 912-8.
284. Jansen, J.R., J.J. Maas, and M.R. Pinsky, Bedside assessment of mean systemic filling pressure. Curr Opin Crit Care, 2010. 16(3): p. 231-6.
285. Maas, J.J., et al., Determination of vascular waterfall phenomenon by bedside measurement of mean systemic filling pressure and critical closing pressure in the intensive care unit. Anesth Analg, 2012. 114(4): p. 803-10.
286. Guyton, A.C., D. Polizo, and G.G. Armstrong, Mean circulatory filling pressure measured immediately after cessation of heart pumping. Am J Physiol, 1954. 179(2): p. 261-7.
287. Maas, J.J., et al., Cardiac output response to norepinephrine in postoperative cardiac surgery patients: interpretation with venous return and cardiac function curves. Crit Care Med, 2013. 41(1): p. 143-50.
288. Appleton, C., et al., Alpha-1 adrenergic control of the venous circulation in intact dogs. J Pharmacol Exp Ther, 1985. 233(3): p. 729-34.
289. Persichini, R., et al., Effects of norepinephrine on mean systemic pressure and venous return in human septic shock. Crit Care Med, 2012. 40(12): p. 3146-53.
290. Moller, S. and J.H. Henriksen, Cardiovascular complications of cirrhosis. Gut, 2008. 57(2): p. 268-78.
291. Rodriguez-Roisin, R. and M.J. Krowka, Hepatopulmonary syndrome--a liver-induced lung vascular disorder. N Engl J Med, 2008. 358(22): p. 2378-87.
292. Wong, F., et al., Role of cardiac structural and functional abnormalities in the pathogenesis of hyperdynamic circulation and renal sodium retention in cirrhosis. Clin Sci (Lond), 1999. 97(3): p. 259-67.
293. Ognibene, F.P., et al., Depressed left ventricular performance. Response to volume infusion in patients with sepsis and septic shock. Chest, 1988. 93(5): p. 903-10.
294. Parker, M.M., et al., Responses of left ventricular function in survivors and nonsurvivors of septic shock. J Crit Care, 1989. 4(1): p. 19-25.

295. Parker, M.M., et al., Right ventricular dysfunction and dilatation, similar to left ventricular changes, characterize the cardiac depression of septic shock in humans. Chest, 1990. 97(1): p. 126-31.
296. Zaky, A., et al., Characterization of cardiac dysfunction in sepsis: an ongoing challenge. Shock, 2014. 41(1): p. 12-24.
297. Abelmann, W.H., et al., Effects of abdominal distention by ascites on lung volumes and ventilation. AMA Arch Intern Med, 1954. 93(4): p. 528-40.
298. Roussos, C. and A. Koutsoukou, Respiratory failure. Eur Respir J Suppl, 2003. 47: p. 3s-14s.
299. Jardin, F., Cyclic changes in arterial pressure during mechanical ventilation. Intensive Care Med, 2004. 30(6): p. 1047-50.
300. Shih, T.H., et al., The change of respiratory compliance before and after removal of ascites in living donor liver transplantation. Transplant Proc, 2014. 46(3): p. 730-2.
301. Canada, E., J.L. Benumof, and F.R. Tousdale, Pulmonary vascular resistance correlates in intact normal and abnormal canine lungs. Crit Care Med, 1982. 10(11): p. 719-23.
302. Magder, S., D. Lagonidis, and F. Erice, The use of respiratory variations in right atrial pressure to predict the cardiac output response to PEEP. J Crit Care, 2001. 16(3): p. 108-14.
303. Annane, D., et al., Norepinephrine plus dobutamine versus epinephrine alone for management of septic shock: a randomised trial. Lancet, 2007. 370(9588): p. 676-84.
304. Sort, P., et al., Effect of intravenous albumin on renal impairment and mortality in patients with cirrhosis and spontaneous bacterial peritonitis. N Engl J Med, 1999. 341(6): p. 403-9.

Chapter Five

The Physiology of Extubation Failure

Abstract

Extubation failure is frequently encountered in the intensive care unit and it is typical that a single, simple mechanism is sought to explain a patient's inability to liberate from mechanical ventilation. Because the heart and lungs share the thoracic space, their interactions are inherently inexorable. As well, change in abdominal pressure with respiration has appreciable effects on venous return. Following extubation, increased work of breathing both incites and perpetuates abnormal physiology in the pulmonary and cardiovascular systems. Understanding these interactions help the clinician fully appreciate the pathophysiology of extubation failure, as well as dyspnea in general, and promote rational therapy.

Key Words: heart-lung interaction, work of breathing, dyspnea, obstructive airways, pulmonary congestion, ventricular interdependence

Introduction

It is commonplace for patients, with varying degrees of underlying obstructive lung disease, heart failure and pulmonary hypertension, to have disease processes rendering them intubated in an intensive care unit. Despite adequate physiological parameters prior to liberation from mechanical ventilation, patients with co-morbid cardiopulmonary disease may worsen immediately following removal of positive pressure. While it is tempting to place blame on a single process, it is often injurious interactions between the heart, lungs and vasculature that maintain and even intensify breathlessness and extubation failure.

This chapter will elaborate the stresses placed upon: a. the pulmonary vasculature, b. the surface of the heart, c. the ventricular septum and d. the abdomen in the setting of respiratory distress after extubation. Previous authors have detailed heart-lung interactions in terms of these aforementioned four stresses [1]; however, this review proposes a positive-feedback model whereby insult to any of the lungs, heart or vasculature induces pathology in the other. Additionally, while other reviews on cardiopulmonary interaction focus, primarily, on the physiology while on positive pressure [2, 3], this review will concentrate on patients breathing spontaneously, after the removal of positive pressure. This paradigm is also useful when clinicians encounter breathless patients in the emergency department on general medical

floor. Simply, this chapter intends to remind the reader of the complex mechanical interrelationships between the lungs and the cardiovascular systems. In doing so, the reader will better appreciate the pathomechanics of mechanical ventilation liberation failure, as well as dyspnea in general and rational therapy.

Obstructive Airways Disease and Impedance to Ventricular Outflow

Airway Resistance and Pulmonary Compliance

Positive pressure tends to distend airways and therefore lower their resistance, particularly during expiration. Putatively, this facilitates lung emptying by stenting open distal airways [4-8]. In patients with underlying airways obstruction, increased airways resistance incites dyspnea. In advanced cases, with decreased pulmonary elastic recoil, the pressure gradient from the alveolus down the airway during active expiration is decreased. Consequently, an equal pressure point is generated in the airway – where the pleural pressure supersedes the airway pressure and leads to dynamic airway collapse [9, 10]. The equal pressure point theory of expiratory airflow limitation explains air-trapping, auto-PEEP and hyperinflation [11, 12] which may ensue by invoking an increasingly aboral 'choke point' [figure 1]. While dynamic hyperinflation and air-trapping are often used interchangeably, there is a subtle distinction. The former is classically associated with impaired pulmonary elastic recoil and emphysema while the latter can occur in disease states typified even by high elastic recoil such as pulmonary ARDS. The air-trapping that occurs in the setting of pulmonary edema and ARDS is the result of high airway resistance which may occur because of edema, inflammation and high closing volumes in the lower lobes [13, 14].

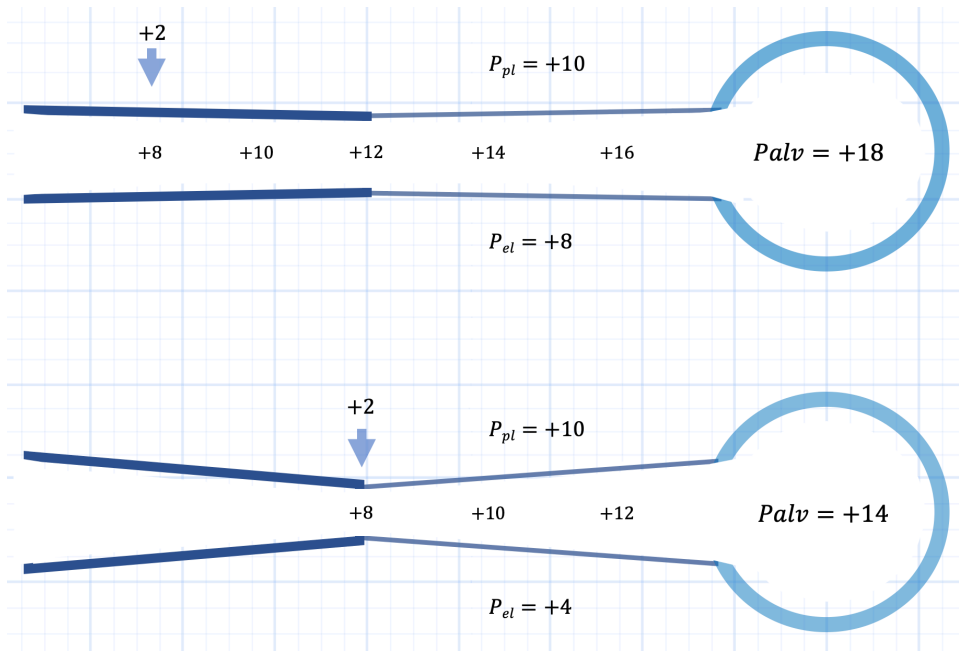

Figure 1: The equal pressure point theory. Top panel: Hypothetical pressures are depicted for a normal lung unit. The thickened portion of the airway signifies rigid cartilaginous tissue and the arrows represent compression pressure. The pleural pressure rises during forced expiration [here to +10], the alveolar pressure then becomes the summation of the pleural pressure and the elastic recoil pressure

[+8] of the lung. The gradient formed results in an equal pressure point within the rigid portion of the airway. Bottom panel: The Ppl is equal, however, the elastic recoil pressure of this lung is one-half the top panel [+4]. Thus, the equal pressure point is closer to the alveolus and no longer protected by rigid cartilage. This increases expiratory resistance, flow-limitation and, potentially, auto-PEEP [see text].

Because the pulmonary pressure-volume curve flattens at high volume, pulmonary compliance is dynamically reduced as a consequence of air-trapping [15]. Poorly compliant lung, by definition, requires greater transpulmonary pressure [i.e. more negative pleural pressure in the spontaneously breathing patient] for any given lung volume change [figure 2]. As elaborated below, diminution in pleural pressure appreciably affects biventricular loading conditions. Air-trapping and dynamic hyperinflation carry a multitude of untoward consequences for the respiratory pump. For instance, because intrinsic positive end-expiratory pressure is generated, an inspiratory threshold stresses the muscles of inspiration [figure 3]. Additionally, the diaphragm becomes less mechanically efficient as it flattens [16, 17]. While these latter effects do not have a direct pathomechanical effect upon hemodynamics, they certainly increase the oxygen cost of breathing as discussed at the outset of chapter 4 and in chapter 9.

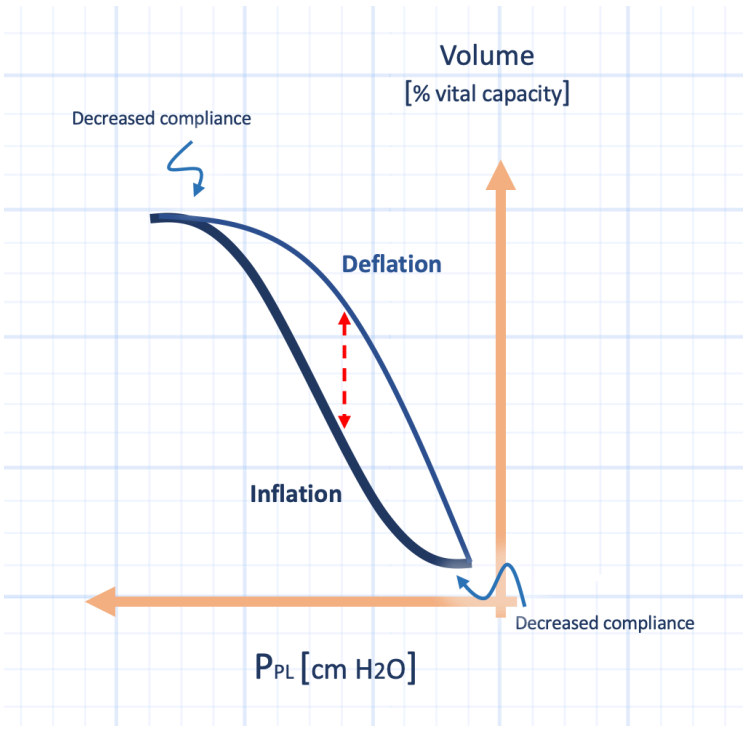

Figure 2: The pulmonary compliance curve reveals that a greater pressure change [x-axis] is required to affect volume change at extremes in lung volume. That is, the compliance is poor at both low and high lung volume [y-axis]. Ppl is pleural pressure with more negative values leftwards on the x-axis. The red-dotted line depicts hysteresis; see chapter 9.

As detailed above, liberation from mechanical ventilation may result in air-trapping which reduces pulmonary compliance; however, withdrawal of positive end-expiratory pressure may also enhance atelectasis in other lung units. Inspection of the pulmonary pressure-volume curve reveals that, like very high lung volumes, low lung volumes are also poorly compliant [18] [figure 2]. This pathophysiology contributes to increasingly negative intra-thoracic pressure and high breathing

work. As well, this may lead to 'pendelluft' physiology and act as a 'stress raiser' as discussed in chapter 9.

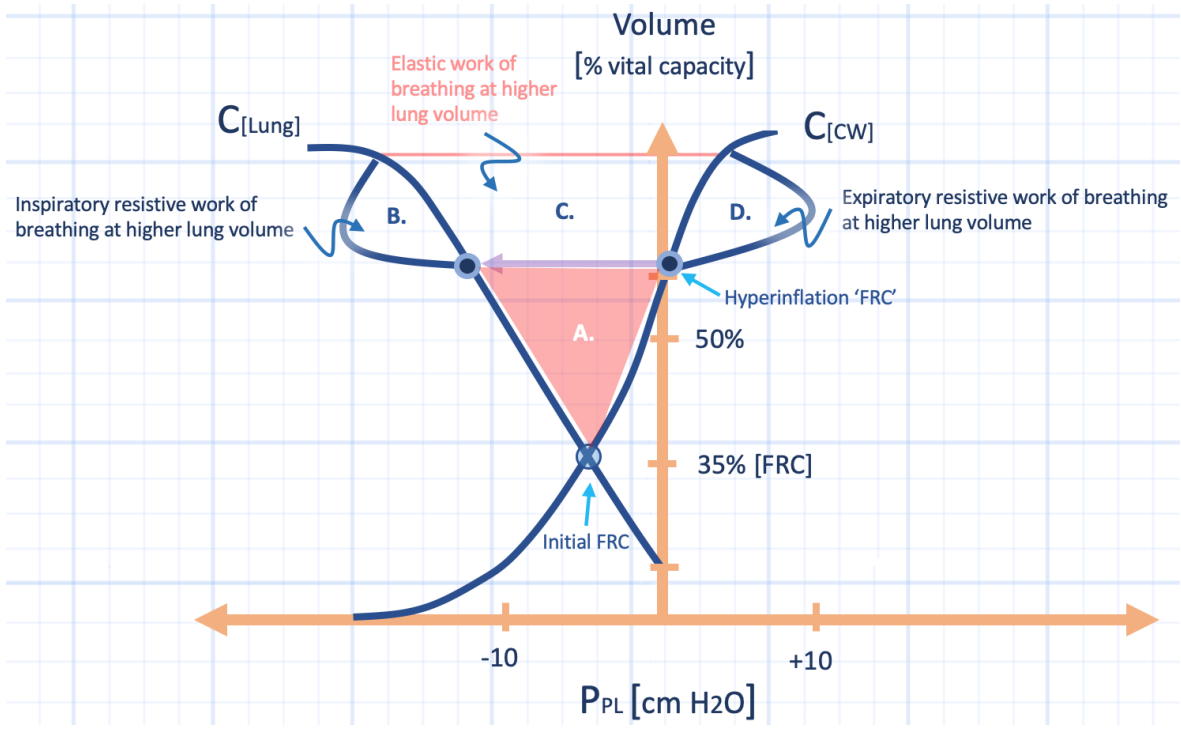

Figure 3: The Campbell diagram in response to air-trapping. The functional residual capacity [FRC] is increased along the chest wall compliance curve [Ccw] which raises intra-thoracic pressure prior to inspiration [hyperinflation 'FRC']. The purple arrow represents the muscular pressure load required to initiate a breath and increase lung volume on the y-axis. Note the large, negative inspiratory pressure required at high lung volume. The shaded triangle A is the work performed on the thorax by auto-PEEP; this work can be offset by application of extrinsic PEEP. The total work per breath is the sum of A-D. See also chapters 1 & 4.

The decrement in pulmonary compliance and increasingly negative pleural pressures described above, each contribute to adverse interaction with the cardiovascular system by increasing ventricular outflow impedance and ventricular wall tension [19-23].

In overly simple terms, impedance may be thought of as the geometric summation of two biophysical properties: resistance and reactance. This is also known as the 2-element Windkessel model described in chapter 2. Vascular resistance is commonly-described by Poiseuille's law, which states that resistance is inversely proportional to the radius of the vessel raised to the fourth power [24, 25]. Reactance, by contrast is inversely related to both vascular compliance and cycle frequency which takes into consideration blood flow resistance afforded by vascular distensibility [26]. While a single measure of right ventricular afterload is complex [27, 28] there is evidence that increased pulmonary vascular resistance [29], decreased pulmonary arterial compliance [30] and increased transmural vascular pressure all effectively afterload the RV [23]. Yet, relative contributions of the resistive versus compliance components to total impedance may differ [21, 28]. Recall from chapter 2 that the 2-element Windkessel model does not fully reproduce impedance as well as the 3-element model and that calculated pulmonary vascular resistance cannot

distinguish between Poiseuille and Starling resistance [24, 29, 31]. Additionally, some authors have suggested adapting the modified LaPlace relationship as a marker of left ventricular afterload [20] to the right ventricle [32, 33].

The effect of exaggerated negative pleural pressure on the pulmonary vasculature has different consequences for the extra-alveolar versus intra-alveolar vessels. The extra-alveolar vessels [the large pulmonary arteries, veins and tributaries that lie outside of the alveolar wall] are directly exposed to pleural pressure. The bronchovascular bundle enters the lungs at the hila via an invagination of the visceral pleura. To the extent the transpulmonary pressure exceeds the vascular transmural pressure, the extra-alveolar vessel dilates during inspiration [34] which lowers vascular resistance; this effect predominates at lung volumes less than FRC [35, 36].

By contrast, the intra-alveolar vessels are directly exposed to alveolar pressure. The effect on pulmonary vascular outflow impedance is largely dependent upon the local alveolar pressure relative to left atrial pressure; West and colleagues initially proposed lung zones to describe the relationship between alveolar pressure and pulmonary vascular pressure [37]. Zone II physiology occurs when alveolar pressure is greater than left atrial pressure. Zone II predominates when alveolar pressure is high, and/or left atrial pressure is low. In this circumstance, the alveolar pressure becomes the pressure against which the right ventricle ejects [38, 39].

That RV outflow impedance increases with air-trapping was illustrated by Harris and colleagues [40, 41]. They found that exercise and voluntary hyperventilation in patients with obstructive airways disease increased pulmonary vascular resistance when compared to healthy controls. Further, they found that the degree to which pulmonary vascular resistance increased with hyperventilation was directly proportional to the inverse of the FEV1. These findings have been subsequently corroborated [42, 43].

While increased impedance to right ventricular outflow seems mostly mediated by increased vascular resistance at the level of the pulmonary capillaries, it is interesting to speculate whether the large negative deflections in thoracic pressure during respiratory distress also decrease pulmonary arterial vascular compliance. It is also possible that right ventricular wall tension rises and impairs ejection. To this end, Scharf and colleagues demonstrated that echocardiographic right ventricular ejection fraction decreased when healthy controls generated negative pleural pressure without changing their lung volume [i.e. a Mueller maneuver] and that the decrease in ejection fraction was accompanied by increased right ventricular size [21]. These results suggest that either increased impedance or decreased ventricular contractility caused the low ejection fraction, though echocardiographic assessment of right ventricular function has its limitations [44]. More recent studies have shown that there may be impaired RV contractility with decreased intra-thoracic pressure in the absence of lung volume change as myocyte fibre velocity shortening of the RV is attenuated during Mueller maneuver [45]; however, it is still unclear whether systolic or diastolic ventricular interdependence during Mueller can account for changes in right ventricular strain rate via echocardiography.

As RV distention is expected to raise RV afterload by increasing ventricular radius, one might surmise that any spontaneous inspiration necessitates increased RV

afterload. However, in the healthy population the right ventricle tends to fill below its stressed volume [46]; consequently, the slope of the right ventricular cardiac function curve approximates 1 [i.e. there is an increase in cardiac output by Frank-Starling with essentially no change in right atrial pressure] such that large decrements in intra-thoracic pressure likely limit RV filling by collapse of the great veins as they enter the thorax. Thus, the contribution of increased RV radius in healthy normal subjects unlikely augments RV afterload [47]. By contrast, one expects greater inspiratory distention of the right heart in patients with underlying RV dysfunction and fluid overload. Interestingly, and discussed in more detail in the following section, inspiratory changes in RV volume may mediate its own preload via ventricular interdependence. That is, to the extent that change in RV geometry impairs LV compliance and raises the left atrial pressure – the back pressure to RV ejection – the RV preload can become its own afterload [48].

Ventricular Interdependence

As the RV outflow impedance rises with heightened work of breathing, elevated stress across the interventricular septum results. Jardin and colleagues demonstrated this effect in a classic study [23]. They found that in patients with status asthmaticus and paradoxic pulse, transmural vascular pressure predicted the pulmonary arterial afterload better than absolute pressure. Also, they demonstrated that septal bowing into the LV during inspiration accounted for the paradoxic pulse. Importantly, this study illustrated the pathomechanics of ventricular interdependence, i.e. how dysfunction in one ventricle afflicts the other. Animal models and clinical investigations have revealed that right ventricular overload can reduce the compliance and increase filling pressures of the left ventricle [49-52]. Interestingly, ventricular interdependence is enhanced by a compliant interventricular septum, when the pericardium is distended and less compliant [53-56] or, similarly, when lower lobe hyperinflation renders the cardiac fossa less distensible [figure 4]. As an example of the latter phenomenon, Butler and colleagues established the hemodynamic importance of lower lung hyperinflation in patients with COPD [57]. Through exercise and hyperventilation, they observed increased juxta-cardiac pressure with lower lobe gas trapping. Not only does this elevate wedge pressure and impair cardiac filling, but it also magnifies ventricular interdependence.

Left Ventricular Afterload

As touched upon briefly above, impedance to left ventricular outflow is increased by diminished pleural pressure [19, 21, 58]. The picture is somewhat less complicated than the right ventricle because the elaborate effects of lung volume on the pulmonary vascular bed do not apply to the aorta. Low pleural pressure increases the peak systolic wall stress across the left ventricular wall and aorta relative to the extra-thoracic arteries [59]. This effect is approximated by LaPlace's Law, which

states that wall tension is directly proportional to transmural wall pressure and cavity radius [20] [see also chapter 1]. A classic study by Buda and co-workers illustrated this effect when they established that the end-systolic volume of the left ventricle was best accounted for by left-ventricular transmural pressure and not absolute aortic pressure [19]. When breathing is normal, pleural effects on the left heart are minimal. During states of severe respiratory distress, however, pleural pressures down to – 60 cm of H_2O may be generated and this has hemodynamic consequences [60, 61]. If, by the mechanisms above, respiratory distress insults LV compliance and output, then the left ventricular end-diastolic pressure [LVEDP] rises. This, in turn, facilitates pulmonary congestion.

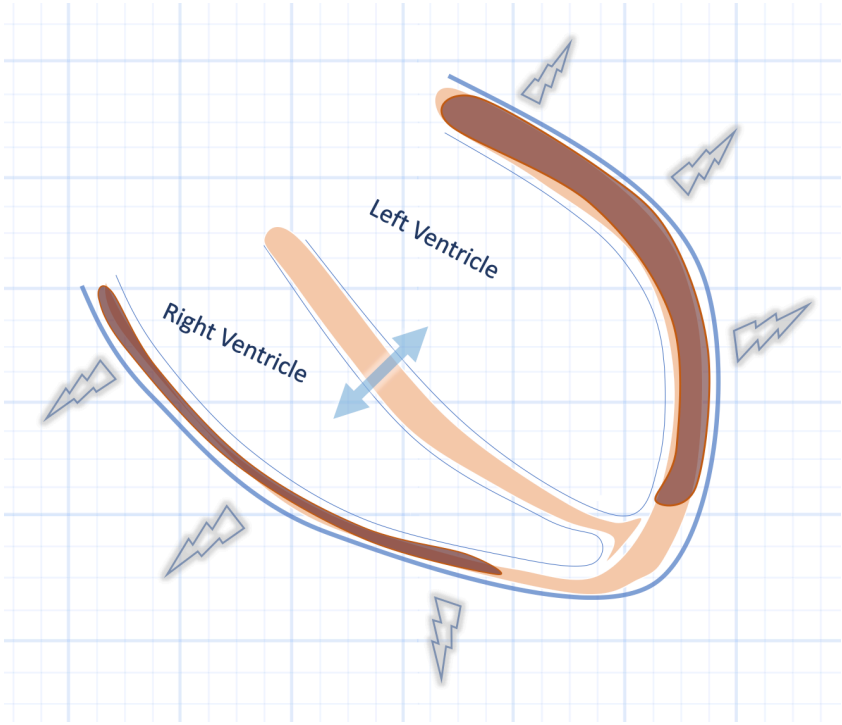

Figure 4: Ventricular interdependence [double-headed blue arrow] is facilitated by stiff ventricular free walls, pericardium, lung hyperinflation, etc. [lightning bolts] and a compliant inter-ventricular septum.

Excessive Lung Water, Pulmonary Mechanics and Work of Breathing

Elevated left ventricular filling pressure complicated by pulmonary congestion and edema are key precipitating events for dyspnea secondary to volume overload. The instigators of high left ventricular end-diastolic filling pressure are protean; as above, ventricular interdependence and high LV afterload may both contribute.

The Evolution of Pulmonary Edema

Early work delineating the pathogenesis of pulmonary congestion and edema focused on discrete stages of fluid overload [62, 63]. Importantly, each of these stages has been associated with increased work of breathing by both decreased pulmonary compliance and increased airway resistance.

Using freeze-fracture technique, Staub and colleagues viewed the histopathological transformation of the lung under increasingly severe volume overload. Based on this work, the 'stages' of increased lung water – in order of sequence – are: pulmonary vascular engorgement, bronchovascular interstitial edema, alveolar interstitial edema followed by frank alveolar flooding [63] [figure 5].

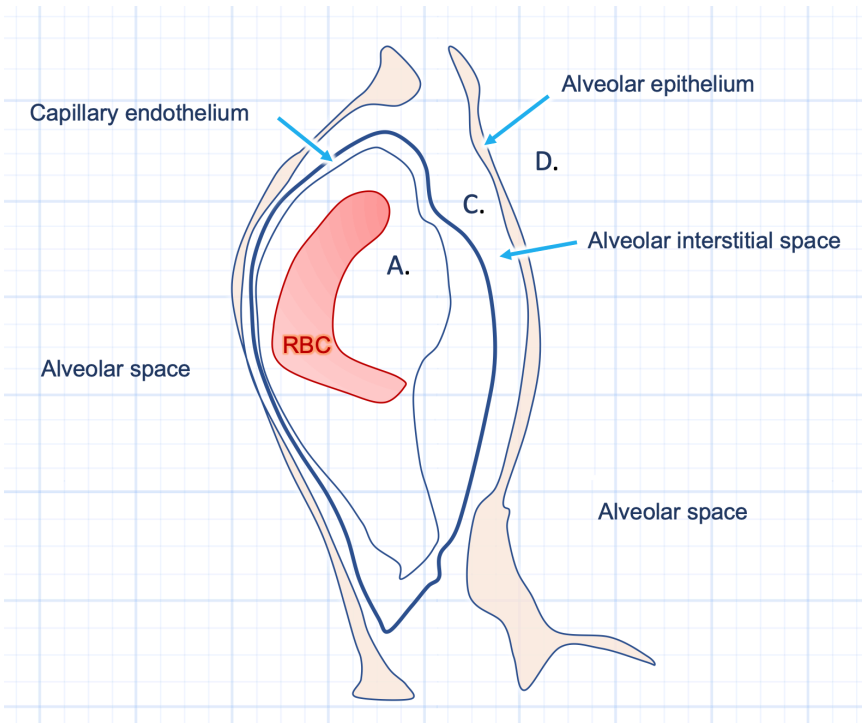

Figure 5: Schematic of an electron micrograph illustrating the 'stages' of pulmonary edema. The first [A] occurs as the blood vessels and capillaries become engorged with excess fluid. As this progresses, water is shifted out of the blood vessels by Starling forces into the [not pictured] peribronchovascular bundles, and then alveolar interstitium [C]. Lastly, fluid exudes into the alveolar spaces [D].

That bronchovascular interstitial edema precedes alveolar interstitial edema is explained by direct exposure of the bronchovascular bundles to pleural pressure. The negative pressure surrounding the extra-alveolar vessels provides a pressure gradient for lymphatic drainage away from the alveolar interstitium towards the hilum [64]; about 500 mL of fluid can be retained in this space [65].

Pulmonary Edema and Work of Breathing

It has been known for decades that even the earliest stage of increased lung water, pulmonary vascular engorgement, is associated with diminished pulmonary compliance in humans; though this effect tends to be small [66]. Remarkably, this decreased compliance was ablated by administering atropine – a drug previously used in the treatment of pulmonary edema. The authors postulated that an abrupt increase in left atrial pressure and pulmonary vascular congestion caused auto-regulatory active vascular tension according to the myogenic theory of blood flow. While pulmonary congestion stiffens the lungs, further investigation revealed that pulmonary compliance falls greatly in later stages of pulmonary edema. In fact, the greatest drop in compliance occurs with frank alveolar flooding [67]. Potentially,

the alveolar bubble froth seen in severe edema decreases alveolar radius and impairs the stabilizing effects of surfactant, impairing pulmonary compliance [68].

Stiff lungs consequent to pulmonary edema increase work of breathing; so too, however, does increased airways resistance, seen with pulmonary volume overload. A number of investigations revealed that airway resistance rises with pulmonary vascular engorgement and edema [67, 68]. Data from animal models [69] propose that in the early stages of increased lung water, elevated airway resistance is mediated reflexively by the vagal nerve. Thereafter, as bronchovascular interstitial edema progresses, the airways are physically impinged upon [70-72]. With frank alveolar edema, bubble froth plugs the small airways and leads to the greatest increase in resistance [68]. On the Campbell diagram, diminished pulmonary compliance and increased airway resistance lower inspiratory pressure and increase the static and dynamic work of breathing [figure 6] [see also chapter 4].

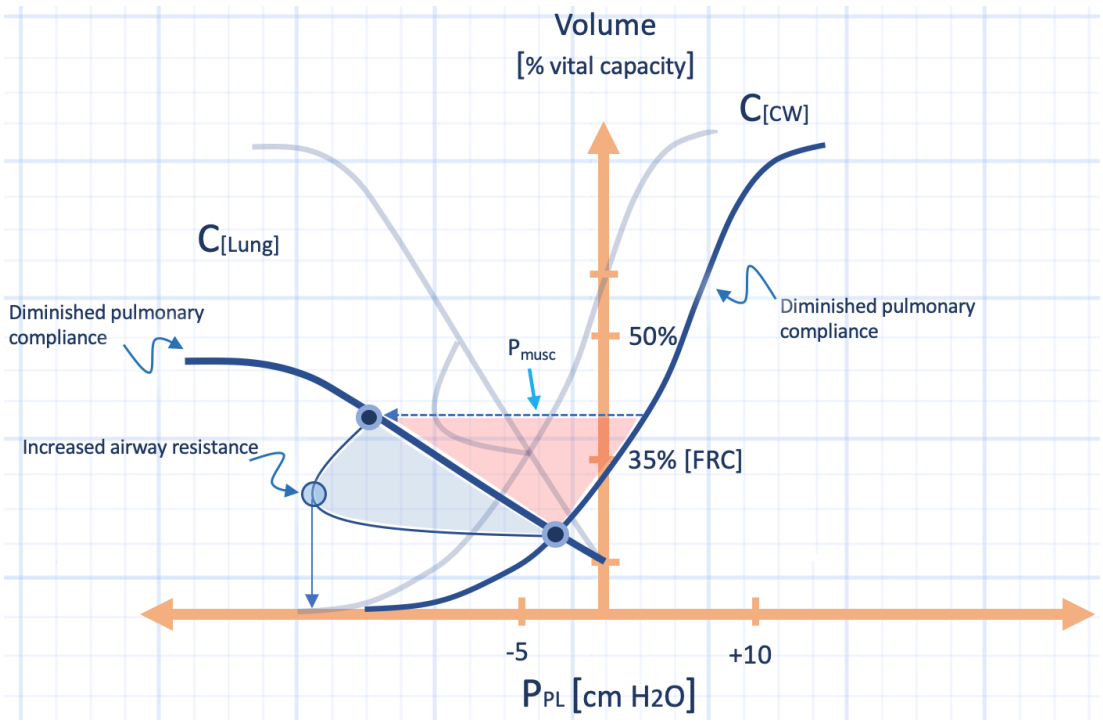

Figure 6: The effect of pulmonary edema on the Campbell diagram. There is decreased lung compliance – [Clung] – and increased airway resistance. The result is diminished intra-thoracic inspiratory pressure. Note, if there is co-morbid obesity or chest wall edema, the chest wall compliance will also fall and widen the pressure differential between the lung and chest wall or the Pmusc [light blue, dotted arrow]. The shaded area is the work of breathing created by the impaired mechanics. These patients tend to rapid-shallow-breath to mitigate the static work of breathing – see chapter 1.

Figure 7 is a simplified diagram illustrating the interactions between the lungs and heart in conditions of both obstructive-lung disease and congested-lung physiology. It is notable that perturbations in right ventricular outflow lead to left ventricular dysfunction, impaired LV filling and worsened lung mechanics and vice versa. Note, this is a simplified depiction and that other interactions may occur. For instance, more recent work has shown that prolonged resistive breathing can increase lung interstitial edema in healthy rats [73]. Presumably, this is secondary to the gradient generated between the alveolar interstitium and pulmonary capillary by prolonged negative airway pressure.

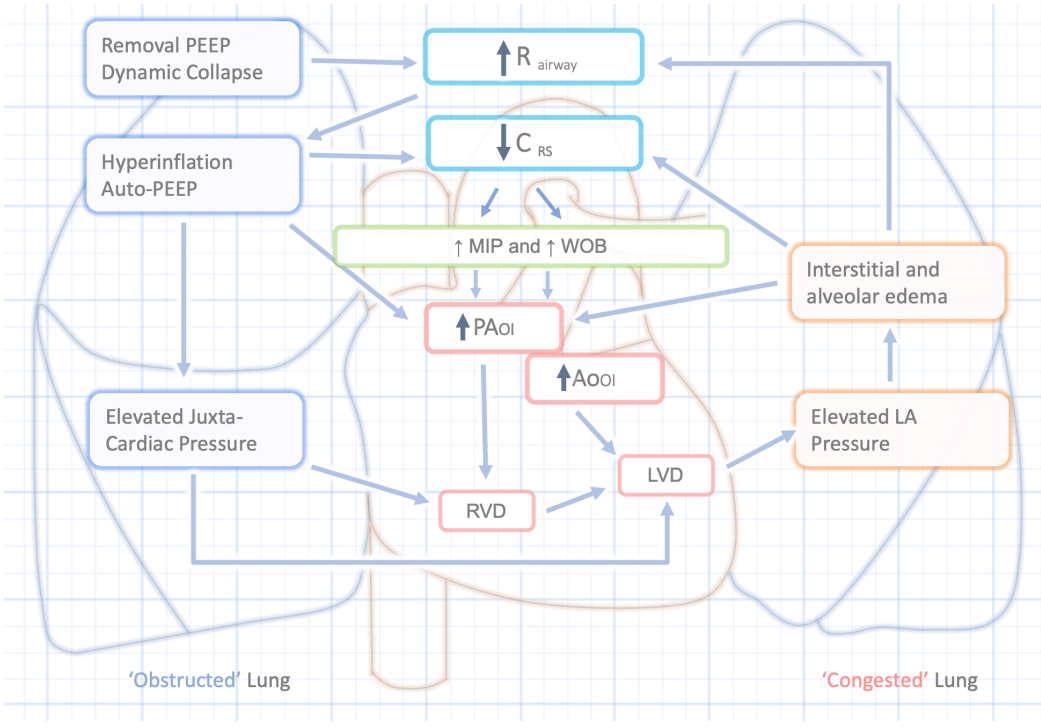

Figure 7: Depiction of selected cardiopulmonary interactions during respiratory distress. R airway is airway resistance, Crs is respiratory system compliance, MIP is maximal inspiratory pressure; WOB is work of breathing. PAoi is pulmonary arterial outflow impedance, Aooi is aortic outflow impedance, RVD is right ventricular dysfunction and LVD is left ventricular dysfunction, LA is left atrial. This diagram highlights interactions which may or may not be at play during dyspnea or removal from mechanical ventilation. See text for details.

Mean Systemic Pressure, Abdominal Pressure and Venous Return

The mean systemic pressure [Pmsf] is the driving pressure to the right heart [see chapter 2]. The Pmsf is, essentially, the pressure in the venous capacitance vessels at cardiac standstill [59, 74-76]. Pmsf is a static pressure determined by both the blood volume and elastic properties of the blood vessels. Venous return to the right heart is defined by the pressure gradient between the mean systemic pressure and the right atrial pressure divided by the resistance to venous return. Negative pleural pressure increases venous return to the right heart by decreasing right atrial pressure. However, venous return will not increase further when the right atrial pressure causes falls below a critical pressure threshold; normally this occurs around 4-6 cm H2O below atmospheric pressure [77]. The mechanisms involved were discussed in previous chapters; the diaphragm acts like a sphincter with moderate respiratory effort and extra-thoracic veins compress – acting as Starling resistors [1, 38, 78] [figure 8].

During spontaneous breathing, diaphragmatic contraction elevates abdominal pressure which, in turn, augments mean systemic pressure [79-81]. Some authors have demonstrated that abdominal blood vessels act analogously to the pulmonary vascular bed [82, 83]. For example, abdominal vessels with zone III physiology decrease their capacitance and squeeze blood into the right atrium in response to increased abdominal pressure [82-84].

The implication of the aforementioned is that volume status has important effects on venous return. Specifically, with volume overload and elevated right atrial pressure, a greater decrement in downstream pressure can occur before venous

return is hindered by great vein collapse. Additionally, more of the abdomen is in zone III physiology; therefore, increased abdominal pressure from diaphragm contraction raises IVC flow [1] [figure 8]. Clinically, in spontaneously breathing patients presenting with significant dyspnea secondary to obstructive airways exacerbation [23] and in those with volume overload [85], venous return to the right heart is increased.

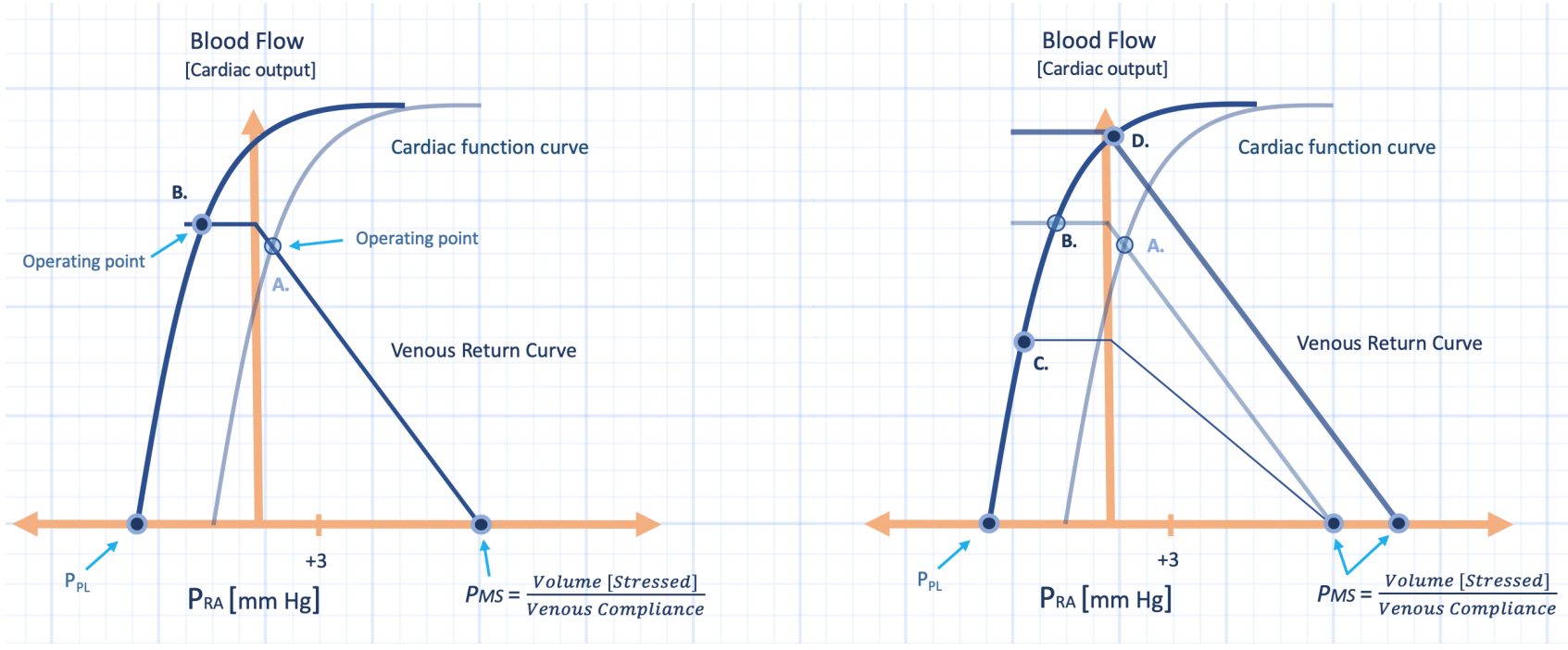

Figure 8: The effect of decreased intra-thoracic pressure [ITP] on venous return. Left panel: The drop in pleural pressure [Ppl] pulls the cardiac function curve leftwards along the x-axis [bold curve]. The operating point moves from point A to point B. The cardiac output [y-axis] increases until maximal venous return occurs [the plateau of the venous return curve]. This occurs when the great veins collapse upon entry to the thorax. Venous return, and therefore cardiac output, cannot rise above point B on the y-axis. Right panel: In addition to decreasing Ppl, the rise in lung volume also changes the venous return characteristics. Instead of changing the operating point from A to B, cardiovascular function is mediated by underlying volume status. In the hypovolemic patient, an increase in the resistance to venous return with abdominal pressurization may drop cardiac output [from operating point A to C]. In the hypervolemic patient, cardiac output may increase [from point A to point D] – see text for details. Pms is mean systemic pressure; Pra is right atrial pressure.

Venous return to the left heart depends upon alveolar blood volume prior to inflation. Lung inflation in zone III physiology decreases pulmonary vascular capacitance, increases its static pressure and augments venous return to the left atrium. Inflation of zone II transiently decreases venous return as blood volume pools in the extra-alveolar vessels [86] [see chapter 2].

Implications for Fluid Overload and Pulmonary Arterial Hypertension

In pulmonary arterial hypertension, reduced pulmonary vascular caliber and cross-sectional area increases right ventricular afterload. Early in disease progression, there is uncoupling of the right ventricular and pulmonary arterial elastances [87]. As the disease worsens, right ventricular failure leads to abdominal visceral congestion, edema and exercise intolerance.

When considering the injurious interactions between the heart and lungs described above, increasingly negative pleural pressure, increased airway resistance and decreased pulmonary compliance all promote right ventricular strain when patients with pulmonary hypertension present with acute decompensation. While there are multiple factors implicated in acute right heart dysfunction [88], ventricular interdependence is of utmost importance [89, 90]. For example, Kasner and colleagues elegantly illustrated the clinical importance of right-to-left ventricular dynamics in mild pulmonary hypertension [50]. Patients with an average mean pulmonary artery pressure of 29 mmHg were compared to patients with diastolic dysfunction in the setting of pacing-induced tachycardia. While both pulmonary hypertension patients and diastolic dysfunction patients decreased their left ventricular stroke volume with tachycardia, only pulmonary hypertension patients significantly increased left ventricular stroke volume with temporary preload reduction. The increase in LV output with temporary IVC occlusion was associated with downward shift of the LV end-diastolic pressure-volume relationship consistent with improved LV diastolic compliance [91] [see chapter 2].

Rational Therapy

Figure 7 reveals that liberation from mechanical ventilation will be most successful when airway resistance and pulmonary compliance are optimized as well as when biventricular loading conditions are ideal. This is further discussed in chapter 10 where the passive leg raise has been observed to help predict liberation from mechanical ventilation.

When broncho-obstruction is an important underlying issue, mitigation of air-trapping and auto-PEEP with bronchodilators is paramount. As hyperinflation abates, the lung becomes more compliant and work of breathing improves [16, 92]. Contemporaneously, RV afterload falls and adverse ventricular interactions are averted. Targeting work of breathing via novel therapeutic avenues is, therefore, of clinical interest. While systemic opiates are typically avoided during acute broncho-obstruction, anecdotal evidence of pre-procedure sedation improving hemodynamics and oxygen saturation is common amongst critical care clinicians. This has led some investigators to trial inhaled opiates; clinical benefit has been observed with nebulized hydromorphone and fentanyl, but not morphine [93].

Further, in patients with acute exacerbation of obstructive airways disease complicated by air-trapping and RV overload, ventricular interdependence can impair LV-filling. This is amplified by pre-existing LV abnormalities, valvulopathy and atrial arrhythmias. Diuresis in these patients may be dangerous as lower lobe air-trapping can impair venous return. Therefore, novel approaches such as inhaled furosemide [94, 95] and inhaled alpha-agonists - to constrict the pulmonary vasculature in the bronchovascular bundle [96, 97] - have been successfully studied. In a similar vein, brain natriuretic peptide may predict successful extubation [98]; as above, this is touched upon in chapter 10.

The cardiopulmonary implications of positive pressure have been reviewed extensively [3, 99], but are important to review in the context of extubation. The effect of positive pressure can be difficult to predict as it has multiple, sometimes conflicting cardiopulmonary effects. First, it increases transpulmonary pressure and lung volume, which increases RV afterload; however, if positive pressure improves oxygenation, RV afterload is reduced by the ablation of pulmonary hypoxic vasoconstriction [59, 100]. Second, mechanical ventilation increases pleural pressure, which may decrease venous return [101]. Lastly, positive pressure also decreases ventricular wall stress and LV afterload [102, 103].

Interestingly, the reduced venous return observed with positive end-expiratory pressure [PEEP] is not simply due to increased right atrial pressure. Multiple investigators have shown that the pressure gradient to the right heart does not change [or changes minimally] with the application of PEEP because mean systemic pressure typically increases to the same degree as right atrial pressure [1, 80, 82, 83, 99, 104]. Therefore, it is the resistance to venous return that increases – in combination with diminution of maximal venous return – following PEEP application [figure 9] [see also chapters 3 &4].

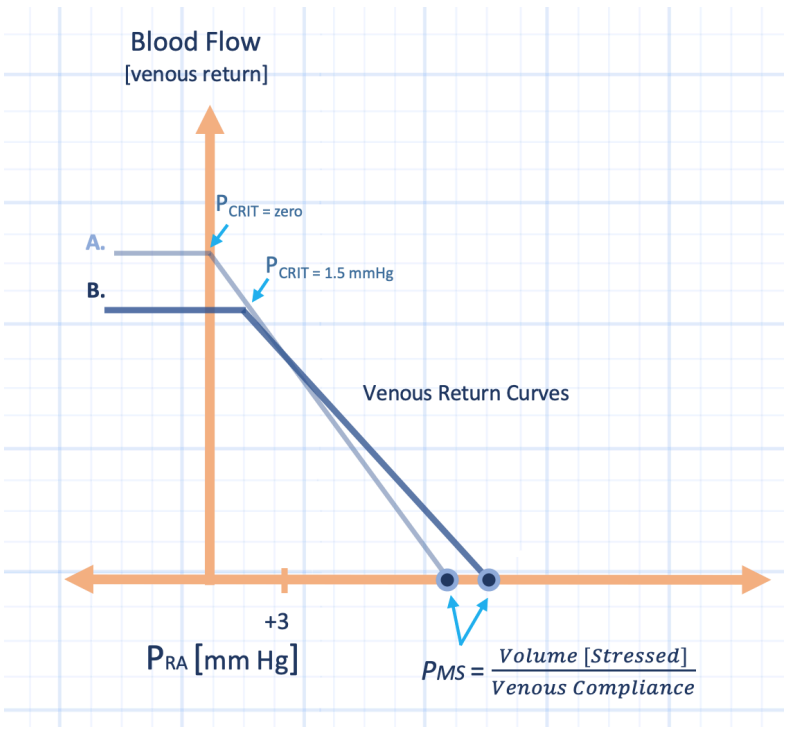

Figure 9: The effect of positive end-expiratory pressure [PEEP] on venous return. Note that the pressure-head for venous return [the x-intercept or mean systemic filling pressure] is increased by PEEP, but so too is the resistance to venous return [the slope]. Additionally the critical collapse pressure [Pcrit] is increased from zero on the baseline venous return curve [A] to roughly 1.5 on curve B. Maximal venous return [the plateau] is reduced.

As a rule of thumb, volume status typically determines whether the effect of positive pressure will predominantly decrease preload or afterload. In states of cardiac congestion, preload is abnormally high; therefore, the ventricle tolerates reduced venous return without significantly impaired stroke volume. Further, as the ventricle is insensitive to preload reduction, decreased transmural pressure facilitates ventricular ejection – diminished afterload predominates [102, 103, 105, 106]. However, the effect of positive airway pressure on the heart and pulmonary vasculature depends on its 'transmission' to the surface of the vascular structures.

Airway resistance, as well as pulmonary and chest wall compliance determine to what degree the juxta-vascular space feels airway pressure [107-111]. In general, increased lung compliance and decreased chest wall compliance exaggerate pleural pressure. While methods of estimating perivascular and juxta-cardiac pressure are validated [112], the important underlying principle is that when approaching a patient ready for extubation, euvolemia is achieved.

In states of volume overload, furosemide is used both to acutely reduce preload and as a diuretic [113]. Similar to positive pressure, pharmacological preload reduction has multiple beneficial effects on ventricular function and work of breathing. The findings of Kasner and co-workers highlight the importance of furosemide in right heart decompensation [50]. Additionally, removal of pulmonary interstitial edema improves pulmonary compliance, airway resistance and relieves West zone IV physiology – when alveolar interstitial pressure supersedes left atrial pressure [114, 115]. Diuresis attenuates abdominal congestion as illustrated by Lemaire and co-workers [85]. This classic study evaluated patients with normal pulmonary mechanics who failed liberation from mechanical ventilation. Continued diuresis over the course of 7 days led to successful extubation in most. It is proposed [1, 82, 83] that relief of zone III physiology in the abdomen reduced venous return and improved cardiac performance at the time of extubation; this is considered in more detail in chapter 10.

Finally, therapy specific for right heart failure, such as inhaled nitric oxide [116] – which reduces right ventricular outflow impedance and improves V/Q matching – is a rational approach to the aberrant physiology described above. It also suggests that inhaled nitroglycerin or prostacyclin may be beneficial. Treatment of right heart failure typically focuses on preload reduction, RV inotropic support, RV afterload reduction, and avoidance of atrial dysrhythmias; this topic has been reviewed elsewhere [88]. Obviously, right ventricular preload and afterload must be optimized prior to removal of positive pressure.

While patients are often given a spontaneous breathing trial with pressure support just prior to liberation from mechanical ventilation, it is important to note that one of the most commonly used indices to predict extubation success – the rapid-shallow breathing index – was validated on T-piece, not pressure support [117]. Notably, Tobin argued that extubation after 'minimal ventilator settings' [i.e. pressure support] may be harmful to patients [118]; the true load placed on the cardiopulmonary system might be masked on pressure support. In patients with co-morbid cardiopulmonary disease, his reasoning is prudent.

Conclusion

In summary, liberation from mechanical ventilation causes abrupt changes in pulmonary airways resistance and thoracic compliance. Because the heart is, essentially, a pressure chamber within the thoracic pressure chamber, fluctuating pleural pressure and lung volume alter biventricular loading. More specifically, aberrant lung physiology stresses the pulmonary vasculature and the surface of the

heart, which increases impedance to flow and impairs biventricular output. Stress across the ventricular septum augments biventricular dysfunction and this reflects back upon the respiratory system completing a vicious cycle. Understanding potentially deleterious interplay between heart and lung in patients with co-morbid cardiopulmonary disorders is imperative. Appreciation of the aforementioned physiology prepares the clinician to anticipate and treat adverse interactions with a rational therapeutic approach prior to liberation from mechanical ventilation.

References

1. Fessler, H.E., Heart-lung interactions: applications in the critically ill. Eur Respir J, 1997. 10(1): p. 226-37.
2. Vargas, M., et al., PEEP role in ICU and operating room: from pathophysiology to clinical practice. ScientificWorldJournal, 2014. 2014: p. 852356.
3. Luecke, T. and P. Pelosi, Clinical review: Positive end-expiratory pressure and cardiac output. Crit Care, 2005. 9(6): p. 607-21.
4. Slats, A.M., et al., Enhanced airway dilation by positive-pressure inflation of the lungs compared with active deep inspiration in patients with asthma. J Appl Physiol (1985), 2008. 105(6): p. 1725-32.
5. Smith, T.C. and J.J. Marini, Impact of PEEP on lung mechanics and work of breathing in severe airflow obstruction. J Appl Physiol (1985), 1988. 65(4): p. 1488-99.
6. Guerin, C., et al., Small airway closure and positive end-expiratory pressure in mechanically ventilated patients with chronic obstructive pulmonary disease. Am J Respir Crit Care Med, 1997. 155(6): p. 1949-56.
7. Kondili, E., et al., Pattern of lung emptying and expiratory resistance in mechanically ventilated patients with chronic obstructive pulmonary disease. Intensive Care Med, 2004. 30(7): p. 1311-8.
8. Kaczka, D.W., et al., Inspiratory lung impedance in COPD: effects of PEEP and immediate impact of lung volume reduction surgery. J Appl Physiol (1985), 2001. 90(5): p. 1833-41.
9. Jayamanne, D.S., H. Epstein, and R.M. Goldring, Flow-volume curve contour in COPD: correlation with pulmonary mechanics. Chest, 1980. 77(6): p. 749-57.
10. Saltzman, H.P., E.M. Ciulla, and A.S. Kuperman, The spirographic "kink". A sign of emphysema. Chest, 1976. 69(1): p. 51-5.
11. O'Donnell, D.E., et al., Effect of dynamic airway compression on breathing pattern and respiratory sensation in severe chronic obstructive pulmonary disease. Am Rev Respir Dis, 1987. 135(4): p. 912-8.
12. Tobin, M.J. and R.F. Lodato, PEEP, auto-PEEP, and waterfalls. Chest, 1989. 96(3): p. 449-51.
13. Vieillard-Baron, A., et al., Pressure-volume curves in acute respiratory distress syndrome: clinical demonstration of the influence of expiratory flow limitation on the initial slope. Am J Respir Crit Care Med, 2002. 165(8): p. 1107-12.
14. Light, R.W. and R.B. George, Serial pulmonary function in patients with acute heart failure. Arch Intern Med, 1983. 143(3): p. 429-33.
15. O'Donnell, D.E. and K.A. Webb, The major limitation to exercise performance in COPD is dynamic hyperinflation. J Appl Physiol (1985), 2008. 105(2): p. 753-5; discussion 755-7.
16. O'Donnell, D.E., Hyperinflation, dyspnea, and exercise intolerance in chronic obstructive pulmonary disease. Proc Am Thorac Soc, 2006. 3(2): p. 180-4.
17. Vassilakopoulos, T., Understanding wasted/ineffective efforts in mechanically ventilated COPD patients using the Campbell diagram. Intensive Care Med, 2008. 34(7): p. 1336-9.
18. Salazar, E. and J.H. Knowles, An Analysis of Pressure-Volume Characteristics of the Lungs. J Appl Physiol, 1964. 19: p. 97-104.
19. Buda, A.J., et al., Effect of intrathoracic pressure on left ventricular performance. N Engl J Med, 1979. 301(9): p. 453-9.
20. Karam, M., et al., Mechanism of decreased left ventricular stroke volume during inspiration in man. Circulation, 1984. 69(5): p. 866-73.
21. Scharf, S.M., et al., Cardiac effects of increased lung volume and decreased pleural pressure in man. J Appl Physiol Respir Environ Exerc Physiol, 1979. 47(2): p. 257-62.
22. Scharf, S.M., Cardiovascular effects of airways obstruction. Lung, 1991. 169(1): p. 1-23.
23. Jardin, F., et al., Mechanism of paradoxic pulse in bronchial asthma. Circulation, 1982. 66(4): p. 887-94.
24. Versprille, A., Pulmonary vascular resistance. A meaningless variable. Intensive Care Med, 1984. 10(2): p. 51-3.
25. Naeije, R., Pulmonary vascular resistance. A meaningless variable? Intensive Care Med, 2003. 29(4): p. 526-9.
26. Milnor, W.R., Arterial impedance as ventricular afterload. Circ Res, 1975. 36(5): p. 565-70.
27. Piene, H., Pulmonary arterial impedance and right ventricular function. Physiol Rev, 1986. 66(3): p. 606-52.
28. Saouti, N., et al., Right ventricular oscillatory power is a constant fraction of total power irrespective of pulmonary artery pressure. Am J Respir Crit Care Med, 2010. 182(10): p. 1315-20.
29. Saouti, N., et al., The arterial load in pulmonary hypertension. Eur Respir Rev, 2010. 19(117): p. 197-203.
30. Wang, Z. and N.C. Chesler, Pulmonary vascular wall stiffness: An important contributor to the increased right ventricular afterload with pulmonary hypertension. Pulm Circ, 2011. 1(2): p. 212-23.
31. Tedford, R.J., Determinants of right ventricular afterload (2013 Grover Conference series). Pulm Circ, 2014. 4(2): p. 211-9.

32. Maughan, W.L., et al., Instantaneous pressure-volume relationship of the canine right ventricle. Circ Res, 1979. 44(3): p. 309-15.
33. Sibbald, W.J. and A.A. Driedger, Right ventricular function in acute disease states: pathophysiologic considerations. Crit Care Med, 1983. 11(5): p. 339-45.
34. Lai-Fook, S.J., A continuum mechanics analysis of pulmonary vascular interdependence in isolated dog lobes. J Appl Physiol Respir Environ Exerc Physiol, 1979. 46(3): p. 419-29.
35. Whittenberger, J.L., et al., Influence of state of inflation of the lung on pulmonary vascular resistance. J Appl Physiol, 1960. 15: p. 878-82.
36. Permutt, S., et al., Effect of lung inflation on static pressure-volume characteristics of pulmonary vessels. J Appl Physiol, 1961. 16: p. 64-70.
37. West, J.B., C.T. Dollery, and A. Naimark, Distribution of Blood Flow in Isolated Lung; Relation to Vascular and Alveolar Pressures. J Appl Physiol, 1964. 19: p. 713-24.
38. Permutt, S. and R.L. Riley, Hemodynamics of Collapsible Vessels with Tone: The Vascular Waterfall. J Appl Physiol, 1963. 18: p. 924-32.
39. Jardin, F., et al., Reevaluation of hemodynamic consequences of positive pressure ventilation: emphasis on cyclic right ventricular afterloading by mechanical lung inflation. Anesthesiology, 1990. 72(6): p. 966-70.
40. Harris, P., N. Segel, and J.M. Bishop, The relation between pressure and flow in the pulmonary circulation in normal subjects and in patients with chronic bronchitis and mitral stenosis. Cardiovasc Res, 1968. 2(1): p. 73-83.
41. Harris, P., et al., The influence of the airways resistance and alveolar pressure on the pulmonary vascular resistance in chronic bronhcitis. Cardiovasc Res, 1968. 2(1): p. 84-92.
42. Naeije, R. and J.A. Barbera, Pulmonary hypertension associated with COPD. Crit Care, 2001. 5(6): p. 286-9.
43. Hilde, J.M., et al., Haemodynamic responses to exercise in patients with COPD. Eur Respir J, 2013. 41(5): p. 1031-41.
44. Vonk-Noordegraaf, A., et al., Right heart adaptation to pulmonary arterial hypertension: physiology and pathobiology. J Am Coll Cardiol, 2013. 62(25 Suppl): p. D22-33.
45. Koshino, Y., et al., Changes in left and right ventricular mechanics during the Mueller maneuver in healthy adults: a possible mechanism for abnormal cardiac function in patients with obstructive sleep apnea. Circ Cardiovasc Imaging, 2010. 3(3): p. 282-9.
46. Pinsky, M.R., J.M. Desmet, and J.L. Vincent, Effect of positive end-expiratory pressure on right ventricular function in humans. Am Rev Respir Dis, 1992. 146(3): p. 681-7.
47. Condos, W.R., Jr., et al., Hemodynamics of the Mueller maneuver in man: right and left heart micromanometry and Doppler echocardiography. Circulation, 1987. 76(5): p. 1020-8.
48. Lockhart, A., et al., Elevated pulmonary artery wedge pressure at rest and during exercise in chronic bronchitis: fact or fancy. Clin Sci, 1969. 37(2): p. 503-17.
49. Bove, A.A. and W.P. Santamore, Ventricular interdependence. Prog Cardiovasc Dis, 1981. 23(5): p. 365-88.
50. Kasner, M., et al., Left ventricular dysfunction induced by nonsevere idiopathic pulmonary arterial hypertension: a pressure-volume relationship study. Am J Respir Crit Care Med, 2012. 186(2): p. 181-9.
51. Weber, K.T., et al., Contractile mechanics and interaction of the right and left ventricles. Am J Cardiol, 1981. 47(3): p. 686-95.
52. Maruyama, Y., et al., Mechanical interactions between four heart chambers with and without the pericardium in canine hearts. Circ Res, 1982. 50(1): p. 86-100.
53. Rabson, J. and S. Permutt, Role of Pericardium in Diastolic Interdependence of Right and Left-Ventricles. Federation Proceedings, 1978. 37(3): p. 778-778.
54. Maughan, W.L., K. Sunagawa, and K. Sagawa, Ventricular systolic interdependence: volume elastance model in isolated canine hearts. Am J Physiol, 1987. 253(6 Pt 2): p. H1381-90.
55. Farrar, D.J., J.C. Woodard, and E. Chow, Pacing-induced dilated cardiomyopathy increases left-to-right ventricular systolic interaction. Circulation, 1993. 88(2): p. 720-5.
56. Little, W.C., F.R. Badke, and R.A. O'Rourke, Effect of right ventricular pressure on the end-diastolic left ventricular pressure-volume relationship before and after chronic right ventricular pressure overload in dogs without pericardia. Circ Res, 1984. 54(6): p. 719-30.
57. Butler, J., et al., Cause of the raised wedge pressure on exercise in chronic obstructive pulmonary disease. Am Rev Respir Dis, 1988. 138(2): p. 350-4.
58. Scharf, S.M., et al., The effects of large negative intrathoracic pressure on left ventricular function in patients with coronary artery disease. Circulation, 1981. 63(4): p. 871-5.
59. Broccard, A.F., Cardiopulmonary interactions and volume status assessment. J Clin Monit Comput, 2012. 26(5): p. 383-91.
60. Stalcup, S.A. and R.B. Mellins, Mechanical forces producing pulmonary edema in acute asthma. N Engl J Med, 1977. 297(11): p. 592-6.
61. Freedman, S., A.E. Tattersfield, and N.B. Pride, Changes in lung mechanics during asthma induced by exercise. J Appl Physiol, 1975. 38(6): p. 974-82.
62. Staub, N.C., H. Nagano, and M.L. Pearce, The sequence of events during fluid accumulation in acute pulmonary edema. Jpn Heart J, 1967. 8(6): p. 683-9.
63. Staub, N.C., H. Nagano, and M.L. Pearce, Pulmonary edema in dogs, especially the sequence of fluid accumulation in lungs. J Appl Physiol, 1967. 22(2): p. 227-40.

64. Bhattacharya, J. and N.C. Staub, Direct measurement of microvascular pressures in the isolated perfused dog lung. Science, 1980. 210(4467): p. 327-8.
65. Gee, M.H. and D.O. Williams, Effect of lung inflation on perivascular cuff fluid volume in isolated dog lung lobes. Microvasc Res, 1979. 17(2): p. 192-201.
66. Giuntini, C., A. Maseri, and R. Bianchi, Pulmonary vascular distensibility and lung compliance as modified by dextran infusion and subsequent atropine injection in normal subjects. J Clin Invest, 1966. 45(11): p. 1770-89.
67. Noble, W.H., J.C. Kay, and J. Obdrzalek, Lung mechanics in hypervolemic pulmonary edema. J Appl Physiol, 1975. 38(4): p. 681-7.
68. Sharp, J.T., et al., Ventilatory mechanics in pulmonary edema in man. J Clin Invest, 1958. 37(1): p. 111-7.
69. Ishii, M., et al., Effects of hemodynamic edema formation on peripheral vs. central airway mechanics. J Appl Physiol (1985), 1985. 59(5): p. 1578-84.
70. Hogg, J.C., et al., Distribution of airway resistance with developing pulmonary edema in dogs. J Appl Physiol, 1972. 32(1): p. 20-4.
71. Pepine, C.J. and L. Wiener, Relationship of anginal symptoms to lung mechanics during myocardial ischemia. Circulation, 1972. 46(5): p. 863-9.
72. Hales, C.A. and H. Kazemi, Small-airways function in myocardial infarction. N Engl J Med, 1974. 290(14): p. 761-5.
73. Toumpanakis, D., et al., Inspiratory resistive breathing induces acute lung injury. Am J Respir Crit Care Med, 2010. 182(9): p. 1129-36.
74. Magder, S. and B. De Varennes, Clinical death and the measurement of stressed vascular volume. Crit Care Med, 1998. 26(6): p. 1061-4.
75. Magder, S., Bench-to-bedside review: An approach to hemodynamic monitoring - Guyton at the bedside. Crit Care, 2012. 16(5): p. 236.
76. Guyton, A.C., D. Polizo, and G.G. Armstrong, Mean circulatory filling pressure measured immediately after cessation of heart pumping. Am J Physiol, 1954. 179(2): p. 261-7.
77. Guyton, A.C., A.W. Lindsey, and B.N. Kaufmann, Effect of mean circulatory filling pressure and other peripheral circulatory factors on cardiac output. Am J Physiol, 1955. 180(3): p. 463-8.
78. Lloyd, T.C., Jr., Effect of inspiration on inferior vena caval blood flow in dogs. J Appl Physiol Respir Environ Exerc Physiol, 1983. 55(6): p. 1701-8.
79. van den Berg, P.C., J.R. Jansen, and M.R. Pinsky, Effect of positive pressure on venous return in volume-loaded cardiac surgical patients. J Appl Physiol (1985), 2002. 92(3): p. 1223-31.
80. Jellinek, H., et al., Influence of positive airway pressure on the pressure gradient for venous return in humans. J Appl Physiol (1985), 2000. 88(3): p. 926-32.
81. Nanas, S. and S. Magder, Adaptations of the peripheral circulation to PEEP. Am Rev Respir Dis, 1992. 146(3): p. 688-93.
82. Takata, M., R.A. Wise, and J.L. Robotham, Effects of abdominal pressure on venous return: abdominal vascular zone conditions. J Appl Physiol (1985), 1990. 69(6): p. 1961-72.
83. Takata, M. and J.L. Robotham, Effects of inspiratory diaphragmatic descent on inferior vena caval venous return. J Appl Physiol (1985), 1992. 72(2): p. 597-607.
84. Robotham, J.L. and M. Takata, Mechanical abdomino/heart/lung interaction. J Sleep Res, 1995. 4(S1): p. 50-52.
85. Lemaire, F., et al., Acute left ventricular dysfunction during unsuccessful weaning from mechanical ventilation. Anesthesiology, 1988. 69(2): p. 171-9.
86. Brower, R., et al., Effect of lung inflation on lung blood volume and pulmonary venous flow. J Appl Physiol (1985), 1985. 58(3): p. 954-63.
87. Granton, J., The right ventricle in pulmonary hypertension: when good neighbors go bad. Am J Respir Crit Care Med, 2012. 186(2): p. 121-3.
88. Lahm, T., et al., Medical and surgical treatment of acute right ventricular failure. J Am Coll Cardiol, 2010. 56(18): p. 1435-46.
89. Janicki, J.S., Influence of the pericardium and ventricular interdependence on left ventricular diastolic and systolic function in patients with heart failure. Circulation, 1990. 81(2 Suppl): p. II15-20.
90. Jardin, F., Ventricular interdependence: how does it impact on hemodynamic evaluation in clinical practice? Intensive Care Med, 2003. 29(3): p. 361-363.
91. Atherton, J.J., et al., Diastolic ventricular interaction in chronic heart failure. Lancet, 1997. 349(9067): p. 1720-4.
92. O'Donnell, D.E., et al., Effects of tiotropium on lung hyperinflation, dyspnoea and exercise tolerance in COPD. European Respiratory Journal, 2004. 23(6): p. 832-840.
93. Boyden, J.Y., et al., Nebulized Medications for the Treatment of Dyspnea: A Literature Review. J Aerosol Med Pulm Drug Deliv, 2014.
94. Ong, K.C., et al., Effects of inhaled furosemide on exertional dyspnea in chronic obstructive pulmonary disease. Am J Respir Crit Care Med, 2004. 169(9): p. 1028-1033.
95. Vahedi, H.S.M., et al., The Adjunctive Effect of Nebulized Furosemide in COPD Exacerbation: A Randomized Controlled Clinical Trial. Respiratory Care, 2013. 58(11): p. 1873-1877.
96. Cabanes, L.R., et al., Bronchial hyperresponsiveness to methacholine in patients with impaired left ventricular function. N Engl J Med, 1989. 320(20): p. 1317-22.
97. Cabanes, L., et al., Improvement in exercise performance by inhalation of methoxamine in patients with impaired left ventricular function. N Engl J Med, 1992. 326(25): p. 1661-5.

98. Zapata, L., et al., B-type natriuretic peptides for prediction and diagnosis of weaning failure from cardiac origin. Intensive Care Med, 2011. 37(3): p. 477-85.
99. Robotham, J.L. and S.M. Scharf, Effects of positive and negative pressure ventilation on cardiac performance. Clin Chest Med, 1983. 4(2): p. 161-87.
100. Canada, E., J.L. Benumof, and F.R. Tousdale, Pulmonary vascular resistance correlates in intact normal and abnormal canine lungs. Crit Care Med, 1982. 10(11): p. 719-23.
101. Jardin, F. and A. Vieillard-Baron, Right ventricular function and positive pressure ventilation in clinical practice: from hemodynamic subsets to respirator settings. Intensive Care Med, 2003. 29(9): p. 1426-34.
102. Grace, M.P. and D.M. Greenbaum, Cardiac performance in response to PEEP in patients with cardiac dysfunction. Crit Care Med, 1982. 10(6): p. 358-60.
103. Rasanen, J., P. Nikki, and J. Heikkila, Acute myocardial infarction complicated by respiratory failure. The effects of mechanical ventilation. Chest, 1984. 85(1): p. 21-8.
104. Fessler, H.E., et al., Effects of Positive End-Expiratory Pressure on the Gradient for Venous Return. American Review of Respiratory Disease, 1991. 143(1): p. 19-24.
105. Calvin, J.E., A.A. Driedger, and W.J. Sibbald, Positive end-expiratory pressure (PEEP) does not depress left ventricular function in patients with pulmonary edema. Am Rev Respir Dis, 1981. 124(2): p. 121-8.
106. Pinsky, M.R., Recent advances in the clinical application of heart-lung interactions. Curr Opin Crit Care, 2002. 8(1): p. 26-31.
107. O'Quin, R.J., et al., Transmission of airway pressure to pleural space during lung edema and chest wall restriction. J Appl Physiol (1985), 1985. 59(4): p. 1171-7.
108. Romand, J.A., W. Shi, and M.R. Pinsky, Cardiopulmonary effects of positive pressure ventilation during acute lung injury. Chest, 1995. 108(4): p. 1041-8.
109. Scharf, S.M. and R.H. Ingram, Jr., Effects of decreasing lung compliance with oleic acid on the cardiovascular response to PEEP. Am J Physiol, 1977. 233(6): p. H635-41.
110. Mesquida, J., H.K. Kim, and M.R. Pinsky, Effect of tidal volume, intrathoracic pressure, and cardiac contractility on variations in pulse pressure, stroke volume, and intrathoracic blood volume. Intensive Care Med, 2011. 37(10): p. 1672-9.
111. Jardin, F., et al., Influence of lung and chest wall compliances on transmission of airway pressure to the pleural space in critically ill patients. Chest, 1985. 88(5): p. 653-8.
112. Teboul, J.L., et al., Estimating cardiac filling pressure in mechanically ventilated patients with hyperinflation. Crit Care Med, 2000. 28(11): p. 3631-6.
113. Dikshit, K., et al., Renal and extrarenal hemodynamic effects of furosemide in congestive heart failure after acute myocardial infarction. N Engl J Med, 1973. 288(21): p. 1087-90.
114. West, J.B., Perivascular edema, a factor in pulmonary vascular resistance. Am Heart J, 1965. 70(4): p. 570-2.
115. West, J.B., C.T. Dollery, and B.E. Heard, Increased Pulmonary Vascular Resistance in the Dependent Zone of the Isolated Dog Lung Caused by Perivascular Edema. Circ Res, 1965. 17: p. 191-206.
116. Bhorade, S., et al., Response to inhaled nitric oxide in patients with acute right heart syndrome. Am J Respir Crit Care Med, 1999. 159(2): p. 571-9.
117. Yang, K.L. and M.J. Tobin, A prospective study of indexes predicting the outcome of trials of weaning from mechanical ventilation. N Engl J Med, 1991. 324(21): p. 1445-50.
118. Tobin, M.J., Extubation and the myth of "minimal ventilator settings". Am J Respir Crit Care Med, 2012. 185(4): p. 349-50.

Chapter Six

The Central Venous Pressure

Abstract

The central venous pressure is a hemodynamic variable comprised of multiple, co-varying, physiological determinants. Simply, the pressure within the central veins is described at the intersection of the venous return curve – which illustrates central venous inflow; and the cardiac function curve – which describes central venous outflow. Venous return and cardiac function are depicted on the Guyton diagram. While this approach makes sense of the CVP and its utility in the clinical arena, the use of the CVP must be first understood in terms of its measurement and specific waveforms. Although the CVP is often contemplated as a quick assessment of 'volume status' and 'fluid responsiveness', such oversimplification of this complex parameter misleads the clinician. By contrast, dynamic assessments of the CVP may provide more functionally relevant appraisal of the cardiovascular system.

Keywords: central venous pressure, venous return, Guyton diagram, preload, fluid responsiveness, volume status, trans-mural pressure, IVC variability

Introduction

The central venous pressure [CVP], for all intents and purposes, can be considered equivalent to the right atrial pressure. Abnormalities in the anatomy between the intra-thoracic great veins and the right atrium would create a difference between the right atrial pressure and central venous pressure, but in the vast majority of patients such an abnormality is not present. This chapter, therefore, considers right atrial pressure and central venous pressure as interchangeable. The focus of this chapter surrounds the clinical significance of the central venous pressure. While there is little debate that static markers of cardiac preload neither provide accurate assessments of volume status nor volume responsiveness [1-5], the CVP remains a frequently misunderstood data point [6, 7]. Knowing the host of determinants of the CVP makes clear why a static CVP value cannot be used to define a patient's volume status or whether provision of fluid will augment cardiac output. To this end, this chapter will begin with pressure measurement principles of the CVP followed by its specific waveforms. A discussion about the determinants of the central venous pressure as well as its relationship to 'volume status' and 'volume responsiveness' is presented to dispel some of the aforementioned misperceptions.

This will be followed by brief discussion on dynamic CVP changes and the commonly-employed surrogate of central venous pressure, the IVC ultrasound examination. Both the CVP and IVC collapse are further discussed in chapter 10.

Principles of Measurement

The pressure exerted by fluid on the walls of its container is a static pressure, that is, the pressure generated independent of liquid flow; furthermore, pressure is a force applied over an area. Recall that a force is proportional to the mass of an object and that mass, in this case, is related to the density and volume of the liquid. From this logic flows the use of liquid length [e.g. cm H_2O or mmHg] to measure the force that a liquid exerts against its walls. The use of cm H_2O versus mmHg is completely historical and because vascular pressure tends to be greater than thoracic pressure. Thus, to make vascular pressure measurement less cumbersome, mercury manometers were utilized, while for low pressure pulmonary measurements, water manometers were used.

Importantly, pressure is referenced to some arbitrary gravitational point [8, 9]. Because clinicians are interested in the pressure within the right atrium – the anatomical and physiological intersection of cardiac function and venous return – the reference point for pressure transduction is the level of the right atrium. The closest approximation to the right atrium, in most patients, is 5 centimetres below the sternal angle. Using the aforementioned reference point, the transducer may remain fixed even if the patient is placed in a small degree of reverse Trendelenburg because the right atrium remains roughly 5 cm below the sternal angle even in this position. However, more frequently the CVP is referenced to the mid-thoracic position on the patient – which is taken to be the mid-axillary line lateral to the sternal angle. Because of right atrial positional changes relative to this point, this reference is only valid when the patient is completely supine [8] [figure 1].

While measuring the central venous pressure requires reference to a gravitational point in space, it also requires a 'zero' reference, or baseline pressure. Simply, this reference is made to atmospheric pressure. Because of this reference point, an artifact is introduced into CVP measurement as a result of the right atrium's residence within the thorax. During spontaneous inspiration, the intra-thoracic pressure falls relative to atmosphere and so too does the central venous pressure. Unfortunately, this gives the impression that the right atrial distending pressure – the transmural pressure – is also decreasing. However, during a spontaneous inspiration, the right atrial transmural pressure very often increases. In other words, the central venous pressure falls relative to atmosphere during spontaneous inspiration but the pressure within the right atrium actually increases relative to the intra-thoracic pressure. This occurs because systemic venous return rises during spontaneous inspiration; the intra-vascular pressure, therefore, remains higher than the ambient intra-thoracic pressure such that the vascular distending pressure is enhanced. If the catheter measuring central venous pressure were referenced to pleural pressure – rather than atmospheric pressure – this increase would be detected as a positive deflection on the ICU monitor! Conversely, during passive

mechanical inspiration, the opposite is seen. One could envision referencing the CVP to an esophageal pressure monitor to achieve this effect [figure 2].

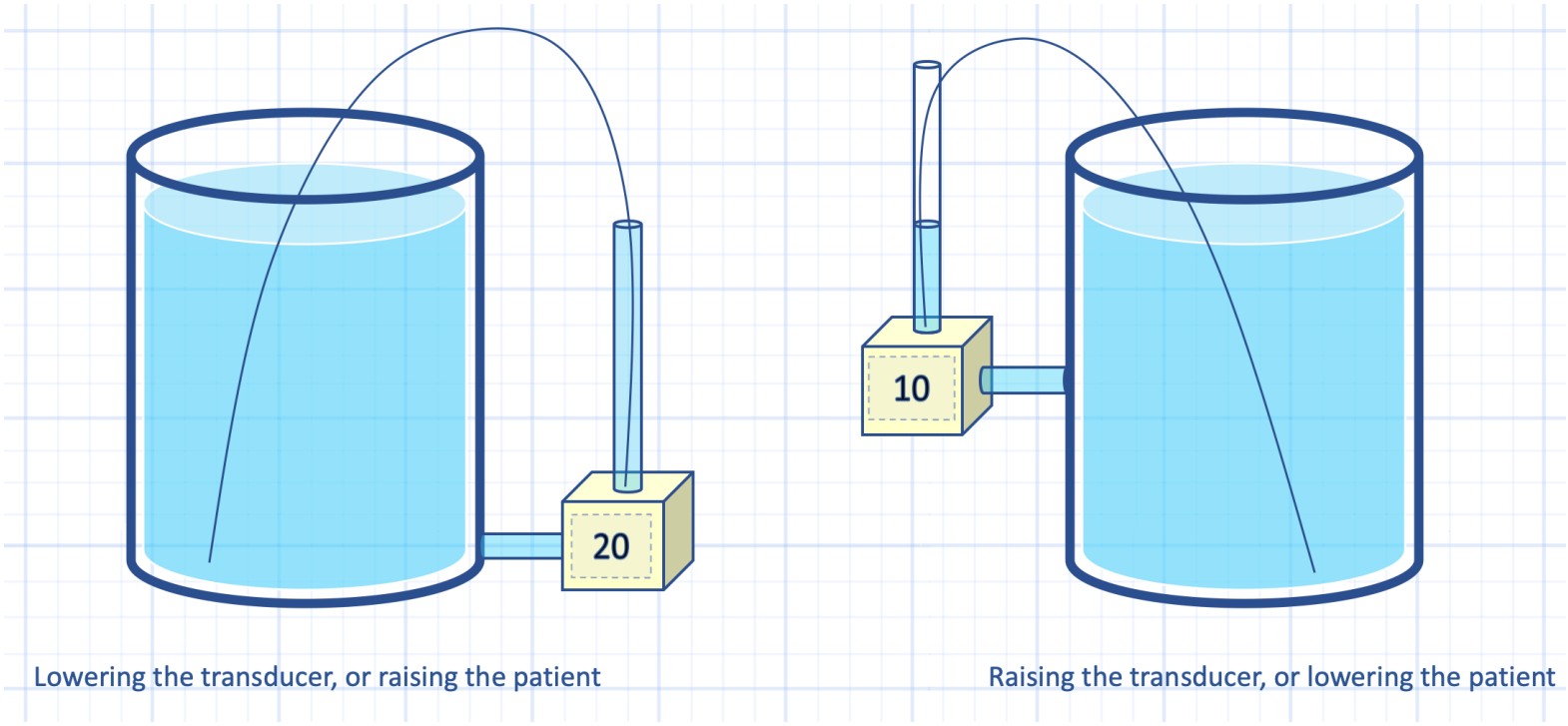

Figure 1: A gravitational reference point is important for the central venous pressure. See text.

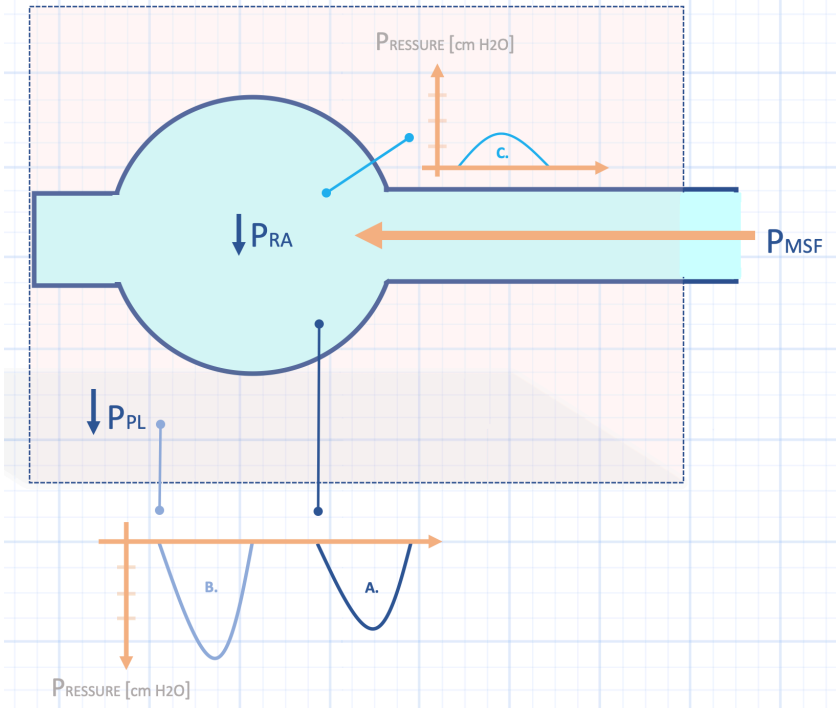

Figure 2: The influence of respiration on central venous pressure. Curve A. represents the typical CVP monitor in the ICU with intra-vascular pressure referenced to atmospheric pressure [outside the thoracic box]. With spontaneous inspiration, pressure falls. B. represents an esophageal pressure monitor as an approximation of pleural pressure [Ppl] referenced to atmospheric pressure. With inspiration, Ppl [B.] falls more than A. as right atrial pressure [Pra] is buffered by venous return [arrow from mean systemic filling pressure - Pmsf]. Subtracting A. from B. [e.g. referencing the CVP monitor to the esophageal balloon] gives pressure waveform C. - an approximation of right atrial trans-mural pressure - which rises!

Because of the aforementioned reference artifact during respiration, vascular pressures should be measured at end-expiration which ensures that intra-thoracic pressure is as close to atmospheric pressure as possible. When this is achieved, the intra-vascular pressure best reflects the true vascular distending pressure. Caveats

to this approach include high levels of PEEP and forced expiration by the patient which raise intra-thoracic and intra-vascular pressure throughout expiration [6, 7, 10]. In these cases, there may be no accurate measurement of central venous pressure without reference to an esophageal balloon.

Lastly, while the application of PEEP may 'artifactually' raise the central venous pressure – that is, increase the intra-vascular pressure but decrease the transmural pressure – the recorded intra-vascular pressure remains the true 'back pressure' to venous return. Therefore, PEEP may shrink right atrial volume, but the increased right atrial pressure and mean systemic filling pressure negatively impact fluid transudation in the capillary beds, favouring interstitial edema [10].

Waveforms

A cardiac cycle typically generates two positive CVP deflections and sometimes three. As well, there are two negative deflections during one cardiac cycle [figure 3]. These waveforms are seen in both the right and left atria. In the left atrium, they are seen in the wedge pressure but may be dampened by the physical distance between the left atrium and the end of the pulmonary artery catheter [11, 12]. The waveforms are important to understand, especially when interpreting Doppler venous velocimetry as discussed in chapter 10.

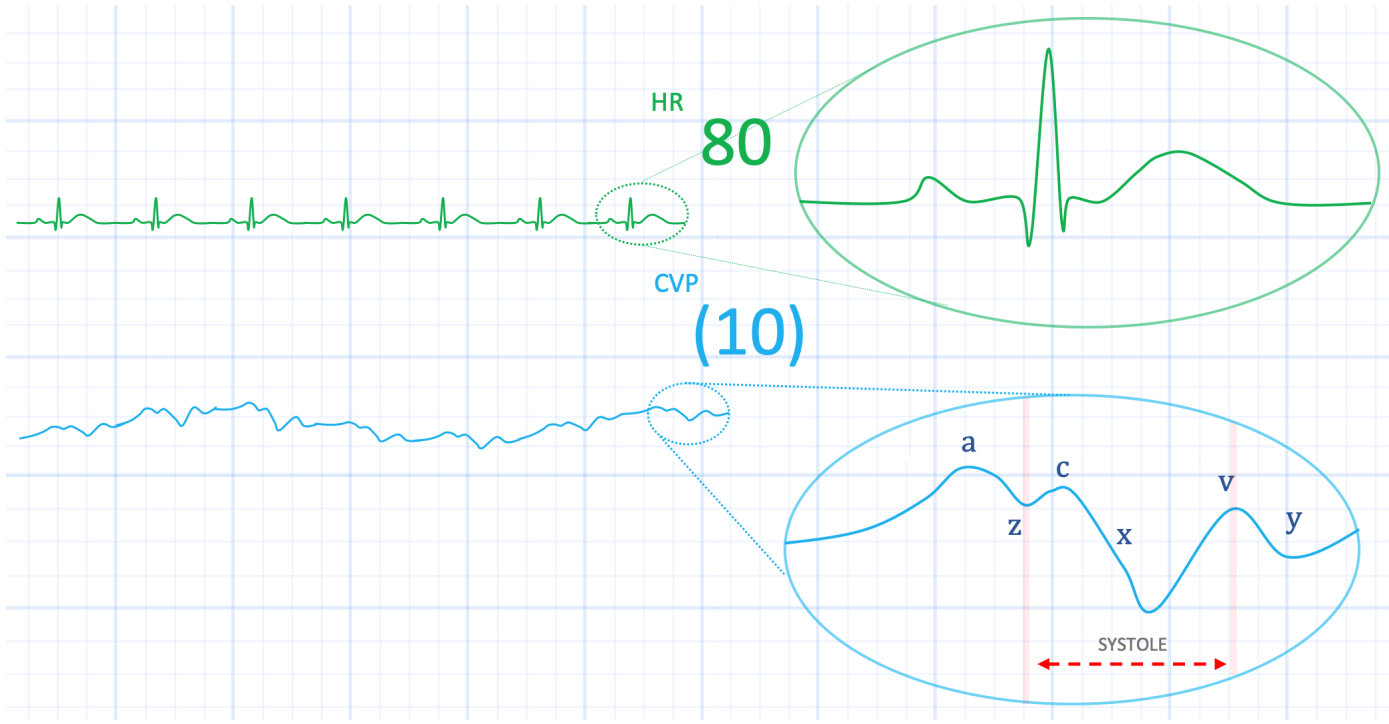

Figure 3: Illustration of an ICU monitor. The central venous pressure waveform for a single cardiac cycle is represented. See text

The a wave

The a wave is the first positive deflection of the CVP and is caused by atrial contraction. Consequently, when atrial contraction is absent, the a wave is absent

or intermittent and diminutive. The pressure at the end of the a wave reflects true end-diastolic ventricular filling pressure as this occurs just before the onset of the QRS complex [i.e. systole]. The a wave pressure change depends on contraction strength, atrial compliance [which may be low at high atrial volume] and volume transfer. The presence of an intermittent, large [or cannon] a wave – especially in conjunction with a low arterial pressure beat synchronous with the cannon a wave – strongly suggests atrioventricular dissociation [12, 13].

The c wave

This is the second positive deflection of the CVP and is infrequently seen as it is below the sensitivity of many pressure-monitoring systems in clinical practice. The c wave is a pressure upstroke within the right atrium that occurs early in systole and presumably depicts reflection of the closed tricuspid valve into the right atrium as intra-ventricular cavity pressure increases. As the a wave marks the end of diastole and the c wave the beginning of systole, it is the nadir between the a wave and c wave [if seen] that marks true end-diastolic pressure; this location on the CVP tracing is sometimes called the z-point [9, 10].

The x descent

The atrial pressure falls from the apex of the a wave and ends at the base of the v wave. This pressure drop results from increased atrial volume during systole. As the ventricle contracts, the tricuspid valve is pulled downwards through systole and this raises atrial capacitance. Consequently, the central venous pressure drops through most of systole. The fall in pressure facilitates venous return through systole until pressure begins to rise again in late systole – marking the beginning of the v wave [9, 12].

The v wave

The v wave is the third positive deflection of the CVP and, as above, is the result of venous pooling in the right atrium in late systole. The v wave will be tall and occupy the x descent if there is tricuspid regurgitation [12]. Importantly, the v wave can be tall in the left atrium simply as a result of high cardiac volume. The reason for tall v waves in the left atrium is the lower compliance of the left atrium and pulmonary veins in comparison with the right atrium; consequently, tall v waves resolve with diuresis. The low compliance causes greater pressure variation in the v waves especially at high left atrial volume.

The y descent

The apex of the v wave marks the beginning of the y descent. The y descent represents falling atrial pressure beginning at the onset of diastole. When the tricuspid valve opens, blood leaves the right atrium and blood volume transfer causes the pressure drop, or y-descent [9, 10, 12]. If right atrial pressure is high [e.g. restrictive filling pattern] and right ventricular pressure is low at the onset of diastole, there is a large drop in pressure and a prominent y descent. If a restrictive filling pattern is accompanied by poor ventricular function, then end-systolic ventricular pressure will be relatively high and a large y descent will not be seen [14, 15]. Therefore, the absence of a large y-descent does not exclude restrictive physiology. Similarly, in cardiac tamponade, when all chamber pressures equalize during diastole, there is minimal pressure difference between the right atrium and ventricle at the apex of the v wave [i.e. the onset of diastole]; therefore, the y descent is diminished or absent in cardiac tamponade. Of note, the lack of y descent only occurs when all chambers of the heart are compressed by a large pericardial effusion. In some instances, for example post-cardiac surgery, there is localized pericardial effusion or clot, so cardiac chamber pressures do not completely equalize during diastole and the y descent may be present despite tamponade-like physiology [15-17].

Determinants of CVP

Simply speaking, the pressure within a distensible chamber depends upon its volume and compliance. At normal right atrial volume, the compliance is quite high, so chamber volume change causes relatively small pressure change, if any at all. In fact, more than two decades ago, the right ventricle was shown to be, essentially, an unstressed structure at physiological volumes [18]. The relationship is, however, curvilinear so when a certain critical volume is reached, there is an abrupt drop in compliance and small volume change causes large pressure change. The volume at which this occurs is much smaller in critically-ill patients and may vary considerably between patients and within a patient over a disease course [18-21].

What then determines right atrial volume? If the right atrium is considered to be like an eddy in a stream, its volume is determined by the relative contributions of inflow and outflow. Within the heart, these properties are determined by venous return and cardiac function, respectively, and they are described graphically by the Guyton diagram.

Venous Return

As described extensively in other chapters [see chapters 2, 8 & 10], the venous return curve represents the return, or circuit, function of the vascular system. It is a linear relationship that characterizes venous return as a function of mean systemic

filling pressure and resistance, across a spectrum of right atrial pressures. Recall that if the curve is shifted rightwards by increased stressed volume or attenuated venous compliance, or if the slope is shifted upwards by diminished resistance, then venous return is enhanced and right atrial pressure should rise [6, 22-24].

Cardiac Function

However, the steady-state blood volume of the central veins – which determines the right atrial pressure – cannot be described by the venous return function alone. The volume in the central veins also depends upon the function of the heart which expels blood from the central veins into the arterial tree. The Frank-Starling mechanism ensures that the inflow of blood to the right heart [i.e. venous return] is ejected forward to the lungs and periphery. The slope of the cardiac function curve defines overall pump function and is determined not just by contractility but also by the heart's diastolic properties, valve function, afterload, heart rate and rhythm [22, 23]. The cardiac function curve simply describes cardiac output on the ordinate at any given right atrial pressure on the abscissa. The point at which the cardiac function curve intersects the venous return curve defines the operating point of the cardiovascular system. Accordingly, the operating point describes the steady-state right atrial pressure and cardiac output for a given venous return and cardiac function [22, 23] [figure 4].

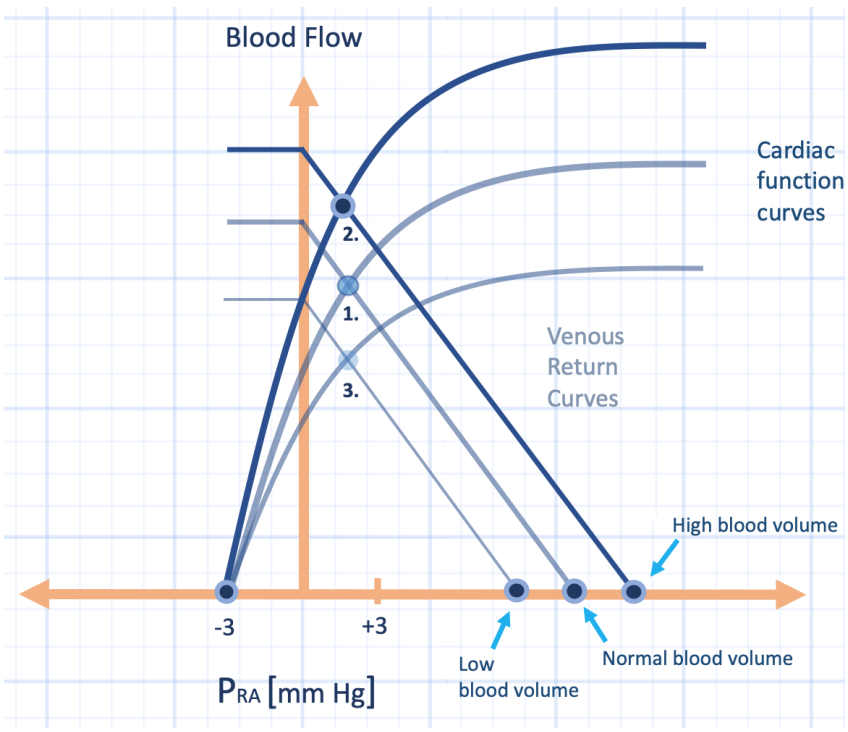

Figure 4: Determinants of the central venous pressure or right atrial pressure [Pra]. Three different hypothetical blood volumes are depicted as three different mean systemic filling pressures and venous return curves. Similarly, three different cardiac function curves are shown with the uppermost, opaque curve representing enhanced function and the lowermost, thin, translucent curve illustrating impaired cardiac function. Three operating points are generated: 1. normal cardiac function and normal blood volume; 2. enhanced cardiac function coupled with high blood volume; 3. impaired cardiac function with low blood volume. All three operating points have the same right atrial pressure [x-axis, roughly 2 mmHg], but different cardiac outputs [y-axis].

The term 'volume status' refers to a patient's degree of volume repletion or depletion, that is, whether the patient is euvolemic, hypovolemic or hypervolemic. Unfortunately, the CVP is often used unquestioningly as a marker for volume status. Based on the aforementioned, the CVP cannot accurately predict 'volume status' nor would anyone who understands this physiology demand this of the central venous pressure. Asking if one may determine a patient's 'volume status' from the central venous pressure is akin to asking if one may determine lactate concentration when given only the patient's pH [6, 7, 10, 11, 25]. We would never ask this question because we know that the pH is a single value with many physiological determinants - only one of which is serum lactate. The same reasoning applies to the central venous pressure and volume status!

Because the CVP depends upon the intersection of the venous return and cardiac function curves and because the shape and position of each curve depend upon multiple co-varying physiological parameters, it is challenging to relate – with certainty – any one determinant to the CVP itself. It is true that a patient who is volume overloaded would tend towards higher CVP just as a patient with a high lactate would tend towards lower pH, but there are other processes that mediate the relationship. Ultimately, there are many other dynamic determinants of both the pH and CVP – they are both complex physiological variables. This is further discussed via analogy to a marionette in chapter 10.

As an example, consider a patient with a right atrial or central venous pressure of 2 mmHg [figure 4]; this value could be the result of: 1. a hypervolemic patient with increased cardiac function [e.g. low afterload, high contractility]; 2. a euvolemic patient with normal cardiac function or; 3. a hypovolemic patient with impaired cardiac function. What is more critical is the trend of a patient's CVP in response to changes in cardiac output; it is imperative that the CVP be interpreted within the context of cardiac output. While a pulmonary arterial catheter can measure cardiac output directly, and is invaluable when interpreting a CVP, newer non-invasive means are available in addition to clinical and biochemical parameters such as skin temperature, mentation, urine output, lactate and central venous oxygen saturation [10].

In contrast to 'volume status', 'volume responsiveness' refers to recruitable stroke volume in response to increased mean systemic filling pressure. When considering the Guyton analysis, stroke volume augmentation following fluid challenge occurs if the operating point lies upon the ascending portion of the cardiac function curve [26]. Unfortunately, because the cardiac function curve slope varies considerably between and within patients, there is no good right atrial pressure that predicts the ascending portion universally. The plateau of the cardiac function curve has been found to occur as low as 2 mmHg [7]. Indeed, the slope of the cardiac function curve shifts upwards and downwards depending on disease state. As well, the cardiac function curve shifts along the venous return curve in response to changes in intra-thoracic pressure. It is expected, therefore, that a single value or set of right atrial pressure values cannot accurately predict volume responsiveness in all

patients [1-3, 5] [figure 5]. Unfortunately, the right atrial pressure continues to be used as a marker for volume responsiveness, as discussed in chapter 10.

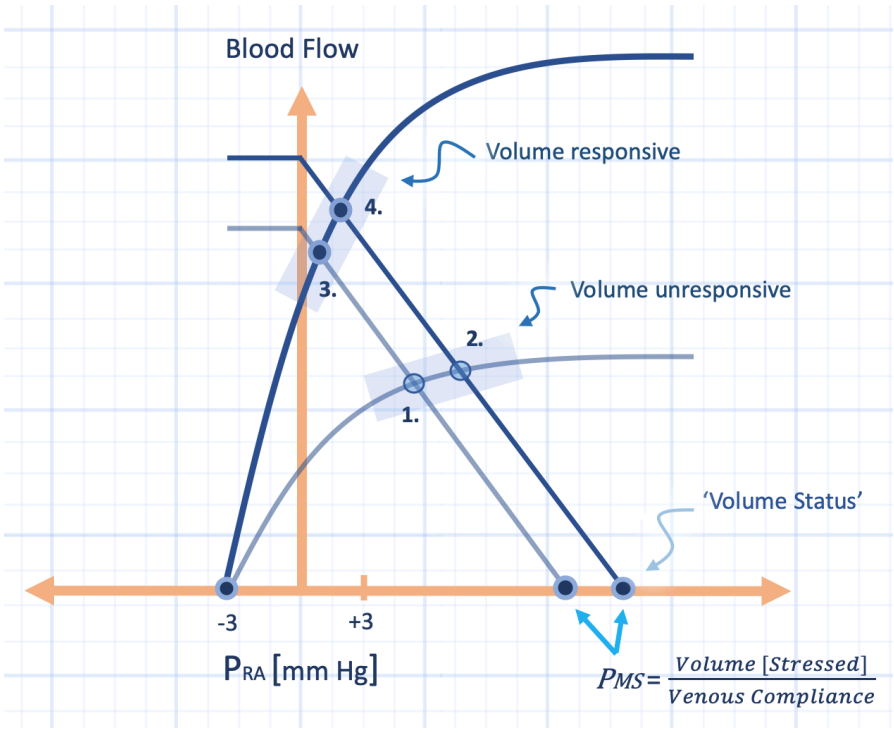

Figure 5: Volume status and volume responsiveness on the Guyton diagram. See also figure 4. Volume status is one determinant of mean systemic pressure [Pms], itself one mediator of venous return. Volume responsiveness is determined by where the operating point is on the cardiac function curve. Here, 4 operating points are generated: 1. normal volume status with impaired cardiac function; this is a non-responsive patient [on plateau of Starling curve] with a low right atrial pressure [Pra, x-axis]. 2. higher blood volume with the same cardiac function. 3. normal blood volume with enhanced cardiac function - this patient is volume responsive. 4. enhanced cardiac function with high blood volume - also volume responsive. Note all 4 operating points may represent different patients or the same patient in response to various interventions; y-axis is cardiac output.

Nevertheless, one study did find that when the CVP is above 10 mmHg, the likelihood of responding to a volume infusion is low and completely absent above 13 mmHg [7]. Should a patient be volume responsive above these values it is prudent to determine why the cardiac function curve is shifted rightwards along the venous return curve, for example with high levels of PEEP, lower lobe gas-trapping or mediastinal edema [6, 7].

When a patient has a CVP less than 10-13 mmHg and there is a desire to administer intravenous fluid, the 'gold-standard' for volume responsiveness is the administration of intravenous fluid followed by measurement of cardiac output. Unfortunately, blood pressure and urine output may not increase even when stroke volume rises. A fluid challenge has been defined as a rapid fluid bolus [within 10-30 minutes] as an attempt to increase central venous pressure by 2 mmHg; responders are considered to have an increase in cardiac index by over 300 ml/min/m2 [26] or by 10-15% [2]. Similarly, a passive leg raise could be done to achieve the same increase in central venous pressure, but care must be given to appropriate levelling of the CVP transducer during this maneuver [27]. An additional test is the 'mini' fluid challenge [28].

Spontaneous Ventilation

As discussed extensively in chapters 3 and 4, the cardiac function curve shifts relative to the systemic venous return curve in response to changes in intra-thoracic pressure. Accordingly, respiratory maneuvers are used to determine the position of the cardiac function curve's plateau relative to the operating point. Recall that the x-intercept of the cardiac function curve tracks intra-thoracic pressure. Thus, a spontaneous inspiratory effort left-shifts the cardiac function curve [29] with respect to the systemic venous return curve on the Guyton diagram. A stable CVP during spontaneous inspiration has been shown to adequately predict the absence of response to a fluid challenge [30], though this is contentious [31, 32]. When considering this graphically, a patient will not augment cardiac output if the operating point lies upon the plateau of the cardiac function curve. If the cardiac function curve shifts leftwards in response to a spontaneous inspiratory effort, the plateau of the cardiac function curve leads to unchanging central venous pressure as the operating point remains on the plateau. Importantly, active expiration may spuriously suggest an inspiratory fall in CVP leading the clinician to think that the patient is operating on the ascending limb of the cardiac function curve. Active abdominal contraction during expiration will increase the right atrial pressure by shifting the cardiac function curve rightwards; the initiation of inspiration and relaxation of abdominal muscles cause the right atrial pressure to fall even though the patient may be truly volume non-responsive [6, 10, 11, 26, 30]. It is therefore imperative that the patient be observed for forced expiration during this test [figure 6].

Regrettably, the presence of CVP change during spontaneous inspiration does not accurately and reliably [31] predict a response to a fluid challenge. This may be due to an inadequate inspiratory effort, or an operating point that is close to the plateau of the cardiac function curve; a fall in central venous pressure is also accentuated if the operating point is near maximal venous return and if inspiratory efforts are excessive [10, 26, 30].

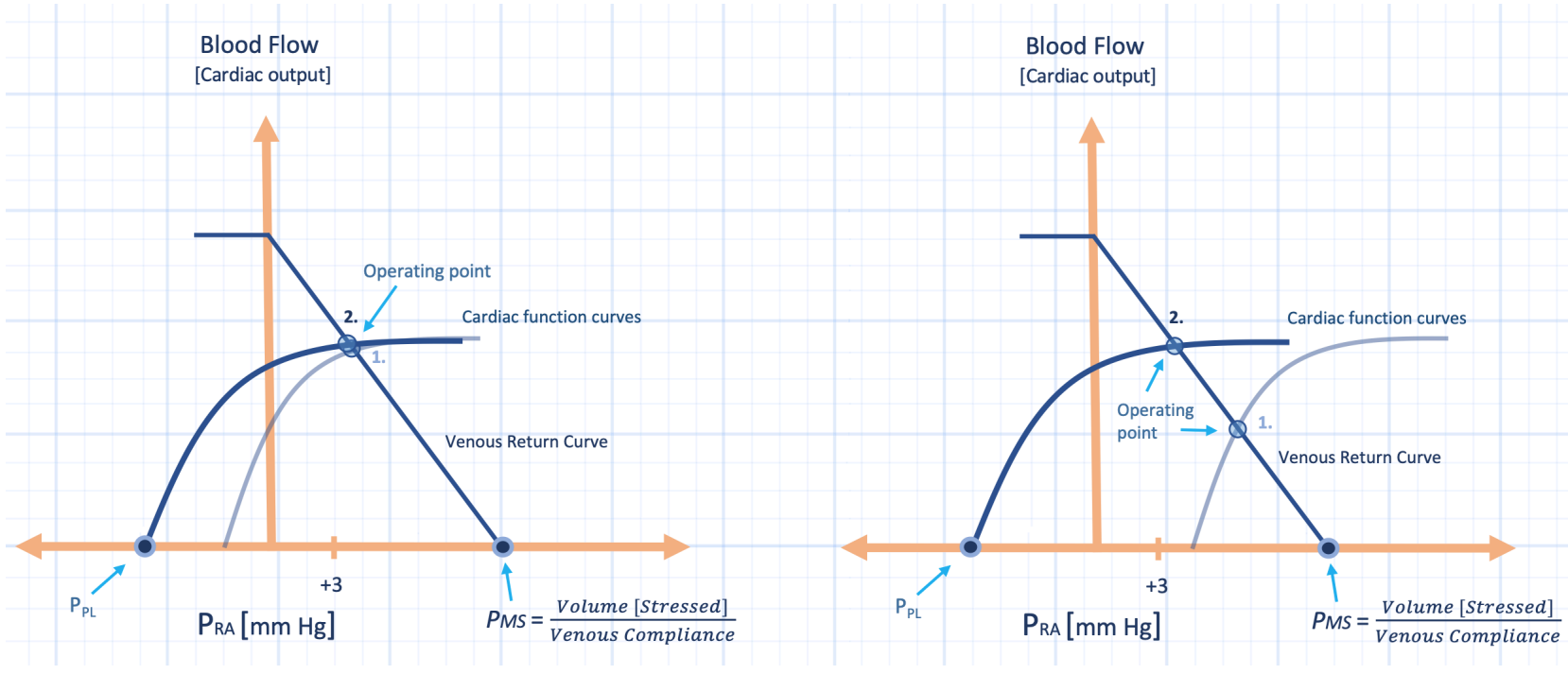

Figure 6: Dynamic changes in the central venous pressure or right atrial pressure [Pra, x-axis]. Left panel: Spontaneous inspiration lowers pleural pressure [Ppl] and pulls the volume unresponsive cardiac function curve leftwards. Because the operating point 1. is initially on the flat portion of the Starling curve, it does not change much with inspiration; that is, the operating point moves to 2. Thus, Pra and cardiac output do not change and this patient is inferred to be volume non-responsive. Right panel: The effect of expiratory muscle recruitment. The patient is volume unresponsive, but the right-shift followed by left shift causes the Pra to rise [1.] and then fall [2.]. This decrease in Pra signals that the operating point is on the ascending portion of the Starling curve, but this is a false positive. Pms is mean systemic pressure; y-axis is cardiac output.

Mechanical Ventilation and PEEP

If a spontaneously breathing patient has a decrease in central venous pressure with inspiration, it is expected that the institution of mechanical ventilation – which shifts the cardiac function curve rightwards – would reduce cardiac output. This is not seen empirically, however, and likely has to do with reflex responses to the application of mechanical ventilation, and especially PEEP [33, 34] [figure 7]. Recall that mechanical ventilation and positive intra-thoracic pressure alter both the cardiac function and venous return curves [22, 35-41]. The mean systemic filling pressure, and therefore venous return curve, is shifted rightwards in response to PEEP preserving cardiac output as long as right atrial pressure stays above Pcrit. Pcrit is the pressure at which collapse of the great veins occurs entering the thorax. Equally important is the adrenergic response observed following the application of both PEEP and intermittent positive pressure ventilation. Sympathetic tone raises the slope of cardiac function curve as a consequence of both augmented inotropy and chronotropy; this defends cardiac output. Thus, predicting diminished cardiac output in response to initiating mechanical ventilation is difficult; there are confounding effects imparted by intra-thoracic pressure on both cardiac function and systemic venous return. By the same argument, observing increased right atrial pressure when instituting mechanical ventilation cannot reliably predict that the operating point is on the ascending portion of the cardiac function curve and, therefore, may not be used to predict fluid responsiveness [6, 10, 26].

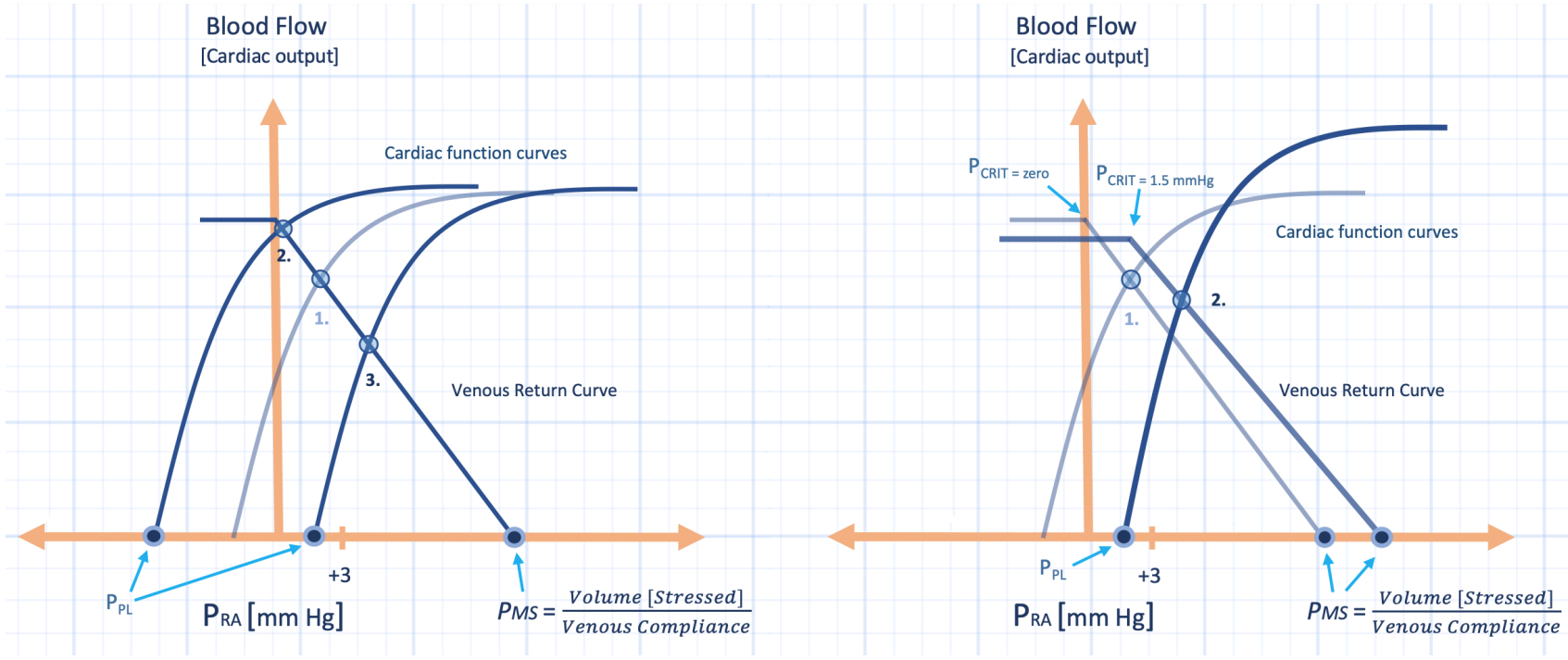

Figure 7: Predicting the effect of positive end-expiratory pressure [PEEP] from dynamic right atrial pressure [Pra] change. Left panel shows the baseline operating point 1. for a patient who inspires spontaneously. The cardiac function curve moves leftwards as pleural pressure [Ppl] falls. The operating point moves to 2, the Pra [x-axis] falls and cardiac output [y-axis] rises because the operating point originated on the ascending [volume responsive] portion of the Starling curve [compare this to figure 6]. Accordingly, a passive, mechanical breath, which raises Ppl, should move the operating point to 3, predicting that if mechanical ventilation is initiated that cardiac output will fall. Right panel shows that initiation of PEEP in this patient is not met by a fall in cardiac output because of compensatory sympathetic tone - which raises mean systemic pressure [Pms] and increases the slope of the Starling curve. The operating point moves from 1. to 2. There is minimal change in cardiac output [y-axis]. Pcrit is the critical collapse pressure of the great veins as discussed in chapters 3 & 4.

A stable CVP during a mechanical breath suggests – but does not prove – that the operating point is upon the plateau of the cardiac function curve and that fluid challenge is unhelpful. However, this is an uncommon clinical event for the following reasons. Recall that the degree to which the cardiac function curve shifts rightwards depends upon how much of the tracheal pressure is felt in the pleural space - a function of lung volume and chest wall compliance [42, 43]. Thus, large tidal volume and/or stiff chest wall results in excessive inspiratory rightward shift and rise in the CVP. Additionally, the venous return curve shifts rightwards with insufflation of the thorax and this also raises inspiratory right atrial pressure [36, 37, 40]. Finally, if right ventricular afterload rises with the breath, downshift of the cardiac function curve would augment atrial pressure with inspiration [44]. Any or all of these effects make a stable right atrial pressure during mechanical inspiration an uncommon event. As an example of the complicated nature by which the right atrial pressure changes during a passive mechanical inspiration, an investigation in stable, post-operative cardiac surgery patients demonstrated that some patients increased their transmural right atrial pressure while others decreased right atrial transmural pressure. While this study did not specifically assess how mechanical inspiratory changes in CVP relate to volume responsiveness, it does illustrate the complicated and sometimes conflicting effects that mechanical ventilation has upon ventricular loading conditions [45].

In a patient who is receiving mechanical ventilation with spontaneous efforts, the situation becomes even more complicated; an example is a patient on CPAP. The application of pressure throughout the respiratory cycle, which occurs with CPAP,

results in a steady-state rightward shift of the cardiac function curve and decreased maximal venous return [36, 37, 40]. However, with spontaneous inspiratory efforts, the cardiac function curve moves leftwards unpredictably. Given the aforementioned shape changes of the cardiac function and venous return curves during the respiratory cycle, dynamic assessments of right atrial pressure while on CPAP are confounded, impairing reliable and accurate assessments of volume status and responsiveness [31].

Ultrasound of the Inferior Vena Cava

While respiratory variation of the inferior vena cava [IVC] is sometimes considered a dynamic assessment, its physiological underpinning lies mostly as a non-invasive surrogate of the central venous pressure, as detailed below. As well, the clinical implication of IVC dilation during passive mechanical ventilation and IVC collapse during spontaneous ventilation, while often confused, is actually different.

During passive mechanical ventilation, that is, in the absence of spontaneous respiratory efforts, IVC dilation with inspiration was observed to be a successful marker of fluid responsiveness [46]. As discussed above, both the cardiac function and venous return curves shift rightwards during passive mechanical inspiration which raises central venous pressure. While abdominal pressure does increase with passive mechanical ventilation, in the absence of diaphragmatic contraction, trans-diaphragmatic pressure does not increase. As a result, the central venous pressure rises beyond that of the intra-abdominal pressure and, therefore, the IVC transmural pressure increases. Because the compliance curve of the IVC is curvilinear, there is dilation when the IVC transmural pressure rises up to an inflection point. When the IVC functions within its compliant zone, this acts as a surrogate for cardiac fluid responsiveness [47]. Note, however, that this test is not a 'direct' assessment of cardiac function.

By contrast, assessment of IVC collapse during spontaneous inspiration is the result of active contraction of the diaphragm and increased trans-diaphragmatic pressure. As the intra-thoracic pressure falls, so too does the CVP which is transmitted to down the IVC. Simultaneously, the intra-abdominal pressure rises and supersedes intra-abdominal IVC pressure. If the transmural pressure of the intra-abdominal IVC decreases, then collapse is seen [48]. As discussed in chapter 2, this physiology creates a Starling resistor and vascular waterfall; the fluttering of the IVC creates the plateau in venous return – maximal venous return. Graphically, this is illustrated when the right atrial pressure approaches the venous return plateau as the cardiac function curve shifts leftwards during spontaneous inspiration [figure 8].

IVC collapse has been employed to estimate right atrial pressure. IVC collapse in healthy subjects with normal inspiratory effort was correlated with right atrial pressure; collapse of more than 50% predicted a right atrial pressure less than 10 mmHg while collapse of less than 50% predicted a right atrial pressure of more than 10 mmHg [49]. Thus, in healthy subjects without excessive inspiratory

activity, the collapse of the IVC can be used as a surrogate for right atrial pressure. Indeed, this physiology makes sense when considering the Guyton analysis – maximal venous return is reached more readily with a low baseline right atrial pressure. Again, this occurs as the cardiac function curve slides leftwards along the plateau portion of the venous return curve. Interestingly, even in healthy controls, diaphragmatic breathing versus chest wall breathing can alter the relationship between IVC collapse and right atrial pressure [50].

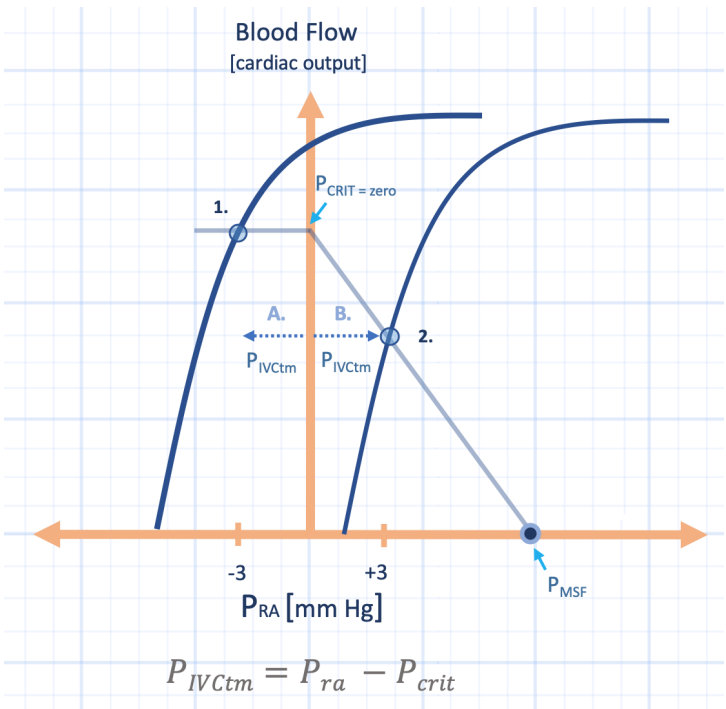

Figure 8: Illustration of inferior vena cava [IVC] collapse and dilation. Spontaneous inspiration pulls the cardiac function curve leftwards; the operating point 1. falls below the critical collapse pressure [Pcrit] and there is IVC collapse. This causes maximal venous return - a plateau of the venous return curve. The transmural pressure of the IVC [P_{IVCtm}] is the right atrial pressure [Pra] less the Pcrit and is depicted by the dotted arrow A. Operating point 1. results in a negative P_{IVCtm} indicating collapse. An increase in intra-thoracic pressure increases the Pra to operating point 2. Here the P_{IVCtm} is positive, indicating IVC dilation as represented by the dotted line B. The P_{IVCtm} is not to be confused with the right atrial transmural pressure illustrated in figure 9.

However, the patients in the ICU and on the floor who have their IVCs interrogated by ultrasonography are far from healthy subjects. They frequently have excessive inspiratory and expiratory efforts. They often have invasive or non-invasive ventilation or may have auto-PEEP and elevated intra-abdominal pressure [figure 9]. These abnormalities change the venous return curve such that the plateau for venous return is pushed downwards and the aforementioned correlation between right atrial pressure and IVC collapse falls apart [51]. Equally important, even in healthy subjects IVC collapse was correlated with central venous pressure which, as discussed in detail above, is not an accurate indicator of volume status or volume responsiveness. In this sense, collapse of the IVC during spontaneous inspiration is not a dynamic measure of the central venous pressure but rather a surrogate marker for static right atrial pressure. Indeed, the use of IVC collapse in spontaneously breathing subjects as a marker for fluid responsiveness has been studied and found to be, at best, moderately useful for predicting recruitable stroke volume [52, 53]. In one investigation, it was most helpful in patients with complete IVC collapse, but 40% of the patients in the study were

likely suffering from hemorrhagic shock. This topic is discussed in further detail in chapters 8 and 10.

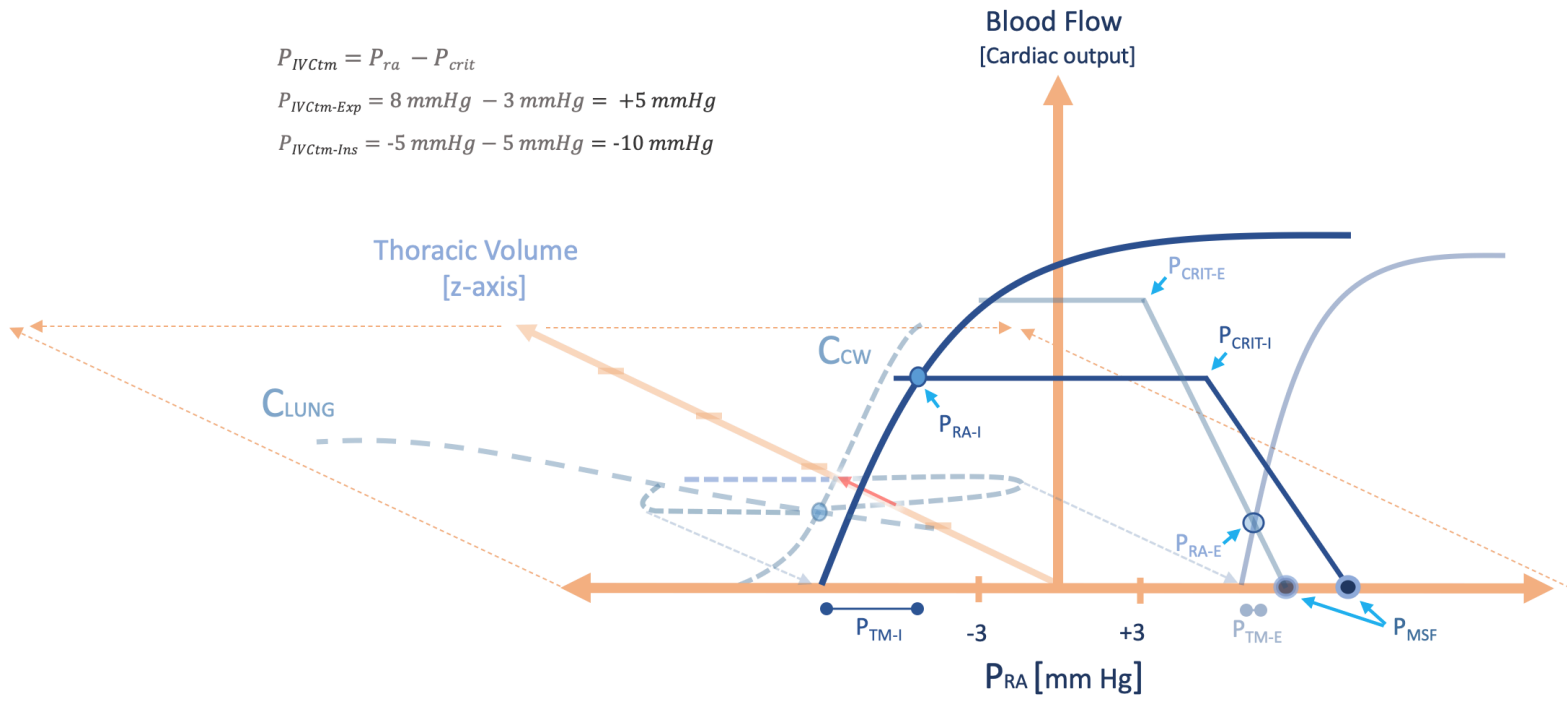

Figure 9: Contrasting IVC transmural pressure and right atrial transmural pressure in decompensated cirrhosis [see chapter 4]. Lung compliance [Clung] and chest wall compliance [Ccw] are reduced from volume overload and tense ascites. Inspiratory and expiratory pleural pressure [Ppl] are exaggerated because of abnormal thoracic mechanics and active expiration. The tense ascites elevates the critical collapse pressure [Pcrit] on the venous return curves. On forced inspiration [opaque curves], the operating point moves to the inspiratory right atrial pressure [Pra-I] which is negative. When referenced to inspiratory pleural pressure [the x-intercept of the cardiac function curve] the transmural pressure of the right atrium [Ptm-I] rises, as illustrated below the x-axis. Note that the right atrial transmural pressure is equivalent to the superior vena cava [SVC] transmural pressure. However, the IVC transmural pressure is the right atrial pressure relative to the inspiratory Pcrit [Pcrit-I]. The IVC transmural pressure here is negative indicating collapse [upper left calculation, roughy -10 mmHg]. Forced expiration increases right atrial pressure to Pra-E. Relative to the pleural pressure on expiration, the transmural pressure of the right atrium [Ptm-E] shrinks [illustrated below x-axis] while the transmural pressure of the IVC [Pra-E relative to Pcrit-E] actually rises [roughly +5 mmHg] indicating IVC dilation. This patient is hypervolemic and volume unresponsive at baseline. The y-axis is cardiac output; Pmsf is mean systemic filling pressure.

Conclusion

The central venous pressure is related to the central venous blood volume by a curvilinear relationship both in the vena cavae and the right heart itself. At physiological volumes, the great veins and right heart are essentially unstressed structures. In critically-ill patients, the relationship between central venous volume and central venous pressure is more direct such small changes in volume result in large changes in pressure. The determinant of central venous volume is the cross-roads of venous return and cardiac function, which may be thought of as the balance between central venous inflow and outflow. When simultaneously plotted on the Guyton diagram, venous return and cardiac function unveil a pictorial description of central venous pressure and cardiac output. This relationship reveals that static CVP measurements cannot accurately reflect volume status or whether or not the patient will augment his or her cardiac output in response to a fluid

challenge. Dynamic right atrial pressure assessment is more physiologically sound with respect to predicting a patient's functional hemodynamic state, but results have been conflicting. This undoubtedly reflects the complex relationship between cardiovascular and respiratory physiologies in sickness and in health.

References

1. Marik, P.E., M. Baram, and B. Vahid, Does central venous pressure predict fluid responsiveness? A systematic review of the literature and the tale of seven mares. Chest, 2008. 134(1): p. 172-8.
2. Marik, P.E., X. Monnet, and J.L. Teboul, Hemodynamic parameters to guide fluid therapy. Ann Intensive Care, 2011. 1(1): p. 1.
3. Marik, P.E. and R. Cavallazzi, Does the central venous pressure predict fluid responsiveness? An updated meta-analysis and a plea for some common sense. Crit Care Med, 2013. 41(7): p. 1774-81.
4. Shippy, C.R., P.L. Appel, and W.C. Shoemaker, Reliability of clinical monitoring to assess blood volume in critically ill patients. Crit Care Med, 1984. 12(2): p. 107-12.
5. Kumar, A., et al., Pulmonary artery occlusion pressure and central venous pressure fail to predict ventricular filling volume, cardiac performance, or the response to volume infusion in normal subjects. Crit Care Med, 2004. 32(3): p. 691-9.
6. Magder, S., Bench-to-bedside review: An approach to hemodynamic monitoring - Guyton at the bedside. Crit Care, 2012. 16(5): p. 236.
7. Magder, S. and F. Bafaqeeh, The clinical role of central venous pressure measurements. J Intensive Care Med, 2007. 22(1): p. 44-51.
8. Courtois, M., et al., Anatomically and physiologically based reference level for measurement of intracardiac pressures. Circulation, 1995. 92(7): p. 1994-2000.
9. Lodato, R.F., Use of the pulmonary artery catheter. Seminars in Respiratory and Critical Care Medicine, 1999. 20(1): p. 29-42.
10. Magder, S., How to use central venous pressure measurements. Current Opinion in Critical Care, 2005. 11(3): p. 264-270.
11. Magder, S., Central venous pressure: A useful but not so simple measurement. Crit Care Med, 2006. 34(8): p. 2224-7.
12. Sharkey, S.W., Beyond the wedge: clinical physiology and the Swan-Ganz catheter. Am J Med, 1987. 83(1): p. 111-22.
13. Kern, M.J., et al., Interpretation of cardiac pathophysiology from pressure waveform analysis: multivalvular regurgitant lesions. Cathet Cardiovasc Diagn, 1993. 28(2): p. 167-72.
14. Shabetai, R., N.O. Fowler, and W.G. Guntheroth, The hemodynamics of cardiac tamponade and constrictive pericarditis. Am J Cardiol, 1970. 26(5): p. 480-9.
15. Reddy, P.S., et al., Cardiac tamponade: hemodynamic observations in man. Circulation, 1978. 58(2): p. 265-72.
16. Takata, M., W. Mitzner, and J.L. Robotham, Influence of the pericardium on ventricular loading during respiration. J Appl Physiol (1985), 1990. 68(4): p. 1640-50.
17. Takata, M., et al., Coupled vs. uncoupled pericardial constraint: effects on cardiac chamber interactions. J Appl Physiol (1985), 1997. 83(6): p. 1799-813.
18. Pinsky, M.R., My paper 20 years later: Effect of positive end-expiratory pressure on right ventricular function in humans. Intensive Care Med, 2014. 40(7): p. 935-41.
19. Pinsky, M.R., J.M. Desmet, and J.L. Vincent, Effect of positive end-expiratory pressure on right ventricular function in humans. Am Rev Respir Dis, 1992. 146(3): p. 681-7.
20. Tyberg, J.V., et al., The relationship between pericardial pressure and right atrial pressure: an intraoperative study. Circulation, 1986. 73(3): p. 428-32.
21. Santamore, W.P., M. Constantinescu, and W.C. Little, Direct assessment of right ventricular transmural pressure. Circulation, 1987. 75(4): p. 744-7.
22. Feihl, F. and A.F. Broccard, Interactions between respiration and systemic hemodynamics. Part I: basic concepts. Intensive Care Med, 2009. 35(1): p. 45-54.
23. Broccard, A.F., Cardiopulmonary interactions and volume status assessment. J Clin Monit Comput, 2012. 26(5): p. 383-91.
24. Guyton, A.C., Determination of cardiac output by equating venous return curves with cardiac response curves. Physiol Rev, 1955. 35(1): p. 123-9.
25. Magder, S., Central venous pressure monitoring. Current Opinion in Critical Care, 2006. 12(3): p. 219-27.
26. Magder, S., Fluid status and fluid responsiveness. Current Opinion in Critical Care, 2010. 16(4): p. 289-96.
27. Monnet, X. and J.L. Teboul, Passive leg raising. Intensive Care Med, 2008. 34(4): p. 659-63.

28. Muller, L., et al., An increase in aortic blood flow after an infusion of 100 ml colloid over 1 minute can predict fluid responsiveness: the mini-fluid challenge study. Anesthesiology, 2011. 115(3): p. 541-7.
29. Magder, S., Clinical usefulness of respiratory variations in arterial pressure. Am J Respir Crit Care Med, 2004. 169(2): p. 151-5.
30. Magder, S., G. Georgiadis, and T. Cheong, Respiratory Variations in Right Atrial Pressure Predict the Response to Fluid Challenge. Journal of Critical Care, 1992. 7(2): p. 76-85.
31. Heenen, S., D. De Backer, and J.L. Vincent, How can the response to volume expansion in patients with spontaneous respiratory movements be predicted? Crit Care, 2006. 10(4): p. R102.
32. Magder, S., Predicting volume responsiveness in spontaneously breathing patients: still a challenging problem. Crit Care, 2006. 10(5): p. 165.
33. Nanas, S. and S. Magder, Adaptations of the peripheral circulation to PEEP. Am Rev Respir Dis, 1992. 146(3): p. 688-93.
34. Magder, S., D. Lagonidis, and F. Erice, The use of respiratory variations in right atrial pressure to predict the cardiac output response to PEEP. J Crit Care, 2001. 16(3): p. 108-14.
35. Marini, J.J., B.H. Culver, and J. Butler, Effect of positive end-expiratory pressure on canine ventricular function curves. J Appl Physiol Respir Environ Exerc Physiol, 1981. 51(6): p. 1367-74.
36. Fessler, H.E., et al., Effects of Positive End-Expiratory Pressure on the Gradient for Venous Return. American Review of Respiratory Disease, 1991. 143(1): p. 19-24.
37. Jellinek, H., et al., Influence of positive airway pressure on the pressure gradient for venous return in humans. J Appl Physiol (1985), 2000. 88(3): p. 926-32.
38. Robotham, J.L. and S.M. Scharf, Effects of positive and negative pressure ventilation on cardiac performance. Clin Chest Med, 1983. 4(2): p. 161-87.
39. Robotham, J.L., et al., A re-evaluation of the hemodynamic consequences of intermittent positive pressure ventilation. Crit Care Med, 1983. 11(10): p. 783-93.
40. Scharf, S.M. and R.H. Ingram, Jr., Influence of abdominal pressure and sympathetic vasoconstriction on the cardiovascular response to positive end-expiratory pressure. Am Rev Respir Dis, 1977. 116(4): p. 661-70.
41. Ingram, R.H., Jr., Effect of carotid artery occlusion and lung inflation on the main pulmonary artery. 1. Proc Soc Exp Biol Med, 1972. 140(4): p. 1424-8.
42. Jardin, F., et al., Influence of lung and chest wall compliances on transmission of airway pressure to the pleural space in critically ill patients. Chest, 1985. 88(5): p. 653-8.
43. O'Quin, R.J., et al., Transmission of airway pressure to pleural space during lung edema and chest wall restriction. J Appl Physiol (1985), 1985. 59(4): p. 1171-7.
44. Jardin, F., et al., Reevaluation of hemodynamic consequences of positive pressure ventilation: emphasis on cyclic right ventricular afterloading by mechanical lung inflation. Anesthesiology, 1990. 72(6): p. 966-70.
45. Lansdorp, B., et al., Mechanical ventilation-induced intrathoracic pressure distribution and heart-lung interactions*. Crit Care Med, 2014. 42(9): p. 1983-90.
46. Barbier, C., et al., Respiratory changes in inferior vena cava diameter are helpful in predicting fluid responsiveness in ventilated septic patients. Intensive Care Med, 2004. 30(9): p. 1740-6.
47. Jardin, F. and A. Vieillard-Baron, Ultrasonographic examination of the venae cavae. Intensive Care Med, 2006. 32(2): p. 203-6.
48. Bodson, L. and A. Vieillard-Baron, Respiratory variation in inferior vena cava diameter: surrogate of central venous pressure or parameter of fluid responsiveness? Let the physiology reply. Crit Care, 2012. 16(6): p. 181.
49. Kircher, B.J., R.B. Himelman, and N.B. Schiller, Noninvasive estimation of right atrial pressure from the inspiratory collapse of the inferior vena cava. Am J Cardiol, 1990. 66(4): p. 493-6.
50. Kimura, B.J., et al., The effect of breathing manner on inferior vena caval diameter. European Journal of Echocardiography, 2011. 12(2).
51. Juhl-Olsen, P., C.A. Frederiksen, and E. Sloth, Ultrasound assessment of inferior vena cava collapsibility is not a valid measure of preload changes during triggered positive pressure ventilation: a controlled cross-over study. Ultraschall Med, 2012. 33(2): p. 152-9.
52. Muller, L., et al., Respiratory variations of inferior vena cava diameter to predict fluid responsiveness in spontaneously breathing patients with acute circulatory failure: need for a cautious use. Crit Care, 2012. 16(5): p. R188.
53. Corl, K., A.M. Napoli, and F. Gardiner, Bedside sonographic measurement of the inferior vena cava caval index is a poor predictor of fluid responsiveness in emergency department patients. Emerg Med Australas, 2012. 24(5): p. 534-9.

Chapter Seven

The Pulmonary Artery Catheter

Abstract

While current trends in the intensive care unit dissuade the use of the pulmonary artery catheter [PAC], the poor performance of the PAC in large clinical trials may be partly a function of inadequate clinician experience. Placement of the PAC requires proficiency with both acquisition and interpretation of the PAC's multiple hemodynamic measurements. Without this knowledge, the intensivist can fall prey to inaccuracies both of measurement and analysis, which leads to imprecise clinical decisions. The parameters gleaned from the PAC can be understood, and errors minimized with better comprehension of cardiovascular-respiratory interaction and other subtleties of cardiopulmonary physiology.

Key words: pulmonary artery catheter, pulmonary artery occlusion pressure, wedge pressure, central venous pressure, cardiac output, pulmonary capillary pressure

Introduction

A preponderance of evidence counsels against routinely using the pulmonary artery catheter [PAC] [1-6]. In fact, evidence indicates that routine pulmonary artery catheterization is harmful [7, 8]. However, there also exists literature revealing that both physicians and nurses with the most exposure to the PAC also have poor understanding of its data acquisition and interpretation [9, 10]. Accordingly, the question raised is whether the observed injury associated with the PAC is intrinsic to the catheter itself or stems from the health professionals using it.

Consequently, there are no absolute indications for placing a PAC. The PAC is not therapy; it is a monitoring utensil. The PAC is a tool for the intensivist and its utility is deeply couched in the clinician's ability to recognize spurious data and apprehend the physiological underpinnings of its measurements. The PAC is arguably most useful in patients with complicated hemodynamic derangements and especially in those with shock and significant co-morbid pulmonary arterial hypertension. Unfortunately, it is the latter group in which placing a PAC can be challenging because of encountered anatomical and physiological abnormalities. Perhaps the most important pre-requisites for PAC floatation are that the clinician placing the PAC is comfortable with data interpretation and that this information cannot be achieved by other, less-invasive means [11].

Anatomy of the Pulmonary Artery Catheter

The standard pulmonary artery catheter is 110 cm in length and has two ports [12-15]. The distal port is located at the tip of the catheter; both the pulmonary artery pressure is transduced and mixed venous oxygen saturation assayed from this port. The tip of a properly placed pulmonary artery catheter lies in a proximal pulmonary arteriole at or below the level of the left atrium [16]. The second port lies 30 cm from the tip and is appropriately called the proximal port. In the majority of patients, the 30 cm port lies within the right atrium. Consequently, it is through this port that the central venous pressure is measured. Furthermore, central venous oxygen saturation may be measured and medicated drips administered via this port.

There are two other connections on the opposite end of the standard PAC. One is a thermistor which is usually a white-and-red channel from which the temperature-time curve is measured – 4 cm from the tip of the PAC – and digitally displayed on a bedside monitor. From the temperature-time curve, the pulmonary artery blood flow, or cardiac output is calculated. The remaining attachment is a conduit through which a small quantity of air is administered to inflate the distal balloon. The balloon lies at the very tip of the PAC and, when inflated, provides a recess into which the tip of the PAC invaginates. This protects the walls of the vasculature from catheter tip abrasion. Further, the balloon helps carry the catheter into the pulmonary arterial tree via blood flow; this is why it is said that one 'floats' a pulmonary artery catheter [17] [figure 1].

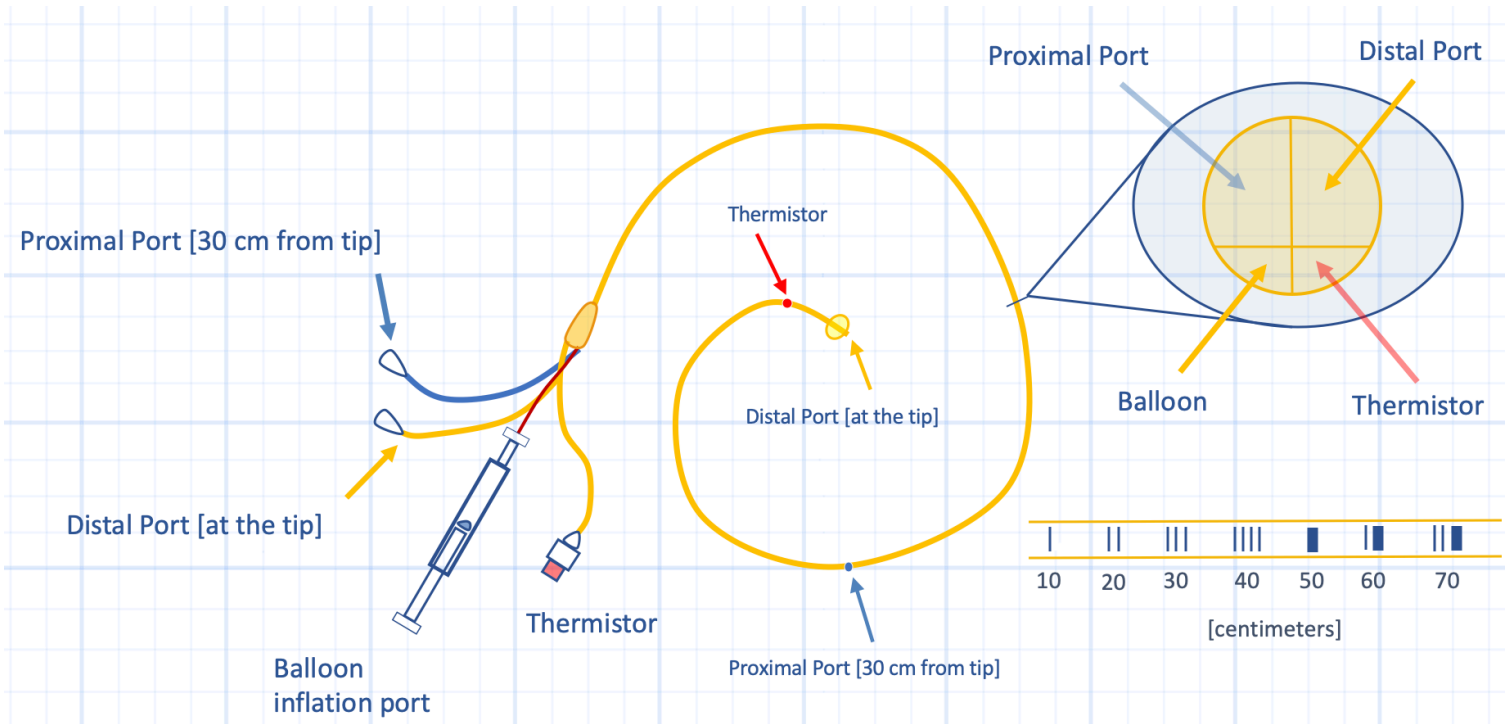

Figure 1: Anatomy of the pulmonary artery catheter; right inset shows cross-section of catheter and centimetre markings. See text for details.

In cross-section, the standard PAC is 2.3 mm in diameter and has four channels, each of which correspond to the aforementioned conduits [the proximal and distal ports, the thermistor and the balloon]. With more sophisticated catheters, the

diameter is larger for additional accessories. For example, some catheters are designed to place a transvenous pacer wire into the right ventricle via an opening 14 cm from the PAC tip [18]. Other PACs provide continuous thermodilution cardiac output via an internal thermal filament that continuously heats the blood; some PACs can calculate right ventricular ejection fraction via high resolution rapid-response thermistors [19, 20]. One of the more commonly-used accessories is the ability to continuously monitor mixed venous oxygen saturation via a distal fiberoptic oximeter [21].

Insertion and Placement of the Pulmonary Artery Catheter

Placing a foreign catheter into a vascular space requires that the physician practice strict, sterile technique and universal precautions. Prior to insertion, the PAC should be inspected for integrity and balloon functionality. All ports of the catheter should be flushed with sterile saline to assess for patency. If a continuous mixed venous fiberoptic oximeter is used, the light source near the catheter tip is calibrated prior to insertion.

In the intensive care unit, the PAC is inserted through an introducer catheter placed in the internal jugular [IJ] vein or subclavian [SC] vein [22-24]. Because of the inherent curl in the catheter, the right internal jugular vein and left subclavian vein are preferred sites for insertion. Each 10 centimetres on the pulmonary artery catheter is marked in succession with thin dark lines. The 50-centimetre mark is a single thick imprint. From the IJ or SC, the superior vena cava is reached at roughly 10-15 cm of depth. Usually at this point, the distal balloon is inflated with 1.5 mL of air from a special syringe that prevents the plunger from expelling more than this small amount of volume. Barring any central caval anatomical abnormality, the pressure waveform in the SVC is identical to the central venous pressure. Careful examination of the waveform and comparison with the ECG can be difficult while placing the catheter; however, at this point of insertion, tall v-waves suggest tricuspid regurgitation [15]. If the transducer is level with the patient's right atrium and appropriately zeroed to atmosphere, a rough right atrial pressure is estimated.

A catheter depth of 30 to 40 cm [slightly less if from a SC insertion site] should place the tip within the right ventricle [25]. With severe pulmonary hypertension or tricuspid regurgitation, the catheter has a tendency to curl within the right atrium, or pass down into the inferior vena cava. In this situation, it has been reported that filling the balloon with 1.5 mL of sterile saline and placing the patient in left-lateral decubitus facilitates dropping the catheter tip down through the tricuspid valve and into the right ventricle [26]. Anecdotally, the author has had some success placing the patient in right lateral decubitus and allowing the air-filled balloon to float up through the tricuspid valve.

The pressure waveform within the right ventricle is usually abruptly different than the CVP tracing but may approach the CVP waveform with significant right ventricular depression [27]. The right ventricular systolic pressure is normally less than 30 mmHg and the right ventricular diastolic pressure is close to zero. Severe deviations from these values suggest underlying right ventricular systolic and/or diastolic dysfunction. The CVP and right ventricular end-diastolic pressure should

be nearly equal. If the right ventricle is enlarged, there is a tendency for the catheter to coil on itself. One should refrain from deeply and repeatedly inserting and withdrawing the catheter as this increases the risk of the catheter knot formation [28].

At 50-55 cm, the catheter should advance through the pulmonic valve and into the main pulmonary artery. This waveform is marked by a diastolic step-up, generated by the pulmonary vascular resistance [25]. The pulmonary arterial diastolic pressure is typically 4-12 mmHg; as well, a distinct dicrotic notch is typically seen in the terminal portion of the systolic waveform – formed by the closure of the pulmonic valve. The value of the dicrotic notch closely tracks the mean pulmonary arterial pressure [29]. The pulmonary arterial systolic pressure should be identical to the right ventricular systolic pressure.

Ten centimetres beyond the acquisition of the pulmonary artery pressure waveform is typically when the pulmonary artery occlusion pressure is obtained. When the balloon obstructs a segmental or lobar artery, blood flow ceases distal to the balloon and a static column of blood between the catheter tip and the J-1 point is created [16, 25, 30]. The J-1 point, or first junction of the pulmonary veins, lies about 1.5 cm from the left atrium where the pulmonary veins converge. The waveform that is obtained with pulmonary artery occlusion is a damped left atrial pressure waveform – similar to the right atrial pressure or CVP tracing. There is a time-delay however, when comparing the pulmonary artery occlusion pressure to the ECG. Further, faithful representation of the left atrial pressure requires that the catheter tip lie in West zone III, which is physiologically defined, but often occurs when the catheter tip is located below the left atrium, radiographically [16]. These important concepts pertaining to the pulmonary artery occlusion pressure are discussed in more detail below [figure 2].

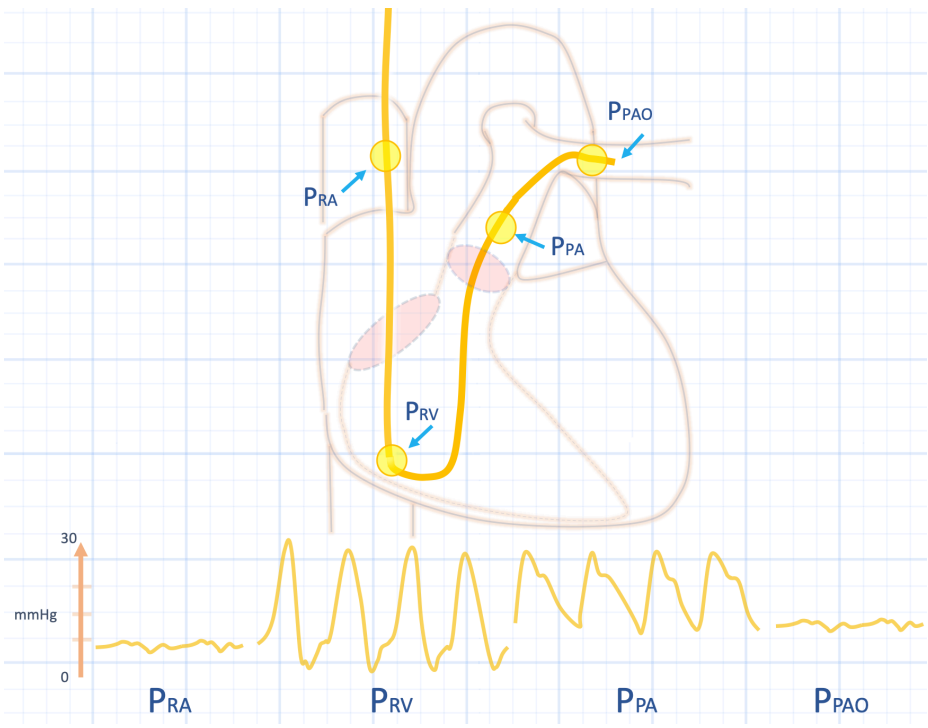

Figure 2: Waveform evolution of pulmonary artery catheter floatation. Pra is right atrial pressure; Prv is right ventricular pressure; Ppa is pulmonary arterial pressure; Ppao is pulmonary artery occlusion pressure. See text for details.

The Central Venous Pressure

The central venous pressure was described specifically in chapter 6; however, it deserves some discussion here as it is a commonly assessed parameter while a PAC is in situ. In chapter 6, central venous pressure was considered an analysis of central venous blood volume with the relationship between volume and pressure being central venous compliance. The question then became, what determines central venous or right atrial volume? The Guyton analysis helps answer this question because it considers the determinants of central venous inflow [i.e. venous return], outflow [i.e. cardiac function] and their intersection.

Superimposed upon venous return and cardiac function is changing intra-thoracic pressure. In a manner similar to measuring the pulmonary artery occlusion pressure [Ppao, as elaborated below] the right atrial distending pressure is best assessed at the end of a passive expiration. The reason is that at the end of a passive expiration, the effect of intra-thoracic pressure on central venous pressure is minimized and, therefore, the intra-vascular pressure is closest to the true transmural vascular pressure [16, 25, 31]. Recall that the transmural pressure is the intra-vascular pressure minus the ambient [intra-thoracic pressure] and that the transmural pressure predicts vascular volume.

During spontaneous inspiration with a PAC in place, the intra-thoracic pressure falls relative to atmospheric pressure; therefore, the right atrial pressure is also diminished. But the right atrial pressure is simultaneously modified by venous return [thoracic inflow] and cardiac function [thoracic outflow]. Venous return tends to enhance right atrial pressure while cardiac output tends to diminish right atrial pressure as depicted by the Guyton analysis. In other words, venous return fills the central venous volume while cardiac function empties central venous volume. But the act of inspiration itself modifies both venous return and cardiac output. While spontaneous inspiration lowers right atrial pressure and augments thoracic inflow [32-34], the concurrent increase in lung volume and, therefore, right ventricular afterload transiently attenuates cardiac output [35-37]. Therefore, spontaneous inspiration coincidently: 1. decreases intra-thoracic pressure which lowers right atrial pressure; 2. increases venous return which enhances right atrial volume and pressure and 3. decreases cardiac output which transiently retains central venous blood volume. Accordingly, though right atrial pressure falls relative to atmosphere – as measured by the PAC – right atrial transmural pressure typically increases [from a transient increase in thoracic venous inflow and decrease in right ventricular outflow]. A similar, but inverse argument is made regarding forced-expiration. Consequently, the most meaningful right atrial pressure from a PAC is made when intra-thoracic pressure is closest to atmospheric pressure – at the end of passive expiration [16, 25] [see chapter 6].

The Pulmonary Artery Pressure

The pulmonary artery systolic and diastolic pressures are measured from the distal port of the PAC when the balloon is fully deflated; these are continuous and useful measurements. The pulmonary arterial pressure is related to the stroke volume of the right ventricle and the impedance of the pulmonary arterial tree. Recall that the impedance of a vascular bed combines both classical 'resistance' which is related to vascular cross-sectional diameter, but also 'reactance' which considers the distensible element [or 'Windkessel' phenomenon] of the blood vessels. This is known as the '2-element model' discussed in more details in chapter 2. Thus, the pulse pressure from a given right ventricular stroke volume is a function of both compliance and vascular runoff through the pulmonary arterial tree [38].

As above, a normal pulmonary artery systolic pressure matches the right ventricular systolic pressure and is less than 30 mmHg. The pulmonary artery diastolic pressure is usually between 4 and 12 mmHg and should closely track the left atrial pressure [15]. In fact, in normal, healthy patients the pulmonary vascular resistance is negligible and zero flow or even slight flow reversal from the pulmonary veins may occur at the very end of diastole [39]. If the pulmonary artery diastolic pressure is 5 mmHg or more than an accurately-measured pulmonary arterial occlusion pressure, then there is likely an abnormality in pulmonary vascular resistance [40, 41]. This is considered in more detail in chapter 10.

Like other vascular pressures measured by a catheter and referenced to atmosphere, the pulmonary artery pressure is affected by intra-thoracic pressure [42, 43]. This introduces measurement artifact when both the right ventricle and pulmonary arterial tree are exposed to the same changes in thoracic pressure. As discussed in chapter 3, this is observed during a Valsalva maneuver or an increase in intra-thoracic pressure without changing lung volume. Because the right ventricle and pulmonary arterial tree are exposed to the same increment in ambient pressure, there is no effective change in right ventricular afterload [44-46]. In fact, and perhaps counterintuitively, to the extent that increased thoracic pressure augments left ventricular ejection, systolic ventricular interdependence may slightly increase RV ejection during the initial phase of Valsalva. In agreement with this physiology are data from stressed respiratory maneuvers. First, Valsalva decreases right ventricular end-systolic volume which suggests reduced impedance to RV ejection [47]; conversely, during the opposite of a Valsalva – the Mueller maneuver – there is increased right ventricular end-systolic volume suggesting increased impedance to RV ejection [48, 49]. Importantly, the aforementioned responses to respiratory maneuvers do not prove changes in pulmonary arterial input impedance as the end-systolic volumes may simply be tracking changes in the end-diastolic volumes or contractility. What is more convincing, however, is the change in pulmonary artery transmural pressure in response to Valsalva. Augmented right ventricular afterload is marked by increased pulmonary arterial transmural pressure [i.e. the pressure within the pulmonary artery relative to the intra-thoracic pressure] as exemplified by patients with dynamic hyperinflation [50], those with electrocardiographic evidence of right heart strain [51] and pulmonary emboli [46]. By contrast, transmural pulmonary arterial pressure falls in response to reduced afterload, as

observed with pulmonary vasodilation [52]. Many studies have documented reduced transmural pulmonary artery pressure as a consequence of Valsalva [53-55], which argues strongly against elevated RV afterload. Notably, Charlier's group erroneously concluded that Valsalva increased pulmonary arterial 'impedance' because calculated pulmonary vascular resistance increased with Valsalva; this illustrates a glaring physiological inaccuracy of the pulmonary vascular resistance [56, 57]. In the case of elevated intra-thoracic pressure without a change in lung volume, systemic venous return is reduced. Consequently, there is less cardiac output ejected into the pulmonary arterial tree. Crucially, diminished cardiac output is not in response to elevated RV afterload nor any true change in the characteristics of the pulmonary vascular bed, but instead a consequence of reduced RV preload. Nevertheless, calculated PVR rises because its denominator [i.e. cardiac output] is reduced [figure 3]. It is not physiologically consistent for an increase in pulmonary arterial impedance to be accompanied by diminished transmural pulmonary arterial pressure!

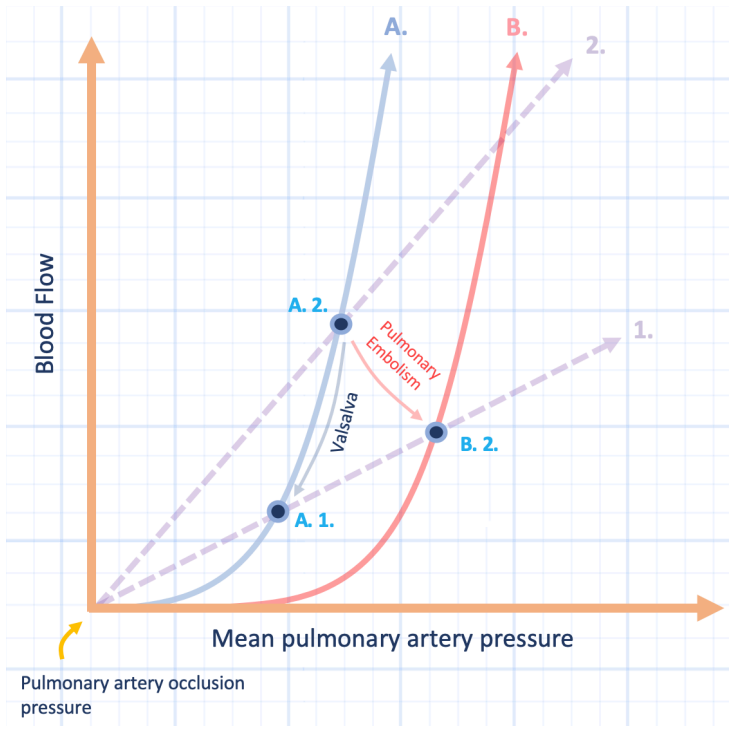

Figure 3: Valsalva & pulmonary embolism on pulmonary pressure-flow curves. The x-axis is the transmural, mean pulmonary artery pressure relative to pulmonary artery occlusion pressure at the origin [Ppao]. The y-axis is blood flow. Starting at point A.2. Valsalva may increase absolute pressure relative to atmosphere, but the mean pressure relative to the pleural pressure shrinks to point A.1. Assuming a linear relationship between pressure and flow, the calculated pulmonary vascular resistance rises [dashed line 2 to 1]; however, the true nature of the pulmonary vasculature has not changed [curved line A]. A pulmonary embolism, by contrast, increases the critical closing pressure of the vascular tree and shifts the pressure-flow curve rightwards [curve A to B; i.e. a true change]. Spuriously, the Valsalva and PE equally increase calculated pulmonary vascular resistance [curve 1].

Thus, the main hemodynamic effect of Valsalva on the RV is an abrupt reduction of ventricular preload; this occurs because the pressure in the thorax rises relative to systemic venous return [53, 58]. In patients with fixed, high RV impedance [e.g. pulmonary arterial hypertension], Valsalva may be dangerous because these patients rely on right ventricular end-diastolic volume to maintain RV stroke volume. Though, when patients with high RV impedance increase intra-thoracic pressure, they may not truly Valsalva, but also lower their lung volume. To the extent that a Valsalva-like maneuver reduces lung volume below FRC, the

pulmonary vascular resistance rises as extra-alveolar vessels shrink and become tortuous [35, 36].

By contrast, in the event of high pulmonary arterial impedance [e.g. acute venous thromboembolism] pulmonary arterial pressure less than that of Valsalva can lead to precipitous RV collapse. Therefore, it is not the absolute pulmonary arterial pressure, per se, that marks the afterload of the right ventricle but rather the systolic right ventricular transmural wall tension [59-61]; this is difficult to measure in clinical practice [38]. While commonly reduced to the law of LaPlace – which describes the tension across the wall of a perfect sphere – the RV wall tension is more complicated.

The pulmonary vascular resistance is a commonly calculated variable that is taken to be a marker of right ventricular afterload [38]. As discussed in chapter 2, the pulmonary vascular resistance is calculated by dividing the driving pressure across the pulmonary vascular tree by the pulmonary blood flow:

$$(1)\quad PVR = \frac{mPAP - Ppao}{cardiac\ output}$$

Equation 1: PVR is pulmonary vascular resistance; mPAP is mean pulmonary arterial pressure; Ppao is the pulmonary artery occlusion pressure.

As illustrated in figure 3, this equation assumes linear relationship between driving pressure and flow in the pulmonary vascular tree. Because of vascular distensibility and parallel recruitment, the pulmonary vascular tree has an exponential relationship between pressure and flow. In an individual vessel at low vascular volume, increasing driving pressure enlarges vascular radius because vessels are elastic; thus, change in flow rises with pressure non-linearly. As well, considering all vessels together, augmenting proximal pulmonary arterial pressure causes parallel recruitment, amplifying flow exponentially. Thus, calculated PVR is altered without change in vasomotor tone [e.g. active constriction or dilation] [56, 57, 62]. As an example, diminished cardiac output following severe hemorrhage [or Valsalva!] may increase calculated pulmonary vascular resistance. Conversely, administering vasoactive medicines that only increase blood flow will mathematically diminish PVR without any change in pulmonary vascular tone. For these reasons, any intervention that changes cardiac output or pulmonary vascular driving pressure, or both must be considered carefully and not simply distilled into the potentially misleading PVR. A true change in pulmonary vascular resistance may be inferred when driving pressure and blood flow change in opposite directions, [or at least when one of driving pressure or blood flow remains constant]. An example is the American Heart Association's definition of a pulmonary vasodilator response: there must be a clinically significant decrement in driving pressure without diminution of blood flow [63, 64]. See also chapter 2 and 10 for more detailed discussions of the calculated pulmonary vascular resistance.

The Pulmonary Artery Occlusion Pressure

The pulmonary artery occlusion pressure, or pulmonary capillary wedge pressure is the pressure measured at the tip of the pulmonary artery catheter when the distal balloon is inflated. With balloon inflation, blood flow ceases distal to the catheter tip; this creates a static column of blood as a conduit through which the left atrial pressure is transduced. Like the central venous pressure measured in the right atrium, the pulmonary artery occlusion pressure assumes an atrial pressure waveform, as discussed in chapter 6. In contrast to right atrial pressure, the pulmonary artery occlusion pressure [Ppao] is slightly phase-shifted with respect to the ECG tracing [15, 16, 25]. Most notably, the Ppao a-wave typically follows the QRS; nevertheless, the a-wave of the Ppao, like the CVP, is still the first positive deflection following the ECG p-wave. Importantly, the Ppao v-wave is located following the ECG t-wave; that is, the rise in systolic left atrial pressure is detected by the Ppao following electrical repolarization. This fact is important because tall v-waves [e.g. mitral regurgitation] may look like the pulmonary arterial systolic waveform, but the latter is entirely within the ECG t-wave. Further, incomplete wedging, as detailed below, may present with positive pressure deflections easily confused with v-waves; however, the partially-transmitted systolic waveform of incomplete wedging also occurs within the ECG t-wave [15, 65] [figure 4].

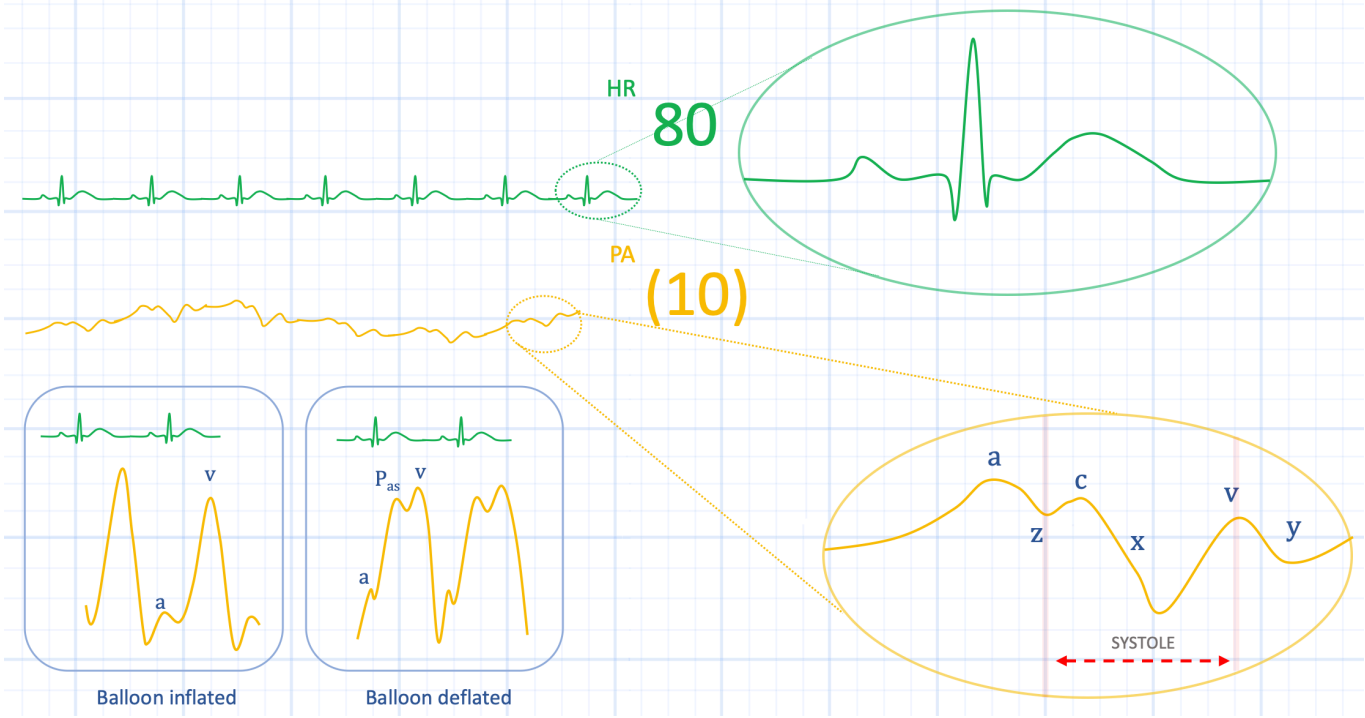

Figure 4: The relationship between the pulmonary artery occlusion pressure [Ppao] and the ECG. As compared to the central venous pressure [see chapter 6] the Ppao is slightly time-delayed relative to the ECG. The inset shows tall v-waves in the Ppao [balloon inflated]; the peak of the v wave is beyond the ECG t-wave. When the balloon is deflated the pulmonary artery systolic pressure is seen again [Pas] with its peak within the ECG t-wave; the v-wave remains. See text for details.

Accurately measuring the Ppao is one of the most difficult-to-achieve parameters gleaned from the PAC. There are two key obstacles to overcome when trying to obtain faithful evaluation of the Ppao: 1. the effect of intra-thoracic pressure and 2. an uninterrupted column of blood between the catheter tip and the left atrium [i.e. West zone III physiology].

As discussed in chapter 6 regarding the central venous pressure, dynamic intra-thoracic pressure changes lead to measurement artifact and interpretation error [30, 31, 66]. Both high intra-thoracic pressure [e.g. forced expiration, intrinsic and extrinsic positive end-expiratory pressure] as well as low inspiratory, intra-thoracic pressure degrade the accuracy of the Ppao.

At end-expiration, or when the lungs are at functional residual capacity, the intra-thoracic pressure is only minimally sub-atmospheric and therefore the measured intra-vascular pressure [i.e. the Ppao] nearly reflects the true vascular distending pressure; the trans-mural pressure. When inspecting respiratory variation of the Ppao tracing, end-expiratory pressure in a patient breathing spontaneously occurs at the peak of the Ppao tracing, barring active expiration. Conversely, in a heavily sedated and potentially paralyzed patient on mechanical ventilation, the end-expiratory pressure is the lowest point of the Ppao tracing. The situation is complicated when the patient is generating spontaneous efforts while receiving supplemental positive pressure or when the patient is bearing down against positive pressure. When the patient is not passive with the ventilator [or when the patient is on non-invasive positive pressure ventilation], defining end-expiration can be difficult and oftentimes requires bedside evaluation of the patient's respiratory status and pressure-tracings, simultaneously. With excessive inspiratory effort, measured Ppao significantly underestimates the true left atrial distending pressure; in contradistinction, high expiratory effort overestimates the Ppao [16, 25, 31]. If the patient can follow commands, sometimes having the patient sip water through a straw can arrest respiratory drive long enough to measure end-expiratory Ppao, but this is often untenable.

Even when the patient is passive with the ventilator, the effect of intrinsic or extrinsic positive end-expiratory pressure [PEEP] may cause overestimation of the Ppao [30, 31, 67, 68]. One way to circumvent this problem is to utilize the 'index of transmission' – an estimation of how much of the airway pressure is 'transmitted' to the vascular compartment [69]. The index of transmission is computed by comparing the change in airway pressure from end-expiration to the plateau pressure to the simultaneously measured change in Ppao; this correction factor may be multiplied the amount of total PEEP as an estimate of how much of the measured Ppao is a result of airway pressure [figure 5].

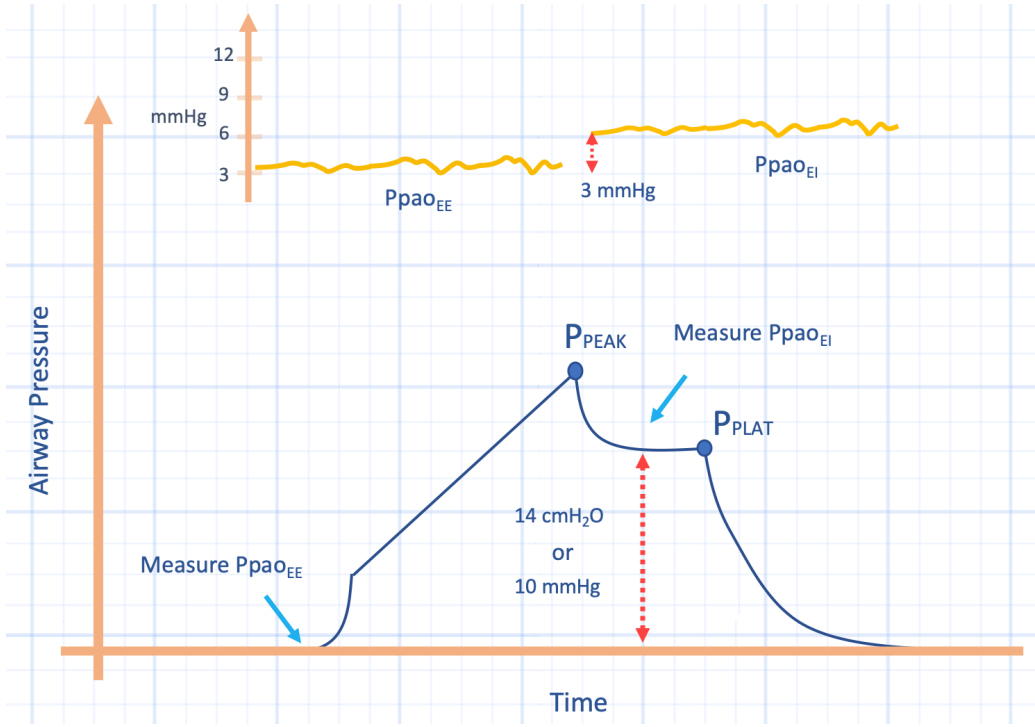

Figure 5: The index of transmission. Ppao is pulmonary artery occlusion pressure; EE is end-expiratory; EI is end-inspiratory. There is a 3 mmHg Ppao change & 10 mmHg change in airway pressure; thus, the index of transmission is 30%. Ppeak is peak airway pressure; Pplat is airway plateau pressure.

Clearly, the index of transmission is valid only in passive, mechanically ventilated patients. What is less clear is that the index of transmission may not be applied to the central venous or right atrial pressure. The reason is that increased pleural pressure affects both pulmonary venous return and left heart function to the same degree and thus the change in Ppao is almost entirely the result of changing intra-thoracic pressure. By contrast, increased intra-thoracic pressure changes right heart function relative to systemic venous return, so the changes in right atrial pressure become confounded. In other words, not only is right atrial pressure changing as a function of intra-thoracic pressure, but also as a function altered systemic venous return [figure 6].

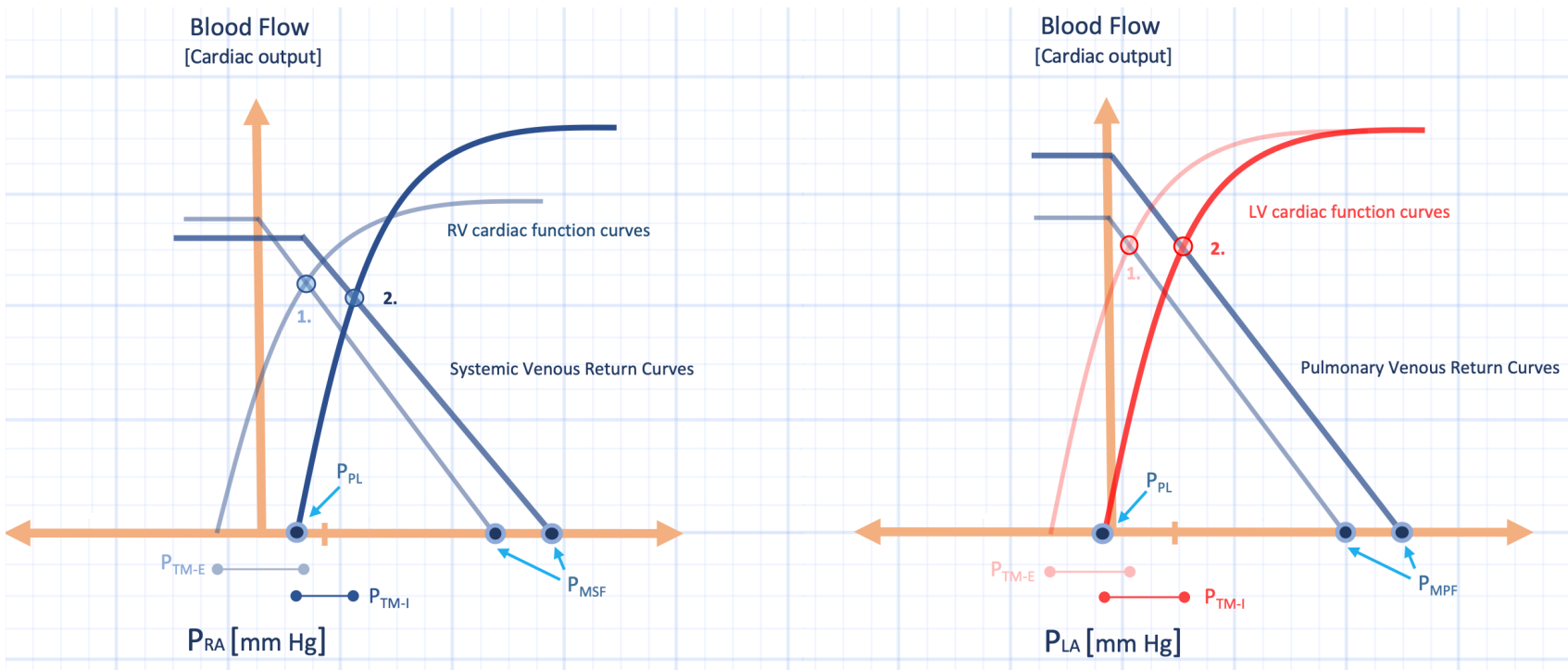

Figure 6: Illustration of the effect of pleural pressure on right atrial pressure [Pra] and left atrial pressure [Pla]. The left panel shows how positive pressure [e.g. positive end-expiratory pressure] affects Pra. The

Pra rises from operating point 1 to operating point 2. Because of simultaneous changes in cardiac function and systemic venous return, the inspiratory trans-mural pressure [Ptm-I] shrinks from expiration to inspiration [below x-axis]. Right panel shows that, in theory, positive pressure affects cardiac function and pulmonary venous return equally, so the change in operating point from 1 to 2 causes no change in the trans-mural distending pressure [below the x-axis].

Yet, the aforementioned supposition assumes that increased airway pressure and, consequently, increased pleural pressure does not change left ventricular function [i.e. the slope of the cardiac function curve] or pulmonary venous return to any significant degree. However, it is possible that augmented pleural pressure shifts the left ventricular cardiac function curve relative to pulmonary venous return [e.g. via diastolic ventricular interdependence or afterload reduction] and that the Ppao, accordingly, changes not solely as a function of increased pleural pressure. This effect is most drastic when chest wall compliance is low, tidal volume is high or a combination thereof; the reason being that juxta-cardiac pressure is heightened in these settings.

In addition to altered intra-thoracic pressure, the Ppao is affected by its position within the pulmonary vascular tree. As there must be an uninterrupted, static column of blood between the pulmonary artery catheter tip and the left atrium, the catheter should lie within the portion of the pulmonary vascular bed where pulmonary arterial, capillary and venous pressure are all greater than alveolar pressure [16]. When alveolar pressure supersedes any portion of the pulmonary vascular tree, then the pulmonary artery catheter effectively measures alveolar pressure and not the left atrial pressure. Therefore, the PAC must lie within West zone III – where blood flow is the greatest. The elegance of the PAC is that the balloon naturally pulls the catheter into the lung zone with the greatest flow, which is typically gravity dependent and zone III physiology. However, upwards of 25-30% of all placed PACs wedge in zone II or zone I [16]. Importantly, these zones are dynamic; a patient may initially have correct placement, but with volume-loss, zone III may become zone II. This change in lung zone may be heralded by damping of the Ppao waveforms which may reverse with fluid challenge. Further, in a patient who is mechanically ventilated and passive with the ventilator, greater respiratory Ppao variation than the pulmonary artery diastolic pressure suggests that the catheter is transducing alveolar pressure [42]. Radiographically, zone III physiology is usually below the left atrium, so the PAC should be located in the region on a portable chest X-ray in the ICU [16].

Considering both intra-thoracic pressure and pulmonary zone physiology ensures that the Ppao accurately reflects the left atrial pressure. However, even when measurement is done perfectly, that is, during a period of calm end-expiration while the catheter is located in zone III, and at the Ppao tracing between the a and c wave [i.e. end-diastole - see chapter 6], the left atrial pressure may uncouple from the left ventricular end-diastolic pressure [LVEDP], discussed next.

Accurate Interpretation of the Ppao

The relationship between the left ventricular end-diastolic volume [LVEDV] and LVEDP was also considered in chapter 2. The relationship is notable for low

elastance [high compliance] at low volumes such that there is little pressure change for large changes in volume. However, as LVEDV increases, the elastance progressively increases with an exponential relationship between LVEDV and LVEDP [70]. This curve is also known as the LV end-diastolic pressure-volume relationship [71]. Importantly, there is no universal curve amongst all patients. Further, the slope and position of the curve changes acutely [e.g. diastolic ventricular interdependence, LV ischemia, adrenergic medications] and chronically [e.g. chronic hypertension, valvulopathies, etc.]. Therefore, it is flawed to ascribe one particular Ppao to any given LV filling state [72]. Commonly, 20-24 mmHg is considered to be the upper limit of normal for the Ppao, but this value varies considerably between patients and within a patient during a particular disease course [72-74]. Arguably, a careful trend of a particular patient's Ppao with respect to his or her cardiac output is most meaningful. As discussed below, the cardiac output is readily obtained from the PAC. Assessment of cardiac performance, that is, the left-ventricle's ability to increase forward flow in response to increased filling pressure is a recapitulation of the Frank-Starling curve. One may, therefore, generate an individual's cardiac function curve with the PAC, bearing in mind that the slope of the curve can and will change during any patient's stay in the ICU.

Pulmonary Capillary Pressure

The Ppao is frequently used to estimate the pulmonary capillary pressure. The upper limit of normal for the hydrostatic pressure of a generic capillary is roughly 20 mmHg [between 32 mmHg on the arterial end and 15 mmHg on the venous end] [75]. The reason that tiny capillaries are able to maintain relatively high hydrostatic pressure compared to, for example, the IVC is that the radius of the capillary is very small. Wall tension is directly proportional to the distending pressure multiplied by the radius. Thus, the tension experienced by capillary endothelial cells is quite small as a result of its small internal diameter. When the capillary hydrostatic pressure increases above 20 mmHg, the Starling fluid flux equation predicts net movement of water out of the capillary and into the interstitium [76].

$$(2)\quad Net\ filtration = k\ x\ [(Pmv\ -\ Ppmv)\ -\ \sigma(umv\ -\ upmv)]$$

Equation 2: Starling fluid filtration equation. K is the filtration coefficient of the membrane which is the product of membrane wall conductivity and surface area; Pmv is microvascular pressure; Ppmv is the perivascular microvascular pressure; σ is the reflection coefficient of the membrane to proteins and has a value between zero and 1; μmv is the microvascular osmotic pressure and μpmv is the perivascular osmotic microvascular pressure. Note, the revised Starling principle is discussed in chapter 10.

By the aforementioned reasoning, it is often held that a Ppao greater than 20 mmHg in the setting of pulmonary edema predicts a hydrostatic etiology, while edema in the context of low Ppao predicts non-hydrostatic edema. This reasoning is incorrect on multiple fronts. First, there is significant lag in radiographic resolution of edema. Thus, a brief period of a high Ppao may result in clinical and radiographic pulmonary edema that persists long after the Ppao has

normalized. For instance, less than 5 minutes of LV ischemia may increase the Ppao to 40 mmHg followed by normalization of the Ppao when ischemia resolves [77]. This physiology is magnified by hypoalbuminemia which is common in critically-ill patients [78]. If these caveats are not recognized, the intensivist may be tempted to label the patient as having non-hydrostatic pulmonary edema.

There is yet another mechanism by which hydrostatic pulmonary edema results in the face of a low Ppao – high pulmonary venous resistance. While this is often thought to complicate the uncommon clinical entity of pulmonary venous occlusive disease [PVOD], pulmonary venous hypertension can commonly complicate ARDS, hypoxemia and other frequent processes in the ICU [79-83]. Normally pulmonary venous resistance makes up about 1/3 of pulmonary vascular bed's total resistance [84, 85]. When pulmonary venous resistance is abnormally high, the Ppao may be quite disparate from the pulmonary capillary pressure. Normally, when the balloon of the pulmonary artery catheter inflate, pressure immediately drops; this pressure fall corresponds to the pulmonary arterial resistance. Then there is a brief inflection point when the blood beyond the inflated pulmonary artery catheter equilibrates with the pulmonary capillary capacitance bed; this pressure reading marks the true pulmonary capillary pressure. Subsequently, as the blood passes through the pulmonary venous resistance beds, pressure gradually falls to the Ppao [85-88]. Clearly if pulmonary venous resistance is increased from roughly 30% to 50-60% of the total pulmonary vascular resistance, the fall in pressure between the pulmonary capillary and Ppao is large. High pulmonary venous resistance may then be misinterpreted as pulmonary edema of non-hydrostatic etiology.

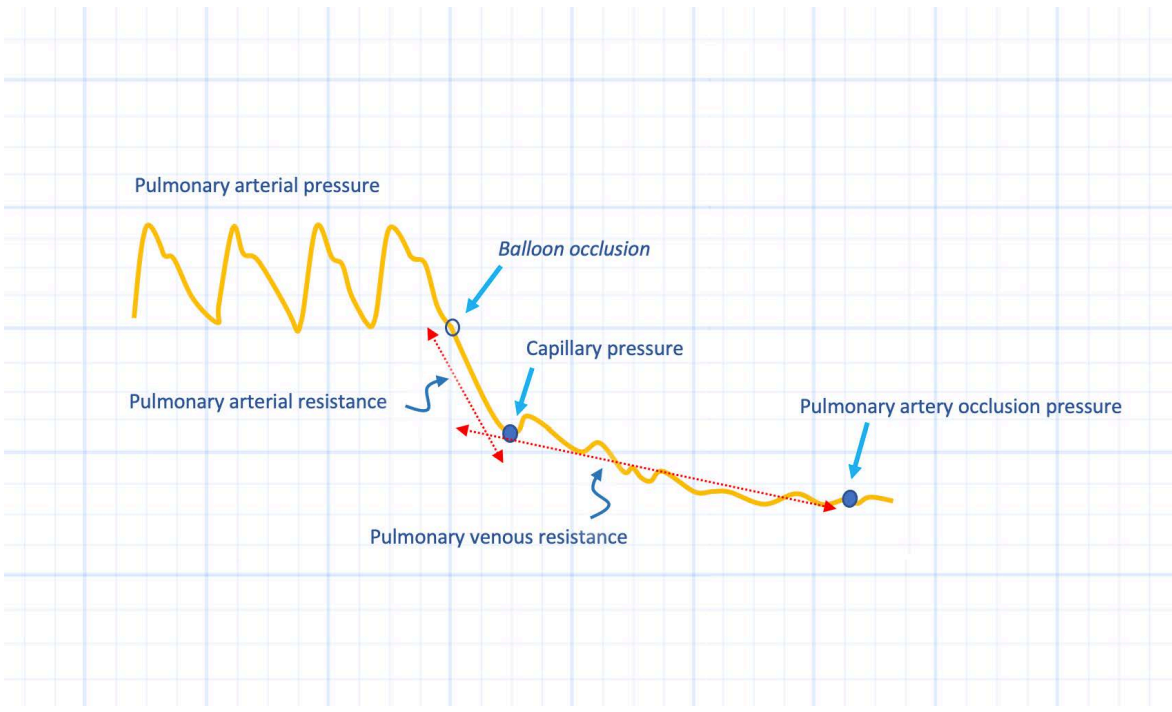

Figure 7: The pulmonary capillary pressure. At the moment of balloon occlusion, pressure falls to the capillary pressure and this descent depicts pulmonary arterial resistance [red dotted line]. From pulmonary capillary pressure to the pulmonary artery occlusion pressure [Ppao] the fall in pressure represents pulmonary venous resistance; normally this is 1/3 of the resistance. In diseases like ARDS, the fall in pressure from capillary pressure to Ppao may be as steep as the arterial decay.

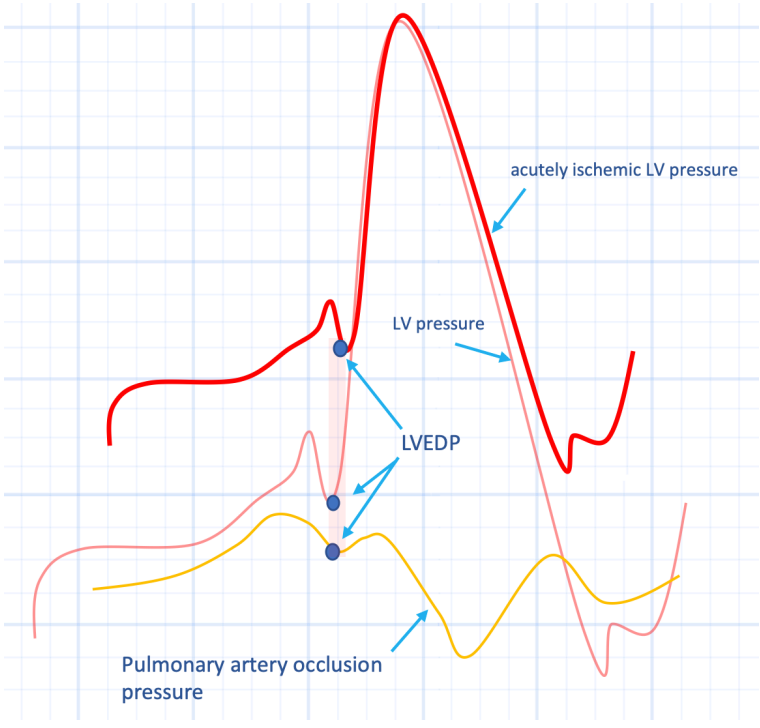

Figure 8: A potential false negative when using pulmonary artery occlusion pressure [Ppao] to detect elevated left ventricular end diastolic pressure [LVEDP]. With LV ischemia, the LV pressure waveform increases [light red to dark red waveform] out-of-proportion to the PAC tracing. The increased LV pressure causes the mitral valve to close prematurely, and the PAC essentially 'misses' the increased LV cavity pressure.

On the other hand, significantly elevated pulmonary capillary pressure may also alter pulmonary capillary tight junctions – leading to non-hydrostatic edema in conjunction with high Ppao [89]. Further, if such a patient has chronically-elevated Ppao [e.g. from chronic heart failure], there may be supra-normal pulmonary lymphatic clearance such that high Ppao may not be responsible for pulmonary congestion and alveolar edema [73, 74].

Cardiac Output

Arguably, the most valuable hemodynamic variable obtained from the pulmonary artery catheter is pulmonary blood flow, a surrogate for cardiac output. Recall that mean systemic arterial blood pressure is a product of cardiac output and systemic vascular resistance [SVR]. As SVR is a nebulous, summative value [see discussion above on pulmonary vascular resistance], directly measuring cardiac output is a critical tool for analyzing the etiology of hypotension the critically-ill. There are two methods for assessing cardiac output via a PAC - the method of thermodilution and the method of Fick.

Thermodilution employs the principle of indicator dilution [90, 91]. If the concentration of an indicator within a fluid is measured as it moves past a given point, the area under its concentration-time curve is inversely related to the flow of the fluid. With regards to the PAC, when room-temperature or cold-saline solution is injected into the proximal port of the PAC [which emerges in the patient's right atrium], the decrease in blood temperature is measured at the thermistor located 4 cm from the tip of the PAC [which should be resting well into the pulmonary artery]. Therefore, the area under the temperature time curve is inversely related to

pulmonary blood flow. From this value, the patient's stroke volume and systemic vascular resistance may be calculated.

$$(3)\quad SV = \frac{cardiac\ output}{heart\ rate}$$

$$(4)\quad SVR = \frac{mean\ systemic\ arterial\ pressure}{cardiac\ output}$$

Equations 3 & 4: SV is stroke volume; SVR is systemic vascular resistance. Cardiac output is assumed to equal pulmonary blood flow.

The method by which the thermodilution curve is achieved is important to consider. First, saline injection technique can significantly alter the temperature-time curve. 10 mL of room-temperature saline should be injected over a period of 2-4 seconds into the proximal port. There is typically little difference between 5 mL and 10 mL, as well as between room-temperature and iced-saline. However, larger volume and colder injection provides a faithful signal-to-noise ratio when generating the temperature-time curve [92-94]. Because small variations may produce variable effects on the temperature-time curve, three saline injections should be done and the average of the three calculated cardiac outputs used. Note that the first injection often over-estimates the cardiac output. The reason is that the first injection often loses temperature to cool the PAC itself; losing temperature from the system diminishes the area under the concentration-time curve which generates higher cardiac output [95]. Because the concentration-time curve is measured over a number of cardiac cycles, premature atrial or ventricular contractions during the injection may alter the temperature-time graphic as will atrial fibrillation and respiratory variation. The three injections should, ideally, all occur at end-expiration [96, 97] as this reduces cardiac output variability by as much as 1 litre/minute. A sudden, very abrupt increase in cardiac output [i.e. the appearance of a temperature-time curve with a very small area] should prompt the nurse or physician to consider inadvertent saline injection into the distal port rather than the proximal port of the PAC.

While loss of temperature to catheter cooling over-estimates cardiac output, so too will right-to-left, or left-to-right shunts. By contrast, tricuspid regurgitation [TR] slurs the temperature-time curve as the injected saline washes to and from the right atrium in a 'pendelblut' effect. The temperature-time curve in the context of tricuspid regurgitation is not a valid means to calculate cardiac output and tends to underestimate the true value [98]. With moderate-to-severe TR, thermodilution should be forgone and the Fick method or serial mixed venous oxygen saturations be utilized, as described below. Of note, backward flow of blood within the central veins occurs independently of tricuspid regurgitation in many patients subjected to mechanical ventilation; this phenomenon also degrades the accuracy of thermodilution-derived cardiac output [99].

The Fick method of cardiac output calculation is predicated upon the following principles: 1. if the rate of disappearance of a flowing substance is known and 2. the concentration of that substance both upstream and downstream from the site of

disappearance is known, then 3. the flow of that substance may be calculated. In the context of the circulation, this substance is oxygen [100]. As such, if the arterial concentration of oxygen is known [e.g. from an arterial blood gas analysis], the mixed venous oxygen concentration is known [e.g. measured from the distal port of the PAC] and the oxygen consumption of the peripheral tissues is known [i.e. measured by a metabolic cart], then the cardiac output is calculated as follows.

$$(5)\quad cardiac\ output = \frac{VO2}{arterial\ oxygen\ saturation - mixed\ venous\ oxygen\ saturation}$$

Equation 5: VO_2 is oxygen consumption; this assumes stable hemoglobin & dissolved oxygen.

However, as can be gleaned from the equation, cardiac output cannot be obtained unless the tissue oxygen consumption is known. Frequently [in lieu of direct measurement], a generic value of 125 mL/L/min is used, but the exact oxygen consumption will vary based on the patient's body habitus, sex, physiological stress, temperature, etc. so this method is a gross estimation at best [95]. What the Fick analysis does reveal is an inverse relationship between cardiac output and the arterial-venous oxygen difference. Consequently, widening difference between arterial oxygen saturation and mixed-venous blood saturation suggests – but does not prove – falling cardiac output.

Accordingly, there are caveats to using the arterial-venous oxygen difference without directly measuring VO_2 [which is essentially the method universally adopted in the ICU]. As the equation above illustrates, if the arterial-venous oxygen difference were to widen [the denominator] in the setting of an increased oxygen consumption [VO_2 - the numerator] there is no true change in the cardiac output. Clinically, elevated oxygen consumption [VO_2] is observed during agitation, fever, chills, rigors, seizures or the shifting of blood flow to more metabolically active tissue beds [101-103]. Note that, in theory, should vasoactive substances shift blood flow from dormant to metabolically-active tissues, the effect is physiologically analogous to elevating VO_2. Additionally, adrenergic agents are thermogenic and may inherently alter tissue oxygen consumption; the relationship between vasoactive medications and critical illness can be quite complicated in this regard [104, 105].

Conversely, if the denominator shrinks [i.e. a narrowed arterial-venous oxygen difference] with a contemporaneous decrement in oxygen utilization [i.e. the numerator], then cardiac output did not change. This physiological scenario can occur with the converse of the above: paralysis, fever-reduction, sedation and the shunting of blood to metabolically inactive muscle beds [106, 107]. Again, blood flow redistribution may be a consequence of vasoactive medications. Additionally, the VO_2 may shrink in the setting of cytopathic tissue hypoxia [108]. Such pathophysiology can occur in septic shock, where the tissues and mitochondria are injured and unable to extract oxygen from capillary blood. To further complicate matters, VO_2 can fall when oxygen delivery becomes very low - so-called flow-dependent oxygen consumption [109]. With cytopathic tissue hypoxia and flow-dependent oxygen consumption, the patient typically has significantly deranged hemodynamics [110].

In summary, the arterial-mixed venous oxygen difference is frequently utilized as a surrogate for cardiac output. While it is sometimes helpful, assuming static oxygen consumption [VO2] leads to inaccurate clinical conclusions. When faithful, accurate cardiac output is needed, every attempt should be made to directly measure VO2.

Complications and Troubleshooting

Complications of PAC placement are uncommon in experienced hands. One common, benign complication is transient arrhythmia. Both brady-arrhythmia and tachy-arrhythmia may develop but occur in less than 5% of PAC placements [111, 112]. Perhaps one of the most feared complications is right bundle branch block in a patient with pre-existing left bundle branch block - i.e. complete heart block. In such patients, the intensivist should have both positive chronotropes and transcutaneous pacemaker at hand while placing the PAC [113, 114]. Equally uncommon complications are catheter-associated thrombus, pulmonary infarction and pulmonary artery rupture [115, 116]. The latter two entities are very rare, but devastating. The key to preventing both infarction and pulmonary artery rupture is to ensure that the distal balloon is inflated only during PAC placement and when obtaining Ppao. The intensivist can never be too conscientious about the distal balloon and must ensure that it is deflated after the Ppao is obtained. For subsequent Ppao measurements, the full 1.5 mL should never be rapidly delivered into the balloon. The syringe should be compressed slowly until the Ppao tracing is obtained. If the amount of air required to obtain the Ppao decreases significantly from the initial Ppao, consider distal migration of the PAC and retraction [117].

Ppao determination may also present problems as a result of catheter tip malposition. One example is the 'over-wedge' which occurs when balloon inflation itself either occludes the distal port of the PAC or the distal port becomes wedged against the lumen of the blood vessel. Because the PAC's patency is maintained by a slow heparin infusion that is pressurized to 300 mmHg, occlusion of the distal lumen will gradually raise the pressure reading to the level of the pressurized heparin infusion! If the over-wedge is secondary to distal port compression into the vascular lumen, this poses risk for vascular rupture; the over-wedge should, therefore, be immediately corrected by balloon deflation and, potentially, catheter reposition [118].

By contrast, 'incomplete-wedge' results when balloon inflation does not entirely occlude pulmonary artery blood flow to the distal vascular bed. When this occurs, pulsatile blood flow is partially transmitted beyond the tip of the PAC and may be incorrectly interpreted as tall v-waves in the Ppao. It also raises the mean Ppao relative to the pulmonary artery diastolic pressure. Sudden narrowing of the pulmonary artery diastolic - pulmonary artery occlusion pressure difference should prompt consideration for incomplete or partial wedging. Further, if 'v-waves' are seen within the ECG t-wave, it strongly suggests partial wedging as true v-waves of the Ppao should occur entirely after the ECG t wave. When positive deflections are seen within the ECG t-wave, it is likely a result of partial transmission of the pulmonary artery systolic wave [119] [see figure 4 & 9].

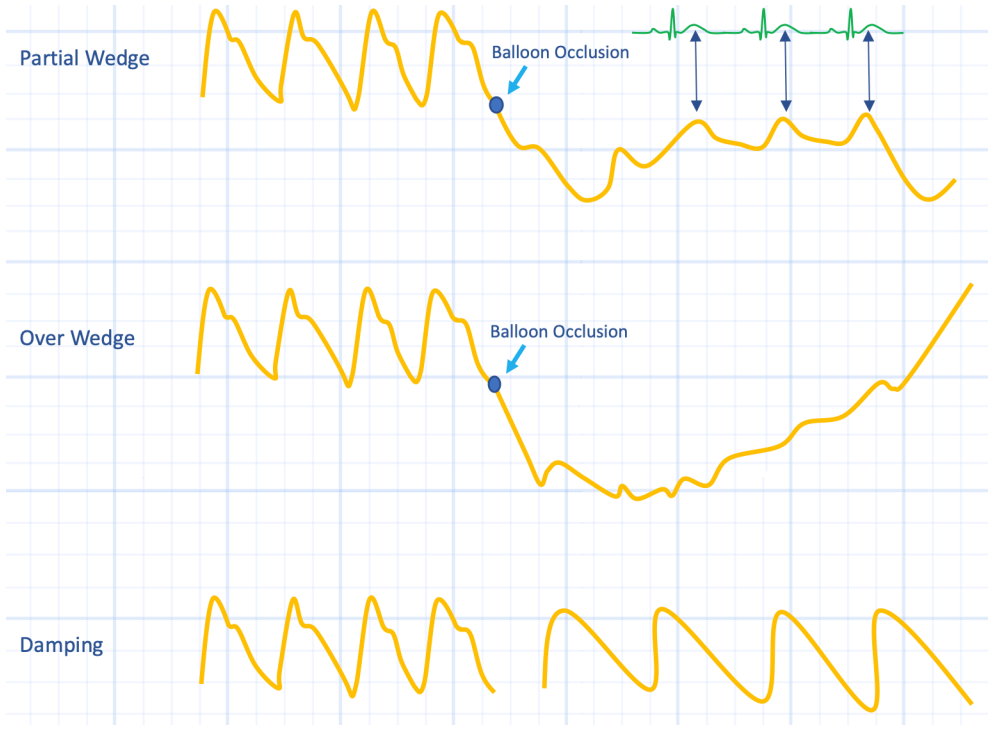

Figure 9: Examples of common pressure tracing problems. See text for details. The pulmonary artery systolic waveform is seen in the partial wedge tracing timed with the ECG t-wave. See figure 4. Damping is loss of fine detail of the pressure tracing with an overly-smooth pressure waveform. Damping commonly occurs with: thrombus at the distal lumen, kinked catheter, air in stopcocks, faulty transducer.

Conclusion

Routine use of the pulmonary artery catheter for critically-ill patients is discouraged and unwarranted. Nevertheless, in patients with multiple organ system dysfunction and complicated hemodynamic derangements, accessing the pulmonary artery via a flow-directed catheter can provide important data. Yet, this data is only useful if the clinician appreciates the multiple caveats inherent in measuring intra-thoracic, intra-vascular pressures, as well as, blood flow and oxygen kinetics in the critically-ill. The complexities of data acquisition and interpretation from the pulmonary artery catheter are better understood with a good grasp of heart-lung interactions in sickness and in health.

References

1. Rhodes, A., et al., A randomised, controlled trial of the pulmonary artery catheter in critically ill patients. Intensive Care Med, 2002. 28(3): p. 256-64.
2. Sandham, J.D., et al., A randomized, controlled trial of the use of pulmonary-artery catheters in high-risk surgical patients. N Engl J Med, 2003. 348(1): p. 5-14.
3. Richard, C., et al., Early use of the pulmonary artery catheter and outcomes in patients with shock and acute respiratory distress syndrome: a randomized controlled trial. JAMA, 2003. 290(20): p. 2713-20.
4. Wheeler, A.P., et al., Pulmonary-artery versus central venous catheter to guide treatment of acute lung injury. N Engl J Med, 2006. 354(21): p. 2213-24.
5. Marik, P.E., Obituary: pulmonary artery catheter 1970 to 2013. Ann Intensive Care, 2013. 3(1): p. 38.
6. Tuman, K.J., et al., Effect of pulmonary artery catheterization on outcome in patients undergoing coronary artery surgery. Anesthesiology, 1989. 70(2): p. 199-206.
7. Gore, J.M., et al., A community-wide assessment of the use of pulmonary artery catheters in patients with acute myocardial infarction. Chest, 1987. 92(4): p. 721-7.
8. Connors, A.F., Jr., et al., Complications of right heart catheterization. A prospective autopsy study. Chest, 1985. 88(4): p. 567-72.
9. Squara, P., D. Bennett, and C. Perret, Pulmonary artery catheter: does the problem lie in the users? Chest, 2002. 121(6): p. 2009-15.
10. Gnaegi, A., F. Feihl, and C. Perret, Intensive care physicians' insufficient knowledge of right-heart catheterization at the bedside: Time to act? Critical Care Medicine, 1997. 25(2): p. 213-220.
11. Pinsky, M.R. and J.L. Vincent, Let us use the pulmonary artery catheter correctly and only when we need it. Critical Care Medicine, 2005. 33(5): p. 1119-1122.
12. Putterman, C., The Swan-Ganz Catheter - a Decade of Hemodynamic Monitoring. Journal of Critical Care, 1989. 4(2): p. 127-146.
13. Cruz, K. and C. Franklin, The pulmonary artery catheter: uses and controversies. Crit Care Clin, 2001. 17(2): p. 271-91.
14. Swan, H.J., The pulmonary artery catheter. Dis Mon, 1991. 37(8): p. 473-543.
15. Sharkey, S.W., Beyond the wedge: clinical physiology and the Swan-Ganz catheter. Am J Med, 1987. 83(1): p. 111-22.
16. Oquin, R. and J.J. Marini, Pulmonary-Artery Occlusion Pressure - Clinical Physiology, Measurement, and Interpretation. American Review of Respiratory Disease, 1983. 128(2): p. 319-326.
17. Swan, H.J.C., et al., Catheterization of Heart in Man with Use of Flow-Directed Balloon-Tipped Catheter. New England Journal of Medicine, 1970. 283(9): p. 447-&.
18. Halpern, N., et al., The technique of inserting an RV port PA catheter and pacing probe. J Crit Illn, 1991. 6: p. 2253-1159.
19. Yelderman, M.L., et al., Continuous thermodilution cardiac output measurement in intensive care unit patients. J Cardiothorac Vasc Anesth, 1992. 6(3): p. 270-4.
20. Vincent, J.L., et al., Thermodilution measurement of right ventricular ejection fraction with a modified pulmonary artery catheter. Intensive Care Med, 1986. 12(1): p. 33-8.
21. Armaganidis, A., et al., Accuracy assessment for three fiberoptic pulmonary artery catheters for SvO2 monitoring. Intensive Care Med, 1994. 20(7): p. 484-8.
22. Kong, R. and M. Singer, Insertion of a pulmonary artery flotation catheter: how to do it. Br J Hosp Med, 1997. 57(9): p. 432-5.
23. Pego, R.F. and M.H. Luria, Left subclavian vein puncture for insertion of Swan-Ganz catheters. Heart Lung, 1979. 8(3): p. 507-10.
24. Bailey, L.L., et al., Improved technique for bedside insertion of the Swan-Ganz pulmonary artery catheter. Ann Thorac Surg, 1976. 21(5): p. 460-1.
25. Wiedemann, H.P., M.A. Matthay, and R.A. Matthay, Cardiovascular-pulmonary monitoring in the intensive care unit (Part 1). Chest, 1984. 85(4): p. 537-49.
26. Venus, B. and M. Mathru, A maneuver for bedside pulmonary artery catheterization in patients with right heart failure. Chest, 1982. 82(6): p. 803-4.
27. Cohn, J.N., et al., Right ventricular infarction. Clinical and hemodynamic features. Am J Cardiol, 1974. 33(2): p. 209-14.
28. Matsuda, T., et al., Images in Anesthesia: accidental knot formation of a pulmonary artery catheter. Can J Anaesth, 2004. 51(10): p. 1010.
29. Thyrault, M., et al., Relation between dicrotic notch and mean pulmonary artery pressure studied by using a Swan-Ganz catheter in critically ill patients. Intensive Care Med, 1998. 24(1): p. 77-80.
30. Pinsky, M.R., Pulmonary artery occlusion pressure. Intensive Care Med, 2003. 29(1): p. 19-22.
31. Schmitt, E.A. and C.O. Brantigan, Common artifacts of pulmonary artery and pulmonary artery wedge pressures: recognition and interpretation. J Clin Monit, 1986. 2(1): p. 44-52.

32. Guyton, A.C., A.W. Lindsey, and B.N. Kaufmann, Effect of mean circulatory filling pressure and other peripheral circulatory factors on cardiac output. Am J Physiol, 1955. 180(3): p. 463-8.
33. Jacobsohn, E., R. Chorn, and M. OConnor, The role of the vasculature in regulating venous return and cardiac output: historical and graphical approach. Canadian Journal of Anaesthesia-Journal Canadien D Anesthesie, 1997. 44(8): p. 849-867.
34. Sylvester, J.T., H.S. Goldberg, and S. Permutt, The Role of the Vasculature in the Regulation of Cardiac-Output. Clinics in Chest Medicine, 1983. 4(2): p. 111-126.
35. Whittenberger, J.L., et al., Influence of state of inflation of the lung on pulmonary vascular resistance. J Appl Physiol, 1960. 15: p. 878-82.
36. Permutt, S., et al., Effect of lung inflation on static pressure-volume characteristics of pulmonary vessels. J Appl Physiol, 1961. 16: p. 64-70.
37. Permutt, S. and R.L. Riley, Hemodynamics of Collapsible Vessels with Tone: The Vascular Waterfall. J Appl Physiol, 1963. 18: p. 924-32.
38. Saouti, N., et al., The arterial load in pulmonary hypertension. Eur Respir Rev, 2010. 19(117): p. 197-203.
39. Harvey, R.M., Y. Enson, and M.I. Ferrer, A reconsideration of the origins of pulmonary hypertension. Chest, 1971. 59(1): p. 82-94.
40. Cozzi, P.J., J.B. Hall, and G.A. Schmidt, Pulmonary artery diastolic-occlusion pressure gradient is increased in acute pulmonary embolism. Critical Care Medicine, 1995. 23(9): p. 1481-4.
41. Naeije, R., et al., The transpulmonary pressure gradient for the diagnosis of pulmonary vascular disease. Eur Respir J, 2013. 41(1): p. 217-23.
42. Teboul, J.L., et al., A Bedside Index Assessing the Reliability of Pulmonary-Artery Occlusion Pressure Measurements during Mechanical Ventilation with Positive End-Expiratory Pressure. Journal of Critical Care, 1992. 7(1): p. 22-29.
43. Hoyt, J.D. and J.W. Leatherman, Interpretation of the pulmonary artery occlusion pressure in mechanically ventilated patients with large respiratory excursions in intrathoracic pressure. Intensive Care Med, 1997. 23(11): p. 1125-1131.
44. Robotham, J.L., et al., Cardiorespiratory interactions in patients with an artificial heart. Anesthesiology, 1990. 73(4): p. 599-609.
45. Pinsky, M.R., Cardiovascular issues in respiratory care. Chest, 2005. 128(5 Suppl 2): p. 592S-597S.
46. Naeije, R., J.M. Maarek, and H.K. Chang, Pulmonary vascular impedance in microembolic pulmonary hypertension: effects of synchronous high-frequency jet ventilation. Respir Physiol, 1990. 79(3): p. 205-17.
47. Claessen, G., et al., Interaction between respiration and right versus left ventricular volumes at rest and during exercise: a real-time cardiac magnetic resonance study. Am J Physiol Heart Circ Physiol, 2014. 306(6): p. H816-24.
48. Scharf, S.M., et al., Cardiac effects of increased lung volume and decreased pleural pressure in man. J Appl Physiol Respir Environ Exerc Physiol, 1979. 47(2): p. 257-62.
49. Scharf, S.M., Cardiovascular effects of airways obstruction. Lung, 1991. 169(1): p. 1-23.
50. Jardin, F., et al., Mechanism of paradoxic pulse in bronchial asthma. Circulation, 1982. 66(4): p. 887-94.
51. Gelb, A.F., et al., P pulmonale in status asthmaticus. J Allergy Clin Immunol, 1979. 64(1): p. 18-22.
52. Muramoto, A., et al., Nifedipine dilates the pulmonary vasculature without producing symptomatic systemic hypotension in upright resting and exercising patients with pulmonary hypertension secondary to chronic obstructive pulmonary disease. Am Rev Respir Dis, 1985. 132(5): p. 963-6.
53. Pinsky, M.R., Determinants of pulmonary arterial flow variation during respiration. J Appl Physiol Respir Environ Exerc Physiol, 1984. 56(5): p. 1237-45.
54. Pinsky, M.R., Instantaneous venous return curves in an intact canine preparation. J Appl Physiol Respir Environ Exerc Physiol, 1984. 56(3): p. 765-71.
55. Charlier, A.A., P.M. Jaumin, and H. Pouleur, Circulatory effects of deep inspirations, blocked expirations and positive pressure inflations at equal transpulmonary pressures in conscious dogs. J Physiol, 1974. 241(3): p. 589-605.
56. Versprille, A., Pulmonary vascular resistance. A meaningless variable. Intensive Care Med, 1984. 10(2): p. 51-3.
57. Naeije, R., Pulmonary vascular resistance. A meaningless variable? Intensive Care Med, 2003. 29(4): p. 526-9.
58. Porth, C.J., et al., The Valsalva maneuver: mechanisms and clinical implications. Heart Lung, 1984. 13(5): p. 507-18.
59. Karam, M., et al., Mechanism of decreased left ventricular stroke volume during inspiration in man. Circulation, 1984. 69(5): p. 866-73.
60. Maughan, W.L., et al., Instantaneous pressure-volume relationship of the canine right ventricle. Circ Res, 1979. 44(3): p. 309-15.
61. Sibbald, W.J. and A.A. Driedger, Right ventricular function in acute disease states: pathophysiologic considerations. Crit Care Med, 1983. 11(5): p. 339-45.
62. Naeije, R., Physiology of the pulmonary circulation and the right heart. Curr Hypertens Rep, 2013. 15(6): p. 623-31.
63. Vonk-Noordegraaf, A., et al., Right heart adaptation to pulmonary arterial hypertension: physiology and pathobiology. J Am Coll Cardiol, 2013. 62(25 Suppl): p. D22-33.

64. McLaughlin, V.V., et al., ACCF/AHA 2009 expert consensus document on pulmonary hypertension: a report of the American College of Cardiology Foundation Task Force on Expert Consensus Documents and the American Heart Association: developed in collaboration with the American College of Chest Physicians, American Thoracic Society, Inc., and the Pulmonary Hypertension Association. Circulation, 2009. 119(16): p. 2250-94.
65. Levinson, D.C., et al., Evidence for retrograde transpulmonary propagation of the V (or regurgitant) wave in mitral insufficiency. Am J Cardiol, 1958. 2(2): p. 159-69.
66. Nadeau, S. and W.H. Noble, Misinterpretation of pressure measurements from the pulmonary artery catheter. Can Anaesth Soc J, 1986. 33(3 Pt 1): p. 352-63.
67. Pinsky, M., J.L. Vincent, and J.M. De Smet, Estimating left ventricular filling pressure during positive end-expiratory pressure in humans. American Review of Respiratory Disease, 1991. 143(1): p. 25-31.
68. Pinsky, M.R., Recent advances in the clinical application of heart-lung interactions. Curr Opin Crit Care, 2002. 8(1): p. 26-31.
69. Teboul, J.L., et al., Estimating cardiac filling pressure in mechanically ventilated patients with hyperinflation. Crit Care Med, 2000. 28(11): p. 3631-6.
70. Pinsky, M.R., Clinical significance of pulmonary artery occlusion pressure. Intensive Care Med, 2003. 29(2): p. 175-8.
71. Sagawa, K., The ventricular pressure-volume diagram revisited. Circ Res, 1978. 43(5): p. 677-87.
72. Raper, R. and W.J. Sibbald, Misled by the wedge? The Swan-Ganz catheter and left ventricular preload. Chest, 1986. 89(3): p. 427-34.
73. Sprung, C.L., et al., The spectrum of pulmonary edema: differentiation of cardiogenic, intermediate, and noncardiogenic forms of pulmonary edema. American Review of Respiratory Disease, 1981. 124(6): p. 718-22.
74. Mchugh, T.J., et al., Pulmonary Vascular Congestion in Acute Myocardial-Infarction - Hemodynamic and Radiologic Correlations. Annals of Internal Medicine, 1972. 76(1): p. 29-&.
75. Landis, E.M., Micro-injection studies of capillary blood pressure in human skin. Heart-a Journal for the Study of the Circulation, 1930. 15(2): p. 209-228.
76. Starling, E.H., On the Absorption of Fluids from the Connective Tissue Spaces. J Physiol, 1896. 19(4): p. 312-26.
77. Sharkey, S.W. and N.B. Aberg, Hemodynamic evidence of painless myocardial ischemia with acute pulmonary edema in coronary disease. Am Heart J, 1995. 129(1): p. 188-91.
78. Gaar, K.A., Jr., et al., Effect of capillary pressure and plasma protein on development of pulmonary edema. Am J Physiol, 1967. 213(1): p. 79-82.
79. Kloess, T., U. Birkenhauer, and B. Kottler, Pulmonary pressure-flow relationship and peripheral oxygen supply in ARDS due to bacterial sepsis. Prog Clin Biol Res, 1989. 308: p. 175-80.
80. Tracey, W.R., et al., Effect of endothelial injury on the responses of isolated guinea pig pulmonary venules to reduced oxygen tension. American Review of Respiratory Disease, 1989. 140(1): p. 68-74.
81. Fang, K., et al., Starling resistor effects on pulmonary artery occlusion pressure in endotoxin shock provide inaccuracies in left ventricular compliance assessments. Critical Care Medicine, 1996. 24(10): p. 1618-25.
82. Pellett, A.A., et al., Pulmonary capillary pressure during acute lung injury in dogs. Critical Care Medicine, 2002. 30(2): p. 403-9.
83. Benzing, A., et al., Inhaled nitric oxide reduces pulmonary transvascular albumin flux in patients with acute lung injury. Anesthesiology, 1995. 83(6): p. 1153-61.
84. Michel, R.P., T.S. Hakim, and H.K. Chang, Pulmonary arterial and venous pressures measured with small catheters in dogs. J Appl Physiol Respir Environ Exerc Physiol, 1984. 57(2): p. 309-14.
85. Takala, J., Pulmonary capillary pressure. Intensive Care Med, 2003. 29(6): p. 890-3.
86. Cope, D.K., et al., Measurement of Effective Pulmonary Capillary-Pressure Using the Pressure Profile after Pulmonary-Artery Occlusion. Critical Care Medicine, 1986. 14(1): p. 16-22.
87. Cope, D.K., et al., Pulmonary capillary pressure: a review. Critical Care Medicine, 1992. 20(7): p. 1043-56.
88. Holloway, H., et al., Estimation of Effective Pulmonary Capillary-Pressure in Intact Lungs. Journal of Applied Physiology, 1983. 54(3): p. 846-851.
89. Staub, N.C., The pathogenesis of pulmonary edema. Prog Cardiovasc Dis, 1980. 23(1): p. 53-80.
90. Ganz, W. and H.J. Swan, Measurement of blood flow by thermodilution. Am J Cardiol, 1972. 29(2): p. 241-6.
91. Weisel, R.D., R.L. Berger, and H.B. Hechtman, Current concepts measurement of cardiac output by thermodilution. N Engl J Med, 1975. 292(13): p. 682-4.
92. Renner, L.E., M.J. Morton, and G.Y. Sakuma, Indicator amount, temperature, and intrinsic cardiac output affect thermodilution cardiac output accuracy and reproducibility. Critical Care Medicine, 1993. 21(4): p. 586-97.
93. Nelson, L.D. and H.B. Anderson, Patient selection for iced versus room temperature injectate for thermodilution cardiac output determinations. Critical Care Medicine, 1985. 13(3): p. 182-4.
94. Pearl, R.G., et al., Effect of injectate volume and temperature on thermodilution cardiac output determination. Anesthesiology, 1986. 64(6): p. 798-801.
95. Tuman, K.J., G.C. Carroll, and A.D. Ivankovich, Pitfalls in interpretation of pulmonary artery catheter data. J Cardiothorac Anesth, 1989. 3(5): p. 625-41.

96. Synder, J.V. and D.J. Powner, Effects of mechanical ventilation on the measurement of cardiac output by thermodilution. Critical Care Medicine, 1982. 10(10): p. 677-82.
97. Stevens, J.H., et al., Thermodilution cardiac output measurement. Effects of the respiratory cycle on its reproducibility. JAMA, 1985. 253(15): p. 2240-2.
98. Cigarroa, R.G., et al., Underestimation of cardiac output by thermodilution in patients with tricuspid regurgitation. Am J Med, 1989. 86(4): p. 417-20.
99. Jullien, T., et al., Incidence of tricuspid regurgitation and vena caval backward flow in mechanically ventilated patients. A color Doppler and contrast echocardiographic study. Chest, 1995. 107(2): p. 488-93.
100. Finch, C.A. and C. Lenfant, Oxygen transport in man. N Engl J Med, 1972. 286(8): p. 407-15.
101. Guffin, A., D. Girard, and J.A. Kaplan, Shivering following cardiac surgery: hemodynamic changes and reversal. J Cardiothorac Anesth, 1987. 1(1): p. 24-8.
102. Zwischenberger, J.B., et al., Suppression of shivering decreases oxygen consumption and improves hemodynamic stability during postoperative rewarming. Ann Thorac Surg, 1987. 43(4): p. 428-31.
103. Krafft, P., et al., Mixed Venous Oxygen-Saturation in Critically Ill Septic Shock Patients - the Role of Defined Events. Chest, 1993. 103(3): p. 900-906.
104. Guerin, J.P., et al., Effects of dopamine and norepinephrine on systemic and hepatosplanchnic hemodynamics, oxygen exchange, and energy balance in vasoplegic septic patients. Shock, 2005. 23(1): p. 18-24.
105. Boerma, E.C. and C. Ince, The role of vasoactive agents in the resuscitation of microvascular perfusion and tissue oxygenation in critically ill patients. Intensive Care Med, 2010. 36(12): p. 2004-2018.
106. Manthous, C.A., et al., Effect of cooling on oxygen consumption in febrile critically ill patients. Am J Respir Crit Care Med, 1995. 151(1): p. 10-4.
107. Marik, P.E. and D. Kaufman, The effects of neuromuscular paralysis on systemic and splanchnic oxygen utilization in mechanically ventilated patients. Chest, 1996. 109(4): p. 1038-42.
108. Fink, M.P., Bench-to-bedside review: Cytopathic hypoxia. Crit Care, 2002. 6(6): p. 491-9.
109. Shibutani, K., et al., Critical level of oxygen delivery in anesthetized man. Crit Care Med, 1983. 11(8): p. 640-3.
110. Walley, K.R., Use of central venous oxygen saturation to guide therapy. Am J Respir Crit Care Med, 2011. 184(5): p. 514-20.
111. Boyd, K.D., et al., A prospective study of complications of pulmonary artery catheterizations in 500 consecutive patients. Chest, 1983. 84(3): p. 245-9.
112. Shah, K.B., et al., A review of pulmonary artery catheterization in 6,245 patients. Anesthesiology, 1984. 61(3): p. 271-5.
113. Morris, D., D. Mulvihill, and W.Y. Lew, Risk of developing complete heart block during bedside pulmonary artery catheterization in patients with left bundle-branch block. Arch Intern Med, 1987. 147(11): p. 2005-10.
114. Thomson, I.R., et al., Right bundle-branch block and complete heart block caused by the Swan-Ganz catheter. Anesthesiology, 1979. 51(4): p. 359-62.
115. Chastre, J., et al., Thrombosis as a complication of pulmonary-artery catheterization via the internal jugular vein: prospective evaluation by phlebography. N Engl J Med, 1982. 306(5): p. 278-81.
116. Siegel, L.C. and R.G. Pearl, Measurement of the longitudinal distribution of pulmonary vascular resistance from pulmonary artery occlusion pressure profiles. Anesthesiology, 1988. 68(2): p. 305-7.
117. Wiedemann, H.P., M.A. Matthay, and R.A. Matthay, Cardiovascular-pulmonary monitoring in the intensive care unit (Part 2). Chest, 1984. 85(5): p. 656-68.
118. Barash, P.G., et al., Catheter-induced pulmonary artery perforation. Mechanisms, management, and modifications. J Thorac Cardiovasc Surg, 1981. 82(1): p. 5-12.
119. Leatherman, J.W. and R.S. Shapiro, Overestimation of pulmonary artery occlusion pressure in pulmonary hypertension due to partial occlusion. Crit Care Med, 2003. 31(1): p. 93-7.

Chapter Eight

Dynamic Means of Cardiovascular Monitoring

Abstract

The operating point of the cardiovascular system is formed at the intersection of venous return and cardiac function. Applying a defined stress to the cardiovascular system may be used to infer the location of the operating point by altering cardiac function relative to venous return, or vice versa. If the operating point falls upon the ascending portion of the cardiac function curve, then the change in both cardiac output and central venous pressure is relatively large for a given stress. These changes are detected as left ventricular stroke volume and vena cavae diameter variation, respectively, and are employed as markers of preload responsiveness. This approach, termed 'functional hemodynamic monitoring,' has relatively recently reached the intensive care unit. Fluency in the heart-lung interaction helps make sense of functional hemodynamic monitoring, recognize the shortcomings of this approach and make informed management decisions while caring for the critically-ill.

Key Words: pulse-pressure variation, intra-thoracic pressure, stroke volume variation, vena cava assessment, passive leg raise, functional hemodynamic monitoring

Introduction

When a defined stress is applied to the cardiovascular system, a variety of dynamic responses may be observed and measured. From the observed response, something clinically meaningful is inferred about the patient's underlying hemodynamic state. This mechanical 'dose-response' relationship in the cardio-circulatory system has been coined 'functional hemodynamic monitoring' [FHM] [1, 2]. A common clinical inquiry regarding a patient's underlying hemodynamic state is whether a patient will augment cardiac output in response to a fluid challenge, or simply, is the patient 'volume responsive?'

Before discussing the varieties and intricacies of FHM, it is imperative that the reader appreciate the following over-arching principle: the validity of the measured hemodynamic response is inexorably linked to the stress applied to the system. In the assortment of FHM discussed in this chapter, the stress applied to the cardiovascular system is often intra-thoracic pressure change. If a clinician desires

to measure and interpret a standardized response [e.g. left ventricular stroke volume variation and its surrogates, vena cava diameter alteration, etc.] to facilitate clinical decision-making, then the patient must receive an equivalent cardio-circulatory stress [e.g. intra-thoracic pressure change] as the validation cohort in which the measures were derived. Consequently, the general principle involved in FHM is a dose-response relationship not at all dissimilar to basic pharmacology. As an analogy, if one were to alter the dose of a medication and observe a different response, this change could be a function of the altered dose rather than something inherently different about the patient. Nevertheless, some clinicians ignore the aforementioned as it pertains to FHM. The sensitivity and specificity of measured hemodynamic responses were derived in the context of specific, predefined stresses applied to the cardiovascular system. When utilizing FHM to assess a patient for fluid responsiveness, the clinician must know that if the applied stress [e.g. intra-thoracic pressure change] deviates from the cohort in which the measured response [e.g. SVV and its surrogates] was derived, the sensitivity and specificity of the measured response is degraded; simply, the change in 'response' of SVV is confounded by the change in the 'dose' of intra-thoracic pressure.

As discussed below, with the exception of trials that included patients with spontaneous respiratory effort, essentially all trials of FHM utilized volume-control mechanical ventilation in patients who were fully passive with the mechanical ventilator. When employing volume-limited modes of mechanical ventilation, there are multiple determinants of intra-thoracic pressure - the presence and degree of patient effort, the applied tidal volume and chest wall compliance [3, 4]. Thus, in addition to receiving a similar tidal volume and having similar chest wall characteristics as the derivation cohort, paralysis or at least very heavy sedation is a pre-requisite to ensure that intra-thoracic pressure reliably changes with each breath. With varying inspiratory effort by the patient, intra-thoracic pressure during inspiration changes unpredictably. Thus, the hemodynamic response is confounded. The 'dose-response' analogy to FHM is echoed in chapter 10.

This chapter will commence with a basic review of cardiovascular physiology as this is the foundation upon which the reader appreciates the distinction between 'volume status,' and 'volume responsiveness.' The chapter then turns to the determinants of the central venous pressure [CVP] and how changing intra-thoracic pressure during mechanical ventilation and spontaneous ventilation impart changes upon the CVP. A discussion of the physiological and clinical significance of dynamic change in both left ventricular output and vena cavae diameter during both spontaneous and mechanical ventilation follows.

Review of Cardiovascular Physiology

While commonly confused at the bedside, 'volume responsiveness' is physiologically distinct from 'volume status,' the latter referring to whether a patient has an excess or deficit of total body salt and water. In fact, while 'volume responsiveness' and 'volume status' are related clinically, they are mechanistically, mutually exclusive.

The aforementioned concepts have been previously discussed in Chapter 6, but are reviewed below.

Venous Return

As commonly taught, flow requires a pressure differential – the components of which are referred to as an upstream and downstream pressure [see chapter 1]. As such, venous return to the right heart has the mean systemic filling pressure [Pmsf – see chapter 2] and the right atrial pressure, respectively. The right atrial pressure is equivalent to the CVP, barring any caval obstruction; this chapter uses them interchangeably.

The upstream pressure, or Pmsf, is defined by the stressed volume of the lumped venous capacitance beds divided by the compliance of this vascular bed. Because 70% of the blood volume lies within the veins and venules [5], and the compliance of the venous vascular beds is roughly thirty times greater than that of the arterial tree at typical venous pressure [6], the transmural pressure of the lumped venous system is quasi-static, irrespective of cardiac activity [2]. Accordingly, when cardiac function ceases, the pressure within the entire circulatory system, including the right atrium, equilibrates to the mean circulatory filling pressure [Pmcf]. The Pmcf is similar to the mean systemic filling pressure [Pmsf] and used interchangeably in this volume; chapter 2 describes the subtle difference between the two. Because blood flow [on the y-axis] is zero at cardiac standstill, the Pmcf or Pmsf is the x-intercept of the venous return curve [figure 1]. In the euvolemic patient, the Pmsf is roughly 5-10 mmHg [7, 8]; because the right atrial pressure in a normal, euvolemic patient is close to atmospheric pressure [zero mmHg], the entirety of venous return to the right heart is driven by a pressure gradient of only 5-10 mm Hg.

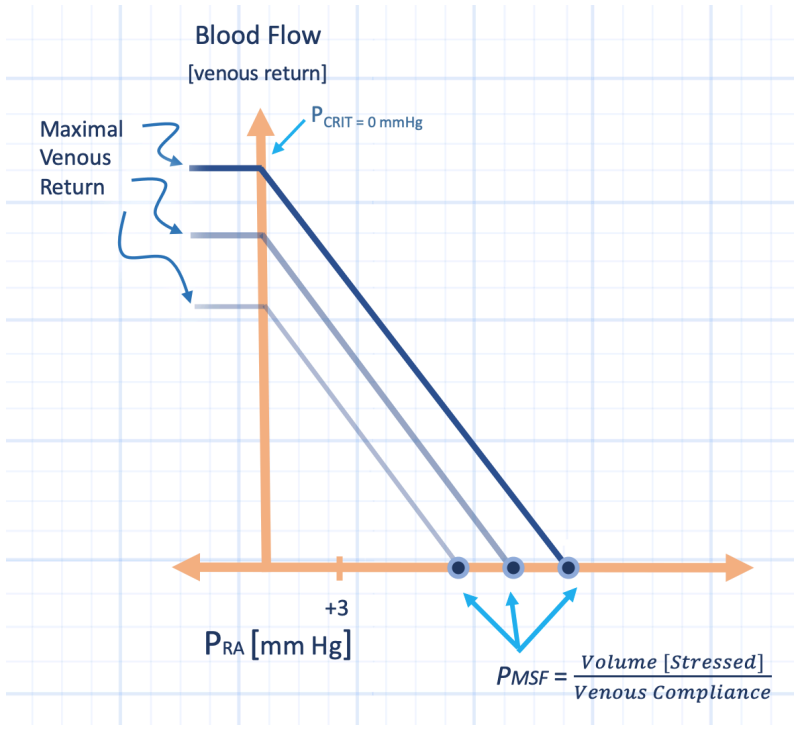

Figure 1: The venous return curve describes the physiology of blood return to the heart. The mean systemic filling pressure, Pmsf, is the x-intercept; its primary determinants are blood volume and venous tone. Thus, hypervolemia shifts the curve rightwards, but so too does enhanced adrenergic tone.

Discussion of venous return is crucial as 'volume status' is a determinant of the Pmsf. Hypervolemia increases the stressed volume of the venous capacitance beds and, therefore, the Pmsf – right-shifting the venous return curve. Conversely, in the hypovolemic patient, the stressed volume of the venous capacitance beds falls; therefore, the Pmsf [i.e. the upstream pressure for venous return] is diminished and the venous return curve shifts leftwards. Importantly, the stressed volume of the venous capacitance beds is dynamic. The capacitance of the veins and venules can change with adrenergic tone such that Pmsf may be relatively low even when a patient is hypervolemic [e.g. venoplegia secondary to sedation or sepsis] and vice versa [9, 10].

Cardiac Function

The cardiac function curve [or 'cardiac response curve' as Arthur Guyton called it] pictorially defines the relationship between right atrial pressure and cardiac output [11, 12]. Unlike the stretch-twitch relationship of a single myocyte, which has a true descending portion, the in vivo heart does not 'fall off' the Starling curve. The basic principle of the cardiac function curve is that greater right atrial pressure raises forward flow until a plateau is reached – beyond which augmenting right atrial pressure does not increase cardiac output. The plateau portion of the curve is largely determined by the myocyte cytoskeleton, pericardium and mediastinal constraint [13]. Note that the slope of the cardiac function curve steepens with improved cardiac function and flattens with diminished function. Slope shifting of the cardiac function curve is determined not simply by cardiac contractility, but also heart rate, rhythm, biventricular afterload and valve function [2, 11].

The Guyton Diagram and the Operating Point

It is the superposition of the venous return curve and the cardiac function curve which defines the steady-state operating point of the cardiovascular system [figure 2]. The operating point of the cardiovascular system determines a patient's CVP and cardiac output as a consequence of venous return and cardiac function. Notably, while the CVP is analyzed on the x-axis, it is not an independent variable. The CVP rises and falls as a function of both changing venous return and cardiac function [13].

Finally, we may now consider 'volume responsiveness;' or arguably of more clinical importance, 'volume un-responsiveness.' A patient augments cardiac output if the operating point is on the ascending portion of the cardiac function curve. By contrast, if the venous return curve intersects near or upon the plateau of the cardiac function curve, the patient is not volume responsive. Careful consideration of this concept unveils a clinical paradox: a patient may be hypervolemic and volume responsive. Conversely, if there is diminished cardiac function, a patient can be volume un-responsive when hypovolemic [figure 2]. Because the slope of the cardiac function curve is hard to know with certainty in a patient in the ICU,

almost any CVP may fall upon the plateau. Up to 25% of patients with a CVP less than 5 mmHg can be unresponsive to fluid loading [14].

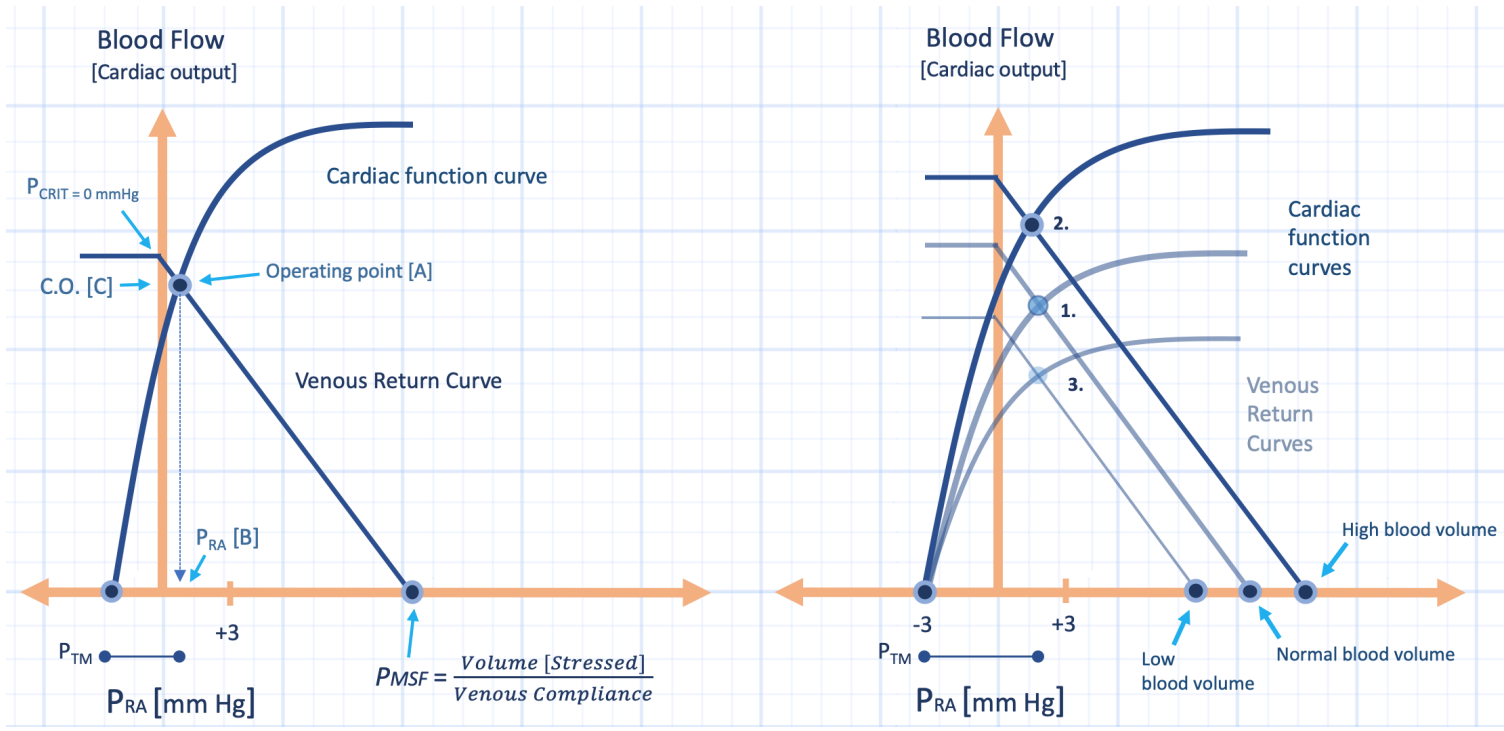

Figure 2: The Guyton diagram. Left panel: The Guyton diagram illustrates the operating point of the cardiovascular system [point A] which defines the cardiac output on the y-axis [point C] and the right atrial pressure or central venous pressure on the x-axis [point B]. The operating point is determined by neither venous return nor cardiac function alone, but both in tandem. Right panel: The relationship between 'volume status' and 'volume responsiveness' via the Guyton diagram. The initial operating point is point 1. Operating point 2 illustrates a hypervolemic patient because of the right-shifted venous return curve [an increase in Pmsf], but the patient also has enhanced cardiac function so the operating point is on the ascending portion of the cardiac function curve, or the patient is volume responsive. Lastly, operating point 3 illustrates a hypovolemic patient with impaired cardiac function, the patient is volume unresponsive. Each patient has a similar CVP [roughly 2 mmHg] and similar right atrial distending pressure [Ptm, blue dumbbell].

The Central Venous Pressure and Intra-thoracic Pressure

The Guyton diagram described above is true only under respiratory arrest. A simple visit to the bedside of a patient with continuous CVP monitoring, making active respiratory efforts reveals that the CVP changes with intra-thoracic pressure; this was discussed in chapter 6. The effect of intra-thoracic pressure upon the Guyton diagram, and therefore the CVP, is understood by considering the x-intercept of the cardiac function curve. As the x-intercept on the Guyton diagram represents no blood flow [i.e. the y-axis is zero], the x-intercept of the cardiac function curve requires circulatory arrest. However, we must additionally consider the right atrium uncoupled from venous return; if venous return were allowed to proceed during cardiac standstill, then the right atrial pressure would become the Pmsf as discussed above. If venous return to the right heart is prohibited while under cardio-circulatory arrest, then the right atrial pressure assumes intra-thoracic pressure. It follows that the x-intercept of the cardiac function curve tracks changes in intra-thoracic pressure, as initially postulated by Guyton, and confirmed by Marini and colleagues [11, 15].

Prior to spontaneous inspiration, the x-intercept of the cardiac function curve is slightly sub-atmospheric because the intra-thoracic pressure at functional residual capacity is normally slightly negative. With spontaneous inspiration, the x-intercept [and therefore cardiac function curve] shifts leftwards relative to the systemic venous return curve. Thus, the effect on central venous pressure depends on three co-varying physiological phenomena: 1. change in intra-thoracic pressure, 2. the characteristics of the venous return curve and 3. the characteristics of the cardiac function curve. If the operating point lies on the ascending portion of the cardiac function curve, the central venous pressure tends to decrease while the cardiac output tends to increase [figure 3].

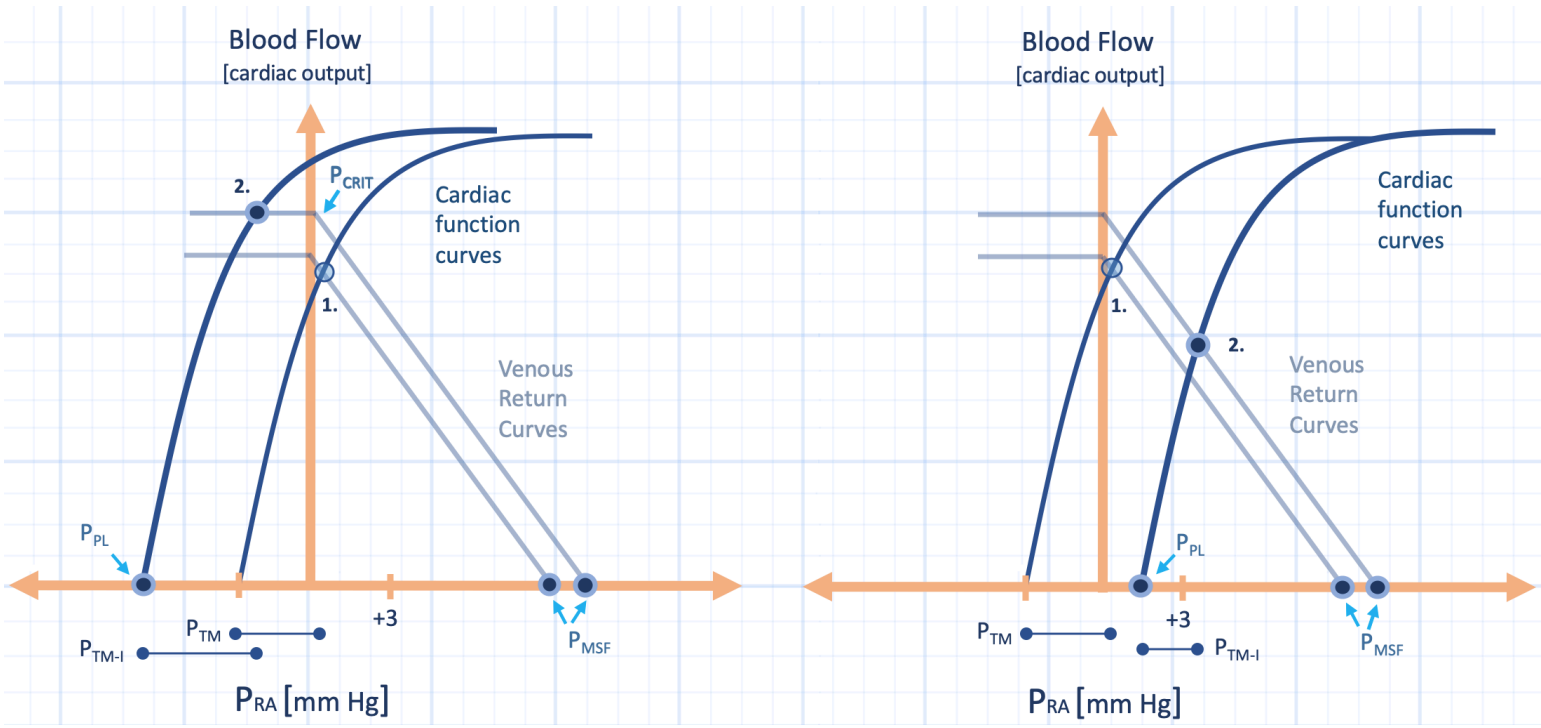

Figure 3: Respiration and the operating point. Left panel: A spontaneous breath shows decreased intra-thoracic pressure [or pleural pressure, Ppl] there is left shift of the cardiac function curve and also right shift in the venous return curve [increased mean systemic filling pressure, Pmsf] as abdominal venous capacitance is decreased with the rise in lung volume. Thus, the operating point moves from point 1 to point 2. There is decreased right atrial pressure [or CVP, x-axis] but increased cardiac output [y-axis] and right atrial distending pressure [blue dumbbell below x-axis, Ptm-I]. Right panel: The effect of a passive, mechanical breath on the operating point. The Ppl increases and the cardiac function curve shifts rightwards. So too does the venous return curve secondary to the effect of diaphragm descent on the abdominal veins. The operating point moves from point 1 to point 2; there is decreased cardiac output [y-axis] and right atrial distending pressure [blue dumbbell below x-axis; Ptm-I]. The right atrial pressure, or CVP, also increases [x-axis]. Pcrit is the critical collapse pressure of the great veins; Ptm is the baseline right atrial trans-mural pressure

By contrast, delivering a mechanical breath to the fully passive patient [i.e. not making respiratory efforts during mechanical ventilation] shifts the cardiac function curve rightwards with respect to the venous return curve [figure 3]. This opposes the effects described above; that is, the CVP rises while cardiac output falls. The degree to which the cardiac function curve shifts rightwards with respect to the venous return curve depends on the change in intra-thoracic pressure. In the fully adapted patient, the increase in intra-thoracic pressure from a mechanical breath is directly related to the ventilator-applied tidal volume and indirectly proportional to the compliance of the chest wall [3, 16, 17]. Thus, with mechanical insufflation of the lungs the 'stress' [i.e. intra-thoracic pressure] applied to the cardiovascular system

increases with higher tidal volume and/or lower chest wall compliance [e.g. ascites, chest wall edema, obesity etc.], and vice versa [3]. If a patient generates inspiratory effort with the ventilator, or bears down against it, the change in intra-thoracic pressure is, essentially, unpredictable. Such fluctuation in intra-thoracic pressure confounds any measured cardiovascular response such as SVV. It is the reason why studies of FHM included patients who were completely adapted with the ventilator, receiving relatively high tidal volumes [8-10 mL/kg] [18-20].

Changes in Left Ventricular Stroke Volume

As it is the left ventricle that ejects blood into the systemic circulation, assessing instantaneous change in its output is much more straightforward than assessing dynamic right ventricular output. There are various direct and indirect assessments of beat-to-beat left ventricular stroke volume; the shared physiology amongst these methods is described in the following section.

The Physiology of Left Ventricular Stroke Volume Variation

Deflections in left ventricular stroke volume during a single, mechanical respiratory cycle are referenced to an end-expiratory [or 'apneic'] baseline [figure 4]. When a ventilated patient is fully passive, initiation of a mechanical breath increases systolic blood pressure – sometimes referred to as 'reverse pulsus paradoxus.' The increase in systolic blood pressure is called dUP [or delta UP] and is the consequence of multiple mechanisms. First, there may be direct transmission of increased intra-thoracic pressure to the aorta and arterial tree [21]; however, the methods used in this study utilized conductance catheter-derived measures of left ventricular stroke volume which are prone to LV volume sampling error [22]. Second, mechanical insufflation of the lungs in a passive patient favours each of the following: improved left ventricular [LV] compliance via reduced right ventricular volume [23], reduced left ventricular afterload [24], increased pulmonary venous return and, therefore, LV preload [4, 25-27]. Diminished right heart volume improving left ventricular filling during intermittent positive pressure ventilation is felt to be a less prominent mechanism [4, 26]; in theory, though, this becomes more dominant as right heart volume rises, as in states of right heart overload. As many of these variables are not related to volume responsiveness and, in fact, are more influential when a patient is hypervolemic, dUP is felt to be a poor marker of fluid responsiveness [28, 29]. This is an important caveat of SVV as discussed below.

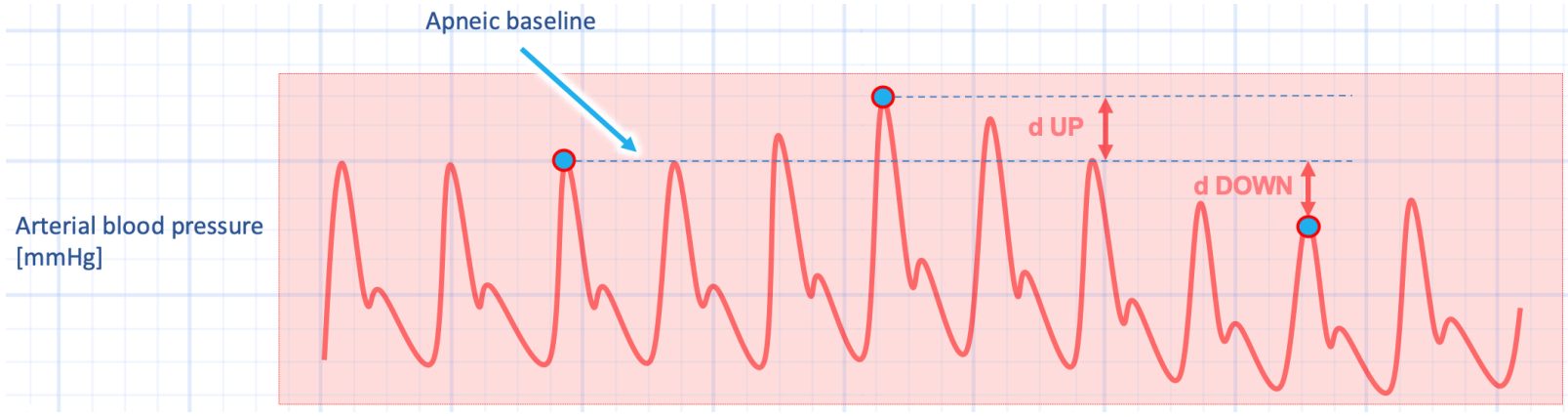

Figure 4: d UP and d DOWN on an arterial line tracing. This waveform applies only to a patient completely passive with the mechanical ventilator; that is, generating no respiratory effort. The degree to which the systolic pressure rises above the apneic baseline is the d UP, while the degree to which the systolic pressure falls below the apneic baseline is known as d DOWN.

By contrast, during mechanical expiration, the inspiratory reduction in RV output reaches the left ventricle and diminishes LV stroke volume. This is observed as reduced aortic systolic pressure during expiration and is referred to as dDOWN [or delta DOWN] [figure 4]. Thus, dDOWN is somewhat analogous to waves reaching the shore, created by a distant boat. It is a delayed effect that is subject to the physiology of the right heart, pulmonary circulation and left heart. Nevertheless, dDOWN most closely approximates volume responsiveness [30-32]. As above, because the gradient for venous return to the right heart is typically less than 10 mm Hg, a small shift in the cardiac function curve relative to the venous return curve markedly drops right ventricular output, but only if the operating point lies on the ascending portion of the cardiac function curve. Then, 2-3 cardiac cycles later, diminished right heart output traverses the pulmonary circuit and reaches the left ventricle. If the operating point of the left heart also lies on the ascending portion of the left ventricular cardiac function curve, left ventricular stroke volume also falls. Accordingly, dDOWN represents biventricular volume responsiveness [33].

Left Ventricular Stroke Volume Variation Caveats

Flowing from the analogy introduced at the outset of this chapter, there are two broad categories of caveats for stroke volume variation. First, if the patient under evaluation receives a different 'dose' of intra-thoracic pressure than the study cohort in which the metric threshold was derived and second, if the patient has significant underlying cardiovascular abnormalities, then the measured cardiovascular 'response' [e.g. SVV, PPV] may mislead when assessing volume responsiveness.

In the initial FHM studies, the patients were assumed to have essentially normal chest wall compliance, all received relatively large tidal volumes and all were completely passive with the ventilator. These parameters, in effect, standardized the 'dose' of intra-thoracic pressure that each patient received with each breath. It also explains why FHM has short-comings when applied to patients generating spontaneous respiratory effort [34-37], when smaller tidal volumes are applied [38, 39], or when there are abnormalities in chest wall compliance [3, 40, 41]. The

reasons for impaired sensitivity and specificity in the aforementioned clinical situations are varied and not fully known. In terms of patients who are breathing completely spontaneously, without the aid of positive pressure ventilation, there is diminished sensitivity, with good specificity [34] when employing left ventricular SVV to predict fluid responsiveness. The likely mechanisms for impaired sensitivity in this situation are collapse of the great veins during inspiration, which limits the cardiovascular stress upon the right ventricle and therefore impairs deflections in LV output and/or insufficient intra-thoracic pressure change during spontaneous inspiration [figure 5]. The latter mechanism helps explain data supporting SVV when deep inspiration is used to exaggerating the stress upon the cardiovascular system [42]. Nevertheless, states of volume overload and right heart dysfunction ostensibly degrade SVV specificity during spontaneous inspiration via ventricular interdependence and reduced LV stroke volume. Right ventricular dysfunction can cause false positive LV stroke volume variation [43]; such patients were specifically excluded from the Soubrier study [34] [figure 5].

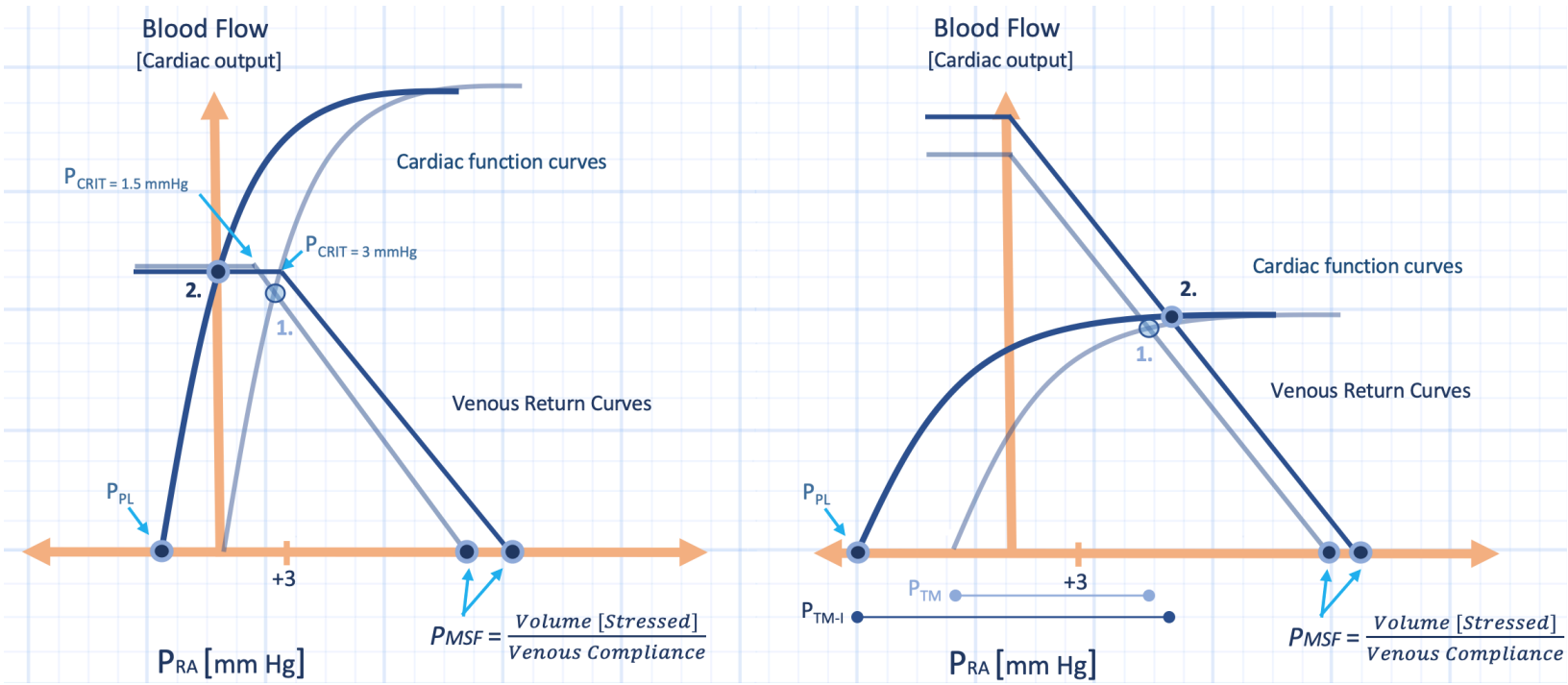

Figure 5: Hypothetical mechanisms of impaired sensitivity and specificity. Left panel: The change in right ventricular output with spontaneous inspiration while on positive end-expiratory pressure. The patient triggers a breath. Note that this patient is fluid responsive because the operating point [1] lies on the ascending portion of the cardiac function curve. However, PEEP lowers maximal venous return and, as this patient inspires, collapse of the great veins occurs [right atrial pressure, Pra, below the critical collapse pressure, Pcrit]. There is little change in right ventricular output on the y-axis [point 2 compared to point 1]; this patient has no variation in stroke volume and is a false negative. Right panel: Spontaneous inspiration in right heart failure; this patient is not on PEEP. This patient is not fluid responsive and has a high mean systemic filling pressure [Pmsf] e.g. from cor pulmonale. Point 1 is on the flat part of the cardiac function curve. With inspiration, there is a large increase in right atrial distending pressure [trans-mural pressure on inspiration Ptm-I; blue dumbbell below x-axis]. Point 2 may cause ventricular interdependence effect upon the left ventricle [e.g. pulsus paradoxus]. If this causes LV output to drop, there would be a false positive variation in its output, i.e. diminished specificity.

With regards to patients generating inspiratory effort while receiving supplemental positive pressure [via either an endotracheal tube or tight-fitting facemask], the physiology of stroke volume variation becomes muddied as inspiratory intra-thoracic pressure can fall below atmospheric pressure, rise above atmospheric pressure or there may be some combination thereof [44]. Because waxing and

waning intra-thoracic pressure tend to have opposing effects on biventricular loading [2, 11, 27, 28, 45, 46], the unpredictable and conflicted nature of cardiac loading during assisted ventilation renders LV SVV a troublesome marker of biventricular volume responsiveness [30, 37, 47]. In fact, Heenen and colleagues found that the area under the receiver-operator curve for the pulmonary capillary wedge pressure out-performed left ventricular SVV when predicting volume responsiveness in patients triggering the ventilator [35].

When patients are passive, but receiving small tidal volumes, SVV has impaired sensitivity as an indicator of fluid responsiveness [3, 38]. This may be due to insufficient intra-thoracic pressure change consequent to low tidal volume [figure 6]. Accordingly, adopting lower SVV thresholds improves sensitivity [48]. By contrast, diminished chest wall compliance exaggerates left ventricular output variation and diminishes specificity; that is, creates false positives [3, 49] [figure 7]. This could lead to excessive fluid administration and if chest wall edema occurs, a self-perpetuating cycle.

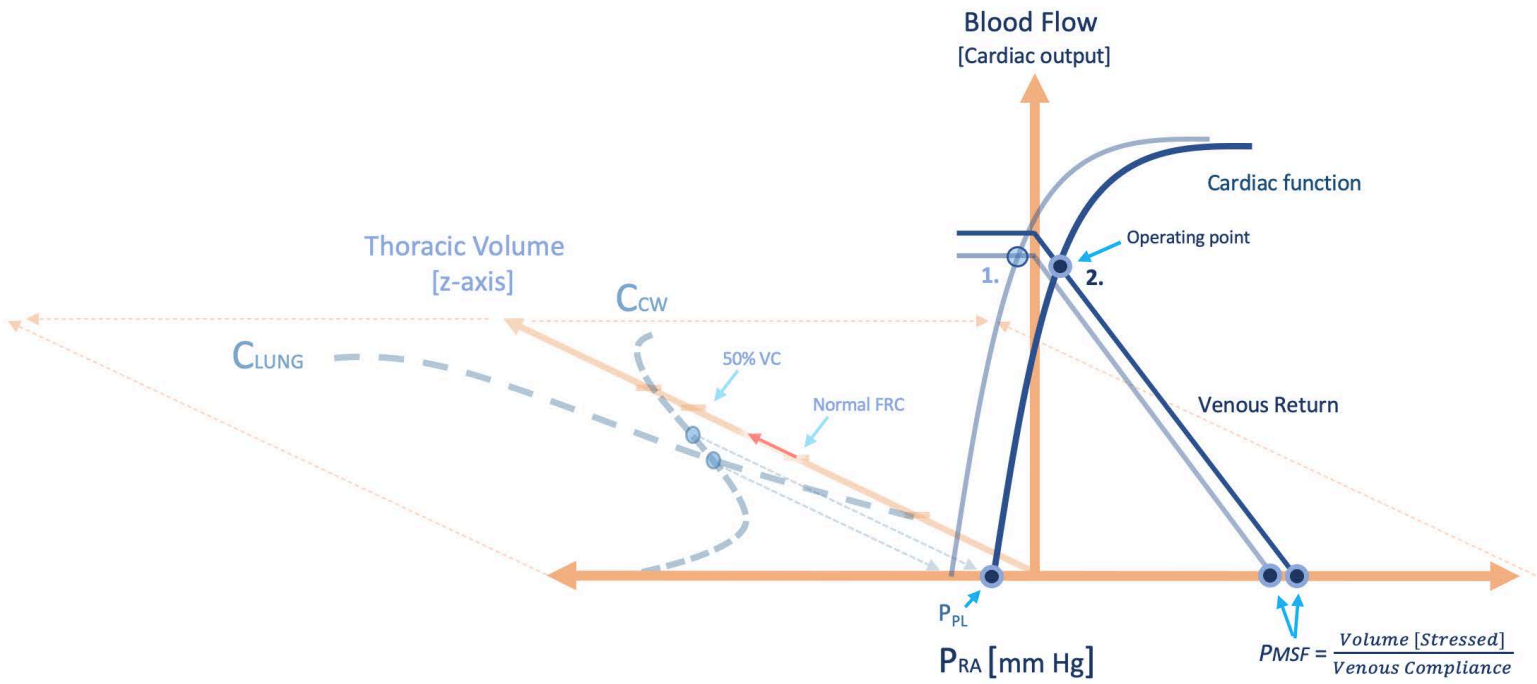

Figure 6A: The effect of a small tidal volume on right ventricular [RV] output. The tidal volume delivered by the ventilator is the red arrow on the z-axis [into the page]. Increased intra-thoracic pressure [or pleural pressure, Ppl] follows the chest wall compliance curve in the passive patient [Ccw]. The cardiac function curve shifts in-step with the rise in Ppl. There is minimal rise in Ppl and afterload and, therefore, minimal fall in RV output [y-axis] between point 1 and point 2 . There is no left ventricular stroke volume variation 1-2 cardiac cycles later. FRC indicated functional residual capacity; VC is vital capacity; Clung is lung compliance. See chapters 3 and 4 for additional details.

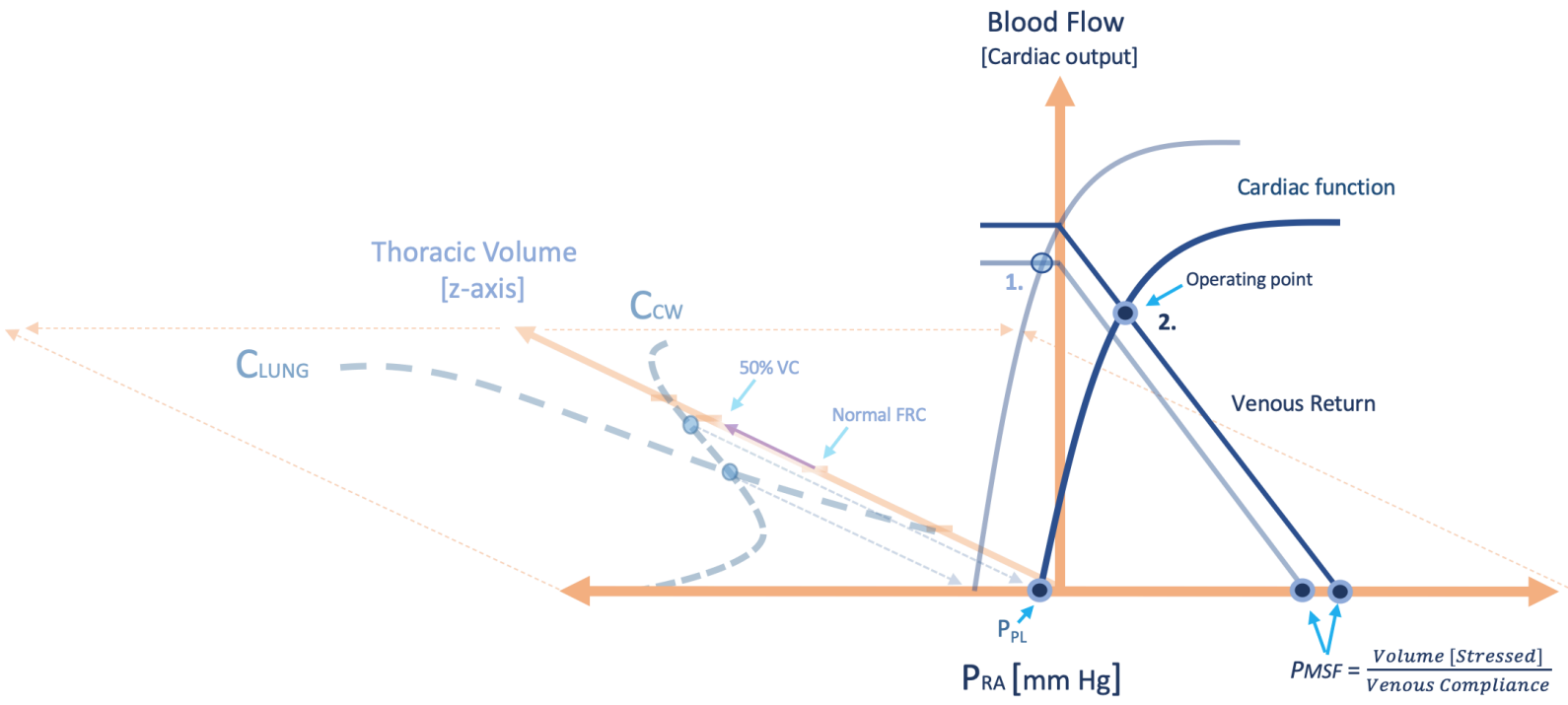

Figure 6B: The effect of large tidal volume on right ventricular [RV] output. The tidal volume delivered by the ventilator is large and indicated as the purple arrow on the z-axis [into the page]. The increase in intra-thoracic pressure, or pleural pressure [Ppl] follows the chest wall compliance curve in the passive patient [Ccw]. The cardiac function curve shifts in-step with the rise in Ppl. The increase in lung volume afterloads the RV and shifts the mean systemic filling pressure [Pmsf] to the right. There is a large drop in RV output [y-axis] between point 1 and point 2, causing left ventricular stroke volume variation 1-2 cardiac cycles later. FRC indicated functional residual capacity; VC is vital capacity; Clung is lung compliance. See chapters 3 and 4 for additional details.

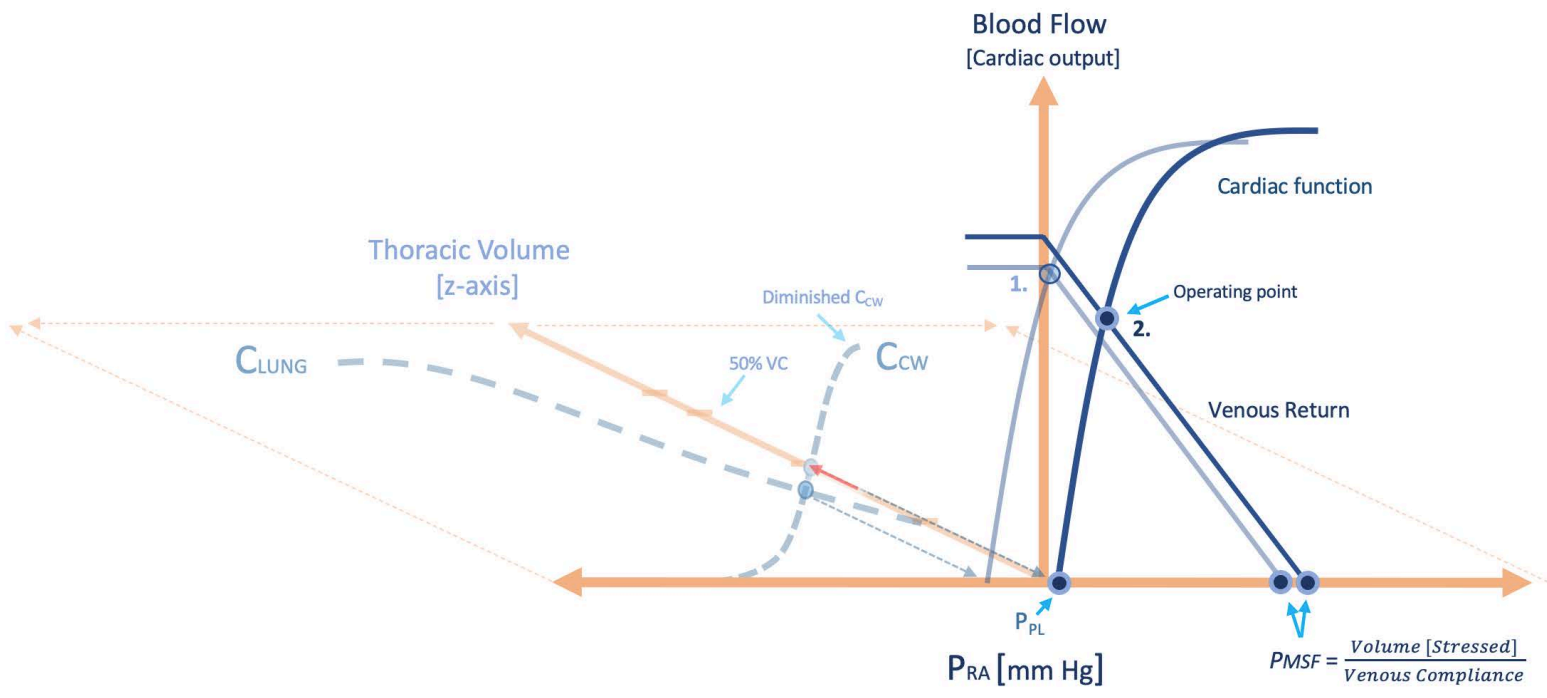

Figure 7: The effect of diminished chest wall compliance [Ccw] on right ventricular [RV] output. The patient is passive with the ventilator and the volume delivered by the ventilator is marked by the red arrow on the z-axis [into the page]. Because of the stiff chest wall, the cardiac function curve moves rightwards instep with the rise in pleural pressure [Ppl] to a similar degree as figure 6B. The operating point moves from point 1 to point 2 in this patient and there is a large reduction in RV output [y-axis], exaggerating the hemodynamic effect of the delivered tidal volume. VC is vital capacity; Clung is lung compliance. See chapters 3 and 4 for additional details.

The second group of caveats to LV SVV is more subtle than the first. As described above, the primary mechanism of SVV and PPV as markers of fluid responsiveness is reduced right ventricular output during mechanical inspiration, then transmitted to the left ventricle during mechanical expiration [28, 33]. The reason this is the dominant mechanism is that small changes in intra-thoracic pressure impart large changes in right heart preload – by diminishing venous return [50, 51]. Thus, left ventricular stroke volume variation assumes that right ventricular preload variation is the key mediator. Nevertheless, intra-thoracic pressure and lung volume both affect right and left heart afterload. For example, increasing lung volume above functional residual capacity afterloads the right heart by increasing pulmonary arterial impedance [52-55]; if this mechanism becomes prominent, then reduced right heart output may not simply reflect preload reserve, but instead afterload sensitivity. On the Guyton diagram, afterload sensitivity is illustrated not by an inspiratory rightwards shift in the cardiac function curve relative to the system venous return curve, but instead by a reduced slope of the cardiac function curve [2]. Clinically, when pulmonary compliance is severely reduced, or in patients with pulmonary arterial hypertension, right ventricular afterload sensitivity may impair the diagnostic characteristics of SVV and PPV [43, 56-60]. While smaller tidal volume could also play a role in these findings, animal studies point towards reduced pulmonary compliance as the culprit [61, 62] [figure 8].

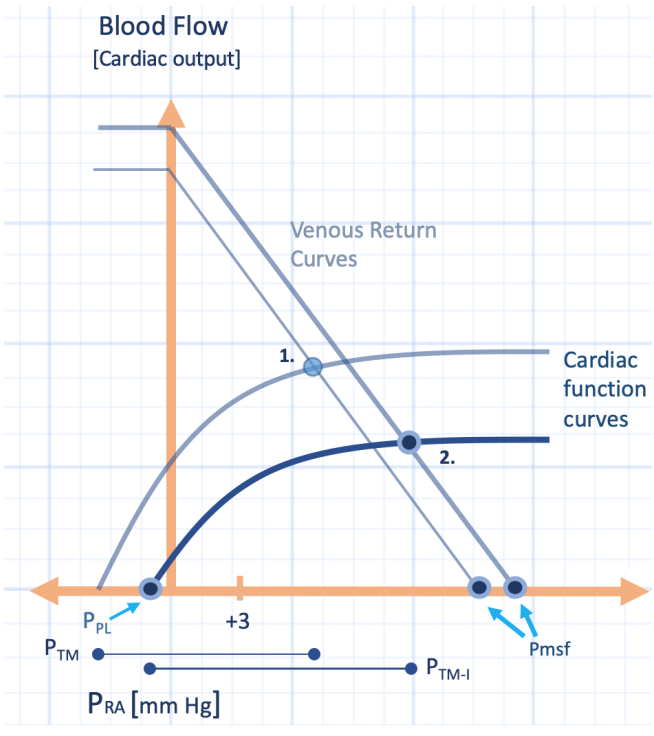

Figure 8: The phenomenon of afterload sensitivity. This patient is not fluid responsive as the operating point 1 lies on the flat portion of the cardiac function curve. However, if this patient has severe ARDS or pulmonary arterial hypertension, increased lung volume with a passive mechanical breath enlarges right ventricular [RV] afterload. Thus, the mechanical breath raises intra-thoracic pressure [or pleural pressure, Ppl] shifting the cardiac function curve rightwards, it also bends the curve downwards because of the afterload effect. RV output falls [y-axis] between point 1 and 2 and this generates stroke volume variation in the left ventricle 1-3 cardiac cycles later. As well, the right atrial trans-mural pressure [Ptm] rises on inspiration [Ptm-I] which may cause LV variation from interdependence.

Additionally, if the left ventricle is afterload sensitive – as in systolic heart failure – then the inspiratory intra-thoracic pressure rise with passive mechanical ventilation both unloads the left ventricle and improves its compliance via ventricular interdependence. These phenomena enhance dUP, creating pulse pressure

variation [3, 63-66] [figure 9]. Further, the initial validation cohorts did not have cardiac arrhythmia, which alters stroke volume as a function of varying diastole length.

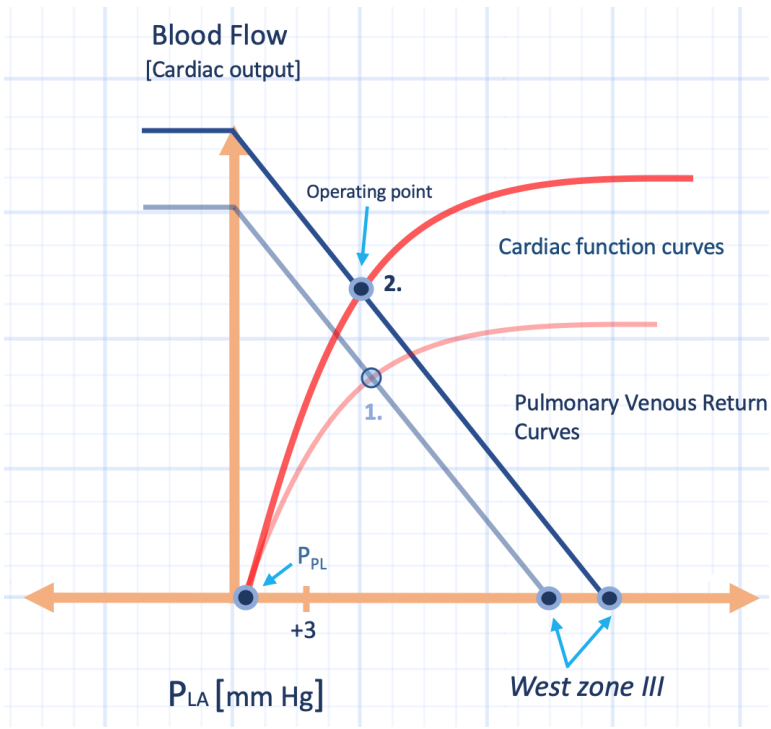

Figure 9: Enhanced d UP in left heart failure. This patient has poor LV function and the operating point begins at point 1. With a mechanical breath there is improved left ventricular afterload and the left ventricular [LV] cardiac function curve shifts upwards; improved function also occurs by increased LV compliance as the right ventricular [RV] volume shrinks during mechanical inspiration. As well, pulmonary venous return is enhanced because of West zone III. There is a large increase in LV output [y-axis] from point 1 to point 2 which augments inspiratory d UP.

Finally, because dUP and dDOWN were derived in patients fully adapted with the ventilator and with a certain heart rate to respiratory rate ratio, excessive respiratory rate also degrades the predictive value of SVV [67] – right heart output no longer reaches the left heart during mechanical expiration to form d DOWN.

Given the caveats above, FHM methods that do not rely upon intra-thoracic pressure change as the cardio-circulatory stress reduce some uncertainty. Bedside tests that alter the venous return function do just this. Passive leg raising, the end-expiratory occlusion test and the mini fluid challenge are three such methods which outperform those that rely on intra-thoracic pressure change as the cardiovascular stress, both in patients breathing spontaneously and with arrhythmia [56, 68, 69], as discussed below.

Methods of Measuring Left Ventricular Stroke Volume Variation

Until this point, the physiology discussed has focused on left ventricular stroke volume variation as a marker of preload responsiveness. Measuring instantaneous left ventricular stroke volume can be done at the bedside in a variety of ways [68, 70]. Perhaps the most direct way is via changes in aortic blood velocity [71, 72] during a single cardiac cycle. If the cross-sectional area of a tube is known [e.g.

obtained by duplex ultrasound] as well as the velocity of a liquid moving through it, then flow is calculated as the product of area and velocity. Of course, this assumes that the area of the aortic outflow tract or the aorta itself does not change during a respiratory cycle.

Bioreactance cardiac output measurement is possible because changes in intra-thoracic blood volume induce phase shifts of oscillating electrical current [68]. This method of stroke-volume calculation is correlated with thermodilution and pulse-contour analysis [73, 74]. However, as above, it is important to understand that performance characteristics are critically-dependent upon the patient population and the cardio-circulatory stress employed [75-77].

Other methods of assessing stroke volume involve the method of pulse-contour analysis, which uses the morphology of a single arterial pressure deflection to derive stroke volume. In general, there are two approaches to pulse-contour analysis: calibrated and un-calibrated. The former may employ lithium dilution or trans-pulmonary thermodilution as calibration methods. By contrast, un-calibrated systems use proprietary algorithms derived from patient demographics to obtain stroke volume from the arterial pulse contour [78-82]. Importantly, these devices may not correlate well with each other and with pulmonary artery catheter-derived cardiac output [78] such that the validation of one technology in one group of patients does not guarantee that another form of pulse contour analysis will perform equally well.

In addition to the method by which stroke volume is calculated, it is also critical to distinguish what stress upon the cardiovascular system is used to instigate stroke volume variation. In general, the term 'variation' implies that the stress is intra-thoracic pressure; in other words, variation induced by the respiratory cycle. This is distinct from stressing venous return [e.g. fluid challenge, passive leg raise or end-expiratory occlusion test] as discussed below. Importantly, the method of FHM impacts the sensitivity and specificity of predicting fluid responsiveness [83-85].

A commonly-used surrogate of left ventricular stroke volume variation is the pulse pressure variation [PPV]. Because aortic pulse pressure [aortic systolic pressure – aortic diastolic pressure] directly reflects left ventricular stroke volume [as a function of central aortic compliance] on a beat-to-beat basis, pulse pressure variation can accurately reflect left ventricular stroke volume variation [3, 33]. Prior to PPV, systolic pressure variation [SPV] was used to detect volume responsiveness and this measure was initially described in the late 1970s [70]. In Perel's classic study, systolic pressure variation was defined as the difference between maximal systolic pressure and minimal systolic pressure as compared to an apneic, systolic baseline [86]. Systolic pressure variation was highly correlated with graded hemorrhage. This physiology was later confirmed in humans [30-32] and discussed in more detail above. However, given concern for the direct effect of intra-thoracic pressure on aortic systolic pressure variation [21, 27], pulse pressure variation [PPV] was introduced. Because intra-thoracic pressure [ITP] affects systolic and diastolic pressures equally over the course of a respiratory cycle, the contribution of ITP is controlled [33]. In other words, because arterial compliance remains stable over the course of a respiratory cycle, changing pulse pressure directly reflects left ventricular stroke volume [27, 87, 88]. In a landmark paper, Michard and colleagues [18] showed that in fully-passive, septic patients, PPV was

superior to SPV for predicting fluid responsiveness. PPV is calculated by subtracting the maximal pulse pressure from the minimal pulse pressure and dividing the difference by the mean of the two [33] [figure 10].

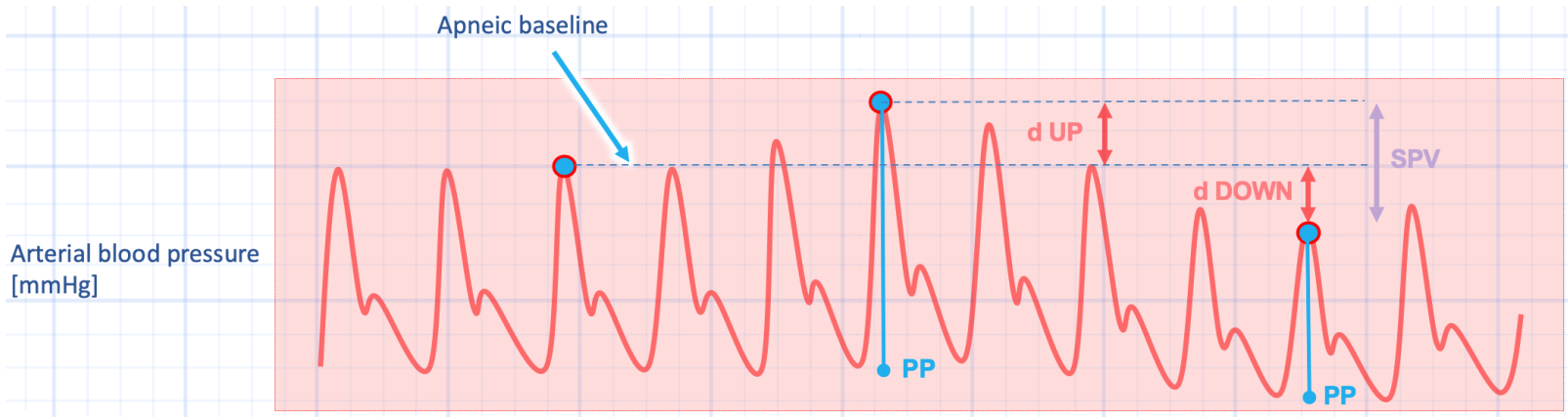

Figure 10: The relationship between d UP, d DOWN, systolic pressure variation [SPV] and pulse pressure variation [PPV]. Delta UP [d UP] is the inspiratory rise in systolic pressure above the apneic baseline, whereas delta DOWN is the expiratory fall in systolic pressure below the apneic baseline. Again, this morphology only applies to patients totally passive with the mechanical ventilator. SPV is the difference between the greatest systolic pressure and lowest systolic pressure – essentially the summation of d UP and d DOWN. PPV is the difference between the maximal and minimal values of pulse pressure [PP] divided by the mean of these two values.

An even less-invasive method of tracking left ventricular outflow variation is plethysmographic waveform analysis; this has been correlated with systolic pressure variation [65, 89]. However, vasomotor tone alters the plethysmographic signal and degrades its utility in the intensive care unit [90, 91].

Assessment of the Vena Cavae

Visualization of the superior and inferior vena cavae via ultrasonography is another means of functional hemodynamic monitoring. Unlike variation in left ventricular output, the clinician transduces vena cavae diameter change in response to intra-thoracic pressure variation. In order to understand how the vena cavae vary in diameter, one must apprehend the central venous pressure in relation to the intra-thoracic pressure and intra-abdominal pressure; that is the vena cavae transmural pressure.

Vena Cavae Transmural Pressure

Having discussed the determinants of central venous pressure and the relationship between CVP, volume status and volume responsiveness at the outset, there is one final principle to be considered: the vena cavae transmural pressure. The transmural pressure of the vena cavae is the pressure within the vessel less the ambient pressure. A critically important distinction between the superior vena cava [SVC]

and the inferior vena cava [IVC] is that the ambient pressure of the SVC is the intra-thoracic pressure whereas the ambient pressure of the IVC is intra-abdominal pressure [92]. When the transmural pressure of the vena cavae increases, their dimensions tend to increase; nevertheless, the relationship between the transmural pressure and diameter of the vena cavae is curvilinear such that at small transmural pressures, there is great capacity for diameter change. Conversely, at high transmural pressure, there is little capacity for diameter change [92].

Assessment of the Inferior Vena Cava

Often there is confusion surrounding IVC assessment at the bedside; this may arise from the difference in physiology between the patient who is fully passive with the ventilator and one in whom spontaneous inspiratory efforts are generated. In the heavily sedated and, potentially, paralyzed patients who are fully adapted with the mechanical ventilator and receiving relatively large tidal volumes, inspiratory IVC dilation was observed to accurately predict volume responsiveness [19]. This brings up two important considerations. First, the reason for vessel dilation is that – during a completely passive mechanical breath – the CVP increases as the cardiac function and venous return curves shift rightwards [figure 3]. The rise in CVP is transmitted down the IVC and the pressure within the vessel rises relative to the intra-abdominal pressure; in other words, the trans-mural pressure of the IVC increases. If the IVC is on the 'ascending limb' of its pressure-radius curve, then there is dilation; this is thought to be a surrogate for cardiac preload responsiveness [93] [figure 11]. Second, this physiology reemphasizes that FHM requires a defined stress upon the cardiovascular system that is consistent and reproducible. The patients in whom IVC dilation predicted preload reserve were all passive with the ventilator and receiving relatively large tidal volumes in volume-controlled ventilation. If there is deviation from this highly specific and reproducible stress upon the cardio-circulatory system, then it is unknown if change in cardiovascular response [i.e. IVC diameter change] is due to true differences in cardiovascular state [e.g. volume responsiveness] or due to variation in stress applied to the system.

By contrast, patients generating spontaneous inspiratory efforts tend to collapse their IVC. The reason IVC collapse occurs is that a Starling resistor is generated – when the pressure within a distensible tube drops below its ambient pressure; that is, transmural pressure falls. Therefore, IVC collapse is encouraged by falling CVP, rising intra-abdominal pressure, or a combination of both [figure 11].

As discussed above, the degree to which the CVP falls during a spontaneous inspiratory effort depends upon three competing variables: 1. the drop in pleural pressure, 2. the venous return function and 3. the cardiac function. This should make intuitive sense – the pressure within the right atrium during spontaneous inspiration is influenced by the pleural pressure pulling the CVP down, the venous return from the lower body pushing the CVP up and the cardiac function ejecting blood from the thorax – also pushing the CVP down. Diminished pleural pressure is depicted by shifting the cardiac function curve leftwards with respect to the

venous return curve [94]; this favours a fall in CVP and the intra-luminal pressure of the IVC [figure 3].

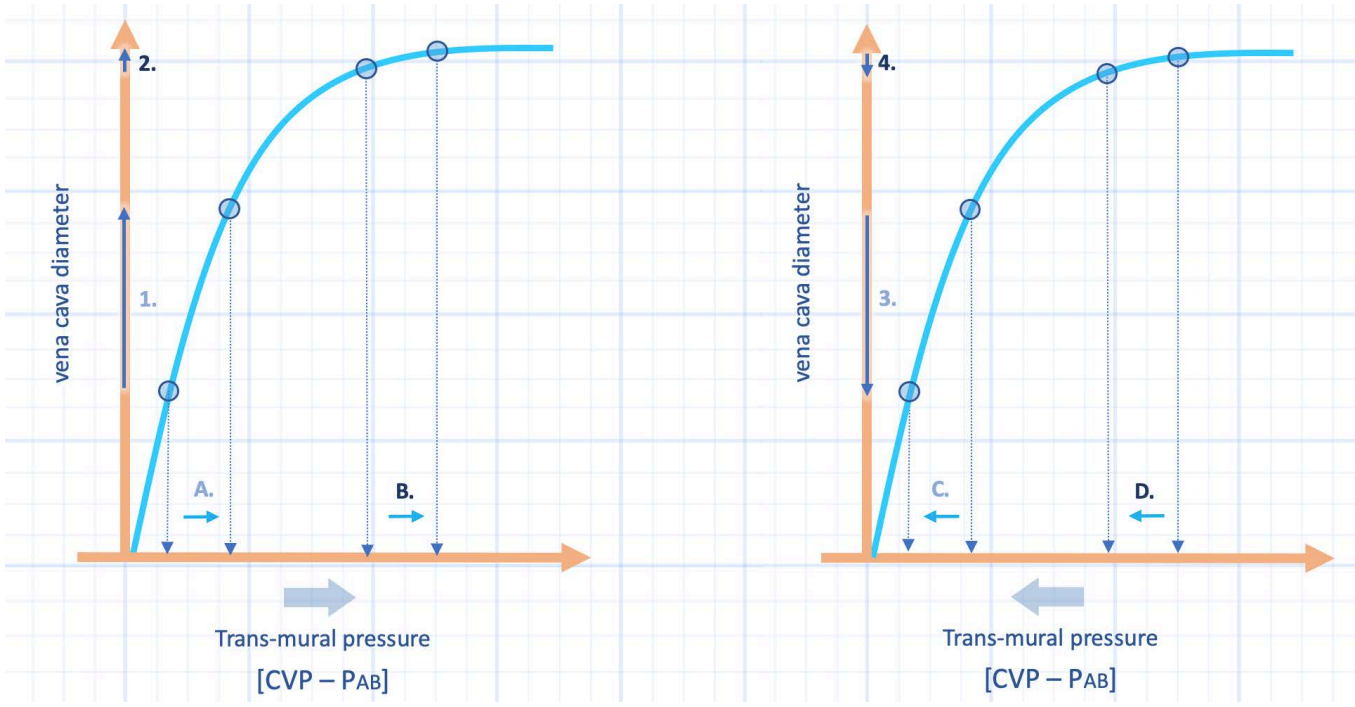

Figure 11: The vena cava compliance curve. Left panel: The patient is passive with the ventilator. For a similar increase in transmural pressure on the x-axis [e.g. an increase in the CVP] – arrow A & B – there is significant difference in vena cava diameter change depending on the baseline transmural pressure – arrow 1 & arrow 2 on the y-axis. Right panel: The vena cava compliance curve in the patient generating inspiratory effort. Compare curves C and D [on the x-axis] caused by diminished transmural pressure; diameter change is on the y-axis [arrows 3 and 4]. CVP is central venous pressure; Pab is abdominal pressure.

But does this inspiratory reduction in central venous pressure tell us anything definitive about a patient's 'volume status' or 'volume responsiveness?' Unfortunately, no [93, 95-100]. The reason is that the central venous pressure [and therefore IVC transmural pressure] depends upon the intersection of venous return and cardiac function – two phenomena each with multiple determinants. 'Volume status' plays a role in venous return in that hypovolemia tends to decrease venous return and therefore, CVP, but venous return also has multiple other determinants unrelated to volume status. This explains the poor relationship between volume status and CVP [97]. 'Volume responsiveness,' by contrast, is determined by how far the operating point is from the plateau of the cardiac function curve. Because the slope of the cardiac function curve is hard to know with certainty, almost any CVP may fall upon the plateau, especially in patients with cardiac abnormalities [e.g. those in the intensive care unit] [14]. Thus, a low CVP may or may not be on the ascending portion of the cardiac function curve [figure 3, see also chapter 6 and 10].

Complicating matters is that increased abdominal pressure facilitates IVC collapse. Because positive end-expiratory pressure, intra-abdominal hypertension and breathing pattern all affect abdominal pressurization [50, 51, 101-103], IVC collapse can uncouple from CVP; this may lead the clinician even further away from the patient's true cardiovascular state.

Thus, inspiratory IVC collapse tells us that the CVP falls below the intra-abdominal pressure. If there is no pathogenic or iatrogenic pressurization of the

abdomen [e.g. PEEP, auto-PEEP, ascites], and inspiration is not stressed [e.g. dyspnea, breathing through an endotracheal tube], then IVC collapse tells us that the CVP is low [104]. Low CVP may be the result of: hypovolemia, high resistance to venous return [e.g. alpha agonist], high venous capacitance [e.g. venodilators, sepsis], and hyper-dynamic cardiac function [e.g. extrinsic or intrinsic adrenergic tone] or any combination thereof.

Assessment of the Superior Vena Cava

As the superior vena cava is an intra-thoracic structure, adequately assessing its respiratory diameter variation necessitates trans-esophageal ultrasonography. Recall that the transmural pressure of the superior vena cava [SVC] is determined by the SVC intra-luminal pressure and intra-thoracic pressure. In patients who are fully passive with the mechanical ventilator, inspiration has seemingly paradoxical responses upon the IVC and SVC. As above, in the absence of inspiratory patient effort, mechanical insufflation of the lungs facilitates IVC dilation. By contrast, in the absence of inspiratory patient effort, mechanical inspiration favours SVC collapse.

While mechanical inspiration increases CVP, as demonstrated by the rightward shift of the cardiac function curve relative to the venous return curve [figure 3], the intra-thoracic, or pleural, pressure rises more than the CVP does. Consequently, the SVC transmural pressure falls. The reason that the CVP does not increase as much as the intra-thoracic pressure is because mechanical inspiration retards venous return from the venous capacitance beds; this reduces SVC intra-luminal pressure relative to the intra-thoracic pressure. The aforementioned explanation may be better gleaned from the Guyton diagram [figure 12]. The transmural pressure of the SVC is equivalent to the right atrial transmural pressure; that is, the CVP [the operating point] minus the intra-thoracic pressure [the x-intercept of the cardiac function curve]. With a mechanical breath, the x-intercept of the cardiac function curve shifts rightwards with the intra-thoracic pressure. While CVP increases with mechanical inspiration, the difference between the CVP and the intra-thoracic pressure falls. Thus, a passive, mechanical breath collapses the SVC; though the degree to which the SVC shrinks depends upon where the SVC lies upon its transmural – diameter relationship [figure 11].

As with assessment of inspiratory IVC dilation in the passive patient, SVC collapse is able to identify patients who are volume responsive [20]. Again, this study emphasizes that in FHM, the validity of the measured response is inexorably linked to the stress applied to the system. Whether assessing the SVC or IVC, the stress administered to the cardiovascular system is the change in intra-thoracic pressure. In volume-control mechanical ventilation, there are multiple determinants of intra-thoracic pressure – the presence and degree of patient effort, the applied tidal volume and chest wall compliance [3, 4]. If a clinician aims to use a standardized response [e.g. vena cavae diameter change] to facilitate clinical decision-making, then the patient must be subjected to an equivalent cardio-circulatory stress [i.e. intra-thoracic pressure change] as the validation cohort. Significant deviation in the

stress applied will cloud the measured response. Thus, in addition to receiving a similar tidal volume and having similar chest wall characteristics as the derivation cohort, paralysis or at least very heavy sedation is a pre-requisite to ensure that intra-thoracic pressure increases reliably with each breath. With varying inspiratory effort, intra-thoracic pressure changes unpredictably; consequently, evaluation for vena cavae diameter change, or any hemodynamic response for that matter, is confounded.

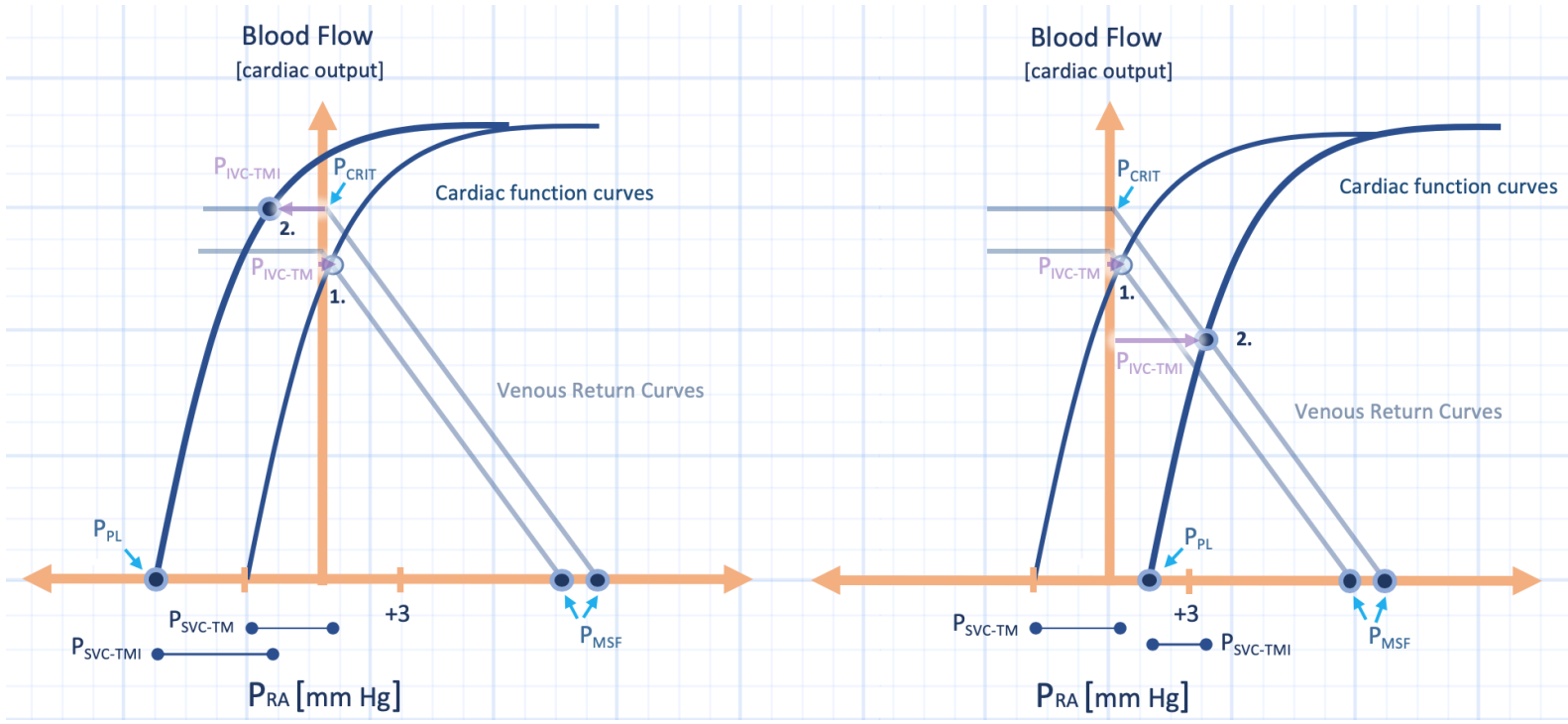

Figure 12: The effect of inspiration on SVC and IVC transmural pressure. Left panel: A spontaneous breath. The SVC transmural pressure at baseline [Psvc-tm, below x-axis] is the right atrial pressure [Pra] less the pleural pressure [the x-intercept of the cardiac function curve – Ppl]. The operating point at baseline is at point 1. The baseline IVC transmural pressure [Pivc-tm] is the Pra relative to the critical collapse pressure [Pcrit] and represented by the small, positive purple arrow. A breath in moves the cardiac function curve leftwards with the Ppl and moves the operating point to 2. This increases the SVC distending pressure [Psvc-tmi] seen below the x-axis. By contrast, it decreases the IVC distending pressure [leftwards, purple arrow, Pivc-tmi] as Pra falls below Pcrit - so the SVC distends and the IVC collapses. Right panel: A passive mechanical breath from operating point 1 to 2. The cardiac function curve shifts rightwards as Ppl rises. Because the SVC is referenced to Ppl, its distending pressure shrinks on inspiration [Psvc-tmi]; because the IVC is referenced to the Pcrit, its distending pressure rises on inspiration [purple arrow, Pivc-tmi] Thus, a passive mechanical breath shrinks the SVC but distends the IVC.

Passive Leg Raising

Thus far, intra-thoracic pressure change has been the stress placed upon the cardiovascular system. While we assume that the physiological consequence of mechanical inspiration is to simply decrease right ventricular preload, and therefore right heart output, the situation is much more complicated. As discussed above, unpredictable and non-standardized intra-thoracic pressure fluctuation confounds left ventricular stroke volume variation. Further, intra-thoracic pressure and lung volume change affect the heart in ways beyond right ventricular preload reduction. As illustrated on the Guyton diagram, the basis of intra-thoracic pressure as a hemodynamic stress is the parallel shift of the cardiac function curve relative to the

systemic venous return curve. However, the slope of the cardiac function curve can also change in response to intra-thoracic pressure and volume; this may confound stroke volume variation. Therefore, shifting the venous return curve relative to the cardiac function curve may circumvent some of the aforementioned caveats. If the operating point of the cardiovascular system falls upon the ascending portion of the cardiac function curve, then shifting the venous return curve rightwards increases cardiac output. By contrast, if the cardiac function curve is intersected at its plateau, then right shift of the venous return curve will not increase cardiac output [figure 13].

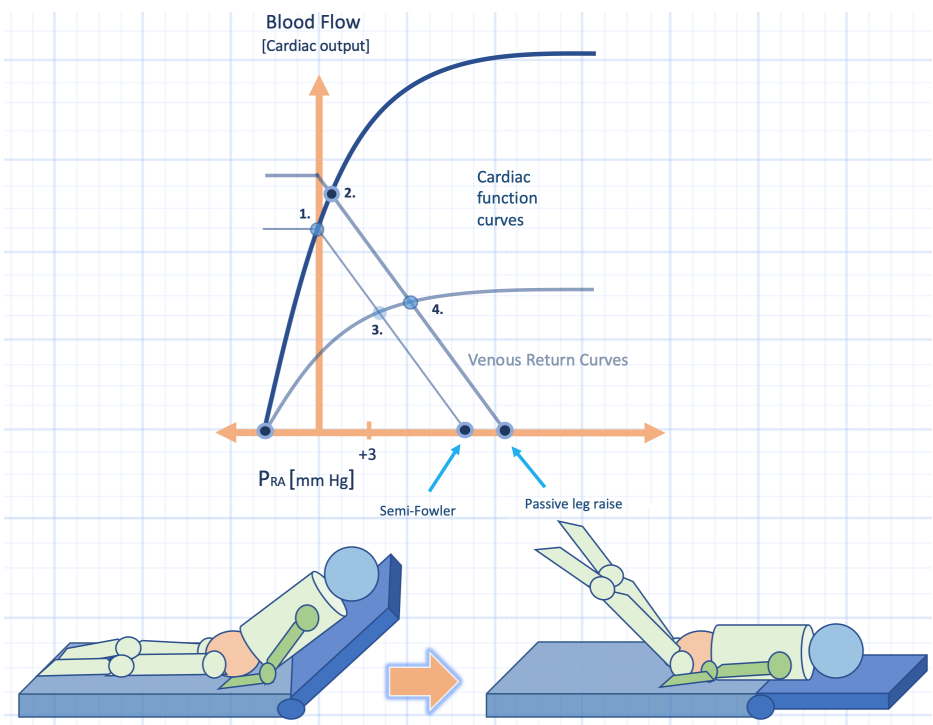

Figure 13: Functional hemodynamic monitoring by augmenting venous return. At semi-Fowler baseline, a fluid responsive patients begins at operating point 1. A passive leg raise [PLR] increases venous return and the operating point moves to 2. Cardiac output [y-axis] rises. By contrast, a fluid non-responsive patient begins at operating point 3. The same leg raise moves the venous return curve to operating point 4 - there is little increase in cardiac output. Pra is right atrial pressure or central venous pressure. Pain should be minimized to prevent adrenergic-induced cardiac augmentation. Compression stockings should be removed and the maneuver should not be performed in patients with elevated intracranial pressure.

Because passive leg raise [PLR] does not alter the cardiac function curve, per se, nor does it rely on intra-thoracic pressure change as the cardiovascular stress, its ability to predict fluid responsiveness in patients breathing spontaneously and with arrhythmia is improved [37, 105]. Importantly, however, in spontaneously breathing patients, direct assessment of aortic flow must be utilized; PPV loses predictive power when performing a passive leg raise [37, 105-109]. However, there is evidence supporting pulse-contour derived stroke volume change during the passive leg raise in spontaneously breathing patients [83, 84].

The PLR is performed by moving the patient from semi-recumbent to the supine position with the legs raised 45 degrees relative to the torso [figure 13]. The technique recruits blood from both the legs and the abdominal compartment; the legs contain about 150 mL of blood volume for recruitment [110]. However, intra-abdominal hypertension may retard venous inflow to the right heart and impair the diagnostic utility of the passive leg raise [111]. The passive leg raise can increase

static markers of cardiac preload as well as LV ejection time [37, 112]. Typically, maximal augmentation of cardiac output in response to PLR occurs within 30 to 90 seconds, so instantaneous flow monitoring is mandatory. PLR should be painless so as to avoid sympathetically-induced cardiac output augmentation; further, PLR should be avoided in patients with head trauma as the maneuver can increase intra-cerebral pressure. Lastly, compression stockings may alter lower extremity blood volume recruitment, so these devices should be removed prior to a passive leg raise [113].

Another test developed to detect volume responsiveness is the end-expiratory occlusion maneuver [84]. Typically, a 15-second end-expiratory pause is applied; this gives time to measure the rise in stroke volume following release of inspiratory intra-thoracic pressure. Continuous cardiac output monitoring is employed and a 5% stroke volume augmentation is a good predictor of preload responsiveness. Because the test is averaged over a number of cardiac cycles, it may be used in patients with arrhythmia and spontaneous breathing activity light enough to allow the test. Additionally, end-expiratory occlusion is superior to PPV in patients with poor respiratory system compliance [56], though results have not been totally generalizable [114].

Conclusion

Functional hemodynamic monitoring is a step forward in the ICU. Predicting the cardiovascular response to volume loading is important and FHM is superior as compared to traditional, static parameters of cardiac preload [68, 98, 99, 115]. Nevertheless, with the explosion in various technologies for assessing stroke volume variation and the dissemination of pocket-sized ultrasound devices, it is more important than ever for intensivists to fully appreciate the physiological underpinnings of these ICU monitoring advancements. The mechanical linkage between the cardiovascular and respiratory systems drives many observations gleaned from these new devices. If the underlying physiology is ignored, inappropriate management decisions could be made; potentially harming critically-ill patients. As with all diagnostic tests, the imperfect sensitivity and specificity of FHM highlight key caveats. As described, imperfect test performance may arise from difference between the cardiovascular stress applied at the bedside as compared to the derivation cohort. Additionally, the multi-faceted nature of heart-lung interaction coupled with unique patient pathophysiology may also muddy test performance. Regardless, intensivists should approach hemodynamic conundra with a pretest probability, apply a useful diagnostic maneuver and reassess thereafter; therein lies the challenge and excitement of intensive care medicine.

References

1. Pinsky, M.R. and D. Payen, Functional hemodynamic monitoring. Crit Care, 2005. 9(6): p. 566-72.
2. Broccard, A.F., Cardiopulmonary interactions and volume status assessment. J Clin Monit Comput, 2012. 26(5): p. 383-91.
3. Mesquida, J., H.K. Kim, and M.R. Pinsky, Effect of tidal volume, intrathoracic pressure, and cardiac contractility on variations in pulse pressure, stroke volume, and intrathoracic blood volume. Intensive Care Med, 2011. 37(10): p. 1672-9.
4. Robotham, J.L. and S.M. Scharf, Effects of positive and negative pressure ventilation on cardiac performance. Clin Chest Med, 1983. 4(2): p. 161-87.
5. Guyton, A.C., A.W. Lindsey, and B.N. Kaufmann, Effect of mean circulatory filling pressure and other peripheral circulatory factors on cardiac output. Am J Physiol, 1955. 180(3): p. 463-8.
6. Baird, R.N. and W.M. Abbott, Elasticity and compliance of canine femoral and jugular vein segments. Am J Physiol, 1977. 233(1): p. H15-21.
7. Guyton, A.C., D. Polizo, and G.G. Armstrong, Mean circulatory filling pressure measured immediately after cessation of heart pumping. Am J Physiol, 1954. 179(2): p. 261-7.
8. Magder, S. and B. De Varennes, Clinical death and the measurement of stressed vascular volume. Crit Care Med, 1998. 26(6): p. 1061-4.
9. Gelman, S., Venous function and central venous pressure: a physiologic story. Anesthesiology, 2008. 108(4): p. 735-48.
10. Rothe, C.F., Physiology of venous return. An unappreciated boost to the heart. Arch Intern Med, 1986. 146(5): p. 977-82.
11. Feihl, F. and A.F. Broccard, Interactions between respiration and systemic hemodynamics. Part I: basic concepts. Intensive Care Med, 2009. 35(1): p. 45-54.
12. Guyton, A.C., Determination of cardiac output by equating venous return curves with cardiac response curves. Physiol Rev, 1955. 35(1): p. 123-9.
13. Magder, S., Central venous pressure: A useful but not so simple measurement. Crit Care Med, 2006. 34(8): p. 2224-7.
14. Magder, S. and F. Bafaqeeh, The clinical role of central venous pressure measurements. J Intensive Care Med, 2007. 22(1): p. 44-51.
15. Marini, J.J., B.H. Culver, and J. Butler, Effect of positive end-expiratory pressure on canine ventricular function curves. J Appl Physiol Respir Environ Exerc Physiol, 1981. 51(6): p. 1367-74.
16. Pinsky, M.R., Recent advances in the clinical application of heart-lung interactions. Curr Opin Crit Care, 2002. 8(1): p. 26-31.
17. Jardin, F., et al., Influence of lung and chest wall compliances on transmission of airway pressure to the pleural space in critically ill patients. Chest, 1985. 88(5): p. 653-8.
18. Michard, F., et al., Relation between respiratory changes in arterial pulse pressure and fluid responsiveness in septic patients with acute circulatory failure. Am J Respir Crit Care Med, 2000. 162(1): p. 134-8.
19. Barbier, C., et al., Respiratory changes in inferior vena cava diameter are helpful in predicting fluid responsiveness in ventilated septic patients. Intensive Care Med, 2004. 30(9): p. 1740-6.
20. Vieillard-Baron, A., et al., Superior vena caval collapsibility as a gauge of volume status in ventilated septic patients. Intensive Care Med, 2004. 30(9): p. 1734-9.
21. Denault, A.Y., et al., Determinants of aortic pressure variation during positive-pressure ventilation in man. Chest, 1999. 116(1): p. 176-86.
22. Boltwood, C.M., Jr., R.F. Appleyard, and S.A. Glantz, Left ventricular volume measurement by conductance catheter in intact dogs. Parallel conductance volume depends on left ventricular size. Circulation, 1989. 80(5): p. 1360-77.
23. Mitchell, J.R., et al., RV filling modulates LV function by direct ventricular interaction during mechanical ventilation. Am J Physiol Heart Circ Physiol, 2005. 289(2): p. H549-57.
24. Buda, A.J., et al., Effect of intrathoracic pressure on left ventricular performance. N Engl J Med, 1979. 301(9): p. 453-9.
25. Brower, R., et al., Effect of lung inflation on lung blood volume and pulmonary venous flow. J Appl Physiol (1985), 1985. 58(3): p. 954-63.
26. Scharf, S.M., et al., Hemodynamic effects of positive-pressure inflation. J Appl Physiol Respir Environ Exerc Physiol, 1980. 49(1): p. 124-31.
27. Robotham, J.L., et al., A re-evaluation of the hemodynamic consequences of intermittent positive pressure ventilation. Crit Care Med, 1983. 11(10): p. 783-93.
28. Magder, S., Clinical usefulness of respiratory variations in arterial pressure. Am J Respir Crit Care Med, 2004. 169(2): p. 151-5.
29. Jardin, F., Cyclic changes in arterial pressure during mechanical ventilation. Intensive Care Med, 2004. 30(6): p. 1047-50.

30. Rooke, G.A., H.A. Schwid, and Y. Shapira, The effect of graded hemorrhage and intravascular volume replacement on systolic pressure variation in humans during mechanical and spontaneous ventilation. Anesth Analg, 1995. 80(5): p. 925-32.
31. Ornstein, E., et al., Systolic pressure variation predicts the response to acute blood loss. J Clin Anesth, 1998. 10(2): p. 137-40.
32. Tavernier, B., et al., Systolic pressure variation as a guide to fluid therapy in patients with sepsis-induced hypotension. Anesthesiology, 1998. 89(6): p. 1313-21.
33. Michard, F. and J.L. Teboul, Using heart-lung interactions to assess fluid responsiveness during mechanical ventilation. Crit Care, 2000. 4(5): p. 282-9.
34. Soubrier, S., et al., Can dynamic indicators help the prediction of fluid responsiveness in spontaneously breathing critically ill patients? Intensive Care Med, 2007. 33(7): p. 1117-24.
35. Heenen, S., D. De Backer, and J.L. Vincent, How can the response to volume expansion in patients with spontaneous respiratory movements be predicted? Crit Care, 2006. 10(4): p. R102.
36. Magder, S., Predicting volume responsiveness in spontaneously breathing patients: still a challenging problem. Crit Care, 2006. 10(5): p. 165.
37. Monnet, X., et al., Passive leg raising predicts fluid responsiveness in the critically ill. Crit Care Med, 2006. 34(5): p. 1402-7.
38. De Backer, D., et al., Pulse pressure variations to predict fluid responsiveness: influence of tidal volume. Intensive Care Med, 2005. 31(4): p. 517-23.
39. Renner, J., et al., Stroke volume variation during hemorrhage and after fluid loading: impact of different tidal volumes. Acta Anaesthesiol Scand, 2007. 51(5): p. 538-44.
40. Jacques, D., et al., Pulse pressure variation and stroke volume variation during increased intra-abdominal pressure: an experimental study. Crit Care, 2011. 15(1): p. R33.
41. Duperret, S., et al., Increased intra-abdominal pressure affects respiratory variations in arterial pressure in normovolaemic and hypovolaemic mechanically ventilated healthy pigs. Intensive Care Med, 2007. 33(1): p. 163-71.
42. Preau, S., et al., Hemodynamic changes during a deep inspiration maneuver predict fluid responsiveness in spontaneously breathing patients. Cardiol Res Pract, 2012. 2012: p. 191807.
43. Mahjoub, Y., et al., Assessing fluid responsiveness in critically ill patients: False-positive pulse pressure variation is detected by Doppler echocardiographic evaluation of the right ventricle. Crit Care Med, 2009. 37(9): p. 2570-5.
44. Banner, M.J., M.J. Jaeger, and R.R. Kirby, Components of the work of breathing and implications for monitoring ventilator-dependent patients. Crit Care Med, 1994. 22(3): p. 515-23.
45. Peters, J., et al., Negative intrathoracic pressure decreases independently left ventricular filling and emptying. Am J Physiol, 1989. 257(1 Pt 2): p. H120-31.
46. Fessler, H.E., Heart-lung interactions: applications in the critically ill. Eur Respir J, 1997. 10(1): p. 226-37.
47. Teboul, J.L. and X. Monnet, Prediction of volume responsiveness in critically ill patients with spontaneous breathing activity. Curr Opin Crit Care, 2008. 14(3): p. 334-9.
48. Freitas, F.G., et al., Predictive value of pulse pressure variation for fluid responsiveness in septic patients using lung-protective ventilation strategies. Br J Anaesth, 2013. 110(3): p. 402-8.
49. Tavernier, B. and E. Robin, Assessment of fluid responsiveness during increased intra-abdominal pressure: keep the indices, but change the thresholds. Crit Care, 2011. 15(2): p. 134.
50. Fessler, H.E., et al., Effects of Positive End-Expiratory Pressure on the Gradient for Venous Return. American Review of Respiratory Disease, 1991. 143(1): p. 19-24.
51. Jellinek, H., et al., Influence of positive airway pressure on the pressure gradient for venous return in humans. J Appl Physiol (1985), 2000. 88(3): p. 926-32.
52. Whittenberger, J.L., et al., Influence of state of inflation of the lung on pulmonary vascular resistance. J Appl Physiol, 1960. 15: p. 878-82.
53. Permutt, S., et al., Effect of lung inflation on static pressure-volume characteristics of pulmonary vessels. J Appl Physiol, 1961. 16: p. 64-70.
54. Permutt, S. and R.L. Riley, Hemodynamics of Collapsible Vessels with Tone: The Vascular Waterfall. J Appl Physiol, 1963. 18: p. 924-32.
55. West, J.B., C.T. Dollery, and A. Naimark, Distribution of Blood Flow in Isolated Lung; Relation to Vascular and Alveolar Pressures. J Appl Physiol, 1964. 19: p. 713-24.
56. Monnet, X., et al., Passive leg-raising and end-expiratory occlusion tests perform better than pulse pressure variation in patients with low respiratory system compliance. Crit Care Med, 2012. 40(1): p. 152-7.
57. Wyler von Ballmoos, M., et al., Pulse-pressure variation and hemodynamic response in patients with elevated pulmonary artery pressure: a clinical study. Crit Care, 2010. 14(3): p. R111.
58. Daudel, F., et al., Pulse pressure variation and volume responsiveness during acutely increased pulmonary artery pressure: an experimental study. Crit Care, 2010. 14(3): p. R122.
59. Magder, S., Further cautions for the use of ventilatory-induced changes in arterial pressures to predict volume responsiveness. Critical Care, 2010. 14(5).
60. Venus, B., L.E. Cohen, and R.A. Smith, Hemodynamics and intrathoracic pressure transmission during controlled mechanical ventilation and positive end-expiratory pressure in normal and low compliant lungs. Crit Care Med, 1988. 16(7): p. 686-90.
61. da Silva Ramos, F.J., et al., Heart-lung interactions with different ventilatory settings during acute lung injury and hypovolaemia: an experimental study. Br J Anaesth, 2011. 106(3): p. 394-402.

62. Wiklund, C.U., et al., Influence of tidal volume on pulse pressure variations in hypovolemic ventilated pigs with acute respiratory distress-like syndrome. Anesthesiology, 2010. 113(3): p. 630-8.
63. Grace, M.P. and D.M. Greenbaum, Cardiac performance in response to PEEP in patients with cardiac dysfunction. Crit Care Med, 1982. 10(6): p. 358-60.
64. Rasanen, J., P. Nikki, and J. Heikkila, Acute myocardial infarction complicated by respiratory failure. The effects of mechanical ventilation. Chest, 1984. 85(1): p. 21-8.
65. Pizov, R., Y. Ya'ari, and A. Perel, The arterial pressure waveform during acute ventricular failure and synchronized external chest compression. Anesth Analg, 1989. 68(2): p. 150-6.
66. Atherton, J.J., et al., Diastolic ventricular interaction in chronic heart failure. Lancet, 1997. 349(9067): p. 1720-4.
67. De Backer, D., et al., Influence of Respiratory Rate on Stroke Volume Variation in Mechanically Ventilated Patients. Anesthesiology, 2009. 110(5): p. 1092-1097.
68. Marik, P.E., X. Monnet, and J.L. Teboul, Hemodynamic parameters to guide fluid therapy. Ann Intensive Care, 2011. 1(1): p. 1.
69. Muller, L., et al., An increase in aortic blood flow after an infusion of 100 ml colloid over 1 minute can predict fluid responsiveness: the mini-fluid challenge study. Anesthesiology, 2011. 115(3): p. 541-7.
70. Cannesson, M., et al., Pulse pressure variation: where are we today? J Clin Monit Comput, 2011. 25(1): p. 45-56.
71. Monnet, X., et al., Esophageal Doppler monitoring predicts fluid responsiveness in critically ill ventilated patients. Intensive Care Med, 2005. 31(9): p. 1195-201.
72. Feissel, M., et al., Respiratory changes in aortic blood velocity as an indicator of fluid responsiveness in ventilated patients with septic shock. Chest, 2001. 119(3): p. 867-73.
73. Raval, N.Y., et al., Multicenter evaluation of noninvasive cardiac output measurement by bioreactance technique. J Clin Monit Comput, 2008. 22(2): p. 113-9.
74. Keren, H., D. Burkhoff, and P. Squara, Evaluation of a noninvasive continuous cardiac output monitoring system based on thoracic bioreactance. Am J Physiol Heart Circ Physiol, 2007. 293(1): p. H583-9.
75. Squara, P., et al., Comparison of monitoring performance of Bioreactance vs. pulse contour during lung recruitment maneuvers. Crit Care, 2009. 13(4): p. R125.
76. Squara, P., Bioreactance for estimating cardiac output and the effects of passive leg raising in critically ill patients. Br J Anaesth, 2014. 112(5): p. 942.
77. Kupersztych-Hagege, E., et al., Bioreactance is not reliable for estimating cardiac output and the effects of passive leg raising in critically ill patients. Br J Anaesth, 2013. 111(6): p. 961-6.
78. Hadian, M., et al., Cross-comparison of cardiac output trending accuracy of LiDCO, PiCCO, FloTrac and pulmonary artery catheters. Crit Care, 2010. 14(6): p. R212.
79. Hamilton, T.T., L.M. Huber, and M.E. Jessen, PulseCO: a less-invasive method to monitor cardiac output from arterial pressure after cardiac surgery. Ann Thorac Surg, 2002. 74(4): p. S1408-12.
80. Pittman, J., et al., Continuous cardiac output monitoring with pulse contour analysis: a comparison with lithium indicator dilution cardiac output measurement. Crit Care Med, 2005. 33(9): p. 2015-21.
81. Felbinger, T.W., et al., Cardiac index measurements during rapid preload changes: a comparison of pulmonary artery thermodilution with arterial pulse contour analysis. J Clin Anesth, 2005. 17(4): p. 241-8.
82. Manecke, G.R., Edwards FloTrac sensor and Vigileo monitor: easy, accurate, reliable cardiac output assessment using the arterial pulse wave. Expert Rev Med Devices, 2005. 2(5): p. 523-7.
83. Biais, M., et al., Changes in stroke volume induced by passive leg raising in spontaneously breathing patients: comparison between echocardiography and Vigileo/FloTrac device. Crit Care, 2009. 13(6): p. R195.
84. Monnet, X., et al., Predicting volume responsiveness by using the end-expiratory occlusion in mechanically ventilated intensive care unit patients. Crit Care Med, 2009. 37(3): p. 951-6.
85. Davies, S.J., et al., Comparison of stroke volume and fluid responsiveness measurements in commonly used technologies for goal-directed therapy. J Clin Anesth, 2013. 25(6): p. 466-74.
86. Perel, A., R. Pizov, and S. Cotev, Systolic blood pressure variation is a sensitive indicator of hypovolemia in ventilated dogs subjected to graded hemorrhage. Anesthesiology, 1987. 67(4): p. 498-502.
87. Gunn, S.R. and M.R. Pinsky, Implications of arterial pressure variation in patients in the intensive care unit. Curr Opin Crit Care, 2001. 7(3): p. 212-7.
88. Morgan, B.C., et al., Hemodynamic effects of intermittent positive pressure respiration. Anesthesiology, 1966. 27(5): p. 584-90.
89. Partridge, B.L., Use of pulse oximetry as a noninvasive indicator of intravascular volume status. J Clin Monit, 1987. 3(4): p. 263-8.
90. Monnet, X., et al., Prediction of fluid responsiveness by a continuous non-invasive assessment of arterial pressure in critically ill patients: comparison with four other dynamic indices. Br J Anaesth, 2012. 109(3): p. 330-8.
91. Landsverk, S.A., et al., Poor agreement between respiratory variations in pulse oximetry photoplethysmographic waveform amplitude and pulse pressure in intensive care unit patients. Anesthesiology, 2008. 109(5): p. 849-55.

92. Jardin, F. and A. Vieillard-Baron, Ultrasonographic examination of the venae cavae. Intensive Care Med, 2006. 32(2): p. 203-6.
93. Bodson, L. and A. Vieillard-Baron, Respiratory variation in inferior vena cava diameter: surrogate of central venous pressure or parameter of fluid responsiveness? Let the physiology reply. Crit Care, 2012. 16(6): p. 181.
94. Magder, S., Bench-to-bedside review: An approach to hemodynamic monitoring - Guyton at the bedside. Crit Care, 2012. 16(5): p. 236.
95. Muller, L., et al., Respiratory variations of inferior vena cava diameter to predict fluid responsiveness in spontaneously breathing patients with acute circulatory failure: need for a cautious use. Crit Care, 2012. 16(5): p. R188.
96. Corl, K., A.M. Napoli, and F. Gardiner, Bedside sonographic measurement of the inferior vena cava caval index is a poor predictor of fluid responsiveness in emergency department patients. Emerg Med Australas, 2012. 24(5): p. 534-9.
97. Shippy, C.R., P.L. Appel, and W.C. Shoemaker, Reliability of clinical monitoring to assess blood volume in critically ill patients. Crit Care Med, 1984. 12(2): p. 107-12.
98. Marik, P.E. and R. Cavallazzi, Does the central venous pressure predict fluid responsiveness? An updated meta-analysis and a plea for some common sense. Crit Care Med, 2013. 41(7): p. 1774-81.
99. Kumar, A., et al., Pulmonary artery occlusion pressure and central venous pressure fail to predict ventricular filling volume, cardiac performance, or the response to volume infusion in normal subjects. Crit Care Med, 2004. 32(3): p. 691-9.
100. Juhl-Olsen, P., C.A. Frederiksen, and E. Sloth, Ultrasound assessment of inferior vena cava collapsibility is not a valid measure of preload changes during triggered positive pressure ventilation: a controlled cross-over study. Ultraschall Med, 2012. 33(2): p. 152-9.
101. Lloyd, T.C., Jr., Effect of inspiration on inferior vena caval blood flow in dogs. J Appl Physiol Respir Environ Exerc Physiol, 1983. 55(6): p. 1701-8.
102. Rubinson, R.M., et al., Inferior Vena Caval Obstruction from Increased Intra-Abdominal Pressure - Experimental Hemodynamic and Angiographic Observations. Archives of Surgery, 1967. 94(6): p. 766-&.
103. Kimura, B.J., et al., The effect of breathing manner on inferior vena caval diameter. European Journal of Echocardiography, 2011. 12(2).
104. Kircher, B.J., R.B. Himelman, and N.B. Schiller, Noninvasive estimation of right atrial pressure from the inspiratory collapse of the inferior vena cava. Am J Cardiol, 1990. 66(4): p. 493-6.
105. Lamia, B., et al., Echocardiographic prediction of volume responsiveness in critically ill patients with spontaneously breathing activity. Intensive Care Med, 2007. 33(7): p. 1125-32.
106. Maizel, J., et al., Diagnosis of central hypovolemia by using passive leg raising. Intensive Care Med, 2007. 33(7): p. 1133-8.
107. Lafanechere, A., et al., Changes in aortic blood flow induced by passive leg raising predict fluid responsiveness in critically ill patients. Crit Care, 2006. 10(5): p. R132.
108. Preau, S., et al., Passive leg raising is predictive of fluid responsiveness in spontaneously breathing patients with severe sepsis or acute pancreatitis. Crit Care Med, 2010. 38(3): p. 819-25.
109. Cavallaro, F., et al., Diagnostic accuracy of passive leg raising for prediction of fluid responsiveness in adults: systematic review and meta-analysis of clinical studies. Intensive Care Med, 2010. 36(9): p. 1475-83.
110. Rutlen, D.L., F.J. Wackers, and B.L. Zaret, Radionuclide assessment of peripheral intravascular capacity: a technique to measure intravascular volume changes in the capacitance circulation in man. Circulation, 1981. 64(1): p. 146-52.
111. Mahjoub, Y., et al., The passive leg-raising maneuver cannot accurately predict fluid responsiveness in patients with intra-abdominal hypertension. Crit Care Med, 2010. 38(9): p. 1824-9.
112. Pozzoli, M., et al., Loading manipulations improve the prognostic value of Doppler evaluation of mitral flow in patients with chronic heart failure. Circulation, 1997. 95(5): p. 1222-30.
113. Monnet, X. and J.L. Teboul, Passive leg raising. Intensive Care Med, 2008. 34(4): p. 659-63.
114. Guinot, P.G., et al., End-expiratory occlusion manoeuvre does not accurately predict fluid responsiveness in the operating theatre. Br J Anaesth, 2014. 112(6): p. 1050-4.
115. Pinsky, M.R., Functional haemodynamic monitoring. Curr Opin Crit Care, 2014. 20(3): p. 288-93.

Chapter Nine

Updates in Respiratory Physiology

Abstract

Mechanical heart-lung interaction is an important set of concepts in the intensive care unit. Respiratory strain and stress underpin the phenomena of volutrauma and barotrauma on both the pulmonary parenchyma and vasculature. Strain and stress also define the energy applied to the lung over time - or power - tying together multiple avenues of lung injury research. Mechanical power also highlights the importance of basic physiology and assists our therapeutic approach. Prone position, positive end-expiratory pressure, airway pressure release ventilation, esophageal manometry, helium-oxygen mixtures, high flow nasal cannula and even fighter pilot flight suits are better understood when viewed through the prism of transpulmonary strain, stress and power. The heretofore principles of heart-lung interaction are expanded upon in this synopsis of clinically-relevant respiratory physiology.

Key Words: strain, stress, mechanical power, ergotrauma, volutrauma, barotrauma, driving pressure, prone position, airway pressure release ventilation, esophageal manometry, respiratory effort, work of breathing, high flow oxygen

Introduction

A pressure chamber within a pressure chamber; the heart within the thorax. Two pumps beating in-and-out of time, varying in physiology and pathophysiology between patients and within one patient during the arc of an illness. As such, when we inspect the size and function of the heart, we must respect its surroundings, for it is the bony thorax, mediastinum and spongy lungs which fashion the stage upon which the heart sets its performance.

Yet cardiovascular physiology and thoracic mechanics are typically taught separately, ripped from each other's intimate grasp; should this be so? Divorcing hemodynamics from respiratory mechanics has resulted in folly. Consider that the acquisition and interpretation error of the pulmonary artery occlusion pressure stems from ignorance of thoracic characteristics and ambient pressures [1, 2]. Will we repeat the same mistakes with less invasive means of hemodynamic assessment?

To consider the intimate linkage of the cardiovascular and respiro-thoracic systems, it may be fruitful to think about them simultaneously [3]. Indeed, the entire thesis of heart-lung.org is to marry two classic diagrams onto a single graphic. While these musings may appear excessively complicated on first blush, I believe that mere appreciation for these interactions is imperative. The model proposed is certainly not meant to completely explain heart-lung interactions, but instead awaken within or remind the learner of their existence.

Hidden Hemodynamics in Respiratory Mechanics

As described at the outset, hemodynamic assessment, by any means, demands familiarity with mechanical heart-lung interaction. The two ventricles communicate in series and in parallel; each ventricle's pressure-volume characteristics and loading conditions pulsate between systole and diastole. And around the heart and pericardium lies the respiratory pump – the lungs within the thorax – itself varying by pressure, volume and frequency. We shouldn't be surprised, therefore, at the fallibility of distilling these exceedingly thorny relations into a simple output measurement [e.g. pulse pressure variation, vena cavae dimension change]; especially, if we desire an index which is universally applicable within the varied pathologies of the intensive care unit. Accordingly, linking the physiologies of the cardiac and thoracic pumps facilitates acquisition and interpretation of hemodynamic data as well as provides rationale for optimizing respiratory mechanics.

Respiratory Mechanics

Respiratory pressure-volume curves are oft-covered subjects in medical school and have merit when analyzing clinically-important heart-lung interaction. The classic diagram, also known as the Rahn diagram, depicts the static [i.e. in the absence of air flow], pressure-volume relationships of the lungs, chest wall and respiratory system [i.e. the lungs and chest wall together [figure 1] [4, 5].

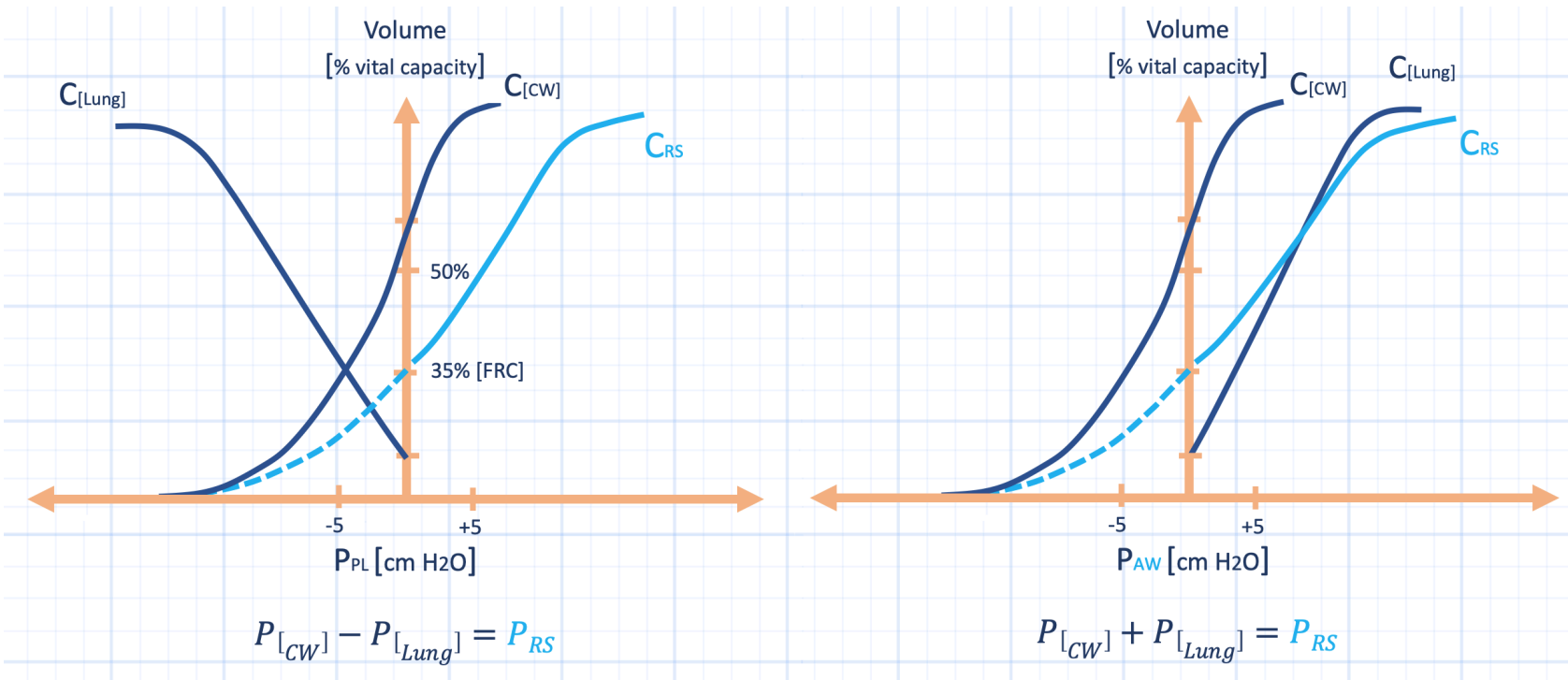

Figure 1: Relationship between 'Rahn diagram' and 'Campbell diagram.' Left panel is Campbell diagram with superimposed respiratory system compliance curve [Crs - light blue] which is a 'summation' of the lung and chest wall in series. For clarity some figures will omit the dashed portion of Crs. Cpulm is pulmonary compliance, Ccw is chest wall compliance, Crs is respiratory system compliance. Right panel is the Rahn diagram. See also chapter 1 figure 10 for more detail.

This diagram is similar to the Campbell diagram, which simply reflects the pulmonary pressure-volume relationship as a mirror image. Thus, the Rahn analysis is helpful when analyzing the patient passive with the ventilator [increase in airway pressure raising lung volume] while the Campbell diagram is better suited for patients breathing spontaneously [fall in airway pressure raising lung volume] [6].

The slope of the respiratory system curve represents the compliance of the lungs and chest wall in series. For each point on the y-axis [e.g. volume applied], the pressure returned by the respiratory system is a summation of the respective recoil pressures of the passive lungs and chest wall, individually. Thus, if the chest wall were to stiffen [e.g. obesity, ascites, intra-abdominal hypertension], its curve shifts down and rightwards and so too does the compliance curve of the respiratory system [7, 8]. Similarly, if the lungs lose compliance [e.g. massive aspiration, alveolar edema, fibrotic lung disease], so too does the compliance curve of the entire respiratory system [8, 9] [see figure 2].

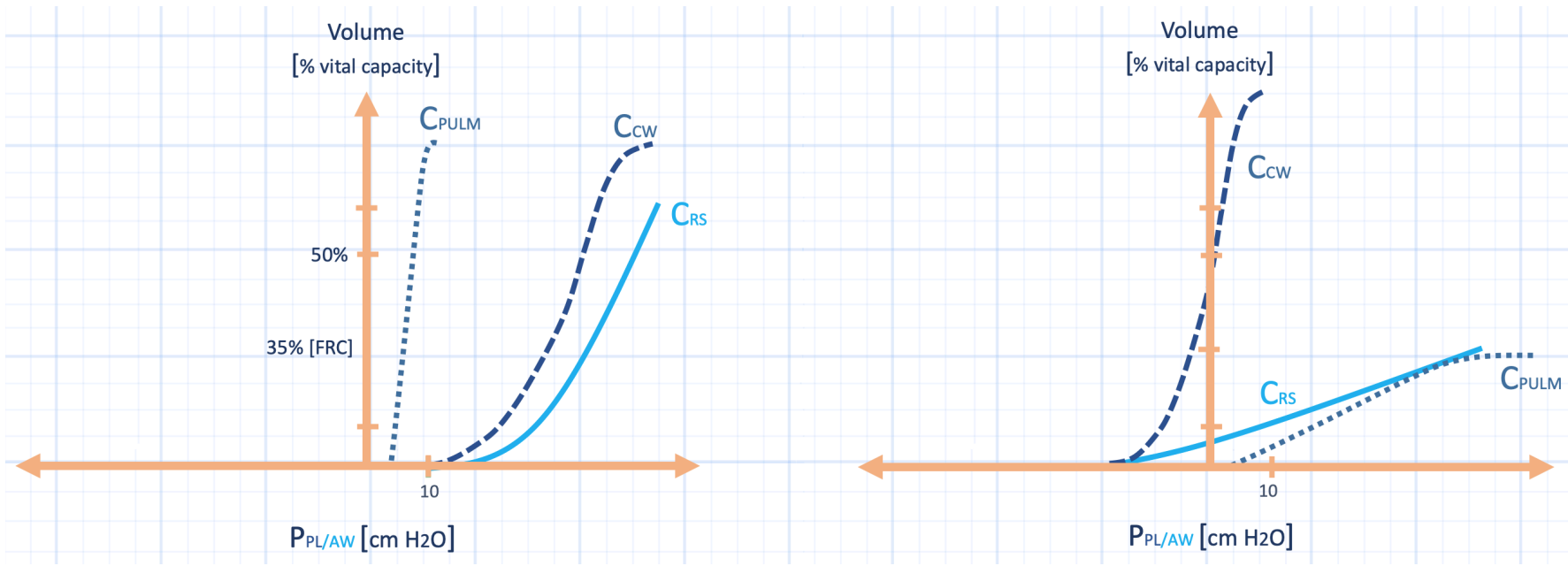

Figure 2: Left panel demonstrates a hypothetical system with normal Cpulm and abnormal Ccw and Crs. Note that the pathologies which stiffen the chest wall are varied and may change the slope of the Ccw [e.g. extra-pulmonary ARDS] or shift it rightwards without changing the slope [paralyzed obese chest wall [4]]. This diagram depicts both. Right panel depicts abnormal pulmonary compliance. Again the pathologies which do this are diverse and the down-shift of the curve is only a model depicting an increased pressure required to achieve a given lung volume [see concept of 'baby lung' [6]].

But what are the clinical correlates of these curves? The compliance curve of the respiratory system provides the static airway pressure of the respiratory system. On the ventilator, this is the plateau pressure [Pplat] at end-inspiration. If one assumes that – during an end-inspiratory hold – there is a continuous column of air from the trachea to the alveolus, then the Pplat also represents the intra-alveolar pressure. Importantly, in the passive patient, the chest wall compliance curve tracks the pleural pressure [Ppl] – approximated by an esophageal balloon [10].

Accordingly, a high Pplat [low respiratory system compliance] may be of two very distinct etiologies [8]. If due to low lung compliance [with unchanged chest wall compliance], the Pplat rises relative to the Ppl. If due to low chest wall compliance, the Pplat and Ppl rise in tandem.

Hidden Hemodynamics

Wherein lie the hemodynamics on the Rahn diagram? Quietly nestled within this graphic sits markers of both right ventricular [RV] afterload and preload. First, as above, if the Pplat represents the end-inspiratory alveolar pressure [PAlv] and the chest wall compliance curve illustrates the pleural pressure, then the lateral distance between these two points – for a given ventilator volume [on the y-axis] – depicts the transpulmonary pressure [Ptp]. The Ptp indicates the pressure across the alveolus and therefore the pulmonary capillary bed. The higher the Ptp, the greater the impedance to RV outflow through the pulmonary vascular tree [11]. Consequently, there should be a direct relationship connecting the area between the Crs and the Ccw curves and RV afterload. A high RV afterload flattens the slope of the RV cardiac function curve; that is, lower its output for any given filling pressure.

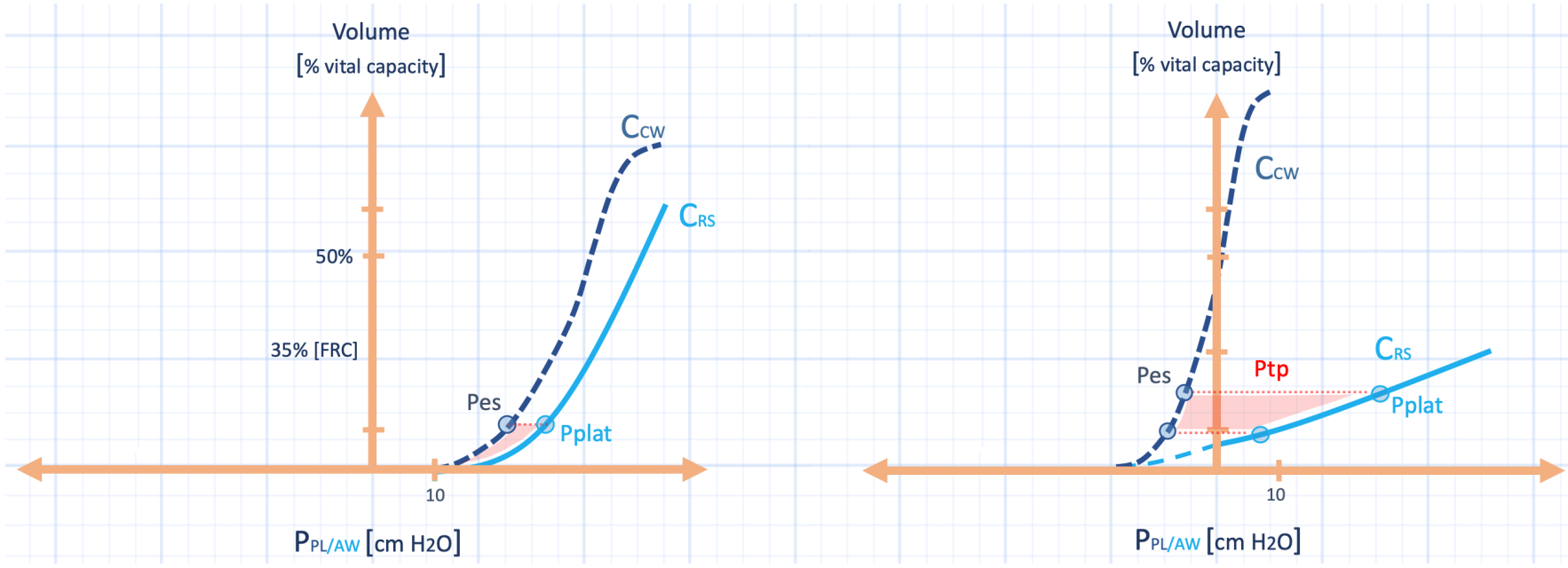

Figure 3: Static work of the respiratory system. This is a recapitulation of figure 2, with Cpulm removed for clarity. Pplat is plateau pressure and Pes is esophageal pressure as an estimate of pleural pressure [Ppl]. Each diagram assumes a starting PEEP of 5 cm H20 and a delivered breath of about 500 mL. Note in left panel, the difference between the Pplat and Pes [the transpulmonary pressure] is low. There is a higher Ppl for this breath and a lower distending pressure across the alveolus and pulmonary capillaries. Right panel, for the same breath, the Ptp is much greater, and the rise in Pes [Ppl] is much less.

Secondly, the degree to which the Ppl rises – in response to mechanical insufflation of the thorax – mediates RV preload. As such, a stiffened chest wall increases Ppl for any given volume on the y-axis, dropping RV preload more impressively – see figure 3.

Implications for Practice

Thus, the clinician must recognize and balance the pre- and afterload effects exerted upon the RV by the respiratory pump [12]. Aim to minimize the area between the respiratory system compliance curve and the chest wall compliance curve; this reduces Ptp and, ostensibly, RV afterload. Selective improvement in pulmonary compliance can achieve this goal. This can be done by minimizing alveolar edema, recruiting atelectatic lung with PEEP [e.g. using the stress-index or driving pressure, see below] or instituting the prone position. Importantly, both PEEP and the prone position diminish preload by raising Ppl and stiffening the chest wall, respectively [13]. It should not escape the reader that the area between the respiratory system and chest wall compliance curves [red-shaded area in figures 3-5] is a partial representation of 'driving power' discussed below. Mitigating pulmonary driving power has salubrious right ventricular effects too.

Secondly, finding hemodynamic data within respiratory physiology explains the plethora of caveats found within the literature on fluid responsiveness. A large area between the chest wall compliance curve and respiratory system compliance curve raises RV afterload throughout a breath. The result is an inspiratory-associated pulse-pressure variation due to afterload sensitivity – cor pulmonale physiology – rather than preload responsiveness [14] [see chapter 8]. Further, appreciating the relationship between volume delivered [y-axis], chest wall compliance and Ppl [on

the x-axis] makes explicit the effect of respiratory mechanics on RV preload. It is established that altering the volume delivered to different degrees of chest wall stiffness has significantly different effects on Ppl, preload and, accordingly, hemodynamic variables [e.g. pulse-pressure variation] [15].

Finally, if the patient begins breathing spontaneously, the analysis is confounded and nearly impossible to apply in a clinically-meaningful way. We must then turn to assessments which raise venous return relative to RV function to assess fluid responsiveness [e.g. passive leg raise, end-expiratory occlusion test, etc.] [16] [see chapter 8].

The Hemodynamics of Prone

Given the above, a brief discussion on the hemodynamic effects of the prone position in severe ARDS [13, 17-20] is warranted. How does prone position alter the cardiovascular system? A good approach to this problem is a Guytonian one, where we consider the consequences of the prone position separately on venous return and cardiac function [3].

Venous Return

The upstream pressure for venous return is the mean systemic filling pressure [Pmsf – see chapter 2]. The Pmsf is directly related to the stressed venous volume and indirectly related to the compliance of the venous tree; it is the x-intercept of the venous return curve [i.e. the pressure within the vascular system when blood flow is ceased] [21-24]. If the stressed venous blood volume is increased [e.g. volume infusion, passive leg raising] or venous compliance decreases, the x-intercept [and therefore the entire venous return curve] shifts rightwards – augmenting venous return. However, the slope of the venous return curve is also important as it depicts the resistance to venous return [25]. Increased resistance to venous return down-shifts the venous return curve without a change in the x-intercept; accordingly, increased resistance diminishes venous return.

The presumed mechanism by which the prone position alters venous return is via abdominal pressurization. Increased intra-abdominal pressure has two competing effects upon venous return. First, it facilitates venous return by increasing the Pmsf [26], illustrated as a rightwards shift of the venous return x-intercept [27]. Second, it may impair venous return by increasing the resistance to venous return. However, the degree to which it increases the resistance to venous return is greatly influenced by the patient's underlying volume status [26, 28]. Simply, when the abdominal venous beds are 'full' [e.g. like West zone III in the lungs], pressurization of the abdomen does not retard venous return to the same degree as a venous tree that is relatively 'empty' [e.g. like West zone I in the lungs] [29]. In summary, because prone position increases intra-abdominal pressure [13], the venous return curve shifts rightwards, favouring venous return, but has variable effects upon resistance

to venous return depending on the patient's underlying volume status. Additionally, the effect on venous return resistance may be complicated by venous Starling resistors within the hepatic circulation – somewhat akin to what happens with PEEP application [30]. The point at which the systemic venous return curve intersects the cardiac function curve defines the steady state cardiac output, such that increased Pmsf without increased resistance to venous return raises cardiac output as long as the operating point lies upon the ascending portion of the cardiac function curve, as described below.

Cardiac Function

Prone positioning has complex and conflicting effects upon right ventricular load. Because prone positioning reduces the compliance of the chest wall [31], the passive patient receiving mechanical ventilation experiences a relatively large increase in intra-thoracic pressure for a given tidal volume [15, 32]. Assuming that the intra-thoracic pressure is transmitted integrally to the pericardial space [33], increased intra-thoracic pressure shifts the cardiac function curve rightwards relative to the systemic venous return curve [34]; to the extent that the cardiac function curve shifts rightwards relative to the right-shift of the Pmsf, as elaborated above, cardiac output falls. Conversely, and less intuitively, augmented intra-thoracic pressure also diminishes right ventricular afterload. The reason is that right ventricular afterload is partly determined by the distending pressure of the lung [i.e. the transpulmonary pressure] which is the pressure within the alveolar compartment less the pressure within the pleural compartment. Consequently, reduced chest wall compliance raises the pleural [or intra-thoracic] pressure relative to the alveolar pressure and this unloads right ventricular ejection [35-37]. Additionally, prone position recruits compressed dorsal lung [38] which lowers pulmonary vascular resistance [39], and improves oxygenation – releasing hypoxemic vasoconstriction in the pulmonary bed [40]. Right ventricular afterload reduction is illustrated by steepening of the cardiac function curve slope [i.e. an up and to the left shift].

This conflicting physiology is summarized in an excellent review by Jardin and Vieillard-Baron [12]. In their summary, they reconcile conflicting data pertaining to the effect of PEEP on right ventricular volume in ARDS, and they do so within the framework of Gattinoni's distinction pulmonary and extra-pulmonary ARDS [8] [see chapter 4]. Briefly, pulmonary ARDS is a consequence of direct pulmonary insult which reduces pulmonary compliance; whereas, extra-pulmonary ARDS arises from systemic unrest and diminishes chest wall compliance. In the former, less of the alveolar pressure is felt by the pleural space [41-43]. Therefore, trans-pulmonary pressure rises and right ventricular afterload is heightened. As above, this favours right ventricular enlargement and diminished cardiac output. In contradistinction, extra-pulmonary ARDS is typified by raised pleural pressure relative to alveolar pressure such that transpulmonary pressure and right ventricular afterload fall; this favours diminished right ventricular volume and improved cardiac output.

Thus, placing a patient in the prone position has important implications for both venous return and right ventricular function. While elevated intra-abdominal pressure raises the pressure head for venous return, improved venous return is only realized in the absence of contemporaneous rise in resistance to venous return. Therefore, careful consideration should be paid to a patient's volume status prior to initiating prone position. Additionally, the degree to which ventilator-applied airway pressure partitions into the alveolar space relative to the pleural space determines to what extent the intra-thoracic milieu diminishes right ventricular preload, afterload or some combination thereof. Careful consideration must be given to underlying cardiac function as well as the relative contributions of the pulmonary and chest wall compliances to the overall compliance of the respiratory system. Integration of these multiple, co-varying physiological elements may explain conflicting hemodynamics both in ARDS and other mechanically-ventilated patient populations [3] [see figures 4 and 5].

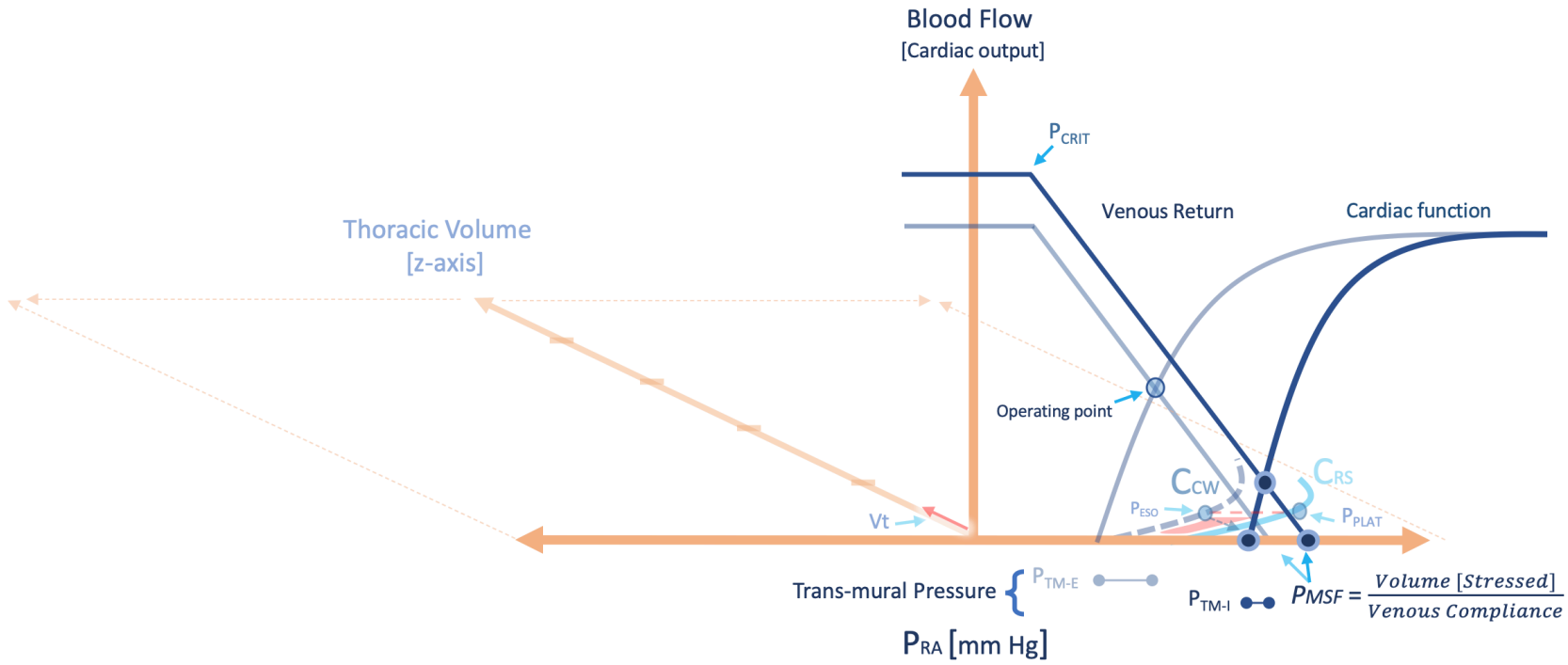

Figure 4: Heart-lung interaction in prone position with extra-pulmonary ARDS. The chest wall compliance curve [Ccw] is stiffened and shifted rightwards - see also figures 2 and 3. The plateau pressure [Pplat] is high, but this is from an elevated pleural pressure [e.g. esophageal pressure, Peso]. The trans-pulmonary pressure [Ptp] is low, therefore, right ventricular afterload is relatively preserved. Because Peso is high, right ventricular preload [i.e. right atrial trans-mural pressure on inspiration and expiration, Ptm-I/E] is diminished [below x-axis]. Pra is right atrial pressure. Y-axis is cardiac output, z-axis is thoracic volume. Crs is respiratory system compliance. Pcrit is the critical collapse pressure of the great veins. PEEP is positive end-expiration pressure. Pra is right atrial pressure. The red arrow on z-axis is tidal volume [Vt]. Note, the red-shade in the x,z plane represents transpulmonary 'driving power' discussed below.

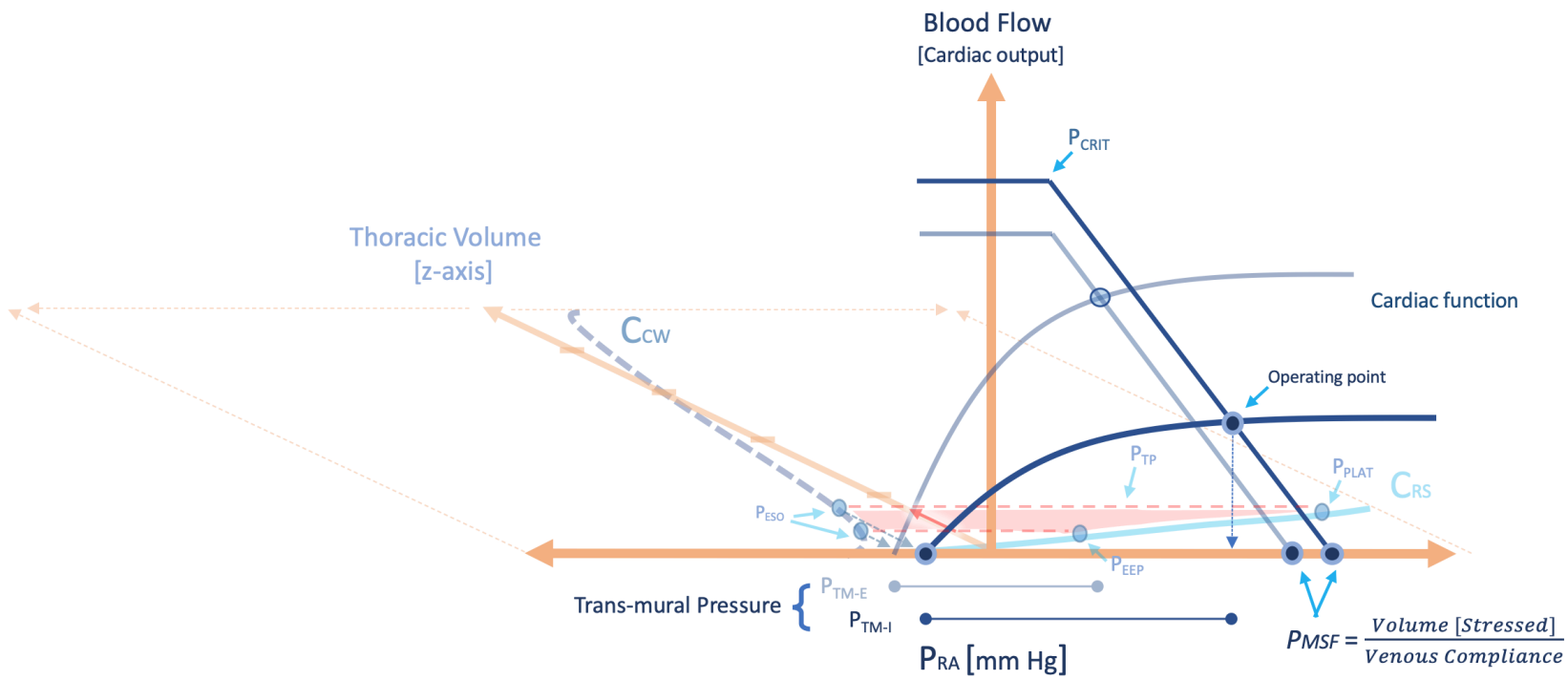

Figure 5: Heart-lung interaction in supine, pulmonary ARDS. Contrary to figure 4, the chest wall is not stiff. Pulmonary compliance is poor, so the respiratory system compliance is poor, plateau pressure [Pplat] and transpulmonary pressures [Ptp] are high. Right ventricular afterload is heightened, so the cardiac function curve is flattened. There is afterload sensitivity - inspiration decreases cardiac output on the y-axis. Right atrial trans-mural pressure is great on inspiration and expiration [Ptm-I/E]. Thus, this patient may have pulse pressure variation by afterload sensitivity and ventricular interdependence [see chapter 8] even though not fluid responsive. Pcrit is the critical collapse pressure of the great veins. PEEP is positive end-expiration pressure. The red arrow on z-axis is tidal volume [Vt]. Pra is right atrial pressure. Note, the red-shade in the x,z plane represents transpulmonary 'driving power' discussed below.

Strain and Stress

Gattinoni and Quintel note that, in the treatment of ARDS, lung inhomogeneity should be mitigated using optimal positive end-expiratory pressure [PEEP] and the prone position [44]. But what is lung inhomogeneity? How does it relate to strain and stress and what are the implications for volutrauma and barotrauma? These questions are considered in the next two sections.

Strain is the volume applied to the lung; importantly, strain is not simply the absolute volume administered by the ventilator, but rather it is the volume applied by the ventilator relative to the volume within the lung available for gas exchange [45]. In progressively severe ARDS, the volume within the lung accessible for ventilation becomes increasingly small. This cryptic lung volume was first appreciated when ARDS was initially studied with CT scans in the 1980s, giving rise to the notion of the 'baby lung' [45]. Consider two 70 kg patients, one with a 'baby lung' size of 200 mL and the other with a baby lung of 800 mL. Applying a 400 mL breath to each of these fictitious patients results in very different strains [2.0 and 0.5, respectively]; consequently, different stress is felt by these lungs despite the same tidal volume.

Stress refers to the fibre tension experienced by the lung; primarily the tensile properties of collagen. In other words, in response to a given strain, there is an internal tension – a molecular rearrangement – generated within the fibrous lung skeleton and this is stress [45, 46]. Clinically, it is approximated by the trans-

pulmonary pressure or the airway pressure less the pleural pressure. Stress and strain are related by a constant, which is specific to the tensile properties of the deformed material. This constant is called the specific elastance and, interestingly, even within severe ARDS the specific elastance of the lung is normal [45, 47]. Simply, the enlarged strain and stress of the lung arises not because the diseased lung is stiff, but rather small [45]. These principles are further discussed in the following section on volutrauma and barotrauma.

Lung Inhomogeneity and Stress Raisers

Appreciation of strain and stress within the context of pulmonary mechanics is important when considering the 'stress raiser' hypothesis. Initially proposed by Mead et al. in 1970, the stress raiser theory considers that local stress is multiplied when directed towards inhomogeneous material [48]. Consider figure 6 below; the inhomogeneous portion of the lung acts as a 'stress raiser' locally on its neighbouring units. An equivalent volume is applied to both lung units in the figure, however, the portions of lung around the 'stress raiser' experience greater regional stress.

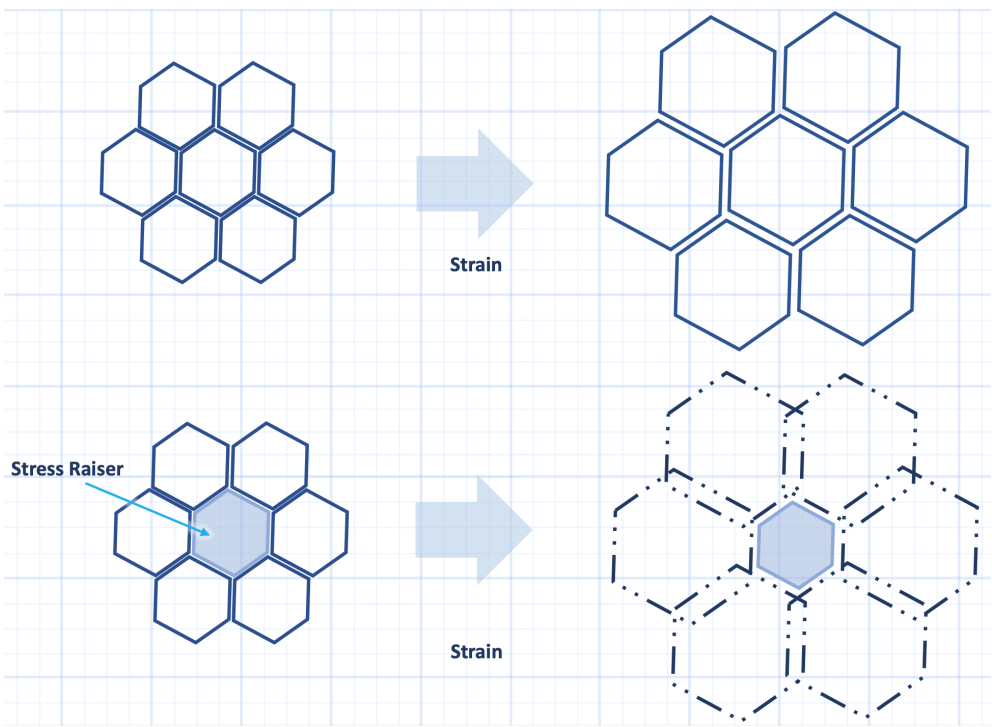

Figure 6: An illustration of a stress raiser. See text for details.

In a porcine model, Cressoni and colleagues found that in normal lungs, ventilator-induced lung injury [VILI] began around areas of the lung which are anatomically inhomogeneous [e.g. at the pleural/alveolar interface, blood vessels and airways] lending credence to the 'stress raiser' hypothesis [49]. Importantly, any structural anomaly may be a stress raiser [e.g. atelectasis, age-related anatomical changes, scar, edema, secretions, consolidation, etc.]

PEEP and Stress Raisers

PEEP is perhaps the easiest means by which lung inhomogeneity – and therefore 'stress raisers' – is attenuated [50, 51]. Using a unique, CT scan voxel analysis, Cressoni and colleagues assessed lung inhomogeneity in ARDS and also in response to increased airway pressure [51]. They found that the scope of lung homogeneity was associated with ARDS severity, dead space fraction and patient outcome. Additionally, they found that augmenting PEEP diminished lung inhomogeneity, in totality. Importantly, however, in the individual patient, PEEP can have variable effects on lung inhomogeneity – that is augment, diminish or unalter it. Nevertheless, two means by which the effect of PEEP on thoracic mechanics is quantitatively or qualitatively judged are the driving pressure and stress index, respectively [see below]. At the optimum level, PEEP prevents intertidal collapse and maintains recruited lung open [52, 53].

Prone Position and Stress Raisers

Transpulmonary pressure, or stress – described above – is not uniform within the normal lung. Because of both gravitational forces and the adaptation of the lung and chest wall to match each other's shape, alveolar stress is greatest at the ventral portion of the lung, when supine [54]. When placed in the prone position, gravitational effects compress the ventral portions of the lung, but the adaptation of the lung to the shape of the chest wall resists the compressive gravitational force [54]. Consequently, alveolar stress from the dorsal to the ventral regions is homogenized. Perfusion of the lungs is similar between the supine and prone positions. Accordingly, ventilation-to-perfusion ratios are more consistent while prone [55].

In severe ARDS, there is increased edema and lung injury throughout, ubiquitously elevating hydrostatic pressure within the lung. This, 'superimposed pressure' may be 4-5 time normal and compresses the dorsal lung [54]. Thus, the dependent lung is degassed giving the impression of dependent opacities. Bone [56] coined this 'sponge lung' to illustrate a boggy mass squeezed under its own weight. Empirically, flipping a patient into the prone position immediately transfers lung density from the dorsal to ventral region. The dorsal lung mass is anatomically greater, hence there is improved ventilation as the enlisted dorsal airspaces exceeds loss of the ventral sections [54] [figure 7].

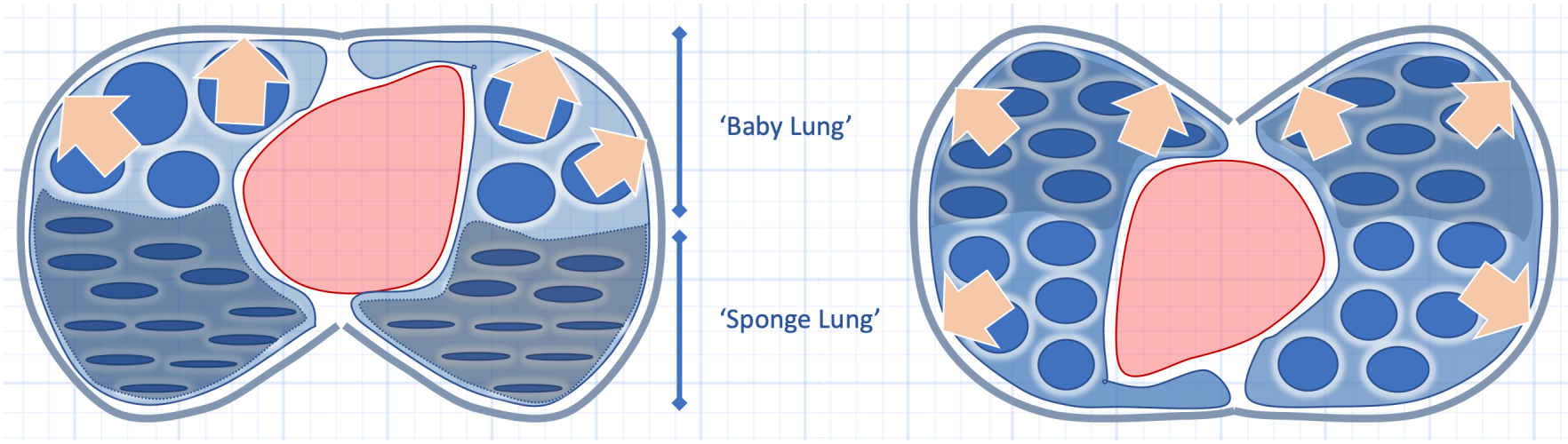

Figure 7: Illustration of how prone position homogenizes the lung by shape-matching the lungs and chest wall. See text for details.

Ultimately, prone-induced improvements in lung homogeneity promote gas exchange [57], hemodynamics [58] and mitigate stress-raisers as described above. These salutary physiological effects may explain the observed benefits of both PEEP and prone positioning in the most severe forms of ARDS [59, 60].

Volutrauma or Barotrauma?

In an excellent, open-access review, Gattinoni, Quintel and Marini ask which is worse, volutrauma or atelectrauma [61]? This concise review provides the pieces from which this section assembles. As well, the concepts of strain and stress, described above, are expanded into their clinical correlates, volume and pressure, respectively.

Volume and Strain

As above, the absolute volume applied to the lung is an important determinant of biological injury. However, equally-important is the absolute volume delivered relative to the baseline volume of the lung [i.e. functional residual capacity or FRC]. The latter is referred to as the 'baby lung' in ARDS because FRC can be quite variable and quite small [45, 62]. FRC in ARDS is typically unknown. From the previous section, reconsider two different patients – one with an FRC of 800 mL and the other with an FRC of only 200 mL because of severe lung injury [i.e. the 'baby lung']. Delivery of 400 mL to the first patient results in a lung strain of 0.5. Lung strain is the tidal volume divided by the FRC [i.e. 400 mL divided by 800 mL]. However, in the second patient, the same tidal volume results in a lung strain of 2.0 [i.e. 400 mL divided by 200 mL]! These two extreme examples illustrate why there is no one-size-fits-all tidal volume for all patients with ARDS. If the volume of the baby lung is unknown, true lung strain is also unknown but it is clear that keeping tidal volume small will also keep lung strain small.

Pressure and Stress

The pressure across a distensible material is known as stress and is directly related to strain [determined as above] [63, 64].

$$(1) \quad stress = k \; x \; strain$$

Equation 1: The relationship between stress and strain. k is specific elastance.

Pressure is often measured clinically as the plateau pressure on the ventilator. Analogous to volume, it is not solely the value of pressure in the airway that is important, but rather the pressure in the airway relative to the pressure around the lung – the pleural pressure. When considering the stress or pressure across the lung [plateau relative to pleural pressure] one anticipates scenarios where both plateau and pleural pressure rise in tandem such that the plateau pressure is very high, but because the pleural pressure is also high, the pressure [i.e. stress] across the lung is normal. An example in the ICU may be morbid obesity where the weight placed upon the chest wall increases both pleural pressure and plateau pressure.

A more physiologically-exciting example is that of fighter pilots wearing anti-gravity suits. To defend against gravity-induced loss-of-consciousness, anti-gravity suits pressurize the thorax as this maintains pressure gradient for blood flow from the left ventricle to the brain. One mechanism of these suits is the application of airway pressures upwards of 80 – 90 cm H_2O! If one considers only the airway pressure this leads one to speciously infer very high lung stress. However, the chest wall stiffens during high-gravity maneuvers. In addition, an inflatable bladder around the abdomen and chest – in some suits – also braces the chest wall and pilots perform straining maneuvers the raise thoracic pressure. As a result, the pleural pressure dramatically rises such that very high airway pressure is tempered by augmented pleural pressure – lung stress is actually normal!

Volutrauma versus Barotrauma

Which is the mechanism of lung injury, volutrauma or barotrauma? They are, in essence, the same thing but only when one considers tidal volume in relation to FRC [i.e. strain] and airway pressure in relation to pleural pressure [i.e. stress] [63]. The equation above is fleshed out into a clinically-relevant relationship in equation 2.

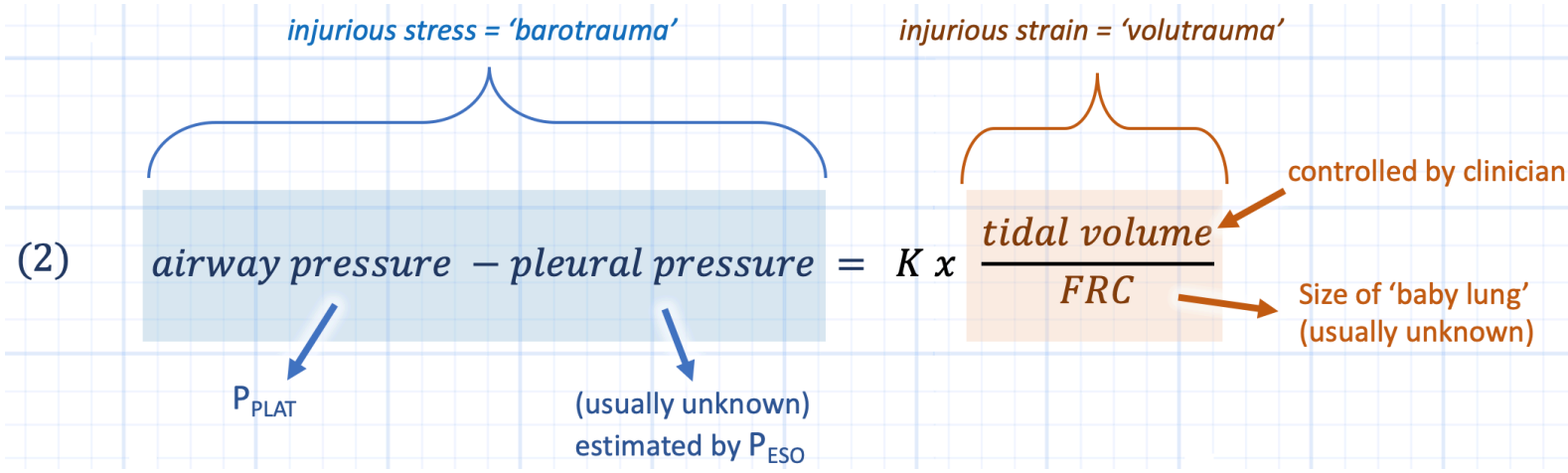

Equation 2: An elaboration of equation 1 above.

One sees that stress and strain are directly related by a constant – known as the 'specific elastance' [k]. Elastance is the inverse of compliance – a measure of the 'stiffness' of the material. In humans, this value is about 12 cm H2O. In other words, increasing the tidal volume of the lung relative to the FRC by a factor of 1.0 [i.e. a strain of 1.0] generates a transpulmonary pressure of 12 cm H2O. Total lung capacity occurs at a lung strain of about 2.5 – which produces in a transpulmonary pressure of about 30 cm of H2O in humans. Interestingly, at least some lung units see their collagen fibres completely distended at a transpulmonary pressure as low as 21 cm H2O [65]; this corresponds to a lung strain of roughly 1.5 to 2.0 – a value known to provoke lung injury in swine [46].

What seems paradoxical is that the specific elastance remains unchanged even in severe ARDS [45, 47]; in other words the numerical relationship between strain and stress stays constant as the functional lung size shrinks. Accordingly, strain and stress rise as FRC falls in ARDS rather than as a consequence of increased in elastance [decreased compliance].

Atelectasis and Stress Raisers

As discussed above, the mechanism by which atelectasis drives lung injury may be secondary to excessive mechanical stress upon the lung [63, 64]. A 'stress raiser' [or riser] occurs when materials of differing elasticity are located adjacent to one another [48]. In this situation, the less compliant area augments radial stress at the interface of the two units upon deformation. An atelectatic unit acts as a stress raiser on surrounding lung parenchyma. In a classic – but theoretical – paper by Mead and colleagues, a stress raiser augmented local stress by a factor of 4.64 [48]. Thus, a transpulmonary pressure of 21 cm H2O – at a stress raiser – is effectively 21 cm H2O x 4.64 or 97 cm H2O! Nevertheless, clinical evidence finds this multiplication factor closer to 2.0 [51]. If we factor stress raisers into the equation above, we see the result is – in essence – a functional increase in lung elastance [decrease in compliance] [61]. Given this factor of 2.0, some have suggested keeping the transpulmonary driving pressure less than 12 cm H2O [66]. As above, stress raisers are diminished by both positive end-expiratory pressure [PEEP] and prone

position – the latter does not, however, increase mechanical power [44], which is considered in more detail below.

Fighter Pilots!

An interesting example of transpulmonary stress and strain comes from fighter pilots because they have continuous positive airway pressure [i.e. CPAP] masks as a part of their flight suit. Strikingly, beyond the clinically-commonplace airway pressure of 5-15 cm of H_2O, a fighter pilot may endure a mask-applied pressure of 90 cm H_2O [67]! How and why is this physiology acceptable? How does this relate to stress and strain described above?

+Gz - Associated Loss of Consciousness

The abbreviation +Gz refers to a head-to-foot inertial force resulting from an equal but opposite acceleration [68]. Inertial forces in this direction occur, for instance, when an aircraft is rapidly directed upwards from a deep dive. More simply, think of organs and tissues - including blood - moving downwards at high velocity; when there is rapid, upwards correction of the aircraft, an inertial force in the +Gz axis keeps all tissue – including blood – moving downwards against the will of the aircraft.

Elevated G force to twice that of gravity, i.e. +2Gz, reduces mean arterial pressure [MAP] by 20-25 mmHg at the level of the head [68]. This MAP reduction holds for each additional increment in G force such that at +4Gz, the MAP at the level of the head falls by roughly 100 mmHg. Accordingly, the typical +Gz level tolerated by relaxed humans is about +3.5Gz before there is +Gz - associated loss of consciousness, or GLOC [69]. Perhaps the first description of GLOC was nearly a century ago in an esoteric chapter entitled "Sensations Experienced by Normal Persons in Machines Heavier than Air" [70].

Fundamentally, GLOC is secondary to cerebral hypoperfusion and has been evaluated via various methods including trans-cranial Doppler [71]. Indeed, there is a dose-dependent reduction in middle cerebral artery flow with increasing +Gz and in subjects with GLOC, reversal of MCA flow was noted! Of interest, the moment of GLOC is not simultaneous to cessation of cerebral blood flow but rather lags by 5 - 10 seconds; this delay is known as the cerebral anoxic reserve [72] – first systematically studied in healthy, young prisoners in the mid-20th century [73].

Prevention of GLOC: Anti-G suits

Basic hemodynamics and heart-lung interaction are exploited in modern aircraft to augment the level and duration of +Gz tolerance. Fighter pilots now readily

withstand up to +12 Gz! From the above, to sustain cerebral perfusion at +12 Gz [assuming a cardiac-to-head distance of 30 cm and a seat at 30 degrees from the vertical] a left ventricular pressure approaching 300 mmHg is needed [68]. Such pressure is achieved using anti-G suits [AGS], positive pressure breathing for +Gz tolerance [PBG] and the anti-G straining maneuver [AGSM] [67].

Initial attempts to maintain high cardiac pressure in the face of +Gz force focused on augmenting venous return [72]. Contemporary AGS apply compression pressures that eclipse 200 mmHg to the extremities and abdomen in response to high +Gz [68, 74]. Mechanistically, wrapping the veins intensifies venous return [75]. Further, mechanical restraint of the arteries increases peripheral arterial resistance directing arterial blood to the head [67]. Lastly, abdominal compression by the AGS physically raises the heart [76] which lowers the pressure gradient to the cerebral circulation.

Venous return and arterial resistance are also enhanced by +Gz training, for example in a centrifuge. Fighter pilots have decreased venous capacitance; that is have higher venous pressure for a given blood volume and they are more sensitive to phenylephrine infusion compared to normal controls [77]. It is, therefore, presumed that their enhanced +Gz tolerance is mediated by alpha-receptors [77].

Prevention of GLOC: Positive pressure breathing for +Gz tolerance

The application of high airway pressure, described in the introductory paragraph, also enhances cerebral perfusion by squeezing arterial blood out of the left ventricle and thorax [78]. The COMBAT-EDGE system administers 16 cm H_2O of airway pressure for each +Gz above 4 to a maximum of 82 cm H_2O at +9Gz [79]. While airway pressure of this degree may concern clinicians, high +Gz force simultaneously raises chest wall weight, thereby limiting the transpulmonary pressure [i.e. 'stress'], or distending pressure of the lung [80]. This is akin to the morbidly obese in the ICU with high airway pressure. Additionally, some flight suits splint the chest wall by inflating a bladder around the anterior chest to the same level as pressure applied to the airway, though this may be redundant [80].

Prevention of GLOC: Anti-G straining maneuver

Supplementing PBG, pilots routinely perform strenuous maneuvers comparable to Valsalva, interspersed with breaths. Additionally, extremity muscle clenching maintains venous return and raises arterial pressure. Collectively, the aforementioned is termed the anti-G straining maneuver. The AGSM increases +Gz tolerance by 2-3 with measured esophageal pressure [Pes, surrogate for pleural pressure] up to 140 cm H_2O [or 100 mmHg] [81]!

Clinical Relevance

Perhaps the most important concept highlighted by the extreme physiology of high +Gz is that of the pressure across a distensible structure, or the transmural pressure [Ptm]. The Ptm makes clear that it is not simply the pressure inside the object [e.g. airway pressure], but rather it is the pressure inside relative to the outside [i.e. airway pressure relative to pleural pressure] that is physiologically meaningful. In a fantastic study [74] of volunteers receiving extraordinary CPAP - with both pulmonary arterial and esophageal catheters in place - the Pes was higher than the applied airway pressure of 95 cm H_2O. In other words, the Ptm fell and lung volume shrunk in the volunteers wearing counter-pressure. This is also why airway pressure may reach 200-300 mmHg during coughing [82, 83].

Additionally, the measured mean pressure in the pulmonary artery rose to 77 mmHg! However, this did not increase the afterload of the right ventricle; the transmural pressure of the pulmonary artery actually fell [74], meaning that RV outflow impedance also fell. In summary, the lesson is that measuring an intravascular or airway pressure is only half the story. The surrounding pressure is an equally important determinant of stress and therefore strain [i.e. change in volume] of the structure.

Lung Injury and the Pulmonary Vasculature

Given the discussion on strain, stress and the pulmonary parenchyma, this brief section draws the reader to the pulmonary vasculature as a mediator of ventilator induced lung injury [VILI]. That the pulmonary vasculature participates in the pathogenesis and propagation of the acute respiratory distress syndrome [ARDS] has been known for decades [84]. Highlighting the importance of the pulmonary vascular tree in ARDS, both a prediction score for acute cor pulmonale [ACP] in ARDS and an expert opinion on the hemodynamic management of ARDS are relevant resources [11, 85].

There are a plethora of 'indirect' insults to the pulmonary vasculature that raise resistance to blood flow during ARDS [86, 87]. These include microthrombi, hypoxemic vasoconstriction, hypercapnia and interstitial edema [86]. Additionally, the 'direct' effect of lung stress and airway mechanics upon the vasculature are also paramount [87]. In a patient, fully adapted with the ventilator [e.g. paralyzed], a mechanical breath raises lung strain and stress as detailed above. Stress on the lung skeleton has opposing effects upon two vascular populations within the lung [88]. The alveolar vessels [e.g. the pulmonary capillaries] are exposed to the alveolar pressure and tend to collapse during lung inflation [i.e. because the alveolar pressure rises relative to the pleural pressure]. By contrast, within the bronchovascular bundles – which originate at the hila and invaginate into the lung parenchyma – are the extra-alveolar vessels. When lung volume rises [even in response to a fully passive, ventilator-delivered breath], these conduits dilate. To the extent that these conduits increase in size, the interstitial pressure surrounding

the extra-alveolar vessels falls. Consequently, the extra-alveolar vessels dilate and elongate [89].

There is a unique sub-population of blood vessels within the lung known as 'corner vessels.' They are anatomically alveolar [they lie at the junction of at least 3 alveolar septae] but are physiologically extra-alveolar because they dilate when lung volume rises [88]. Indeed, under West zone I conditions, the corner vessels are responsible for continued, local blood flow [90]. When lung stress is abnormally high – as during ARDS – over-distention of inhomogeneous lung causes excessive West zone I, particularly during inflation. This forces blood through corner vessels, raises their transmural pressure and enhances interstitial edema, particularly when vessels are abnormally leaky as in ARDS [11, 88]. While the Mead model detailed above considers the effects of stress raisers on neighbouring lung units during inflation, asymmetrical radial forces are exerted in an equal, but opposite direction during exhalation [48]. Accordingly, the interstitial space adjacent to a stress raiser during alveolar emptying is predicted to experience traction forces multiplied by a factor of 4.64 [48, 88]. Therefore, if alveoli empty at an end-inspiratory distending pressure of 30 cm H_2O, the interstitial pressure surrounding the corner vessel may fall by 140 cm H_2O [or 100 mmHg]! In theory, it follows that the transmural pressure of corner vessels can amplify to levels known to fracture capillaries [91] [see figure 8].

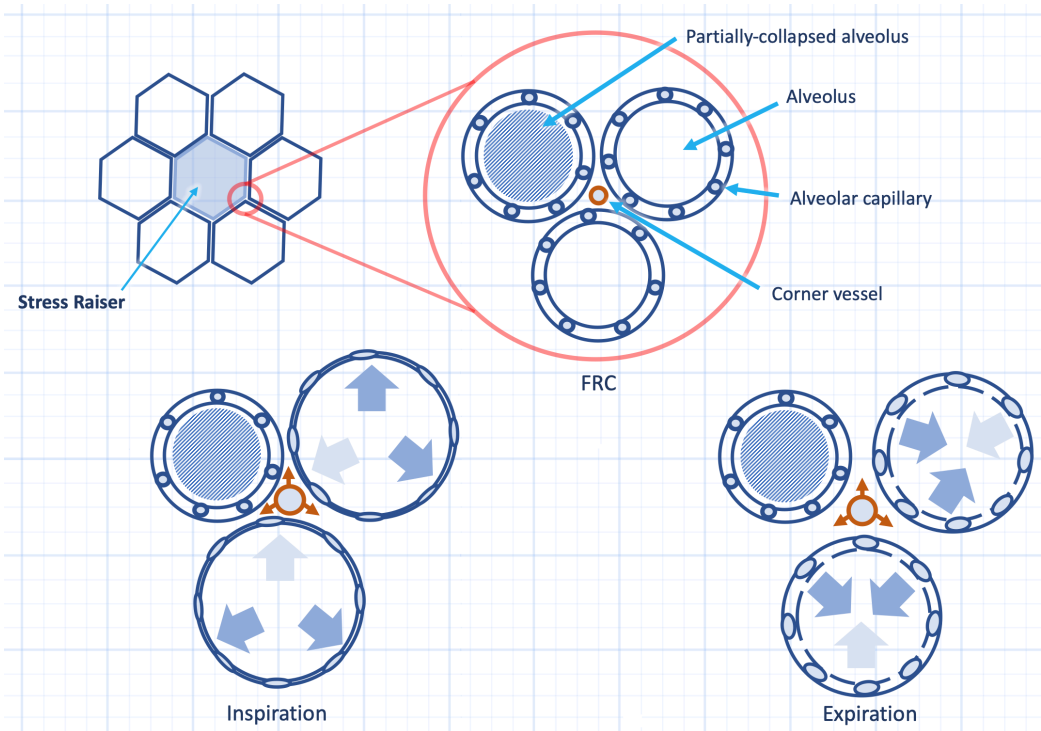

Figure 8: Hypothetical effect of stress raiser on corner vessel during inspiration from functional residual capacity [FRC] back to expiration. See text for details.

In summation, the strain and stress applied to the airways can exacerbate vascular injury via cyclical stress on the microvasculature. Empirically, increased pulmonary arterial blood flow, cycle time and pressure have all been demonstrated to exacerbate hemorrhagic edema and VILI [88, 92-95]. Additionally, in a VILI model, lowering left atrial pressure exacerbated lung injury [96]. From above, it may be deduced that diminished left atrial and pulmonary venous pressure increase the fractions of West zone I and II – exacerbating cyclical fluctuation in microvascular stress. By this reasoning, West zone III acts as 'vascular PEEP.'

As the aforementioned vascular injury heightens right ventricular [RV] afterload, the RV may dilate [i.e. diastolic dysfunction or volume overload] and experience paradoxical septal motion [i.e. systolic dysfunction or pressure overload]. When both RV diastolic and systolic dysfunction are present on an echocardiogram, acute cor pulmonale [ACP] is diagnosed [97]. Prior to lung protective ventilation [LPV], the incidence of ACP in ARDS was upwards of 60%. In contemporary studies, it is about 20% [87]. Fortunately, scoring systems help predict the likelihood of ACP [85] [see table 1].

Table 1: Acute Cor Pulmonale Prediction Score

Risk Factor	Risk
Pneumonia as ARDS cause	0 risk factors - 20%
Driving pressure at least 18 cm H_2O	1 risk factor - 31%
PaO_2 : FiO_2 ratio of less than 150 mmHg	2 risk factors - 39%
$PaCO_2$ of at least 48 mmHg	3 risk factors - 44%
	4 risk factors - 64%

Non-invasive indices of fluid responsiveness in ARDS pose problems as RV output varies in response to respiratory-induced augmentation in afterload, rather than diminished preload [98]. Trans-esophageal echocardiography may mitigate such error by continuous assessment of RV size, SVC collapsibility [i.e. in the paralyzed patient] and RV outflow mean acceleration time [98]. The latter index is the ratio of the maximal RV outflow velocity to the acceleration time; its fall is directly associated with RV systolic function and inversely related to RV afterload [99].

Another venerable monitoring utensil is the pulmonary artery catheter [PAC] [see chapter 7]. Importantly, because of near-ubiquitous tricuspid regurgitation during mechanical ventilation [100] [especially in ARDS [101]], thermodilution cardiac output can be inaccurate. Similarly, pulmonary vascular resistance is described as a 'meaningless variable' [102, 103] [see chapters 2, 7 and 10]. Instead, untoward hemodynamic effects of mechanical ventilation upon the RV may be inferred from diminished pulmonary arterial pulse pressure and/or increased isovolumic contraction pressure [figure 9] [104].

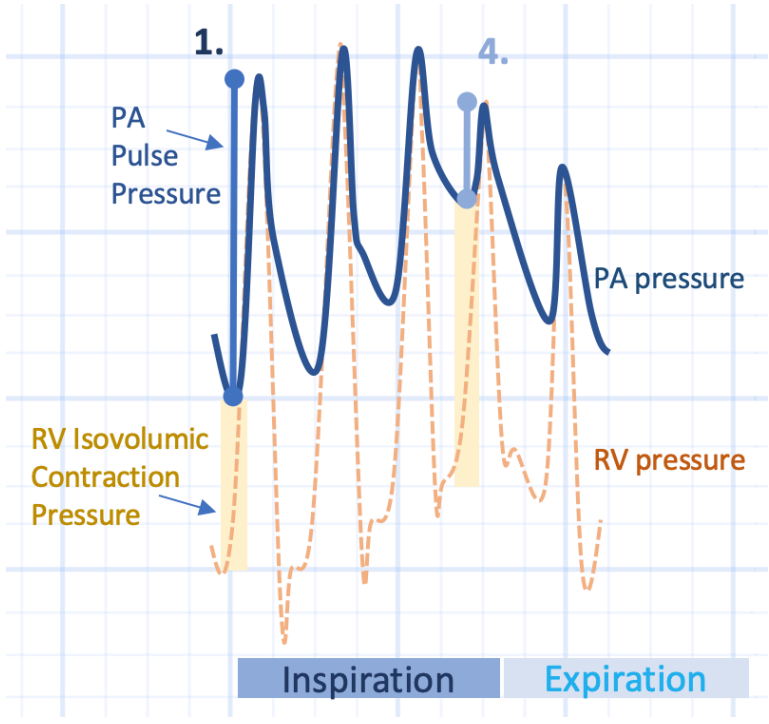

Figure 9: Isovolumic contraction pressure. Simultaneous pulmonary artery and right ventricular pressure tracing. Beat 1. is at the beginning of inspiration, when stroke volume is greatest and afterload for the right ventricle is lowest. This is illustrated as a large pulmonary artery [PA] pulse pressure and low right ventricular [RV] isovolumic contraction pressure, respectively. At the end of inspiration, beat 4, RV stroke volume is at its lowest and afterload at its highest, as shown by small pulse pressure and large isovolumic contraction pressure, respectively. The shaded, rectangular bar is the RV isovolumic contraction pressure, or the rise in pressure from RV end-diastole to the opening of the pulmonic valve.

Therapy

Ultimately, the above underscores the importance of lung protective ventilation; adhering to the adage 'what's good for the lung is good for the RV' [101] certainly applies. As discussed in much more detail below, minimizing the strain and stress applied to the lung diminishes the driving power and, therefore, might have salutary effects on the RV. To minimize driving power, one can titrate PEEP using driving pressure or the stress index as quantitative and qualitative surrogates of alveolar distention, respectively [see below]. Further, prone position homogenizes the lung without augmenting driving power. Regarding hemodynamics, the clinician can consider norepinephrine to maintain right coronary artery perfusion in shocked ARDS patients, approach fluids judiciously and weigh arterial vasodilators and extra-corporeal support in severe ARDS [11, 87]. Nevertheless, what remains unanswered is whether specifically monitoring and treating ACP in ARDS improves outcome.

Driving Pressure and Stress Index

Given that the problem with the lung in the acute respiratory distress syndrome [ARDS] is not that it is stiff, but rather, small [105] it is important that the clinician have tools to help gauge pulmonary over-distension. As discussed above, in the 1980s, CT scans of ARDS patients revealed diminished functional lung size with dependent densities [9]. These images led to the notion of the 'baby lung;' the size

of aerated lung in ARDS patients approximated the size of a child's lung. As expected, the degree of dependent consolidation correlates with shunt fraction, hypoxemia and pulmonary hypertension [106]. However, in any given patient, it is difficult to predict the exact size of the 'baby lung.' The larger the mismatch between the size of the ventilator-delivered volume and the size of the 'baby lung,' the larger the difference in strain and stress. As a materials analogy, consider two balloons comprised of the same elastic material [i.e. their specific elastances are equivalent], but one has a capacity of 800 mL and the other a capacity of 200 mL. Delivering 400 mL of volume to each of these balloons results in different strains [i.e. the change in volume change relative to baseline volume] and therefore stress [i.e. the increase in balloon pressure relative to its ambient pressure]. In the intubated patient [free of respiratory effort], this physiology is represented by a calculated difference in respiratory system compliance [Crs]; that is, for a given change in thoracic [lung and chest wall] volume, the airway pressure change is also different.

Given the above, a complex statistical analysis of previously published randomized controlled trials on tidal volume [Vt] limitation and positive end-expiratory pressure [PEEP] in ARDS patients was undertaken [107]. The authors hypothesized that change in airway pressure in response to a volume-limited ventilator-delivered breath would be the best physiological surrogate to assess the strain of the 'baby lung.' This is the driving pressure [ΔP] [equation 3]:

$$(3)\quad \Delta P = \frac{tidal\ volume\ (Vt)}{Crs}$$

Equation 3: The relationship between driving pressure, tidal volume and respiratory system compliance

Or, the driving pressure equals the end-inspiratory plateau pressure [Pplat] minus the positive end expiratory pressure [PEEP], such that [equation 4]:

$$(4)\quad Pplat - PEEP = \frac{tidal\ volume\ (Vt)}{Crs}$$

Equation 4: Driving pressure is the plateau pressure [Pplat] less positive end-expiratory pressure [PEEP]

Contemplating this equation certainly causes some mathematical consternation because it is confusing as to what the independent [clinician-controlled] and dependent [system output] variables are. For this, an illustration proves fruitful [figure 10].

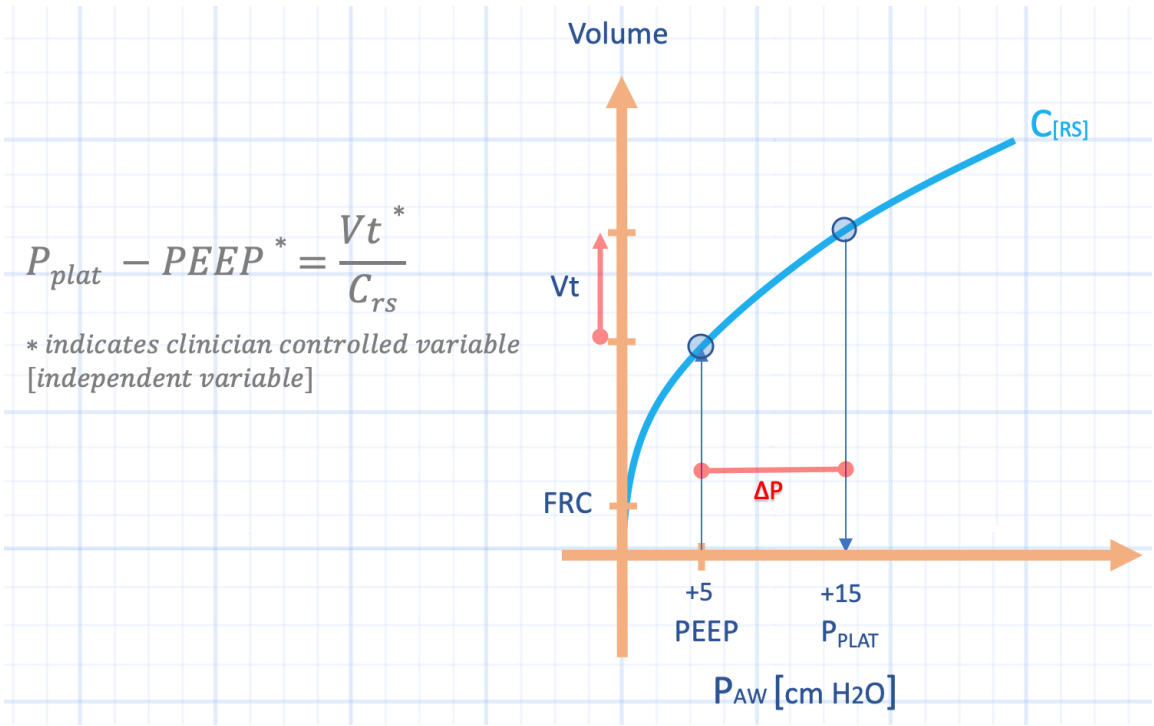

Figure 10: The relationship between tidal volume and driving pressure [ΔP]. There are two independent variables, Vt [ΔV] and PEEP; these are both selected by the clinician in a volume-targeted mode of ventilation. Thus, the true dependent variable is the Pplat while the Crs is a derived variable that forms the slope of the ΔV/ΔP relationship. Paw is airway pressure; PEEP is positive end-expiratory pressure; FRC is functional residual capacity; Crs is respiratory system compliance.

The first complicating matter here is that both Vt and Crs modify driving pressure. In volume control, the clinician directly controls the former, and indirectly the latter. Accordingly, decreasing Vt diminishes ΔP but so too does improving Crs – for example by PEEP titration. Because ΔP follows both changing Vt and Crs, it confounds what a change in Pplat [and therefore ΔP] represents, physiologically. One can envision a situation where diminished Vt [which lowers ΔP] also leads to compressive atelectasis, which impairs Crs [and raises ΔP]. The converse is, theoretically, also possible. Nevertheless, if Vt is held constant and PEEP titration causes over-distension, the slope of the Crs bends down and rightwards [see figure 11]. If there is recruitment of lung, the slope of the Crs bends up and leftwards [see figure 11]. It follows that after PEEP titration, if ΔP remains the same, or falls, then Crs has not worsened.

The second complicating matter here is that Crs reflects the pressure difference between the alveolus and the atmosphere; that is, the distending pressure across the thorax. But this does not represent the true stress on the lung, which is the transpulmonary pressure [Ptp] or the alveolar pressure minus the pleural pressure [9, 108]. Accordingly, a patient with normal pulmonary compliance, but very low chest wall compliance [e.g. obesity, extra-pulmonary ARDS, ascites] will have large ΔP [curve A above], without great stress across the lung [8, 109]. This is important, because it is the stress and strain on the lung which increases lung injury risk and is also an important determinant of right ventricular hemodynamics [9, 12]. This criticism was astutely raised in response to the original paper with the suggestion of measuring esophageal pressure as a surrogate for pleural pressure [110]. The authors responded, somewhat anemically, "...the measurement of esophageal pressures would just reveal a fixed elastic component (chest wall), in series with lung elastance," which lacks substance, because this is true for all patients who are passive with a mechanical ventilator. The question posed to the authors is

distinguishing how much of the chest wall elastance contributes to the calculated airway pressure. The effect of the chest wall on airway pressure can be clinically significant [111, 112].

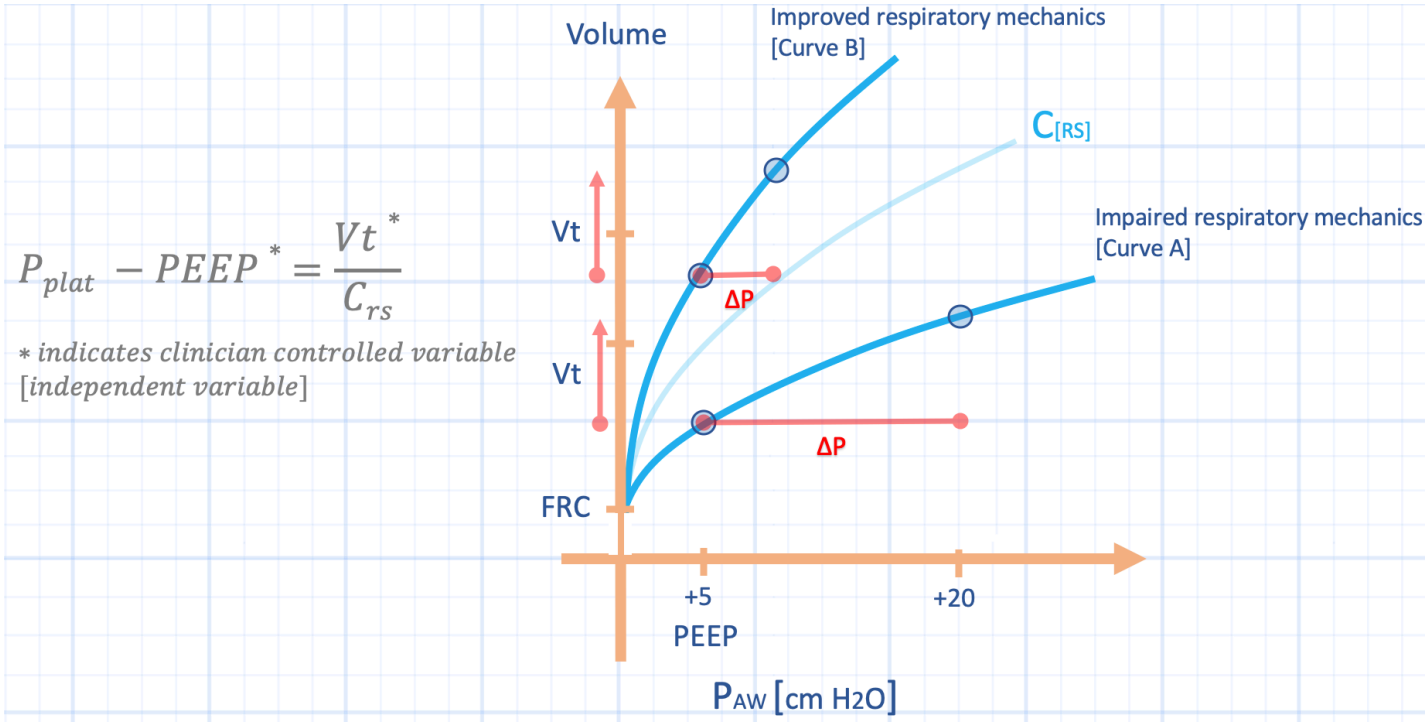

Figure 11: The relationship between tidal volume, airway pressure and respiratory system compliance. Note the tidal volume is the same for both Crs scenarios. See text for details. Paw is airway pressure; PEEP is positive end-expiratory pressure; Vt is tidal volume; FRC is functional residual capacity; Crs is respiratory system compliance; ΔP is driving pressure.

One method for qualitatively evaluating respiratory mechanics – which flows from the physiology above – is the stress index [113]. If the terminal portion of the pressure-time curve on the ventilator demonstrates curvature away from the pressure axis [which approximates curve B, figure 12] the stress index < 1; that is, tidal recruitment. By contrast, if the terminal portion of the pressure-time curve bends towards the pressure axis on the ventilator, curve A in figure 12 is approximated; this represents tidal over-distension [stress index > 1]. Note that on the ventilator, pressure is on the y-axis, not on the x-axis as in figures 10 and 11. Also, on the ventilator, time in on the x-axis rather than volume. A crucial point here is that when measuring the stress index, flow must be constant [square wave delivery] because when flow is constant, volume and time are linear analogs [114]. In other words, flow must be constant so that deformation of the pressure curve reflects altered elastic properties of the lung rather than changing flow.

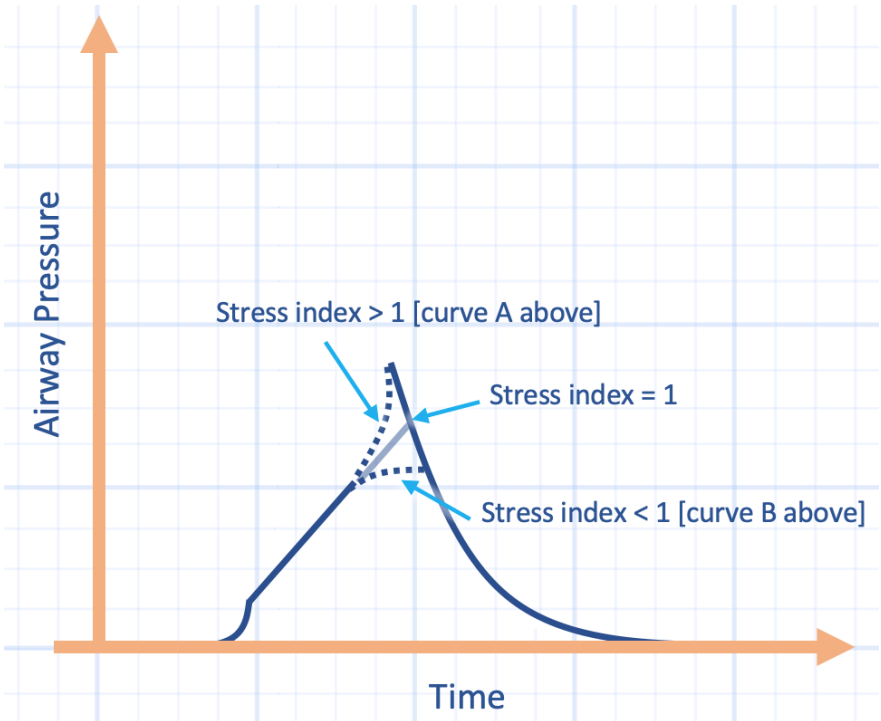

Figure 12: The pressure time curve and the stress index. See text on how this relates to the pressure volume curve in figure 11 [i.e. curve A versus B].

The Respiratory System Pressure-Volume Curve

More than 20 years ago Amato and colleagues reported a significant mortality reduction in ARDS patients who had their ventilator settings guided by the pressure-volume [PV] curve [115]. The 28-day mortality reduction was profound [71% versus 38%] in favour of the patients who had their positive end-expiratory pressure [PEEP] set 2 cm H_2O above the lower inflection point [LIP] ascertained from the PV curve. In addition, the intervention group had their plateau pressure [Pplat] capped at 20 cm H_2O. While this trial may have been practice-changing at the time, the unusually-high mortality rate for the conventional group [i.e. 71%] coupled with simultaneous titration of PEEP and Pplat precluded definitive implementation of PV-curve-based ventilator tuning [116]. Furthermore, the landmark ARDSNet trial [117] swiftly followed as the fountainhead for modifying lung volume and airway pressure in the ARDS patient.

The Curve Basics

The PV curve is typically measured without an esophageal balloon meaning that the relationship is an amalgam of the lung and chest wall together – the 'respiratory system.' As pressure rises on the x-axis, volume follows on the y-axis as a function of the respiratory system compliance [see figure 13]. Classically, the curve is measured at zero PEEP, forming a sigmoid shape because of lung recruitment at low pressure-volume and hyperinflation at high pressure-volume. In other words, at low pressure-volume, there is a lower inflection point [LIP] created by alveolar opening pressure. Below the LIP, there is little volume change on the y-axis. However, after

the LIP pressure investment, volume rises. Initially, the LIP was thought to be the end of alveolar recruitment and PEEP was set 2 cm H_2O above this level.

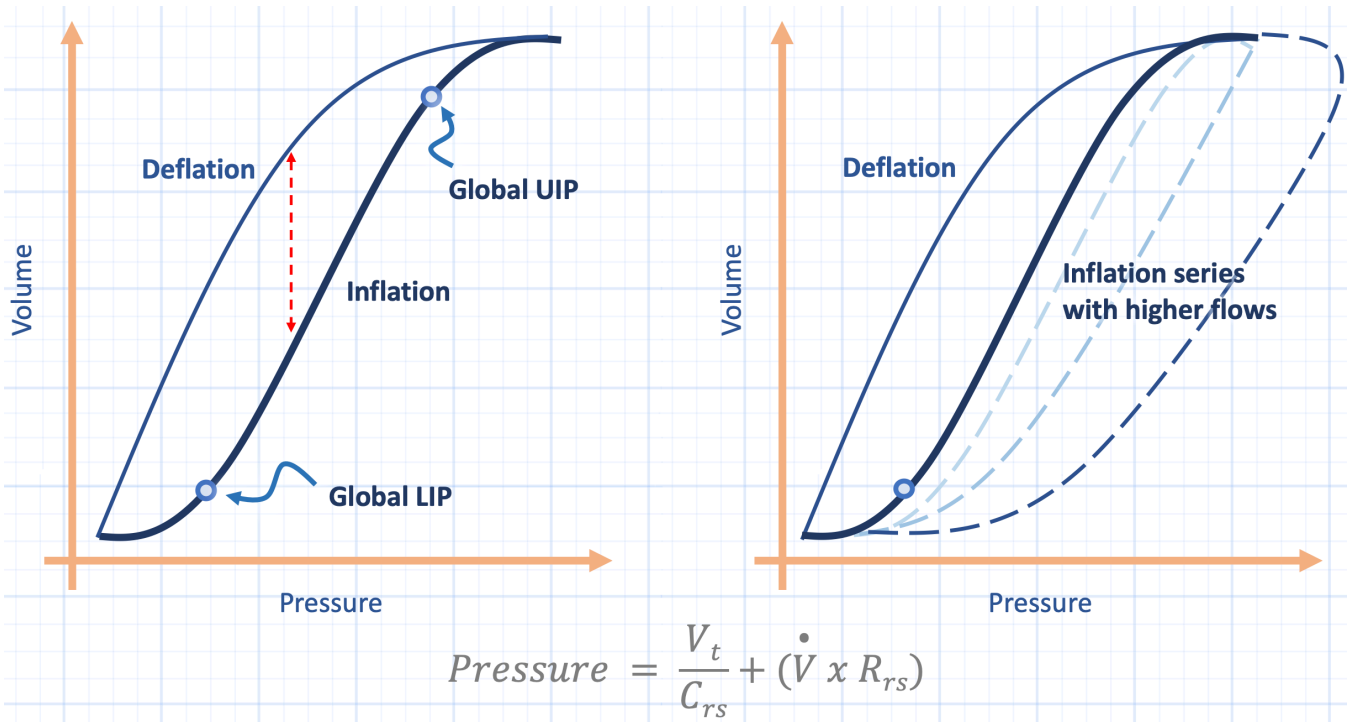

Figure 13: The pressure-volume curve. Left panel shows the basic curve with hysteresis as the red dotted line. Right panel shows measuring the curve and how flow rate affects the curve. This is driven by the equation of motion below the PV curves. Pressure on the x-axis is a function of the respiratory system compliance [Crs] but also flow [V-dot]. Vt is tidal volume, Rrs is respiratory system resistance.

To the contrary, the upper inflection point [UIP] reveals the moment when increased airway pressure no longer raises volume on the y-axis. The UIP was felt to mark the moment of alveolar over-distension; ergo, safe ventilation was bounded between the LIP and UIP.

Conspicuously, there is a pressure difference between inflation and deflation in the pressure volume curve. This is known as 'hysteresis' and occurs primarily because inflation pressure must overcome the attraction between water molecules at the water-air interface. Surfactant mitigates inter-molecular attraction of water such that as pressure falls on deflation, larger volume is achieved [118]. For simplicity of discussion, only inflation PV curves will be considered herein. This should not, however, belie the importance of the deflation limb [119, 120].

Measuring the Curve

The point of the PV curve is to provide information on the static characteristics of the respiratory system. Thus, like an end-inspiratory hold on a ventilator, gas flow [and patient effort] should be removed from the equation [figure 13, right panel]. There are 3 basic techniques to measure the static pressure-volume curve: the 'super-syringe' method, the multiple occlusion method and the constant flow technique [118, 121]. The former two may be thought of as a series of 'end-inspiratory' holds – such that measurements are made at zero airflow, while the latter allows for a constant, low-flow during measurement. Consequentially, gas

flow less than 10 L/min [122, 123] should be used to mitigate the effects of dynamic airway pressure, yet even flow values less than 2 L/min can have small effects on the LIP of the PV curve [124]!

Curve Caveats

Even if the PV curve of the respiratory system is measured perfectly, there can be significant variability of LIP measurement between observers [125, 126]. Moreover, in the absence of an esophageal balloon, the chest wall contribution is ignored which may be important in the obese and/or extra-pulmonary ARDS [8, 127]. Further, patients must be deeply-sedated and, potentially, paralyzed to ensure that no respiratory effort contributes to airway pressure. Lastly, animal, clinical and mathematical models have suggested continuous recruitment of alveoli along the inflation curve beyond the LIP. Conversely, some alveoli may reach their strain limit before the UIP [128-131]. Indeed, Venegas et al. found that the derivative of the equation of best-fit for the PV curve was Gaussian, suggesting a broad distribution of alveolar recruitment along the entire curve [131].

Recent Data

In line with the mathematical models of Venegas and Hickling [119, 129, 131], a recent and inspiring clinical study revealed that regional PV curves exist within the lung and distribute around the global PV curve [132] [see figure 13]. Scaramuzzo and colleagues studied 41 PV curves from 12 patients with acute respiratory failure with or without ARDS. The patients were deeply-sedated and pharmacologically paralyzed in the supine position; electrical impedance tomography [EIT] was used to measure regional volumes along the ventral-dorsal axis. The key findings are illustrated in figure 14.

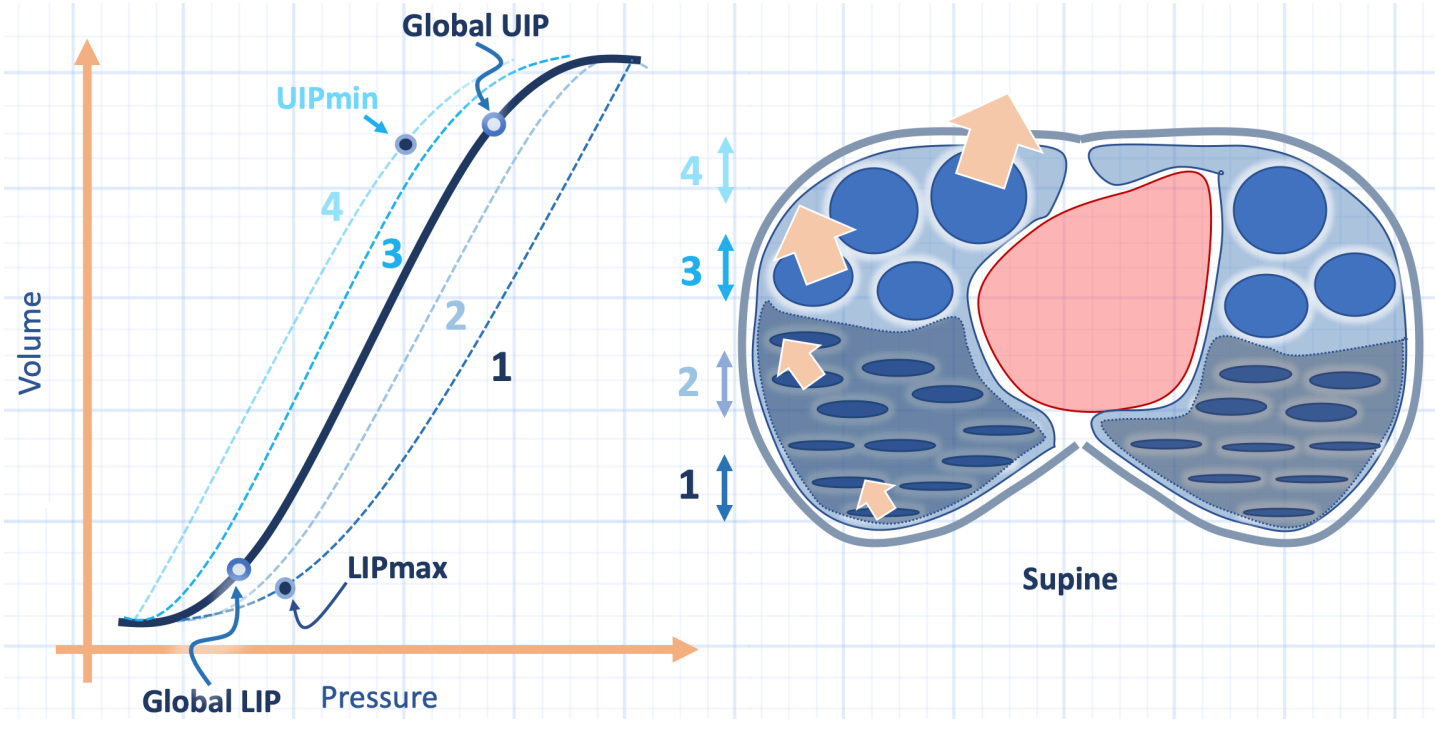

Figure 14: Illustration of local pressure-volume curves within the lung. See text for details. LIP is lower inflection point, UIP is upper inflection point.

In brief, the global PV curve had a LIP lower than that of the opening pressure required to open the dorsal-most lung unitsThus, if the global LIP were used, the dependent lung may still act as 'stress raisers' – aggravating the risk of atelectrauma. Conversely, the global UIP was found to be higher than the regional UIP of the ventral-most lung units, placing these units at risk for over-distension if the global UIP is used to limit end-inspiratory pressure. This has implications for the 'stress index.' As described previously, the global UIP marks the point at which the pressure-time curve bends towards the pressure axis [i.e. stress index > 1]. Accordingly, at a stress index of exactly 1, some of the ventral-most lung units may be over-distended. Previous data has suggested that the stress index may result in slight over-application of PEEP [133, 134].

Lastly, one may theorize how pronation may affect the regional versus global PV curves. The prone position shifts the chest wall PV curve rightwards and stiffens the chest wall [i.e. change its slope] [7]. With simultaneous homogenization of the pulmonary parenchyma in the prone position [44, 54], one expects the regional curves to cluster more closely around the global curve. Thus, higher absolute pressures would be required with less disparity between the global and regional values – potentially making the stress index a valuable tool for titrating PEEP in the prone position [figure 15].

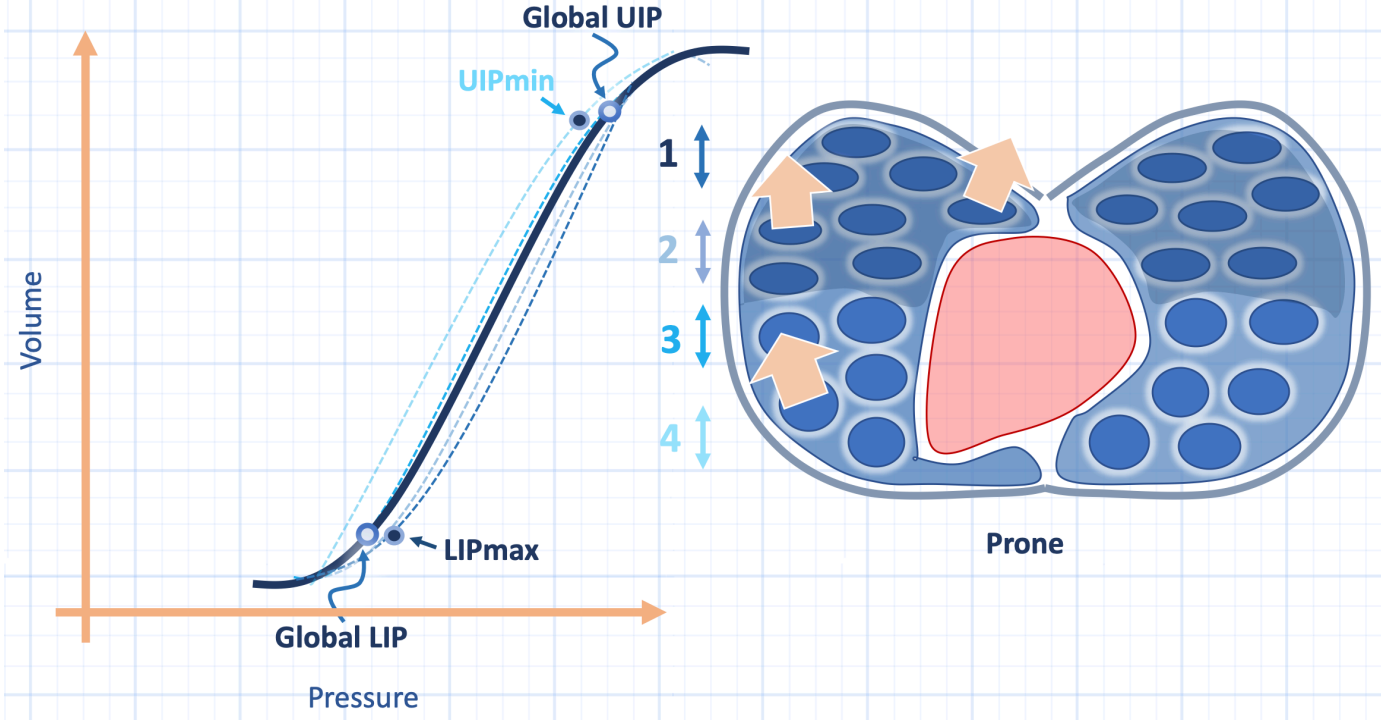

Figure 15: Hypothetical affect of prone position on regional pressure-volume curves. See text for details. LIP is lower inflection point, UIP is upper inflection point.

Ergotrauma

In a succinct and relatively recent treatise, Gattinoni and Quintel outline the modern management of the acute respiratory distress syndrome [ARDS] [44]. It is

critical, they reason, that treating ARDS requires reducing lung inhomogeneity, as discussed above, but also the mechanical power applied to the lungs as discussed herein.

The Lung Skeleton

The fibrous skeleton of the lung is composed of two fibre systems. First, there is an axial system which is anchored to the hilum and branches along the airways towards the alveolar ducts [45]. Second, there is a peripheral system which is tethered to the visceral pleura and tracks inwardly towards the lung acini. These two systems associate at the alveoli and generate a continuous 'lung skeleton' [45]. Elastin and collagen are the major components of this skeleton and it is to this fibrous scaffold that the epithelial and endothelial cells of the lungs tether. When the skeleton of the lung is distended, the lung parenchyma and accompanying cellular scaffolds are altered. Excessive energy distributed to the skeleton may lead to a myriad of injuries, both indirectly via activation of mechanoreceptors but also by direct mechanical stress [45, 135].

Energy and Work

Accordingly, the energy applied to the lung's fibrous skeleton may be a key determinant of ventilator induced lung injury [VILI]. As Gattinoni notes, VILI is more precisely coined ventilation induced lung injury, as it may also be the consequence of spontaneous ventilation [136].

The total energy absorbed by the lung during a single breath is quantified by the joule; the joule is a measure of work. Consider that work is defined as a force required to move an object a given distance.

$$(5)\quad work = force\ x\ distance$$

Equation 5: The equation for work.

Because pressure is a force applied over a given area, and because volume is an area applied over a distance the following is derived:

$$(6)\quad work = [pressure\ x\ area]\ x\ \frac{volume}{area}$$

And, therefore:

$$(7)\quad work = pressure\ x\ volume$$

Equations 6 & 7: The relationship between work, pressure and volume.

Accordingly, upon the lung, work is graphically depicted as the area bounded by the pressure-volume relationship [figure 16]. Further, there are two types of work applied to the lung during a breath – static and dynamic [see also chapter 1]. Static work is the energy required to maintain volume while dynamic work is the requisite portion of energy driving gas flow and overcoming tissue resistance [e.g. tissues sliding over each other]. At the onset of a breath, a greater fraction of work is dedicated to gas flow and tissue resistance [figure 16 - red shaded area]. As the breath continues a larger proportion of work is partitioned into maintaining lung volume [figure 16 - blue shaded area]. At the termination of the breath, all of the work is invested in the new volume; this is when flow – and therefore the fraction of dynamic energy – is zero.

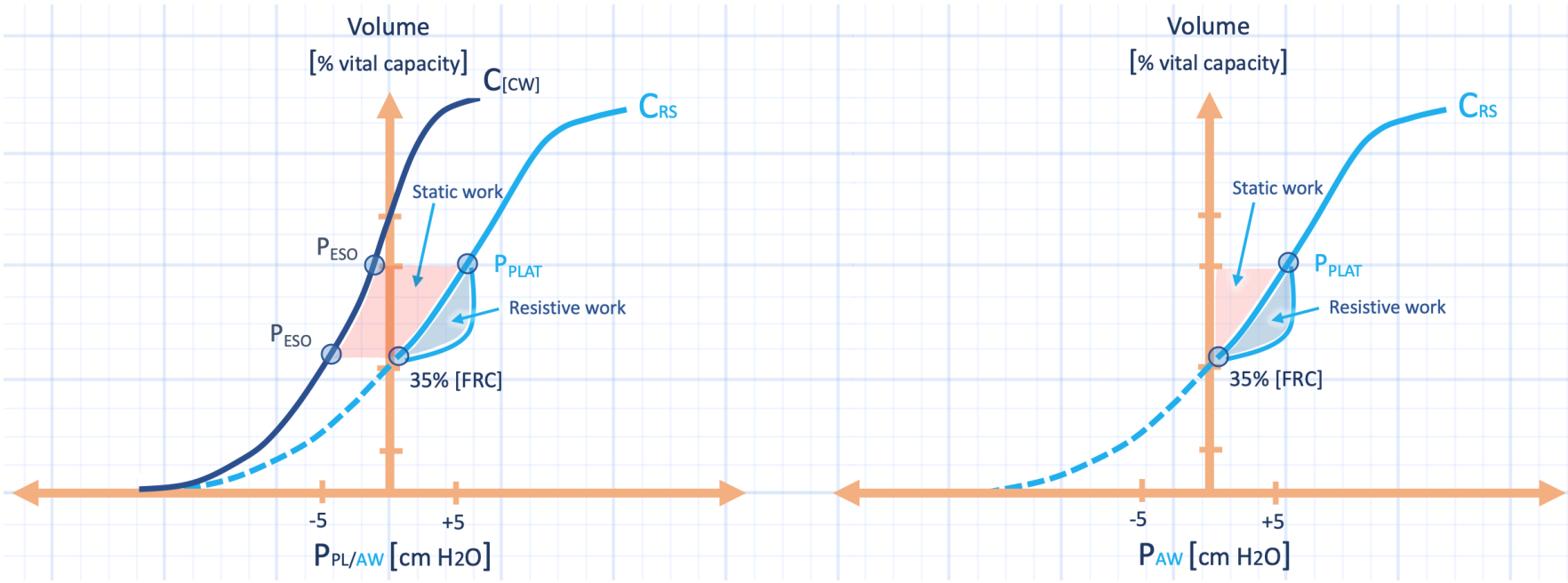

Figure 16: Work and power. Left panel: The work across the lung for a single breath. The work across the lung is bounded between the respiratory system compliance curve [Crs] and chest wall compliance curve [Ccw]. Static or elastic work is red-shaded, dynamic or resistive work is blue shade. Peso is esophageal pressure as a surrogate for pleural pressure [Ppl]. Pplat is the plateau pressure. This breath starts from zero positive end-expiratory pressure. FRC is functional residual capacity. Paw is airway pressure from the Crs curve. Work for one breath multiplied by the respiratory rate is power. Right panel: The work across the respiratory system. The reasoning is similar to the lung in the left panel, however, the pressure reference is is atmospheric pressure rather than esophageal pressure.

The summation of the static and dynamic work gives the total work for a single breath. However, when the total work is multiplied by the respiratory rate, the entire work per unit time is obtained and this is the mechanical power applied to the lung.

Perhaps the leap forward offered by mechanical power is its conceptual parsimony – tying together multiple, incongruent instigators of VILI into a single explanatory variable [64, 137]. And this conceptual frugality is matched by its face-validity in first principles as above; i.e., power is work over time, work is a force over a distance, necessitating energy transfer, and energy is needed to break stuff – like lung tissue.

From a clinical perspective, tidal volume [i.e. displacement of the lung or its 'strain'] and transpulmonary pressure [i.e. the pressure difference between the airway and

the pleural space or 'stress'] have been undeniably essential mediators of ventilator – or ventilation – induced lung injury. Yet, they alone cannot explain other known arbiters of harm. For example, with constant tidal volume and airway pressure, increased respiratory rate exacerbates lung injury [63, 88]. Further, with tidal volume, driving pressure and respiratory rate all equal, rapidly delivered volume – i.e. increased flow or strain rate – also promotes lung injury [138, 139]. Importantly, all of these facilitators of VILI are contained – and therefore explained – within the model of the mechanical power applied to the lung [140, 141].

Mechanical Power

Since the publication of the landmark ARDSNet trial [142], the focus of VILI prevention – clinically – has been minimizing lung volume and plateau pressure. These variables represent markers of the static work of a single breath. However, respiratory rate, flow and even temperature are also VILI co-mediators [143, 144]. Accordingly, the dynamic work applied to the lung also facilitates some aspect of lung injury. To address these findings, Cressoni and colleagues have proposed a unifying hypothesis – mechanical power – which considers both static and dynamic energy applied to the lung over time [145].

In their porcine model, Cressoni and colleagues applied a tidal volume – known to be lethal – at varying respiratory rates. All other respiratory variables were maintained constant and all animals received paralytics. Consequently, mechanical power varied only by respiratory rate and flow. The difference between the lowest and highest respiratory rate was 5-fold [3 breaths/minute versus 15 breaths per minute], yet the power increased 11-fold because flow rises with higher respiratory frequency. The power threshold for VILI was 12 joules/minute. In confirmatory testing, a respiratory rate of 35 breaths per minute was selected for all animals, but at two different tidal volumes – one tidal volume that superseded the VILI threshold and one which did not. Again, only those ventilated with mechanical power above 12 joules/minute developed VILI. Mechanical power was also associated with final lung weight, increasing lung elastance, and diminished PaO_2 to FiO_2 ratio. Animals ventilated below this threshold developed only isolated lung densities [145].

There are clinical repercussions of this model should it extrapolate to the bedside. First, peak pressure does indeed matter with respect to VILI as the peak pressure is a measure of dynamic work. Second, it raises theoretical concerns with pressure-targeted modes of ventilation in ARDS as this method of ventilation prevents the clinician from completely controlling: lung volume, transpulmonary pressure or gas flow. Third, mitigation of mechanical power provides mechanistic plausibility for the – albeit contentious – therapeutic effects of early paralysis in ARDS [146, 147]. Absence of respiratory effort allows total control over lung volume, gas flow and minimizes transpulmonary pressure. Lastly, this model may explain the disappointing results of high-frequency oscillatory ventilation [148]. While tidal volume is extraordinarily reduced, the total mechanical power necessitated for lung oscillation may supersede the VILI threshold. Finally, the mechanical power

applied to the lung's fibrous skeleton may be cryptically high in other unconventional methods of mechanical ventilation, for example, airway pressure release ventilation [APRV] as considered in more detail below.

The Mechanical Power Equation

The equation for mechanical power is shown at the bottom of figure 17. While complicated on first-blush, it is simply a mathematical representation of the ventilator pressure-time waveform, as elaborated below.

For simplicity, we will consider inspiration in a patient passive with the ventilator and in a volume-limited mode of mechanical ventilation. The equation of motion [63, 137, 140, 149, 150] shows that at any moment in time, the airway pressure is the summation of two principle components [three if you consider positive end-expiratory pressure, PEEP]. These two components are: 1. the pressure required to overcome airway and tissue resistance and 2. the pressure required to increase the volume of the lung and chest wall. These two components evolve over a breath and may be thought of analogously to kinetic and potential energy, respectively. In other words, there is pressure dedicated to 1. movement, for example, of gas [i.e. kinetic energy] and 2. increasing the volume of an elastic structure [i.e. potential energy].

These components are often visualized on a pressure-volume curve, also depicted in figure 17. The kinetic component is the parallelogram shaded in blue – this is often referred to as 'resistive pressure' and the area defined by the blue shade is the 'resistive work.' Additionally, the potential energy from the tidal volume-related 'elastic work' is shaded in red. Finally, when PEEP is applied, the additional elastic work component is in pink.

As the area of each of these three subcomponents represent work, they are summed to obtain the total work for a single inspiration. The areas are computed by simple geometry because the PEEP-related elastic work [in pink] is a square, the tidal volume-related elastic work [in red] is a triangle and the resistive work, in blue, is approximated by a parallelogram.

The dimensions of each of these shapes are read from the pressure-volume graph. Recall that the area of a square and parallelogram are base x height and a triangle is one-half base x height. Note that the 'height' of the triangle [its pressure cathetus] is calculated by multiplying its base [its volume cathetus] by the slope of its hypotenuse. The slope of the hypotenuse is the compliance or elastance of the respiratory system [Ers – elastance is the change in pressure for a change in volume – the inverse of compliance]. The 'base' of the parallelogram [in pressure] is the gas flow x tissue resistance while its height is Vt.

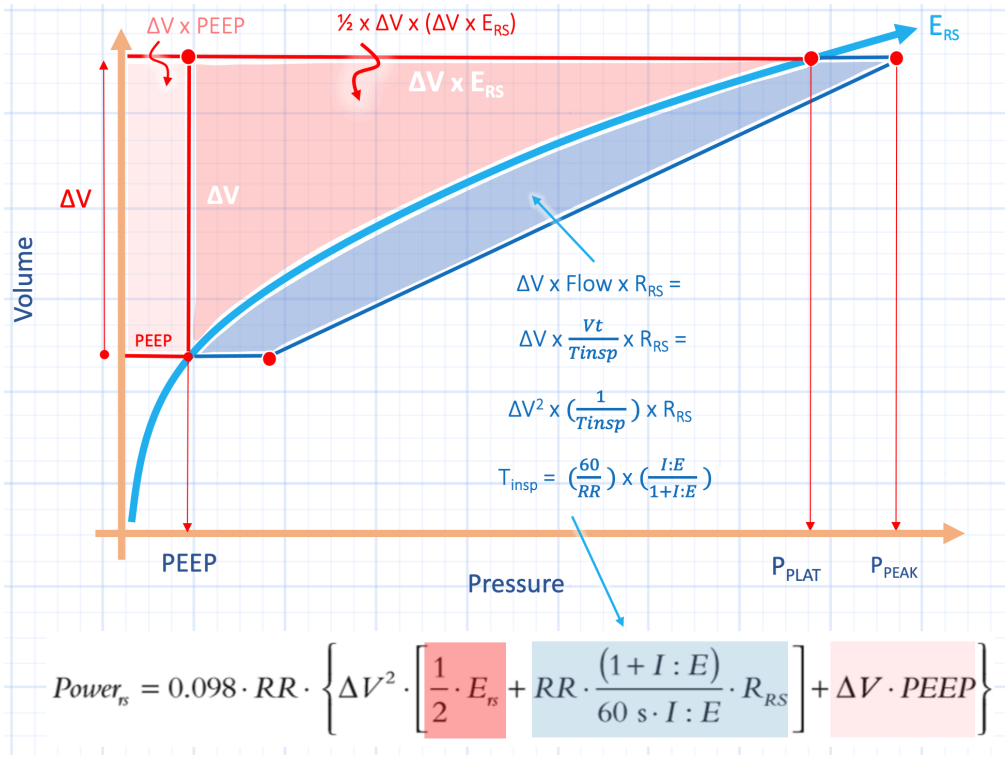

Figure 17: Mechanical power across the respiratory system. See text for details. Note that compliance and elastance are inversely related. If volume is known and elastance is known, then multiplying volume by elastance gives pressure. Tinsp is inspiratory time; I:E is the inspiratory-to-expiratory time ratio. PEEP is positive end-expiratory pressure; Pplat is plateau pressure; Ppeak is peak inspiratory pressure; Ers is respiratory system elastance; Rrs is respiratory system resistance; RR is respiratory rate.

Accordingly, when these areas are summed, the power equation takes shape – including the seemingly strange tidal volume [ΔV] squared term. When the work of one breath is multiplied by the respiratory rate, then power over time is given.

Relation to the Pressure Waveform on a Ventilator

As described above, the pressure-volume curve – so often used in basic respiratory physiology papers – can be transmuted into the pressure-time curve displayed on a ventilator. This is achieved by moving pressure from the x-axis to the y-axis and changing volume to time on the x-axis. Volume and time are interchangeable when there is constant flow [i.e. square-wave flow] such that volume and time become linear analogues [i.e. if flow is constant, then the same amount of volume is delivered per unit time]. As seen in figure 18, you have undoubtedly already subdivided a breath into its elastic and resistive work components; for example, when performing an end-inspiratory hold to differentiate peak and plateau pressures.

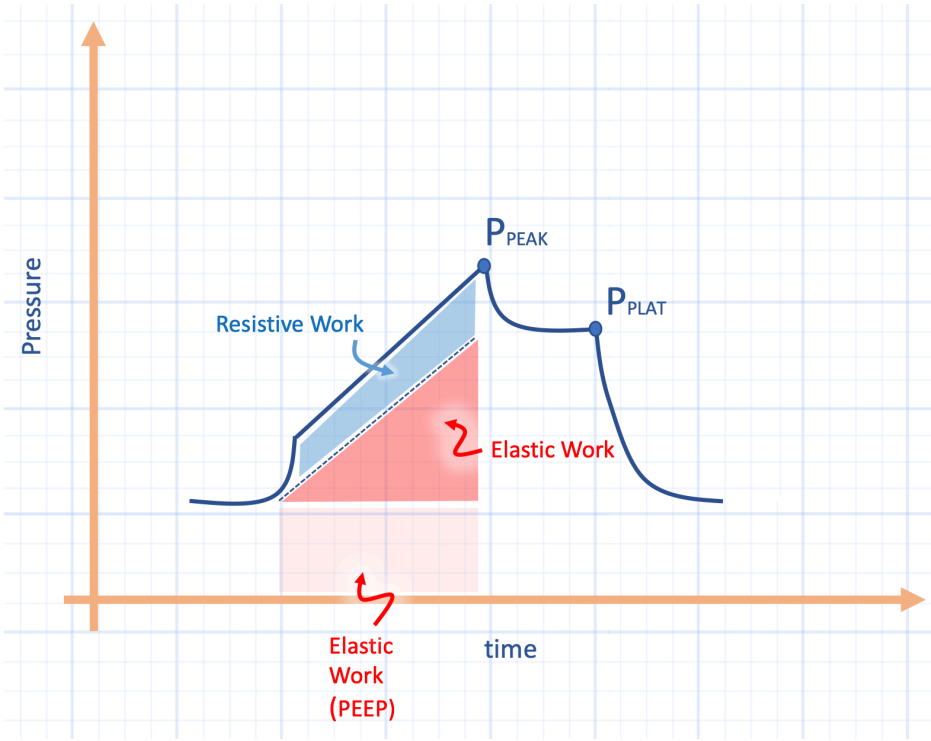

Figure 18: Pressure-time waveform from the ventilator. Colour-coding and abbreviations match figure 17. Volume can become time when flow is constant.

While mechanical power deserves attention, it is not without criticism [151] especially in light of two recent papers on the interaction between tidal volume and power [152] and PEEP and power [153]. While all of power seems important, should we preferentially focus on the 'driving power' as coined by Marini [137]?

The mechanical power applied to the lung is a risk factor for ventilator or ventilation-induced lung injury [VILI] [63, 140, 141, 153]. But can the work done to the lung over time be homogenized into a single value? Could different components of the power equation carry different VILI risk beyond their mathematical inequalities [140]?

One possible avenue to explore these questions is to study positive end-expiratory pressure [PEEP], which should linearly increase mechanical power and, therefore, VILI [64]. But others criticize this reasoning – noting that PEEP should have a 'U-shaped' effect [137, 151]. In other words, increasing PEEP linearly increases mechanical power, but not necessarily VILI.

A recent porcine investigation provides some answers to the questions above [153]; but before explicating these results, a primer on the effect of PEEP on power is justified.

PEEP and the Viscoelastic Lung

The degree of stress developed in a viscous material [think putty], is quite different from a purely elastic material [think rubber band] when submitted to strain [see figure 19] [139]. Recall that strain is an increase in length – or volume – relative to baseline [62, 154]. In a viscous material, the stress felt is proportional to strain velocity, while in an elastic material the stress is proportional to the strain and the material's inherent 'stiffness' or specific elastance.

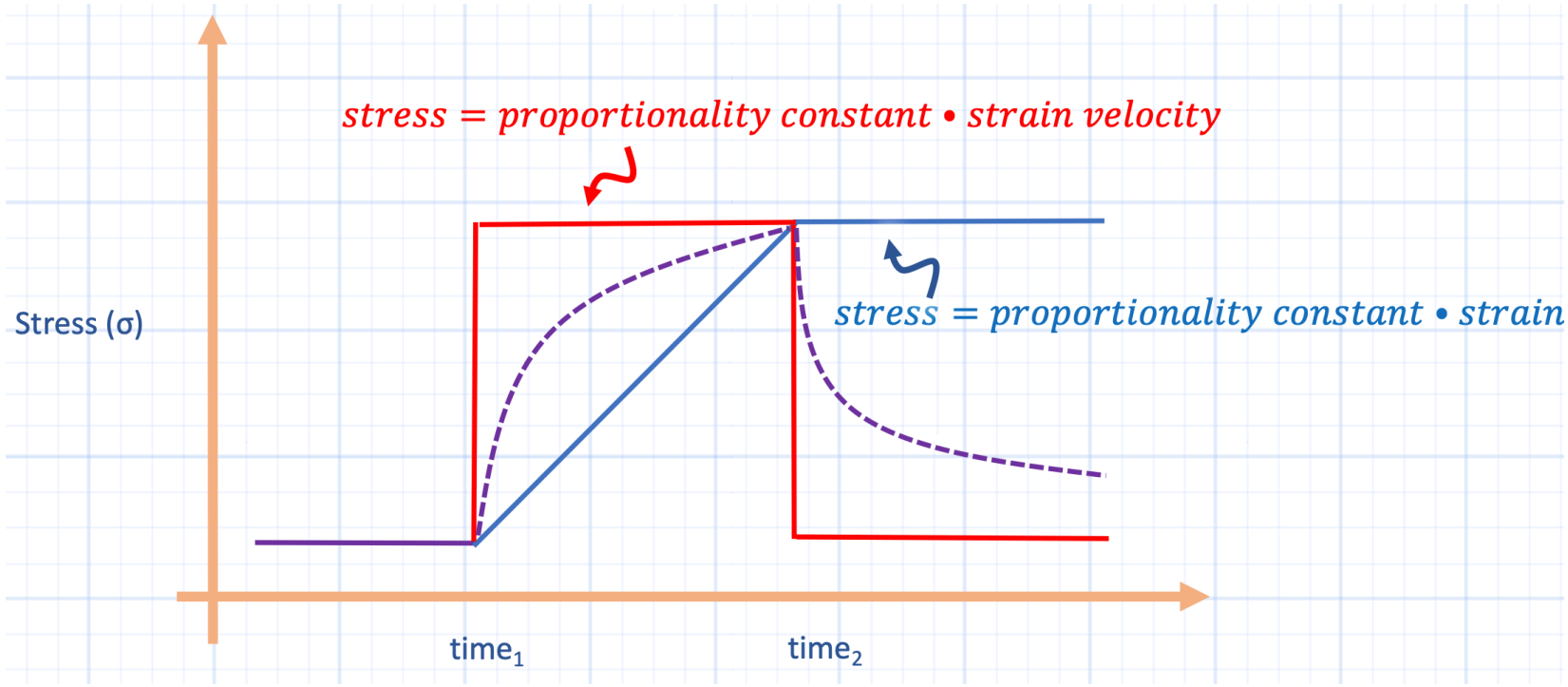

Figure 19: Stress in elastic [blue] versus viscous [red] material. Purple dashed line is viscoelastic material. See text for details.

In a purely elastic material, the energy required to stress the object is stored in potential energy which is recaptured upon strain release. In a viscous material, this energy is lost as heat and rearrangement of the underlying material structure.

The lung is viscoelastic – its stress response to a given strain is somewhere between a purely viscous and elastic material [139, 155]. Accordingly, the absolute strain and the strain velocity mediate stress and, therefore, lung injury. How does PEEP affect absolute strain and strain velocity?

First, when total strain remains constant [i.e. constant change in lung volume], but this total strain is composed of increasing levels of PEEP [e.g. 100% tidal strain versus 75% tidal strain and 25% PEEP strain], there is less VILI with larger PEEP fraction [138] – when all other variables like respiratory rate and I:E ratio are constant. Presumably, because smaller tidal strain means a smaller volume change per unit time [i.e. strain rate], there is less viscous-mediated stress across the lung and less lung injury [139].

Second, PEEP 'homogenizes' the lung [as does pronation]. More simply, PEEP reduces the number of 'stress raisers' [44] as discussed above. Stress raisers locally amplify stress around adjacent materials of differing elastance. Mathematically, stress raisers augment the local stress by 4.6 [48] though this is probably closer to 2.0, clinically [51, 64].

In summary, PEEP reduces strain rate which eases viscous stress and PEEP homogenizes the lung which reduces local specific elastance or elastic stress.

PEEP and Mechanical Power

A recent porcine study investigated the effect of 6 levels of PEEP with tidal volume, flow and respiratory rate all held constant [153]. One group received zero end-expiratory pressure [ZEEP] while the other 5 groups entertained progressively higher PEEP. Amongst the 5 groups that received PEEP, mechanical power and VILI risk rose linearly. Importantly, however, the ZEEP group had equivalent mechanical power to the low PEEP groups, but had lung injury comparable to the high PEEP groups. Thus, while overall mechanical power is an important determinant of VILI, it is not absolute, because the ZEEP group had relatively low power. A hypothetical illustration of ZEEP versus PEEP and mechanical power is seen in figure 20.

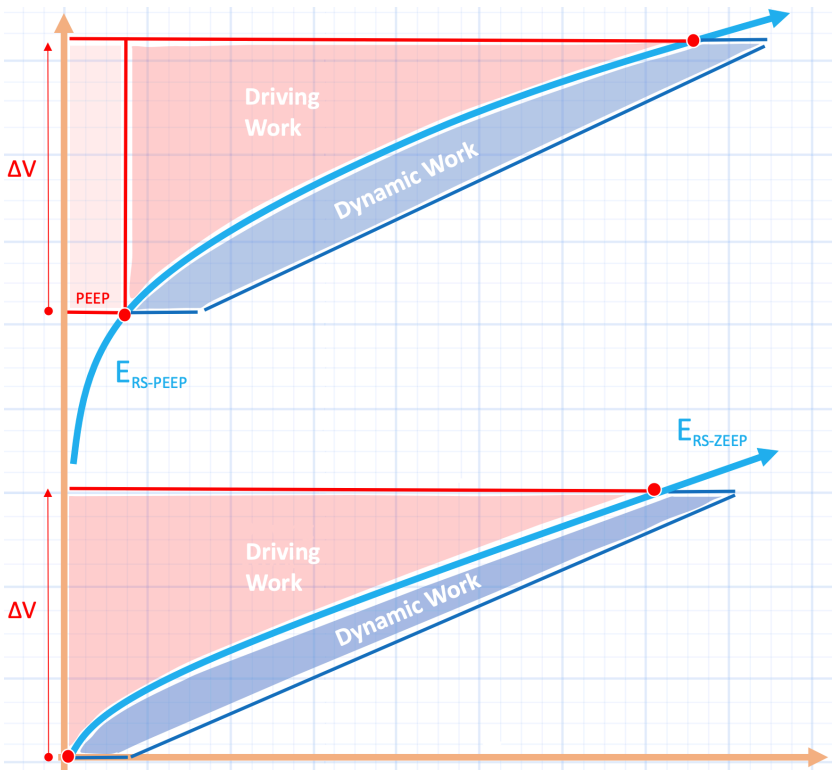

Figure 20: Hypothetical effect of positive end-expiratory pressure and mechanical power. Bottom waveform is zero end-expiratory pressure [ZEEP] and Ers is respiratory system elastance [or compliance]. Top panel is the effect of positive end-expiratory pressure [PEEP]. Note that the total area is similar, but the larger driving work and power may be more injurious. The y-axis is volume and ΔV is tidal volume. The x-axis is pressure.

Moreover, the fraction of power dedicated to tidal ventilation [i.e. 'driving power'] seemingly better correlated with VILI. In the ZEEP group at baseline, nearly 60% of the total power per breath was due to the elastic, tidal volume component, while in the low PEEP groups, this fraction fell to about 40%. The fall in driving power likely resulted from improved pulmonary compliance via lung recruitment – decreasing driving pressure [see figure 20]. Considering the discussion above, PEEP improved the elastic stress – given that the strain rate was constant – which reduced local stress raisers and mitigated VILI.

With high PEEP, driving power slightly increased; ostensibly because of impaired lung compliance by over-distension.

Operationalizing Driving Power

Given the above, we are led back to Marini's prescient description of the 'driving power [137].' If this is the most important sub-component of the mechanical power, how could one go about operationalizing this at the bedside?

First, concentrating on the three key determinants of the driving power is sensible [i.e. tidal volume, respiratory rate and lung elastance]. Previously, Gattinoni's group found that tidal volume affected total power exponentially by a factor of 2.0, while respiratory rate increased power exponentially by a factor of 1.4 [140]. Further, reducing both respiratory rate and tidal volume decrease all of the other power sub-components [e.g. resistive, elastic-PEEP and elastic-tidal volume]. Ideally, tidal volume is reduced with knowledge of the 'baby lung' volume so as to reduce strain [62].

The next component of the driving power – the lung elastance – can be reduced by increasing PEEP. Titrating the effect of PEEP on lung elastance may be executed by either the stress index or driving pressure – as described above. Thus, increasing PEEP-related mechanical power seems prudent only when offset by diminished driving power. If PEEP fails to decrease pulmonary elastance – and therefore driving power – then prone position should be considered [11, 44].

Once driving power is optimized, then the resistive work is minimized. Importantly, PEEP decreases airway resistance by increased lung volume. As well, reduced I:E ratio should also reduce VILI risk as flow, like tidal volume, augments mechanical power exponentially by a factor of 2.0 [140].

Shorthand Equations for Respiratory System Power

Calculating mechanical power based on the equation described above is cumbersome. There are, however, shorthand equations that make power calculation facile; these mathematical heuristics derive from simplified geometric calculations of respiratory system work for a single breath [in joules]. This geometric approach is used to explain two simple equations – the second of which was recently studied in a cohort of mechanically-ventilated, critically-ill patients [135].

Basic Geometry of Work

As described above, the work for a single breath is the area between the pressure-volume curve. Of note, when a patient is passive with the ventilator, in volume control with a square-wave flow delivery, every pressure-time waveform illustrates work.

Figure 17 above shows that the work for a single breath is approximated by summing the area of three shapes nestled within the breath:

1.) a triangle [in red] representing the elastic work above positive end expiratory pressure [PEEP]

2.) a parallelogram [in blue] representing dynamic work [e.g. gas flow, moving tissues]

3.) a rectangle [in pink] representing the elastic work of PEEP

When these three geometric figures are added, the rather foreboding equation within the braces at the bottom of figure 17 results. When work [in joules, within the braces] is multiplied by the respiratory rate [outside of the braces], then work over time – or power – is obtained. The 0.098 converts [L x cm H_2O] to joules [140, 145].

Shorthand Equation 1

While the equation in figure 17 most accurately measures power applied to the respiratory system, it is clearly cumbersome to calculate at the bedside. Additionally, it requires measuring both the resistance and elastance [i.e. stiffness] of the respiratory system. For this reason, Gattinoni and colleagues proposed the following, clinically-friendly equation [140] [see figure 21].

Here, the same geometries carry from figure 20, however, this approach employs a 'subtraction method' to calculate breath work. As tidal volume [ΔV, y-axis] is outside of the brackets in the equation, it is multiplied first with peak pressure [Ppeak] and this gives the area of the entire rectangle bounded by ΔV and Ppeak [i.e. width x length]. However, when ΔV is multiplied by the second term within the brackets [highlighted in purple], the area of the purple triangle is given. The base of the purple triangle is geometrically-equivalent to the plateau pressure less the PEEP [i.e. the driving pressure, Pdrive] and the height of the purple triangle is the ΔV, outside of the brackets. This is divided by 2 to calculate the area of the triangle [i.e. $\frac{1}{2}$ base x height]. Accordingly, this subtraction method gives the same area as highlighted in figure 17 which is multiplied by respiratory rate and the conversion factor 0.098 to obtain power in joules/min.

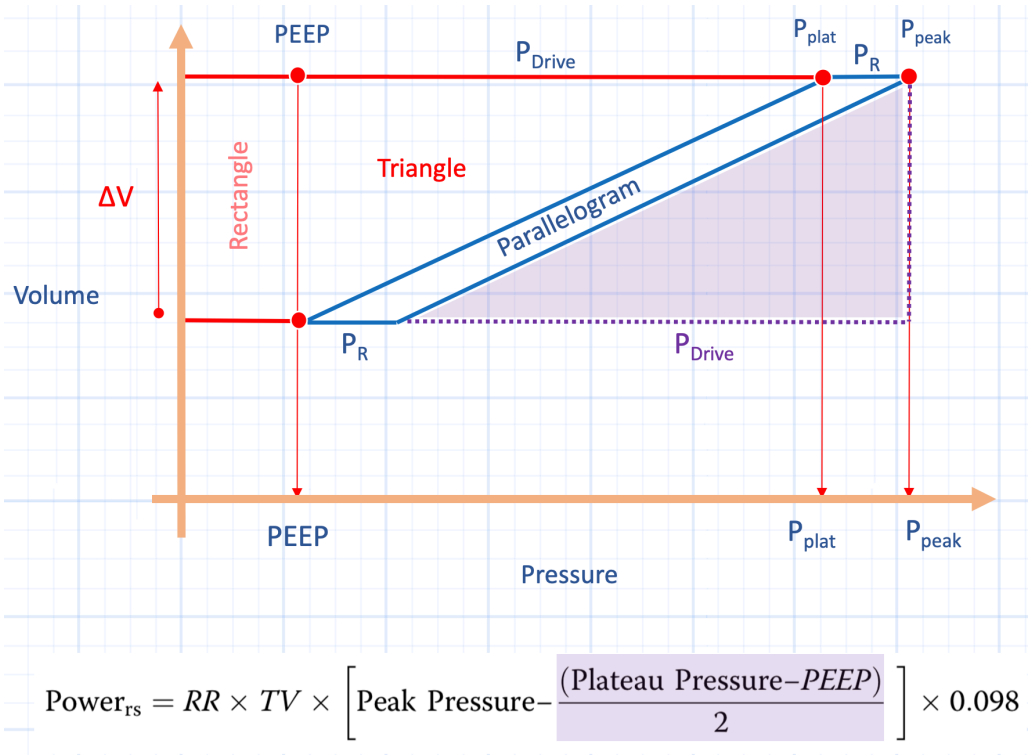

$$\text{Power}_{rs} = RR \times TV \times \left[\text{Peak Pressure} - \frac{(\text{Plateau Pressure} - PEEP)}{2}\right] \times 0.098$$

Figure 21: Geometry behind shorthand equation 1. The y-axis is volume and x-axis is pressure. PEEP is positive end-expiratory pressure; Pplat is plateau pressure; Ppeak is peak airway pressure; Pdrive is driving pressure; Pr is resistance pressure; ΔV and TV are both tidal volume; RR is respiratory rate.

Shorthand Equation 2

While more clinically-intuitive, shorthand equation 1 still requires a ventilator-maneuver; that is, an inspiratory hold to parse out the plateau pressure from the peak pressure. In a recent investigation, Gattinoni's group proposed an equation that requires no hold maneuver [156]; thus, real-time power may be displayed continuously.

Figure 22 shows that this approach essentially requires summing 3 separate triangles to obtain the breath's work. The height of each triangle is tidal volume [ΔV, y-axis]. Consequently, ΔV is outside of the parentheses and distributed to 3 separate terms – the bases of the 3 triangles. The base of the right triangle [A] is the peak pressure [Ppeak]; the base of the obtuse scalene triangle [B] is PEEP and the base of the obtuse, scalene triangle [C] is ventilatory flow [F] divided by 6.

What is the origin of flow/6? This is the pressure due to resistance [Pr] and requires an assumption in the absence of an inspiratory hold. The assumption is that the resistance is the mean value of resistance in ventilated patients [i.e. 10 $cmH_2O \cdot sec/litres$] or 1/6 $cmH_2O \cdot min/litres$ [156]. Accordingly, multiplying this assumption by the flow [F, litres/min] gives the estimated Pr [base of C – see figure 22].

Finally, the denominator – 20 – is a constant resulting from $\frac{1}{2}$ [from the area of the triangles] multiplied by the conversion factor 0.098.

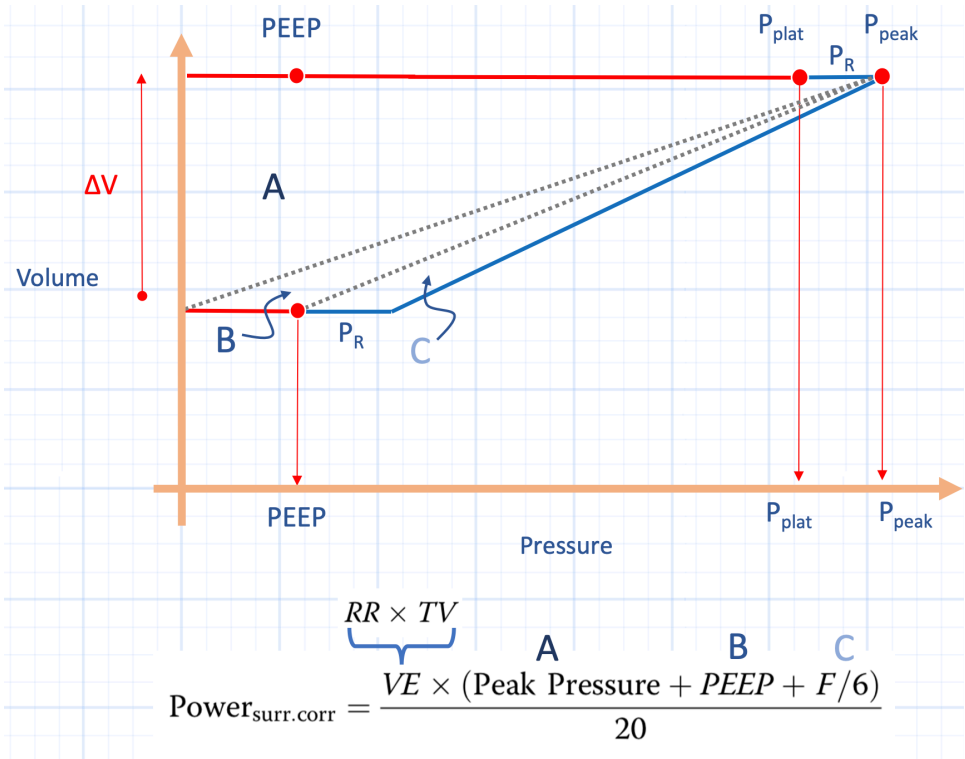

Figure 22: Geometry of shorthand equation 2. See text for details. Both ΔV and TV are tidal volume; VE is minute ventilation; PEEP is positive end-expiratory pressure; Pplat is plateau pressure; Ppeak is peak airway pressure; Pr is resistance pressure; RR is respiratory rate; F is flow.

Clinical Implications

Shorthand equation 2 was recently validated in 200 ventilated, ICU patients from 7 previously-published trials [156]. These patients had mechanical power of the respiratory system calculated by the initial method [figure 17] at PEEP values of 5 and 15 cm H_2O. At both PEEP levels, the R^2 comparing shorthand equation 2 to the full equation was quite excellent – 0.98 and 0.97, respectively. The shorthand equation slightly underestimated mechanical power to the respiratory system by 0.5 – 1.35 joules/min.

Importantly, to presume the aforementioned geometries, patients should be passive [i.e. no respiratory muscles contributing to the pressure waveform] and with constant-flow delivery in volume control. Currently, the power threshold for ventilator induced lung injury [VILI] in humans is unknown. Indeed, Marini recently stated that he does not target a certain power to avoid lung injury [157]. Nevertheless, the VILI threshold for porcine lungs is 12 joules/min, as described above. Given that human lungs have twice the specific elastance of porcine lungs [46], a rough, extrapolated threshold is 24 joules/min. Critically, these thresholds represent power across the lung and not the lung and chest wall together; the equations above calculate the power across the respiratory system [i.e. lungs and chest wall together].

The power across the lung itself is approximated by multiplying the power across the respiratory system by the fraction of lung stiffness to total respiratory system stiffness [i.e. the El/Ers ratio]. Normally this ratio is 0.5. In pulmonary ARDS, the ratio can rise to 0.8 [64]. Given that the range of mechanical power of the respiratory system reported by Serpa Neto et al. was 11.7–31.2 joules/min [158] – the estimated power across normal lungs [El/Etot of 0.5] in this cohort is 5.85 – 15.6

joules/min. If these patients are assumed to have pulmonary ARDS [El/Etot of 0.8] then the estimated pulmonary power is 9.36 – 25 joules/min.

Airway Pressure Release Ventilation

While the lung in the throes of acute respiratory distress syndrome [ARDS] is shrunken, edematous and inflamed, a basic management maneuver is to 'recruit' lost pulmonary surface area. In other words, unfold alveolar-capillary units with the ventilator like a respiro-thoracic party horn. One 'unconventional' way to maximize and maintain lung volume is airway pressure release ventilation [APRV].

Imagine applying 30 cm H2O of continuous positive airway pressure [CPAP] to a spontaneously breathing patient; then every 5 seconds or so, the airway pressure is released from 30 to atmospheric pressure [0 cm H2O] for roughly 0.5 seconds. Following this momentary release, 30 cm of H2O is rapidly re-applied. Importantly, the patient breathes on his or her own throughout. This is, essentially, APRV [see figure 23].

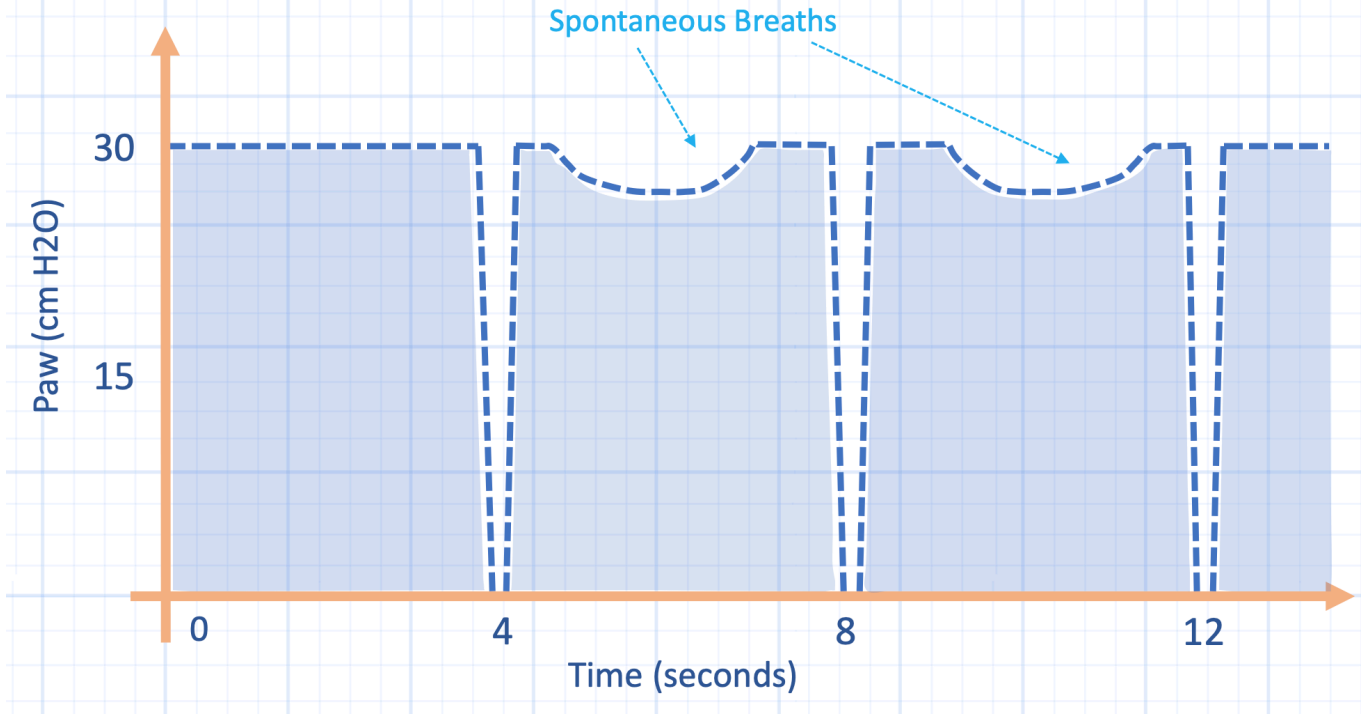

Figure 23: Hypothetical airway pressure waveform in P-APRV. Y-axis is airway pressure [Paw] and x-axis is time in seconds. P-High of 30 cm H2O and P-Low of zero cm H2O. T-High is about 4 seconds and T-Low is very short. Spontaneous breaths are seen as downward deflections in the airway pressure on y-axis.

Yet this facile description belies the complicated literature surrounding APRV, largely for the same reason that mechanical ventilation, in general, drives new trainees bonkers – erratic clinical application and nomenclature between different ventilators, institutions and investigations [159, 160]. What was called APRV in the late 1980s is quite different from its application today; what is called APRV on one ventilator today may be called something quite different on another contemporary ventilator [e.g. BiLevel, BiVent, BiPhasic and DuoPAP] [161].

For the above reasons, this section makes a key distinction between 2 broad APRV 'types,' originally coined by Habashi in 2005 [159, 162]. First, APRV approaches that 'fix' settings are termed F-APRV while those approaches that personalize APRV settings – based on respiratory mechanics between patients and within one patient across the arc of an illness – are designated P-APRV.

Fixed or Personalized?

The 4 main settings of APRV establish the duration and degree of its 2 different pressure sets; that is, the value of the high pressure [P-High] and the time spent at said high pressure [T-High]. Similarly, the clinician selects the value and duration of the lower pressure [P-low and T-low, respectively]. These settings suggest APRV as a type of BiPAP with long inspiratory time. However, the change in applied airway pressure is not – save for very uncommon varieties – triggered by the patient. APRV applies inverse-ratio, pressure-limited, time-cycled breath-types whilst allowing the patient to breathe spontaneously throughout [163].

Ironically, fixed forms of APRV [F-APRV] can be quite variable. Generally, F-APRV encompasses settings that include a relatively long T-low. Indeed, the duration of T-Low may be so prolonged that the waveform appears similar to BiPAP [164]. Accordingly, F-APRV, as defined by Habashi, encompasses settings that include relatively short T-High [i.e. less than 90% of the entire cycle time] and maintain T-Low that is invariant in the face of changing respiratory mechanics. P-APRV, by contrast, is defined by T-High that is at least 90% of the total cycle time, T-Low that is titrated to changing respiratory mechanics and P-Low that is set to zero [159] [see figure 24].

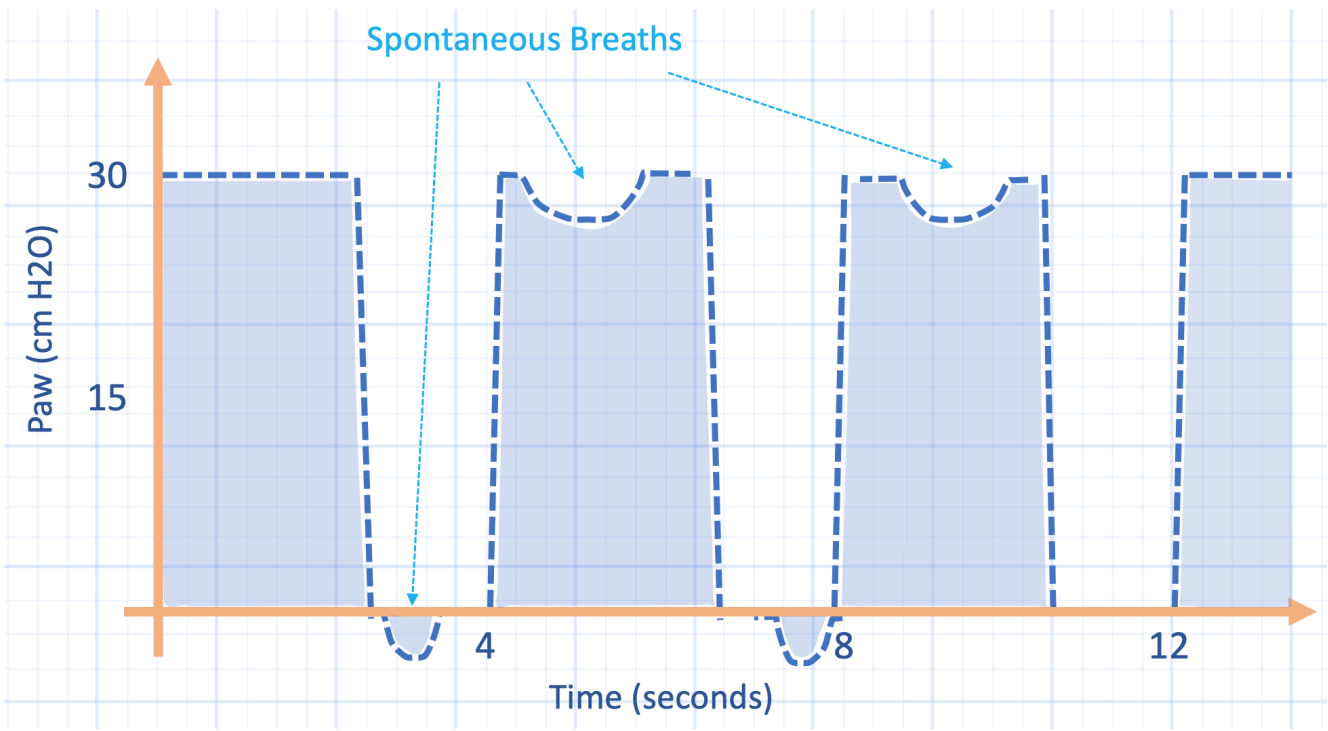

Figure 24: Example of F-APRV. P-High is 30 cm H_2O and P-Low is zero cm H_2O. T-High and T-Low are now almost equal. With longer T-Low, spontaneous breaths can be seen at P-Low.

T-Low, P-Low and Time Constants

A key aspect of P-APRV is that the duration of time at P-Low is very short. How short? This depends upon the respiratory mechanics of the patient. As the ultimate goal of APRV is to 'open the lung and keep it open', and release duration [i.e. T-Low] varies inversely with expiratory lung volume [EELV], then short T-Low is desired. In other words, brief T-Low generates large EELV and vice versa. Intuitively, long T-low allows more time for lung volume to empty while short T-low prevents lung empty – causing auto-PEEP.

Accordingly, one reasonable criticism of APRV is that it generates 'hidden PEEP' – and it does [see below]. Certainly hidden PEEP strains and stresses the lung [154]. Can a clinician titrate how much stress and strain are generated by changing T-Low? This is an important question given that excessive strain and stress are the mediators of volutrauma and barotrauma, respectively [62].

One mathematical approach assumes lung emptying acts as a single compartment composed of resistance [e.g. airway] and compliance [e.g. alveolus], in series [165]. In this simplified system, respiratory characteristics decay mono-exponentially with time.

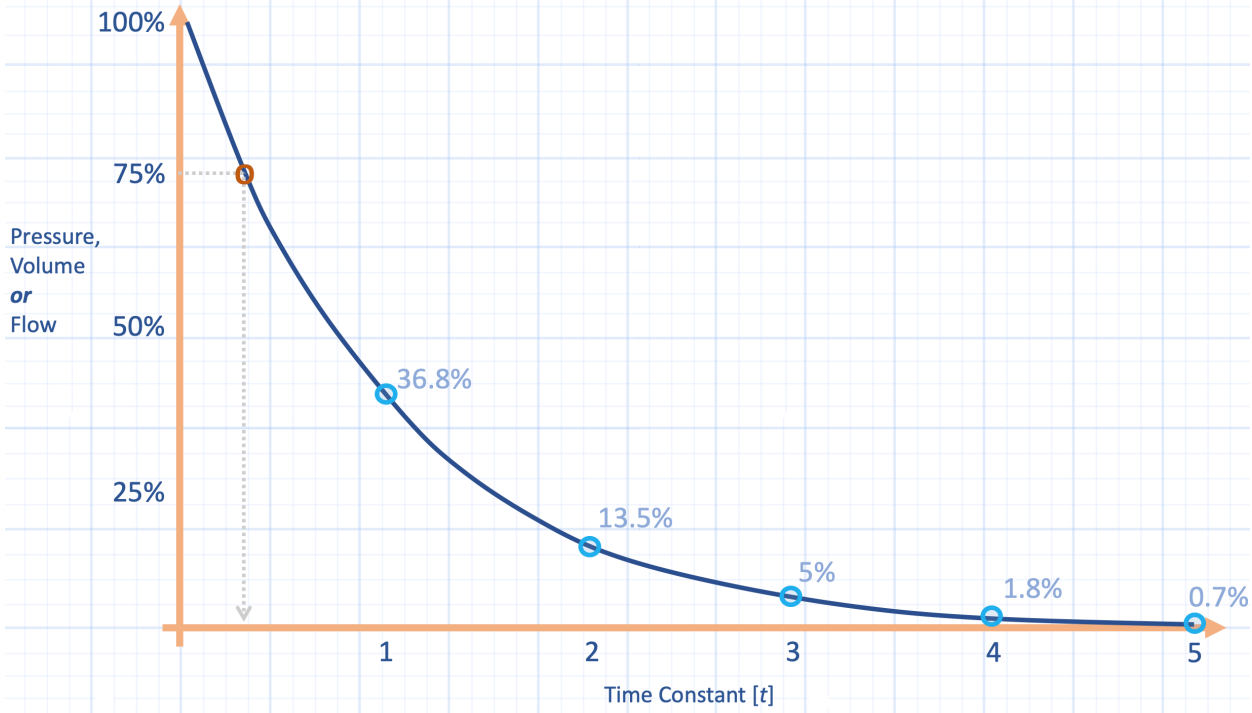

Figure 25: Time constants. See text for details - the dotted-line at 75% will become important below when discussing how T-Low is set in P-APRV.

The time it takes for pressure, volume or flow to fall by 63% of its value is the time constant [t] and is estimated for the respiratory system as the product of respiratory system compliance [Crs] and resistance [Rrs] [161]. For example, if an ARDS patient has a Crs of 30 mL/H_2O and a total Rrs of 15 cmH_2O/L/s [166], then t is 0.030 L/H_2O x 15 cmH_2O/L/s [note mL to L change for compliance] = 0.45 seconds. Accordingly, airway pressure is expected to decay by 63% following 0.45 seconds of expiration. If the initial airway pressure were 30 cm H_2O, then

following 0.45 seconds of expiration, the predicted fall in airway pressure is 19 cm H_2O [i.e. to 11 cm of H_2O]. Following another time constant, airway pressure drops by another 63% [i.e. from 11 to 4 cm H_2O]. Implicit in these calculations is that the P-Low is set to atmospheric pressure [0 cm H_2O] which maximizes expiratory pressure and volume drop and therefore carbon dioxide excretion. Indeed, P-Low of zero is inherent to the P-APRV definition [159].

Problems with Time Constants

There are a few problems with using t to predict auto-PEEP during P-APRV. The first is that the lung is not a simple 'tube and bag' model upon which mono-exponential decay is based [165]. The lung contains many units in parallel of differing resistance and compliance. As well, resistance and compliance are tied physiologically. For example, airway caliber depends upon lung volume – with higher lung volumes tethering open peripheral airways. Complicating matters, the compliance of the respiratory system also changes with volume. Additionally, calculated resistance is affected by compliance because the stiffness of the lungs partly determines flow, independent of airway caliber. Only when all time constants are equal is total resistance independent of compliance [167]. Uniform time constants are unlikely in the diseased ARDS lung with multiple abnormal lung compartments in parallel. Indeed, this has been demonstrated in multiple studies of total airway resistance in ARDS [167-170]. Further, both resistance and compliance are dynamic throughout the course of ARDS and its treatment. Thus, resistance and compliance must be repeatedly measured to adjust T-Low which is clinically burdensome. Finally, because different ventilators handle air-trapping differently, there can be substantial variation in the amount of auto-PEEP after 1 time constant solely as a function of the type of ventilator [171]!

Expiratory Flow Decay, Micro-strain and Micro-stress

Rather than calculate the time constant [t] one may simply use the change in expiratory flow as a surrogate of pressure decay. Thus, if expiratory flow falls by 50% one expects that airway pressure diminishes by 50% - assuming mono-exponential decline. Indeed, in a number of fascinating animal studies [172-174], various expiratory flow-to-peak expiratory flow ratios [EF-PEFR] were studied in APRV for their effects upon alveolar recruitment and micro-strain.

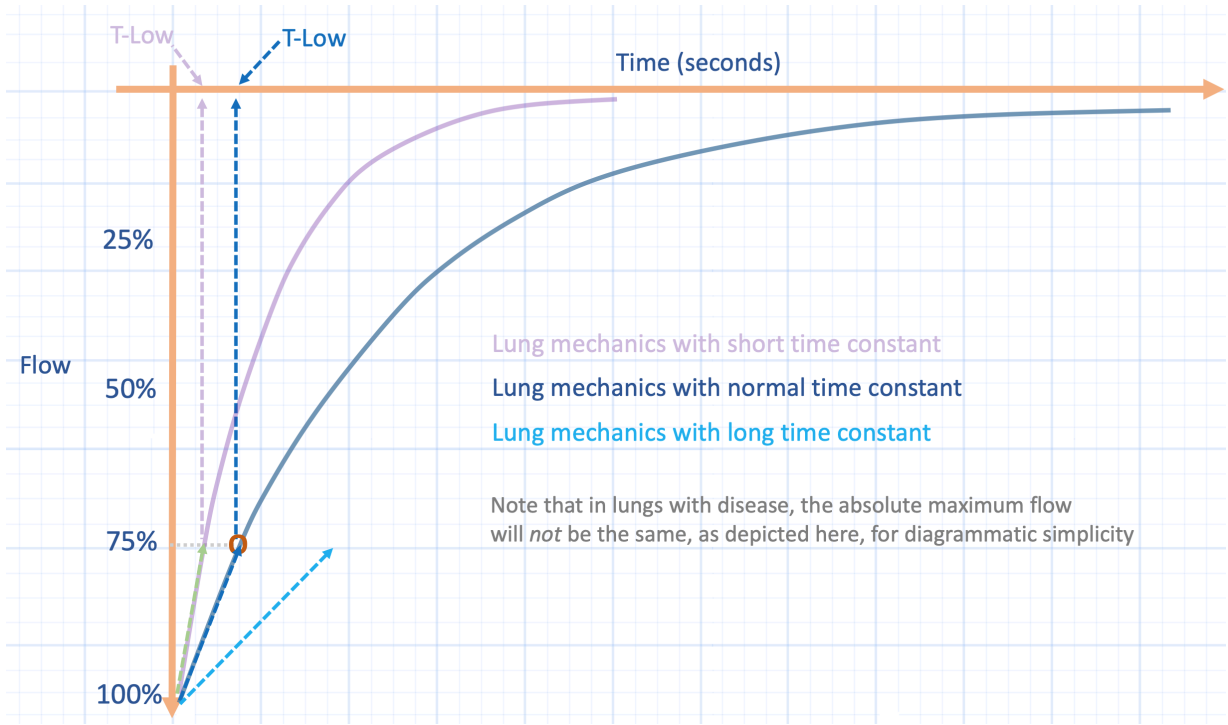

Figure 26: Expiratory flow curve on ventilator. This is simply figure 25 inverted because expiratory flow is depicted this way on a ventilator. Lungs with short [t] in light purple. T-Low changes between short [t] lungs and normal t lungs when EF-PEFR of 75% is used as the cutoff to cycle to P-High. Note the distinction between T-Low and [t]; the latter sets the slope of decay, the former is controlled by the clinician - set to when flow is 75% of its maximum value. For reference, healthy, non-intubated patients reported [t] as 0.4 – 0.5 (s); ARDS [t] reported as 0.6 – 0.7 (s) [170].

Each investigation found that when the EF-PEFR was 75% [i.e. when expiratory flow had fallen to 75% of its peak value] that alveoli – studied by unique microscopy techniques – showed the greatest expiratory area and the smallest amount of micro-strain. As compared to low tidal volume ventilation [LTV] with high positive end-expiratory pressure [PEEP], micro-strain was similar but there was more absolute alveolar micro-recruitment in the EF-PEFR 75% APRV group. Micro-strain was defined as the change in volume from expiration to inspiration normalized to its expiratory value. Additionally, 75% EF-PEFR redistributed gas volume from the respiratory bronchioles to the alveoli as compared to LTV [173]. For these reasons, it is argued, P-APRV should maintain T-Low at a value resulting in an EF-PEFR of 75%.

Notably, an EF-PEFR of 75% is expected to be much less than 1 [t] given the 25% fall in flow [recall that 1 [t] diminishes the variable of interest by 63%]; a brief T-Low recruits end-expiratory lung volume and generates auto-PEEP. Further, if end-expiratory volume rises, then strain will, mathematically, fall [the denominator is larger]. Lastly, while micro-strain [change in alveolar volume] may fall, this does not necessarily speak to micro-stress. Stress is the pressure across the alveolus and is related to strain by elastance [or stiffness] of the structure being deformed [62]. In the animal models described, surfactant wash-out models of ARDS were employed which are expected to increase the surface tension of the alveolus – an increased micro-elastance – and therefore the pressure across it by LaPlace's approximation.

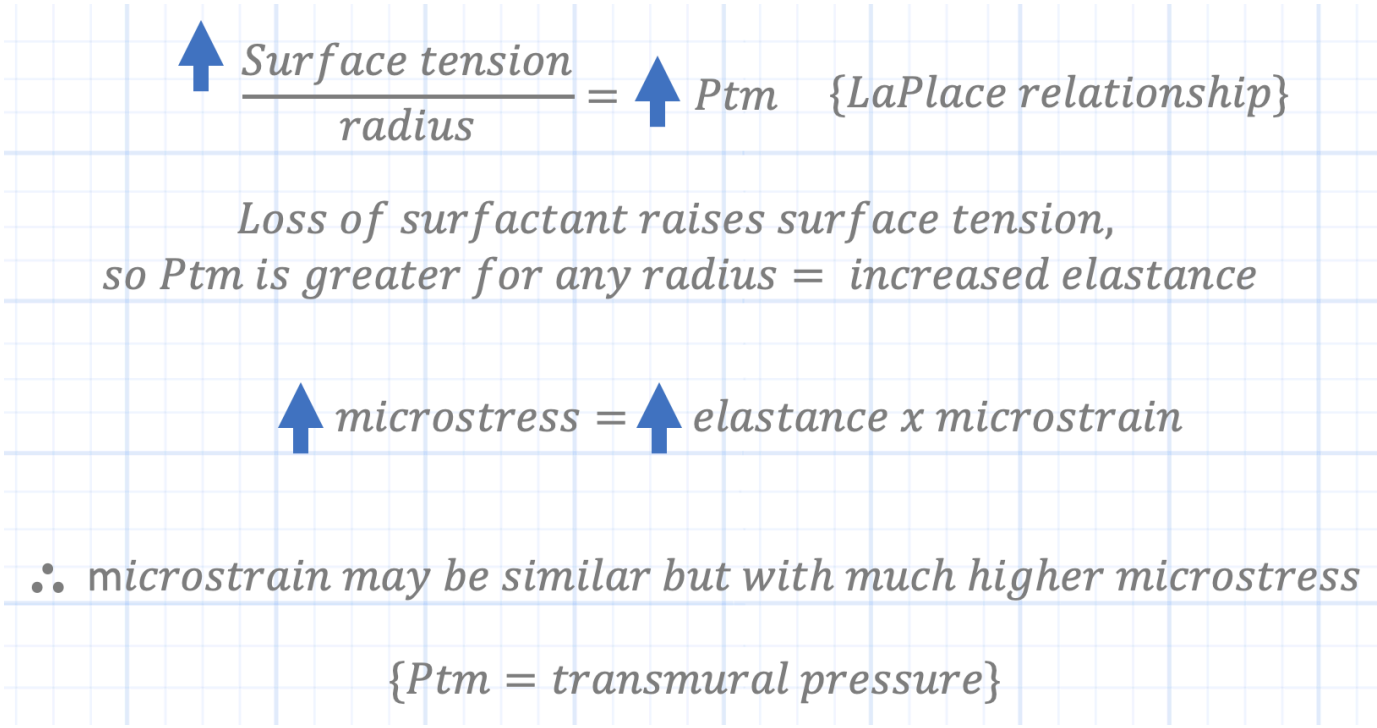

Figure 27: Theoretical relationship between microstrain [i.e. change in alveolar volume] and microstress [i.e. change in trans-mural alveolar pressure] at the level of the alveolus. See text for details.

While the authors did not employ micro-transducers to measure alveolar pressure relative to interstitial/pleural pressure [i.e. measure micro-stress], a crude inference can be made by assessing the area of the non-airway, non-alveolar spaces visualized in their micrographs. This value was not reported, but is deduced by subtracting the area of the conducting airways and alveoli from 100%. In other words, the fraction of space on microscopy that is not airway or alveolus reflects the summation of the interstitium, blood vessels and lymphatics. In the control group, this space made up 33% of the end-expiratory microscopic area while in the EF-PEFR of 75% group, it was only 27%. Thus, while end-expiratory alveolar area/ recruitment was similar between the control and the EF-PEFR 75% groups, it came at the expense of 'compressing' the blood vessels, lymphatics and interstitium – by 6% [173]. While this serves as a visual transduction of trans-alveolar pressure [i.e. 'micro-stress'] it is, admittedly, speculative. Yet, the micro-recruitment observed in the EF-PEFR 75% group occurred at a meaningfully higher pressure-time product [double the LTV group] and tidal volume [double the LTV group] [172]. Thus, a reasonable supposition is that enhanced micro-recruitment and diminished micro-strain amplified micro-stress – considered in more detail below.

P-High, T-High and APRV Breath Types

Turning from the physiological considerations of T-Low, appreciation for time spent at P-High and spontaneous breaths are equally important when employing APRV in ARDS. As above, P-ARPV as defined by Habashi, requires more than 90% of the respiratory cycle time at P-High – to optimize alveolar recruitment. Typically, T-High is around 5 seconds while P-High is close to the patient's plateau pressure if switched from conventional ventilation.

How do the spontaneous breaths of APRV fit into the rotation between P-Low and P-High? Different breaths types in APRV have previously been defined and form the basis for analysis of ergotrauma below [175, 176]:

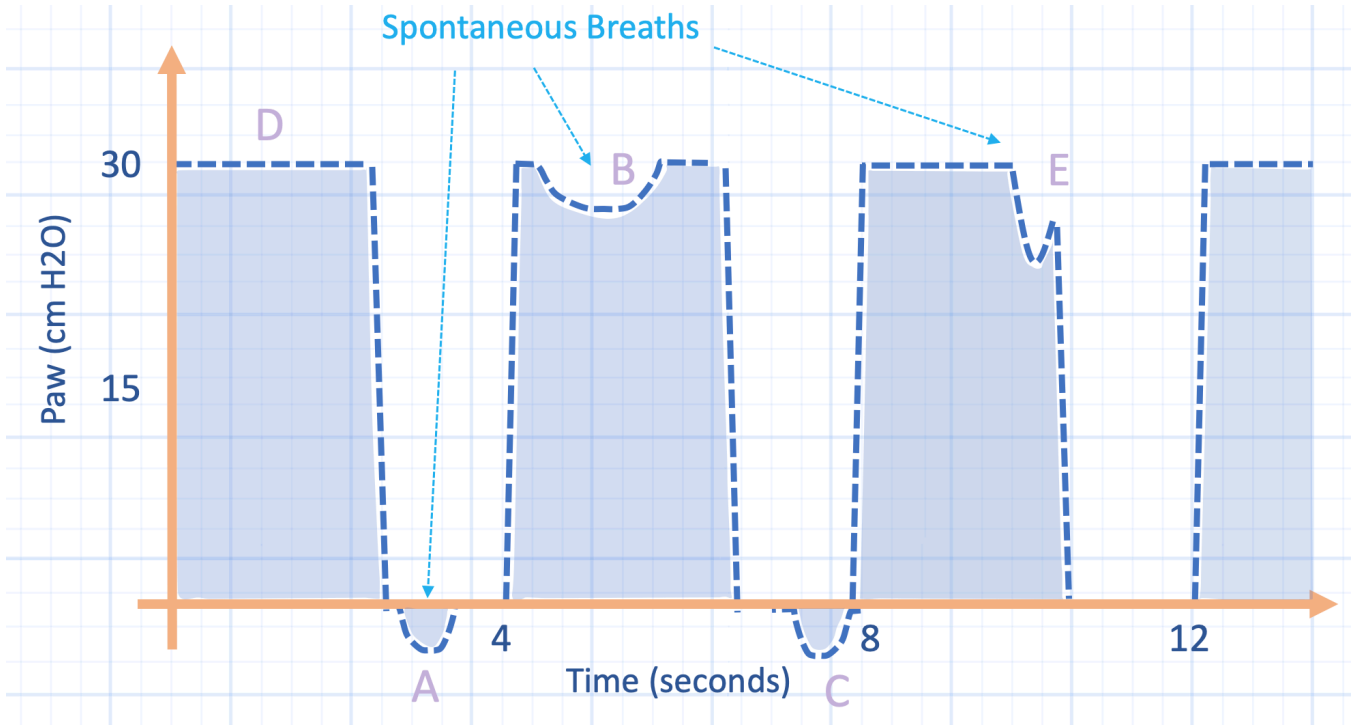

Figure 28: Breath types during APRV. A. breath - spontaneous at P-Low; B. breath - spontaneous at P-High; C. breath - spontaneous at the initiation of P-High; D. breath - ventilator breath from P-Low to P-High; E. breath - spontaneous breath initiated at transition from P-High to P-Low. Note that only the D breath is purely from the ventilator.

As seen, breath type varies as a function of the duration of T-High relative to T-Low. Indeed, shortening T-Low essentially abolishes all breaths except B and D types [177]. As T-High increases relative to T-Low, ventilation and work is transferred from the ventilator to the patient [177]. As P-ARPV demands T-Low values less than 1 [t] in duration, presumably all breaths are either B type [i.e. spontaneously during P-High] or D type [i.e. ventilator-controlled P-Low to P-High].

Lung Stress in Pulmonary and Extrapulmonary ARDS

Initially described in the late 1990s, the distinction between direct pulmonary insults [i.e. pulmonary ARDS] and indirect pulmonary insults [i.e. extra-pulmonary ARDS] is important [178] [see also chapter 4]. Additionally, direct pulmonary insults [e.g. gastric acid aspiration] may have a different molecular phenotype from indirect, extra-pulmonary insults such as trauma or pancreatitis. Yet, for this discussion, the original, mechanical distinction is most important; i.e. the proportional difference in lung stress relative to total respiratory system stress.

The stiffness of the lungs and chest wall together is quantified as the elastance of the respiratory system [Ers], while the stiffness of only the lungs is lung elastance [El]. In pulmonary ARDS, the ratio of the lung stiffness to the total respiratory system stiffness is high – upwards of 80% [El/Ers = 0.8] [63, 64]. By contrast, in extra-pulmonary ARDS, the relationship between lung stiffness and total system

stiffness is low; this value can be as low as 20% [El/Ers = 0.2]. The El/Etot ratio is important; when it is multiplied by the pressure change applied at the airway [i.e. driving pressure], then the change in trans-pulmonary pressure [Ptp] or stress across the lung is given. As well, using an elastance-based Ptp calculation [which assumes pleural pressure at expiration to be zero], multiplying the absolute airway pressure by the El/Etot gives the absolute trans-pulmonary pressure.

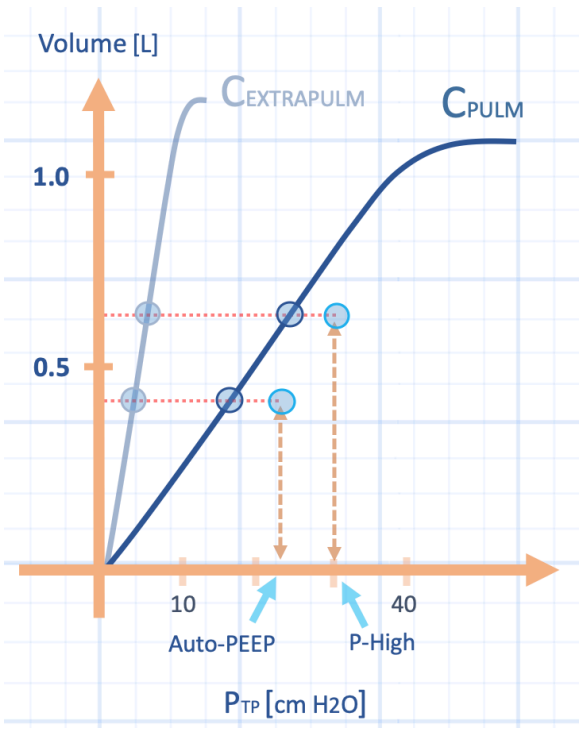

Figure 29: A hypothetical D-type breath in P-APRV. P-High of 30 cm H_2O results in a P-Low of 22.5 cm H_2O or a driving pressure of 7.5 cm H_2O. This causes a ΔPtp of 6 cm H_2O in pulmonary ARDS [7.5 x 0.8, blue curve] compared to a ΔPtp of only 1.5 cm H_2O in extra-pulmonary ARDS or obesity [7.5 x 0.2, orange curve]. Note x-axis is Ptp [transpulmonary pressure or whole lung stress], y-axis is volume in litres. The floating light blue circles represent the airway pressure. Assumptions are: respiratory system compliance is 20 mL/cmH_2O, EF-PEFR-75%, P-Low is zero. El/Etot is 0.2 for extra-pulm, El/Etot is 0.8 for pulm ARDS, pleural pressure begins at zero cm H_2O.

Knowing the Ptp during a D-breath at P-High defines the envelope of the area under the pressure-volume curve – or work – applied to the lung by the ventilator [64]. Critically, in a recent trial comparing APRV to conventional, low tidal volume ventilation [LTV] in ARDS, an apparent failure of randomization allocated a disproportionate number of patients with extra-pulmonary ARDS to APRV [only 25% had direct causes]. By contrast, 39% had pulmonary or direct causes of ARDS in the LTV group [179]. Therefore, the APRV patients in this trial experienced less lung stress at any given airway pressure; accordingly, the favourable APRV findings may be tenuous.

Ergotrauma in APRV: a theoretical model

As previously described, the work performed on the lung during a single breath is divided into dynamic [e.g. gas flow] and static components [e.g. lung volume]. The summation of the dynamic and static work over time determines the mechanical power – in joules per minute – applied to the lung [64, 137]. Thus, VILI secondary

to mechanical power – ergotrauma – provides unification of multiple avenues of VILI research [63]; neither static pressure or volume alone drive VILI, but also baseline stretch [i.e. PEEP, auto-PEEP] as well as airway resistance, gas flow and respiratory rate. Augmenting any of these variables boosts the power applied to the lung skeleton and, in theory, VILI risk. But how does this relate to P-APRV?

First, the static work of the D-type breaths, is defined by the envelope between the auto-PEEP generated at T-Low, and the Ptp generated at P-High [figure 30]. But there is also a dynamic component to D-type breaths described as gas flow multiplied by airway resistance. This parcel is illustrated to the right of the lung elastance curve. Notably, a D-breath in APRV demands gas volume delivered over a very short period of time – that is, high inspiratory flow. Gas supplied swiftly supports turbulent flow which increases effective resistance and, therefore, dynamic work. Indeed, high flow rate is a known determinant of VILI [137]. The area of the dynamic and static envelopes is the work for a single D-type breath, but the power is solved by this area multiplied by its frequency of application to the lung [i.e. 60 / T-High (sec) + T-Low (sec)].

Second, B-type breaths must also be considered in the power calculation. Because B-breaths occur at P-High, they increase Ptp and lung volume beyond that of the D-breath [figure 30]. This additional work allotment, like a D breath, comprises static and dynamic elements. Ostensibly, the dynamic work is reduced at higher lung volume given tethering of airways. Yet, like the D-breath, the static and dynamic parcels of work must be multiplied by their rate to determine joules/minute, or mechanical power. Crucially, the elastic work for each spontaneous B-breath includes the elastic work that is generated when the lung is placed at a higher volume by the D-breath; why? Using Hook's Law as an analogy [63], consider a malleable material stretched from its baseline length (l) [e.g. (l) + x] and then extended repeatedly beyond x [i.e. repetitions between x and higher length y]. The total power applied is [(l) + y] multiplied by the stretch frequency. Thus, the work for a single B-breath is the static and dynamic work of the B-breath multiplied by the patient's spontaneous respiratory rate. The theoretical total mechanical power is given in the figure. From this analysis it is understood that the power applied to the directly-insulted ARDS lung during APRV can become extremely high.

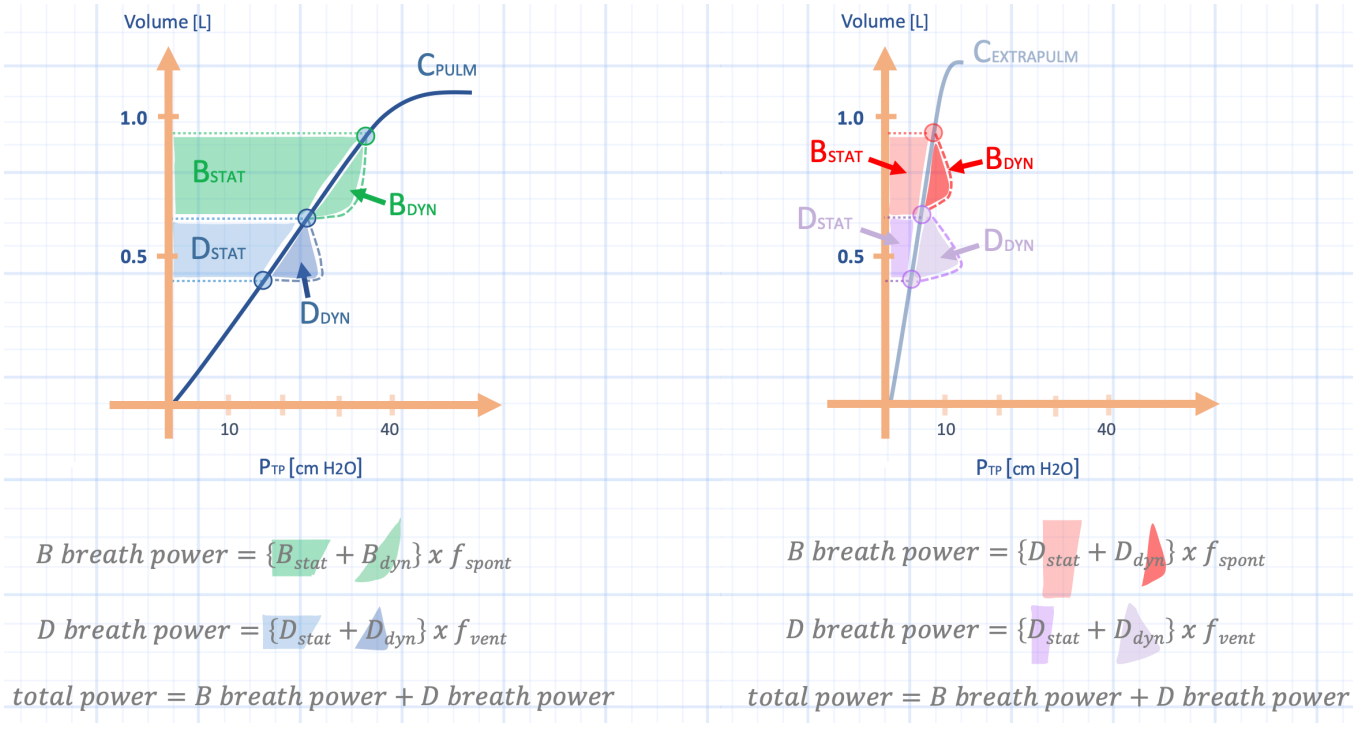

Figure 30: Theoretical model for P-APRV power calculation. Left panel is pulmonary ARDS. The area of the dynamic and static envelopes is the work for a single breath type [D versus B], but the power is solved by this area multiplied by its frequency. Dstat & Ddyn are static & dynamic work of breathing for D breath, respectively. Bstat & Bdyn are static & dynamic WOB for B breath, respectively. f-spont is spontaneous respiratory rate. f-vent = 60 / T-High (sec) + T-Low (sec). x-axis is Ptp or transpulmonary pressure while y-axis is volume in litres. Right panel is theoretical power calculation for P-ARPV in extra-pulmonary ARDS.

Empirical Evidence

There is sparse data for stress across the lung during APRV let alone mechanical power. In one report, a patient receiving F-APRV [with a relatively long P-Low] engaged in mostly D and B breaths – similar to what one would expect during P-ARPV [177]. Importantly, an esophageal balloon was placed so both an approximation of lung stress [i.e. Ptp] was tracked with lung strain [i.e. lung volume]. Close inspection of the airway pressure curve relative to esophageal pressure [Pes] curve at the end of D and B-breaths reveals that both Ptp and lung volume doubled during a B-breath. This is consistent with increased stress and strain during spontaneous breathing in APRV [163, 177].

Work of breathing [WOB] in joules per litre during APRV has been calculated in a small cohort of patients receiving F-APRV [175]. One patient in this investigation – 'subject 9' – engaged in mostly B and D type breaths. Here, spontaneous WOB was 1.25 joules/Litre while the ventilator delivered roughly 2.75 joules/Litre of work for a total of roughly 4.0 J/L [normal work of breathing is 0.3 to 0.6 J/L [180]]. As minute ventilation was 12 L/min, the overall power applied to the lung was 48 joules/minute! The power threshold for VILI is not known in humans; in a swine model, it was 12 J/min [141]. As human lungs have twice the specific elastance as swine [181], one would expect this threshold to at least double in humans, but these comparisons are extremely tenuous.

Caveat and Conclusion

An intriguing investigation demonstrated that the fall in pleural pressure [Ppl] during spontaneous effort is not distributed evenly across all pleural surfaces in ARDS – as in health [182]. Rather, the lower lobes experience disproportionately low Ppl leading to cryptic stress, strain and pendelluft – sloshing of air from the ventral to the dorsal lung units at the onset of inspiration. The observed Ppl was much lower than the Pes; accordingly, the aforementioned calculations may actually underestimate the total power during B-type breaths. Nevertheless, the high auto-PEEP generated by APRV may diminish lower lobe stress and strain during spontaneous breathing [183]; in other words, while the total power in APRV is high, the 'driving power' may not be.

Thus, widely opening the lung during inspiration and expiration reduces microstrain, but the pressure required can multiply the mechanical power experienced by the lung – especially if supplemented by spontaneous breaths. Evidence for aggressive recruitment – an attempt to reduce lung inhomogeneity and stress raisers – reveals a cryptic cost. Should we adopt a lower the threshold for prone position – which homogenizes stress raisers without increased power – than APRV? Further, should we be open to closing the lung and keeping it closed [184]?

Driving Pressure in Airway Pressure Release Ventilation

Given that 'driving power' may be more important than total power applied to the lung, one wonders if the driving pressure can be gleaned from APRV. A letter [185] in response to the investigation by Zhou and colleagues [179], therefore, deserves some thought. This brief communication proposed an equation for estimating the amount of intrinsic PEEP [PEEPi] generated during APRV and argued that the driving pressure in APRV is likely less than that reported in the study by Zhou et al.

Ultimately, the mathematical approach proposed by Taylor and Camporota estimates the amount of trapped volume in the lung at the end of the expiratory time [T-Low] and multiplies this residual volume by the elastance [or stiffness] of the lung to give the residual pressure, PEEPi.

(8) $PEEPi = residual\ volume\ x\ elastance$

Equation 8: PEEPi is intrinsic positive end-expiratory pressure

How can we calculate the remaining ['residual'] volume at the end of the expiratory time during APRV? One can understand by inspecting the expiratory flow waveform on a ventilator [see figure 31]. If we assume that it takes 4 time constants to fully empty and multiply this time by the peak expiratory flow rate [PEFR] then we get the total expired volume if the lung were left to empty completely.

Geometrically, this is one-half the rectangular area [i.e. the blue highlighted triangle] defined by the PEFR and the duration of 4 time constants.

But in APRV, the lung isn't allowed to fully empty, so the 'residual volume' described above is the total triangular volume in figure 31 less the actual released volume [in red]. This remaining area of the triangle - in purple - defines the amount of volume left in the lung at the end of T-Low. If this value is multiplied by the elastance [i.e. stiffness, the inverse of compliance], then the recoil pressure remaining in the airway – that is, the PEEPi – is revealed.

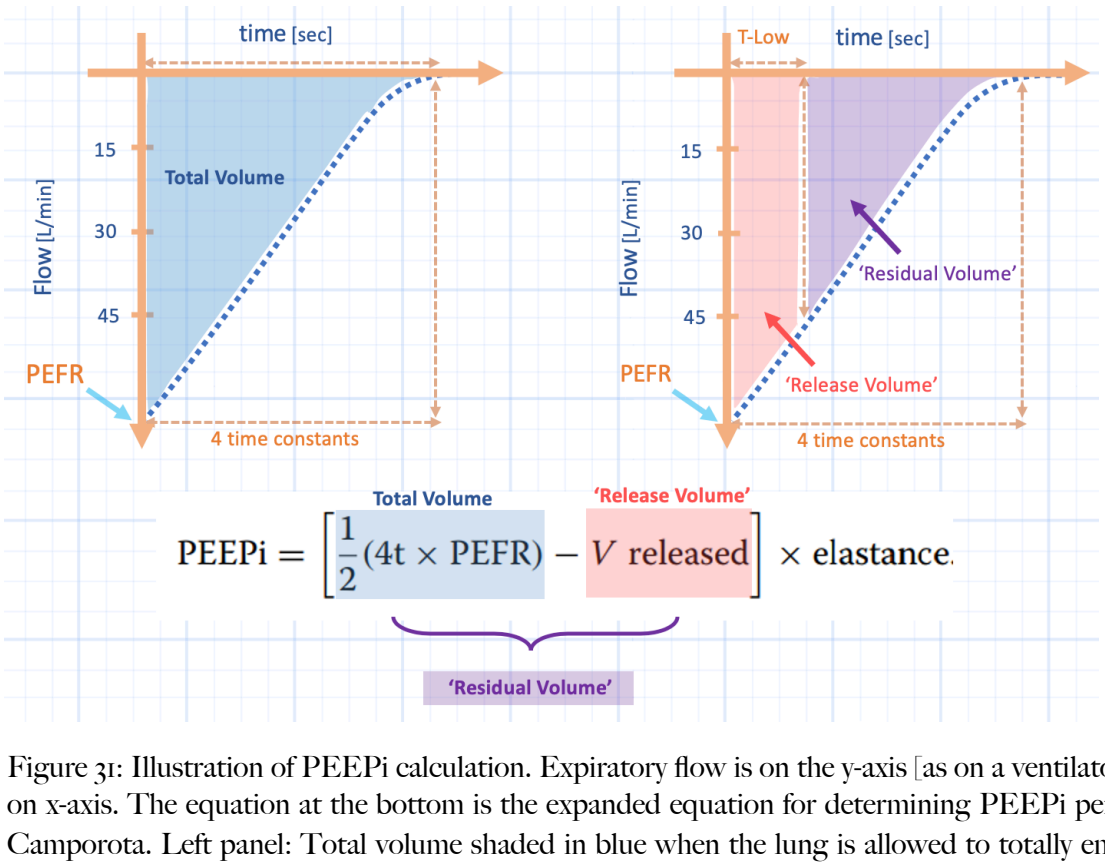

Figure 31: Illustration of PEEPi calculation. Expiratory flow is on the y-axis [as on a ventilator] with time on x-axis. The equation at the bottom is the expanded equation for determining PEEPi per Taylor and Camporota. Left panel: Total volume shaded in blue when the lung is allowed to totally empty - over 4 time constants [t]. Note that this is 1/2 the area of a rectangle formed by the boundaries of peak expiratory flow [PEFR] and 4 time constants. Right panel: When APRV is applied and T-Low results in 25% fall in flow - the released volume in red is subtracted from the total volume in blue. This leaves the residual volume in purple. If this value is multiplied by the stiffness of the lung, then PEEPi is given.

Caveats

There are both practical and theoretical problems with the above. The practical problems are that airway resistance and compliance [and therefore elastance] are burdensome to calculate correctly at the bedside. In a patient on APRV, determining these respiratory variables, essentially, mandates switching the patient to volume control. Further, accurate calculation typically requires heavy sedation and, potentially, paralysis to maintain synchrony during end-expiratory and inspiratory holds. Finally, patients with the same respiratory mechanics and identical APRV settings can have different PEEPi levels based solely on the ventilator given inherent differences in device manufacture.

Theoretically, as described above, time-constants are problematic because both calculated resistance and compliance are physiologically-coupled. Only when all lung units are homogenous does compliance totally uncouple from resistance and

this is simply impossible in ARDS. Additionally, both calculated airway resistance [and compliance] are volume-dependent – for example resistance falls as lung volume rises, presumably due to the tethering open of airways. Similarly, compliance [i.e. elastance] is also volume dependent; should these calculations be made on a standardized level of PEEP? If, during the elastance [or resistance] calculation, the clinician uses an extrinsic PEEP [PEEPe] of 10 cm H_2O, can the stiffness [and resistance] of the lung at this clinician-selected PEEPe be used interchangeably with the stiffness [and resistance] of the lung at the PEEPi generated during APRV?

A Simpler Method

Also as described above, a simpler assumption [with less physiological and mathematical coupling] is to presume that flow, volume and pressure all decay mono-exponentially. Using this approach, if flow falls by 25% then pressure [from P-High] also falls by 25%. As an example, if PEFR is 60 L/min and at the end of T-low, the expiratory flow is 45 L/min then flow has fallen by 25%. If P-High were set to 30 cm H_2O and we assume that it too fell by 25%, then PEEPi becomes 22.5 cm H_2O; the driving pressure is 30 cm H_2O – 22.5 cm H_2O or 7.5 cm H_2O. Accordingly, the estimated PEEPi – and driving pressure – becomes the following:

$$(9)\quad \frac{End-expiratory\ flow}{PEFR}\ x\ PHigh\ =\ PEEPi$$

or

$$(10)\quad \left[1\ -\ \frac{End-expiratory\ flow}{PEFR}\right]\ x\ PHigh\ =\ Driving\ Pressure$$

Equation 9 & 10: A simplified proposal for deriving PEEPi and driving pressure. Here end-expiratory flow rate is the flow at the end of T-Low and PEFR is peak expiratory flow rate. PHigh is the pressure high setting during APRV.

Driving Pressure Problems

Yet the problem with both of the aforementioned calculations is that driving pressure still only speaks to the change in pressure within the 'airway compartment' and cannot definitively provide the true stress across the lung, over time. It is entirely possible that a patient with severe ARDS secondary to trauma-induced pancreatitis and a patient with equally severe ARDS from bilateral aspiration pneumonia have the same respiratory mechanics. However, their transpulmonary pressures – and therefore stress across the lung – may be markedly different. With disparate stress across the lung, the driving power felt by the lung skeleton may be dissimilar despite equal driving pressure [see figure 3]. As above, PEEP lowers driving power upon the lung only to the extent that PEEP homogenizes

pulmonary stress raisers and improves pulmonary elastance. If PEEP does not homogenize the lung, then it simply raises the power felt by the lung during both the mechanical and spontaneous breaths of APRV. Finally, and as elaborated next, the measured end-expiratory airway pressure may not capture PEEPi hidden behind closed airways.

Esophageal manometry in APRV

A recent letter [186] posed a rather provocative question – 'Are we really preventing lung collapse with APRV?' The authors cited a case report of esophageal manometry used in conjunction with airway pressure release ventilation [APRV] in an obese patient with severe, extra-pulmonary ARDS.

The authors found that at the most rapid T-low [i.e. 0.1 s], the transpulmonary pressure [i.e. the airway pressure minus the esophageal pressure] was most negative. Consistently, as T-Low lengthened [i.e. from 0.1s to 0.7 s], the trans-pulmonary pressure was less negative. In other words, the transpulmonary pressure suggested the most collapse when T-low was 0.1 s. Additionally, when the T-low was the longest [i.e. 0.7 s], there appeared to be less collapse, but collapse nonetheless. Thus, all of the transpulmonary pressures at the end of T-low were negative. The percent of peak expiratory flow rate for these different T-low times ranged from 87% at 0.1s to 75% at 0.7 s.

The fact that shorter expiratory times [i.e. more rapid T-lows] caused increasingly negative transpulmonary pressure – suggesting more collapse – deserves consideration. The theory underpinning APRV is that short T-low causes auto-PEEP and prevents collapse. How could this result be so contradictory? Ostensibly, the measured end-expiratory transpulmonary pressures were under-estimated [i.e. too low]; in fact, they were all probably quite positive and their negative values were due to problems when measuring both auto-PEEP and esophageal pressure. In other words, the measured airway pressures were lower than what they actually were and the esophageal pressure was higher than it actually was – this combination resulted in spuriously low transpulmonary pressure.

As discussed in chapter 1, PEEP may be hidden behind closed airways at end-expiration [see figure 15 in chapter 1]. The resultant pre-mature airway closure leaves the patient with distended alveoli with high auto-PEEP 'hidden' from the central airways and therefore not recorded by the ventilator. The hallmark of hidden auto-PEEP is that the airway pressure gradually trends upwards during an expiratory-hold maneuver as the gas hidden behind the closed airways gradually leaks out and raises the central airway pressure.

Further, in the letter, the patient's transpulmonary pressure at the end of P-High gradually fell from a T-Low of 0.7 s to about 0.4 s and then rose again. What does this mean? Consider an analogy with conventional volume control; if PEEP is increased and plateau pressure decreases [i.e. the driving pressure falls], then lung has been recruited and that the compliance has improved. If the P-High trans-

pulmonary pressure is considered analogous to the plateau pressure, its reduction as T-low decreased suggests that pulmonary compliance improved, probably as a consequence of auto-PEEP recruiting lung. Indeed, this represents a novel way to titrate T-Low in APRV – simply decrease T-low until the transpulmonary pressure at the terminus of P-High reaches its minimum [see figure 32].

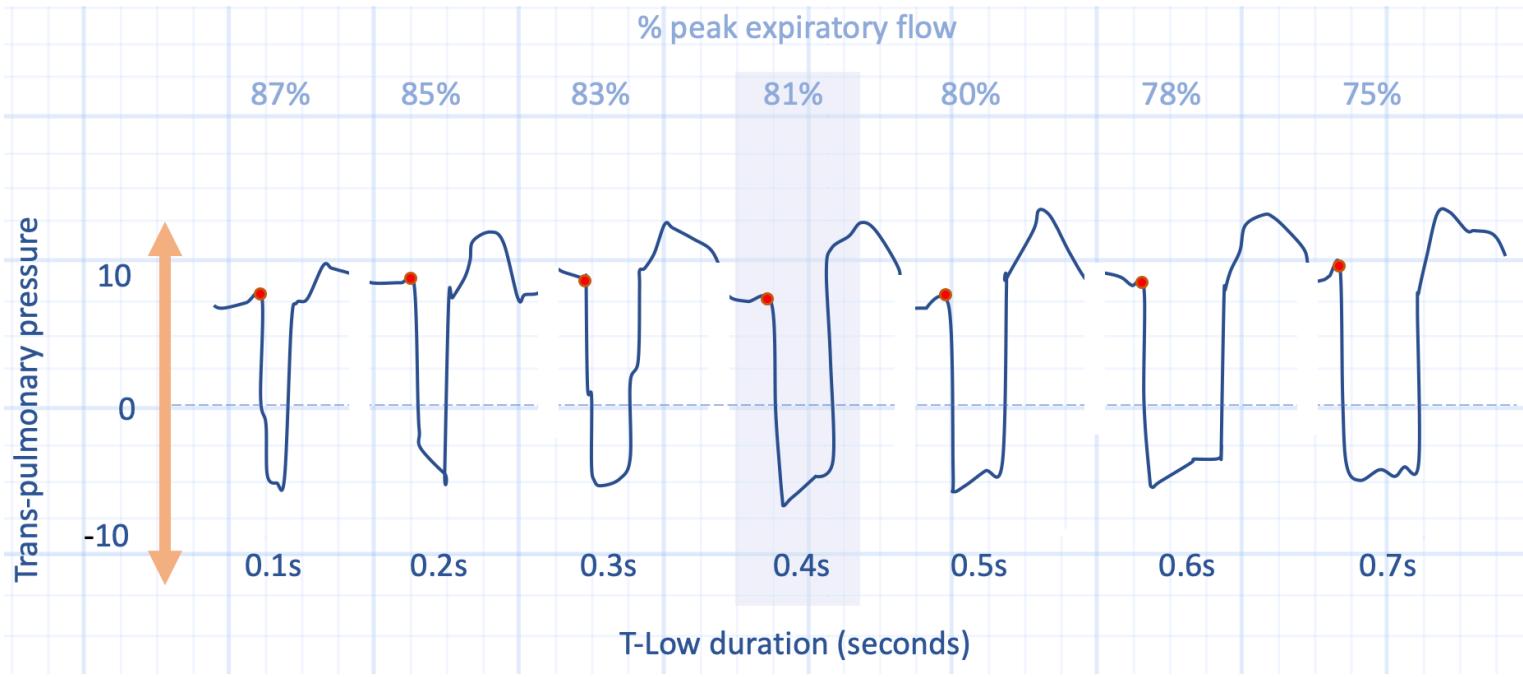

Figure 32: A novel way to titrate T-Low. This figure depicts 7 different P-High-to-P-Low releases at different T-Low durations. As T-low is decreased [to cause auto-PEEP] leftwards along the x-axis, the trans-pulmonary [y-axis] pressure at the very end of P-High [red dots] gradually falls to a minimum at 0.4s of T-Low and then rises again. The falling trans-pulmonary, P-High implies improving lung compliance and may occur at a higher % decay of peak expiratory flow target than commonly recommended [e.g. often 75% is targeted].

Lastly, mediastinal weight adds a fixed load to the esophagus which increases esophageal pressure; yet, the change in esophageal pressure likely represents an 'average' change in pleural pressure. Some have advocated simply subtracting 3 –to-7 cm H2O from the absolute value obtained by esophageal manometry [187].

In summary, in APRV, the airway pressure can be higher than measured [because of occult auto-PEEP], and the esophageal pressure lower [because of mediastinal weight]. Accordingly, observed transpulmonary pressure at the end of T-Low is much lower [i.e. more negative] than its true value. Thus, titrating T-Low based on its absolute transpulmonary pressure is problematic. Instead, a better indicator for T-Low optimization may be the minimum value of the transpulmonary P-High as shown in figure 32.

Helium and Oxygen

Given the aforementioned discussion on ventilator-induced lung injury [VILI] and ergotrauma [145], should we also consider the peak pressure as a therapeutic target

in ARDS? That is, if the model of Cressoni and colleagues proves true, it may be prudent to minimize dynamic power felt by the lung.

The magnitude of the dynamic pressure applied to the effortless, mechanically-ventilated patient can be simplified to the equation at the bottom of figure 33; there is pressure [ΔP] required to drive both laminar and turbulent airflow [188]. For simplicity, this analysis neglects 'transitional' airflow which lies between laminar and turbulent airflow in its effects on dynamic pressure.

Physiology of Helium-Oxygen Mixtures

Replacing nitrogen with helium has two effects on gas properties. First, because helium is much less dense than nitrogen, helium-oxygen is considerably less dense than air. Second, and often neglected, is that helium is slightly more viscous than nitrogen, consequently, helium-oxygen is mildly more viscous than air [188, 189]. As illustrated in figure 33, these differences in density [p] and viscosity [u] have complicated and somewhat conflicting effects upon the pressure required [ΔP] for a given ventilator-applied gas flow.

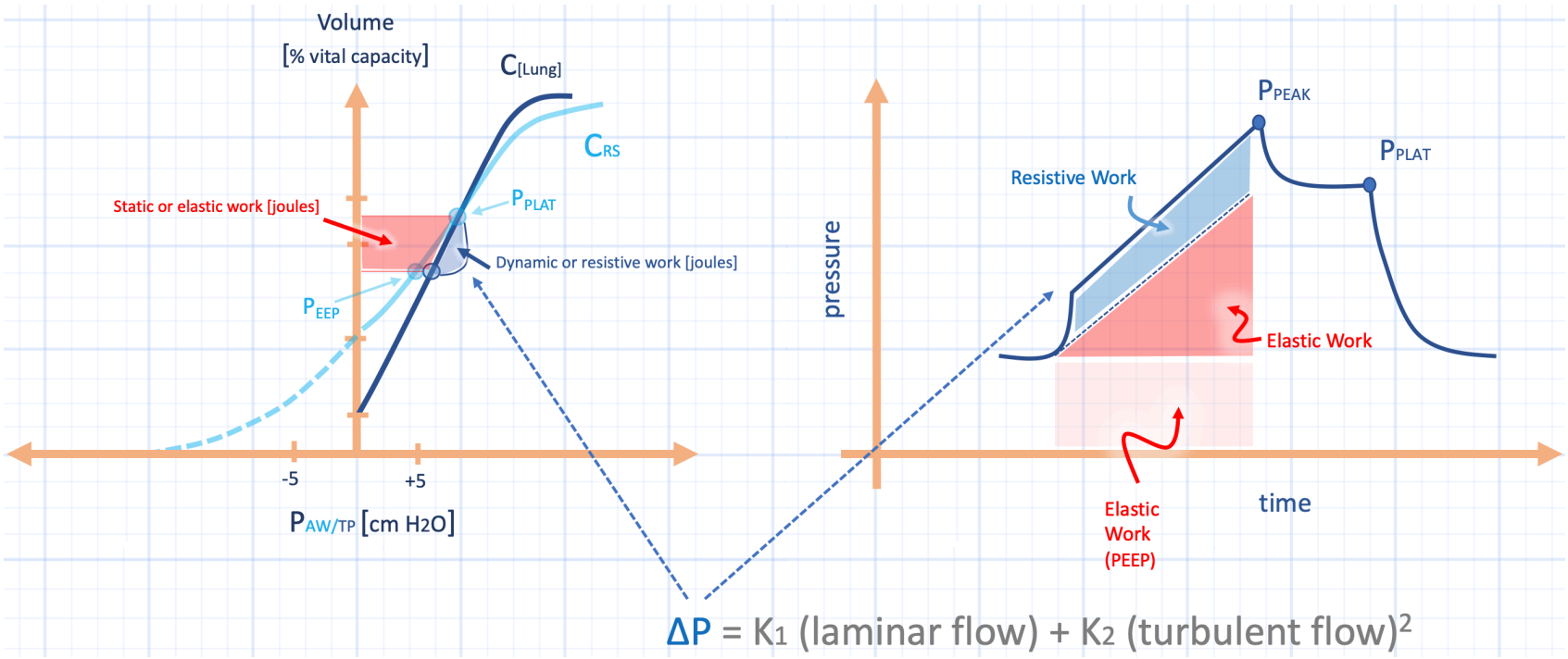

Figure 33:The left panel reveals the work applied to the lung, parsed into its static [red] and dynamic [blue] components. The left figure is modified from classic physiology diagrams such as the Rahn diagram. The respiratory system compliance curve [Crs] is shown in reference to the pulmonary compliance curve [Cpulm]. The pressure obtained on Cpulm is the transpulmonary pressure; the pressure obtained on Crs is the airway pressure [Paw]. The Ptp is slightly larger than the trans-respiratory pressure at positive end-expiratory pressure [PEEP] because the Ptp is referenced to the pleural pressure which is slightly sub-atmospheric on the chest wall compliance curve [not pictured]; compare to figure 16. If pressure is moved from the x-axis to the y-axis and volume is moved from the y-axis and changed to time on the x-axis, the clinically-relevant ventilator waveform is formed on the right. Importantly, volume can become time only if flow is constant [i.e. square wave delivery]; constant flow means that the same volume is delivered per unit time. Also, the ventilator waveform represents not the Ptp but the pressure across the respiratory system [trans-respiratory] in the passive patient. As above, if esophageal pressure [as a surrogate for pleural pressure] were subtracted from the airway pressure, Ptp is obtained. Ptp is transpulmonary pressure; Ppeak is peak pressure; Pplat is plateau pressure; PEEP is positive end-expiratory pressure; ΔP is the dynamic pressure gradient [blue].

Helium-oxygen reduces Reynold's number [Re] which is the ratio of inertial forces [density-dependent, viscosity-independent] to viscous forces [viscosity-dependent, density-independent] in a perfect tube [189]. The lower the Re, the more likely laminar flow is to occur; the higher the Re, the more likely turbulent flow is to occur. In figure 34, lower Re increases laminar flow fraction as depicted by the emboldened arrow towards laminar flow; this greatly reduces ΔP because it is the square of turbulent airflow that is proportional to ΔP.

Yet helium-oxygen directly affects the laminar and turbulent flow existing within a given Re milieu; the constants that mediate laminar [K1] and turbulent [K2] airflow explain how. Helium-oxygen reduces density which lowers K2; but Helium-oxygen slightly increases K1 because of slightly greater viscosity. It should not escape the reader that both K1 and K2 are highly and inversely related to the radius of the airway through which gas flows [188]. Thus, airway caliber plays a pivotal role in the ΔP value.

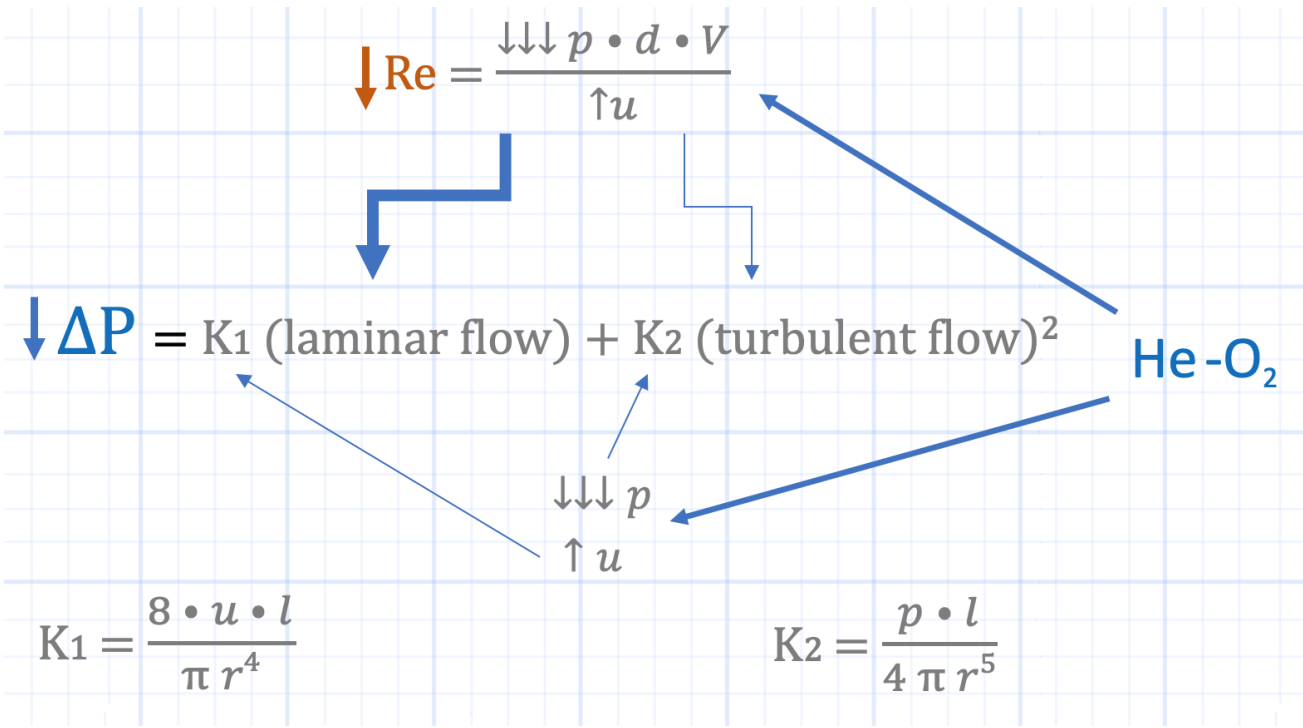

Figure 34: Re is Reynold's number; p is gas density; d is tube diameter; V is gas velocity; u is gas viscosity; l is tube length; r is tube radius; ΔP is the dynamic pressure gradient. Helium-oxygen diminishes gas density to a larger degree than it raises gas viscosity [see text].

Inspiratory Effects

The effect of helium-oxygen on peak inspiratory pressure [Ppeak] has been demonstrated in a number of trials of obstructive airways disease. Indeed, in one small study, helium-oxygen dramatically reduced the mean Ppeak by 32 cm H2O [190]. Additionally, Lee and colleagues showed that Ppeak fell by 10 cm H2O [191] and Tassaux et al. noted an average fall of 5 cm H2O [192]. While the differences between these trials may be related to disease severity, fraction of helium utilized, as well as tidal volume and flow rate, they consistently show that in the effortless, ventilated patient, helium-oxygen reduces dynamic, inspiratory pressure. The overall effect shrinks resistive work and therefore mechanical power.

Expiratory Effects

In addition to diminished Ppeak, helium-oxygen reliably reduces intrinsic positive end-expiratory pressure [PEEPi]. Expiratory flow through an obstructed airway can be modelled with the orifice flow equation [figure 35] [188].

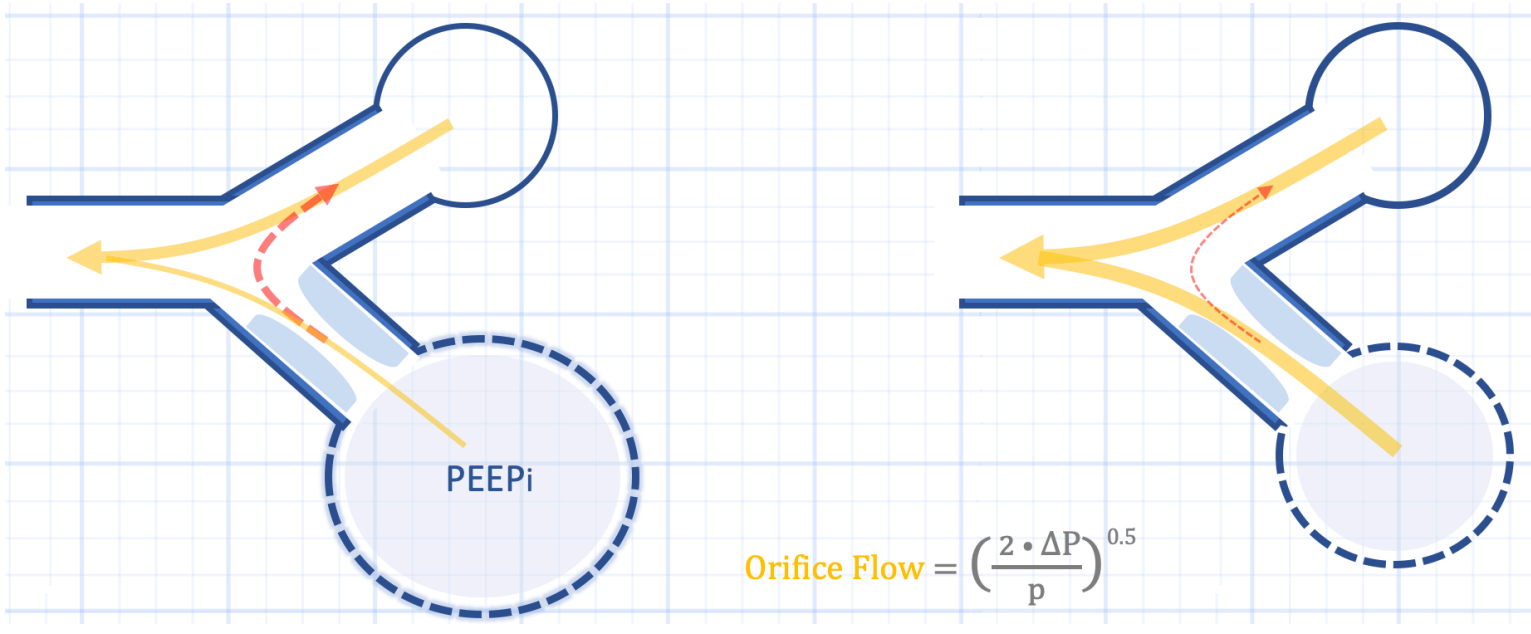

Figure 35: Orifice flow is inversely related to gas density (p). Low gas density enhances expiratory flow. An obstructed lung unit [bottom left] prolongs the unit's time constant, delays emptying and leads to intrinsic PEEP [PEEPi]. Pendelluft [red dashed arrow] occurs at end-expiration from lung units of long to short time constants. Homogenous emptying in response to helium-oxygen prevents this physiology [right]. ΔP is the dynamic pressure gradient.

Orifice flow is inversely related to gas density, such that expiratory flow through a narrowing rises as gas density falls. Accordingly, helium-oxygen diminishes PEEPi and dynamic hyperinflation, which was observed in the aforementioned studies [191-193]. To the extent that PEEPi is abolished, static breathing work falls as well. Indeed, Lee et al. reported that Ppeak, PEEPi and Pplat all fell significantly with helium-oxygen administration [191]. As well, diminished PEEPi also improved cardiac output and attenuated pulse pressure variation in their analysis!

Another consequence of PEEPi is that at end expiration, there can be continued airflow from lung units with prolonged time constants [bottom lung unit on the left of figure 35]. If some of this flow is directed to lung units without PEEPi [red dashed line] then air sloshes within the lung – so called 'pendelluft' physiology. This is wasted ventilation and effectively raises dead space. If lung units empty more homogenously, then the end-expiratory pendelluft phenomenon should also cease [194]. While helium-oxygen commonly diminishes PEEPi and lowers $PaCO_2$, not all authors have found this to be due to homogenization of time constants [193].

In summary, lowering gas density has salutary effects on both inspiratory and expiratory phases of the respiratory cycle. By reducing Ppeak, PEEPi and Pplat, dynamic and elastic work is reduced. Accordingly, the total mechanical power applied to the lung skeleton is diminished which may mitigate VILI. Lung units of

differing time-constants have been found in ARDS [195], so this physiology may be germane beyond obstructive airways disease. The obvious drawback is that the density-dependent benefits of helium-oxygen come at the expense of FiO_2 and limits application to severely hypoxemic patients. Accordingly, helium-oxygen as an adjunct to extracorporeal oxygenation may hold clinical merit [196].

Asthmatic Mechanics

An acute exacerbation of asthma is typified by an inability to completely evacuate the alveolus [197-199]. Ultimately, this results at the cross-roads of three synchronic events: 1. Decreased pressure gradient for expiratory flow 2. Increased resistance to expiratory flow and 3. Diminished time for expiration. While some will lump the first two problems into a 'prolonged respiratory time constant,' this only applies to the passive patient [200] in a straightforward manner.

Difficulty generating a pressure gradient for expiration [from the alveolus towards the mouth] is the result of diminished pulmonary elastic recoil – commonly thought to characterize only emphysema – culminating in less alveolar pressure for any given lung volume [201, 202]. Further, during an exacerbation of asthma, the chest wall can also retard expiration, from persistent activation of inspiratory muscles during expiration [203]. Importantly, overly active muscles of inspiration are externally off-loaded by a ventilator [204] – one potential method by which external airway pressure combats air-trapping.

In addition to the above, expiratory airway resistance also prevents adequate emptying of the lungs. The reasons resistance rises are manifold: smooth muscle constriction, deposition of mucous, fibrin and blood as well as dynamic airway compression [200] – all of which may lead to early airway closure [205] [see figure 1, chapter 5]. Early airway closure may be an unrecognized event in asthma, yet gas trapped behind closed airways will 'hide' from the ventilator during an end-expiratory hold – leading to an inappropriately low auto-PEEP value for degree of hyperinflation [206-208] [see figure 15, chapter 1].

Finally, high respiratory rate – by itself – can prevent full expiration, simply because expiratory time becomes too short. In passive patients, where expiration follows a typical exponential decay, expiratory time that is less than 3-4 pulmonary time constants favours incomplete alveolar emptying [200].

It has been known for at least 40 years that the functional residual capacity [FRC] can double during an acute exacerbation of asthma [209] – approaching the equilibrium volume of the chest wall [see figure 36]. Additionally, during an asthma exacerbation, gas volume from FRC to end-inspiration of 20 mL/kg was associated with pulmonary and hemodynamic risk [210].

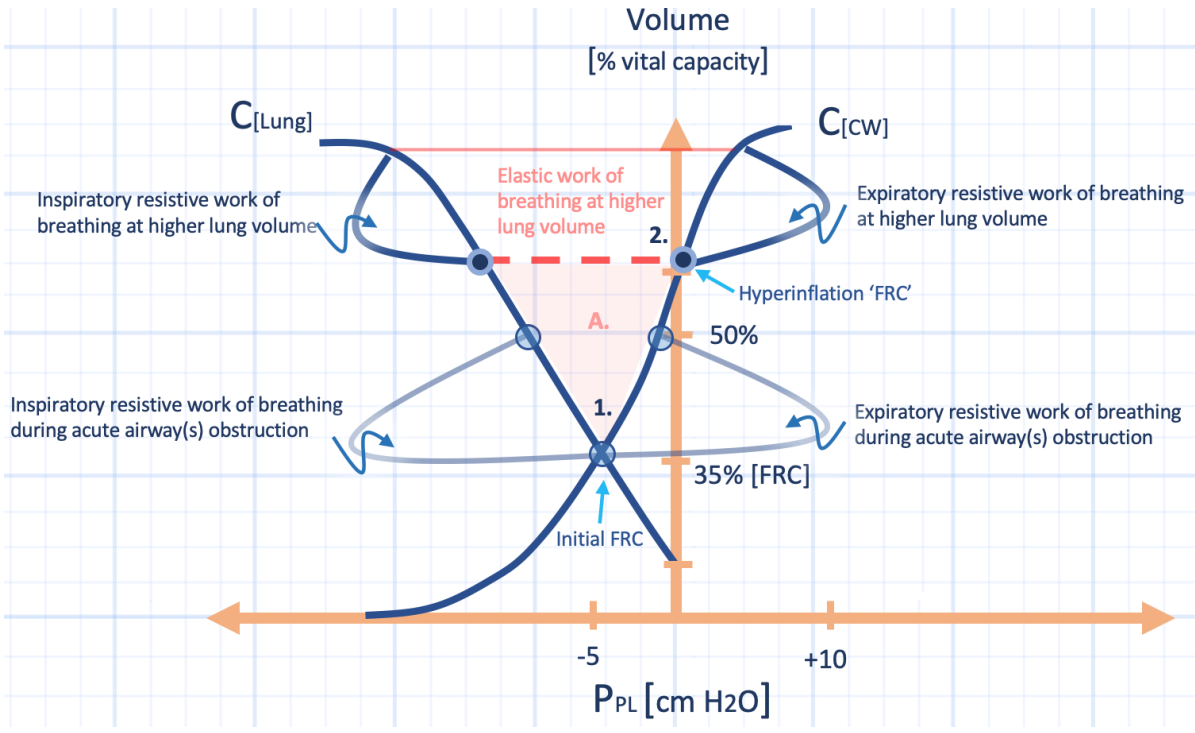

Figure 36: The Campbell diagram during an asthma exacerbation. The initial functional residual capacity [FRC] is at point 1. With increased airways resistance, and air-trapping, the FRC moves upwards to point 2. From this higher FRC, auto-PEEP performs work on the lungs and chest wall [area shaded A]. This is the triggering work that must be performed to initiate airflow and may be offset by extrinsic PEEP. The pink dashed line is muscular effort needed to overcome static work done by auto-PEEP and generate airflow at higher volume. Note this difference between effort and work performed by respiratory muscles. See also figure 37.

Can't Inspire

Yet the opposite side of the coin is also true; the acute asthmatic cannot inspire. With creeping hyperinflation, the lung and chest wall lose their mechanical advantage and inspiration insidiously becomes energetically inefficient. Crucially, rising work-of-breathing is synchronous with air-trapping – long before the patient doubles his or her FRC. The reason is that dynamic hyperinflation generates auto-PEEP – as a function of trapped volume and respiratory system compliance. Auto-PEEP demands an energetic investment prior to inspiratory flow. Additionally, the respiratory muscles operate at an unfavorable position on their length-tension curve and stored elastic recoil of the chest wall is lost as it expands. Finally, breathing takes place at the upper, less compliant portion of the respiratory system, which makes inspiratory work of breathing unfavourable [211].

Applying PEEP unloads the muscles of inspiration when the patient initiates a breath. Ironically, PEEP by itself acts as pressure support in that it both promotes inspiration and, to the extent that there is waterfall physiology [described below], PEEP is functionally absent during expiration [211]!

All IPAP, no EPAP

While it is generally accepted that PEEP is beneficial during an asthma exacerbation when there is inspiratory effort [197-199, 212], it has been argued that

the application of PEEP during passive, controlled ventilation is dangerous [198, 199]. The suggestion that PEEP is harmful – in the absence of inspiratory effort – undoubtedly traces back to a landmark study by Tuxen in 1989 [213]. In this study, 6 paralyzed patients [4 with asthma] were ventilated with ZEEP and PEEP levels of 5, 10 and 15 cm H_2O. Importantly, auto-PEEP was not measured, nor were patients studied for expiratory flow limitation. Each level of PEEP progressively increased lung volume without any beneficial effects; from this, PEEP was deemed hazardous. Interestingly, Tuxen referenced case reports that did find physiological benefit to PEEP in asthmatics on controlled ventilation, but were explained away as fortuitous – unrelated to PEEP.

Chasin' Waterfalls

While the results of Tuxen have been considered conclusive for decades [198, 199], the thoughtful contemporaneous commentary by Marini [204] seems largely forgotten. In it, Marini argues that when expiratory flow limitation is absent [i.e. no 'waterfall' physiology], then yes, PEEP will only increase end-expiratory lung volume [214]. But when there is 'waterfall' physiology – when the downstream pressure from the alveolus is not the mouth, but rather a 'choke point' in the airway [200] – then the application of PEEP at the mouth will have no effect on airflow until PEEP is equal to the value of the collapse pressure at the choke point. This is called 'waterfall physiology' because the flow of gas through the airway is independent of the pressure at the mouth, just as the flow of water over the cusp of a waterfall is unaffected by the level of water in the river below. However, were the level of the river rise to the level of the waterfall's crest, then the river would start to affect flow – just as raising PEEP at the mouth to the choke point pressure would only then begin to retard expiration [211].

Waterfall physiology explains why obstructive patients purse-lip breath [215] – as above, the generated PEEP unloads inspiration, but has no functional effect on expiration so long as the generated PEEP is below the airway closing pressure. Waterfall physiology also explains why subsequent investigations in obstructed patients [including asthma] have found that PEEP may worsen hyperinflation in some, but also have no effect on lung volume until about 80% of the auto-PEEP value is achieved at the mouth [216-218]. Additionally, in others, the application of PEEP can even open closed airways and release trapped volume [216, 219, 220] – consistent with some of the case reports [221] initially referenced by Tuxen!

How is this operationalized at the bedside? We turn to Marini's suggestion in 1989 – increase PEEP incrementally with iterative assessments of the plateau pressure [Pplat – in theory, one could also use the stress index]. If PEEP and Pplat rise equally, then there is hyperinflation. If Pplat does not rise, or even drops – then you might be chasin' waterfalls.

Auto-PEEP

An interesting case report submitted as a letter to the editor of the New England Journal of Medicine in 1993 provides colourful background physiology for the aforementioned discussion on asthmatic mechanics [222]. In the report, the authors describe continuous positive airway pressure [CPAP] generated by placing one's head out of the window of a speeding automobile – hence, true 'auto' PEEP.

The patient is a middle-aged woman who presented to the emergency department with combined pulmonary edema and obstructive airways disease. She required immediate intubation given her comatose state as well as her arterial blood gas - pH of 6.89, $PaCO_2$ of 89 mmHg, PaO_2 of 60 mmHg and an oxygen saturation of 70%!

Notably, she was raced to the hospital by her husband and she described great improvement in her mental state when she stuck her head out of the window of their speeding car. Her husband stated that he was driving 80 miles per hour [130 km/h] and that as he slowed upon hospital arrival, his wife's mental status worsened.

The authors used Bernoulli's equation to estimate the gauge pressure generated by air moving at 80 mph. The equation is, essentially, the kinetic energy of air:

$$(11)\quad \frac{1}{2}\ x\ density\ of\ air\ x\ (velocity\ of\ air)^2$$

Equation 11: The assumptions here are that air is incompressible, non-viscous and irrotational. Given that the vehicle was moving at 36 metres per second and that the density of air is 1.21 kg per m3, the pressure applied to the patient's face was roughly 8 cm H_2O.

As elaborated above, applying CPAP has salutary inspiratory and expiratory effects for a patient with air-trapping and expiratory flow limitation. The inspiratory threshold load generated by dynamic hyperinflation is a function of respiratory system compliance [see figure 37]. The patient generated extra inspiratory effort to overcome her intrinsic positive end-expiratory pressure [PEEP] and trigger airflow. Technically, this initial load upon the respiratory system is not truly 'work' [in joules] because no change in lung volume occurs with the inspiratory effort; it is an undesirable isometric exercise for the respiratory system and it diminishes the energetic efficiency of inspiratory muscles. CPAP carries this inspiratory load for the patient, improves inspiratory energetic efficiency and, therefore, reduces the oxygen demands of the respiratory pump.

The expiratory effects of CPAP may be less intuitive, but if the patient has expiratory flow limitation, it suggests that there is a 'choke point' pressure acting as the effective downstream pressure of expiration – not the pressure at the mouth. If, for example, the patient had large segments of her lung with an intrinsic pressure of 10 cm H_2O at the end of expiration [i.e. PEEPi], then those lung segments were likely limited by a 'choke point' pressure of approximately 10 cm H_2O. The 8 cm H_2O of CPAP provided by the automobile is functionally absent from those 'choked' lung units. Thus, and somewhat paradoxically, CPAP acts in a manner akin to pressure support in that it promotes inspiration beyond that of expiration!

While the difference between work and power have been discussed above, there has been no specific discussion on respiratory effort and efficiency – which are commonly confused with work. Indeed, a recent publication [223] addressing the beneficial effects of high flow nasal cannula in patients with chronic obstructive pulmonary disease [COPD] focuses this examination.

In a small group of patients with hypercapnic respiratory faiure, a nasogastric tube was placed – prior to extubation – to monitor the electrical activity of the diaphragm [EAdi in microvolts – uv]. Just prior to extubation, the patient received an end-expiratory hold maneuver; the peak fall in airway occlusion pressure on inspiration was matched to the peak rise in the electrical activity of the diaphragm which created an index. In other words, continuously measured electrical activity of the diaphragm was used as a surrogate for the pressure generated by the muscles of respiration [Pmusc]. The effort exerted by the muscles of respiration [as estimated by the EAdi] was measured after extubation – first on NHF, then on conventional oxygen therapy.

While on NHF, the pressure time product [PTP] estimated from the electrical activity of the diaphragm was, on average, in the low 130s $cmH_2O \cdot s/min$ and this increased to 211 $cmH_2O \cdot s/min$ on conventional oxygen therapy.

While the authors report the PTP as 'work of breathing,' this is not exactly correct. Work requires displacement [a force deployed over a distance, in joules] [108]. However, the pressure time product [PTP] can rise when lung volume – displacement – does not change. An extreme example is a Mueller maneuver [see chapters 1, 3 and 4] which is when the muscles of inspiration are contracted against a closed glottis. This maneuver causes great effort and energy expenditure by the respiratory muscles, but there is no volume change and, therefore, no work done. The important point here is that PTP tracks energy consumption by the muscles of respiration more closely than breathing work [187]. Accordingly, the reason that PTP is often used as an index of respiratory effort – rather than work – is because it accounts for respiratory energy consumption that occurs during isometric contractions; for example, when overcoming auto-PEEP. PTP also accounts for the time spent during an inspiratory effort which is also directly related to energy use. Because PTP is the integral of the respiratory muscle pressure change over time, its units are $cmH_2O \cdot s/min$ and not $cmH_2O/s/min$ as listed by the authors.

An interesting paper from 2014 [224] highlights the difference between breathing work and breathing effort. In patients with COPD and hyperinflation with auto-PEEP, EAdi, esophageal pressure and tidal volume were measured in response to the addition of external PEEP. The addition of external PEEP from 2 cm H_2O to 8 cm H_2O while on pressure support increased tidal volume by about 20% and decreased both Pmusc and the EAdi by a similar amount. Consequently, if volume increases and pressure falls, then work [the area defined by the pressure-volume loop] may actually change minimally. Importantly, however, respiratory effort [e.g.

the PTP] falls because the effort required to overcome auto-PEEP is diminished by external PEEP. If work is unchanged at a lower respiratory effort/energy consumption, then the efficiency of breathing has improved. The concept of work [in joules] relative to its efficiency is important because this value must stay at-or-below the amount of energy delivered to the muscles of respiration [i.e. oxygen delivery] to maintain adequate ventilation energetics [225] [figure 37].

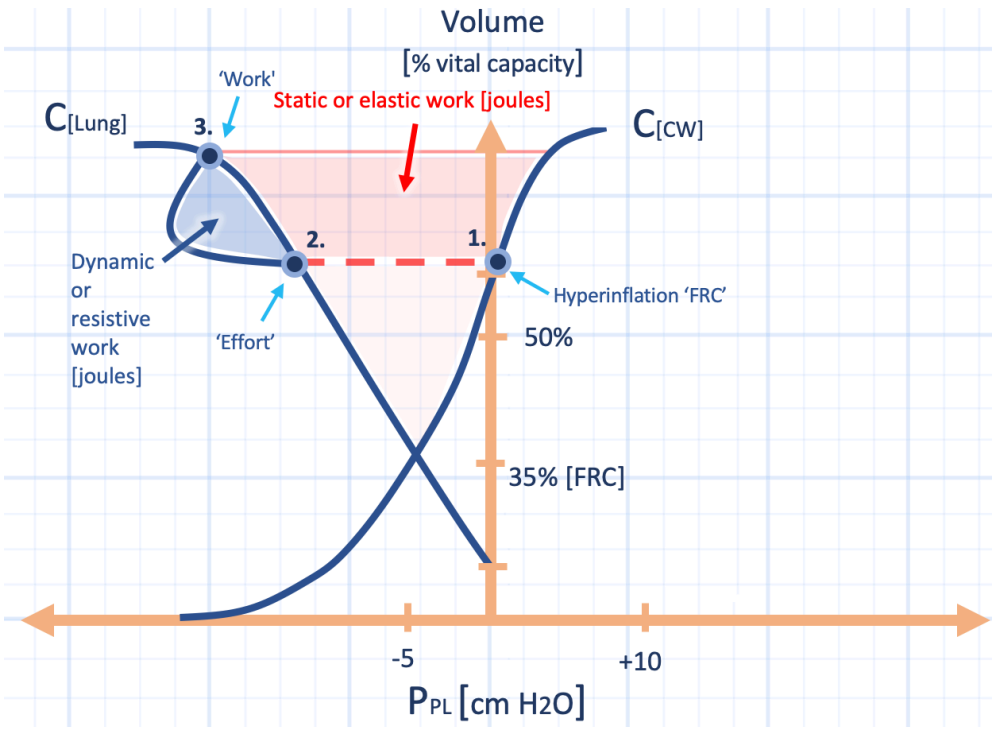

Figure 37: The difference between effort and work on the Campbell diagram. Hyperinflation functional residual capacity [FRC] is elevated in a COPD exacerbation. Moving from point 1 to point 2 represents effort but no work, because the inspiratory muscles are not changing lung volume; however, this increases the pressure time product. Work is seen from point 2 to 3 and is composed of dynamic [blue shade] and elastic [red shade] components. Work is performed because lung volume rises along the y-axis. Ccw is chest wall compliance and Clung is lung compliance. Ppl is pleural pressure. See also figure 36.

Interestingly, in the investigation by Bellani and colleagues [224], the amount of external PEEP applied to lower EAdi to a value similar to the EAdi seen in Di mussi et al. was 8 cm H_2O [EAdi fell to 15 uV in both cohorts], somewhat consistent with the level of high-flow oxygen applied [60 L/min is expected to supply about 5 cmH_2O of external PEEP with the mouth closed]. Thus, improved PTP during NHF was due to diminished isometric energy needed to overcome auto-PEEP.

Because PTP is correlated with oxygen consumption [VO_2], its fall during NHF lowers carbon dioxide production by the muscles of respiration. As described next, carbon dioxide production [VCO_2] is directly proportional to the arterial tension of carbon dioxide [$PaCO_2$]. While PTP fell in the paper by Di mussi et al. [from 211 $cmH_2O \cdot s/min$ to roughly 130 $cmH_2O \cdot s/min$ – normal values are considered to be between 50 and 150 $cmH_2O \cdot s/min$] this is expected to lower the $PaCO_2$. Yet diminished $PaCO_2$ was not seen during NHF which may have been due to contemporaneous fall in minute ventilation or, perhaps, increased dead space from hyperoxygenation [226].

That high flow oxygen applied via nasal cannula lends itself to treating hypoxemic respiratory failure may be obvious. With adequate heat and humidification, oxygen can be employed relatively comfortably at very high flow rates – upwards of 60 L/min – to the nares. At such rates, patient effort is minimized and much less ambient air is entrained. Accordingly, precise fractions of inspired oxygen may be delivered up to 1.0. Further, high oxygen flow creates positive end-expiratory pressure [PEEP] and recruits end-expiratory lung volume [227, 228]. It is estimated that for every 10 L/min of oxygen flow applied, 0.7 cm of H_2O of PEEP is generated with the mouth closed. If the mouth is open, this value falls to 0.35 cm H_2O for each 10 L/min of flow [229]. Lung recruitment with nasal high flow [NHF] oxygen undoubtedly improves PaO_2/FiO_2 ratio in patients with hypoxemic respiratory failure – even in obese post-operative patients who are at high risk for losing end-expiratory lung volume [227]. Additionally, in the FLORALI trial, there was benefit in patients with mild and moderate acute lung injury without hypercapnia as compared to non-invasive ventilation [230].

The Partial Pressure of Arterial Carbon Dioxide

Notably, patients with hypercapnia were specifically excluded from the FLORALI trial as non-invasive ventilation [NIV, e.g. BiPAP] has a strong evidence base in patients with hypercapnic respiratory failure [231]. Nevertheless, NHF does provide some assistance with arterial carbon dioxide tension. Thus, patients with hypercapnia and intolerance of NIV may benefit from NHF. When considering the mechanistic details, it is important to refresh ourselves with the determinants of the partial pressure of arterial carbon dioxide [$PaCO_2$].

$$PaCO_2 = k \bullet \frac{VCO_2}{(f \times Vt) \bullet (1 - \frac{Vd_{ana} + Vd_{alv}}{Vt})} \quad \text{i.e.} \approx \frac{production}{excretion}$$

M_{VE} — Dead space fraction

$$PaCO_2 = \frac{VCO_2}{(60 \times 0.15) \bullet (1 - \frac{0.15}{0.15})} = \frac{VCO_2}{(9\ L/min) \bullet (1 - 1.0)} = \frac{VCO_2}{(zero)} = \infty$$

M_{VE} — Dead space fraction

Figure 38: Top panel: The determinants of $PaCO_2$. Mve is minute ventilation. Bottom panel: The effect of rapid-shallow breathing. Consider a patient breathing 60 breaths per minute with a tidal volume of 150 mL – the minute ventilation is 9 L/min [i.e. 60 x 0.150]. However, if we assume anatomic dead space to be roughly 150 mL, then the patient's alveolar ventilation is zero! The patient is only washing gas in and out of anatomical dead space - dead space fraction is 100%! $PaCO_2$ rises to infinity and death soon follows.

As seen in figure 38, $PaCO_2$ is directly related to tissue carbon dioxide production which makes intuitive sense. A patient with malignant hyperthermia, massive tissue oxygen consumption [VO_2] and consequent supra-normal tissue carbon dioxide production [VCO_2] will have much higher $PaCO_2$ - unless the carbon dioxide is excreted by the lungs via alveolar ventilation.

Accordingly, alveolar ventilation is located in the denominator and is inversely-related to $PaCO_2$ [232]. Alveolar ventilation is the fraction of minute ventilation [Mve] that bathes the alveoli. Thus, a portion of each inspiration does not participate in gas exchange – known as 'wasted ventilation' or 'dead space' [232]. The dead space fraction is the total amount of dead space volume [Vd] out of each tidal volume [Vt]; that is, [Vd / Vt]. In turn, the normal dead space volume [Vd] is composed to two sub-types of dead space – anatomic dead space [Vd-ana] and alveolar dead space [Vd-alv]. Normally, the dead space volume Vd makes up 20-30% of each breath and this is almost entirely Vd-ana [233]. In other words, alveolar ventilation is 70-80% of the minute ventilation.

From the equation above, it should be clear that reducing $PaCO_2$ is enhanced by: reducing VCO_2, increasing Mve [increasing respiratory rate or tidal volume] or reducing the dead space fraction [Vd/Vt].

Reducing dead space fraction is worth some elaboration, particularly in the setting of the commonly encountered patient with rapid-shallow breathing. Note that the dead space fraction [Vd/Vt] necessarily rises as tidal volume [Vt] falls. Thus, any therapy that enhances deep tidal volumes lowers dead space fraction and enhances carbon dioxide excretion [e.g. think Kussmauls' respirations].

What may be less intuitive is that rapid breathing also raises Vd-alv [232]. Rapidly ventilating an alveolus/lung unit above and beyond its degree of perfusion [i.e. increasing V/Q ratio] also causes dead space, but this is not anatomical, it is alveolar. In summary, treating rapid breathing lowers alveolar dead space [Vd-alv], treating shallow breathing increases dead space fraction [i.e. increases Vt, lowers Vd / Vt].

Work of Breathing and Alveolar Ventilation

How might NHF lower $PaCO_2$? Probably all of the aforementioned mechanisms contribute. First, patients in extremis can easily increase oxygen consumption VO_2 – and therefore VCO_2 – by 3-to-4 fold [225, 234]. In a recent study of patients with hypoxemic respiratory failure, NHF reduced the Ti/Ttot from 0.5 to 0.4 [235]. The Ti/Ttot is the ratio of inspiratory time to total breath cycle and is a surrogate for respiratory effort. A normal value is 0.33; values between 0.5 and 0.6 are considered unsustainable as fatigue and respiratory failure will set in [236]. In this study the pressure-time product also fell significantly with NHF [235]. Presumably, while VCO_2 was not measured, it decreased with respiratory muscle rest.

NHF has other salutary effects on carbon dioxide balance. Nearly all investigations reveal that respiratory rate falls on NHF [228]. As above, this reduces alveolar dead space [Vd-alv] by lowering 'wasted ventilation' [232]. Further, in healthy volunteers, Vt increased which lowered their dead space fraction [237]. Importantly, however, while asleep, the same volunteers on NHF reduced their Vt, and therefore Mve, leading the authors to speculate that changes in minute ventilation on nasal high flow are sleep-wake dependent [237].

Not all investigations observed increased tidal volume, but many showed reduced respiratory rate with stable or decreased $PaCO_2$ – consistent with diminished VCO_2 and/or increased efficiency of carbon dioxide excretion. An additional mechanism is nasopharyngeal dead space wash-out by high flow [238] which ameliorates Vd-ana. Notably, applying NIV via a tight-fitting face mask increases Vd-ana [227, 228]!

In summary, it is entirely possible that NHF reduces all of the following: VCO_2, Vd-ana, Vd-alv and – to the extent that tidal volume [Vt] increases – Vd/Vt.

Heliox Boost?

As described above, gas mixtures of helium and oxygen increase the fraction of laminar flow relative to turbulent flow and lower the resistance of the turbulent flow that remains. These effects increase airflow and, therefore, Vt for any given driving pressure and inspiratory time. Also, breathing effort falls and, potentially, VCO_2. To the extent that helium-oxygen abolishes auto-PEEP, and PEEP from nasal high flow stents open collapsed airways, diaphragmatic advantage returns and ventilation enhanced. Nevertheless, in the hypercapnic patient who is wholly intolerant or unable to cooperate with NIV, urgent endotracheal intubation should be considered before NHF plus helium-oxygen.

Conclusion

The pressure and volume across the respiratory system is supplemented by materials science with analogy to stress and strain, respectively. Further, work on the lungs and respiratory system is extended to energy over time, or power. These principles tie together disparate threads of ventilation induced lung injury research. Explication of non-invasive ventilation, high flow oxygen supplementation and unique modes of invasive ventilation through the lens of work and power are exciting avenues of future investigation. Finally, abnormal transmission of energy and power across the lungs must also affect the cardiovascular system. Mechanical heart-lung interaction thus merges the principle of energetic 'coupling' between the respiratory and cardiovascular systems. Accordingly, diagnosing and trending injurious pulmonary energy might be supplemented by hemodynamic monitoring.

References

1. Gnaegi A, Feihl F, Perret C: Intensive care physicians' insufficient knowledge of right-heart catheterization at the bedside: Time to act? Crit Care Med 1997, 25(2):213-220.
2. Pinsky MR, Vincent JL: Let us use the pulmonary artery catheter correctly and only when we need it. Crit Care Med 2005, 33(5):1119-1122.
3. Kenny J-E: Predicting the Haemodynamic Response to Prone Positioning: A Novel and Simultaneous Analysis of the Guyton and Rahn Diagrams. Critical Care Horizons 2017, 1(1):1-7.
4. Rahn H, Otis AB, et al.: The pressure-volume diagram of the thorax and lung. The American journal of physiology 1946, 146(2):161-178.
5. West JB: Challenges in teaching the mechanics of breathing to medical and graduate students. Advances in Physiology Education 2008, 32(3):177-184.
6. Banner MJ, Jaeger MJ, Kirby RR: Components of the work of breathing and implications for monitoring ventilator-dependent patients. Critical care medicine 1994, 22(3):515-523.
7. Behazin N, Jones SB, Cohen RI et al: Respiratory restriction and elevated pleural and esophageal pressures in morbid obesity. J Appl Physiol (1985) 2010, 108(1):212-218.
8. Gattinoni L, Pelosi P, Suter PM et al: Acute respiratory distress syndrome caused by pulmonary and extrapulmonary disease. Different syndromes? American journal of respiratory and critical care medicine 1998, 158(1):3-11.
9. Gattinoni L, Pesenti A: The concept of "baby lung". Intensive care medicine 2005, 31(6):776-784.
10. Rodarte JR, Scharf SM, Pinsky MR et al: Chapter 2 - Lung and Chest Wall Mechanics. In: Respiratory-Circulatory Interactions in Health and Disease. CRC Press; 2001: 9-32.
11. Vieillard-Baron A, Matthay M, Teboul J et al: Experts' opinion on management of hemodynamics in ARDS patients: focus on the effects of mechanical ventilation. Intensive care medicine 2016, 42(5):739-749.
12. Jardin F, Vieillard-Baron A: Right ventricular function and positive pressure ventilation in clinical practice: from hemodynamic subsets to respirator settings. Intensive care medicine 2003, 29(9): 1426-1434.
13. Jozwiak M, Teboul JL, Anguel N et al: Beneficial hemodynamic effects of prone positioning in patients with acute respiratory distress syndrome. American journal of respiratory and critical care medicine 2013, 188(12):1428-1433.
14. Magder S: Further cautions for the use of ventilatory-induced changes in arterial pressures to predict volume responsiveness. Critical Care 2010, 14(5).
15. Mesquida J, Kim HK, Pinsky MR: Effect of tidal volume, intrathoracic pressure, and cardiac contractility on variations in pulse pressure, stroke volume, and intrathoracic blood volume. Intensive care medicine 2011, 37(10):1672-1679.
16. Monnet X, Bleibtreu A, Ferre A et al: Passive leg-raising and end-expiratory occlusion tests perform better than pulse pressure variation in patients with low respiratory system compliance. Critical care medicine 2012, 40(1):152-157.
17. Magder S: Is all on the level? Hemodynamics during supine versus prone ventilation. American journal of respiratory and critical care medicine 2013, 188(12):1390-1391.
18. Albert RK, Hubmayr RD: The hemodynamic effects of prone positioning in patients with acute respiratory distress syndrome remain to be defined. American journal of respiratory and critical care medicine 2014, 189(12):1567.
19. Jozwiak M, Teboul JL, Monnet X: Reply: Prone positioning actually exerts benefits on hemodynamics! American journal of respiratory and critical care medicine 2014, 189(12):1567-1568.
20. Magder S: Reply: Reply: Prone positioning actually exerts benefits on hemodynamics! American journal of respiratory and critical care medicine 2014, 189(12):1568-1569.
21. Magder S: Bench-to-bedside review: An approach to hemodynamic monitoring - Guyton at the bedside. Crit Care 2012, 16(5):236.
22. Feihl F, Broccard AF: Interactions between respiration and systemic hemodynamics. Part I: basic concepts. Intensive care medicine 2009, 35(1):45-54.
23. Broccard AF: Cardiopulmonary interactions and volume status assessment. Journal of clinical monitoring and computing 2012, 26(5):383-391.
24. Guyton AC, Polizo D, Armstrong GG: Mean circulatory filling pressure measured immediately after cessation of heart pumping. The American journal of physiology 1954, 179(2):261-267.
25. Sylvester JT, Goldberg HS, Permutt S: The Role of the Vasculature in the Regulation of Cardiac-Output. Clin Chest Med 1983, 4(2):111-126.
26. Robotham JL, Takata M: Mechanical abdomino/heart/lung interaction. Journal of sleep research 1995, 4(S1):50-52.

27. van den Berg PC, Jansen JR, Pinsky MR: Effect of positive pressure on venous return in volume-loaded cardiac surgical patients. J Appl Physiol (1985) 2002, 92(3):1223-1231.
28. Takata M, Wise RA, Robotham JL: Effects of abdominal pressure on venous return: abdominal vascular zone conditions. J Appl Physiol (1985) 1990, 69(6):1961-1972.
29. Jellinek H, Krenn H, Oczenski W et al: Influence of positive airway pressure on the pressure gradient for venous return in humans. J Appl Physiol (1985) 2000, 88(3):926-932.
30. Berger D, Moller PW, Weber A et al: Effect of PEEP, blood volume, and inspiratory hold maneuvers on venous return. American journal of physiology-heart and circulatory physiology 2016, 311(3):H794-H806.
31. Pelosi P, Tubiolo D, Mascheroni D et al: Effects of the prone position on respiratory mechanics and gas exchange during acute lung injury. American journal of respiratory and critical care medicine 1998, 157(2):387-393.
32. Lansdorp B, Hofhuizen C, van Lavieren M et al: Mechanical ventilation-induced intrathoracic pressure distribution and heart-lung interactions*. Critical care medicine 2014, 42(9):1983-1990.
33. Morgan BC, Guntheroth WG, Dillard DH: Relationship of Pericardial to Pleural Pressure during Quiet Respiration and Cardiac Tamponade. Circulation research 1965, 16:493-498.
34. Marini JJ, Culver BH, Butler J: Effect of positive end-expiratory pressure on canine ventricular function curves. Journal of applied physiology: respiratory, environmental and exercise physiology 1981, 51(6):1367-1374.
35. Vieillard-Baron A, Loubieres Y, Schmitt JM et al: Cyclic changes in right ventricular output impedance during mechanical ventilation. J Appl Physiol (1985) 1999, 87(5):1644-1650.
36. Jardin F, Brun-Ney D, Cazaux P et al: Relation between transpulmonary pressure and right ventricular isovolumetric pressure change during respiratory support. Catheterization and cardiovascular diagnosis 1989, 16(4):215-220.
37. Jardin F, Delorme G, Hardy A et al: Reevaluation of hemodynamic consequences of positive pressure ventilation: emphasis on cyclic right ventricular afterloading by mechanical lung inflation. Anesthesiology 1990, 72(6):966-970.
38. Gattinoni L, Pelosi P, Vitale G et al: Body position changes redistribute lung computed-tomographic density in patients with acute respiratory failure. Anesthesiology 1991, 74(1):15-23.
39. Whittenberger JL, Mc GM, Berglund E et al: Influence of state of inflation of the lung on pulmonary vascular resistance. Journal of applied physiology 1960, 15:878-882.
40. Orchard CH, Sanchez de Leon R, Sykes MK: The relationship between hypoxic pulmonary vasoconstriction and arterial oxygen tension in the intact dog. The Journal of physiology 1983, 338:61-74.
41. O'Quin RJ, Marini JJ, Culver BH et al: Transmission of airway pressure to pleural space during lung edema and chest wall restriction. J Appl Physiol (1985) 1985, 59(4):1171-1177.
42. Jardin F, Genevray B, Brun-Ney D et al: Influence of lung and chest wall compliances on transmission of airway pressure to the pleural space in critically ill patients. Chest 1985, 88(5): 653-658.
43. Venus B, Cohen LE, Smith RA: Hemodynamics and intrathoracic pressure transmission during controlled mechanical ventilation and positive end-expiratory pressure in normal and low compliant lungs. Critical care medicine 1988, 16(7):686-690.
44. Gattinoni L, Quintel M: How ARDS should be treated. Critical Care 2016, 20(1):1.
45. Gattinoni L, Pesenti A: The concept of "baby lung". Intensive care medicine 2005, 31(6):776-784.
46. Protti A, Cressoni M, Santini A et al: Lung stress and strain during mechanical ventilation: any safe threshold? American journal of respiratory and critical care medicine 2011, 183(10):1354-1362.
47. Gattinoni L, Pesenti A, Bombino M et al: Relationships between lung computed tomographic density, gas exchange, and PEEP in acute respiratory failure. Anesthesiology 1988, 69(6):824-832.
48. Mead J, Takishima T, Leith D: Stress distribution in lungs: a model of pulmonary elasticity. Journal of applied physiology 1970, 28(5):596-608.
49. Cressoni M, Chiurazzi C, Gotti M et al: Lung inhomogeneities and time course of ventilator-induced mechanical injuries. The Journal of the American Society of Anesthesiologists 2015, 123(3):618-627.
50. JHaitsma J, Lachmann B: Lung protective ventilation in ARDS: the open lung maneuver. Minerva anestesiologica 2006, 72(3):117.
51. Cressoni M, Cadringher P, Chiurazzi C et al: Lung inhomogeneity in patients with acute respiratory distress syndrome. American journal of respiratory and critical care medicine 2014, 189(2):149-158.
52. Caironi P, Cressoni M, Chiumello D et al: Lung opening and closing during ventilation of acute respiratory distress syndrome. American journal of respiratory and critical care medicine 2010, 181(6):578-586.
53. Cressoni M, Chiumello D, Carlesso E et al: Compressive Forces and Computed Tomography–derived Positive End-expiratory Pressure in Acute Respiratory Distress Syndrome. The Journal of the American Society of Anesthesiologists 2014, 121(3):572-581.

54. Gattinoni L, Taccone P, Carlesso E et al: Prone position in acute respiratory distress syndrome. Rationale, indications, and limits. American journal of respiratory and critical care medicine 2013, 188(11):1286-1293.
55. Henderson AC, Sá RC, Theilmann RJ et al: The gravitational distribution of ventilation-perfusion ratio is more uniform in prone than supine posture in the normal human lung. Journal of applied physiology 2013, 115(3):313-324.
56. Bone RC: The ARDS lung: new insights from computed tomography. Jama 1993, 269(16): 2134-2135.
57. Chatte G, Sab J-M, Dubois J-M et al: Prone position in mechanically ventilated patients with severe acute respiratory failure. American journal of respiratory and critical care medicine 1997, 155(2):473-478.
58. Vieillard-Baron A, Charron C, Caille V et al: Prone positioning unloads the right ventricle in severe ARDS. CHEST Journal 2007, 132(5):1440-1446.
59. Sud S, Friedrich JO, Adhikari NK et al: Effect of prone positioning during mechanical ventilation on mortality among patients with acute respiratory distress syndrome: a systematic review and meta-analysis. Canadian Medical Association Journal 2014, 186(10):E381-E390.
60. Goligher EC, Kavanagh BP, Rubenfeld GD et al: Oxygenation response to positive end-expiratory pressure predicts mortality in acute respiratory distress syndrome. A secondary analysis of the LOVS and ExPress trials. American journal of respiratory and critical care medicine 2014, 190(1):70-76.
61. Gattinoni L, Quintel M, Marini JJ: Volutrauma and atelectrauma: which is worse? In.: BioMed Central; 2018.
62. Gattinoni L, Marini JJ, Pesenti A et al: The" baby lung" became an adult. Intensive care medicine 2016, 42(5):663-673.
63. Tonetti T, Vasques F, Rapetti F et al: Driving pressure and mechanical power: new targets for VILI prevention. Annals of translational medicine 2017, 5(14).
64. Gattinoni L, Marini JJ, Collino F et al: The future of mechanical ventilation: lessons from the present and the past. Critical Care 2017, 21(1):183.
65. Protti A, Andreis DT, Milesi M et al: Lung anatomy, energy load, and ventilator-induced lung injury. Intensive care medicine experimental 2015, 3(1):34.
66. Kassis EB, Loring S, Talmor D: Esophageal pressure: research or clinical tool? Medizinische Klinik-Intensivmedizin und Notfallmedizin 2018:1-8.
67. Lauritzsen LP, Pfitzner J: Pressure breathing in fighter aircraft for G accelerations and loss of cabin pressurization at altitude—a brief review. Canadian Journal of Anesthesia/Journal canadien d'anesthésie 2003, 50(4):415-419.
68. Burns JW, Ivan DJ, Stern CH et al: Protection to+ 12 Gz. Aviation, space, and environmental medicine 2001, 72(5):413-421.
69. Parkhurst M, Leverett Jr S, Shubrooks Jr S: Human tolerance to high, sustained+ G z acceleration. Aerospace medicine 1972, 43(7):708-712.
70. Burton RR: G-induced loss of consciousness: definition, history, current status. Aviation, space, and environmental medicine 1988.
71. Ossard G, Clere J-M, Kerguelen M et al: Response of human cerebral blood flow to+ Gz accelerations. Journal of applied physiology 1994, 76(5):2114-2118.
72. Wood EH: Prevention of the pathophysiologic effects of acceleration in humans: fundamentals and historic perspectives. IEEE Engineering in Medicine and Biology Magazine 1991, 10(1): 26-36.
73. Smith BA, Clayton EW, Robertson D: Experimental arrest of cerebral blood flow in human subjects: the red wing studies revisited. Perspectives in biology and medicine 2011, 54(2).
74. Balldin U, Wranne B: Hemodynamic effects of extreme positive pressure breathing using a two-pressure flying suit. Aviation, space, and environmental medicine 1980, 51(9 Pt 1):851-855.
75. Burns JW, Parnell MJ, Burton RR: Hemodynamics of miniature swine during+ Gz stress with and without anti-G support. Journal of applied physiology 1986, 60(5):1628-1637.
76. Rushmer RF: A roentgenographic study of the effect of a pneumatic anti-blackout suit on the hydrostatic columns in man exposed to positive radial acceleration. American Journal of Physiology–Legacy Content 1947, 151(2):459-468.
77. Convertino VA: High sustained+ Gz acceleration: physiological adaptation to high-G tolerance. Journal of gravitational physiology: a journal of the International Society for Gravitational Physiology 1998, 5(1):P51-54.
78. Buda AJ, Pinsky MR, Ingels Jr NB et al: Effect of intrathoracic pressure on left ventricular performance. New England Journal of Medicine 1979, 301(9):453-459.
79. Travis TW, Morgan TR: US Air Force positive-pressure breathing anti-G system (PBG): subjective health effects and acceptance by pilots. Aviation, space, and environmental medicine 1994, 65(5 Suppl):A75-79.

80. Grönkvist M, Bergsten E, Kölegård R et al: G tolerance and pulmonary effects of removing chest counterpressure during pressure breathing. Aviation, space, and environmental medicine 2005, 76(9):833-840.
81. Eiken O, Kölegård R, Bergsten E et al: G protection: interaction of straining maneuvers and positive pressure breathing. Aviation, space, and environmental medicine 2007, 78(4):392-398.
82. Sharpey-Schafer E: The mechanism of syncope after coughing. British medical journal 1953, 2(4841):860.
83. Green N: Lung volumes during+ Gz acceleration and the effects of positive pressure breathing and chest counter-pressure. Journal of gravitational physiology: a journal of the International Society for Gravitational Physiology 1994, 1(1):P41.
84. Zapol WM, Snider MT: Pulmonary hypertension in severe acute respiratory failure. New England Journal of Medicine 1977, 296(9):476-480.
85. Dessap AM, Boissier F, Charron C et al: Acute cor pulmonale during protective ventilation for acute respiratory distress syndrome: prevalence, predictors, and clinical impact. Intensive care medicine 2016:1-9.
86. Guérin C, Matthay MA: Acute cor pulmonale and the acute respiratory distress syndrome. Intensive care medicine 2016:1-3.
87. Repessé X, Charron C, Vieillard-Baron A: Acute respiratory distress syndrome: the heart side of the moon. Current opinion in critical care 2016, 22(1):38-44.
88. Marini JJ, Hotchkiss JR, Broccard AF: Bench-to-bedside review: microvascular and airspace linkage in ventilator-induced lung injury. Critical Care 2003, 7(6):435.
89. Goshy M, Lai-Fook SJ, Hyatt RE: Perivascular pressure measurements by wick-catheter technique in isolated dog lobes. Journal of applied physiology 1979, 46(5):950-955.
90. Lamm W, Kirk KR, Hanson WL et al: Flow through zone 1 lungs utilizes alveolar corner vessels. Journal of applied physiology 1991, 70(4):1518-1523.
91. Mathieu-Costello O, Willford DC, Fu Z et al: Pulmonary capillaries are more resistant to stress failure in dogs than in rabbits. Journal of applied physiology 1995, 79(3):908-917.
92. Broccard AF, Hotchkiss JR, Kuwayama N et al: Consequences of vascular flow on lung injury induced by mechanical ventilation. American journal of respiratory and critical care medicine 1998, 157(6):1935-1942.
93. Broccard AF, Hotchkiss JR, Suzuki S et al: Effects of mean airway pressure and tidal excursion on lung injury induced by mechanical ventilation in an isolated perfused rabbit lung model. Critical care medicine 1999, 27(8):1533-1541.
94. Hotchkiss Jr JR, Blanch L, Murias G et al: Effects of decreased respiratory frequency on ventilator-induced lung injury. American journal of respiratory and critical care medicine 2000, 161(2):463-468.
95. Hotchkiss Jr JR, Blanch L, Naveira A et al: Relative roles of vascular and airspace pressures in ventilator-induced lung injury. Critical care medicine 2001, 29(8):1593.
96. Broccard AF, Vannay C, Feihl F et al: Impact of low pulmonary vascular pressure on ventilator-induced lung injury*. Critical care medicine 2002, 30(10):2183-2190.
97. Jardin F, Dubourg O, Bourdarias J-P: Echocardiographic pattern of acute cor pulmonale. CHEST Journal 1997, 111(1):209-217.
98. Repessé X, Charron C, Vieillard-Baron A: Assessment of the effects of inspiratory load on right ventricular function. Current opinion in critical care 2016, 22(3):254-259.
99. Vieillard-Baron A, Loubieres Y, Schmitt J-M et al: Cyclic changes in right ventricular output impedance during mechanical ventilation. Journal of applied physiology 1999, 87(5):1644-1650.
100. Jullien T, Valtier B, Hongnat J-M et al: Incidence of tricuspid regurgitation and vena caval backward flow in mechanically ventilated patients: a color Doppler and contrast echocardiographic study. CHEST Journal 1995, 107(2):488-493.
101. Repessé X, Charron C, Vieillard-Baron A: Acute cor pulmonale in ARDS: rationale for protecting the right ventricle. CHEST Journal 2015, 147(1):259-265.
102. Versprille A: Pulmonary vascular resistance. A meaningless variable. Intensive care medicine 1984, 10(2):51-53.
103. Naeije R: Pulmonary vascular resistance. A meaningless variable? Intensive care medicine 2003, 29(4):526-529.
104. Jardin F, Brun–Ney D, Cazaux P et al: Relation between transpulmonary pressure and right ventricular isovolumetric pressure change during respiratory support. Catheterization and cardiovascular diagnosis 1989, 16(4):215-220.
105. Gattinoni L, Marini JJ, Pesenti A et al: The "baby lung" became an adult. Intensive care medicine 2016.
106. Gattinoni L, Pesenti A, Baglioni S et al: Inflammatory pulmonary edema and positive end-expiratory pressure: correlations between imaging and physiologic studies. Journal of thoracic imaging 1988, 3(3):59-64.

107. Amato MB, Meade MO, Slutsky AS et al: Driving pressure and survival in the acute respiratory distress syndrome. The New England journal of medicine 2015, 372(8):747-755.
108. Akoumianaki E, Maggiore SM, Valenza F et al: The application of esophageal pressure measurement in patients with respiratory failure. American journal of respiratory and critical care medicine 2014, 189(5):520-531.
109. Gattinoni L, Chiumello D, Carlesso E et al: Bench-to-bedside review: chest wall elastance in acute lung injury/acute respiratory distress syndrome patients. Crit Care 2004, 8(5):350-355.
110. Costa EL, Slutsky AS, Amato MB: Driving pressure as a key ventilation variable. The New England journal of medicine 2015, 372(21):2072.
111. Talmor D, Sarge T, Malhotra A et al: Mechanical ventilation guided by esophageal pressure in acute lung injury. The New England journal of medicine 2008, 359(20):2095-2104.
112. Brochard L: Measurement of esophageal pressure at bedside: pros and cons. Current opinion in critical care 2014, 20(1):39-46.
113. Grasso S, Terragni P, Mascia L et al: Airway pressure-time curve profile (stress index) detects tidal recruitment/hyperinflation in experimental acute lung injury. Critical care medicine 2004, 32(4):1018-1027.
114. Bekos V, Marini JJ: Monitoring the mechanically ventilated patient. Critical care clinics 2007, 23(3):575-611.
115. Amato MBP, Barbas CSV, Medeiros DM et al: Effect of a protective-ventilation strategy on mortality in the acute respiratory distress syndrome. New England Journal of Medicine 1998, 338(6):347-354.
116. Grinnan DC, Truwit JD: Clinical review: respiratory mechanics in spontaneous and assisted ventilation. Critical Care 2005, 9(5):472.
117. Network ARDS: Brower RG, Matthay MA, Morris A, Schoenfeld D, Thompson BT, Wheeler A. Ventilation with lower tidal volumes as compared with traditional tidal volumes for acute lung injury and the acute respiratory distress syndrome. The New England journal of medicine 2000, 342(18):1301-1308.
118. Harris RS: Pressure-volume curves of the respiratory system. Respiratory care 2005, 50(1):78-98; discussion 98-79.
119. Hickling KG: Best compliance during a decremental, but not incremental, positive end-expiratory pressure trial is related to open-lung positive end-expiratory pressure: a mathematical model of acute respiratory distress syndrome lungs. American journal of respiratory and critical care medicine 2001, 163(1):69-78.
120. Rimensberger PC, Pristine G, Mullen JBM et al: Lung recruitment during small tidal volume ventilation allows minimal positive end-expiratory pressure without augmenting lung injury. Critical care medicine 1999, 27(9):1940-1945.
121. Bigatello LM, Davignon KR, Stelfox HT: Respiratory mechanics and ventilator waveforms in the patient with acute lung injury. Respiratory care 2005, 50(2):235-245; discussion 244-235.
122. Lu Q, Vieira SR, Richecoeur J et al: A simple automated method for measuring pressure–volume curves during mechanical ventilation. American journal of respiratory and critical care medicine 1999, 159(1):275-282.
123. Bachofen H, Hildebrandt J: Area analysis of pressure-volume hysteresis in mammalian lungs. Journal of applied physiology 1971, 30(4):493-497.
124. Mankikian B, Lemaire F, Benito S et al: A new device for measurement of pulmonary pressure-volume curves in patients on mechanical ventilation. Critical care medicine 1983, 11(11):897-901.
125. Scott Harris R, Hess DR, Venegas JG: An objective analysis of the pressure-volume curve in the acute respiratory distress syndrome. American journal of respiratory and critical care medicine 2000, 161(2):432-439.
126. O'Keefe GE, Gentilello LM, Erford S et al: Imprecision in lower" inflection point" estimation from static pressure-volume curves in patients at risk for acute respiratory distress syndrome. Journal of Trauma and Acute Care Surgery 1998, 44(6):1064-1068.
127. De Jong A, Verzilli D, Jaber S: ARDS in Obese Patients: Specificities and Management. Critical Care 2019, 23(1):74.
128. Salmon R, Primiano Jr F, Saidel G et al: Human lung pressure-volume relationships: alveolar collapse and airway closure. Journal of applied physiology 1981, 51(2):353-362.
129. Hickling KG: The pressure–volume curve is greatly modified by recruitment: a mathematical model of ARDS lungs. American journal of respiratory and critical care medicine 1998, 158(1): 194-202.
130. Jonson B, Richard J-C, Straus C et al: Pressure–volume curves and compliance in acute lung injury: evidence of recruitment above the lower inflection point. American journal of respiratory and critical care medicine 1999, 159(4):1172-1178.
131. Venegas JG, Harris RS, Simon BA: A comprehensive equation for the pulmonary pressure-volume curve. Journal of applied physiology 1998, 84(1):389-395.

132. Scaramuzzo G, Spadaro S, Waldmann AD et al: Heterogeneity of regional inflection points from pressure-volume curves assessed by electrical impedance tomography. Critical Care 2019, 23(1): 119.
133. Gattinoni L, Carlesso E, Cressoni M: Selecting the 'right' positive end-expiratory pressure level. Current opinion in critical care 2015, 21(1):50-57.
134. Chiumello D, Cressoni M, Carlesso E et al: Bedside Selection of Positive End-Expiratory Pressure in Mild, Moderate, and Severe Acute Respiratory Distress Syndrome*. Critical care medicine 2014, 42(2):252-264.
135. Hotchkiss JR, Simonson DA, Marek DJ et al: Pulmonary microvascular fracture in a patient with acute respiratory distress syndrome*. Critical care medicine 2002, 30(10):2368-2370.
136. Mascheroni D, Kolobow T, Fumagalli R et al: Acute respiratory failure following pharmacologically induced hyperventilation: an experimental animal study. Intensive care medicine 1988, 15(1):8-14.
137. Marini JJ, Jaber S: Dynamic predictors of VILI risk: beyond the driving pressure. In.: Springer; 2016.
138. Protti A, Andreis DT, Monti M et al: Lung stress and strain during mechanical ventilation: any difference between statics and dynamics? Critical care medicine 2013, 41(4):1046-1055.
139. Protti A, Votta E, Gattinoni L: Which is the most important strain in the pathogenesis of ventilator-induced lung injury: dynamic or static? Current opinion in critical care 2014, 20(1):33-38.
140. Gattinoni L, Tonetti T, Cressoni M et al: Ventilator-related causes of lung injury: the mechanical power. Intensive care medicine 2016, 42(10):1567-1575.
141. Cressoni M, Gotti M, Chiurazzi C et al: Mechanical power and development of ventilator-induced lung injury. Anesthesiology: The Journal of the American Society of Anesthesiologists 2016, 124(5):1100-1108.
142. Laffey JG, Kavanagh BP: Ventilation with lower tidal volumes as compared with traditional tidal volumes for acute lung injury. The New England journal of medicine 2000, 343(11):812; author reply 813-814.
143. Suzuki S, Hotchkiss JR, Takahashi T et al: Effect of core body temperature on ventilator-induced lung injury. Critical care medicine 2004, 32(1):144-149.
144. Rich PB, Reickert CA, Sawada S et al: Effect of rate and inspiratory flow on ventilator-induced lung injury. journal of trauma injury infection and critical care 2000, 49(5):903-911.
145. Cressoni M, Gotti M, Chiurazzi C et al: Mechanical power and development of ventilator-induced lung injury. The Journal of the American Society of Anesthesiologists 2016.
146. Papazian L, Forel J-M, Gacouin A et al: Neuromuscular Blockers in Early Acute Respiratory Distress Syndrome. New England Journal of Medicine 2010, 363(12):1107-1116.
147. National Heart L, Network BIPCT: Early neuromuscular blockade in the acute respiratory distress syndrome. New England Journal of Medicine 2019, 380(21):1997-2008.
148. Ferguson ND, Cook DJ, Guyatt GH et al: High-Frequency Oscillation in Early Acute Respiratory Distress Syndrome. New England Journal of Medicine 2013, 368(9):795-805.
149. Otis AB, Fenn WO, Rahn H: Mechanics of breathing in man. Journal of applied physiology 1950, 2(11):592-607.
150. Marini JJ, Crooke PS: A general mathematical model for respiratory dynamics relevant to the clinical setting. American Review of Respiratory Disease 1993, 147:14-14.
151. Huhle R, Neto AS, Schultz MJ et al: Is mechanical power the final word on ventilator-induced lung injury?—no. Annals of translational medicine 2018, 6(19).
152. Santos RS, Maia LdA, Oliveira MV et al: Biologic impact of mechanical power at high and low tidal volumes in experimental mild acute respiratory distress syndrome. Anesthesiology: The Journal of the American Society of Anesthesiologists 2018, 128(6):1193-1206.
153. Collino F, Rapetti F, Vasques F et al: Positive end-expiratory pressure and mechanical power. Anesthesiology: The Journal of the American Society of Anesthesiologists 2019, 130(1):119-130.
154. Gattinoni L, Pesenti A: The concept of "baby lung". Intensive care medicine 2005, 31(6):776-784.
155. Marini JJ: Dissipation of energy during the respiratory cycle: conditional importance of ergotrauma to structural lung damage. Current opinion in critical care 2018, 24(1):16-22.
156. Giosa L, Busana M, Pasticci I et al: Mechanical power at a glance: a simple surrogate for volume-controlled ventilation. Intensive care medicine experimental 2019, 7(1):61.
157. Marini JJ: How I optimize power to avoid VILI. Critical Care 2019, 23(1):326.
158. Neto AS, Deliberato RO, Johnson AE et al: Mechanical power of ventilation is associated with mortality in critically ill patients: an analysis of patients in two observational cohorts. Intensive care medicine 2018, 44(11):1914-1922.
159. Jain SV, Kollisch-Singule M, Sadowitz B et al: The 30-year evolution of airway pressure release ventilation (APRV). Intensive care medicine experimental 2016, 4(1):11.
160. Henzler D: What on earth is APRV? Critical Care 2011, 15(1):115.
161. Daoud EG, Farag HL, Chatburn RL: Airway pressure release ventilation: what do we know? Respiratory care 2012, 57(2):282-292.

162. Habashi NM: Other approaches to open-lung ventilation: airway pressure release ventilation. Critical care medicine 2005, 33(3):S228-S240.
163. Mireles-Cabodevila E, Kacmarek RM: Should airway pressure release ventilation be the primary mode in ARDS? Respiratory care 2016, 61(6):761-773.
164. Davis K, Johnson DJ, Branson RD et al: Airway pressure release ventilation. Archives of Surgery 1993, 128(12):1348-1352.
165. Melo e Silva CsA, Ventura CEGdS: A simple model illustrating the respiratory system's time constant concept. Advances in physiology education 2006, 30(3):129-130.
166. koutsoukou a, armaganidis a, stavrakaki-kallergi c et al: Expiratory flow limitation and intrinsic positive end-expiratory pressure at zero positive end-expiratory pressure in patients with adult respiratory distress syndrome. American journal of respiratory and critical care medicine 2000, 161(5):1590-1596.
167. Bates J, Rossi A, Milic-Emili J: Analysis of the behavior of the respiratory system with constant inspiratory flow. Journal of Applied Physiology 1985, 58(6):1840-1848.
168. Pelosi P, Cereda M, Foti G et al: Alterations of lung and chest wall mechanics in patients with acute lung injury: effects of positive end-expiratory pressure. American journal of respiratory and critical care medicine 1995, 152(2):531-537.
169. Vieillard-Baron A, Prin S, Schmitt J-M et al: Pressure–volume curves in acute respiratory distress syndrome: clinical demonstration of the influence of expiratory flow limitation on the initial slope. American journal of respiratory and critical care medicine 2002, 165(8):1107-1112.
170. Al-Rawas N, Banner MJ, Euliano NR et al: Expiratory time constant for determinations of plateau pressure, respiratory system compliance, and total resistance. Critical Care 2013, 17(1):R23.
171. Daoud EG, Chatburn RL: Comparing surrogates of oxygenation and ventilation between airway pressure release ventilation and biphasic airway pressure in a mechanical model of adult respiratory distress syndrome. Respiratory investigation 2014, 52(4):236-241.
172. Kollisch-Singule M, Emr B, Smith B et al: Mechanical breath profile of airway pressure release ventilation: the effect on alveolar recruitment and microstrain in acute lung injury. JAMA surgery 2014, 149(11):1138-1145.
173. Kollisch-Singule M, Emr B, Smith B et al: Airway pressure release ventilation reduces conducting airway micro-strain in lung injury. Journal of the American College of Surgeons 2014, 219(5):968-976.
174. Kollisch-Singule M, Jain S, Andrews P et al: Effect of airway pressure release ventilation on dynamic alveolar heterogeneity. JAMA surgery 2016, 151(1):64-72.
175. Kallet RH: Patient-ventilator interaction during acute lung injury, and the role of spontaneous breathing: part 2: airway pressure release ventilation. Respiratory care 2011, 56(2):190-206.
176. Calzia E, Lindner KH, Witt S et al: Pressure-time product and work of breathing during biphasic continuous positive airway pressure and assisted spontaneous breathing. American journal of respiratory and critical care medicine 1994, 150(4):904-910.
177. Neumann P, Golisch W, Strohmeyer A et al: Influence of different release times on spontaneous breathing pattern during airway pressure release ventilation. Intensive care medicine 2002, 28(12): 1742-1749.
178. Gattinoni L, Pelosi P, Suter PM et al: Acute respiratory distress syndrome caused by pulmonary and extrapulmonary disease: different syndromes? American journal of respiratory and critical care medicine 1998, 158(1):3-11.
179. Zhou Y, Jin X, Lv Y et al: Early application of airway pressure release ventilation may reduce the duration of mechanical ventilation in acute respiratory distress syndrome. Intensive care medicine 2017, 43(11):1648-1659.
180. Banner MJ, Jaeger MJ, Kirby RR: Components of the work of breathing and implications for monitoring ventilator-dependent patients. Critical care medicine 1994, 22(3):515-523.
181. Protti A, Cressoni M, Santini A et al: Lung stress and strain during mechanical ventilation: any safe threshold? American journal of respiratory and critical care medicine 2011, 183(10):1354-1362.
182. Yoshida T, Torsani V, Gomes S et al: Spontaneous effort causes occult pendelluft during mechanical ventilation. American journal of respiratory and critical care medicine 2013, 188(12): 1420-1427.
183. Morais CC, Koyama Y, Yoshida T et al: High Positive End-Expiratory Pressure Renders Spontaneous Effort Non-Injurious. American journal of respiratory and critical care medicine 2018(ja).
184. Pelosi P, Rocco PRM, de Abreu MG: Close down the lungs and keep them resting to minimize ventilator-induced lung injury. Critical Care 2018, 22(1):72.
185. Taylor D, Camporota L, Zhou Y et al: Estimation of true driving pressure during airway pressure release ventilation. Intensive care medicine 2018, 44(8):1364-1365.
186. Sato R, Hamahata N, Daoud EG: Are we really preventing lung collapse with APRV? Critical Care 2019, 23(1):178.

187. Mauri T, Yoshida T, Bellani G et al: Esophageal and transpulmonary pressure in the clinical setting: meaning, usefulness and perspectives. Intensive care medicine 2016, 42(9):1360-1373.
188. Hess DR, Fink JB, Venkataraman ST et al: The history and physics of heliox. Respiratory care 2006, 51(6):608-612.
189. McGarvey JM, Pollack CV: Heliox in airway management. Emergency medicine clinics of North America 2008, 26(4):905-920.
190. Gluck EH, Onorato DJ, Castriotta R: Helium-oxygen mixtures in intubated patients with status asthmaticus and respiratory acidosis. Chest 1990, 98(3):693-698.
191. Lee DL, Lee H, Chang H-W et al: Heliox improves hemodynamics in mechanically ventilated patients with chronic obstructive pulmonary disease with systolic pressure variations. Critical care medicine 2005, 33(5):968-973.
192. Tassaux D, Jolliet P, Roeseler J et al: Effects of helium-oxygen on intrinsic positive end-expiratory pressure in intubated and mechanically ventilated patients with severe chronic obstructive pulmonary disease. Critical care medicine 2000, 28(8):2721-2728.
193. Diehl J-L, Peigne V, Guérot E et al: Helium in the adult critical care setting. Annals of intensive care 2011, 1(1):24.
194. Arnal J, Gainnier M, Grandfond A et al: Effect of helium–oxygen mixture on time constant inequalities in COPD patients during controlled ventilation. Critical Care 2002, 6:1-1.
195. Vieillard-Baron A, Prin S, Schmitt JM et al: Pressure-volume curves in acute respiratory distress syndrome: clinical demonstration of the influence of expiratory flow limitation on the initial slope. American journal of respiratory and critical care medicine 2002, 165(8):1107-1112.
196. Beurskens CJ, Wösten-van Asperen RM, Preckel B et al: The potential of heliox as a therapy for acute respiratory distress syndrome in adults and children: a descriptive review. Respiration 2015, 89(2):166-174.
197. Leatherman J: Mechanical ventilation for severe asthma. Chest 2015, 147(6):1671-1680.
198. Oddo M, Feihl F, Schaller M-D et al: Management of mechanical ventilation in acute severe asthma: practical aspects. Intensive care medicine 2006, 32(4):501-510.
199. Laher AE, Buchanan SK: Mechanically ventilating the severe asthmatic. Journal of intensive care medicine 2018, 33(9):491-501.
200. Junhasavasdikul D, Telias I, Grieco DL et al: Expiratory flow limitation during mechanical ventilation. Chest 2018, 154(4):948-962.
201. Gelb AF, Zamel N: Lung elastic recoil in acute and chronic asthma. Current opinion in pulmonary medicine 2002, 8(1):50-53.
202. Gelb AF, Yamamoto A, Verbeken EK et al: Unraveling the pathophysiology of the asthma-COPD overlap syndrome: unsuspected mild centrilobular emphysema is responsible for loss of lung elastic recoil in never smokers with asthma with persistent expiratory airflow limitation. Chest 2015, 148(2):313-320.
203. Cormier Y, Lecours R, Legris C: Mechanisms of hyperinflation in asthma. European Respiratory Journal 1990, 3(6):619-624.
204. Marini JJ: Should PEEP be used in airflow obstruction? In.; 1989.
205. Irvin CG, Bates JH: Physiologic dysfunction of the asthmatic lung: what's going on down there, anyway? Proceedings of the American Thoracic Society 2009, 6(3):306-311.
206. Leatherman JW, Ravenscraft SA: Low measured auto-positive end-expiratory pressure during mechanical ventilation of patients with severe asthma: hidden auto-positive end-expiratory pressure. Critical care medicine 1996, 24(3):541-546.
207. Stewart TE, Slutsky AS: Occult, occult auto-PEEP in status asthmaticus. In. Crit Care Med. 1996 Mar;24(3):379-80.
208. Marini JJ: Dynamic Hyperinflation and Auto–Positive End-Expiratory Pressure: Lessons Learned over 30 Years. American journal of respiratory and critical care medicine 2011, 184(7): 756-762.
209. McFadden Jr E, Kiser R, DeGroot WJ: Acute bronchial asthma: relations between clinical and physiologic manifestations. New England Journal of Medicine 1973, 288(5):221-225.
210. Williams TJ, Tuxen DV, Scheinkestel CD et al: Risk factors for morbidity in mechanically ventilated patients with acute severe asthma. American Review of Respiratory Disease 1992, 146(3):607-615.
211. Tobin MJ, Lodato RF: PEEP, auto-PEEP, and waterfalls. Chest 1989, 96(3):449-451.
212. Smith TC, Marini JJ: Impact of PEEP on lung mechanics and work of breathing in severe airflow obstruction. Journal of Applied Physiology 1988, 65(4):1488-1499.
213. Tuxen DV: Detrimental effects of positive end-expiratory pressure during controlled mechanical ventilation of patients with severe airflow obstruction. Am Rev Respir Dis 1989, 140(1):5-9.
214. Gay PC, Rodarte JR, Hubmayr RD: The effects of positive expiratory pressure on isovolume flow and dynamic hyperinflation in patients receiving mechanical ventilation. American Review of Respiratory Disease 1989, 139(3):621-626.

215. Ingham Jr RH, Schilder DP: Effect of pursed lips expiration on the pulmonary pressure-flow relationship in obstructive lung disease. American Review of Respiratory Disease 1967, 96(3): 381-388.
216. Caramez MP, Borges JB, Tucci MR et al: Paradoxical responses to positive end-expiratory pressure in patients with airway obstruction during controlled ventilation. Critical care medicine 2005, 33(7):1519.
217. Marini JJ: Positive end-expiratory pressure in severe airflow obstruction: More than a "one-trick pony"? Critical care medicine 2005, 33(7):1652-1653.
218. Hoffman RA, Ershowsky P, Krieger BP: Determination of auto-PEEP during spontaneous and controlled ventilation by monitoring changes in end-expiratory thoracic gas volume. Chest 1989, 96(3):613-616.
219. Eumorfia K, Alexopoulou C, Prinianakis G et al: In Patients with Obstructive Pulmonary Disease During Controlled Ventilation, PEEP Decreases Dynamic Hyperinflation: Is This Response Really "Paradoxical"? Critical care medicine 2005, 33(12):2860.
220. Kondili E, Alexopoulou C, Prinianakis G et al: Pattern of lung emptying and expiratory resistance in mechanically ventilated patients with chronic obstructive pulmonary disease. Intensive care medicine 2004, 30(7):1311-1318.
221. Qvist J: High level PEEP in severe asthma. N Engl J Med 1982, 307:1347-1348.
222. McKee JD, Spevetz A, Simony P: Auto PEEP. New England Journal of Medicine 1993, 329(3): 212-213.
223. Spadaro S, Stripoli T, Volta CA et al: High-flow nasal cannula oxygen therapy decreases postextubation neuroventilatory drive and work of breathing in patients with chronic obstructive pulmonary disease. Critical Care 2018, 22(1):180.
224. Bellani G, Coppadoro A, Patroniti N et al: Clinical assessment of auto-positive end-expiratory pressure by diaphragmatic electrical activity during pressure support and neurally adjusted ventilatory assist. Anesthesiology: The Journal of the American Society of Anesthesiologists 2014, 121(3):563-571.
225. Roussos C, Macklem PT: The respiratory muscles. The New England journal of medicine 1982, 307(13):786-797.
226. Aubier M, Murciano D, Milic-Emili J et al: Effects of the administration of O2 on ventilation and blood gases in patients with chronic obstructive pulmonary disease during acute respiratory failure. The American review of respiratory disease 1980, 122(5):747-754.
227. Papazian L, Corley A, Hess D et al: Use of high-flow nasal cannula oxygenation in ICU adults: a narrative review. Intensive care medicine 2016, 42(9):1336-1349.
228. Nishimura M: High-flow nasal cannula oxygen therapy in adults: physiological benefits, indication, clinical benefits, and adverse effects. Respiratory care 2016, 61(4):529-541.
229. Parke RL, Eccleston ML, McGuinness SP: The effects of flow on airway pressure during nasal high-flow oxygen therapy. Respiratory care 2011, 56(8):1151-1155.
230. Frat J-P, Thille AW, Mercat A et al: High-flow oxygen through nasal cannula in acute hypoxemic respiratory failure. New England Journal of Medicine 2015, 372(23):2185-2196.
231. Dwarakanath A, Elliott MW: Noninvasive ventilation in the management of acute hypercapnic respiratory failure. Breathe 2013, 9(5):338-348.
232. Kreit JW: Alterations in Gas Exchange Due to Low–Tidal Volume Ventilation. Annals of the American Thoracic Society 2015, 12(2):283-286.
233. Robertson HT: Dead space: the physiology of wasted ventilation. European Respiratory Journal 2015, 45(6):1704-1716.
234. Macklem P: Respiratory muscles: the vital pump. Chest 1980, 78(5):753-758.
235. Mauri T, Turrini C, Eronia N et al: Physiologic effects of high-flow nasal cannula in acute hypoxemic respiratory failure. American journal of respiratory and critical care medicine 2017, 195(9):1207-1215.
236. Banner MJ: Respiratory muscle loading and the work of breathing. Journal of cardiothoracic and vascular anesthesia 1995, 9(2):192-204.
237. Mündel T, Feng S, Tatkov S et al: Mechanisms of nasal high flow on ventilation during wakefulness and sleep. Journal of applied physiology 2013, 114(8):1058-1065.
238. Möller W, Celik G, Feng S et al: Nasal high flow clears anatomical dead space in upper airway models. Journal of applied physiology 2015, 118(12):1525-1532.

Chapter Ten

Updates in Cardiovascular Physiology

Abstract

While the central venous pressure is neither able to reliably predict the slope of the cardiac function curve nor determine volume status, there is value in knowing the genesis of the central venous pressure [CVP]. A venerable model to help explain the determinants of the CVP, or right atrial pressure [Pra], is the Guyton diagram. The foundation of the CVP explains numerous physiological phenomena in the intensive care unit such as ventricular size during cardiac arrest, collapse and distension of the inferior vena cava, great vein Doppler pulsations, stroke volume variation, hemodynamic response to extra-corporeal membrane oxygenation and many other facets of therapy and monitoring. The Guyton diagram also nicely displays atrial transmural pressure which explains 'venous excess,' right ventricular wall tension and the right ventricular afterload. Finally, tying the Guyton diagram to the Campbell diagram highlights interrelation between the heart and the thorax. This link explains certain therapies during cardiopulmonary resuscitation and suggests that energetic uncoupling between the alveolus and pleural space may also uncouple the heart from both arteries and veins.

Key Words: central venous pressure, right atrial pressure, volume tolerance, volume responsiveness, IVC collapse, ventriculoarterial coupling, stroke volume variation, mean systemic filling pressure, pulmonary vascular resistance

In Defence of the Central Venous Pressure

In the waning days of my fellowship I received a hemoptysis consult in the cardiac care unit. Sifting through CT scans, I overheard two house-officers giving sign-out for the evening. When reviewing the central venous pressure [CVP], one of the residents referred to it as a 'random number generator.' I spied them and recalled being on morning rounds as a sleep-deprived intern. I was mercilessly grilled on the nuances of the central venous pressure and its measurement. I paused and thought: is this what we're teaching housestaff? That this measurement is random?

The Venetian Marionette

Years ago, while strolling the promenade along Venice Beach, I saw a young street performer - a puppeteer, with an oddly dressed marionette. From the corner of my eye, it appeared that his control over his puppet was poor. The marionette haphazardly bobbed up and down, extremities akimbo in utter randomness. On close inspection, however, the puppeteer was actually quite good, with fine control. Focused traction of each string created nuanced movements, even in the face of a waxing and waning ocean breeze.

The CVP is a physiological marionette - its value being pulled in different directions by multiple biological strings. On first blush, it may seem random, especially with waxing and waning intra-thoracic pressure, but the informed intensivist must make sense of this dance.

Strings Attached

The stressed venous volume, venous compliance and the resistance to venous flow are three such physiological strings and collectively known as venous return. Importantly, these variables have multiple determinants and each can be altered in various ways following a plethora of ICU interventions [1, 2]. Together the stressed venous volume and venous compliance form the mean circulatory filling pressure which is the pressure head for venous return to the right heart [3-5]. The stressed venous volume is directly increased with volume infusion or indirectly with alpha-agonists. Alpha-agonists cause venoconstriction which recruits unstressed venous volume into stressed venous volume [6, 7]. In either case, augmenting mean circulatory filling pressure favours venous return to the right heart and higher central venous pressure. Pure alpha receptor agonism, however, also increases the resistance to venous return which retards blood flow towards the thorax. By contrast, beta-2 agonism lowers venous resistance and 'opens the flood gates' for the right heart, as it were [1]. Importantly, the opposite is also true – venodilation, volume loss, sympatholysis [e.g. relief of hypoxemia, sedation] diminish the pressure head for venous return and, consequently, lower the CVP.

But the strings of venous return are only half of the story because cardiac contractility, afterload, heart rate, rhythm and valve function are another group of strings pulling the CVP up or down. Collectively this group of strings is called cardiac function. Intuitively, any intervention that improves cardiac function favours ejection of blood from the thorax and lowers the CVP. Conversely, any state that impairs cardiac function retains blood within the central compartment and raises the CVP.

While Arthur Guyton described in great detail the determinants of venous return, perhaps his greatest contribution was a graphical analysis that superimposed both the venous return function and cardiac function onto a single graph [3, 8]. Thus, the Guyton diagram teaches us that interpreting the CVP requires knowledge of both cardiac pump function [e.g. from a full bedside echocardiogram] and venous return function [i.e. from a clinical exam] – just as interpretation of a patient's pH requires knowledge of both the $PaCO_2$ and venous bicarbonate [9] [figure 1].

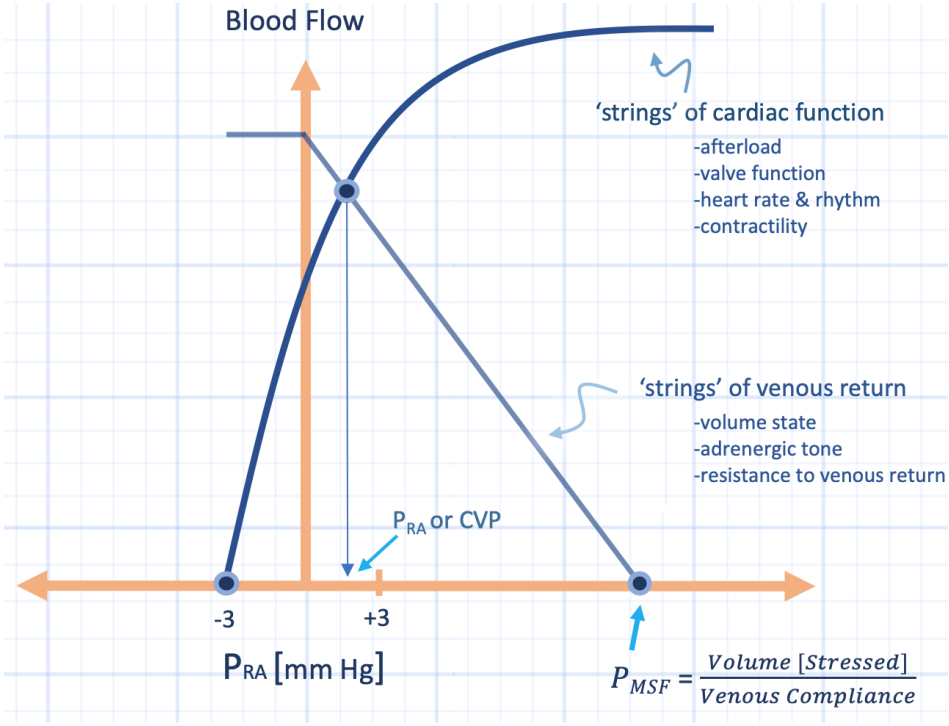

Figure 1: The strings of the central venous or right atrial pressure. See text for details. While the CVP is the x-axis and the x-axis usually represents the independent variable, the CVP is physiologically dependent - being pulled up and down by various mechanisms. Pmsf is mean systemic filling pressure; Pra is right atrial pressure.

The Importance of the CVP

Am I arguing that a static CVP value be used to predict a patient's volume status, or volume responsiveness? Absolutely not [10-12]. However, there is tremendous meaning in the CVP as the starting point for a basic lesson in hemodynamics. The CVP is the fulcrum of cardiovascular physiology at the bedside; understanding the genesis of the CVP lays the foundation for interpreting hemodynamic interventions and bedside echocardiography in the ICU. There is no magic to IVC collapse and distention, they follow the same biophysical principles as the CVP. Ultrasound of the IVC is a visual method to qualitatively track dynamic changes of the central venous pressure relative to the intra-abdominal pressure. When the CVP falls below intra-abdominal pressure, the IVC tends to collapse and when the CVP rises above the intra-abdominal pressure the IVC tends to distend, both as a function of IVC compliance [13].

Further, in a number of elegant studies, Maas and colleagues have used instantaneous CVP and cardiac output monitoring to construct venous return curves at the bedside [14-16]. This has, once again, confirmed Guyton's early work, but also gives us a potential, objective measure of 'volume status' by extrapolating the venous return curve to the x-intercept [i.e. determination of the mean systemic filling pressure] [15]. Additionally, this work has confirmed that vasoactive agents used in the ICU [e.g. norepinephrine] may exert more of their hemodynamic effect by altering venous return [17-20].

So, the next time you infuse volume into a patient, but also change the ventilator settings, increase the fraction of inspired oxygen, sedate the patient and alter the

dose or composition of a vasoactive substance, realize that each of these interventions pulls the strings of both venous return and cardiac function. At first blush, the effect upon the CVP may be seemingly aimless, but like the skilled Venetian puppeteer jigging his marionette within the ebb and flow of an ocean breeze, the dance of the CVP is anything but random.

The Mean Systemic Filling Pressure

It's 4 in the morning. I am somewhere between Riga and Stockholm. The moon is full and bright and rippling across the black, Baltic Sea. This warm, June darkness is cut like onyx by deep vibrations of a cruise ship and its collections of giggling Swedes; they karaoke 'Spaceman' by The Killers in perfect English. I'm perched portside, caught in a yawning ocean breeze, surrounded by a symphony of Slavic slangs and cigarette smoke. My mind turns to the innards of the ship and I imagine another physiological analogy.

The Hull as the Thorax

Consider sitting deep within the hull of this cruise ship, ignorant to the outside. A leak is sprung and ocean rushes in. Thinking quickly, you activate the bilge pump which, appropriately, ejects the ocean outside again. You note that the bilge pump has a number of settings from 'low' to 'high' corresponding to the rate at which it evacuates ocean from inside the hull. When the pump's setting is 'low,' ocean water rises inside the hull – you feel the water's pressure around your ankles. When you increase pump activity to 'high,' the pressure and volume of ocean water around your feet abate. Knowing only this, can you infer the size of the body of water beyond the hull? Are you in the relatively small Baltic or the immense Pacific? Lake Ontario? The Hudson River? Wreck Beach?

The answer is that you cannot know; the amount of ocean water within the hull of the ship is a function of the size of the body of water outside of the hull and its inflow, but also on the efficacy of the bilge pump. Thus, the analogy unfolds – we have approximated volume status [the vastness of the ocean], venous return [the ocean rushing into the boat], the thorax [the hull of the boat], the heart [the bilge pump], the central venous pressure, as well as great vein and cardiac chamber volume [the pressure and volume of the ocean water accumulating within the hull of the boat].

Yet, I see clinicians use right atrial pressure, IVC volume/collapse and left ventricular volume as markers of a patient's volume status. Looking only into the thorax for patient's volume status is as preposterous as estimating the size of an ocean based on the amount sea water accumulating within the hull of a leaky ship.

Volume Status and Venous Return

Approximately 70% of the total blood volume lies within the venous system, another 20% in the arterial system and about 10% in the capillaries [21]; this total blood volume is estimated as 70-80 mL/kg. When the heart is stopped and blood volume distributes itself from the poorly compliant, high pressure arteries, to the highly compliant, low pressure veins, an equilibrium pressure is achieved known as the mean circulatory filling pressure [Pmcf – see chapter 2]. The value of the Pmcf is typically between 7 and 10 mmHg and independent of species and habitus [3, 21, 22]. This pressure is a function of the stressed 'volume status' of the patient and venous compliance; it is the pressure head 'driving' venous return towards the right heart. On the venous return curve, this pressure is marked by the x-intercept, because this is the equilibrium pressure that persists throughout the circulation when blood flow [y-axis] is zero.

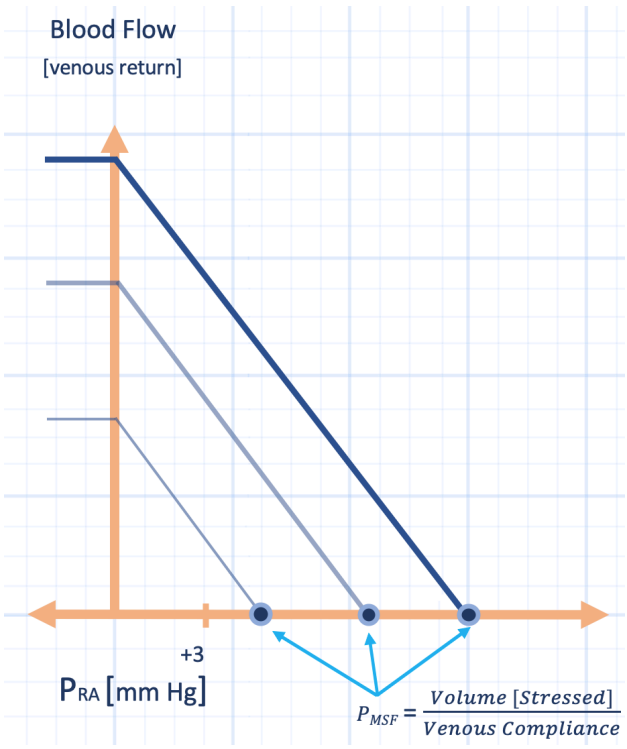

Figure 2: Venous return curves. These three curves might represent 3 different volume states with the leftmost being hypovolemic and rightmost being hypervolemic. Pmsf is mean systemic filling pressure; Pra is right atrial pressure.

The notion of stressed volume may be thought of analogously to that of a water bed, or inflating a beach ball. A certain volume of fluid must be added before the elastic walls are stretched – this volume is the unstressed volume. When the fluid volume begins stretching the walls, an elastic recoil pressure is generated. Accordingly, the volume that contributes to this elastic recoil is known as the stressed volume. In humans undergoing hypothermic, circulatory arrest, the stressed volume was estimated to be about 20 mL/kg or roughly 1.5 L of blood volume [23]. Importantly, the stressed volume is not fixed, and highly dependent upon adrenergic tone, especially alpha-adrenergic tone [1]. Thus, the Pmcf is directly, but not wholly, related to a patient's overall blood volume.

Measuring the Mean Circulatory Filling Pressure

If we desire to know the size of the ocean, we must look beyond the hull of the thorax. Is there a way to measure the Pmcf? First, as above, one can stop the heart and allow the pressures in the arteries, veins and heart equilibrate to the Pmcf. This has been attempted in patients who have died in the ICU, as well as in patients undergoing fibrillatory arrest prior to the placement of a defibrillator [24, 25]. Repesse and colleagues found the Pmcf to be 13 mmHg +/- 5.5 mmHg, 1 minute following clinical death [24]. Because alpha-adrenergic tone plays a key role in the fraction of the stressed blood volume, norepinephrine infusion before death was associated with a higher Pmcf. Interestingly, fluid balance was not associated with Pmcf following death, which may reflect the importance of vascular tone and the plethora of interventions which alter the adrenergic system within the ICU [e.g. sedation, vasopressors, steroids, mechanical ventilation etc.]. As elaborated by Rothe [2], a range of Pmcf may be seen at any given volume status, all as a function of adrenergic tone. In this data, euvolemia can see a Pmcf vary between 8 and 14 mmHg depending upon absence or presence of adrenergic activity, respectively.

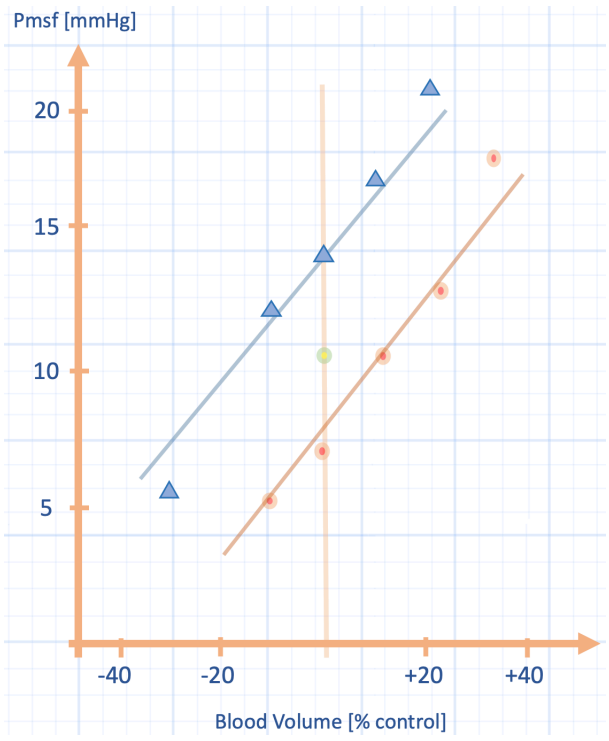

Figure 3: Relationship between blood volume [x-axis], Pmsf [y-axis] and adrenergic tone. Blue triangles represent adrenergic activity while orange circles represent the absence of adrenergic activity. The vertical midline represents euvolemia or baseline blood volume; the green circle on the vertical midline represents baseline adrenergic tone.

While cessation of cardiac activity is considered the gold-standard for measuring Pmcf, it is clearly not feasible, clinically. Fortunately, there are three other methods of approximating the Pmcf which do not require cardiac arrest; these methods are considered next.

As described in chapter 2, there is a slight difference between the mean circulatory and systemic filling pressures [Pmsf]. For brevity, they are used interchangeably. The experimental method by which the Pmsf is determined is cessation of cardiac activity; that is, arterial, capillary, venous and cardiac pressures equilibrate to the Pmsf. As above, this settling pressure is determined by the stressed blood volume and vascular compliance. However, there are 3 ways by which the Pmsf has been

approximated in vivo, without ceasing cardiac activity. The first exploits mechanical heart-lung interaction by simultaneously measuring right atrial pressure and cardiac output in response to a series of increasing inspiratory holds. Progressive escalation of intra-thoracic pressure raises right atrial pressure and diminishes venous return/cardiac output. If these values are plotted, a linear venous return curve is generated and Pmsf is extrapolated as the x-intercept – see figure 4.

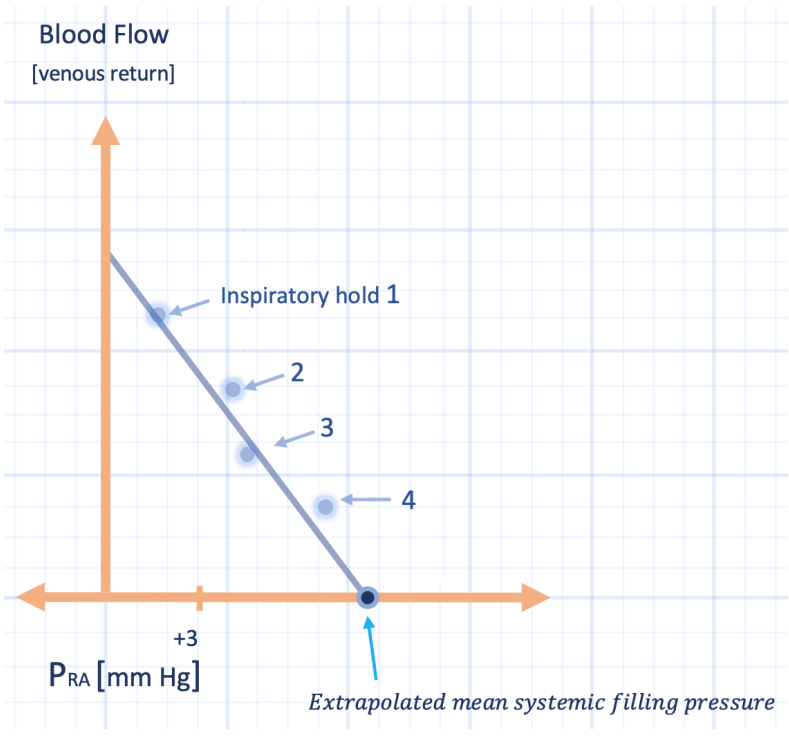

Figure 4: Extrapolating the mean systemic filling pressure. See text for details. Inspiratory holds in a ventilated patient are used to raise the CVP [x-axis], lower cardiac output or venous return [y-axis] and extrapolate the x-intercept of venous return. Pmsf is mean systemic filling pressure; Pra is right atrial pressure

Pinsky proposed this analysis decades ago in a dog model and confirmed the method of extrapolation to Pmsf measured by cardiac standstill [26]. Maas and colleagues have utilized inspiratory holds and extrapolation of the venous return curve as a method to determine Pmsf and found the average Pmsf in euvolemic post-cardiac surgery patients to be approximately 20 mmHg [14].

A second method to measure Pmsf is to use the arm as a surrogate for the entire circulation. If a radial arterial line is in place, very rapid insufflation of a blood pressure cuff causes the venous and arterial pressures in the arm to fall towards the Pmsf; indeed, this has also been studied by Pinsky's group [27] and found to correlate with the method of extrapolation described above.

Lastly, a mathematical approximation of the Pmsf has been proposed by Parkin and described in a superb review – an imperative read [28]. The Pmsf can be derived from the right atrial pressure, cardiac output and some basic anthropometric variables. In the study which evaluated radial arterial pressure as a surrogate for Pmsf, Parkin's formula was also studied. While there was considerable variability, the actual values of Pmsf, by all three methods, were close in value [i.e. 15 – 20 mmHg] [27].

Interestingly, the methods above all resulted in unexpectedly higher values of Pmsf [i.e. closer to 20 mmHg rather than 10 mmHg]. As noted by Repesse and

colleagues, methods that utilize mechanical heart-lung interactions to extrapolate Pmsf assume that the venous return curve is linear [i.e. mechanical ventilation does not change the resistance to venous return] and that Pmsf itself will not change in response to an inspiratory hold. Importantly, mechanical ventilation is known to increase the right atrial pressure and the Pmsf – that is, the gradient for venous return does not vary [29-31]. The mechanism by which mechanical inspiration increases Pmsf is probably in response to sympathetic tone and/or redistribution of venous blood volume [32, 33]. Further, the application of positive end-expiratory pressure has complicated effects on the resistance to venous return, which may include Starling resistors in the hepatic circulation [34].

Therapeutic Control of the Mean Systemic Filling Pressure

If Pmsf can be assessed, one may consider whether its manipulation has any clinical import. As above, direct relationship between a patient's blood volume and the Pmsf is tenuous because of the dynamic nature of the stressed volume in response to adrenergic tone. A low Pmsf may indicate hypovolemia, but also venoplegia or some combination thereof. Accordingly, clinical context is imperative. Another potential implication of measuring Pmsf is the ability to calculate venous tone or compliance. Measuring Pmsf after injecting a known volume of crystalloid allows venous compliance to be calculated and, therefore, whether therapy should focus on adrenergic agents [i.e. to correct high venous compliance] or not [21]. Yet, norepinephrine has multiple conflicting effects on cardiac output including: augmenting Pmsf, increasing the resistance to venous return and flattening of the cardiac function curve if afterload is increased by alpha tone [7, 35].

Volume administration does increase Pmsf [7]. Interestingly, however, in fluid responsive patients, the gradient between the Pmsf and central venous pressure rises, whilst in fluid non-responsive patients, the gradient between the Pmsf and central venous pressure is unchanged [36].

Crucially, these considerations raise the – often muddied – difference between volume status and volume responsiveness. As above, volume status is but one portion of the Pmsf and the Pmsf cannot reveal whether the venous return curve intersects the ascending or plateau portion of the cardiac function curve – that is, speak for volume responsiveness [see figure 5].

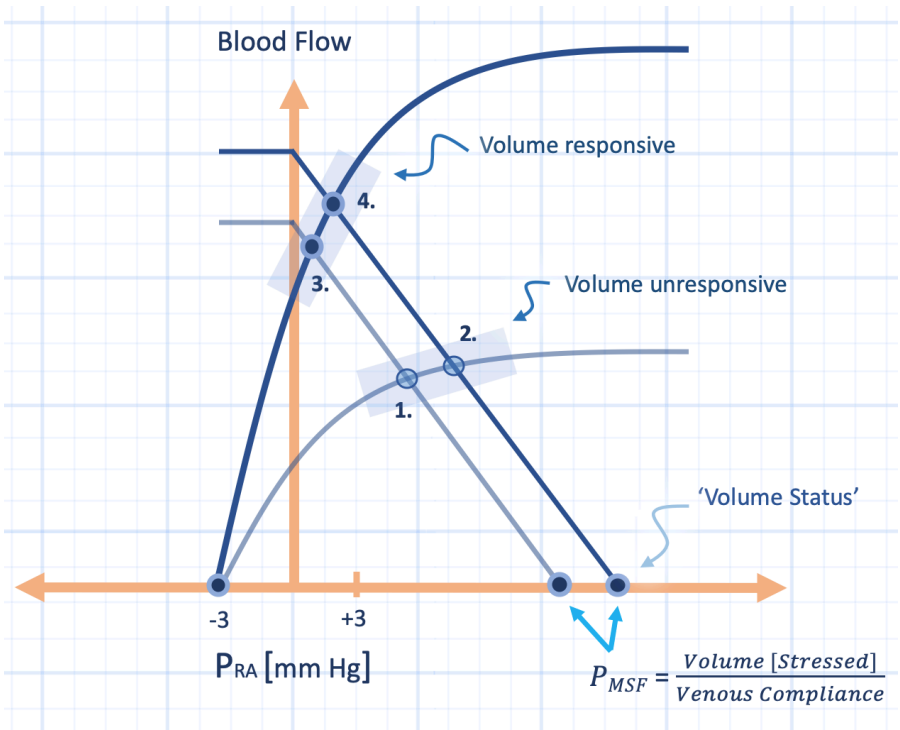

Figure 5: Volume status and Responsiveness. Points 1 & 2 are two different CVP or right atrial pressures in a volume unresponsive patient at two different volume states [e.g. euvolemic and hypervolemic, respectively]. Points 3 & 4 show the same patient, but now volume responsive at the same two volume states. The difference between points 1 and 4 could be a patient given a fluid bolus and started on an epinephrine infusion. Pmsf is mean systemic filling pressure; Pra is right atrial pressure

Implications for Echocardiography in Cardiac Arrest

Given the aforementioned discussion on Pmsf, it shouldn't be surprising that a porcine model demonstrated right ventricular [RV] dilation in the setting of hypovolemic cardiac arrest [37]. When heart function ceases, the right atrial and right ventricular pressure assume the Pmsf as circulatory pressures equilibrate. Thus, the Pmsf partially determines the distending pressure of the RV [the pressure surrounding the RV, which tends to be negative at functional residual capacity, also determines the RV transmural pressure].

In the hypovolemic, arrested pigs, the right atrial pressure – and therefore the Pmsf – averaged 7 mmHg. While the ischemic RV is expected to stiffen somewhat, a distending pressure of 7 mmHg is still expected to provide a significant RV volume [38] because of the high compliance of the RV. This is of particular consequence in humans as Pinsky has shown that the RV normally operates as an un-stressed chamber [39]. Further, the Pmsf in the arrested circulation rises in response to intrinsic and extrinsic adrenergic tone, for example, provision of epinephrine [7] [figure 6].

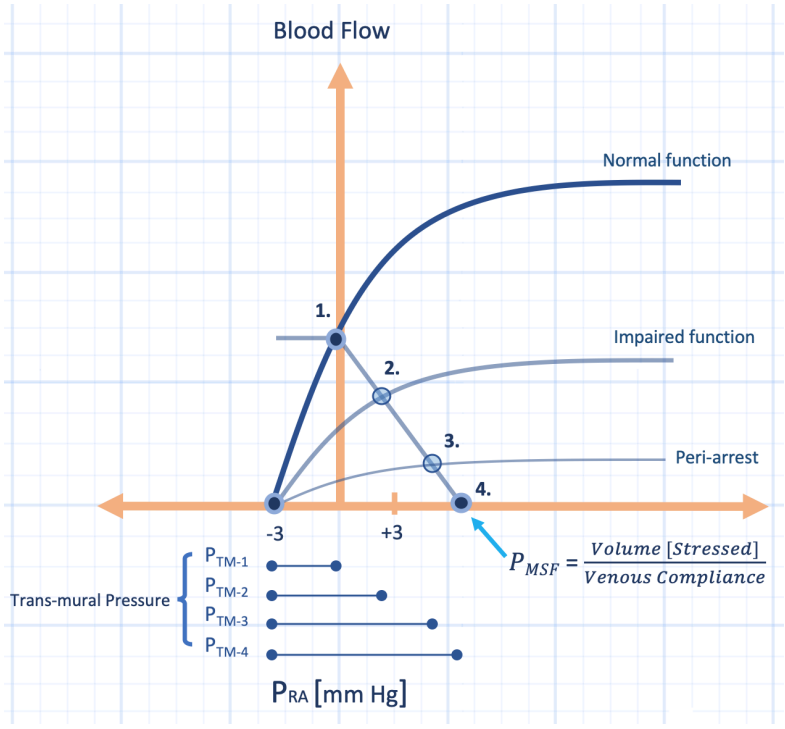

Figure 6: Trans-mural right atrial pressure during hypovolemic arrest. Point 1 represents normal cardiac function in hypovolemia while point 4 represents cardiac arrest, when right atrial pressure becomes the mean systemic filling pressure [here 7 mmHg]. Note how trans-mural right atrial pressure [Ptm] rises from roughly +3 mmHg at baseline [Ptm-1] to +10 mmHg [Ptm-4] during arrest. As the right ventricle is unstressed, 10 mmHg distending pressure dilates the right heart. Provision of epinephrine could raise the Pmsf even more. Pmsf is mean systemic filling pressure; Pra is right atrial pressure.

Inspiratory Collapse of the Inferior Vena Cava

With the dissemination of small, portable, ultrasound devices, it seems that it is every clinician's dream to place an ultrasound probe on a patient's costal border and find something meaningful; what exactly is inferior vena cava [IVC] collapse with inspiration telling us?

Starling Resistor

The reason IVC collapse occurs is that a Starling resistor is generated – when the pressure within a distensible tube drops below the pressure without the tube. It seems straightforward, therefore, that collapse depends on two competing pressures: 1. the pressure within the IVC, which is related to the central venous pressure [i.e. the right atrial pressure barring any caval obstruction] and 2. the pressure within the abdominal cavity. Collapse of the IVC is enhanced by a: fall in 1., rise in 2., or a combination of both.

Pressure Inside the Tube

Why does the pressure within the IVC decrease with a spontaneous inspiration? The right atrium is a thin-walled, compliant structure and the pressure within the

right atrium falls with the pleural pressure during a spontaneous inspiratory effort. This drop in CVP is transmitted down the IVC. The degree to which the CVP falls during spontaneous inspiration depends upon three competing variables: 1. as above, the decrease in pleural pressure 2. the venous return function and 3. the cardiac function. This should make intuitive sense. As discussed in chapter 8, the pressure within the right atrium during spontaneous inspiration is influenced by the pleural pressure pulling the CVP down, the venous return from the body pushing the CVP up and the cardiac function ejecting blood from the thorax, also pushing the CVP down. This physiology is understood by analysis of the Guyton diagram which overlays venous return and cardiac function onto a single graph. The intersection of the two curves defines the operating point of the cardiovascular system – the pressure at the operating point is the central venous pressure. A drop in pleural pressure is depicted by shifting the cardiac function curve leftwards with respect to the venous return curve [3].

But does this inspiratory reduction in central venous pressure tell us anything definitive about a patient's 'volume status' [i.e. whether the patient is euvolemic or not] or 'volume responsiveness' [i.e. whether the patient augments cardiac output with fluid administration]? Unfortunately, no [10-13, 40, 41]. The reason is that the central venous pressure is dependent upon the intersection of venous return and cardiac function – two physiological phenomena each with multiple determinants. 'Volume status' plays a role in venous return in that a hypervolemia tends to increase venous return and therefore, CVP, but venous return has other determinants. This also explains the lack of relationship between volume status and CVP [11]. 'Volume responsiveness' is determined by how far the operating point is from the plateau of the cardiac function curve. Because the slope of the cardiac function curve is hard to know with certainty, almost any CVP may fall upon the plateau, especially in patients with cardiac abnormalities [e.g. those in the intensive care unit] [42].

Pressure Outside the Tube

Complicating matters is the increase in abdominal pressure which facilitates IVC collapse. Because positive end-expiratory pressure, intra-abdominal hypertension and breathing pattern all affect abdominal pressurization [29, 43-45], IVC collapse can be confounded. Phenomena that raise intra-abdominal pressure elevate the critical collapse pressure of the great veins [i.e. Pcrit]. This is normally roughly atmospheric pressure [i.e. 0 mmHg] [see figure 7].

Thus, inspiratory IVC collapse tells us that the CVP is falling below the intra-abdominal pressure. If there is no pathogenic or iatrogenic pressurization of the abdomen [e.g. PEEP, auto-PEEP, ascites], and inspiration is not stressed [e.g. dyspnea, breathing through an endotracheal tube], then IVC collapse tells us that the CVP is low. Recall from chapter 8 that a low CVP may be the result of: hypovolemia, high resistance to venous return [e.g. alpha agonist effects], high venous compliance [e.g. venodilators, sepsis], and hyper-dynamic cardiac function [e.g. extrinsic or intrinsic adrenergic tone].

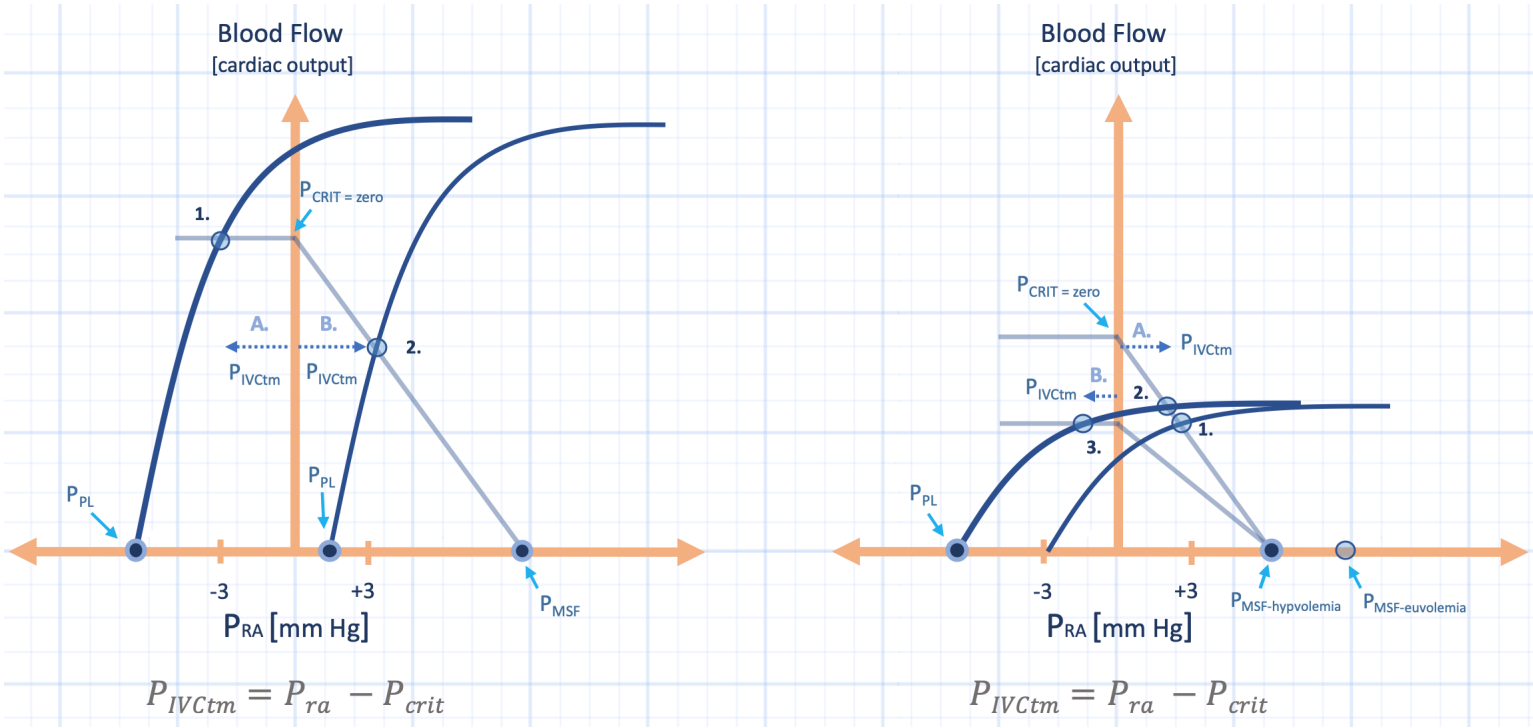

Figure 7: The physiology of IVC collapse. Left panel shows hypothetical normovolemic and volume responsive patient moving from forced expiration [operating point 2] to forced inspiration [operating point 1]. Note that on forced expiration, at point 2, the transmural pressure of the IVC [IVCtm] is positive such that the IVC distends. This is illustrated by the dotted line B. On inspiration, operating point 1, the pleural pressure [Ppl] falls and the IVCtm [dotted line A] is negative because the right atrial pressure, Pra, falls below Pcrit. Right panel shows hypothetical hypovolemic and volume unresponsive patient. At baseline operating point 1, the venous return curve intersects the plateau of the cardiac function curve. On inspiration, operating point 2, the Pra remains above the Pcrit; i.e. the IVCtm is positive and there is IVC distension [dotted line A], despite there being hypovolemia. If inspiration increased the resistance to venous return [e.g. by collapsing hepatic venous Starling resistors] then there could be IVC collapse [dotted line B] at operating point 3; IVC collapse or distension can dissociate from volume status and responsiveness.

PEEP and IVC Collapse

PEEP has conflicting effects on all of the four general elements that determine IVC size and collapse – venous return, cardiac function, intra-thoracic pressure [ITP] and intra-abdominal pressure [IAP]. An often overlooked, but relevant, investigation is that of Juhl-Olsen and colleagues [46]. Healthy volunteers had their volume status altered and IVC collapsibility was measured at varying degrees of PEEP and pressure support. While there are multiple avenues of discussion, a few interesting observations are noted below:

Healthy volunteers lying in the horizontal tended to increase the IVC collapsibility index with the application of 10 cm H2O of PEEP from a baseline of 0.15 to about 0.20. When PEEP rose to 20 cmH2O, the collapsibility index fell to an intermediary value between 0.15 and 0.20.

When placed in Trendelenburg, given 1 L of normal saline and administered 20 cmH2O of PEEP, their IVC collapsibility was also about 0.15; i.e. an equivalent collapse to their supine, volume unloaded physiology without PEEP.

How might these results be reconciled? A detailed evaluation of end-expiratory pressure and its effects on the 4 key determinants of IVC size and collapsibility [venous return, cardiac function, ITP and IAP] can help.

While initially postulated decades ago and then demonstrated by Fessler and colleagues, the venous return curve is changed when PEEP is applied [30, 47, 48]. First, PEEP increases the mean systemic filling pressure – the pressure head for venous return to the right heart [49]. The mechanisms are probably both increased adrenergic tone and redistribution of venous blood from the thorax to lower capacitance venous beds [1, 32, 34, 48, 50]. Nevertheless, this effect of PEEP is expected to maintain venous return and, accordingly, IVC size at end-expiration. Further, volume status alters venous return in that diminished blood volume increases the resistance to venous return and a high venous blood volume blunts resistance to venous return [51, 52]. Thus, increased venous blood volume and the application of PEEP is expected to augment the pressure head for venous return.

PEEP and Intra-thoracic Pressure

PEEP is also expected to raise intra-thoracic, or pleural pressure. At end-expiration, PEEP acts upon the compliance of the lung and chest wall together [i.e. the respiratory system] to increase thoracic volume. How much of the PEEP is felt by the pleural space depends upon the relative compliances of the lungs and chest wall, individually. In health, the compliance of the lungs and chest wall are roughly similar such that 50% of the applied PEEP is used to 'lift' the lungs and the other 50% is used to 'lift' the chest wall. Consequently, 50% of the PEEP ends up as pleural pressure, stenting open the thoracic wall [48, 53]. Clearly, in diseases of the lungs and chest wall, these values vary. The rise in ITP increases the right atrial pressure and favours dilation of the IVC. On the Guyton diagram, increased ITP moves the x-intercept of the cardiac function curve rightwards.

PEEP and Intra-abdominal Pressure

Yet, if PEEP is expected to increase the pressure head for venous return, as well as raise the ITP, how could its application increase IVC collapsibility? It is important to appreciate that the aforementioned physiology relates only to end-expiration. Of equal importance is how PEEP changes inspiratory physiology. As seen on the venous return curve, PEEP lowers maximal venous return, as represented by the plateau of this curve and raises the critical collapse pressure [Pcrit] which is the pressure at which maximal venous return occurs. When right atrial pressure falls below the Pcrit, along the plateau of maximal venous return, a Starling resistor is formed [52]. As above, a Starling resistor is when the pressure within a distensible tube falls below its ambient pressure. What happens here is the tube transiently collapses and then immediately reopens as the upstream pressure [mean systemic filling pressure] rises above the collapsing pressure. This occurs rapidly and cyclically; the result is not cessation of flow, but maximal flow. The mechanism of IVC collapse and Starling resistor physiology in response to increased IAP is likely complicated and dependent upon hepatic contact pressure as well as relative blood volume in the splanchnic and non-splanchnic circulations [34, 54].

Thus, when the patient inspires, and intra-thoracic pressure falls, the cardiac function curve drags leftwards and is more likely to fall into Starling resistor physiology [see figure 8].

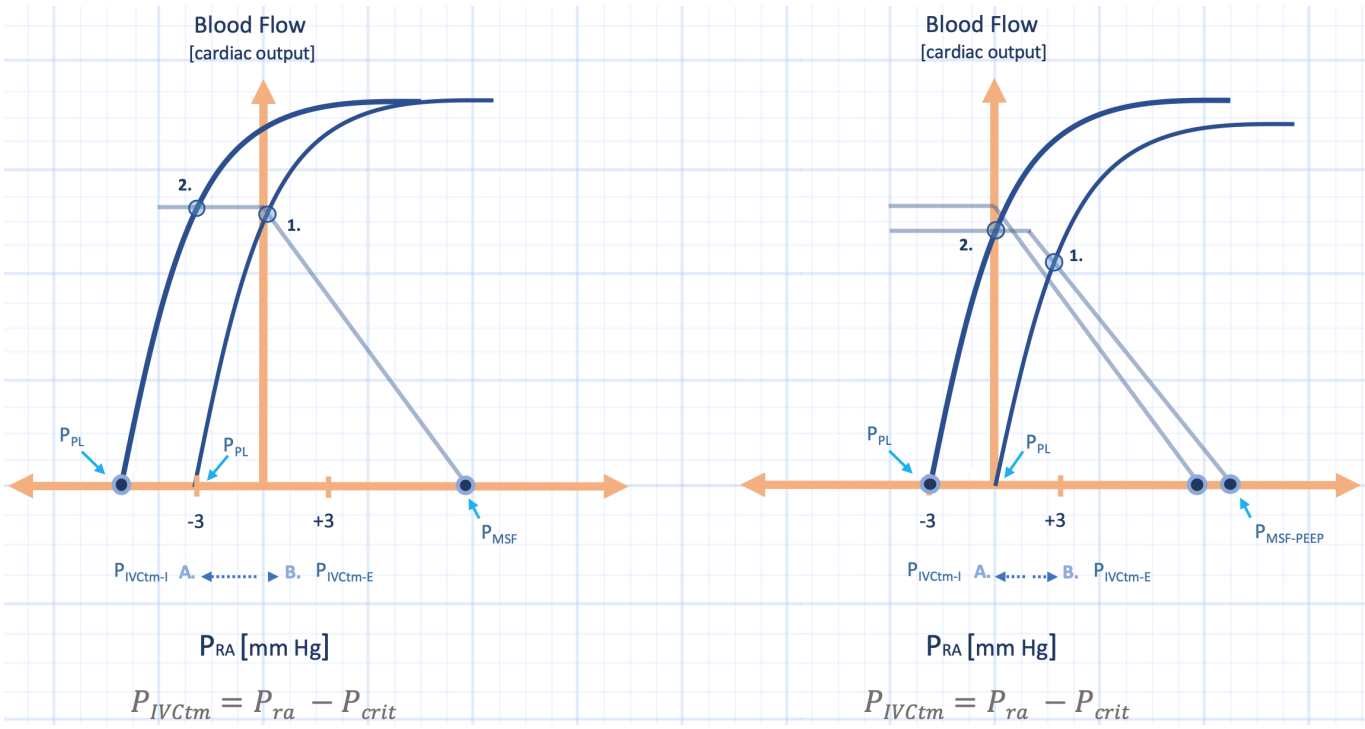

Figure 8: Inspiration and positive end-expiratory pressure [PEEP] effects on IVC collapse. Left panel shows normal inspiration in healthy adult [from operating point 1 to 2]. The pleural pressure [Ppl] falls and the right atrial pressure falls below Pcrit [here atmospheric pressure] such that collapse occurs - see the IVC transmural pressure on inspiration [PIVCtm-i, A.] below the graph. Compare this to the IVC transmural pressure on passive expiration [PIVCtm-e, B.]. Right panel, hypothetical effect of low-moderate PEEP which increases the mean systemic pressure [Pmsf] and the Pcrit. Expiration to inspiration follows point 1 to 2. There is more IVC distension on expiration here such that the IVC dilates and collapses to a greater degree [compare A & B in right panel and left panel]. In the right panel, the Pcrit is roughly 1.5 mmHg. Pra is right atrial pressure. Importantly, for figures 9-11, PIVCtm is always referenced to Pcrit.

PEEP and Cardiac Function

To simplify this analysis, only the effect on right ventricular function [RV] is considered. As described above, while PEEP increases the ambient cardiac pressure, the provision of pressure to the airways also alters RV function. As a rule of thumb, PEEP above 10-15 cm H_2O afterloads the RV and even diminishes its contractility because of increased lung volume [55, 56]. In other words, the RV enlarges in size due to increased outflow impedance. If we assume that a supine, healthy person has a left atrial pressure of roughly 5 mmHg [7 cm H_2O] or less, then a pulmonary distending pressure [transpulmonary pressure] greater than 7 cm H_2O is expected to collapse the pulmonary veins, generate West zone II physiology and afterload the right heart in all areas of the lung anterior to the supine left atrium. Indeed, if 50% of PEEP – in healthy individuals – is added to the pleural pressure [Ppl], then 15 cmH_2O of PEEP applied at the mouth generates an end-expiratory trans-pulmonary pressure [PEEP – Ppl] of 15 cmH_2O – 7.5 cm H_2O = 7.5 cmH_2O. Thus, all of the lung anterior to the left atrium are West zone II – an afterloaded state for the RV.

The effect of high RV afterload is to flatten the cardiac function curve [lower its slope or impair its function]. When this individual inspires, the cardiac function curve shifts leftwards with ITP, but because of the RV's impaired ability to eject blood into the lung, IVC collapse is less likely [see figures 9 & 10].

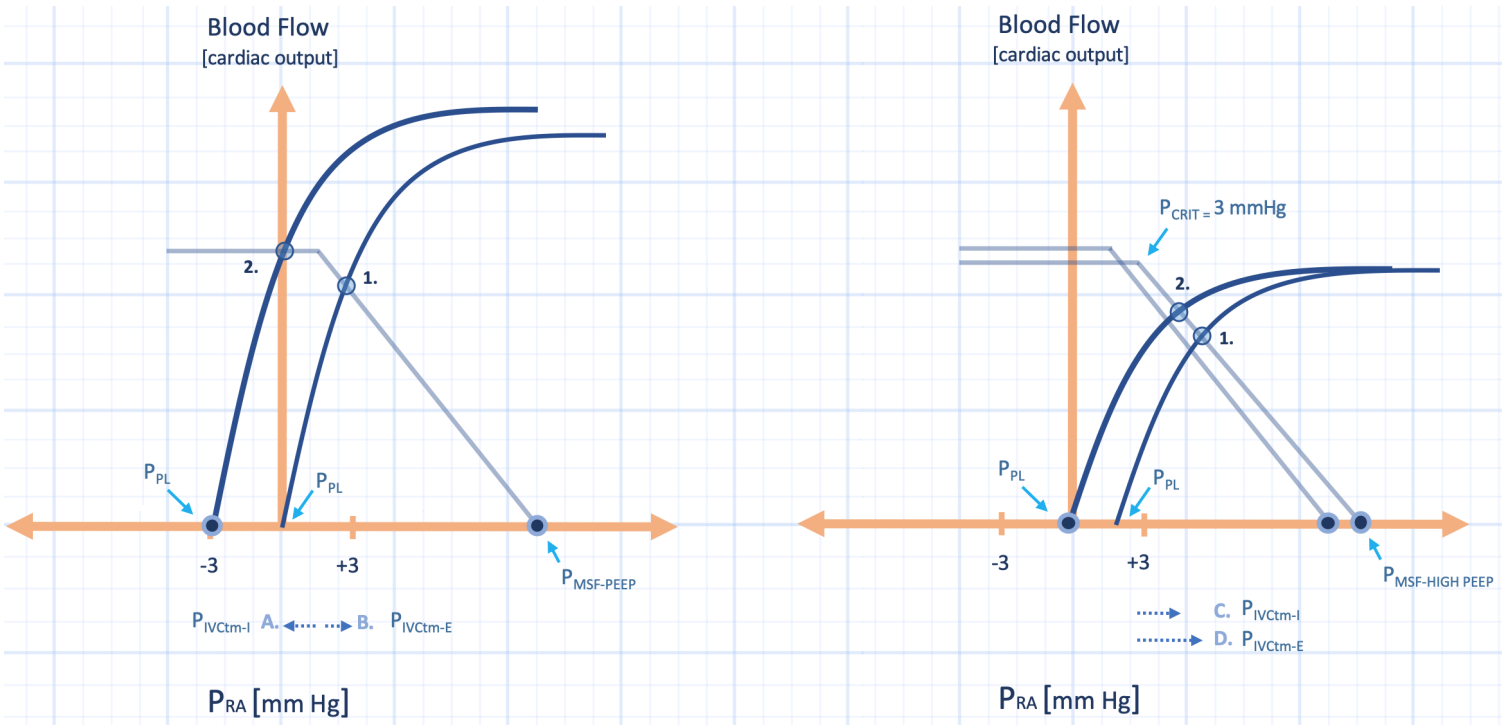

Figure 9: Hypothetical effect of high PEEP in a healthy adult. The left panel is identical to the right panel of figure 8; that is, the effect of low-moderate PEEP on expiration to inspiration from operating point 1 to 2. The IVC transmural pressure on inspiration is negative [PIVCtm-i, A, below x-axis], while it is positive on expiration [PIVCtm-e, B.]. Right panel shows the hypothetical effect of high PEEP. RV afterload rises, so the cardiac function curve flattens. The IVC transmural pressure remains positive from expiration to inspiration [i.e. from point 1 to 2]. Compare the transmural pressures to the left panel [i.e. A to B versus C to D]. Ppl is pleural pressure, Pra is right atrial pressure. See also figure 10.

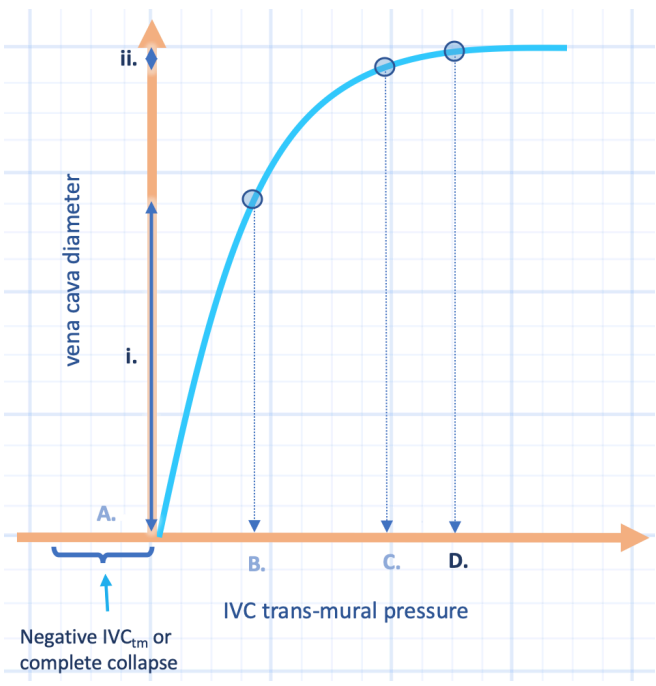

Figure 10: The IVC compliance curve. The transmural pressures indicated on this graph correspond to figure 9. Moving from point A to B illustrates a negative IVC transmural pressure to a positive one; i.e. figure 9 left panel. Note the large change in IVC volume this engenders [i.] arrow on y-axis. By contrast, higher transmural pressures, for example, from point C to D in figure 9 causes a smaller change in IVC diameter [ii.] arrow on y-axis. The y-axis is IVC volume while the x-axis is transmural pressure [IVCtm].

Returning to the findings of Juhl-Olsen described above [46], the provision of higher PEEP in the horizontal position might increase IVC collapsibility during inspiration because of diminished maximal venous return; to the contrary, PEEP above 15 cmH2O may afterload the RV and attenuate IVC collapse [see figures 8-10].

In the volume loaded volunteers in Trendelenburg, the lung is in West zone III, so the RV afterload effect of high PEEP is diminished. Therefore, the effect of reduced maximal venous return dominates and higher PEEP facilitates inspiratory IVC collapse [see figure 11].

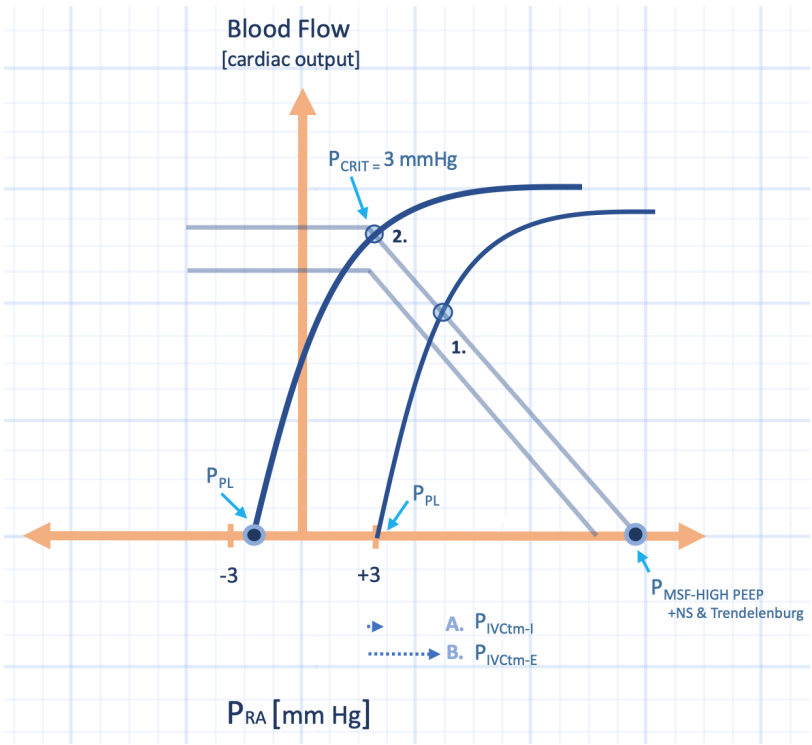

Figure 11: Hypothetical effect of high PEEP with volume loading and Trendelenburg position. The mean systemic pressure [Pmsf] rises without much change in venous return resistance. The pleural pressure [Ppl] rises. Inspiration to expiration is illustrated by operating point 1 to 2, respectively. The IVC transmural pressure from inspiration [PIVCtm-i, A] to expiration [PIVCtm-e, B] has more variability as the RV afterload is attenuated via pulmonary vascular recruitment and dilation in these healthy controls.

The aforementioned illustrates the complexity of inspiratory IVC collapse in healthy volunteers. Without considering all factors affecting IVC collapse, study of heterogeneous and physiologically complicated patients will continue to yield conflicting results [13, 40, 41, 57, 58] and more debate will ensue.

Have we not learned from the central venous pressure and pulmonary artery occlusion pressure [see chapters 6 and 7]? If we insist that simplified surrogates of intricate, intertwined physiologies be employed in patient management, then disappointment and danger await.

The roots of venous excess [59] took hold within the fertile soil of a contrary interpretation of Guyton's classic work on venous return [60]. However, Guyton's original curves have been independently-replicated, even with techniques different from his original experimental design [61-63]. The issue raised was not whether the relationship between flow from the venous beds and right atrial pressure was true. Rather the concern was cause and effect – a chicken and egg argument – between right atrial pressure and blood flow [60]. It is often interpreted that – in the steady state – a fall in right atrial pressure 'sucks' in blood from the venules and veins. The critique, by contrast, is that it is the pump which is the primum movens of both cardiac output and venous return. In other words, it is entirely the heart distributing parcels of blood from the great veins to the great arteries which determines flow and the observed fall in right atrial pressure is simply an epiphenomenon of the heart's action. Accordingly, per this critique, in the steady state, there is a functional relationship between blood flow from the periphery and right atrial pressure, that is perfectly described by Guyton's curve, but the fall in right atrial pressure and rise in venous return are not cause and effect [see figure 12].

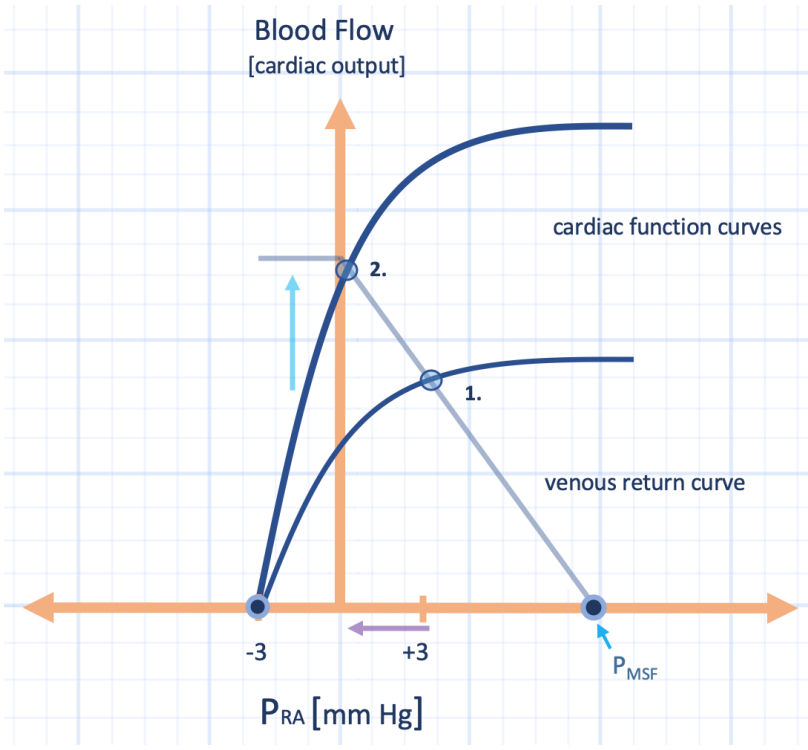

Figure 12: An increase in cardiac function from point 1 to point 2. Note that right atrial pressure [x-axis] falls [purple arrow] and blood flow [cardiac output or venous return] increases on y-axis [light blue arrow]. Does venous return increase because right atrial pressure falls, or does blood flow increase and right atrial pressure fall as a consequence? Pra is right atrial pressure, Pmsf is mean systemic filling pressure.

A critical reappraisal isffored via an independent experiment [63] where the relationship between blood flow and right atrial pressure was assessed, but with right atrial pressure [the dependent variable] on the y-axis, and flow [the independent variable] on the x-axis; in other words, a 'flipped' Guyton curve [60].

This depiction is more mathematically precise in that the right atrial pressure, or the central venous pressure, is ultimately the dependent variable, dancing in response to changes in vascular and cardiac function.

A Criticism of a Criticism

Whether or not the above is true has previously been litigated by physiologists of great scientific stature [64-66]. Guyton considered the argument unhelpfully circular [59, 67]. My concern with the aforementioned really distills down to a critical distinction between transient and steady-state effects. Indeed, it is clearly highlighted in the critical analysis [60] that the arguments put forth apply only to the vasculature when it is in the steady state, i.e. when:

1. volume contained within the peripheral vasculature is constant

2. that regional compliances do not change,

3. that flow is not redistributed among the parallel organ vasculatures

4. that no other energy sources [muscle pumping, respiratory pumping] are present [60].

Upon reviewing these conditions, it is clear how rare it is to find a patient in the operating theatre or intensive care unit in the steady state. Nearly every intervention [e.g. fluid bolus, vasoactive infusion, dynamic shock, change in intra-thoracic pressure/breathing, etc.] violates theses constraints rendering the criticisms described at the outset as clinically moot. It is therefore critical that 'venous return' not be brushed aside as a 'myth' based on an argument valid only during a highly controlled experimental paradigm. When a litre of saline is infused into a peripheral vein, when a deep inspiratory effort is made, both the up [i.e. mean systemic filling pressure], and down [i.e. right atrial] stream pressures of venous return are real, important and the primum movens of flow. Thus, venous return must be understood by students as a true and separate – albeit transient – entity from cardiac output. This is supported by our collective experiences and empirical evidence [64, 68-72].

Venous Excess

The idea of venous excess as a 'tangible' cardiovascular variable grew forth from the short-comings of venous return described above; that is, venous return is not distinct from cardiac output and that right atrial pressure does not have a causative role in blood flow [59]. Accordingly, it is argued that the equation that describes venous return as an upstream and downstream pressure is too nebulous for medical students to comprehend. For instance, the authors argue that mean systemic filling pressure is unhelpful because it cannot be measured and it cannot be physically located within the venous system [59].

Rather than being a valid scientific argument against the mean systemic filling pressure, it strikes me rather as venous xenophobia. To dismiss a principle or concept because it does not fit within the norms of what one considers 'real' on the arterial side of the circulation lays bare a sad vascular relativism. Ask the cocksure physiologist to pinpoint exactly where – anatomically – the mean arterial pressure lies and the certainty and 'realness' of a readily measured variable becomes less incontrovertible. Let this not be the arbiter of what is worthy of physiological consideration; equally, let us not be fooled into thinking that what can be measured is facilely understood.

The proponents of venous excess also argue that venous return ignores the importance of venous capacitance; but it does not. Venous capacitance is an integral part of the mean systemic filling pressure – the 'upstream' pressure for flow returning to the heart [1, 2, 6, 7, 73, 74]. A low venous capacitance indicates a higher venous pressure for a given volume, while a high venous capacitance is just the opposite.

The idea of venous excess itself, however, is a good one – in a sense providing a measure of 'stretch' in the great veins and right heart. This may then act as an 'error signal' for example, triggering the release of atrial natriuretic peptide if stretch is too great [59]. But 'venous excess' is much better gleaned from a Guytonian analysis – as the transmural right atrial pressure [see figure 13]. The importance of using a Guyton diagram to illustrate venous excess is apparent when one considers the super-position of the respiratory pump [e.g. deep inspirations, application of PEEP]. When the intra-thoracic pressure changes, there is dissociation between the pressures across the right heart [e.g. right atrial pressure relative to the pleural pressure] from the pressure within the right heart. This discrepancy is easily visualized on the Guyton diagram and is a superior way to describe 'venous excess' to students, who may speciously equate an increase in absolute right atrial pressure with an increase in its distending pressure [see also chapter 6].

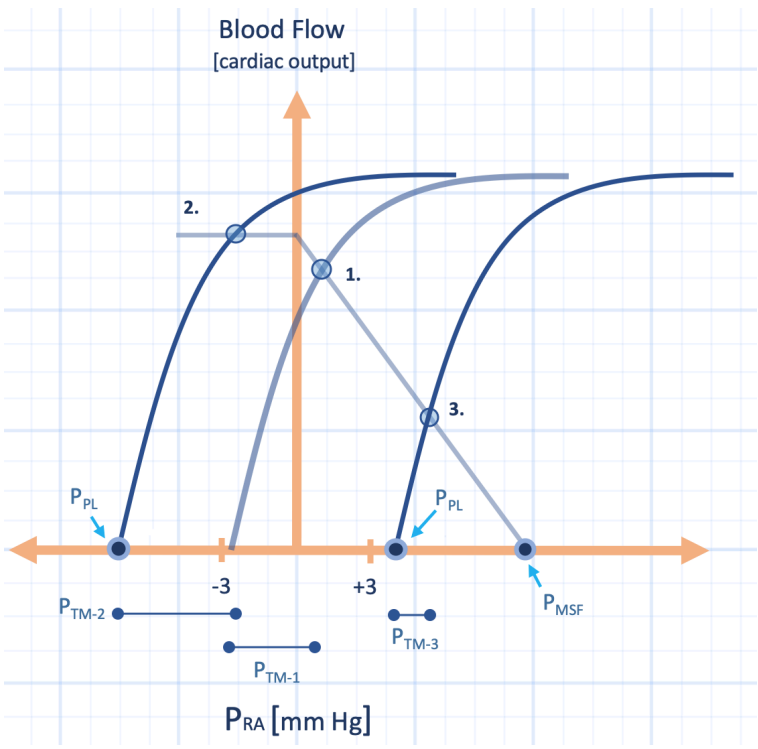

Figure 13: The effect of intra-thoracic or pleural pressure [Ppl] on right heart transmural pressure [Ptm]. Baseline is operating point 1. The right atrial pressure [Pra] at point 1 is slightly positive, the transmural pressure is the blue dumbbell below the graphic [Ptm-1]. The intra-thoracic [or surrounding] pressure is

estimated as the x-intercept of the cardiac function curve. Point 2 represents a deep inspiration. Note that absolute right atrial pressure falls [Pra is now negative], but that the transmural pressure [or venous excess] has increased, marked by the dark blue dumbbell below the x-axis [Ptm-2]. By contrast, operating point 3 represents elevated Ppl [e.g. Valsalva]. While the measured right atrial pressure has increased to point 3, the transmural pressure [venous excess] has fallen, as indicated by the dumbbell below the x-axis [Ptm-3]. This graphic assumes no change in vascular capacitance with change in intra-thoracic pressure for diagram simplicity.

Venous Doppler and Volume Tolerance

At the outset of this chapter, I humbly defended the central venous pressure [CVP]. With the birth of fluid responsiveness physiology [75], there has been a slow and solemn drumbeat ushering the CVP up the squeaking planks of the hemodynamic gallows [10, 76]. Importantly, I was not proposing the CVP as a marker of fluid responsiveness or volume status; instead, I aimed to remind the reader that the CVP remains germane to cardiovascular physiology! Dismissing the CVP as 'useless' is analogous to deeming 'stroke volume' or 'renal perfusion pressure' as forgettable – for neither variable definitively speaks about a given hemodynamic state.

It is now possible that the CVP will rise again, in the context of venous Doppler velocimetry. The venous Doppler waveform is an ultrasonographic transduction of the CVP, right heart hemodynamics and, therefore, a potential non-invasive indicator of venous congestion and 'volume tolerance.'

The Central Venous Pressure Waveform

Classically, teaching of the CVP waveform [or right atrial pressure, Pra] begins with the a-wave [see figure 14] [9, 77-79]. Note that, while the a-wave is the rise in Pra due to atrial contraction, it is the end of ventricular diastole. The key determinants of the height of the a-wave are atrial volume and compliance. Because the relationship between atrial volume and pressure is curvilinear [80, 81], higher atrial volume leads to increasingly great pressure. Thus, large a-waves typically indicate a large atrial volume. The cannon a-waves of atrioventricular dissociation – atrial contractions against a closed tricuspid valve - are taught for examination purposes, but are rare clinically.

As the atrium relaxes, the pressure falls towards the end-diastolic pressure [EDP]. This, z-point, is found at the base of the a-wave just prior to the – commonly indistinguishable – c-wave [9, 77, 82]. When systole begins, there is a moment when right ventricular [RV] pressure rises against closed tricuspid and pulmonic valves [i.e. isovolumic contraction]. Here, the tricuspid valve projects backwards into the right atrium resulting in a brief increase in pressure – the c-wave – until the pulmonic valve opens and ventricular blood ejects into the pulmonary tree; systole progresses [83].

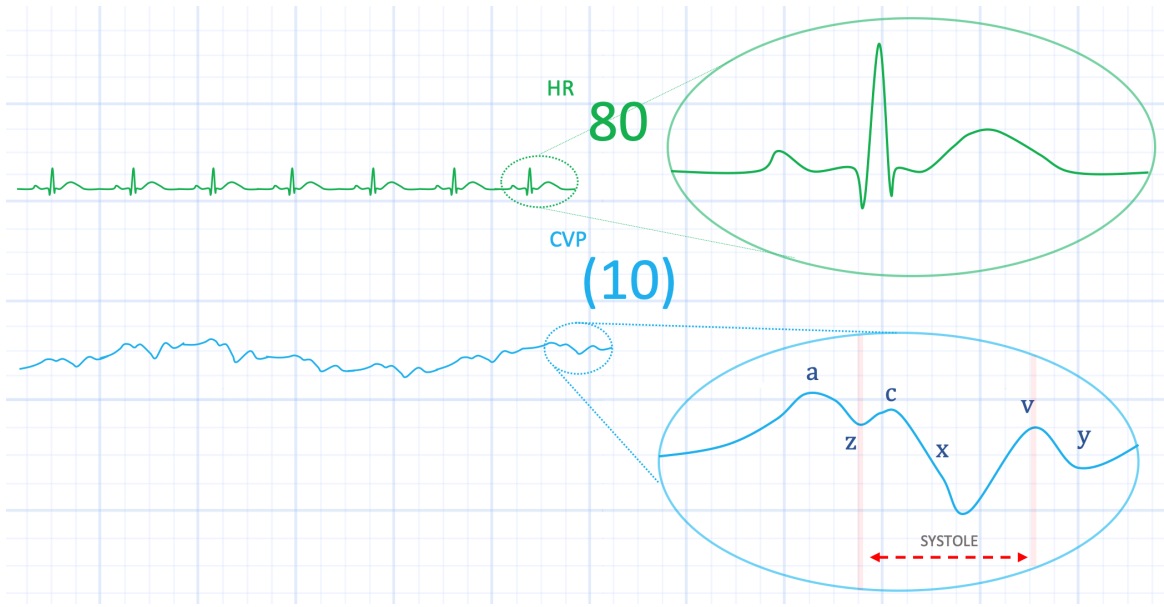

Figure 14: The central venous pressure [CVP] or right atrial pressure [Pra] trace. See text for details.

During systole, the tricuspid annulus is pulled downwards towards the apex of the heart. This motion lowers the pressure in the right atrium – termed the x-descent [83]. It follows that this fall in right atrial pressure during systole is primarily determined by 1. systolic function and 2. tricuspid valve competency. Accordingly, if there is either poor ventricular function or a leaking tricuspid valve, the x-descent is partially or wholly erased.

As systole progresses, the tricuspid annulus shifts backwards towards the cardiac base while meeting on-going venous return within the right atrium; consequently, pressure rises – the v-wave. Like the a-wave, the height of the v-wave is primarily determined by atrial volume and compliance. Normally, the v-wave is not as high as the a-wave [9, 77, 78]. If, however, the atrium is volume overloaded, and/or poorly compliant, then the v-wave may be quite tall – potentially leading to a great y-descent.

When the tricuspid valve opens, diastole begins. The RV accepts volume from the atrium, so the Pra tumbles into the y-descent. Early diastolic 'suction' may facilitate the y-descent [78]; as well, the fall in pressure is particularly susceptible to respiratory variation – more so than the x-descent. This may be due to anatomical connection between the diaphragm and pericardium [84]. That is, with an inspiratory fall in the diaphragm, the capacitance of the pericardium and right ventricle increase and the y-descent is enhanced. Normally, the RV is highly compliant. Indeed, it acts as a 'non-stressed' chamber [39] such that following the y-descent there is little pressure change until atrial contraction at end-diastole.

Venous Doppler Velocimetry

What does the CVP or Pra tracing have to do with venous Doppler interrogation? When a clinician executes pulsed wave Doppler analysis within a vein, there is an immediate up and down-stream pressure to flow through the area of insonation [see figure 15]. But what if the down-stream pressure varies with time – as the Pra does? This is the genesis of the multi-phasic venous Doppler waveform [see figure

15]. In other words, the CVP [i.e. Pra] tracing is visually transduced at the bedside! This can be performed within the superior vena cava [SVC] [85], hepatic vein [HV] [86] and even the internal jugular vein [IJ] [87]. A similar approach is employed in a pulmonary vein to interrogate left atrial physiology [88].

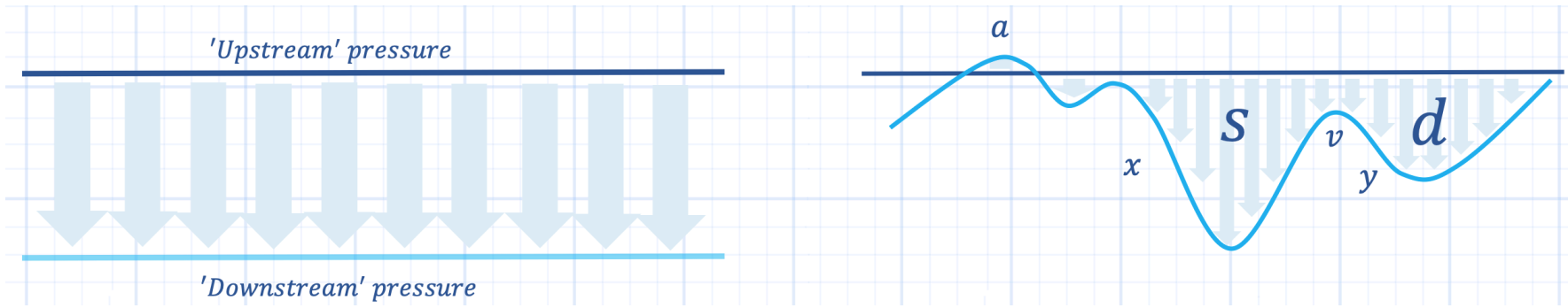

Figure 15: Potential mechanism of S and D waves. Left panel: Generic depiction of flow detected by pulsed wave Doppler with static upstream [dark blue] and downstream [light blue] pressures resulting in monophasic waveform. Right panel: Pulsed wave Doppler with variable downstream pressure [light blue - right atrial pressure]. S is systolic wave towards heart, D is diastolic wave towards heart. This analysis assumes a constant upstream pressure [in dark blue]; it also assumes a constant vessel diameter. Recall, flow = [vessel area] x velocity; thus, velocity can change with no change in flow, if the vessel area changes.

Considering the SVC, it is well-established that the Doppler waveform behaves in a similar manner to the Pra tracing [85]. For example, in healthy individuals, inspiration increases both the x and y-descents, but the latter more so [85]. In the SVC tracing, there can be small amounts of 'reverse' flow which occur during atrial contraction and sometimes during the peak of the v-wave. In health, the degree of reverse flow is < 10% throughout the respiratory cycle [85].

In the setting of pulmonary hypertension, tricuspid regurgitation and/or poor RV function, the venous Doppler profile follows the aberrations of the Pra tracing [89, 90]. With increased atrial volume, the a-wave enlarges thus augmenting reverse flow. Further, the systolic Doppler wave [i.e. x-descent] is progressively lost with poor RV function [90]. As well, if the tricuspid valve is incompetent, then there may be reverse flow throughout all of systole [83] [see figure 16]! If atrial volume remains high at the end of systole, then the v-wave may lead to reverse flow and the diastolic Doppler wave [i.e. the y-descent] is prominent [90].

Very similar physiology occurs in the hepatic veins [HV], however, in health there tends to be slightly more reverse flow than in the SVC [85]. Further, local pressure may alter the HV waveform considering that it is surrounded by the liver, within the abdominal cavity. Thus respiratory variation can render acquisition of the HV waveform more difficult [85]; for example, with Valsalva, intra-abdominal hypertension or when collapse of the IVC 'cuts-off' the HV waveform from right atrial pressure variations [83].

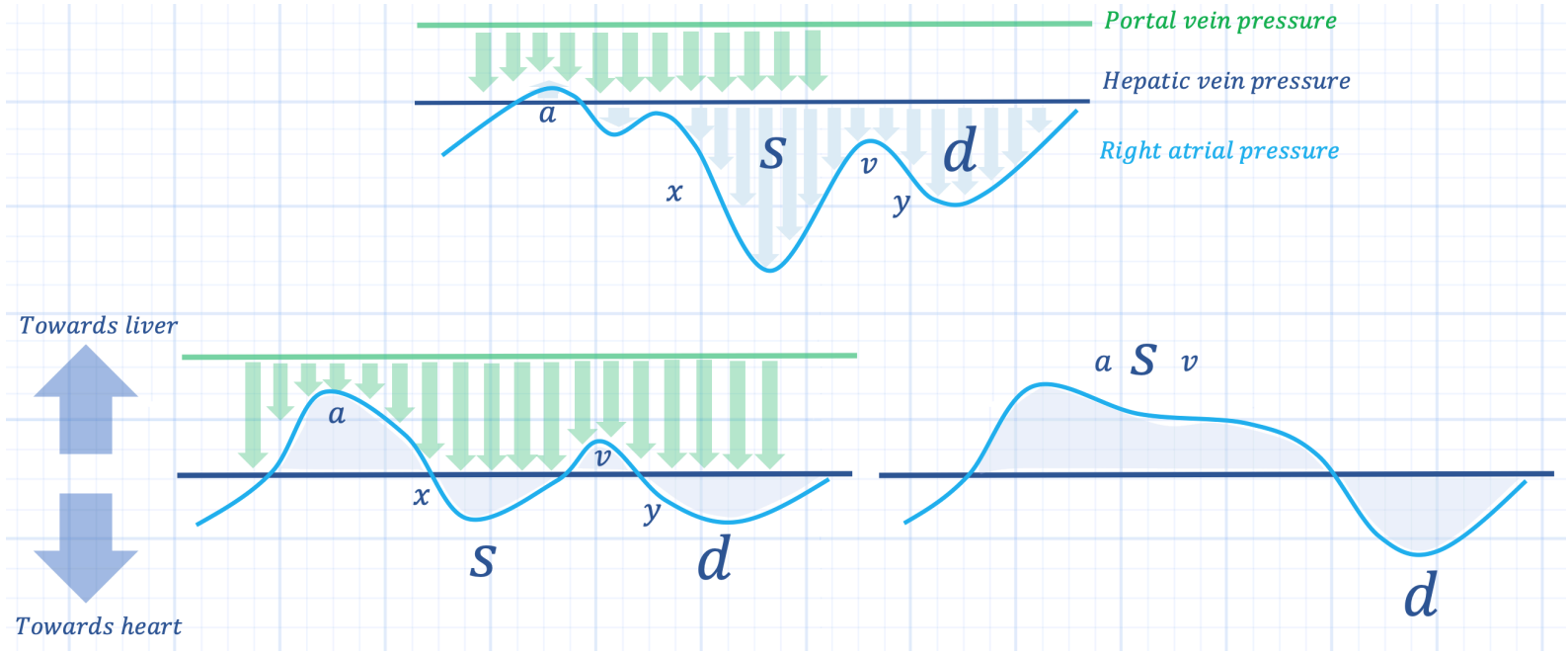

Figure 16: Schematic of portal vein [PV] and hepatic vein pulsed wave Doppler interrogation. Top panel shows potential mechanism of velocity waveforms. Normal with minimal PV flow pulsatility [green flow profile]. Bottom left panel: Worsening disease with atrial congestion [tall a-wave] and diminished x-descent or S wave from systolic back-leak [i.e. TR]. PV pulsatility is enhanced because of atrial pressure reflection towards the PV. Bottom right panel: Severe TR with fused aSv wave; there is no x-descent because of severe back-leak during systole. Note that the fraction of flow towards the heart is diminished relative to back flow. This depicts worsening congestion of the abdominal organs.

Volume Tolerance Includes Volume Responsiveness

Because the CVP marks the outlet pressure for venous return, capillary filtration and lymphatic drainage [78], its value is important for assessing organ congestion. Indeed, abnormal Pra tracings are even reflected back into the portal vein. For example, portal vein flow normally undulates gently with a minimum at end-diastole and maximum during systole. This occurs, primarily, because end-diastolic a-wave flow-reversal in the HV is reflected backwards into the liver, transiently shrinking the portal venous stream. Conversely, systole and early diastole 'pull' venous blood through the hepatic and, therefore, portal veins [83]. Accordingly, excessive portal pulsations suggest high retrograde venous flow, for example, an RV under duress [see figure 16] [91]. Similar physiology has been observed within the intra-renal veins [92, 93].

In summary, right-heart venous Doppler provides an index of 'volume tolerance' for the abdominal organs just as pulmonary venous Doppler qualitatively assesses left atrial pressure and risk of pulmonary edema. These measurements, I believe, supplement the idea of 'volume responsiveness' which specifically refers to the heart's ability to augment its stroke volume in response to preload. I think of 'volume responsiveness' as a sub-component of 'cardiac volume tolerance;' a heart on the flat portion of its Starling curve is volume 'intolerant.' Conversely, a heart on the steep portion of its Starling curve may be feeding kidneys that are volume intolerant by venous Doppler. Thus, assessment of both arterial and venous sides of the circulation may provide nuance in fluid management.

What is ventriculoarterial coupling and how does it relate to Guyton's formulation of the circulatory system? How might venous Doppler of the great veins fit into these frameworks and could the un-coupling of venous-from-cardiac power act as an underlying explanatory theory for aberrant venous Doppler morphology?

The Arterial Load: Ea

The arterial load – typically termed 'afterload' – is a complex matter. It is most certainly not simply the calculated 'systemic vascular resistance [SVR].' SVR is derived from a simplistic model of the circulatory system – one that does not account for other elements that determine true arterial load. For instance, the vasculature carries both a compliance – describing its distensibility – as well as a 'characteristic impedance' which, along with 'classical resistance' [i.e. SVR] make up the '3-element Windkessel' model of arterial load [see chapter 2].

Yet the challenge with the 3-element model is measurement at the bedside. Fortunately, groundbreaking work by Sunagawa et al. over 30 years ago revealed that the slope of the left-ventricular end-systolic pressure [ESP] relative to the stroke volume [SV] is an adequate surrogate for total arterial load [94-96]. Accordingly, the value of the ESP divided by the SV is the arterial elastance [Ea]. The Ea is a 'lumped' index that reflects all elements of the Windkessel model. Ea has units of mmHg per mL because it describes the change in central aortic pressure relative to a change in blood volume. Ea is represented by the purple line in figure 17; a normal value is 2.2 +/- 0.8 mmHg/mL [97]. An increase in arterial elastance [e.g. hypertensive emergency] shifts the Ea curve up-and-rightwards [see figure 17] while a decrease in Ea [e.g. vasodilation] shifts the Ea curve down-and-leftwards [98, 99].

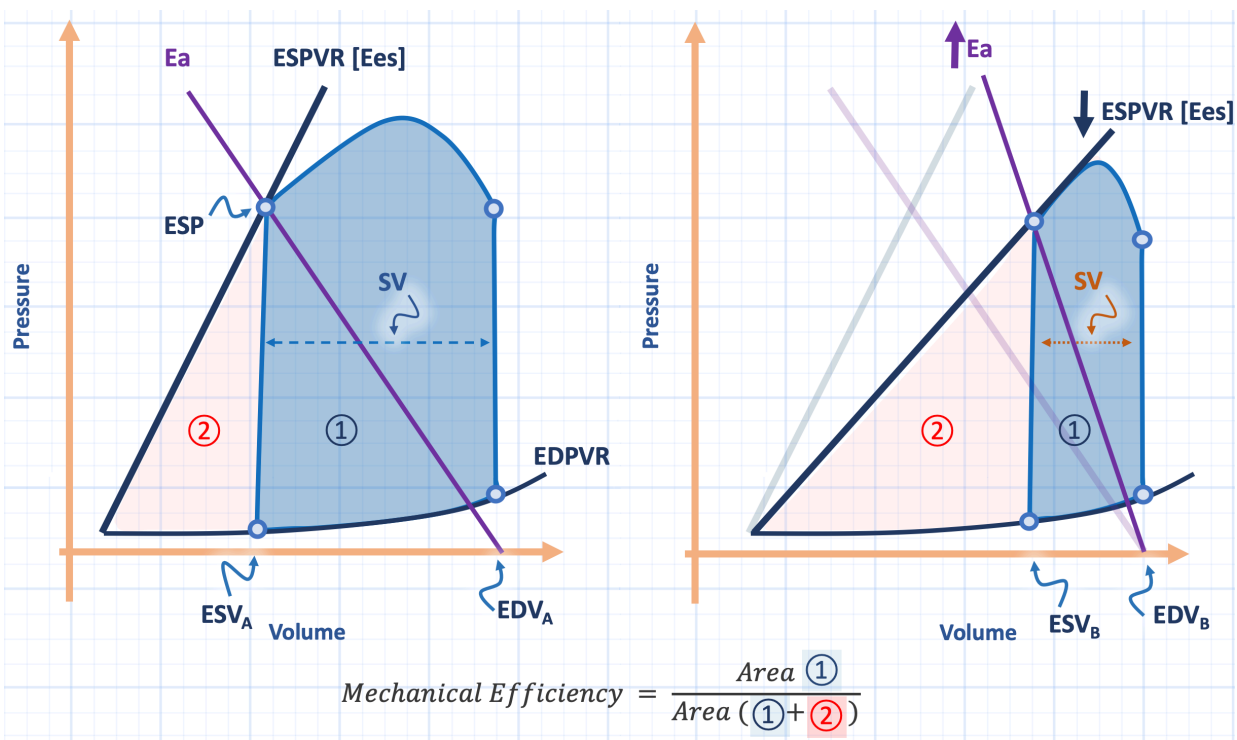

Figure 17: Mechanical efficiency and ventriculoarterial coupling. Left panel represents normal coupling between the arterial load [Ea-purple] and ventricular function [ESPVR-Ees - dark blue]. SV is stroke volume, ESV is end-systolic volume, EDV is end-diastolic volume, EDPVR is end-diastolic pressure volume relationship. Stroke work is the blue shaded area [circled 1] while potential work is the red-shaded area [circled 2]. B reveals an elevated Ea/Ees or ventriculo-arterial un-coupling.

The Left Ventricular Function: Ees

By similar reasoning to the Ea, the left ventricular end-systolic elastance [Ees] is a measure that describes the 'stiffness' of the left ventricle at end-systole. The Ees is, therefore, a 'lumped' index of left ventricular performance comprising contractility as well as geometric and other structural properties of the LV [95, 100]. Importantly, however, acute changes in Ees reflect changes in LV contractility that are load-independent, unaffected by contemporaneous changes in preload and afterload. The LV Ees is also indicated in figure 17 and a normal value is essentially identical to the Ea, that is, 2.3 +/- 1.0 mmHg/mL [97]. An increase in contractility [e.g. cardiac beta-2 receptor stimulation] shifts the Ees curve up-and-leftwards, while a decrease in contractility [e.g. septic cardiomyopathy] shifts it down-and-rightwards [see figure 17, right panel] [97-99].

Ventriculoarterial Coupling and Cardiac Efficiency

Given that Ea and Ees have identical units and nearly equal values, their relationship – the Ea/Ees ratio – is normally 1.0 +/- 0.36 [95]. A normal Ea/Ees ratio is visualized in the left panel of figure 17 while an abnormal [i.e. increased or uncoupled] ratio is seen in its right panel. Note that an increase in Ea, a decrease in Ees, [or both], increases the Ea/Ees ratio and, therefore, the end-systolic volume [compare ESVa to ESVb in figure 17]. Increased end-systolic volume decreases stroke volume [SV], ceteris paribus.

What is also evident from figure 17 is that impaired coupling between the ventricle and the arteries [i.e. an increased Ea/Ees ratio] diminishes cardiac efficiency [35]. The efficiency of the heart is visualized as the ratio between the work required for the stroke volume [i.e. stroke work – blue shade in figure 17] relative to the total work for the contraction. The total work for a cardiac contraction is equal to the potential work [in red shade – circled 2] plus the stroke work [in blue shade – circled 1]. Thus, the less-efficient heart leaves excess potential work behind during cardiac contraction; this concept is revisited below under the guise of 'veno-cardiac coupling.'

How is any of the above clinically-relevant? A recent, fascinating paper evaluated the effect of volume expansion as well as norepinephrine and dobutamine infusions upon ventriculoarterial coupling [VAC] in patients with un-resuscitated septic shock [35]. The authors used the oft-cited, single-beat method described by Chen et al. to non-invasively measure the Ees [101]. As outlined earlier, the authors observed that early volume-expansion with 30 mL/kg acutely-improved Ees and cardiac

efficiency. How might intravenous fluids improve an index of cardiac contractility? It may have been secondary to increased coronary perfusion and, accordingly, myocardial oxygen delivery. It is also possible that a relatively cold [i.e. room temperature] crystalloid infusion increased adrenergic tone. Lastly, despite being validated invasively on 43 patients, the single-beat method of Chen et al. may be inapplicable to septic patients and/or sensitive to the afterload-reducing effects of intravenous fluids [102-104].

Ventriculoarterial Coupling and Guytonian Physiology

But how does the uncoupling of the ventricle(s) from their arterial tributaries relate to Guyton's framework of the cardiovascular system? Figure 18 communicates this relationship [99]. If the y-axis becomes stroke volume – rather than cardiac output – one observes that the uncoupled ventricle has a smaller SV for a given filling pressure. Accordingly, whether the uncoupling is right-sided, left-sided, or both – the outcome is that the 'lumped' Frank-Starling curve is shifted down-and-rightwards [see also chapter 2].

Yet if we focus only on how the cardiac pump interacts with the arterial tree, we ignore half of the cardiovascular picture; venous return also cooperates with the pump! In other words, there is energy stored within the venous vasculature that is transferred to the pump function – which then interacts with the arteries as per above. Figure 18 demonstrates how the venous return must also be considered. A patient with a certain volume status and stressed venous volume – as measured by the mean systemic filling pressure – who then suffers ventriculoarterial uncoupling would see right atrial pressure rise as the impaired pump accepts venous return. As elaborated below, the patient with impaired VAC exhibits diminished cardiac performance [105] because the right atrial filling pressure rises relative to the mean systemic filling pressure – easily visualized in figure 18.

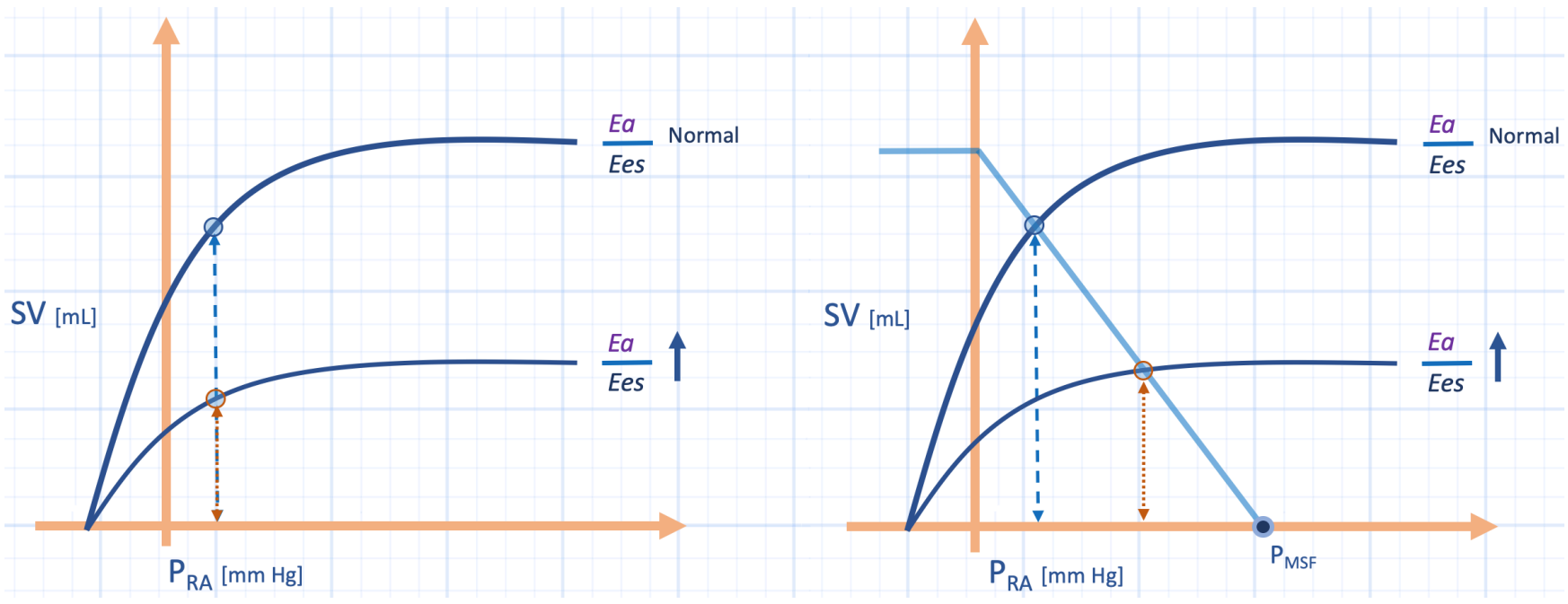

Figure 18: Relationship between Ea/Ees ratio and Guyton diagram. Left panel represents the effect of increasing the Ea/Ees ratio on the Frank-Starling curve; the y-axis is stroke volume [rather than cardiac output - SV x HR] and x-axis is right atrial pressure. The top Starling curve corresponds to figure 17 left

panel and the bottom Starling curve to figure 17 right panel. Figure 18 right panel represents the addition of mean systemic filling pressure [Pmsf] and venous return to the heart with ventriculoarterial decoupling. The light blue curve represents the venous return function.

Veno-Cardiac Coupling

Above, the basics of ventriculoarterial coupling [VAC] were described and related to the Guyton diagram. Below, the notion of cardiac performance [Eh] is explored in relation to venous Doppler velocimetry. Subsequently, I hypothesize that 'veno-cardiac uncoupling' – a concept analogous to VAC – is a symptom of poor cardiac performance [Eh]. Lastly, I postulate that abnormal venous Doppler velocimetry indicates 'veno-cardiac un-coupling'; aberrant transmission of mechanical power from the venous vasculature to the heart and arterial tree.

Cardiac Performance: Eh

In an imperative read, Parkin and Learning describe essential tenets of cardiovascular physiology for the intensive care unit [105]. The principles they espouse build upon those initially posed by Guyton [106, 107]. One such premise is cardiac performance [Eh] [108-110]. Essentially, Eh is the slope of the Frank-Starling curve and is described mathematically as the difference between the mean systemic filling pressure [Pmsf] and the right atrial pressure relative to the mean systemic filling pressure. More concretely, when cardiac performance is excellent, the right atrial pressure falls away from the Pmsf; that is, the difference between them is great. A large difference between these two values raises the value of the numerator of the Eh equation, thus cardiac performance and the slope of the Frank-Starling curve are both considerable [see figure 19]. By contrast, poor Eh is realized when the right atrial pressure encroaches upon the Pmsf, that is, there is a small difference between them [see figure 19].

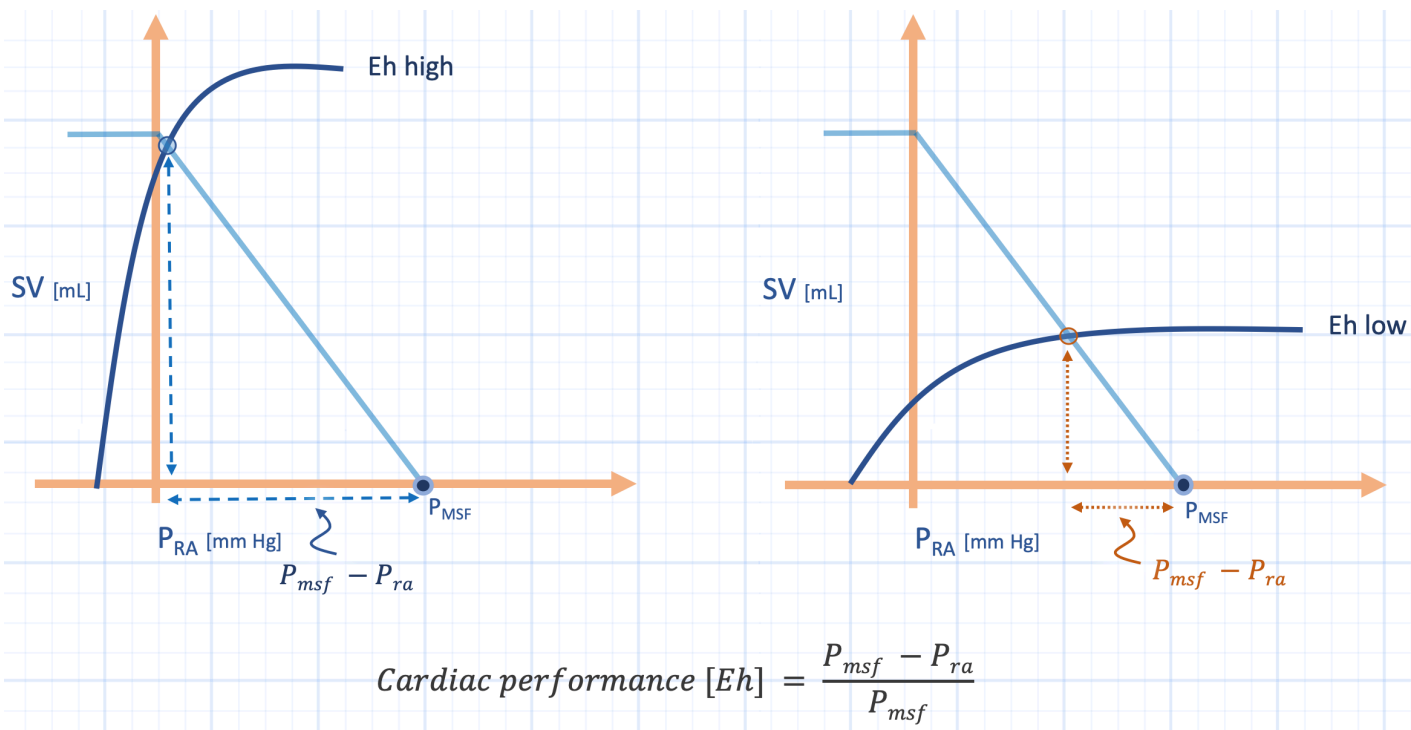

Figure 19: Cardiac performance. Left panel represents high cardiac performance [Eh] while the right panel represents low cardiac performance. SV is stroke volume, Pra is right atrial pressure, Pmsf is mean systemic filling pressure, the light blue line is venous return while the dark blue curve is the Frank-Starling curve. Pmsf is determined largely by volume status and venous capacitance; in both patients, Pmsf is the same.

Venous Doppler and Eh

The physiology of great vein Doppler velocimetry is described above. A simplified approach to the genesis of the great vein Doppler waveform is to consider it an 'inverse' trace of the central venous pressure [CVP or right atrial pressure]. More simply, as CVP falls during a single cardiac cycle, venous velocity rises and vice versa. Consequently, one sees a normal, biphasic systolic and diastolic inflow velocity in conjunction with the x and y descents of the CVP waveform.

It is tempting, therefore, to suppose that as the CVP approaches its upstream pressure [i.e. Pmsf] that venous velocity profiles in distal venous beds become 'atrialized.' For example, the portal or intra-renal veins – which typically harbour gentle, undulating velocity patterns – adopt pulsatile velocity profiles that reflect the contour of the CVP. From figure 19, one sees that as Eh worsens, the CVP nears the Pmsf. Ostensibly, the patient in the left panel of figure 19 possess a normal intra-renal venous velocity pattern while the patient in the right panel of figure 19 exhibits a pulsatile, discontinuous intra-renal venous velocity pattern even though their values of Pmsf are identical!

Mechanical Power and Veno-Cardiac Coupling

Could falling Eh be the physiological explanation for the pulsatile velocity patterns seen in heart failure patients [92, 93] and post-cardiac surgery patients [91, 111-113], or are there more universal principles at play?

If we consider the venous return curve with a perfectly performing heart [i.e. Eh = 1.0, or a vertical line], then the area under this [volume-pressure] curve represents the total energy of the cardiovascular system [figure 20]. Recall that energy over time is power [in watts] such that if stroke volume becomes cardiac output [i.e. volume over time], then the area under the curve is total power. Thus, an increase in Pmsf increases the total power 'available' to the cardiovascular system. From the Guytonian perspective, the heart can only 'impede' venous return, should the heart not keep right atrial pressure near maximal venous return – typically atmospheric pressure [107, 114].

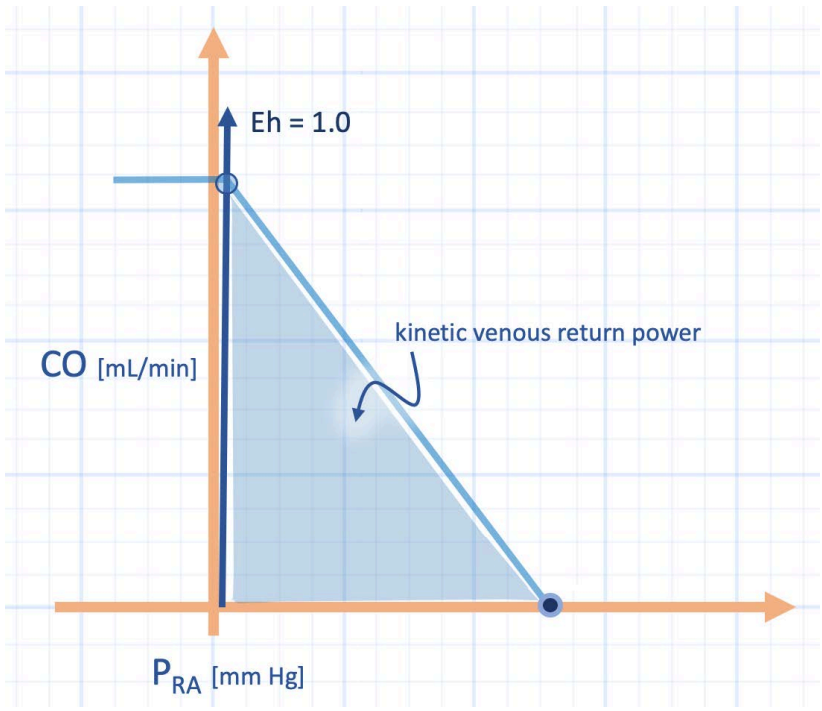

Figure 20: Hypothetical venous return power analysis. The y-axis is cardiac output [HR x stroke volume], while x-axis is Pra or right atrial pressure. A perfectly performing heart has an Eh of 1.0 and allows total power of venous return to be kinetic. Pmsf is mean systemic filling pressure.

An imperfectly performing heart has its slope flattened [figure 21]. The area under the cardiac function curve also represents the power performed over time to fill the heart. There is an additional power representing energy transferred from the venous capacitance beds towards the heart; in effect, this is the conversion of 'potential energy' to 'kinetic energy' from the elastic recoil of the venous vasculature. Thus, when Eh is poor [figure 21], there is a large portion of cardiac filling power relative to kinetic venous return power; that is, 'veno-cardiac uncoupling.' This may explain the reflected Doppler velocities seen in the great veins of patients with poor cardiac function and/or high Pmsf relative to cardiac function. This means a large fraction of 'potential venous return power' [red shade] acting upon the veins, venules and organs. Could this be an arbiter of organ dysfunction – analogous to the mechanical power as a mediator of lung injury?

Interestingly, the physiology espoused by Parkin and Learning [105] has been used to study cardiac power relative to Pmsf as a predictor of volume responsiveness [108, 109]; cardiac power is defined as cardiac output multiplied by mean arterial pressure. As expected, cardiac power efficiency levels off in step with the plateau of the Frank-Starling curve [109].

Venous Doppler at the Bedside

The clinical implications of the above are relatively simple. Reversal of great vein velocity patterns may represent elevated cardiac and potential venous return power relative to kinetic venous return power; what I term 'veno-cardiac uncoupling'. It is plausible that imbalance between forward and reverse-focused cardiovascular power mediates organ injury.

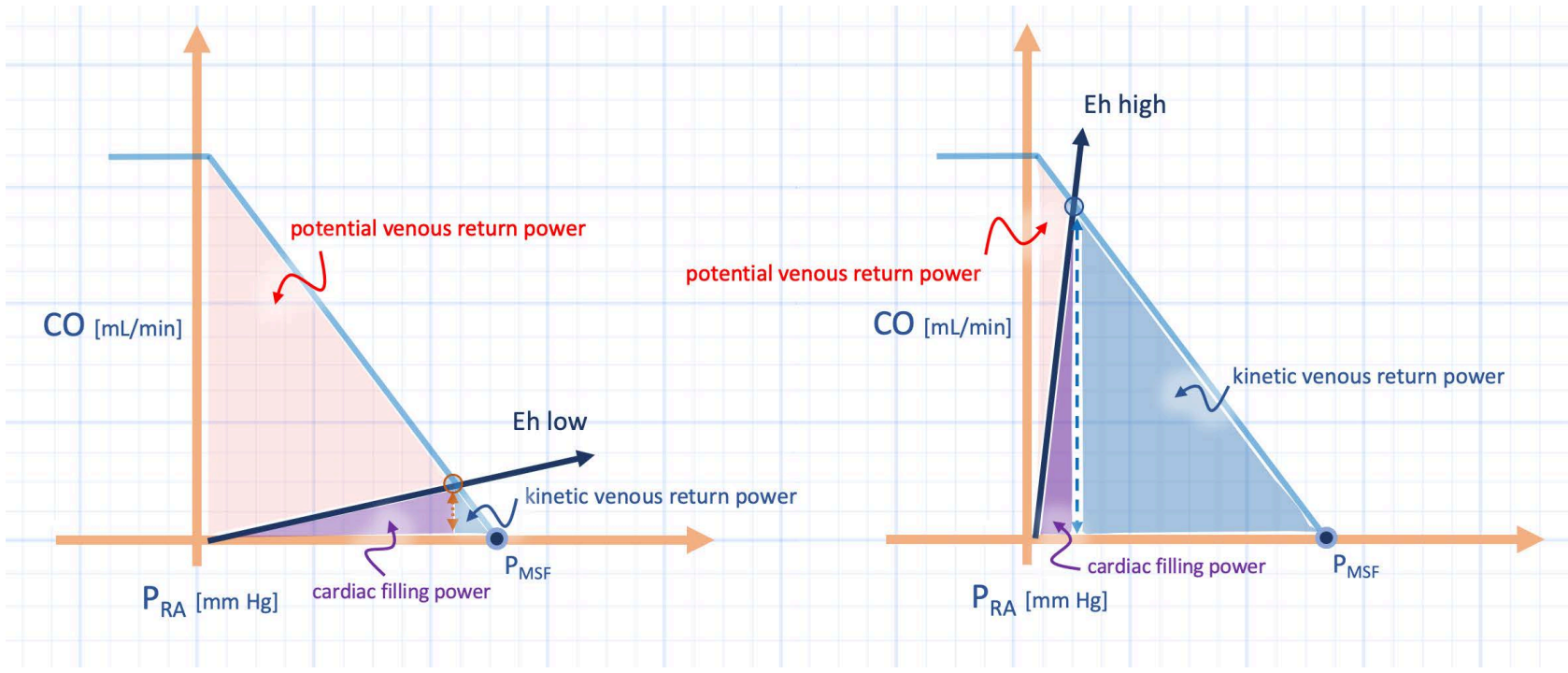

Figure 21: Hypothesis of veno-cardiac uncoupling. Axes are the same as figure 20. Left panel represents poor cardiac performance and 'veno-cardiac un-coupling.' Relate this to ventriculoarterial uncoupling in right panel of figure 17. The purple shade is cardiac filling power which ostensibly characterizes the work below the EDPVR in figure 17. The high potential venous return power relative to kinetic venous power might underpin backwards venous velocity reflections. Right panel represents good cardiac performance or high efficiency. Thus there is low cardiac filling power relative to kinetic venous return power. As well, there is low total potential venous return power [red shade].

Additionally, while hypervolemia favours excessive 'potential venous return power,' veno-cardiac coupling is also decided by Eh. This may explain why portal vein pulsatility was recently observed to appear or disappear without large vascular volume shifts [e.g. immediately after induction of anesthesia or upon transfer from the operating room to the ICU] [115]. Further, inhaled vasodilators can abolish venous Doppler velocity pulsations by improving cardiac function [91] without any acute change in volume status.

Of additional interest, the idea that the mechanical power applied to the venous system is injurious directly flows from the lungs is illustrated in figure 22. Reconsider the first few sections of chapter 9. Elastic driving power across the lung is indicated by the shaded area between the respiratory system compliance curve and the chest wall compliance curve. As this area increases, stress across the pulmonary vasculature rises and the RV afterload heightens. Flattening of the cardiac function curve pushes the operating point towards the Pmsf, that is, cardiac efficiency falls and a greater fraction of the total venous return power remains as 'potential power' directed against the venous system. One would expect Doppler venous pulsatility in the great veins. Thus, there is energetic uncoupling from the airway, across the alveolus to the right ventricle and then directed towards the venous system. This implies that 'reverse venous power' is directly proportional to Pmsf and inversely proportional to the difference between the Pmsf and Pra.

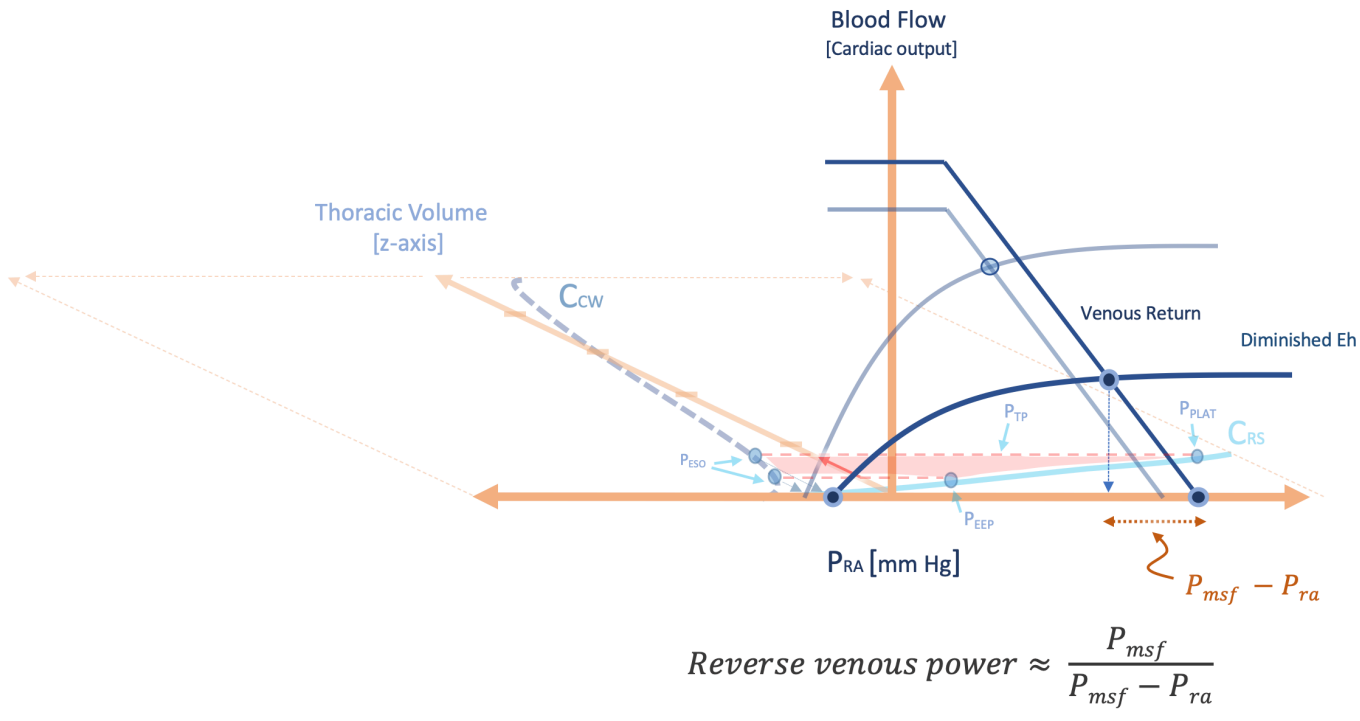

Figure 22: Energetic uncoupling from alveolus to venous system. The high driving power across the lung [red shade in x,z plane] increases RV afterload which reduces the RV efficiency [Eh], note the difference between the mean systemic filling pressure [Pmsf] and right atrial pressure [Pra] shrinks. The x-axis is Pra, the z-axis is thoracic volume. Crs is respiratory system compliance, Ptp is transpulmonary pressure, Peso is esophageal pressure. Ccw is chest wall compliance. In theory, this patient has great vein velocity pulsations that may improve by optimizing respiratory mechanics [e.g. prone position]. See also chapter 9 figure 5. Reverse venous power is a hypothetical equation to predict power directed 'backwards' in the vascular system.

At least one potential caveat to the above is that it assumes that venous return and cardiac function are independent. A recent study on intravenous fluids found that volume infusion – that is, increasing Pmsf and venous return – also improved Eh [35]! Further, venous Doppler pulsations are modified by factors beyond atrial pressure reflections. For example, portal vein pulsatility is also mediated by arterial pressure reflections through the mesenteric artery [116, 117] as well as body habitus [118].

Accordingly, the results of all diagnostic tests – including Doppler ultrasound – must be interpreted and applied within a specific clinical context!

Stroke Volume Variation and the Concept of Dose-Response

Awareness of the undulating pattern of an arterial line tracing is high amongst health professionals in the intensive care unit; certainly, this is an aftereffect of a cacophony of studies and reviews pertaining to pulse pressure variation and fluid responsiveness [see also chapter 8]. But what exactly generates pulse pressure variation? What are its limitations and why do these limitations exist?

Functional Hemodynamic Monitoring

Functional hemodynamic monitoring [FHM] assesses the functional state of the cardiovascular system by measuring a response to a defined stress [119]. The measured response may be either a 'venous-side' [e.g. vena cavae diameter change] or an 'arterial-side' [e.g. stroke volume variation, SVV] variable [5]. The defined stress is often a change in intra-thoracic pressure [ITP]. A commonly queried hemodynamic state is whether cardiac output will rise in response to a volume challenge.

The general principle involved in FHM is a dose-response relationship similar to basic pharmacology. So, if one alters the dose of a medication and observes a different clinical response, the change in response may be due to the altered dose. Similarly, because the diagnostic characteristics of SVV were derived in the context of a specific, predefined stress applied to the cardiovascular system [e.g. ITP change], observing a change in SVV 'response' is confounded by a change in the 'dose' of ITP.

Intra-thoracic Pressure

In the passive, ventilated patient – one not generating any respiratory effort – the change in ITP is related directly to the ventilator-applied tidal volume and indirectly to the compliance of the chest wall [120-122]. Thus, the ITP experienced by the cardiovascular system increases with higher tidal volume and/or lower chest wall compliance [e.g. obesity, ascites, chest wall edema, etc.], and vice versa [121]. If a patient generates his or her own inspiratory effort with the ventilator or bears down against it, the change in ITP is, essentially, unpredictable. Such ITP fluctuation confounds the measured cardiovascular response [e.g. SVV]. It is the reason why studies of FHM included patients who were completely passive with the ventilator and receiving relatively high tidal volumes [8-10 mL/kg] [123-125].

Intra-thoracic Pressure and Cardiovascular Physiology

As described at the beginning of this chapter, cardiac output is determined at the cross-roads of venous return and cardiac function. These two physiological phenomena may be plotted simultaneously to generate the Guyton diagram [3, 8]. The intersection of venous return and cardiac function defines the operating point of the cardiovascular system; the operating point determines the central venous pressure [on the x-axis] and cardiac output [on the y-axis] [4]. A passive, mechanical breath [i.e. an increase in ITP] right-shifts the cardiac function curve relative to the venous return curve. Consequently, if the operating point lies upon the ascending [volume-responsive] portion of the cardiac function curve, an increase in ITP transiently reduces right ventricular output. By contrast, if the operating point intersects the plateau of the cardiac function curve [volume-unresponsive], an increase in ITP does not diminish cardiac output. While this physiology applies to the right ventricle, 2-3 cardiac cycles later, the right heart output is experienced by the left heart – a delay imposed by the pulmonary transit time. Therefore, increased

ITP is a physiological stress that is assayed by beat-to-beat evaluation of left ventricular SVV; the magnitude of SVV suggests where upon the cardiac function curve the venous return curve intersects [75] and, consequently, alludes to volume responsiveness.

Left Ventricular Stroke Volume Variation

Because aortic pulse pressure [aortic systolic pressure – aortic diastolic pressure] directly relates to left ventricular stroke volume [as a function of central aortic compliance], pulse pressure variation [PPV] is frequently used as a surrogate of left ventricular SVV [12]. Deflections in pulse pressure during a single, mechanical respiratory cycle are referenced to an end-expiratory baseline. In the patient passive with the ventilator, a mechanical breath initially increases systolic blood pressure - referred to as reverse pulsus paradoxus, dUP [or delta UP] and is the consequence of multiple mechanisms. First, there may be direct transmission of the increased ITP to the aorta and arterial tree [126]. Second, mechanical insufflation of the lungs in a passive patient favours each of the following: improved left ventricular compliance via reduction of right ventricular volume [127], reduced left ventricular afterload [128] and, most prominently, increased pulmonary venous return and, therefore, LV preload [129, 130]. As many of these variables are not related to volume responsiveness, dUP is felt to be a poor marker of fluid responsiveness [131]. By contrast, during mechanical expiration, the inspiratory reduction in RV output reaches the left ventricle. This is reflected as an expiratory reduction in aortic systolic pressure and is referred to as dDOWN [or delta DOWN].

Caveats and Considerations

First, in the initial clinical FHM studies, patients were assumed to have normal chest wall compliance, all received relatively large tidal volumes and all were completely passive with the ventilator. These parameters, in effect, standardized the 'dose' of ITP. As a consequence, PPV performs poorly in patients generating spontaneous inspiratory effort [132-135], when smaller tidal volumes are applied [136, 137], or when there are abnormalities in chest wall compliance [121, 138, 139].

Second, the primary mechanism of SVV as a marker of fluid responsiveness is the inspiratory reduction in right ventricular output transmitted to the left ventricle during mechanical expiration [75, 131]. This is the primary mechanism because small changes in ITP affect large changes in venous return [29, 31]. However, increased lung volume also afterloads the right heart such that diminished right heart output may not reflect preload reserve, but instead afterload sensitivity. As such, reduced pulmonary compliance and pulmonary arterial hypertension may accentuate afterload sensitivity and diminish SVV and PPV as predictors of fluid responsiveness [140-145]. Additionally, if the left ventricle is afterload sensitive [e.g. systolic heart failure], ITP can unload the heart, facilitate dUP and create PPV [121, 146-148]. The predictive value of SVV and PPV is also impaired in patients with

cardiac arrhythmia [SVV due to variable diastole length], and excessive respiratory rate [149].

Finally, means of FHM that vary the venous return function may reduce some of the aforementioned uncertainty. Passive leg raising and end-expiratory occlusion are two such methods which outperform tests that rely on ITP change as the cardiovascular stress, both in patients breathing spontaneously and with arrhythmia [140, 150].

Systolic Time Intervals

Remarkably, non-invasive cardiology did not begin with ultrasound but rather as investigations into systolic time [151]. Indeed, studies on the duration of systole began in 1875 with Garrod who showed that the left ventricular ejection time [LVET] – the time that the aorta is open and ejecting blood – varies inversely with heart rate [152]. In 1904, Bowen used the carotid pulse tracing to measure left ventricular ejection in man [153]. Subsequently, in 1923, Katz and Feil described a technique of deconstructing systole into subcomponents using simultaneous recordings from a phonocardiogram, electrocardiogram [ECG] and the pulse of a central artery such as the common carotid artery [151, 154-158].

Using the aforementioned analysis of the ECG and common carotid pulse, systole can be reduced into two distinct time periods [159, 160] – the pre-ejection period [PEP] and the LVET. PEP is defined as the period of time between the onset of electrocardiographic systole and the opening of the aortic valve. As above, the LVET begins with the aortic valve opening and terminates at its closure – marked by the onset of the second cardiac sound, or the dicrotic notch in the pulse tracing of a central artery [see figure 23] [151, 157, 158].

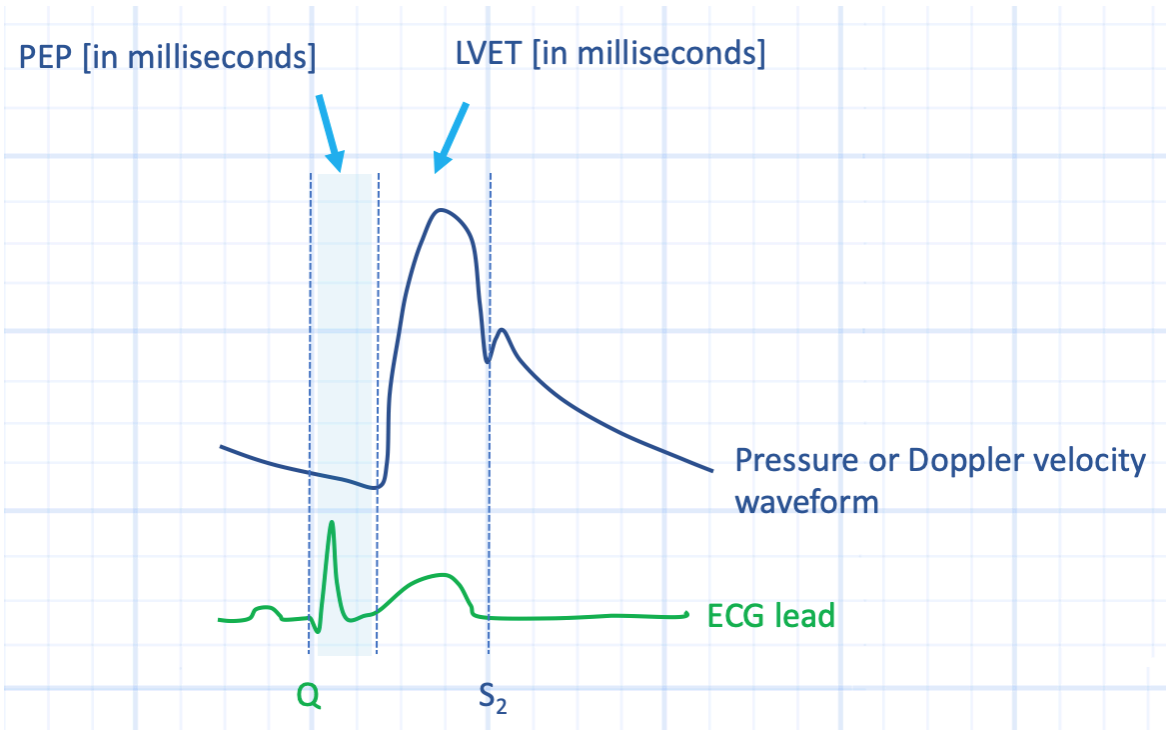

Figure 23: Relationship between ECG and arterial pressure pulse. See text for details.

Electromechanical Systole or QS2

The summation of the PEP and LVET gives the total time of systole – electromechanical systole. As it is bounded by a Q wave and the second heart sound, the duration of total systole has been dubbed 'QS2' [157]. QS2 is remarkably constant – even across a wide variety of cardiac disorders [157, 159-161]. Perhaps the most clinically relevant change in QS2 occurs in response to inotropes. Increased inotropic state is reliably reflected by decreased QS2, whereas diminished inotropic state prolongs QS2 [155, 157]. These findings are true whether or not the inotropes are intrinsic [e.g. anxiety, pheochromocytoma] or extrinsic [e.g. the provision of digitalis or adrenalin] [155, 157, 160, 161].

The Pre-Ejection Period

As seen in figure 23, the PEP begins with electrical systole and ends when the aortic valve opens and ejects blood into the arterial tree. Classically, the opening of the aortic valve has been defined as the upstroke in the pulse waveform of the common carotid artery. There is a small delay between the pressure upstroke in the central aorta and the common carotid by 18-20 milliseconds [151] but there are multiple validations equating the duration of the LVET to the pressure upstroke in the central aorta and carotid arteries [151, 157, 158]. Additionally, the PEP may be defined by relating the onset of systole on the electrocardiogram to both M-mode of the aortic valve [158] as well as Doppler of the aortic outflow tract [162, 163] or the carotid artery [164].

The PEP, essentially, reflects the time the ventricle is in isovolumic contraction. Accordingly, the PEP is prolonged when myocardial contractility is impaired and the change in pressure with respect to time [dP/dt] is low [151, 155, 157, 158]. Interestingly, PEP also rises when stroke volume falls acutely, probably because there is less myocardial fibre stretch and less contraction potentiation via the Frank-Starling mechanism [165]. Classically, stroke volume has been measured via indicator-dilution methods, but the rise in PEP in response to falling stroke volume has also been confirmed more recently using impedance cardiography and Doppler-derived cardiac output [162].

Left Ventricular Ejection Time

As above, the LVET represents the duration that the aortic valve is open and ejecting blood. When corrected for heart rate, the LVET shows a strong and direct relationship with stroke volume [SV]. For example, early studies that employed indicator-dye dilution techniques to measure SV revealed good correlations between SV and LVET in healthy controls and heart failure patients [159, 161].

LVET also tracked changes in stroke volume in response to head-up tilt and tourniquet application to mimic venous pooling [165]. Further, in patients with pulsus paradoxus and confirmed tamponade physiology, inspiratory changes in LVET tracked stroke volume [161]. These data matched earlier animal studies [166, 167]. Additionally, in patients with varying stroke volume secondary to complete heart block, LVET tracked stroke volume very well [168].

Nevertheless, an absolute LVET cannot guarantee an absolute stroke volume. The reasons for this are multifactorial but lie within the relationship between ejection time, ventricular volume and competing hemodynamic influences such as afterload and contractility [159, 169, 170]. One can think of the LVET as being directly related to the 'distance' of myocardial fibre shortening and indirectly related to the 'velocity' of fibre shortening [i.e. time is distance divided by velocity]. Consider administering dobutamine to a patient with dilated cardiomyopathy; this should increase contractility, lower afterload and, consequently, increase the 'distance' of myocardial fibre shortening. While this is expected to increase LVET, the extent to which dobutamine also augments the velocity of shortening, the time required to traverse the greater distance is shortened – causing less change in the LVET.

The PEP-to-LVET Ratio

Across numerous cardiac populations, the most robust metric for predicting LV performance is the PEP/LVET. This static ratio predicts LV ejection fraction well [155, 158]. A normal ratio is such that the PEP occupies about one-third of total systole. When the PEP increases relative to the LVET, beyond about 45%, there is a strong likelihood that the LVEF is less than 40-45% [151, 157]. This has been demonstrated more recently using standard TTE [163] as well as carotid artery Doppler [171]. Interestingly, SV changes in response to upright position and diuresis [162, 165] are marked by increased PEP/LVET ratio.

Application in the ICU

The corrected systolic flow time [cSFT] is, effectively, the LVET corrected for heart rate. Like the studies of LVET in the 1960s and 70s described above, changes in cSFT have been used successfully as a surrogate for SV when assessing the slope of a patient's Starling curve in response to provocative maneuvers [172, 173]. Given that both PEP and LVET diverge in response to LV preload change, perhaps the PEP/LVET ratio may better refine hemodynamic prediction with Doppler ultrasound in the ICU.

Cardiopulmonary Resuscitation

Given the growing interest and evidence for guiding chest compressions by transesophageal echocardiography [174], the physiological nuance of CPR is important to explain and, potentially, improve support for the pulseless patient.

The Cardiac and Thoracic Pumps

"External cardiac massage" as we know it today was introduced in 1960 [175]. As initially described, the goal of CPR was to compress and release the ventricles between the sternum and thoracic spine. Classically this mechanistic explanation of CPR is termed the 'cardiac pump' theory [176]. It posits that during chest compression, the heart is compressed, intraventricular pressure gradients are generated, the atrioventricular valves close and the semilunar valves open. Accordingly, blood is expelled into the great arteries. During chest decompression, falling pressure within the ventricles opens the atrioventricular valves and 'sucks' blood into the ventricles, much like heart function in vivo.

This explanation was quickly challenged, however, based on both canine and human data. In the former, CPR was marked by nearly identical pressures in all heart chambers and esophageal pressure – a surrogate for intra-thoracic pressure [ITP] – during chest compression [177, 178]. In other words, no pressure gradient formed between heart chambers as would be predicted by the cardiac pump theory. Further, the rise in pressure within all chambers of the heart mirrored the rise in ITP. Nevertheless, on chest compression, ITP rises relative to extra-thoracic pressure and this gradient determines blood flow under the banner of the 'thoracic pump' theory. Early data supporting the thoracic pump theory in humans arose from the description of 'cough CPR' whereby consciousness could be maintained in a patient with ventricular fibrillation as long as cough continued [179]. Clearly during cough there is minimal cardiac compression, but a large intrathoracic to extrathoracic pressure gradient.

The mechanism of blood flow described by the thoracic pump theory is less intuitive but posits that chest compression raises intra-thoracic aortic pressure relative to extra-thoracic aortic pressure and this drives blood out of the chest [176]. Parenthetically, this mechanism also underpins the anti-G straining maneuver that fighter pilots use during high +Gz forces in flight, as described in chapter 9. While, intrathoracic venous pressure also rises relative to extrathoracic venous pressure, the extrathoracic venous system does not significantly increase its pressure on account of venous valves and the relatively high compliance of the lumped venous system [176]. That is, because the lumped arterial compliance is 30 times lower than the venous system [180], if an equivalent parcel of blood is delivered out of the thorax and into the great vessels during chest compression, the pressure within the extrathoracic arteries is expected to rise 30 times more than within the extrathoracic veins.

Evidence for Thoracic versus Cardiac Pump Theory

Determining which of the aforementioned models drives blood flow during CPR is readily investigated with ultrasonography. Nevertheless, both transthoracic and transesophageal ultrasound during human CPR, like the methods used to study CPR before them, have yielded mixed results with respect to the dominant mechanism of blood flow [181-183]. Some studies revealed little ventricular compression and no valve closure during hemodynamically successful CPR, while others provided evidence supporting the cardiac pump theory [184]. The reason that both mechanisms have been supported is likely that both are functioning simultaneously during CPR – the thoracic and cardiac pump theories are not mutually exclusive. Differences in compression location, force, chest wall characteristics and volume-status all likely account for disparate experimental results [185-187].

CPR Adjuncts

Despite both mechanisms being important during CPR, many adjuncts have been developed based on optimizing the thoracic pump. Ostensibly, maximizing and minimizing ITP with chest compression and decompression, respectively, raises blood flow – treating the thorax, essentially, as a billow. ITP is augmented by simultaneous ventilation-compression CPR, vest CPR and abdominal compression [188-190]. The latter two effectively reduce chest wall compliance, which heightens ITP. Further, abdominal compression afterloads the left heart, facilitates aortic back pressure as well as coronary perfusion [190]. These methods have improved hemodynamics in animal models but have been lacklustre in human trials [191]. By contrast, active compression-decompression CPR minimizes ITP during decompression. It does so by actively recoiling the chest using a plunger-like mechanism affixed to the chest wall [192]. Similarly, an inspiratory-threshold device placed via a facemask or in-line with an endotracheal tube selectively raises inspiratory resistance. As a result, a partial vacuum is created during chest recoil [193]. Purportedly, active decompression and inspiratory threshold mechanisms facilitate venous return during chest wall recoil. While these devices had initial success in human trials, subsequent studies have been mixed [194].

A unique approach to optimizing the thoracic pump is the application of interspersed abdominal compression [195]. This technique involves compressing the abdomen during chest wall decompression. In theory, abdominal compression raises mean circulatory pressure – the pressure head for venous return [196]. If this occurs while right atrial pressure is falling, i.e. during chest wall recoil, the gradient for venous return is magnified. However, there are important caveats. First, abdominal compression raises venous return only when the venous vasculature is relatively full [51]. If the patient is hypovolemic, force applied to the abdomen may raise resistance to venous return and diminish great vein blood flow [54]. This underscores some success during CPR while applying volume infusion or passive leg raise [197]. Additionally, reducing ITP only enhances venous return in the absence of great vein collapse at the thoracic inlet. In a patient without end-expiratory pressure, venous return is limited at roughly atmospheric pressure by great vein collapse [3]. If a patient has a low right atrial pressure [30] and/or if the

patient is hypovolemic with high resistance to venous return, reducing ITP will not augment blood flow as great vein Starling resistors are limiting [198].

Time on Chest

Ultimately, the disappointment of some of the CPR adjuncts in humans may simply be a function of time. Delaying adequate CPR from 6 to 12 minutes significantly increased coronary perfusion pressure requirement and diminished the likelihood of spontaneous circulation return [184]. Simply, the longer the heart itself is starved of perfusion, the greater the degree of myocardial tetany and irreversible structural damage. Thus, the emphasis on good quality CPR with minimal interruption [199].

Veno-Arterial Extra-Corporeal Membrane Oxygenation

Perhaps the most memorable patient of both my pulmonary and critical care fellowships was that of a very young woman who suffered propofol-related infusion syndrome [PRIS]. As a consequence of PRIS, she endured multiple cardiac arrests and was placed on Veno-Arterial Extra-Corporeal Membrane Oxygenation [VA-ECMO] during cardiopulmonary resuscitation. Because of the rapid resuscitation she received from my colleagues, she survived to discharge – neuro-cognitively intact – despite spending an entire evening without cardiac activity. The details of her case may be reviewed here [200]. The aforementioned use of VA-ECMO highlights its life-preserving capability and underscores the importance of its hemodynamic workings.

Veno-Arterial versus Veno-Venous Extra-Corporeal Membrane Oxygenation

VA-ECMO is hemodynamically distinct from veno-venous extra-corporeal membrane oxygenation [VV-ECMO]. The latter is often used as a salvage therapy for severe ARDS in patients with preserved cardiac function as reviewed here [201]. VV-ECMO removes venous blood, performs gas exchange through an external circuit and then returns the blood back to the venous system. By contrast, VA-ECMO removes venous blood, performs gas exchange through an external circuit, and then returns the 'revitalized' blood to the arterial tree. VA-ECMO, therefore, bypasses the heart and the lungs completely and may be used in advanced cardiac-arrest algorithms as described in the case above. Importantly, should VA-ECMO be employed in advanced cardiac failure, the hemodynamic repercussions must be anticipated; this may be accomplished using the paradigm given to us by Arthur Guyton.

A Guytonian Primer

A fantastic model – borne from the principles Arthur Guyton – was formed by Sunagawa et al [202]; this model was further developed by Sakamoto and colleagues as a framework for understanding VA-ECMO [203]. Before turning to these advanced concepts, a basic review of venous return and cardiac function is warranted.

The circulatory system is described by the simultaneous workings of both venous return and cardiac function. With respect to the right heart, venous return is partially determined by an upstream pressure – the mean systemic pressure [Pmsf]. This crucial pressure is decided by the 'volume status' of the venous beds and the fraction of said volume that is 'stressed' [which is largely dependent upon adrenergic tone]. Additionally, venous return is determined by the resistance to venous return; many exceptional reviews exist on this topic [1, 3, 7, 74] [see figures 1, 5].

Venous return, however, is only half of the cardiovascular story as valvular competence, heart rate and rhythm, contractility, diastolic properties and afterload also mediate circulatory homeostasis. All of these properties together are described by the summative cardiac function curve which is also known as the Frank-Starling curve or cardiac response curve [4, 5, 204]. The intersection of cardiac function and venous return defines the central venous pressure [77] which is one determinant of IVC volume [13].

The left heart faces a similar physiology with the pressure head for venous return originating within the pulmonary circuit [129]; pulmonary venous return is then mediated by the cardiac function of the left heart and left atrial pressure is determined at the physiological intersection thereof. As above, the slope of the cardiac function curve is determined not just by contractility, but by multiple variables one of which is afterload [4]. Thus, increased left heart afterload shifts down, or flattens, the slope of the cardiac function curve.

Guyton and VA-ECMO

As elaborated by the model put forth by Sakamoto et al., VA-ECMO short-circuits the normal hemodynamic path [203]. When VA-ECMO is initiated, blood is removed from the venous bed, which attenuates mean systemic filling pressure and diminishes venous return to the right heart. Exogenous or endogenous adrenergic tone opposes this effect, but the flow at which venous blood is removed by VA-ECMO is a major determinant of diminished venous return. Attenuated blood flow to the right heart mitigates each of the following: right atrial pressure, IVC volume and pulmonary blood flow. These effects are important if a pulmonary artery catheter is employed. Further, change in pulmonary blood flow may alter gas exchange within the native circuit [205].

After blood passes through the external VA-ECMO circuit, it is returned to the arterial tree; the increase in arterial blood volume raises the afterload of the left ventricle [LV]. As a consequence, the LV cardiac function curve flattens and left atrial pressure, for any given value of pulmonary venous return, rises [203]. As VA-ECMO is often initiated in patients with poor, or absent LV function, this effect may be profound. However, as above, because pulmonary blood flow and pulmonary venous return are diminished, the rise in left atrial pressure is blunted. Nevertheless, acute pulmonary edema upon initiation of VA-ECMO is described [206].

Interestingly, an important prediction of the Sakamoto model is that left atrial pressure – and therefore the risk of pulmonary edema – remains high in states of right ventricular [RV] failure, even when LV function is supra-normal [203]. As they offer no mechanistic explanation, it is tempting to speculate. While VA-ECMO lowers right atrial pressure, with RV failure it is possible that RV volume and pressure remain high despite blood being shunted to the arterial tree. Potentially, through ventricular interdependence, LV diastolic function is impaired and compounded by the rise in LV afterload imposed by VA-ECMO physiology. Thus, augmenting VA-ECMO flow decongests the failing RV, but at the cost of elevated LV afterload. In such patients, it may be beneficial to consider a ventricular assist device [VAD] rather than ECMO [203].

The aforementioned physiology is also important when weaning a patient from VA-ECMO [207]. If RV or biventricular failure is present, it is imperative that the clinician recognize that increased venous return has, potentially, disastrous hemodynamic consequences. These patients should have their RV function optimized with careful consideration for each of the following: volume status, inotropic support, pulmonary vasodilators, and pulmonary mechanics including the mode of and settings of mechanical ventilation [208]. Consultation with a specialist in the management of pulmonary hypertension may also be beneficial.

Weaning-Induced Cardiac Dysfunction

Perhaps the landmark investigation elaborating an evolving cardiac dysfunction during the spontaneous breathing trial [SBT] is that of Lemaire and colleagues – published in 1988 [209]. One particularly memorable patient of mine – who miserably failed extubation despite a normal Tobin Index – led me to Lemaire's classic investigation and prompted this summary of the dizzying physiology at play as a patient switches from mechanically-assisted to unassisted breathing. Notably, the second author on Lemaire's landmark study – Jean-Louis Teboul – has published an elegant review of their initial work [210] which should be mandatory reading.

Left Atrial Pressure Rising

A maelstrom of mechanisms ceaselessly spiral towards increased left ventricular [LV] filling pressure when a patient is transitioned from assisted ventilation to a T-piece SBT [211]. In patients with preserved LV diastolic filling properties, increased left ventricular end-diastolic volume [LVEDV] raises the left-ventricular end-diastolic pressure [LVEDP]. The LVEDP is commonly obtained from a pulmonary artery catheter as the pulmonary artery occlusion pressure [Ppao] - see figure 24.

While it is tempting to simply ascribe increased LVEDV to increased preload from the right ventricle [RV] after positive pressure is removed, diminished cardiac contractility and increased LV afterload also augment LVEDV and therefore the LV filling pressure.

Each of these mechanisms are completely plausible as breathing work and adrenergic tone rise during the SBT exercise [210]. In patients with pre-existing coronary artery disease, flow resistance renders the heart susceptible to ischemia especially as the demands of respiratory muscles intensify [212]; impaired cardiac contractility is particularly troubling in patients with diminished ejection fraction [213]. Yet, rising LV afterload also retards blood egress from the LV and raises its filling pressure. Increased blood pressure during the SBT should raise concern for this mechanism, but the absence of elevated blood pressure does not rule out heightened LV outflow impedance [i.e. afterload] [214]. Deep negative inspiratory efforts during systole raise the transmural LV and aortic pressure which afterloads the LV and raises its LVEDV and LVEDP [128].

Equally-insulting to the LV, and probably occurring commonly, is the presence of diastolic incompetence. Diastolic dysfunction of the LV was noted even in the initial Lemaire investigation as a subset of patients demonstrated little-or-no increase in LVEDV, but a marked rise in transmural LVEDP. This indicates steepening of the left ventricular end-diastolic pressure-volume relationship.

Importantly, Moschietto and colleagues noted that patients who failed SBT were unable to increase their mitral annular tissue Doppler velocity [Ea] which is a non-invasive echocardiographic index of LV relaxation [215]. By contrast, those who passed their SBT were able to increase LV relaxation. Similar physiology has been noticed in patients with exercise-induced diastolic dysfunction [216]. Crucially, in Moschietto's study, early LV filling velocity increased in both those who passed and failed the SBT – the key difference being that early LV filling increased in those who passed the SBT because of their ability to increase LV relaxation. In other words, the rise in early diastolic filling in those who failed the SBT was due not to more rapid relaxation, but instead, increased left atrial pressure.

The underlying etiology of evolving diastolic dysfunction during SBT may be that of pre-existing LV stiffness, dynamic LV ischemia and, interestingly, an encroaching interventricular septum secondary to an enlarged right ventricle [217], as described below.

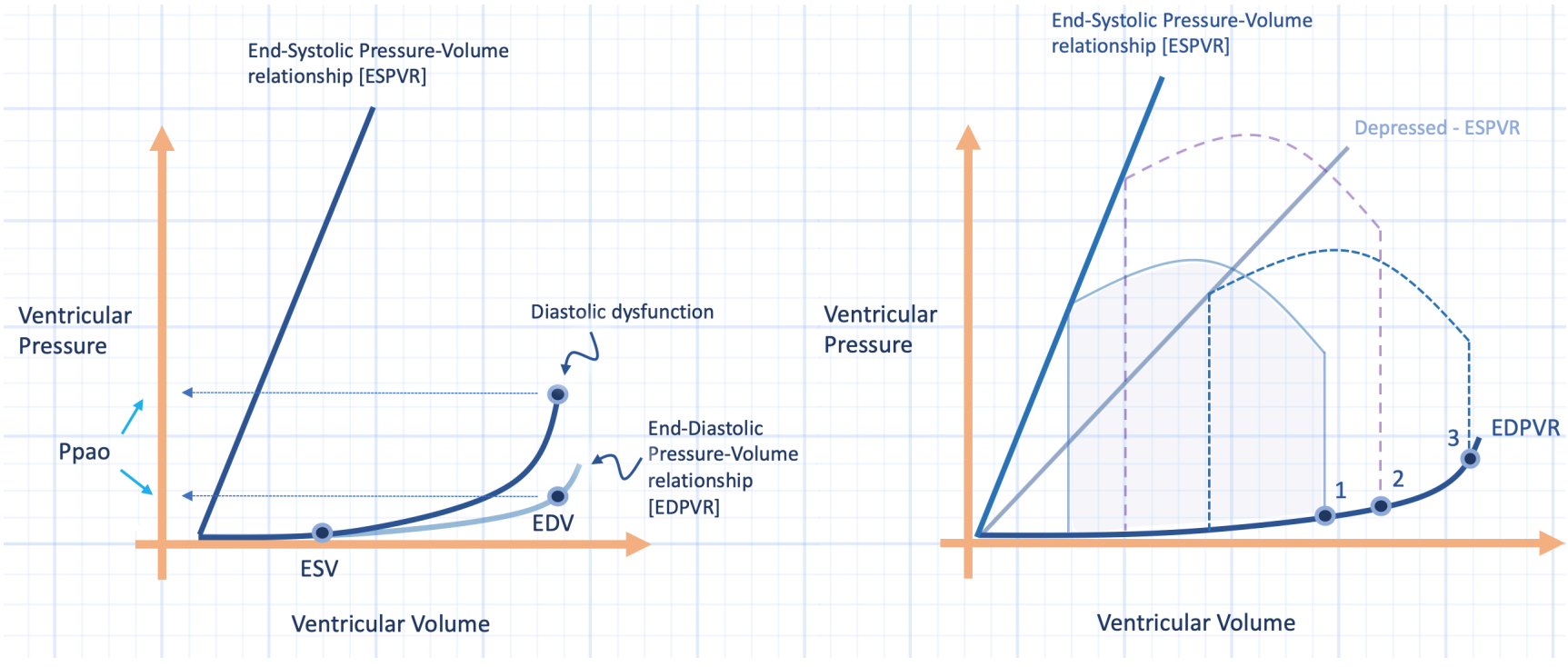

Figure 24: Mechanisms of rising pulmonary artery occlusion pressure [Ppao]. Left panel: EDV is end diastolic volume increasing on the x-axis with rise of left ventricular end diastolic pressure [LVEDP] or pulmonary artery occlusion pressure [Ppao] on y-axis. The darkened EDPVR represents diastolic dysfunction, or a stiffened LV which may result from RV enlargement. Note that for the same EDV on the x-axis, the LVEDP is increased on y-axis. Right panel: The shaded blue loop represents normal state with EDV at point 1. The purple-dashed loop is increased afterload with EDV at point 2. The blue-dashed loop represents diminished LV contractility with EDV at point 3.

The Engorged Right Ventricle

While it is commonly taught that removing positive pressure increases the gradient for venous return, this isn't entirely true [30]. Assisted breathing with positive end-expiratory pressure [PEEP] doesn't diminish the gradient for venous return, rather, it increases the Pcrit which is the critical collapsing pressure of the great vessels as they enter the thorax. When positive pressure is removed, maximal venous return during spontaneous inspiration rises [figure 25].

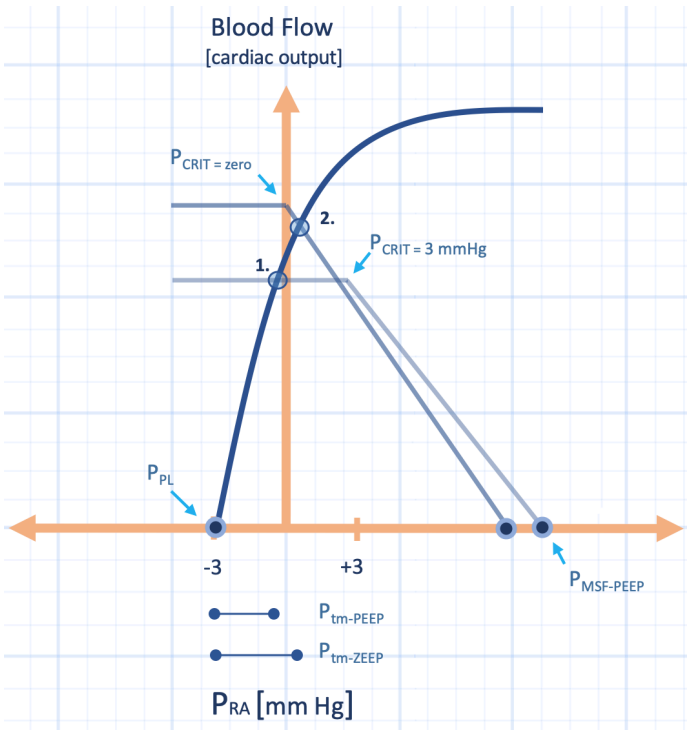

Figure 25: Removing PEEP to ZEEP. Point 1 shows a hypothetical operating point on positive end-expiratory pressure [PEEP]. Right atrial transmural pressure on PEEP [Ptm-PEEP] is shown below the x-axis. Moving the patient to zero end-expiratory pressure [ZEEP] increases maximal venous return and the operating point to 2. The critical collapse pressure of the great veins [Pcrit] falls. With PEEP removal, Pcrit falls from about 3 mmHg to atmospheric pressure. As well, the transmural pressure of the right atrium increases [Ptm-ZEEP]. Pra is right atrial pressure; Pmsf is mean systemic filling pressure.

As venous return increases and negative inspiratory pressures take hold, the right ventricular [RV] blood volume rises. As above, the interventricular septum may encroach upon and stiffen the LV during diastole [217]. Within a few cardiac cycles, this heightened RV preload is transmitted to the LV and LVEDV and LVEDP rise, placing the patient at risk for weaning-induced pulmonary edema [218].

While an enlarged RV results from high inflow, poor outflow also contributes to its size. To the extent that hypoxemia and hypercapnia progress, the RV afterloads [210]. Additionally, rapid breathing in patients with expiratory airflow limitation [e.g. airway edema, ARDS, COPD, obesity] can cause gas-trapping [219-221], raising RV outflow impedance [222]. If the lower-lobe lung volume increases, the mediastinum can compress, which couples RV and LV filling – accentuating the effects of ventricular interdependence [223].

Predicting Cardiac Dysfunction

Given the above, predicting 'weaning-induced pulmonary edema' [WIPE] is important. Towards this end, a recent paper described the incidence of WIPE and its clinical associations [224]. Amongst 81 patients undergoing an SBT via T-piece, 29 had at least 1 episode of WIPE – all of whom failed SBT. Logistic regression revealed that the odds ratio of WIPE was greatest for those with known COPD [OR 8.7], followed by known 'cardiopathy' [defined as dilated, hypertrophic, hypokinetic or with significant valvular disease – OR 4.5] and also obesity [OR 3.6]. Employing the passive leg raise [PLR] to predict preload independence as a risk for WIPE [225] had been previously investigated by this group. Thus it was used to predict WIPE again. When PLR revealed preload independence [i.e. no augmentation of cardiac in response to a PLR], diuretics were given. Nine remained preload independent and of those, 7 had WIPE again. Of the 7 whose PLR revealed conversion to preload-dependence following diuretics, 6 went on to pass a subsequent SBT.

Importantly, preload independence does not necessarily reveal a patient's volume status; volume status and volume responsiveness may diverge. Preload independence, does alert the clinician to a patient whose venous return curve [at any volume status] is intersecting the plateau of the cardiac function curve. Such a patient has little cardiac reserve and is, accordingly, at risk for WIPE.

In addition to the PLR, data exists for BNP elevation as well as hemo-concentration as WIPE predictors [218]. While beyond the scope of this brief synopsis, diagnosing WIPE is important as treatment with diuretics and/or afterload reduction is required for liberation from mechanical ventilation.

The Revised Starling Principle

The use of hyperoncotic albumin to draw fluid from the interstitial space permeates dark corners of the critical care community. The 'pull and push' of 25% albumin followed by furosemide remains somewhat cryptic lore – its use often spoken of in hushed-tones, as if this special physiology may be called upon only in the direst of situations and only by the most venerable clinicians. It is a physiology that I have invoked whilst managing patients with cirrhosis – or others in whom the mystical creature of 'hypervolemic, yet volume deplete' is raised.

Yet the data for this practice is mixed and contemporary, brilliant reappraisals of the original Starling principle of capillary filtration have seriously challenged the reasoning behind this practice [226-230].

The Original

In the late 19th century, Starling noted that isotonic saline injected into a dog's hind limb was reabsorbed whereas, serum was not. From this, he deduced that the capillaries and post-capillary venules are semipermeable membranes. Movement of fluid then became a competition between transendothelial hydrostatic pressure [i.e., the pressure within the capillary [Pc] less the hydrostatic pressure within the interstitial space [Pi]] and the colloid osmotic pressure difference between the capillary and interstitial space [πc – πi]. The colloid osmotic pressure is determined largely by albumin and the degree to which albumin permeates the endothelium is reflected in the Staverman's osmotic reflection coefficient [σ] which ranges from 0 [fully permeable] to 1 [impermeable]. We are left with the following, simplified, equation determining net fluid flux [Jv]:

$$(1)\quad Jv = [Pc - Pi] - \sigma[\pi c - \pi i]$$

Equation 1: Fluid flux, Jv. [I have knowingly omitted the hydraulic conductivity Lp]

If a 'sum-of-forces' approach is adopted, the following pictorial analysis is employed [figure 26]. Note that the force favouring filtration is Pc while the summative force opposing filtration is Pco; their relationship is expressed by the following equation.

$$(2)\quad Pco = \sigma[\pi c - \pi i] + Pi$$

Equation 2: The opposing filtration pressure [Pco]

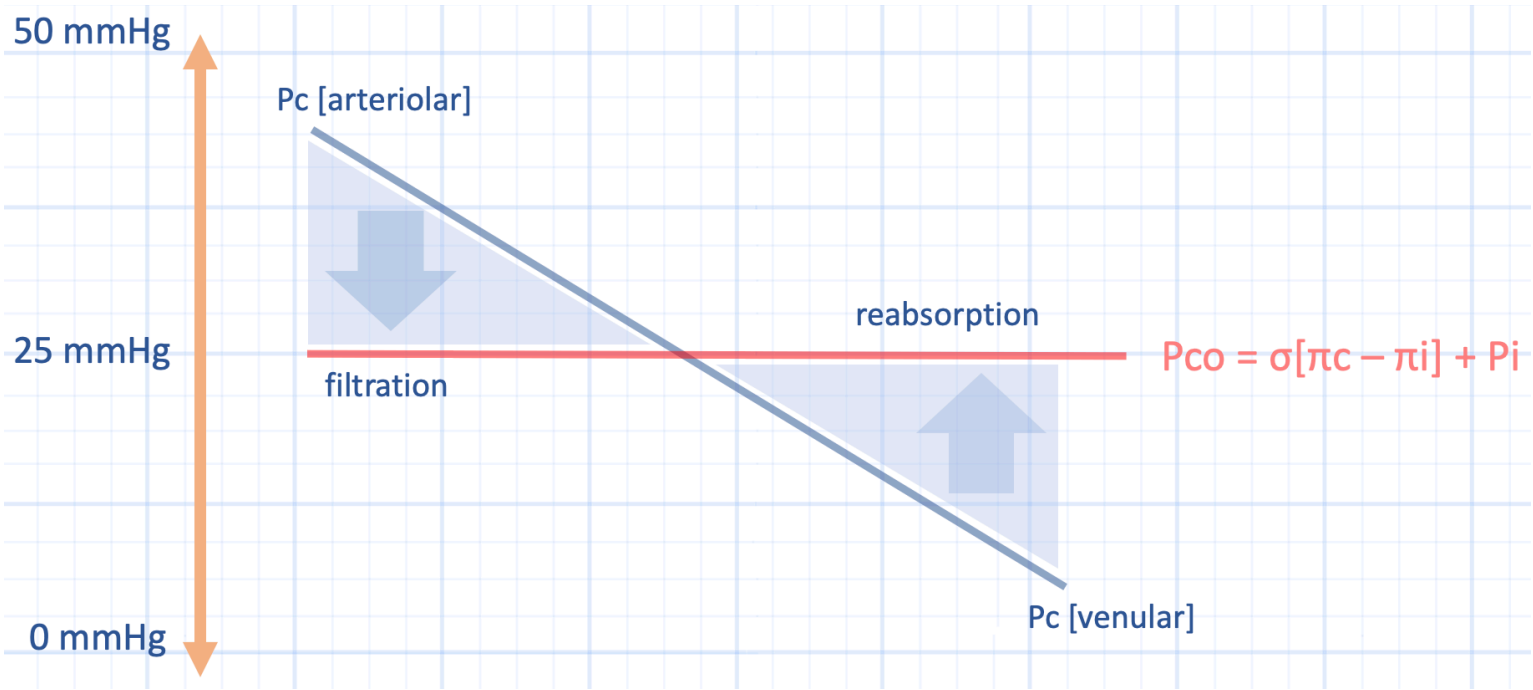

Figure 26: Sum of forces approach. The hydrostatic pressure within the capillary [Pc] is represented by the sloped, blue line. The sum-of-pressures opposing the Pc is the Pco, represented by the red line. When the Pc is above the Pco, filtration occurs, when the Pc is below the Pco, absorption occurs. This is the traditional Starling model.

The capillary filtration opposition pressure [Pco] should be intuitive, for if the capillary colloid osmotic pressure [πc] rises or if the interstitial osmotic pressure [πi] falls, fluid should be retained within the capillary. Similarly, if the pressure surrounding the capillary [Pi] rises, filtration is opposed. The Pco is illustrated by the red line in figures 26-30; if its value rises, filtration is opposed [reabsorption is enhanced] while if its value falls, filtration is enhanced. In the early 20th century, Pc was first successfully measured and found to be roughly 35-45 mmHg at the arterial end and 12-15 mmHg at the venular end. At that time, it was not possible to simultaneously measure πi and it was assumed to be quite low. Similarly, σ was assumed to be 1.0. Based on said assumptions, it was concluded that the Pc falls below the Pco in the middle of the capillary and, therefore, filtration predominates at the arterial end while absorption emerges at the venular end.

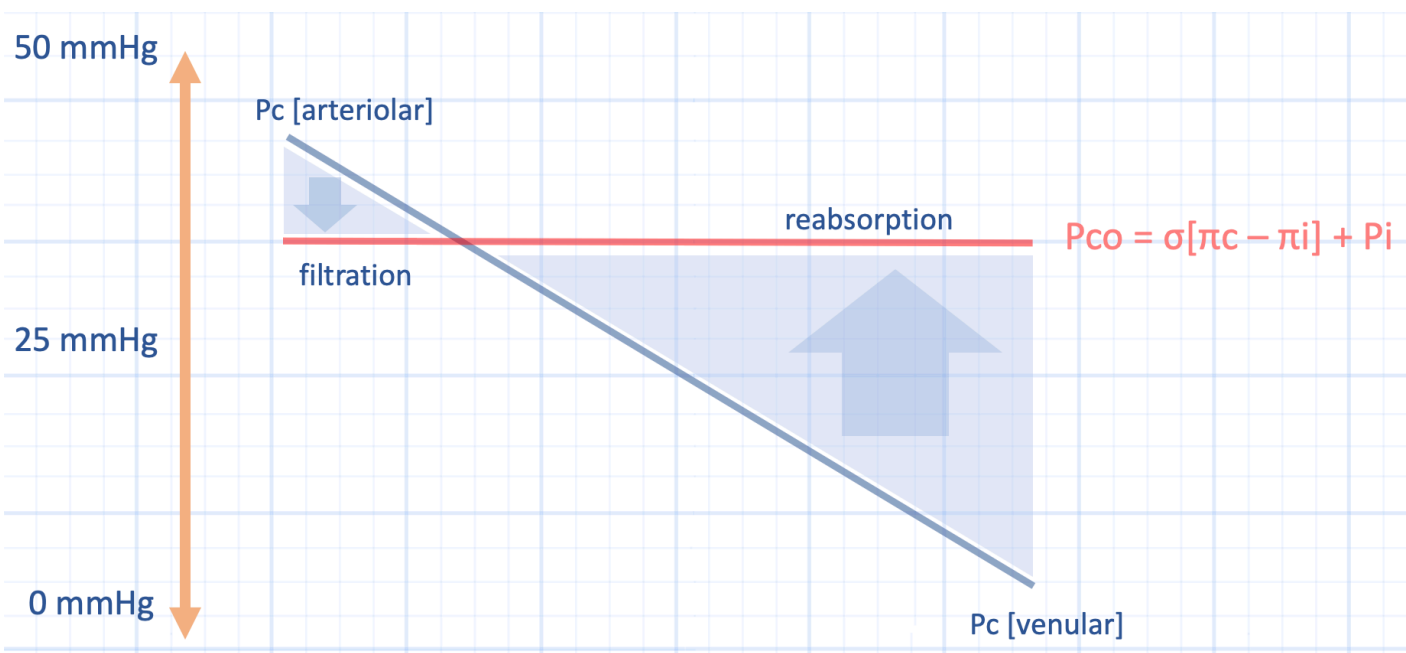

Figure 27: Hypothetical rise in the opposition pressure. Note that the Pco may rise in response to an increase in πc or Pi or a fall in πi. This favours absorption.

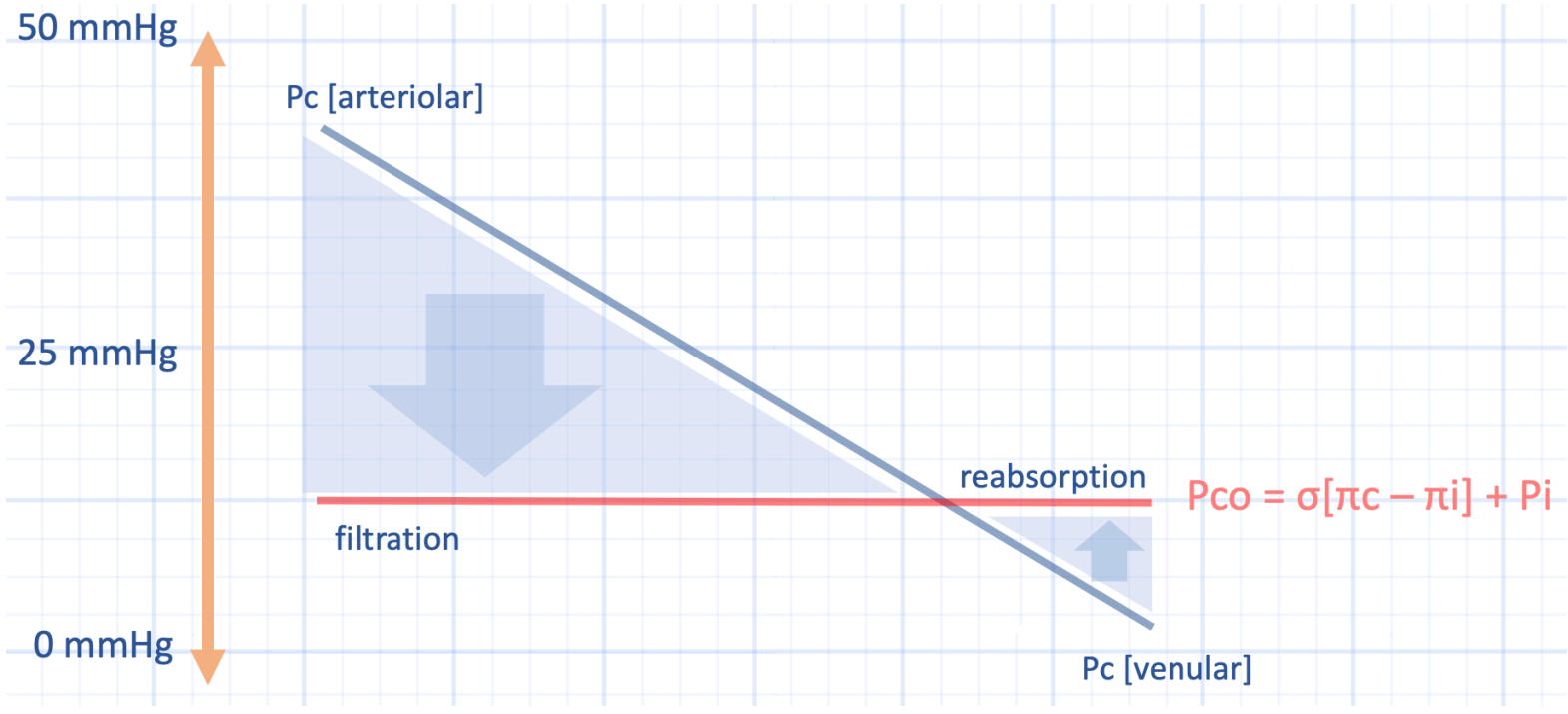

Figure 28: Hypothetical fall in the opposition pressure. Pco will fall secondary to a fall in πc or Pi, or a rise in πi. This favours filtration.

Revised Model

However, when techniques became available to simultaneously measure all of the Starling forces, the Pco was found to be surprisingly low – due to the relatively high πi [i.e. 16 mmHg, note that increasing πi lowers the Pco] and low Pi [actually sub-atmospheric at heart level] such that the Pc remains above Pco throughout the entirety of the capillary. Importantly this is also true for tissues with the lowest Pc [e.g. lung]. In other words, there is no absorption. This has been found true for most tissues. There are notable exceptions to the steady-state 'no-absorption' rule, and these tissues include the intestinal mucosa [but not the mesentery], as well as the renal cortex and medulla [229]. These tissues manage to keep the πi quite low [which raises the Pco] such that absorption is observed [figure 29].

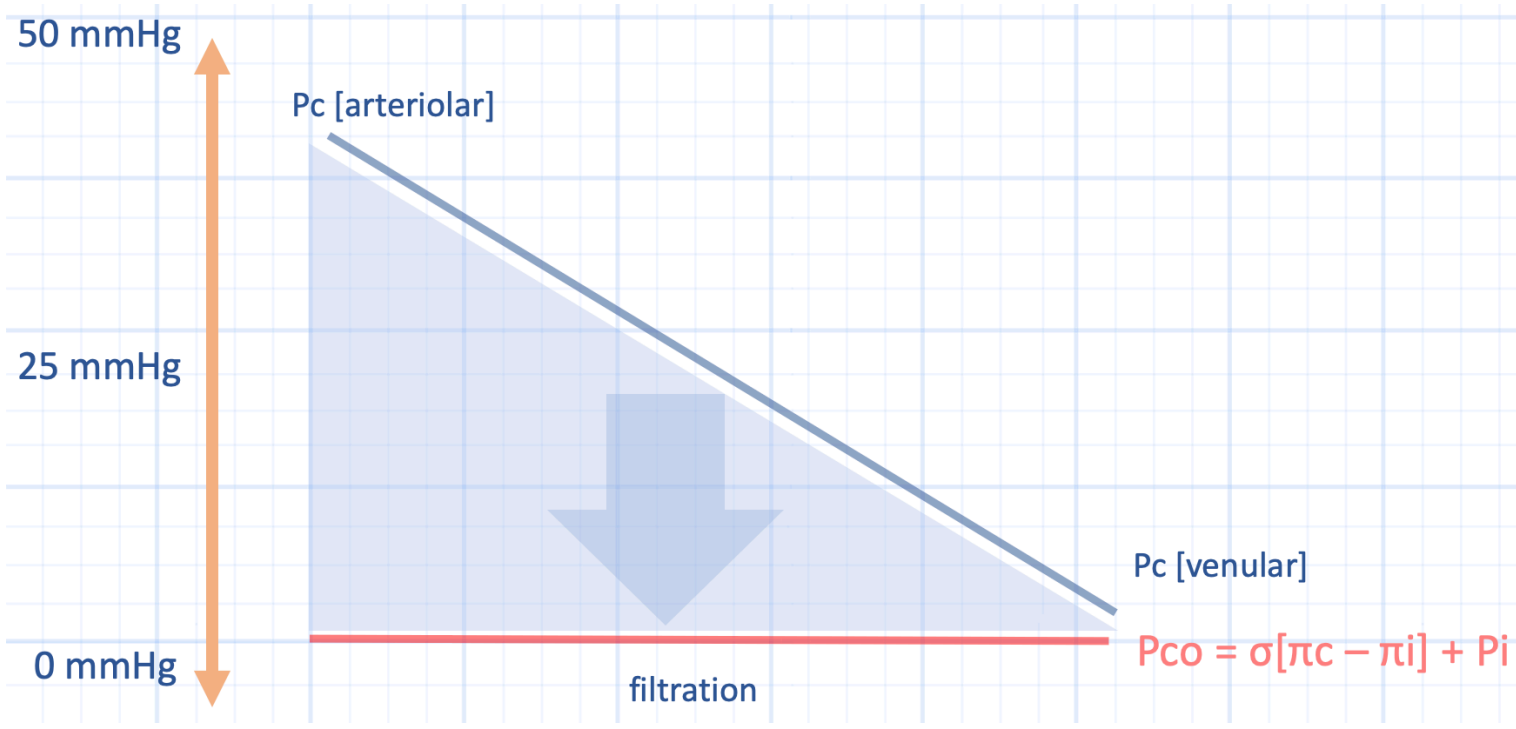

Figure 29: The no-absorption rule [in the steady state]. Note that this occurs in the vast majority of capillaries. The high πi and low Pi both diminish the Pco such that Pc is > Pco throughout the capillary and filtration dominates [downward blue arrow].

Transient versus Steady State

Capillary absorption can be seen in tissues which normally do not absorb along their length when there is a transient fall in Pc. However, within minutes, the sum-of-forces returns to net filtration. This fact highlights the important linkage between Jv [i.e. fluid filtration], πi and Pi. When Jv falls, in response to a drop in Pc, the colloid oncotic pressure of the interstitium πi, rises with time and the Pi falls. Consequently, the Pco falls and net filtration across the capillary is regained; this effect typically occurs within 30 minutes before net filtration is, again, achieved. In theory, the converse is also true, that a transient rise in Pc momentarily augments filtration, but over a period of minutes the Pco rises in compensation – an effect which buffers the initial increase in Jv.

Another Revision

Importantly, even when the revised model with simultaneously-measured 'sum-of-forces' is utilized, there remains an order of magnitude difference between the predicted lymphatic flow and the observed lymphatic flow. Per the above model, the predicted filtration, and therefore afferent lymph drainage, should be much higher than what is observed. If the venular side of the capillary does not reabsorb in the steady-state, where is the excess filtrate going? It appears that the colloid oncotic pressure difference which determines Jv, is not actually a trans-endothelial force per se, but rather an intra-endothelial force. This realization arose in response to the presence of the endothelial glycocalyx [EG]. The EG is a mesh of mucopolysaccharides associated with proteoglycans and glycosaminoglycans. The EG acts as a brushy border within capillaries separating red blood cells and other

large proteins from the sub-endothelial surface. In health, the EG may have a volume of 1700 mL [231]. It is likely that the Staverman osmotic reflection coefficient represents the ability of this border to reflect albumin from the subendothelial space [227]. Thus, the modified Starling equation becomes:

$$(3)\quad Jv = [Pc - Pi] - \sigma[\pi c - \pi sg]$$

Equation 3: The modified Starling equation for fluid flux. See text for details. Sub-glycocalyx space [πsg]

Normally, the colloid oncotic pressure of the sub-glycocalyx [πsg] is quite low, but this force is entirely within the capillary such that Jv across the endothelium is a function of Pc and Pi while the colloid osmotic difference across the EG simply retards filtration. The aforementioned principles still hold in terms of transient and steady-state effects, however, this raises the possibility that the hyperoncotic effect of albumin is simply to dehydrate the subendothelial space and EG rather than draw any significant amount of fluid from the interstitium [230] [figure 30].

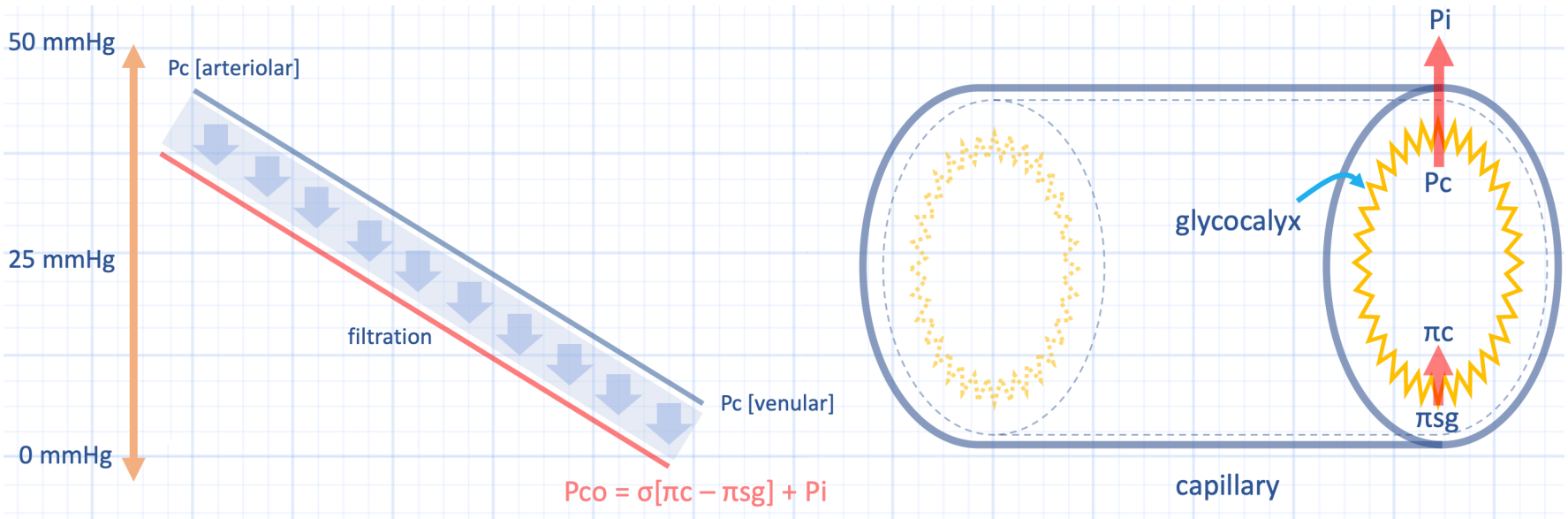

Figure 30: The glycocalyx model showing filtration throughout the capillary, but at a lower value due to the difference between the colloid osmotic pressure within the capillary [πc], less the low colloid osmotic pressure in the sub-glycocalyx space [πsg].

Implications for Practice

The revised Starling-Glycocalyx model explains why there is little difference in hemodynamic outcome and infused volume between colloid and isotonic crystalloid in many trials. Because the colloid oncotic pressure differential is an 'intra-endothelial' force rather than 'trans-endothelial,' the volume expansion effect of colloids is diminished as predicted by the traditional model. It is argued that the greater the Pc falls, the stronger the argument for isotonic crystalloid – which will 'rehydrate' the EG [227]. The revised model thereby turns our focus to the pressure differential [Pc – Pi] as the key determinant of capillary filtration. Many patients in the intensive care unit are inflamed – for a variety of reasons. Inflammation dilates

pre-capillary arterioles which increases Pc. Simultaneously, inflammation changes the characteristics of the interstitium; the extracellular matrix increases its compliance. Thus, Pi is diminished and the transendothelial pressure differential rises [232]. Ostensibly, edema treatment should focus on the underlying cause of inflammation. It also suggests a protective mechanism of alpha agonists [e.g. norepinephrine] which constrict arterioles and, therefore, attenuate Pc.

The aforementioned physiology also calls into question the use of hyperoncotic albumin to draw fluid from the interstitial space, especially in the inflamed ICU patient [i.e. with a reduced Staverman coefficient]. An albumin bolus raises Pc favouring filtration, however, the hyperoncotic effect of 25% albumin [which has an oncotic pressure roughly 4 times that of human plasma] is argued to oppose filtration and even cause resorption. In septic patients, 200 mL of 20% albumin increased the plasma volume by 430 mL, with maximum effect occurring in the first 30 minutes [233]. There was an equally transient improvement in oxygenation during this time [226]. However, it is entirely possible that the increase in plasma volume was due to dehydration of the EG layer rather than imbibing interstitial fluid [230]. Additionally, the transient improvement in oxygenation may reflect improved tissue oxygen delivery with consequent increase in mixed venous oxygen saturation, as well as, diminished dead space perfusion. Importantly, the FADE Trial [234] is set to expand our knowledge here, but should albumin-furosemide not prove fruitful [235, 236], it may well confirm that many of us, myself included, have been suffering from a 'colloid delusion' [237].

Blood Pressure

Why is blood pressure measured by units of length [i.e. millimetres of mercury, mmHg]? What decides systolic and diastolic pressure? What are the determinants of tissue perfusion and what are the clinical implications of this physiology? Can we deceive ourselves into thinking a particular mean arterial pressure [MAP] is beneficial when, in fact, it is depriving tissue of life? In this brief section, I hope to provide foundation for the above – reasons to reexamine and remarkable references [238-242] for further reading around the omnipresent clinical metric with which we are so familiar.

First Principles

Pressure is a force deployed over an area. For example, the force of one's body [one's mass times gravitational acceleration towards the centre of the Earth – also known as weight] can apply more or less pressure to a snow bank depending upon the area of one's footwear – the premise behind snow shoes. Historically, when the force of blood applied across the area of the central arteries [i.e. blood pressure] was transduced to a manometer, a mass of mercury [i.e. mercury's density multiplied its volume] moved up the height of a column – measured in millimetres.

Recall that pressure sensed in this manner is equal to the product of the density of the fluid, gravitational acceleration and height achieved [i.e. pressure = pgh]. Because gravitational acceleration is part of the equation, the elevation at which the pressure is transduced, matters. However, like many of my physiological expositions, the clinical relevance is small. Blood pressure measured by mercury manometry at the peak of Mount Everest is only reduced by 0.2% [240].

Systole and Diastole

Peak systolic pressure is determined by the peak blood volume present in the central arteries during systole and the compliance of the vessels. Importantly, vascular compliance decreases with age and total volume. In other words, at a high baseline blood volume, ejection of additional blood causes greater pressure change than if the same volume entered the central arteries at a lower baseline volume [240]. This physiology is accentuated with each decade of life as the vessels become stiffer [243].

The diastolic pressure is determined by the rate of pressure decay in the central arteries and the time allowed for diastole to transpire. For example, rapid decay time [i.e. short time constant] combined with long diastole favours low diastolic pressure and vice versa. But what is a time constant of the central arteries? If we assume that the decay from peak systole is mono-exponential, it takes roughly 5 time constants for a distensible structure to return to its baseline state of deformation. A time constant is the product of compliance and downstream resistance. Therefore, a poorly compliant aorta [e.g. old, unhealthy, high volume], coupled with a low downstream resistance [e.g. vasodilator, sepsis, high metabolic demands] radically reduces the decay-time from systole to diastole. If this is coupled with a long duration of diastole [e.g. beta-blocker], then the final diastolic pressure can be quite low [figure 31].

An important clinical implication of the above is that of calculated 'vascular resistance'; this has been covered previously in the context of pulmonary vascular resistance [244-246] [see chapters 2, 7 and below]. True downstream resistance may be stable, or even decrease, but if the compliance of the central arteries worsens, then the systolic blood pressure, the mean arterial pressure [MAP] and, consequently, the calculated vascular resistance will rise for a given flow. This was demonstrated in a canine study where the aorta was reinforced with plastic [decreased compliance] [247]. While there was no change in downstream arteriolar constriction [i.e. 'true' resistance], the calculated vascular resistance rose by 20% because of the stiffened aorta. Clinically, an overloaded patient with a high heart rate could 'congest' the aorta and acutely stiffen the central vascular space.

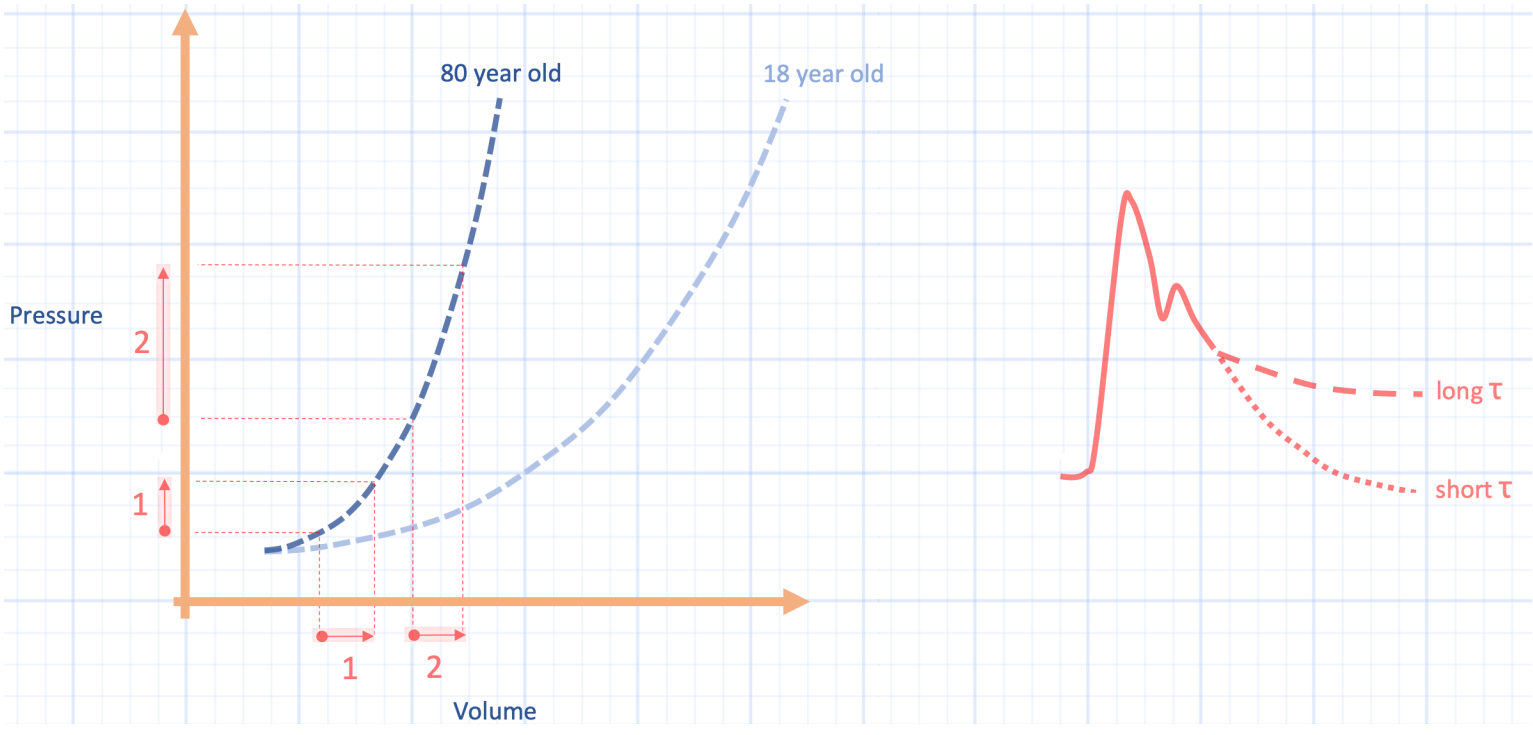

Figure 31: Determinants of systole and diastole. Left panel shows importance of vascular compliance. Volume [x-axis] or flow [assuming stable heart rate] may be the same [compare hypothetical stroke volume 1 to 2 under abscissa], yet change in pulse pressure from diastole to systole along the y-axis is different because of vascular compliance. This has implications for calculated vascular resistance [see text]. Right panel illustrates the difference between long and short time-constant physiology [tau (t) is time constant].

Determinant not Indicator

Blood pressure is a determinant but not an indicator of tissue perfusion [239, 240]. What does this mean? While targeting a specific MAP is recommended in sepsis and septic shock – this may represent a form of 'tangible bias' [238, 241, 242]. In other words, we perceive variables that we can know and measure as more important than they are. Thus, we mistake blood pressure – which we can measure – as an important indication of tissue perfusion, which it is not, per se. If we consider an extreme example – Resuscitative Endovascular Balloon Occlusion of the Aorta [REBOA] – whereby the aorta is occluded by an endovascular balloon in the setting of traumatic blood loss, we raise the measurable MAP, but vastly diminish tissue perfusion [i.e. everything distal to the balloon].

While the example of REBOA is obviously physiological hyperbole, it reminds us that regional organ perfusion is determined not simply by its pressure head [MAP] but also by local resistance. In the setting of REBOA, the local resistance is infinitely high. Increasing MAP at the expense of local perfusion may also be achieved by excessive alpha-receptor agonism which we have all, no doubt, observed in the ICU as skin mottling and/or digital ischemia. How do we reconcile this dissonant clinical scenario where we may be placated by an acceptable MAP yet dispirited by signs of tissue starvation?

As an analogy, consider the quintessential New York City water towers that dot rooftops of the Manhattan skyline. These towers must be filled [e.g. cardiac output] with water and maintain a constant pressure-head [e.g. MAP] for the units in the building [e.g. the tissues]. Some of the units may require large flow – say for manufacturing – and have a low resistance. While other units may require

intermittent flow – say for residential – and have relatively high resistance. Accordingly, it is the local demand that determines local resistance and local perfusion. It is expected that cardiac output – the rate of fill of the tower – be independent from the flow in specific units of the building. Increasing flow into the water tank won't increase the perfusion of a vacant apartment unit! Yet if the water tower runs dry, it is imperative that it be re-filled by increasing its inflow rather than by demanding that all of the building units pinch off their faucets.

In other words, driving up MAP by high-dose vasopressors can be deceptively reassuring. If there is evidence of poor tissue perfusion and if the vital organs are tolerant of further fluid, then augmenting cardiac output with additional volume is physiologically appropriate.

All Perfusion Is Local

To reiterate, mean arterial pressure [MAP] is a determinant, but not an indicator, of perfusion [240, 248]. With the recent 65 Trial [249], deeper exploration of tissue perfusion is warranted. Accordingly, this section provides a new way of visualizing the relationship between macro and micro hemodynamics – a conceptual approach which, hopefully, helps the clinician ponder therapeutic control of the circulation.

Independent and Dependent Variables

The first independent variable of the circulation is blood flow, or cardiac output; therefore, in figure 32, cardiac output is plotted on the x-axis. In vivo, blood flow is stimulated by tissue oxygen demand [248, 250]. Therapeutically, cardiac output is increased by either augmenting preload and/or using vasoactive medications [see figure 1].

The second independent variable of the circulation is tissue conductance. Conductance is the inverse of resistance; in other words, elevated tissue conductance is equivalent to decreased resistance [e.g. vasodilation] and vice versa. For simplicity, this analysis considers a simplified two-tissue system each with variable conductance [i.e. tissue conductance is the slope of the blue and red lines in figure 32]. In vivo, tissue conductance is changed by both systemic [e.g. adrenal release of catecholamines] and local factors [e.g. autoregulation]. Therapeutically, tissue conductance may be mediated by the provision of vasoactives [e.g. norepinephrine, phenylephrine, etc.]. Importantly, tissue conductance is both highly dynamic and tissue-specific. Muscle, splanchnic tissue, the heart and kidney all have different baseline and capacities to adjust conductance [248, 251]. Accordingly, each tissue may respond differentially in the face of identical changes in MAP.

The first dependent variable of the circulation is MAP – plotted on the y-axis in figure 32. MAP is forged by blood flowing against 'total vascular resistance' [purple

line, figure 32]. For simplicity, this analysis ignores the other components of the 3-element model of vascular impedance. Thus, the change in 'total vascular resistance' [purple line] is completely propelled by changes in tissue conductance. Consequently, 'total vascular resistance' depicts the summed conductance of both tissue 1 [blue line, figure 32] and tissue 2 [red line, figure 32].

Crucially, MAP acts as an intermediary, independent variable for regional tissue flow – the second dependent variable of the circulation and plotted on the y-axis of figure 32. Note that regional tissue flow is a function of changing MAP and the tissue's unique conductance. The figure shows what happens when cardiac output rises [e.g. provision of intravenous fluids]. Cardiac output and, accordingly, MAP rises along the lumped vascular resistance curve. The increase in MAP then acts as an intermediary to increase regional tissue flow along each tissue's individual conductance curve.

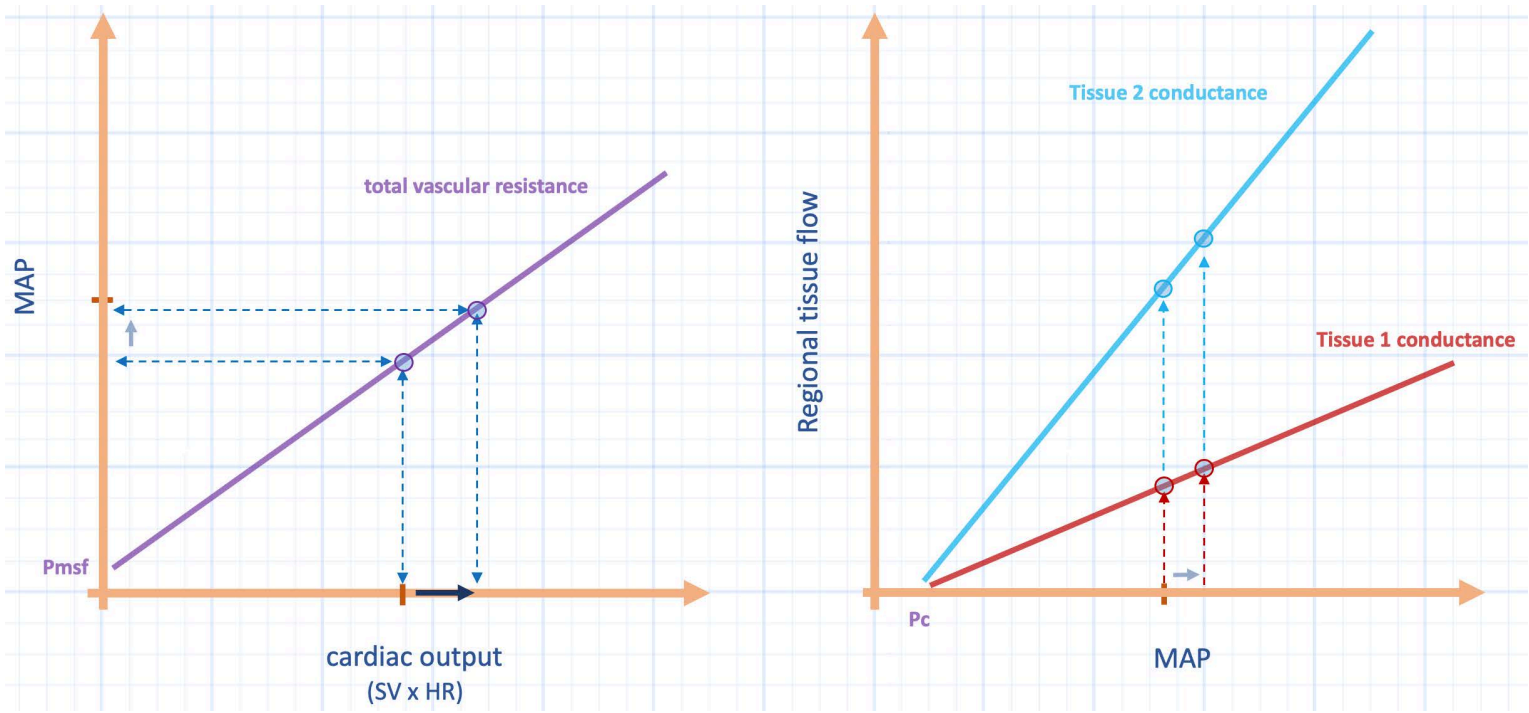

Figure 32: Macrovascular-microvascular perfusion. Left panel is relationship between cardiac output and mean arterial pressure [macrovascular]. Right panel is relationship between mean arterial pressure and regional tissue flow [microvascular]. Tissue 1 & tissue 2 are two hypothetical tissues for illustration. SV is stroke volume; HR is heart rate; Pmsf is mean systemic filling pressure; Pc is closing pressure.

Macro-microvascular Dissociation

Figure 33 is identical to figure 32, however, figure 33 is combined into a single 3-dimensional plot. The x-z plane describes how cardiac output [x-axis] changes MAP [z-axis] which simultaneously acts upon the conductance of each individual tissue to drive local flow [y-axis]. Again, individual tissue conductance [i.e. slopes of blue and red lines, y-z plane] combine to determine the lumped 'total vascular resistance' [slope of purple line, x-z plane].

From this graphic, it is clear that changing macrovascular hemodynamics [i.e. cardiac output on x-axis] has variable effects on microvascular hemodynamics [regional tissue flow on y-axis]. In other words, macro-microvascular dissociation is

normal and expected; 'coherence' should not be assumed to exist [252]! Investigations trying to relate the two are almost certainly doomed to fail.

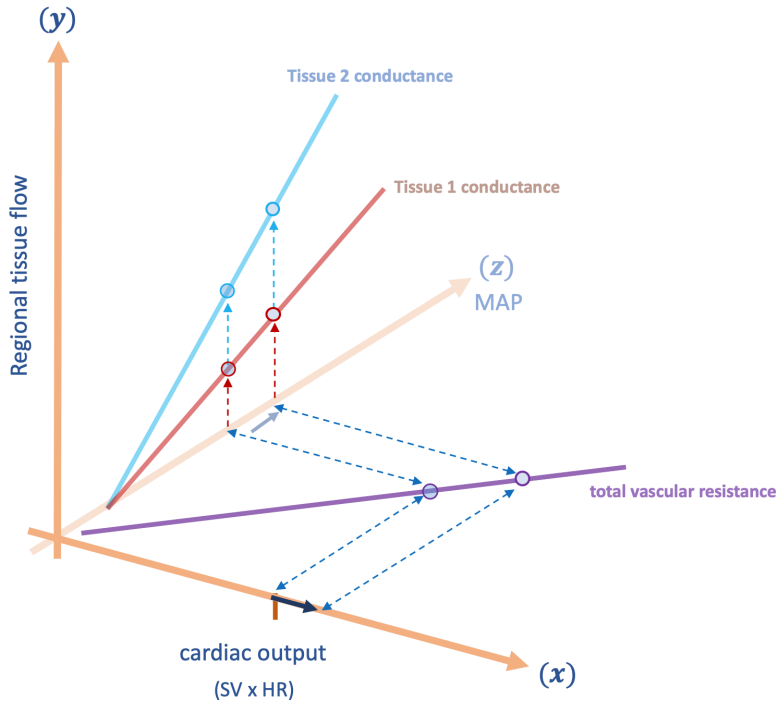

Figure 33: Combined macrovascular-microvascular perfusion diagram. This is the same as figure 32, combined into 3D graphic. It shows the relationship between macrovascular hemodynamics on the x,z-plane and microvascular hemodynamics on the y,z-plane. Mean arterial pressure is the z-axis directed into the page. Faded lines and points represent baseline condition and emboldened lines and points represent response to intervention [here an increase in cardiac output].

Selective Vasoconstriction

Figure 34 shows the hypothetical effect of selectively vasoconstricting tissue 2 [i.e. decreased conductance of tissue 2]. The fall in tissue conductance on the y-z plane increases 'total vascular resistance' on the x-z plane. If cardiac output is unchanged, then MAP rises – increasing the regional flow of tissue 1 [red curve] while decreasing the flow to tissue 2 [blue curve]. An imperfect clinical correlation is the provision of angiotensin II [253, 254] which selectively reduces the conductance of the kidney. This highlights the local complexities of 'tissue perfusion.' Diminished conductance and, therefore, flow in an organ like the kidney, may paradoxically improve glomerular perfusion because of the unique physiology of the kidneys. At the same time, a selective fall in conductance of vascular beds supplying the fingers or the visceral organs could lead to digital and mesenteric ischemia, respectively.

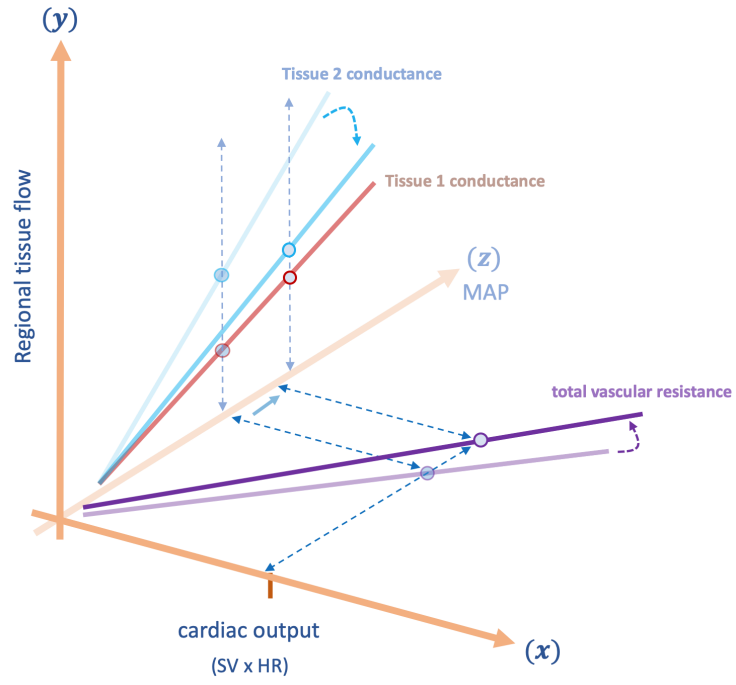

Figure 34: A selective reduction in conductance [increased resistance] of tissue 2. Faded points and lines represent baseline while emboldened points and lines represent effect of intervention. MAP rises [z-axis], but only tissue 1 sees an increase in flow. See text for details.

Global Vasoconstriction

Figure 35 illustrates globally reduced tissue conductance. A clinical example might be high dose phenylephrine [238] or methylene blue. Here, diminished tissue conductance greatly augments total vascular resistance on the x-z plane. If cardiac output is unchanged, then MAP [y-axis] rises significantly; however, despite a boosted MAP, regional tissue flow [y-axis] falls for both tissues. If cardiac output were to drop [e.g. from high afterload], regional tissue flow would diminish further [not pictured]. Note that norepinephrine could have a similar effect; cardiac output may rise [255] or fall [35] in response to norepinephrine.

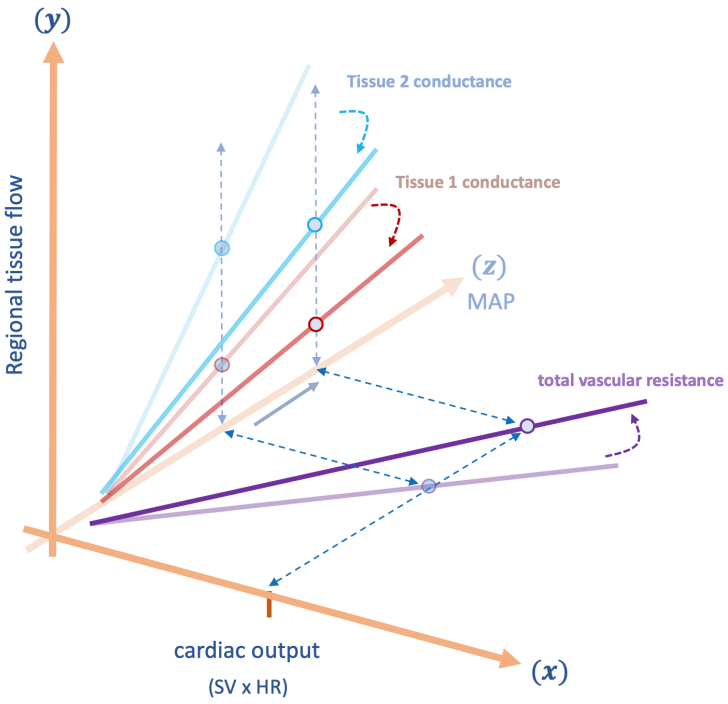

Figure 35: Global vasoconstriction depicted as reduced conductance [increased resistance] of tissue 1 and 2. Faded points and lines represent baseline while emboldened points and lines represent effect of

intervention. MAP rises considerably [z-axis], but regional tissue flow [y-axis] falls for both tissues. See text for details.

Global Vasodilation

On the other hand, if all tissues increased their conductance in exact proportion, the fall in MAP [z-axis] is offset and local tissue flow [y-axis] is preserved or even improved [see figure 36]. This physiology may be how some individuals live with unusually low mean arterial pressures [240, 248]. Thus, the key insult to tissues secondary to vasodilation is when some vascular beds increase their conductance relative to others; the latter tissues have their local flow impaired the most. This is especially prominent for tissues with a high baseline conductance, like the kidneys.

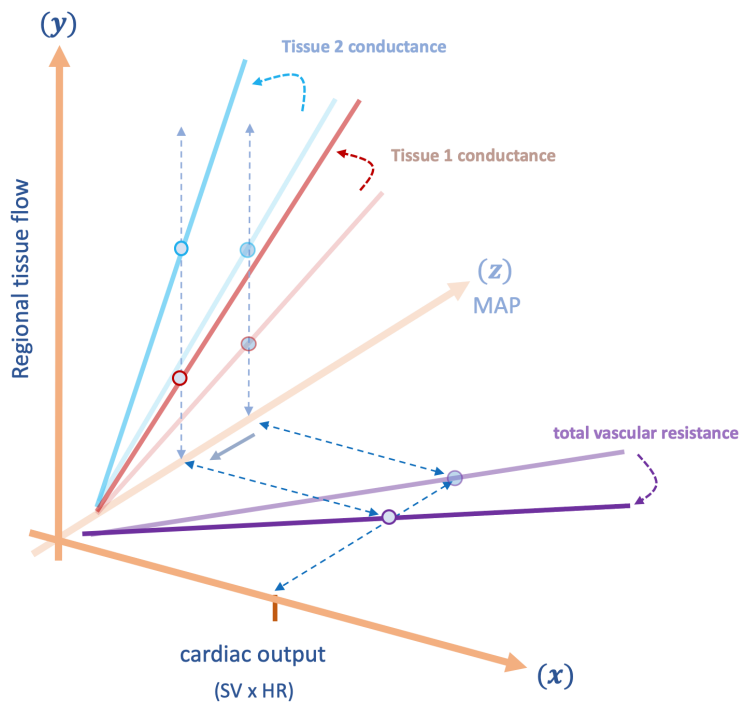

Figure 36: Global vasodilation. Both tissues increase their conductances in proportion. Faded points and lines represent baseline while emboldened points and lines represent effect of intervention. Had only tissue 1 increased its conductance, the fall in MAP [z-axis] would have decreased tissue 2 regional flow; because both tissues increase conductance, the fall in MAP is met by increased flow for both tissues [y-axis]. See text for details.

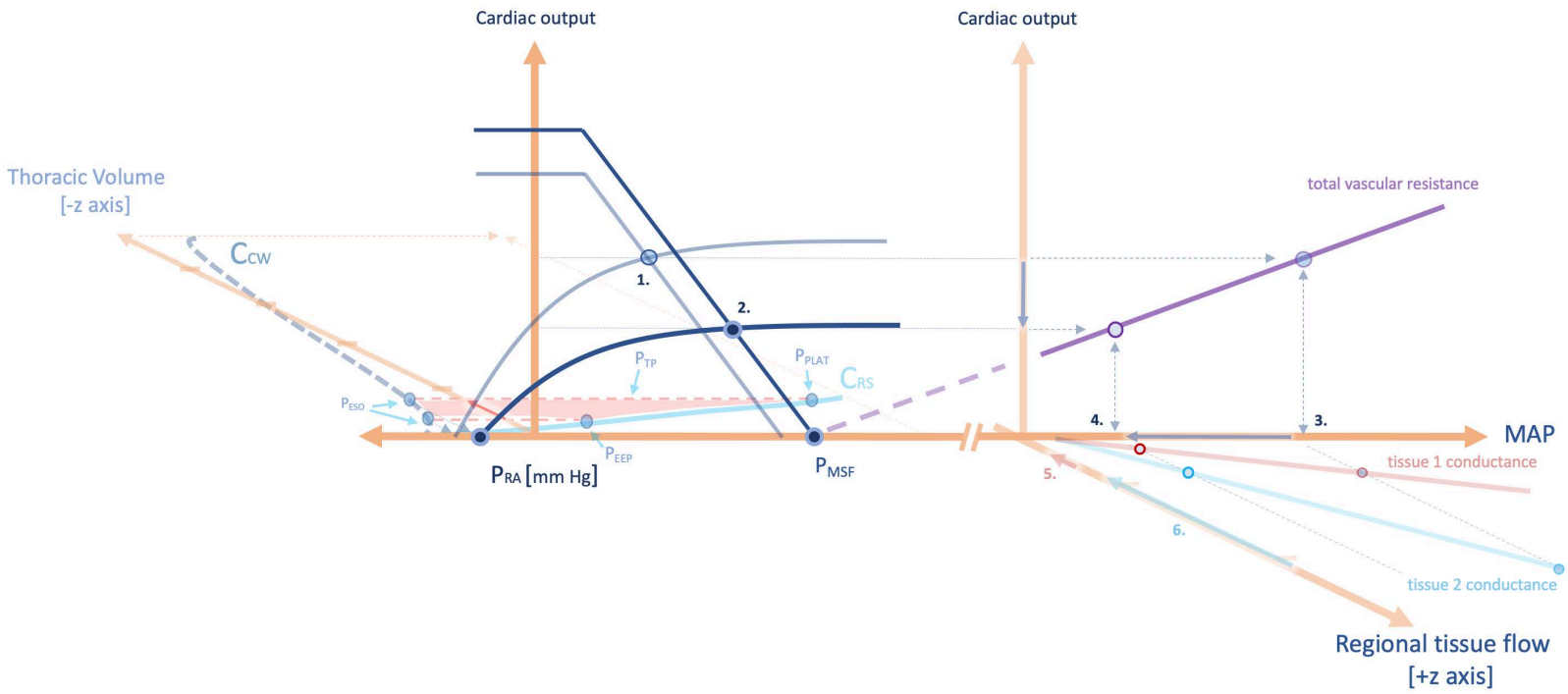

Figure 37: From mechanical heart-lung interaction to tissue perfusion. This is a combination of figure 22 and 33. Left panel shows a large trans-pulmonary pressure [Ptp] generated when a ventilator breath is given [red arrow in -z axis; red shade is elastic pulmonary driving power], this flattens the cardiac function curve slope such that cardiac output on the y axis falls from point 1 to point 2; here the x-axis is right atrial pressure [Pra]. Right panel shows that fall in cardiac output on the y-axis translates into a fall in mean arterial pressure [MAP, x-axis]. The fall in MAP follows the total vascular resistance in purple from point 3 to 4. Diminished MAP translates into diminished tissue perfusion in tissue 1 down its conductance curve [arrow 5 on +z axis] and in tissue 2 [arrow 6 on +z axis]. This graphic assumes no compensatory change in adrenergic tone which would affect venous return, cardiac function and tissue conductance disparately. These relationships highlight the complexity and variable outcomes in hemodynamic research! Pplat is plateau pressure, Peso is esophageal pressure; Crs is respiratory system compliance and Ccw is chest wall compliance. Pmsf is mean systemic filling pressure.

In summary, MAP is determined by lumped vascular resistance while simultaneously driving local tissue perfusion based on regional tissue conductance. Diminished tissue conductance can raise MAP yet impair local flow, while increased tissue conductance may lower MAP with preserved local flow. For these reasons, resuscitation based on markers of regional perfusion [e.g. capillary refill] and the concept of 'permissive hypotension,' [256] carry some physiological weight.

We might think about hemodynamics as the late Tip O'Neil famously described running for office: all perfusion, like politics, is local.

The Folly of Pulmonary Vascular Resistance

When interpreting hemodynamic studies of drugs which, potentially, alter the resistance of the pulmonary vascular tree, we often turn to the calculated pulmonary vascular resistance [cPVR] as our guide. For instance, a vasopressor determined to increase the cPVR is wholly avoided in a patient with pulmonary arterial hypertension. We envision the vascular conduits of the lungs crushed under

pharmacological assault – blood vessels pinched and puckered like one's lips biting into tart citrus. Conversely, a drug noted to lower the cPVR is championed for those with truly high impedance to blood flow through the lungs. Under the influence of this drug, we envision the vascular conduits of the lungs liberated – pulmonary blood vessels yawning wide, singing praise in a soft chorus of hemodynamic hallelujah. But is this calculated variable telling us – specifically – what is happening within the pulmonary vascular bed? Is there a mechanistic link between this derived variable and the physiological forces operating between the right ventricle and left atrium?

The Calculated Pulmonary Vascular Resistance

The cPVR is composed of 4 measured variables from a pulmonary artery catheter [PAC]. The pulmonary artery systolic pressure [PAs] and pulmonary artery diastolic pressure [PAd] determine the mean pulmonary artery pressure [mPAP]. One might consider the mPAP as the 'pressure head' for blood flow through the lungs. The pulmonary artery occlusion pressure [Ppao] – oft referred to as the 'wedge pressure' – can be thought of as the 'pressure sink' or down-stream pressure for pulmonary blood flow. The difference between the mPAP and the Ppao is referred to as the 'transpulmonary pressure' [TPP] and this gradient forms the numerator of the cPVR. The denominator of the cPVR is blood flow through the lungs, which at steady state is equal to total cardiac output; blood flow is typically determined by thermodilution.

$$(4)\quad TPP = [mPAP\ -\ Ppao]$$

Equation 4: TPP is transpulmonary pressure gradient which is composed of the mean pulmonary artery pressure [mPAP] and pulmonary artery occlusion pressure [Ppao].

$$(5)\quad PVR = \frac{TPP}{cardiac\ output}$$

or

$$(6)\quad PVR = \frac{[PAs\ + PAd]\ -\ Ppao}{cardiac\ output}$$

Equations 5 & 6: The mPAP is determined by the pulmonary artery systolic pressure [PAs] and PA diastolic pressure [PAd]. Dividing the TPP by the cardiac output gives the calculated pulmonary vascular resistance [cPVR]. I have omitted the fixed constants 1/3 and 2/3 for simplicity.

The Pulmonary Vascular Resistance is a Meaningless Variable

The misuse and misunderstanding of the PVR was described at least 30 years ago [245], reconsidered over 10 years ago [246] and elegantly demystified in this

physiological treatise [244]. To appreciate why this provocative claim is raised, consider how the cPVR changes in the two following thought experiments.

Figure 38 contemplates slowly cross-clamping the left main pulmonary artery and following what the PAC 'sees.' There is an increase in all of: the PAs, PAd and therefore the mPAP. Importantly, the numerator [TPP] rises and there is diminished cardiac output. Consequently, the cPVR rises and this experiment is referred to as a 'true' increase in pulmonary vascular resistance because the pathophysiology actually lies within the pulmonary tree. This is somewhat akin to an acute PE.

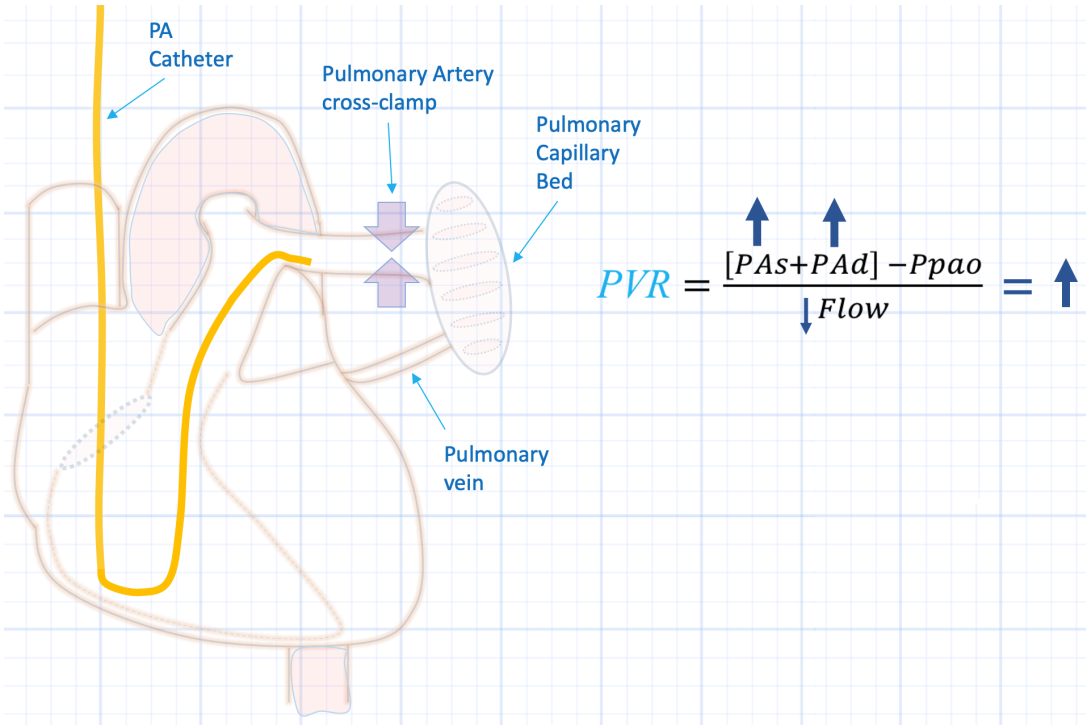

Figure 38: Thought experiment 1. Partially cross-clamping the left main pulmonary artery results in the pulmonary artery catheter [PAC, yellow] 'seeing' a higher PAs and PAd. This increases the TPP, reduces blood flow and, therefore, increases the cPVR; a clinical example here might be an acute PE.

Figure 39 considers slowly cross-clamping the descending aorta, just below the diaphragm. Now what does the PAC 'see'? Here, left ventricular outflow is impaired, so the Ppao and, therefore, pulmonary venous pressure increases. This, consequently, recruits and dilates the pulmonary vascular bed [i.e. why one sees 'cephalization' on a CXR]. Now, the pulmonary blood vessels maximally distend to their elastic limits. In other words, the pulmonary blood vessels are stiff [257] [high elastance, low compliance] such that when the right ventricle ejects blood into the pulmonary arteries, the PAs increases disproportionately owning to a stroke volume thrown against tense blood vessels. This is akin to why the peak pressure on a ventilator rises when the lungs are stiff – an incredibly salient point and the basis of this entire section. While the pulmonary tree is dilated [and therefore resistance is low], it is simultaneously stiff and this disproportionately increases the mPAP to the Ppao – the pressure gradient across the pulmonary bed rises and blood flow falls. The cPVR rises, but the pathophysiology lies entirely outside of the thorax. This is an 'apparent' increase in PVR – lowering the LV afterload [i.e. unclamping the aorta] attenuates the calculated PVR without any direct effect on

the pulmonary vascular bed. Figure 39 is clinically similar to acute left ventricular heart failure.

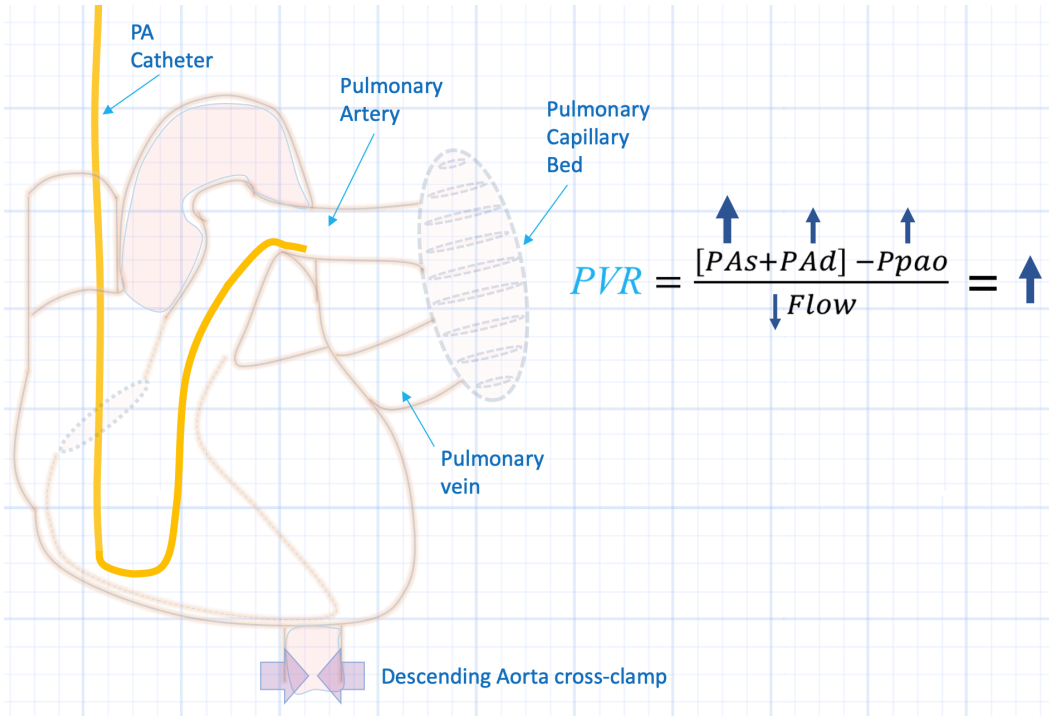

Figure 39: Thought experiment 2. Partially cross-clamping the descending aorta results in high Ppao, pulmonary venous pressure and the pulmonary vasculature recruits, distends and becomes stiff. Now, the PAC 'sees' a higher PAs as blood is ejected into a poorly compliant vascular bed. While this [like thought experiment 1] increases the TPP, the Ppao and PAd rise in tandem, preserving the PAd - Ppao difference. Note that the cPVR rises - just as much as in thought experiment 1, yet the locus of pathology is entirely different! A clinical example here might be acute systolic heart failure with flash pulmonary edema.

How do we distinguish a difference between physiology 1 and physiology 2? The answer lies in the PAd – Ppao difference [244, 258]. In example 2 [e.g. WHO II pulmonary hypertension], the PAd – Ppao difference remains small because the PAd and Ppao rise together; the difference is normally less than 6 mmHg. In example 1 [e.g. WHO I pulmonary hypertension], the PAd rises much more than the Ppao.

Implications for Practice

It should be clear from the aforementioned, that it is not adequate to imply mechanisms from the cPVR alone, especially with respect to the pulmonary vascular tree. Noting an increase in the cPVR following an intervention should be followed with an inquiry into why the cPVR increased. Was it driven by a change in the pressure gradient [numerator] and if so, how? Did the PAd increase with respect to the Ppao [i.e. a true increase in resistance – thought experiment 1], or did the transpulmonary gradient rise solely because of increased PAs with preserved PAd-Ppao gradient [i.e. an apparent increase in resistance – thought experiment 2].

Consider a study seeking to determine if a drug [e.g. phenylephrine] increases PVR. Should the study only report the cPVR, we are physiologically unable to precisely distinguish the effects of phenylephrine on the pulmonary tree unless we

know the PAd – Ppao gradient. Perhaps this drug is causing thought experiment 2 physiology?

Conversely, consider a study seeking to determine if a drug [e.g. a phosphodiesterase inhibitor] reduces PVR. Should the study only report cPVR, we are physiologically unable to determine if this drug is specifically reducing resistance within the thorax. Perhaps only the LV afterload falls [e.g. aortic cross-clamp removed] such that the pulmonary vascular tree decongests and the apparent reduction in PVR is just that – apparent.

In conclusion, the cPVR is not meaningless, but it is certainly confounded. Avoid folly, be clear in your approach – demand the PAd-Ppao!

The Right Ventricular Afterload

We are sometimes told that paralysis is important when intubating patients with pulmonary arterial hypertension to blunt the Valsalva maneuver. The reasoning being that elevated pulmonary arterial pressure from 'bearing-down' raises right ventricular afterload; that is, putting the right heart in danger of distension and failure. Is this accurate?

Left and Right Ventricular Stress

Trainees are commonly quizzed on the physiology of systolic wall stress or tension which is considered to be the most accurate assessment of ventricular afterload [4] [see also chapter 7]. While stress is not the same as pressure, they are related. In a perfect sphere, Laplace's law tells us that the tension experienced by the wall of a sphere is directly proportional the pressure gradient across the sphere as well as its radius but inversely proportional to the thickness of the wall [4]. This approximates the wall stress of the ellipsoid left ventricle [LV] fairly well – though more specific equations have been derived [259] – because wall tension is related to a force vector acting perpendicular to the wall; in the LV, the cardiac muscle shortens circumferentially. In the normal LV, the peak wall tension occurs at the very end of isovolumic contraction, just prior to the aortic valve opening [260]. At this point the transmural LV cavity pressure is greatest with respect to the LV radius. While LV cavity pressure does rise beyond aortic valve opening, radius is concomitantly decreasing during ejection. Accordingly, wall stress falls despite rising intra-cavitary pressure.

By contrast, the relationship between the right ventricular cross-sectional area [i.e. its radius] and its wall stress is muddied. The right ventricle [RV] is not ellipsoid, but rather crescent-shaped and, during ejection, the RV contracts in a peristaltic fashion; the infandibular outflow tract contracts last and sees the highest ejection pressure compared to the RV free wall [261]. Accordingly, the force against which the RV acts does not lie perpendicular to its contraction as it does in the normal

LV. Also, in significant distinction to the LV, peak wall tension of the RV is hard to define because of the RV's different pressure-volume relationship and ventricular systolic interdependence [262, 263]. Despite this, groups have tried to define peak RV wall stress using modifications of the Laplace law [264, 265]. As a result, there is some inherent value in the Laplace formulation when approaching the RV, because pathophysiological events that increase RV volume [i.e. its 'radius'] or the pressure against which the RV ejects, both augment RV wall tension to some degree. This provides a model from which one can consider the concept of RV afterload.

Pulmonary Vascular Resistance

The commonly-taught afterload for the right ventricle is the calculated pulmonary vascular resistance [cPVR]; as per the previous sections and chapters, there are problems with this dogma [245, 246]. Deriving resistance as a simple relationship between pressure and flow applies to non-pulsatile, non-branching, cylindrical tubes – the pulmonary vascular tree is anything but [258]. Mathematically, the PVR generates a linear relationship. If pressure is on the x-axis and flow on the y-axis, the origin is the left atrial pressure [Pla] and the slope of the line defines the PVR. But the pressure-flow relationship for the pulmonary vascular bed is not linear, it is curvilinear [266]. The reasons for the curvilinear relationship lie within the physiology of the vascular bed in totality as well as the individual vessels. First, in any vascular bed, a critical closing pressure must be surpassed prior to flow generation. This effect shifts the pressure-flow relationship along the [pressure] x-axis, away from the origin. In the pulmonary vascular system, this effect is caused by Starling resistors, that is, vascular beds where the perivascular pressure [e.g. alveolar pressure] eclipses the intravascular pressure. This phenomenon has been called 'Starling resistance' to distinguish it from classical 'Pouiseulle' resistance described below [245]. Because Starling resistance shifts the pressure-flow relationship in parallel along the x-axis, PVR calculation using Pla as the downstream pressure overestimates the true vascular 'resistance' faced by the RV [267] [figure 40]. This physiology is considered in more detail below within the context of pulmonary embolism.

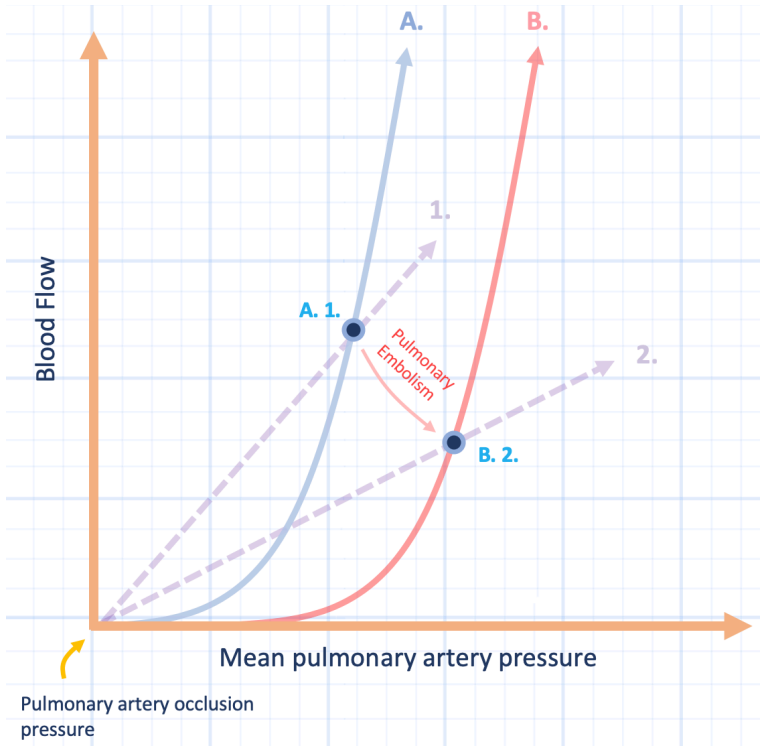

Figure 40: Hypothetical pressure-flow relationship for a pulmonary embolism. The true pressure-flow plot for the pulmonary vascular system at baseline is the blue, curved plot A. The cPVR at baseline is the slope of the dotted line 1. Note that the slope of the dotted line 1 is less [i.e. pulmonary vascular conductance has decreased, or resistance has increased] than the slope of the blue curved line [i.e. cPVR overestimates true 'resistance']. A pulmonary embolism moves the system from point A1 to B2. The truth is that there is an increase in Starling resistance [blue curve A shifts rightwards to red curve B]. Yet the cPVR is now the slope of the dotted line 2. Again, this over-estimates the true load seen by the right ventricle.

Second, individual blood vessels are distensible. Consequently, as the driving pressure within a single vessel rises, the radial pressure of the vessel enlarges and therefore so does its radius. Vessel distension also depends on the vessel's compliance; an increase in radius lowers the vessel's resistance. Thus, pressure and resistance are physiologically linked in a manner whereby flow increases in a curvilinear fashion as a function of increased driving pressure [266]. Additionally, at the other end of the radius-pressure curve, increased pressure is generated for any given flow, as described in the previous section. This gives the impression that the vessel is constricting when in reality it is becoming more tense.

While the pressure-flow relationship is approximately linear over a limited range of physiological flows [268], ignoring the recruitment, dilation and stiffening of pulmonary blood vessels in the critically-ill means that a calculated change in PVR may or may not reflect any true change in pulmonary vascular vasomotor tone. This is clinically meaningful when interventions are thought to change pulmonary hemodynamics based only on PVR calculation. Consider a vasoactive substance that increases blood flow, yet because of pulmonary vascular recruitment and dilation there is only a small increase in mean pulmonary arterial pressure [mPAP]. The cPVR drops, but has there been a change in vasomotor tone? Will giving the same vasoactive substance to a patient in heart failure also lower the resistance to flow through the lungs? Would that medication improve pulmonary hemodynamics in severe ARDS? Type I pulmonary arterial hypertension [PAH]? The answer to all is probably no – but here's the rub – you can't know.

In response to these caveats, calculation of the PVR in the clinical setting has been considered 'meaningless' [245]. Regardless, PVR should be interpreted with

caution [246]. The aforementioned also explains why testing for vasodilator response in patients with PAH has moved away from PVR and towards the mPAP response with respect to a change in pulmonary blood flow. When there is a clinically meaningful fall in mPAP in the context of little change – or an increase – in pulmonary blood flow, then there has likely been true change in pulmonary vasomotor tone [246]. As above, another interesting approach is the pulmonary arterial diastolic-pulmonary artery occlusion pressure difference [244] which, in health, is essentially 0 mmHg [269]. If this value is higher than 5 mmHg, then there is likely increased resistance to flow through the pulmonary circulation. Lastly, all of the above underscore the importance of critically appraising papers that report the effect of vasopressors and inotropes on the pulmonary vascular tree – simply reporting a change in cPVR does not suffice.

Impedance

As blood flow is pulsatile, pulmonary vascular resistance [PVR] does not adequately account for the right ventricular hydraulic load – as discussed above [258]. In the early 1960s, vascular input impedance was first measured and reported [270]. Input impedance records the relationship between pulsatile pressure and flow; it is, unfortunately difficult in terms of both acquisition and interpretation [271]. Therefore, models have been proposed to help characterize impedance more simply. The foundation of these models was proposed by Frank well-over 100 years ago [271]; it is known as the Windkessel model and it takes into consideration both PVR and arterial compliance. Thus, the pulmonary circulation is viewed simply as having two biophysical properties acting in parallel – 1. capacitance which accepts RV stroke volume during systole and is characterized by compliance and 2. resistance which mediates vascular run-off and is described by the PVR. This is sometimes referred to as the 2-element Windkessel model and illustrated via an 'impedance triangle' [272, 273].

But the 2-element Windkessel was deemed inadequate as measures of impedance took hold 50 years ago. Consequently a third element was added to better explain the relationship between pulsatile pressure and flow – the characteristic impedance [Zc] [274]. Zc relates the acceleration of a mass of blood against a compliant vessel. In other words, at the onset of ventricular ejection, cardiac myocytes face a continuous column of dense blood which must be 'lifted' against distensible vessels – Zc accounts for this property in the 3-element Windkessel model. In this model, Zc acts first, in series, with compliance and resistance acting in parallel, as per the 2-element model [274, 275] [see chapter 2].

The relevance of the 3-element model is that it highlights multiple, potentially conflicting hemodynamic variables within the pulmonary circulation. Consider the commonly encountered patient in the ICU with elevated left atrial pressure [Pla]. Study of impedance has revealed that patients with high left heart filling pressures actually have decreased PVR – presumably due to passive congestion and recruitment of the pulmonary vascular tree [244]. However, the congestion also increases the volume of the blood vessels rendering them stiff [i.e. having a reduced

compliance]. The stiff blood vessels increase the pulse pressure which raises the mean pulmonary arterial pressure [mPAP] and, therefore, the transpulmonary gradient [mPAP – Pla]. This calculation may lead the clinician to spuriously think that there is increased 'resistance' [e.g. vascular remodelling or vasoconstriction] within the pulmonary circulation when, in actuality, there is passive congestion that will resolve with salt and water removal [244]. In such patients, the difference between the pulmonary arterial diastolic pressure and Pla is likely a better indication of changes in pulmonary vascular resistance [244], as detailed above.

Pulmonary Arterial Transmural Pressure

Given the complexity of impedance, are there any methods to simply deduce the hydraulic load faced by a ventricle? This problem was elegantly explored by Robotham's group in the late 1980s with respect to the left ventricle [276, 277]. Simply, they reasoned that increased systemic impedance – whatever the cause – would raise the transmural pressure of the aorta. The transmural pressure is the pressure within a vessel less its ambient pressure. Conversely, diminution of systemic impedance would lower aortic transmural pressure. Most importantly, rather than measuring the transmural pressure of the aorta with invasive catheters, they 'transduced' its value by measuring its diameter change [276, 277]. An increased systemic impedance would, therefore, raise the transmural pressure of the aorta and cause it to dilate. By contrast, attenuated systemic impedance leads to diminished aortic volume. One must not confuse aortic dilation with decreased resistance. An extreme increase in systemic afterload is abdominal aortic cross-clamp which would undoubtedly dilate the thoracic aorta. Conversely, sodium nitroprusside infusion reduces systemic afterload and increases peripheral vascular run-off. This intervention diminishes aortic diameter [278].

Similar reasoning has been applied to the transmural pressure of the pulmonary artery. Indeed, the distending pressure of the pulmonary artery rises when pulmonary vascular impedance is high such as hyperinflation and pulmonary emboli [279-281]. Conversely, interventions that diminish pulmonary circulatory impedance reduce pulmonary arterial transmural pressure [282]. Despite this data and the exploding interest in ICU echocardiography, there is a paucity of investigation into the effect of pulmonary arterial impedance upon echocardiographically-measured pulmonary artery diameter.

Valsalva, PVR and Pulmonary Arterial Impedance

During true Valsalva, lung volume does not change despite increased pressure within the entirety of the thorax. As a result, the pressures within the alveolus, all vascular structures, the pleural space and all chambers of the heart rise equally with respect to atmosphere. Importantly, this does not change the hydraulic load upon the RV because there is no pressure differential between the right heart and the alveolus – as occurs when lung volume changes [283]. Of most relevance, the effect

of Valsalva was studied [284] and erroneously concluded to raise right ventricular afterload because Valsalva augmented the calculated PVR. As discussed above, this highlights one of the many problems when using mathematically derived variables as surrogates for true physiological phenomena. The calculated PVR increased because the pressure within the thorax rose relative to blood flow, but most importantly, the study documented diminished pulmonary arterial transmural pressure during Valsalva. Reduced pulmonary arterial transmural pressure with Valsalva has also been observed by Pinsky [26, 33] [figure 41]. As above, this reveals decreased impedance to flow with Valsalva despite increased cPVR. Because increasing intra-thoracic pressure drops venous return, RV wall stress – as discussed above – is actually lessened by the Valsalva maneuver. Valsalva is dangerous in patients with PAH not because of augmented afterload but because these patients require preload to maintain RV output, akin to patients with high left ventricular outflow impedance – for example, aortic stenosis.

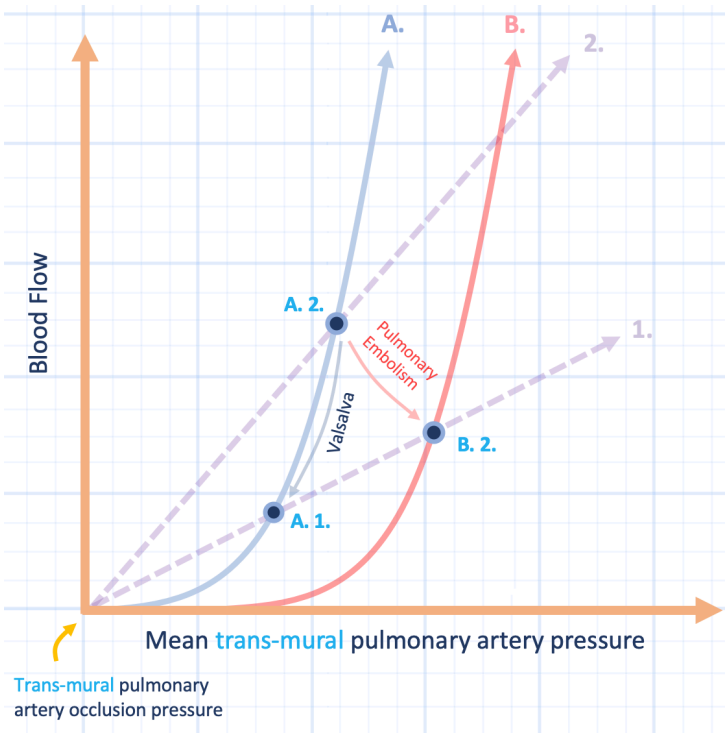

Figure 41: Valsalva on a pulmonary pressure-flow plot. When referenced to atmospheric pressure, the mean pulmonary artery pressure rises and cardiac output falls, spuriously suggesting that the cPVR rises. If referenced to an esophageal balloon [to obtain trans-mural pressure on x-axis], the pressure across the pulmonary vasculature actually falls from A2 to A1. Referencing this to pulmonary artery occlusion pressure [Ppao] still suggests a rise in resistance [slope of dotted line 2 compared to dotted line 1] even though the true nature of the pressure flow plot has not changed [blue curve A]!

Pulmonary Embolism and Syncope

The transient and reversible loss of consciousness that may accompany pulmonary embolism [PE] is well-documented [285-291]. This brief section will not address the controversy regarding the prevalence of PE in 'unexplained' syncope; rather, it will focus on pathomechanisms and serve as the foundation for later sections on pulmonary thromboembolism physiology.

Basics

Loss of consciousness typically requires that the mean arterial pressure fall by 30 – 40 mmHg for at least 7 seconds [292]. The dreadful experiments [i.e. the 'Red Wing Studies'] that confirmed this were considered in chapter 9 [see Fighter Pilots section]. An acute fall in MAP demands either an abrupt drop in cardiac output [i.e. flow] and/or in vascular resistance. When the central aortic pressure, or MAP, falls below the auto-regulatory threshold of the cerebrovascular system, cerebral perfusion plunges into darkness, so to speak.

Yet how, exactly, does PE lead to a transient fall in MAP? As expected, it's complicated and it depends upon the underlying reserve of the patient's cardiopulmonary system [293-296].

Stroke Volume in PE: free from cardiopulmonary disease

As above, the response of the right ventricle to a PE depends upon co-morbidities. To consider the effects of a PE in a patient free of cardiopulmonary disease [CPD] helps clarify the pathophysiology.

Right ventricular [RV] stroke volume [SV] is directly proportional to its end-diastolic volume, and indirectly proportional to pulmonary vascular load [293, 297]. In other words, RVSV tends to rise as the RV fills in end-diastole, but falls if there is a high outflow impedance [e.g. pulmonary vascular obstruction]. In a healthy RV, a relatively large obstruction is required to impair RVSV. In a classic set of observational studies [294], it was documented that 25-35% obstruction by angiography is required to increase mean pulmonary arterial pressure [mPAP] and cause RV dilatation; even anatomically profound obstruction [i.e. > 50%] is well adapted to by the healthy heart [298]. In animal models of PE, similar degrees of obstruction of the pulmonary vascular bed and mPAP elevation resulted in little, if any fall in SV [297, 299, 300]. Why?

RVSV is maintained by increased RV end-diastolic volume; preload is maintained as a consequence of adrenergic effects on the peripheral venous beds, which maintain the gradient for venous return [293]. Additionally, elevated RV contractility lowers RV end-systolic volume [RVESV] and helps maintain SV [298, 300]. Importantly, acute hypoxemia is a profound adrenergic stimulus which sustains the aforementioned adaptive mechanisms [301, 302].

Yet, there clearly is an obstruction threshold beyond which RV compensatory mechanisms fail. In one animal investigation, this was noted to be about 1000 dynes • sec / cm^5 [295]. Above this, there is disproportionate rise in RV end-systolic volume relative to RV end-diastolic volume in response to rising preload [299]. When SV falls in the face of growing RV end-diastolic pressure, RV failure has commenced.

How does this fall in RVSV translate to the left heart? There are, essentially, two broad mechanisms – so called, 'series' and 'parallel' effects [293, 297]. The 'series'

effect simply means that as RVSV falls, so too must LV preload as 2-3 cardiac cycles after RV output changes, the LV preload responds accordingly. More simply, the LV can only eject what it receives from its ventricular partner. 'Parallel' effects occur when the RV directly impinges upon the function of the LV and these are well-known and validated mechanisms of impaired LV output [303-305]. Via coupled pericardial restraint [306], increased RV diameter stiffens [i.e. decreases the compliance of] the LV; this has been convincingly demonstrated in animal and human models of pulmonary hypertension [307, 308]. The effect may also be mediated via a fall, or even reversal, in the trans-septal pressure gradient [309]. Additionally, coronary venous congestion [e.g. from high right atrial pressure] also stiffens the LV [310].

Attenuated SV by the mechanisms above – and if not buffered by tachycardia – leads to diminished central arterial blood volume. Accordingly, without an acute, compensatory rise in peripheral vascular resistance, MAP and cerebral perfusion fall.

Stroke Volume in PE: with cardiopulmonary disease

The mechanisms above also apply to the unhealthy cardiopulmonary system, yet their effects are magnified. In patients with PE and underlying cardiopulmonary disease, the average percent obstruction of the pulmonary vasculature observed is much lower with greater mPAP elevation and diminished cardiac output [294]. That large obstructions are rare in those with inadequate cardiopulmonary reserve suggests that obstruction beyond 50% is a terminal event in these patients. Additionally, in the unhealthy, falling stroke volume is less likely to be compensated by the reflex mechanisms that increase vascular resistance and MAP [311]. It is possible that some anti-hypertensive medications blunt the rise in central aortic pressure in the face of falling cardiac output [311]; the implications for right coronary perfusion pressure are discussed below.

Transient Nature of Syncope

While the aforementioned describes diminished flow into the central arterial space and an ensuing fall in MAP, it doesn't quite address how cerebral perfusion and, therefore, consciousness returns.

One potential mechanism is that a large PE induces neurocardiogenic syncope [292]. As above, an abrupt rise in RV volume and pressure can 'squeeze out' the LV; high contractility from adrenergic tone, coupled with diminished LV preload favours a vasodepressor response from the brain – the Bezold-Jarisch reflex [312]. Ensuing vasodilation drops MAP and consciousness is lost, only to return when the patient is supine and venous return rises. Indeed, extreme brady-dysrhythmias in response to large PE have been documented [291].

A second, non-mutually exclusive, mechanism is a rapid fall in pulmonary vascular resistance following the initial embolic event. Animal models have shown that while the anatomic location of a PE may change minimally after it initially wedges itself into the pulmonary circulation, hemodynamics and angiographic blood flow distribution may spontaneously improve [313]. This suggests recruitment and dilation of adjacent pulmonary vascular beds – allowing blood flow to find its way to the left heart. Notably, the supine position might promote parallel recruitment up to the lung apices. Clearly, this is blunted in a patient with diminished cross-sectional pulmonary vascular area [e.g. severe emphysema]. Thus, cardiopulmonary reserve and peripheral vasoconstrictive reflexes to maintain MAP may define the slim difference between transient and permanent loss of consciousness following pulmonary embolism.

Pulmonary Embolism and Pulmonary Vascular Resistance

What if I told you that, in acute PE, the initiation of intravenous norepinephrine [NE] decreases the calculated pulmonary vascular resistance [cPVR]? Would you believe me? Certainly, you would trust that an infusion of a thrombolytic does so. Of great interest, both NE and thrombolytics decrease the cPVR in acute PE [295, 296, 314-318]. But why is this? Could it be that NE induces the pulmonary circulation to open itself like an accordion – with an airy sigh and harmonic hum of blood stirring swiftly through dilated vascular bellows? Or might the cPVR be fooling us? Perhaps the concord of sounds we hear across the lungs is not driven by a dilating squeeze box, but rather express the synthetic sounds of simplified physiological assumptions? As described above and in previous chapters, you might know how this song concludes. By the end of this section, I hope to show how both NE and thrombolysis lower cPVR in acute PE, but how only the latter truly lowers the lifted load of the RV.

Basics

This section requires analysis of pulmonary artery pressure-flow [PQ] relationships [295, 296, 319]. These are graphical representations of the 'pulmonary vascular resistance' in its broadest sense. Here, the x-axis is blood flow [Q – cardiac output, the independent variable] and the y-axis is mean pulmonary artery pressure [P – the dependent variable]. Thus, the slope of a line on the PQ plot represents the change in P [in the numerator] for a given change in Q [in the denominator]; this is the calculated pulmonary vascular resistance [see figure 42].

Thought Experiment

Imagine that a patient has a normal mean pulmonary artery pressure [mPAP] at a normal cardiac output for a given pulmonary artery occlusion pressure [Ppao or 'wedge pressure']; this value is the green point on the PQ plot in figure 42. The slope of the line connecting the Ppao to the mPAP is the cPVR at this point [green dotted line].

Now imagine that this unfortunate patient suffers a very large PE. The mPAP rises and the cardiac output falls as depicted by the red point in figure 42. Assuming a constant Ppao, it is easily visualized that the slope of the line connecting the mPAP to the Ppao rises; that is, the cPVR increases [red dotted line]. In other words, for a given change in flow on the x-axis, the change in pressure on the y-axis is greater.

Finally, imagine initiating a NE infusion. The alpha effects of the drug improve the gradient for venous return [293], stimulating the right heart Frank-Starling mechanism and the mild inotropic effects increase the contractility of the heart. Accordingly, blood flow along the x-axis increases and so too does the mPAP as more blood fills the pulmonary circuit. This is illustrated by the orange point in figure 42; the dotted line connecting it to the constant Ppao demonstrates that the cPVR has decreased. In other words, as compared to the cPVR during acute PE [red dotted line], the change in pressure for a given change in blood flow is less with NE.

While the aforementioned is hypothetical, this physiology has been demonstrated in multiple animal models of acute PE treated with NE [295, 296, 314-316].

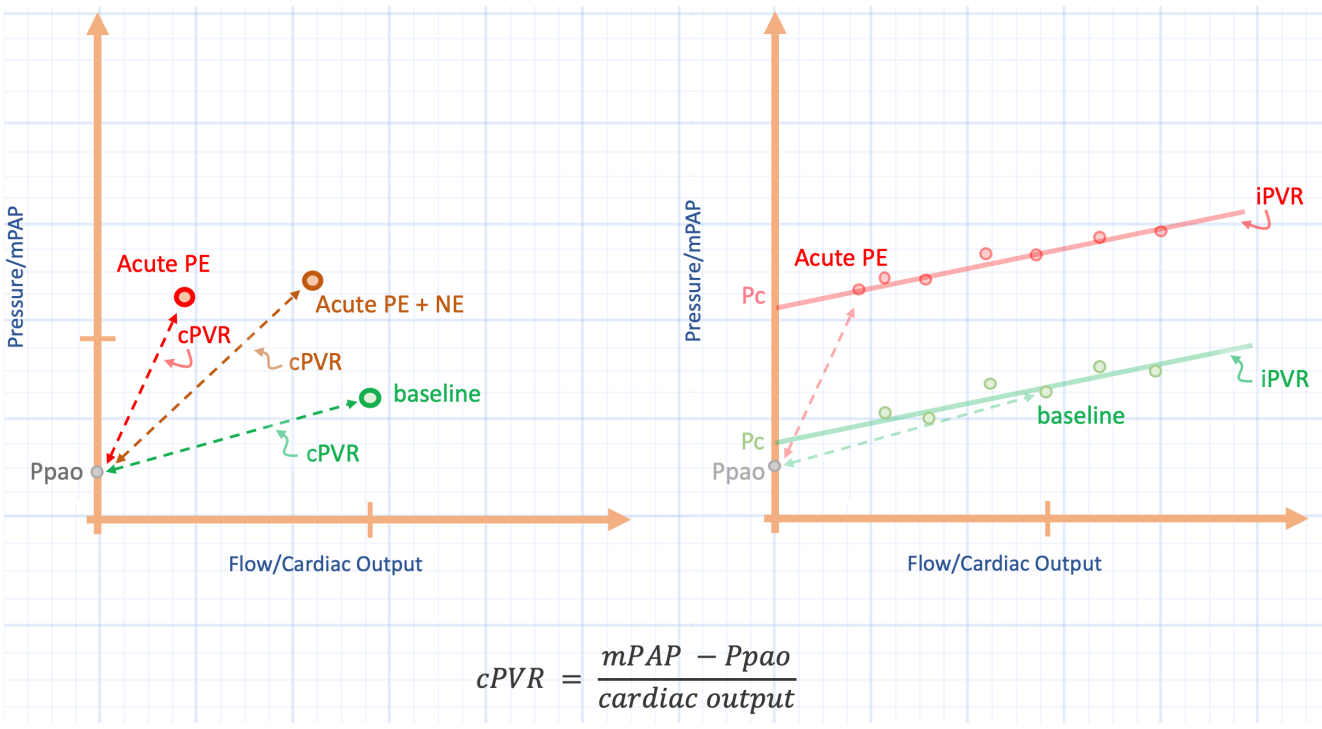

Figure 42: Pulmonary vascular pressure-flow [PQ] plots. Note that in contrast to figure 40 & 41, pressure is on the x-axis, so the slope here is resistance and not conductance as it was in the previous figures. Left panel shows the calculated pulmonary vascular resistance [cPVR] [slope of dotted line] at baseline [green], following PE [red] and with subsequent infusion of NE [orange]. Right panel shows extrapolated PQ plots for baseline [green] and following PE [red]. See text for details. Pc is closing pressure, Ppao is pulmonary artery occlusion pressure, mPAP is mean pulmonary artery pressure, iPVR is incremental pulmonary vascular resistance. Compare the iPVR to the cPVR for the right panel.

The Caveat

The rub is that the Ppao is often not the downstream pressure in the pulmonary circuit and certainly not so during acute PE. The downstream pressure is actually a 'closing pressure' [Pc] that must be overcome before flow occurs, and it is typically greater than the Ppao. The reason for this can be modelled using 'Starling resistors'; an example is the zones of West in the lung. While a particular portion of the lung may have a transpulmonary pressure [alveolar pressure minus the pleural pressure] of 15 mmHg with a Ppao of only 4 mmHg, the closing pressure [i.e. the pressure above which flow occurs, Pc] for the total lung is not 15 mmHg, but rather a conductance weighted-average of each lung section – illustrated mathematically by Mitzner decades ago [320, 321].

A way to measure the Pc of the pulmonary circulation is to measure multiple pressure-flow coordinates at a stable Ppao and extrapolate the line to the y-intercept of the PQ plot [295]. The Pc is typically slightly higher than the Ppao at most physiological values, but as the Ppao rises, the closing pressure and Ppao begin to equalize. In healthy dogs, this occurs at a Ppao of roughly 19 mmHg [321].

PE, NE and the PQ

How does an acute PE affect the PQ plot? Its most notable consequence is that it increases the closing pressure of the pulmonary circulation, with minimal effect on the slope of the PQ plot [see figure 43] [295, 296, 315, 322]. The slope of the red line from the mPAP to the closing pressure [rather than to the Ppao] has been coined the 'incremental' pulmonary vascular resistance [iPVR] to distinguish is from the cPVR, which is referenced to the Ppao. Thus PE, raises the Pc with minimal effect on the iPVR.

And what happens when NE is added to the mix? When a whole PQ plot is generated for a given dose of NE in PE, it lines up almost entirely upon the slope of the PE without NE [315]; accordingly, NE does not alter the iPVR [see figure 43]. Thus, the problem with the cPVR is easily seen graphically – the slope of the orange dotted line [cPVR for NE] falls when referenced to the Ppao. Yet, when correctly referenced to its Pc, there really is no change.

Thrombolysis

As anticipated, the effect of thrombolytics is to lower the closing pressure back to its baseline state following an acute PE [295, 317]. Lytics change the iPVR slightly, but its greatest benefit to the RV is by lowering the Pc – akin to 'opening' a very large Starling resistor [323] [see figure 43].

Alas, the dissonance of the cPVR still grates. With time, I pray, non-invasive measures of RV-pulmonary artery coupling [324] will ring truth like a warm, struck bell. Send not to know for whom the bell tolls; cPVR, it tolls for thee.

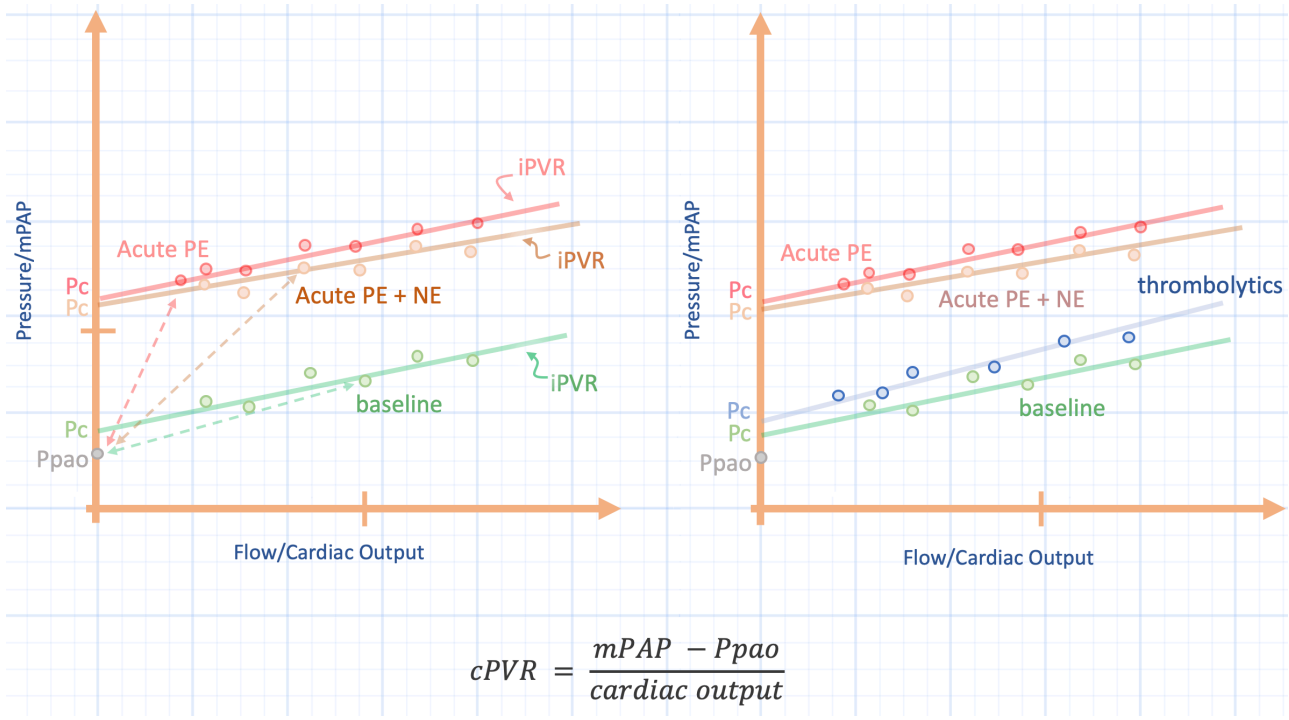

Figure 43: The effect of norepinephrine and tPA on pressure-flow [PQ] plots. Left panel shows the effect of NE infusion in PE using a full PQ plot; compare the iPVR [solid line] to cPVR [dotted line] during PE [red] and the addition of NE [orange]. Right panel shows the effect of tPA [blue]. See text for details. Pc is closing pressure, Ppao is pulmonary artery occlusion pressure, mPAP is mean pulmonary artery pressure, iPVR is incremental pulmonary vascular resistance.

Commonly, we are sold that acute PE burns the right ventricular candle at both ends. This is because perfusion of the right coronary artery [RCA] is mediated by both its upstream, mean arterial pressure [MAP] and downstream right ventricular end-diastolic pressure [RVEDP]. Given that PE may decrease the former and increase the latter, perfusion of the RCA is particularly precarious in the face of an acute, substantial RV outflow obstruction. Additionally, unlike the left coronary artery, the RCA is perfused during both systole and diastole. Consequently, high RV cavity pressure especially impairs normal RCA systolic perfusion [325] likely by congesting the Thebesian vessels [326].

Yet, the immediate effects of PE upon the human RV are more-or-less a mystery; studying patients who present minutes-to-hours after a PE undoubtedly represents a selection bias [294]. Another blatant confound is underlying cardiopulmonary co-morbidities [294, 298, 327]. So when we encounter the ubiquitous claim of RV ischemia and/or infarction [RVI] contributing to the pathophysiology of PE [293, 295, 297, 328], we may rightfully wonder if RVI is a pure and inevitable consequence of PE. To better clarify this question and avoid the aforementioned confounds, this brief section – unless otherwise stated – considers animal models of PE and human studies with subjects free from cardiopulmonary disease.

Pressure-Volume Loops and Oxygen Demand

The normal human mean pulmonary arterial pressure [mPAP] is 14 mmHg at rest [329]. Pulmonary emboli obstructing 25-30% of the pulmonary vasculature increases the mPAP moderately – to roughly 20-30 mmHg or 1.5-to-2 times normal – in healthy adults [294]. At this level of obstruction, RV size usually grows [293]. Remarkably, however, stroke volume [SV] is preserved or elevated with this PE severity [298]. How?

The investigators found that increased cardiac output was strongly and negatively associated with the partial pressure of arterial oxygen [PaO_2]. Given that hypoxemia is a strong adrenergic stimulus, sympathetic tone likely maintained SV by two general mechanisms:

1. Increasing end-diastolic volume [EDV] secondary to augmented venous return [293, 302]

2. Lowering end-systolic volume [ESV] by enhancing RV contractility [see figure 44].

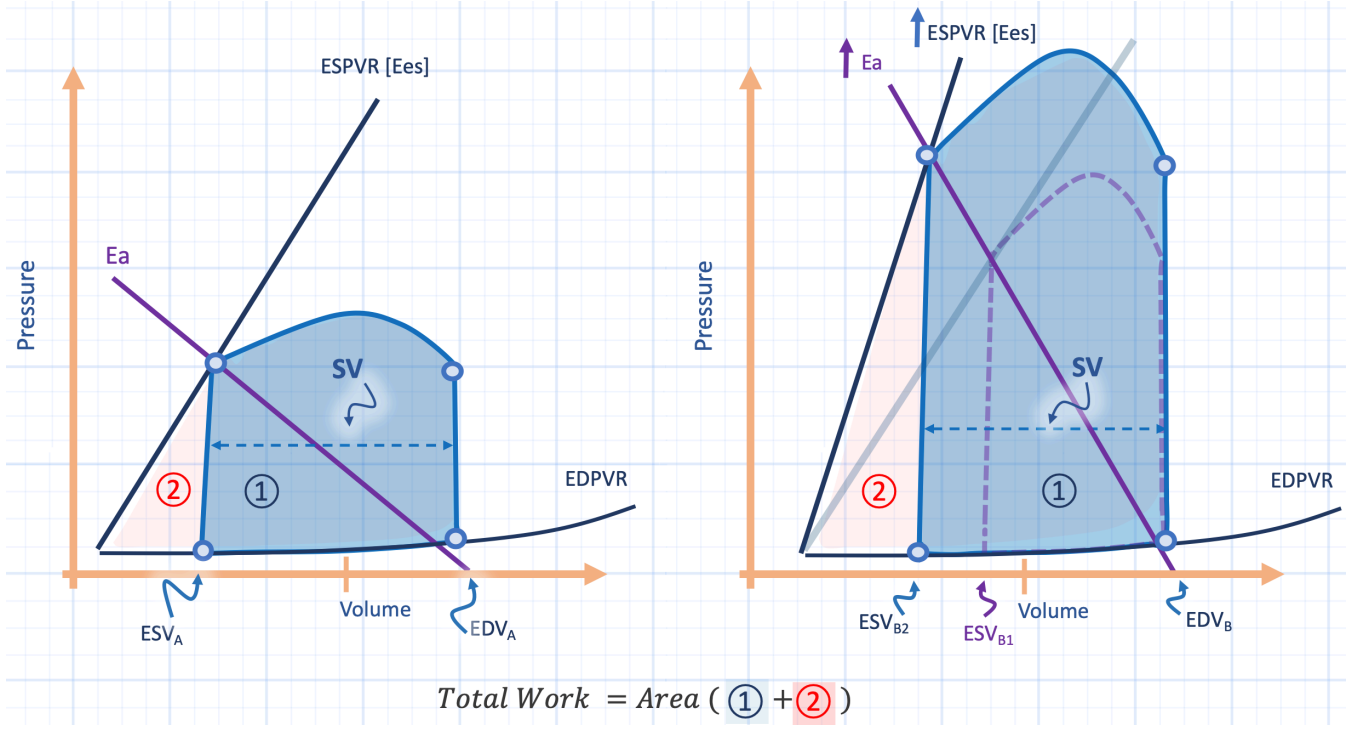

Figure 44: Effects of PE on RV pressure-volume [PV] loop. Note, this assumes that the RV has a similar qualitative PV loop as the LV [see chapter 2]. Left panel shows baseline and right panel shows the effect of PE [increased Ea, arterial elastance - slope of purple line]. Without concomitant increase in RV contractility [end-systolic pressure volume relationship, ESPVR], end-systolic volume would rise to ESVB1 [purple]. With augmented ESPVR, ESV falls to ESVB2 and stroke volume [SV] is preserved. EDPVR is end-diastolic pressure volume relationship, EDV is end-diastolic volume. Total work is proportional to myocardial oxygen demand and represents sum of areas of blue and red shade.

As seen in the figure, PE 'uncouples' RV function from the pulmonary artery [PA]; this topic was considered above for the left ventricle. The increase in 'pulmonary vascular resistance' or – more accurately – impedance [330] secondary to PE is

graphically modelled as increased pulmonary arterial elastance [Ea]. A selective rise in Ea pulls ESV up with it – to the detriment of SV – and RV-PA uncoupling has commenced. Yet, as above, enhanced RV systolic elastance [Es] [i.e. increased contractility] pushes ESV back down. If this is coupled with increased venous return to raise EDV, then one sees how SV is preserved or even increased! Yet this new, compensated state has increased total RV work [i.e. the total shaded area] which is directly proportional to myocardial oxygen demand [99].

Given that RV work – and therefore oxygen demand – rises with acute PE, one might expect RCA flow to grow in tandem. Measurements of RCA flow in more severe cases of RV outflow obstruction will enlighten, described next.

Oxygen Demand and Right Coronary Flow

Interestingly, in healthy adults following a very large acute PE [i.e. > 50% by angiography] an mPAP above 40 mmHg was never observed. Indeed, 'severe' pulmonary hypertension was graded as a value between 30 and 40 mmHg [294, 298] or about 2-to-3 times normal. At this level, RVEDP was essentially always elevated [298]. What can we say about RCA perfusion here? Does the elevated RVEDP impair RCA flow?

In a series of interesting animal studies, mPAP was increased to the aforementioned levels [i.e. 2-3 times normal] and then to the point of RV failure [defined as decreasing SV in the face of rising RVEDP] [297, 299, 300]. Absolute RCA flow, flow-demand ratios and biopsies for evidence of biochemical ischemia were obtained. At all levels of mPAP and even during RV failure, when RVEDP was elevated, total RCA flow increased. Further, when the pericardium was intact, there was no biochemical evidence of RCA ischemia, even during RV failure! Interestingly, the oxygen supply – demand ratio did progressively fall with worsening RV outflow impedance. This was measured as the ratio of RCA flow to RV tension-time index [297]. Thus, as predicted by the pressure-volume loops, demand rose and even outpaced supply, despite the absence of biochemical ischemia.

Importantly, a more recent porcine study replicated that aforementioned [331]. Similar degrees of mPAP were achieved with no biochemical or histopathological evidence for RV ischemia, even after many hours. Notably, serum troponin levels rose, but on histopathology, myocardial necrosis was limited to islands around adrenergic nerve terminals – suggesting that cell death was not secondary to oxygen debt, but rather adrenergic toxicity [332].

In aggregate, the animal studies in which frank RV ischemia was observed, almost ubiquitously required not simply a fall in SV or rise in RVEDP, but also decreased MAP [325, 328, 333, 334].

The Caveat

As stated at the outset, the reasoning above is restricted to animal models and relatively healthy humans. Obviously, patients treated for PE frequently have cardiopulmonary comorbidities including RCA obstruction. Indeed, even in animal models, RV dysfunction occurred sooner when RCA flow was compromised [325] and case series of humans with RV infarction do exist, even in those without RCA obstruction. Nevertheless, hypotension and cardiac arrest often muddy the precipitating force behind RV myocardial injury [335].

Clinical implication

In totality, and most simply, the above highlight the importance of hypotension in acute PE. It may be that the primum movens of RV ischemia is decreased MAP [328]. This also explains why hypotension is a better prognosticator than angiographic obstruction [293] and why therapies that boost MAP such as balloon occlusion of the aorta [326], intra-arterial injection of blood [i.e. to raise MAP!] [326] and norepinephrine [314] have salutary effects on the RV in acute PE.

Conclusion

The pressure-flow plot of the cardiovascular system models many physiological phenomena germane to caring for the critically-ill. For example, ventricular size during cardiac arrest, collapse and distension of the inferior vena cava, great vein Doppler pulsations, stroke volume variation and other aspects of hemodynamic monitoring. But tying the Guyton diagram to the Campbell diagram focuses the interrelations of the heart and the lungs. This mechanical link intimates that energetic uncoupling between the alveolus and pleural space might also uncouple the heart from the vascular system. The thorax is the nexus of mechanical power applied not only to the lung, but also the heart. Accordingly, injurious energetics within the chest reach the tissues via hemodynamics. Both the 'forward' arterial and 'reverse' venous systems are risked by aberrant thoracic power. Future investigation might reveal that efficient energy transfer within the moving organs optimizes these systems; new models are prerequisites for these avenues of inquiry.

References

1. Gelman S: Venous function and central venous pressure: a physiologic story. Anesthesiology 2008, 108(4):735-748.
2. Rothe CF: Physiology of venous return. An unappreciated boost to the heart. Archives of internal medicine 1986, 146(5):977-982.
3. Magder S: Bench-to-bedside review: An approach to hemodynamic monitoring - Guyton at the bedside. Crit Care 2012, 16(5):236.
4. Feihl F, Broccard AF: Interactions between respiration and systemic hemodynamics. Part I: basic concepts. Intensive care medicine 2009, 35(1):45-54.
5. Broccard AF: Cardiopulmonary interactions and volume status assessment. Journal of clinical monitoring and computing 2012, 26(5):383-391.
6. Jacobsohn E, Chorn R, OConnor M: The role of the vasculature in regulating venous return and cardiac output: historical and graphical approach. Can J Anaesth 1997, 44(8):849-867.
7. Funk DJ, Jacobsohn E, Kumar A: The role of venous return in critical illness and shock-part I: physiology. Critical care medicine 2013, 41(1):255-262.
8. Guyton AC: Determination of cardiac output by equating venous return curves with cardiac response curves. Physiological reviews 1955, 35(1):123-129.
9. Magder S: How to use central venous pressure measurements. Curr Opin Crit Care 2005, 11(3): 264-270.
10. Marik PE, Cavallazzi R: Does the central venous pressure predict fluid responsiveness? An updated meta-analysis and a plea for some common sense. Critical care medicine 2013, 41(7): 1774-1781.
11. Shippy CR, Appel PL, Shoemaker WC: Reliability of clinical monitoring to assess blood volume in critically ill patients. Critical care medicine 1984, 12(2):107-112.
12. Kumar A, Anel R, Bunnell E et al: Pulmonary artery occlusion pressure and central venous pressure fail to predict ventricular filling volume, cardiac performance, or the response to volume infusion in normal subjects. Critical care medicine 2004, 32(3):691-699.
13. Bodson L, Vieillard-Baron A: Respiratory variation in inferior vena cava diameter: surrogate of central venous pressure or parameter of fluid responsiveness? Let the physiology reply. Crit Care 2012, 16(6):181.
14. Maas JJ, Geerts BF, van den Berg PC et al: Assessment of venous return curve and mean systemic filling pressure in postoperative cardiac surgery patients. Critical care medicine 2009, 37(3):912-918.
15. Jansen JR, Maas JJ, Pinsky MR: Bedside assessment of mean systemic filling pressure. Current opinion in critical care 2010, 16(3):231-236.
16. Maas JJ, de Wilde RB, Aarts LP et al: Determination of vascular waterfall phenomenon by bedside measurement of mean systemic filling pressure and critical closing pressure in the intensive care unit. Anesthesia and analgesia 2012, 114(4):803-810.
17. Maas JJ, Pinsky MR, de Wilde RB et al: Cardiac output response to norepinephrine in postoperative cardiac surgery patients: interpretation with venous return and cardiac function curves. Critical care medicine 2013, 41(1):143-150.
18. Persichini R, Silva S, Teboul JL et al: Effects of norepinephrine on mean systemic pressure and venous return in human septic shock. Critical care medicine 2012, 40(12):3146-3153.
19. Rastegarpanah M, Magder S: Role of sympathetic pathways in the vascular response to sepsis. Journal of critical care 1998, 13:169-176.
20. Datta P, Magder S: Hemodynamic response to norepinephrine with and without inhibition of nitric oxide synthase in porcine endotoxemia. American journal of respiratory and critical care medicine 1999, 160(6):1987-1993.
21. Aya HD, Cecconi M: Can (and should) the venous tone be monitored at the bedside? Current opinion in critical care 2015, 21(3):240-244.
22. Starr I: Role of the" static blood pressure" in abnormal increments of venous pressure, especially in heart failure. ii. clinical and experimental studies. The American Journal of the Medical Sciences 1940, 199(1):40-54.
23. Magder S, De Varennes B: Clinical death and the measurement of stressed vascular volume. Critical care medicine 1998, 26(6):1061-1064.
24. Repessé X, Charron C, Fink J et al: Value and determinants of the mean systemic filling pressure in critically ill patients. American Journal of Physiology-Heart and Circulatory Physiology 2015, 309(5):H1003-H1007.
25. Schipke J, Heusch G, Sanii A et al: Static filling pressure in patients during induced ventricular fibrillation. American Journal of Physiology-Heart and Circulatory Physiology 2003, 285(6):H2510-H2515.
26. Pinsky MR: Instantaneous venous return curves in an intact canine preparation. Journal of applied physiology: respiratory, environmental and exercise physiology 1984, 56(3):765-771.

27. Maas JJ, Pinsky MR, Geerts BF et al: Estimation of mean systemic filling pressure in postoperative cardiac surgery patients with three methods. Intensive care medicine 2012, 38(9): 1452-1460.
28. Parkin WG, Leaning MS: Therapeutic control of the circulation. Journal of clinical monitoring and computing 2008, 22(6):391-400.
29. Fessler HE, Brower RG, Wise RA et al: Effects of Positive End-Expiratory Pressure on the Gradient for Venous Return. Am Rev Respir Dis 1991, 143(1):19-24.
30. Fessler HE: Heart-lung interactions: applications in the critically ill. The European respiratory journal 1997, 10(1):226-237.
31. Jellinek H, Krenn H, Oczenski W et al: Influence of positive airway pressure on the pressure gradient for venous return in humans. J Appl Physiol (1985) 2000, 88(3):926-932.
32. Luecke T, Pelosi P: Clinical review: Positive end-expiratory pressure and cardiac output. Crit Care 2005, 9(6):607-621.
33. Pinsky MR: Determinants of pulmonary arterial flow variation during respiration. Journal of applied physiology: respiratory, environmental and exercise physiology 1984, 56(5):1237-1245.
34. Berger D, Moller PW, Weber A et al: Effect of PEEP, blood volume, and inspiratory hold maneuvers on venous return. American journal of physiology-heart and circulatory physiology 2016, 311(3):H794-H806.
35. Guarracino F, Bertini P, Pinsky MR: Cardiovascular determinants of resuscitation from sepsis and septic shock. Critical Care 2019, 23(1):118.
36. Cecconi M, Aya HD, Geisen M et al: Changes in the mean systemic filling pressure during a fluid challenge in postsurgical intensive care patients. Intensive care medicine 2013, 39(7): 1299-1305.
37. Aagaard R, Granfeldt A, Bøtker MT et al: The Right Ventricle Is Dilated During Resuscitation From Cardiac Arrest Caused by Hypovolemia: A Porcine Ultrasound Study. Critical care medicine 2017.
38. Kuehne T, Gleason BK, Saeed M et al: Combined pulmonary stenosis and insufficiency preserves myocardial contractility in the developing heart of growing swine at midterm follow-up. Journal of Applied Physiology 2005, 99(4):1422-1427.
39. Pinsky MR: My paper 20 years later: Effect of positive end-expiratory pressure on right ventricular function in humans. Intensive care medicine 2014, 40(7):935-941.
40. Muller L, Bobbia X, Toumi M et al: Respiratory variations of inferior vena cava diameter to predict fluid responsiveness in spontaneously breathing patients with acute circulatory failure: need for a cautious use. Crit Care 2012, 16(5):R188.
41. Corl K, Napoli AM, Gardiner F: Bedside sonographic measurement of the inferior vena cava caval index is a poor predictor of fluid responsiveness in emergency department patients. Emergency medicine Australasia : EMA 2012, 24(5):534-539.
42. Magder S, Bafaqeeh F: The clinical role of central venous pressure measurements. Journal of intensive care medicine 2007, 22(1):44-51.
43. Lloyd TC, Jr.: Effect of inspiration on inferior vena caval blood flow in dogs. Journal of applied physiology: respiratory, environmental and exercise physiology 1983, 55(6):1701-1708.
44. Rubinson RM, Vasko JS, Doppman JL et al: Inferior Vena Caval Obstruction from Increased Intra-Abdominal Pressure - Experimental Hemodynamic and Angiographic Observations. Arch Surg-Chicago 1967, 94(6):766-&.
45. Kimura BJ, Dalugdugan R, Gilcrease GW et al: The effect of breathing manner on inferior vena caval diameter. Eur J Echocardiogr 2011, 12(2).
46. Juhl-Olsen P, Frederiksen CA, Sloth E: Ultrasound assessment of inferior vena cava collapsibility is not a valid measure of preload changes during triggered positive pressure ventilation: a controlled cross-over study. Ultraschall Med 2012, 33(2):152-159.
47. Fessler HE, Brower RG, Wise RA et al: Effects of positive end-expiratory pressure on the canine venous return curve. The American review of respiratory disease 1992, 146(1):4-10.
48. Fessler HE: Effects of CPAP on venous return. Journal of sleep research 1995, 4(S1):44-49.
49. van den Berg PC, Jansen JR, Pinsky MR: Effect of positive pressure on venous return in volume-loaded cardiac surgical patients. J Appl Physiol (1985) 2002, 92(3):1223-1231.
50. Peters J, Hecker B, Neuser D et al: Regional blood volume distribution during positive and negative airway pressure breathing in supine humans. J Appl Physiol (1985) 1993, 75(4):1740-1747.
51. Takata M, Wise RA, Robotham JL: Effects of abdominal pressure on venous return: abdominal vascular zone conditions. J Appl Physiol (1985) 1990, 69(6):1961-1972.
52. Robotham JL, Takata M: Mechanical abdomino/heart/lung interaction. Journal of sleep research 1995, 4(S1):50-52.
53. Gattinoni L, Chiumello D, Carlesso E et al: Bench-to-bedside review: chest wall elastance in acute lung injury/acute respiratory distress syndrome patients. Crit Care 2004, 8(5):350-355.
54. Takata M, Robotham JL: Effects of inspiratory diaphragmatic descent on inferior vena caval venous return. J Appl Physiol (1985) 1992, 72(2):597-607.
55. Biondi JW, Schulman DS, Soufer R et al: The effect of incremental positive end-expiratory pressure on right ventricular hemodynamics and ejection fraction. Anesthesia and analgesia 1988, 67(2):144-151.
56. Cassidy S, Eschenbacher W, Robertson C et al: Cardiovascular effects of positive-pressure ventilation in normal subjects. Journal of applied physiology 1979, 47(2):453-461.

57. Corl KA, George NR, Romanoff J et al: Inferior vena cava collapsibility detects fluid responsiveness among spontaneously breathing critically-ill patients. Journal of Critical Care 2017, 41:130-137.
58. Airapetian N, Maizel J, Alyamani O et al: Does inferior vena cava respiratory variability predict fluid responsiveness in spontaneously breathing patients? Critical Care 2015, 19(1):400.
59. Reddi B, Carpenter R: Venous excess: a new approach to cardiovascular control and its teaching. Journal of applied physiology 2005, 98(1):356-364.
60. Brengelmann GL: A critical analysis of the view that right atrial pressure determines venous return. Journal of applied physiology 2003, 94(3):849-859.
61. Greene AS, Shoukas AA: Changes in canine cardiac function and venous return curves by the carotid baroreflex. American Journal of Physiology-Heart and Circulatory Physiology 1986, 251(2):H288-H296.
62. Hatanaka T, Potts JT, Shoukas AA: Invariance of the resistance to venous return to carotid sinus baroreflex control. American Journal of Physiology-Heart and Circulatory Physiology 1996, 271(3):H1022-H1030.
63. Levy MN: The cardiac and vascular factors that determine systemic blood flow. Circulation research 1979, 44(6):739-747.
64. Magder S: Point: Counterpoint: The classical Guyton view that mean systemic pressure, right atrial pressure, and venous resistance govern venous return is/is not correct. Journal of applied physiology 2006, 101(5):1523-1525.
65. Brengelmann G: Counterpoint: the classical Guyton view that mean systemic pressure, right atrial pressure, and venous resistance govern venous return is not correct. Journal of applied physiology 2006, 101(5):1525-1526.
66. Pinsky MR: The classical Guyton view that mean systemic pressure, right atrial pressure, and venous resistance govern venous return is/is not correct. Journal of applied physiology 2006, 101(5):1528-1530.
67. Guyton AC, CE Coleman T: Circulatory physiology: cardiac output and its regulation. 1973.
68. Deschamps A, Magder S: Baroreflex control of regional capacitance and blood flow distribution with or without alpha-adrenergic blockade. American Journal of Physiology-Heart and Circulatory Physiology 1992, 263(6):H1755-H1763.
69. Deschamps A, Fournier A, Magder S: Influence of neuropeptide Y on regional vascular capacitance in dogs. American Journal of Physiology-Heart and Circulatory Physiology 1994, 266(1):H165-H170.
70. Deschamps A, Magder S: Effects of heat stress on vascular capacitance. American Journal of Physiology-Heart and Circulatory Physiology 1994, 266(5):H2122-H2129.
71. Mitzner W, Goldberg H: Effects of epinephrine on resisitive and compliant properties of the canine vasculature. Journal of applied physiology 1975, 39(2):272-280.
72. Moller PW, Winkler B, Hurni S et al: Right atrial pressure and venous return during cardiopulmonary bypass. American journal of physiology-heart and circulatory physiology 2017, 313(2):H408-H420.
73. Henderson WR, Griesdale DE, Walley KR et al: Clinical review: Guyton–the role of mean circulatory filling pressure and right atrial pressure in controlling cardiac output. Crit Care 2010, 14(6):243.
74. Funk DJ, Jacobsohn E, Kumar A: Role of the venous return in critical illness and shock: part II-shock and mechanical ventilation. Critical care medicine 2013, 41(2):573-579.
75. Michard F, Teboul JL: Using heart-lung interactions to assess fluid responsiveness during mechanical ventilation. Crit Care 2000, 4(5):282-289.
76. Marik PE, Baram M, Vahid B: Does central venous pressure predict fluid responsiveness? A systematic review of the literature and the tale of seven mares. Chest 2008, 134(1):172-178.
77. Magder S: Central venous pressure: A useful but not so simple measurement. Critical care medicine 2006, 34(8):2224-2227.
78. Magder S: Central venous pressure monitoring. Curr Opin Crit Care 2006, 12(3):219-227.
79. Magder S: Right Atrial Pressure in the Critically Ill: How to Measure, What Is the Value, What Are the Limitations? Chest 2017, 151(4):908-916.
80. McNaughton DA, Abu-Yousef MM: Doppler US of the liver made simple. Radiographics 2011, 31(1):161-188.
81. Khurram IM, Maqbool F, Berger RD et al: Association between left atrial stiffness index and atrial fibrillation recurrence in patients undergoing left atrial ablation. Circulation: Arrhythmia and Electrophysiology 2016, 9(3):e003163.
82. Magder S: Central venous pressure monitoring. Current opinion in critical care 2006, 12(3): 219-227.
83. Scheinfeld MH, Bilali A, Koenigsberg M: Understanding the spectral Doppler waveform of the hepatic veins in health and disease. Radiographics 2009, 29(7):2081-2098.
84. Magder S, Erice F, Lagonidis D: Determinants of the Y Descent and its Usefulness as a Predictor of Ventricular Filling. Journal of Intensive Care Medicine 2000, 15(5):262-269.
85. Appleton CP, Hatle LK, Popp RL: Superior vena cava and hepatic vein Doppler echocardiography in healthy adults. Journal of the American College of Cardiology 1987, 10(5): 1032-1039.

86. Abu-Yousef MM: Normal and respiratory variations of the hepatic and portal venous duplex Doppler waveforms with simultaneous electrocardiographic correlation. Journal of ultrasound in medicine 1992, 11(6):263-268.
87. Sivaciyan V, Ranganathan N: Transcutaneous doppler jugular venous flow velocity recording. Circulation 1978, 57(5):930-939.
88. Tabata T, Thomas JD, Klein AL: Pulmonary venous flow by Doppler echocardiography: revisited 12 years later. Journal of the American College of Cardiology 2003, 41(8):1243-1250.
89. Hou Y, Sun D-D, Yuan L-J et al: Clinical application of superior vena cava spectra in evaluation of pulmonary hypertension: a comparative echocardiography and catheterization study. Ultrasound in Medicine and Biology 2016, 42(1):110-117.
90. Ghio S, Recusani F, Sebastiani R et al: Doppler velocimetry in superior vena cava provides useful information on the right circulatory function in patients with congestive heart failure. Echocardiography 2001, 18(6):469-477.
91. Tremblay J-A, Beaubien-Souligny W, Elmi-Sarabi M et al: Point-of-care ultrasonography to assess portal vein pulsatility and the effect of inhaled milrinone and epoprostenol in severe right ventricular failure: A report of 2 cases. A&A Case Reports 2017, 9(8):219-223.
92. Iida N, Seo Y, Sai S et al: Clinical implications of intrarenal hemodynamic evaluation by Doppler ultrasonography in heart failure. JACC: Heart Failure 2016, 4(8):674-682.
93. Tang WW, Kitai T: Intrarenal venous flow: a window into the congestive kidney failure phenotype of heart failure? JACC: Heart Failure 2016, 4(8):683-686.
94. Sunagawa K, Maughan WL, Burkhoff D et al: Left ventricular interaction with arterial load studied in isolated canine ventricle. American Journal of Physiology-Heart and Circulatory Physiology 1983, 245(5):H773-H780.
95. Chantler PD, Lakatta EG, Najjar SS: Arterial-ventricular coupling: mechanistic insights into cardiovascular performance at rest and during exercise. Journal of applied physiology 2008, 105(4):1342-1351.
96. Kelly RP, Ting C-T, Yang T-M et al: Effective arterial elastance as index of arterial vascular load in humans. Circulation 1992, 86(2):513-521.
97. Guarracino F, Ferro B, Morelli A et al: Ventriculoarterial decoupling in human septic shock. Critical Care 2014, 18(2):R80.
98. Guarracino F, Baldassarri R, Pinsky MR: Ventriculo-arterial decoupling in acutely altered hemodynamic states. Critical Care 2013, 17(2):213.
99. Walley KR: Left ventricular function: time-varying elastance and left ventricular aortic coupling. Critical care 2016, 20(1):270.
100. Borlaug BA, Kass DA: Ventricular–vascular interaction in heart failure. Cardiology clinics 2011, 29(3):447-459.
101. Chen C-H, Fetics B, Nevo E et al: Noninvasive single-beat determination of left ventricular end-systolic elastance in humans. Journal of the American College of Cardiology 2001, 38(7): 2028-2034.
102. Yotti R, Bermejo J, Benito Y et al: Validation of noninvasive indices of global systolic function in patients with normal and abnormal loading conditions: a simultaneous echocardiography pressure–volume catheterization study. Circulation: Cardiovascular Imaging 2014, 7(1):164-172.
103. Kumar A, Anel R, Bunnell E et al: Preload-independent mechanisms contribute to increased stroke volume following large volume saline infusion in normal volunteers: a prospective interventional study. Critical Care 2004, 8(3):R128.
104. García MIM, González PG, Romero MG et al: Effects of fluid administration on arterial load in septic shock patients. Intensive care medicine 2015, 41(7):1247-1255.
105. Parkin WG, Leaning MS: Therapeutic control of the circulation. Journal of clinical monitoring and computing 2008, 22(6):391-400.
106. Parkin W, Wright C: Three dimensional closed loop control of the human circulation. International journal of clinical monitoring and computing 1991, 8(1):35.
107. Magder S: Volume and its relationship to cardiac output and venous return. Critical care 2016, 20(1):271.
108. Gupta K, Sondergaard S, Parkin G et al: Applying mean systemic filling pressure to assess the response to fluid boluses in cardiac post-surgical patients. Intensive care medicine 2015, 41(2): 265-272.
109. Sondergaard S, Larsson JS, Möller PW: The haemodynamic effects of crystalloid and colloid volume resuscitation on primary, derived and efficiency variables in post-CABG patients. Intensive Care Medicine Experimental 2019, 7(1):13.
110. Sondergaard S, Parkin G, Aneman A: Central venous pressure: soon an outcome-associated matter. Current Opinion in Anesthesiology 2016, 29(2):179-185.
111. Denault AY, Beaubien-Souligny W, Elmi-Sarabi M et al: Clinical Significance of Portal Hypertension Diagnosed With Bedside Ultrasound After Cardiac Surgery. Anesthesia & Analgesia 2017, 124(4):1109-1115.
112. Beaubien-Souligny W, Denault A, Robillard P et al: The Role of Point-of-Care Ultrasound Monitoring in Cardiac Surgical Patients With Acute Kidney Injury. Journal of Cardiothoracic and Vascular Anesthesia 2018.
113. Beaubien–Souligny W, Benkreira A, Robillard P et al: Alterations in Portal Vein Flow and Intrarenal Venous Flow Are Associated With Acute Kidney Injury After Cardiac Surgery: A

Prospective Observational Cohort Study. Journal of the American Heart Association 2018, 7(19):e009961.
114. Magder S, Scharf SM: Venous return; Magder, Sheldon, and Steven M. Scharf. "Venous return." Lung Biology in Health and Disease 157 (2001): 93-112.
115. Eljaiek R, Cavayas Y, Rodrigue E et al: High postoperative portal venous flow pulsatility indicates right ventricular dysfunction and predicts complications in cardiac surgery patients. British journal of anaesthesia 2019, 122(2):206-214.
116. Nihei Y, Sasanuma H, Yasuda Y: Experimental evaluation of portal venous pulsatile flow synchronized with heartbeat intervals. Journal of Medical Ultrasonics 2011, 38(3):141-149.
117. Nihei Y, Sasanuma H, Yasuda Y: Experimental evaluation of portal venous pulsatile flow synchronized with heartbeat intervals: effects of vascular clamping on portal hemodynamics. Journal of Medical Ultrasonics 2013, 40(1):9-18.
118. Gallix B, Taourel P, Dauzat M et al: Flow pulsatility in the portal venous system: a study of Doppler sonography in healthy adults. AJR American journal of roentgenology 1997, 169(1): 141-144.
119. Pinsky MR, Payen D: Functional hemodynamic monitoring. Crit Care 2005, 9(6):566-572.
120. Pinsky MR: Recent advances in the clinical application of heart-lung interactions. Current opinion in critical care 2002, 8(1):26-31.
121. Mesquida J, Kim HK, Pinsky MR: Effect of tidal volume, intrathoracic pressure, and cardiac contractility on variations in pulse pressure, stroke volume, and intrathoracic blood volume. Intensive care medicine 2011, 37(10):1672-1679.
122. Jardin F, Genevray B, Brun-Ney D et al: Influence of lung and chest wall compliances on transmission of airway pressure to the pleural space in critically ill patients. Chest 1985, 88(5): 653-658.
123. Michard F, Boussat S, Chemla D et al: Relation between respiratory changes in arterial pulse pressure and fluid responsiveness in septic patients with acute circulatory failure. American journal of respiratory and critical care medicine 2000, 162(1):134-138.
124. Barbier C, Loubieres Y, Schmit C et al: Respiratory changes in inferior vena cava diameter are helpful in predicting fluid responsiveness in ventilated septic patients. Intensive care medicine 2004, 30(9):1740-1746.
125. Vieillard-Baron A, Chergui K, Rabiller A et al: Superior vena caval collapsibility as a gauge of volume status in ventilated septic patients. Intensive care medicine 2004, 30(9):1734-1739.
126. Denault AY, Gasior TA, Gorcsan J, 3rd et al: Determinants of aortic pressure variation during positive-pressure ventilation in man. Chest 1999, 116(1):176-186.
127. Mitchell JR, Whitelaw WA, Sas R et al: RV filling modulates LV function by direct ventricular interaction during mechanical ventilation. American journal of physiology Heart and circulatory physiology 2005, 289(2):H549-557.
128. Buda AJ, Pinsky MR, Ingels NB, Jr. et al: Effect of intrathoracic pressure on left ventricular performance. The New England journal of medicine 1979, 301(9):453-459.
129. Brower R, Wise RA, Hassapoyannes C et al: Effect of lung inflation on lung blood volume and pulmonary venous flow. J Appl Physiol (1985) 1985, 58(3):954-963.
130. Scharf SM, Brown R, Saunders N et al: Hemodynamic effects of positive-pressure inflation. Journal of applied physiology: respiratory, environmental and exercise physiology 1980, 49(1): 124-131.
131. Magder S: Clinical usefulness of respiratory variations in arterial pressure. American journal of respiratory and critical care medicine 2004, 169(2):151-155.
132. Soubrier S, Saulnier F, Hubert H et al: Can dynamic indicators help the prediction of fluid responsiveness in spontaneously breathing critically ill patients? Intensive care medicine 2007, 33(7):1117-1124.
133. Heenen S, De Backer D, Vincent JL: How can the response to volume expansion in patients with spontaneous respiratory movements be predicted? Crit Care 2006, 10(4):R102.
134. Magder S: Predicting volume responsiveness in spontaneously breathing patients: still a challenging problem. Crit Care 2006, 10(5):165.
135. Monnet X, Rienzo M, Osman D et al: Passive leg raising predicts fluid responsiveness in the critically ill. Critical care medicine 2006, 34(5):1402-1407.
136. De Backer D, Heenen S, Piagnerelli M et al: Pulse pressure variations to predict fluid responsiveness: influence of tidal volume. Intensive care medicine 2005, 31(4):517-523.
137. Renner J, Cavus E, Meybohm P et al: Stroke volume variation during hemorrhage and after fluid loading: impact of different tidal volumes. Acta anaesthesiologica Scandinavica 2007, 51(5): 538-544.
138. Jacques D, Bendjelid K, Duperret S et al: Pulse pressure variation and stroke volume variation during increased intra-abdominal pressure: an experimental study. Crit Care 2011, 15(1):R33.
139. Duperret S, Lhuillier F, Piriou V et al: Increased intra-abdominal pressure affects respiratory variations in arterial pressure in normovolaemic and hypovolaemic mechanically ventilated healthy pigs. Intensive care medicine 2007, 33(1):163-171.
140. Monnet X, Bleibtreu A, Ferre A et al: Passive leg-raising and end-expiratory occlusion tests perform better than pulse pressure variation in patients with low respiratory system compliance. Critical care medicine 2012, 40(1):152-157.

141. Wyler von Ballmoos M, Takala J, Roeck M et al: Pulse-pressure variation and hemodynamic response in patients with elevated pulmonary artery pressure: a clinical study. Crit Care 2010, 14(3):R111.
142. Daudel F, Tuller D, Krahenbuhl S et al: Pulse pressure variation and volume responsiveness during acutely increased pulmonary artery pressure: an experimental study. Crit Care 2010, 14(3):R122.
143. Magder S: Further cautions for the use of ventilatory-induced changes in arterial pressures to predict volume responsiveness. Critical Care 2010, 14(5).
144. Venus B, Cohen LE, Smith RA: Hemodynamics and intrathoracic pressure transmission during controlled mechanical ventilation and positive end-expiratory pressure in normal and low compliant lungs. Critical care medicine 1988, 16(7):686-690.
145. Mahjoub Y, Pila C, Friggeri A et al: Assessing fluid responsiveness in critically ill patients: False-positive pulse pressure variation is detected by Doppler echocardiographic evaluation of the right ventricle. Critical care medicine 2009, 37(9):2570-2575.
146. Grace MP, Greenbaum DM: Cardiac performance in response to PEEP in patients with cardiac dysfunction. Critical care medicine 1982, 10(6):358-360.
147. Rasanen J, Nikki P, Heikkila J: Acute myocardial infarction complicated by respiratory failure. The effects of mechanical ventilation. Chest 1984, 85(1):21-28.
148. Pizov R, Ya'ari Y, Perel A: The arterial pressure waveform during acute ventricular failure and synchronized external chest compression. Anesthesia and analgesia 1989, 68(2):150-156.
149. De Backer D, Taccone FS, Holsten R et al: Influence of Respiratory Rate on Stroke Volume Variation in Mechanically Ventilated Patients. Anesthesiology 2009, 110(5):1092-1097.
150. Marik PE, Monnet X, Teboul JL: Hemodynamic parameters to guide fluid therapy. Annals of intensive care 2011, 1(1):1.
151. Lewis RP, Rittogers S, Froester W et al: A critical review of the systolic time intervals. Circulation 1977, 56(2):146-158.
152. Garrod AH: On some points connected with the circulation of the blood, arrived at from a study of the sphygmograph-trace. Proceedings of the Royal Society of London 1875, 23(156-163):140-151.
153. Bowen WP: Changes in heart-rate, blood-pressure, and duration of systole resulting from bicycling. American Journal of Physiology-Legacy Content 1904, 11(1):59-77.
154. Katz L, Feil H: Clinical observations on the dynamics of ventricular systole: I. Auricular fibrillation. Archives of Internal Medicine 1923, 32(5):672-692.
155. Boudoulas H: Systolic time intervals. European heart journal 1990, 11(suppl_I):93-104.
156. Atkins CE, Snyder PS: Systolic time intervals and their derivatives for evaluation of cardiac function. Journal of veterinary internal medicine 1992, 6(2):55-63.
157. Weissler AM: Systolic-time intervals. New England Journal of Medicine 1977, 296(6):321-324.
158. Hassan S, Turner P: Systolic time intervals: a review of the method in the non-invasive investigation of cardiac function in health, disease and clinical pharmacology. Postgraduate medical journal 1983, 59(693):423-434.
159. Weissler AM, Peeler RG, Roehll Jr WH: Relationships between left ventricular ejection time, stroke volume, and heart rate in normal individuals and patients with cardiovascular disease. American heart journal 1961, 62(3):367-378.
160. Weissler AM, Harris WS, Schoenfeld CD: Systolic time intervals in heart failure in man. Circulation 1968, 37(2):149-159.
161. Weissler AM, Harris WS, Schoenfeld CD: Bedside technics for the evaluation of ventricular function in man. American Journal of Cardiology 1969, 23(4):577-583.
162. Cybulski G, Michalak E, Koźluk E et al: Stroke volume and systolic time intervals: beat-to-beat comparison between echocardiography and ambulatory impedance cardiography in supine and tilted positions. Medical and Biological Engineering and Computing 2004, 42(5):707-711.
163. Reant P, Dijos M, Donal E et al: Systolic time intervals as simple echocardiographic parameters of left ventricular systolic performance: correlation with ejection fraction and longitudinal two-dimensional strain. European Journal of Echocardiography 2010, 11(10):834-844.
164. Polak JF, Alessi-Chinetti JM, Estes JM et al: Left ventricular ejection time derived from the common carotid artery Doppler waveform: association with left ventricular ejection fraction and prediction of heart failure. Journal of ultrasound in medicine 2015, 34(7):1237-1242.
165. Stafford R, Harris W, Weissler A: Left ventricular systolic time intervals as indices of postural circulatory stress in man. Circulation 1970, 41(3):485-492.
166. Remington JW, Hamilton W, Ahlquist RP: Interrelation between the length of systole, stroke volume and left ventricular work in the dog. American Journal of Physiology-Legacy Content 1948, 154(1):6-15.
167. Braunwald E, Sarnoff S, Stainsby W: Determinants of duration and mean rate of ventricular ejection. Circulation Research 1958, 6(3):319-325.
168. Harley A, Starmer CF, Greenfield JC: Pressure-flow studies in man. An evaluation of the duration of the phases of systole. The Journal of clinical investigation 1969, 48(5):895-905.
169. Shaver JA, Kroetz FW, Leonard JJ et al: The effect of steady-state increases in systemic arterial pressure on the duration of left ventricular ejection time. The Journal of clinical investigation 1968, 47(1):217-230.
170. Lewis RP, Boudoulas H, Welch TG et al: Usefulness of systolic time intervals in coronary artery disease. American Journal of Cardiology 1976, 37(5):787-796.

171. Kelm DJ, Perrin JT, Cartin-Ceba R et al: Fluid overload in patients with severe sepsis and septic shock treated with early-goal directed therapy is associated with increased acute need for fluid-related medical interventions and hospital death. Shock (Augusta, Ga) 2015, 43(1):68.
172. Barjaktarevic I, Toppen WE, Hu S et al: Ultrasound Assessment of the Change in Carotid Corrected Flow Time in Fluid Responsiveness in Undifferentiated Shock. Critical care medicine 2018.
173. Mackenzie DC, Khan NA, Blehar D et al: Ultrasound measurement of carotid flow time changes with volume status. Critical Care 2014, 18(1):P131.
174. Teran F, Dean AJ, Centeno C et al: Evaluation of out-of-hospital cardiac arrest using transesophageal echocardiography in the emergency department. Resuscitation 2019, 137:140-147.
175. Kouwenhoven WB, Jude JR, Knickerbocker GG: Closed-chest cardiac massage. Jama 1960, 173:1064-1067.
176. Weisfeldt ML, Chandra N: Physiology of cardiopulmonary resuscitation. Annual review of medicine 1981, 32:435-442.
177. Mackenzie GJ, Taylor SH, McDonald AH et al: Haemodynamic Effects of External Cardiac Compression. Lancet 1964, 1(7347):1342-1345.
178. Weale FE, Rothwell-Jackson RL: The efficiency of cardiac massage. Lancet 1962, 1(7237): 990-992.
179. Criley JM, Blaufuss AH, Kissel GL: Cough-induced cardiac compression. Self-administered from of cardiopulmonary resuscitation. Jama 1976, 236(11):1246-1250.
180. Hainsworth R: Vascular capacitance: its control and importance. Reviews of physiology, biochemistry and pharmacology 1986, 105:101-173.
181. Werner JA, Greene HL, Janko CL et al: Visualization of cardiac valve motion in man during external chest compression using two-dimensional echocardiography. Implications regarding the mechanism of blood flow. Circulation 1981, 63(6):1417-1421.
182. Redberg RF, Tucker KJ, Cohen TJ et al: Physiology of blood flow during cardiopulmonary resuscitation. A transesophageal echocardiographic study. Circulation 1993, 88(2):534-542.
183. Ma MH, Hwang JJ, Lai LP et al: Transesophageal echocardiographic assessment of mitral valve position and pulmonary venous flow during cardiopulmonary resuscitation in humans. Circulation 1995, 92(4):854-861.
184. Andreka P, Frenneaux MP: Haemodynamics of cardiac arrest and resuscitation. Current opinion in critical care 2006, 12(3):198-203.
185. Hackl W, Simon P, Mauritz W et al: Echocardiographic assessment of mitral valve function during mechanical cardiopulmonary resuscitation in pigs. Anesthesia and analgesia 1990, 70(4): 350-356.
186. Barsan WG, Levy RC: Experimental design for study of cardiopulmonary resuscitation in dogs. Annals of emergency medicine 1981, 10(3):135-137.
187. Georgiou M, Papathanassoglou E, Xanthos T: Systematic review of the mechanisms driving effective blood flow during adult CPR. Resuscitation 2014, 85(11):1586-1593.
188. Krischer JP, Fine EG, Weisfeldt ML et al: Comparison of prehospital conventional and simultaneous compression-ventilation cardiopulmonary resuscitation. Critical care medicine 1989, 17(12):1263-1269.
189. Halperin HR, Tsitlik JE, Gelfand M et al: A preliminary study of cardiopulmonary resuscitation by circumferential compression of the chest with use of a pneumatic vest. The New England journal of medicine 1993, 329(11):762-768.
190. Christenson JM, Hamilton DR, Scott-Douglas NW et al: Abdominal compressions during CPR: hemodynamic effects of altering timing and force. The Journal of emergency medicine 1992, 10(3):257-266.
191. Lurie K, Plaisance P, Sukhum P et al: Mechanical advances in cardiopulmonary resuscitation. Current opinion in critical care 2001, 7(3):170-175.
192. Lurie KG, Lindo C, Chin J: CPR: the P stands for plumber's helper. Jama 1990, 264(13):1661.
193. Frascone RJ, Bitz D, Lurie K: Combination of active compression decompression cardiopulmonary resuscitation and the inspiratory impedance threshold device: state of the art. Current opinion in critical care 2004, 10(3):193-201.
194. Wang CH, Tsai MS, Chang WT et al: Active Compression-Decompression Resuscitation and Impedance Threshold Device for Out-of-Hospital Cardiac Arrest: A Systematic Review and Meta-Analysis of Randomized Controlled Trials. Critical care medicine 2014.
195. Babbs CF: CPR techniques that combine chest and abdominal compression and decompression: hemodynamic insights from a spreadsheet model. Circulation 1999, 100(21):2146-2152.
196. Scharf SM, Ingram RH, Jr.: Influence of abdominal pressure and sympathetic vasoconstriction on the cardiovascular response to positive end-expiratory pressure. The American review of respiratory disease 1977, 116(4):661-670.
197. Jimenez-Herrera MF, Azeli Y, Valero-Mora E et al: Passive leg raise (PLR) during cardiopulmonary (CPR) - a method article on a randomised study of survival in out-of-hospital cardiac arrest (OHCA). BMC emergency medicine 2014, 14:15.
198. Magder S: Fluid status and fluid responsiveness. Curr Opin Crit Care 2010, 16(4):289-296.
199. Meaney PA, Bobrow BJ, Mancini ME et al: Cardiopulmonary resuscitation quality: [corrected] improving cardiac resuscitation outcomes both inside and outside the hospital: a consensus statement from the American Heart Association. Circulation 2013, 128(4):417-435.

200. Mayette M, Gonda J, Hsu JL et al: Propofol infusion syndrome resuscitation with extracorporeal life support: a case report and review of the literature. Annals of intensive care 2013, 3(1):32.
201. Brodie D, Bacchetta M: Extracorporeal membrane oxygenation for ARDS in adults. The New England journal of medicine 2011, 365(20):1905-1914.
202. Sunagawa K, Sagawa K, Maughan WL: Ventricular interaction with the loading system. Annals of biomedical engineering 1984, 12(2):163-189.
203. Sakamoto K, Saku K, Kishi T et al: Prediction of the impact of venoarterial extracorporeal membrane oxygenation on hemodynamics. American journal of physiology Heart and circulatory physiology 2015, 308(8):H921-930.
204. Feihl F, Broccard AF: Interactions between respiration and systemic hemodynamics. Part II: practical implications in critical care. Intensive care medicine 2009, 35(2):198-205.
205. Schwartzstein RM, Parker MJ: Rising PaCO(2) in the ICU: using a physiologic approach to avoid cognitive biases. Chest 2011, 140(6):1638-1642.
206. Lafc G, Budak AB, Yener AU et al: Use of extracorporeal membrane oxygenation in adults. Heart, lung & circulation 2014, 23(1):10-23.
207. Cavarocchi NC, Pitcher HT, Yang Q et al: Weaning of extracorporeal membrane oxygenation using continuous hemodynamic transesophageal echocardiography. The Journal of thoracic and cardiovascular surgery 2013, 146(6):1474-1479.
208. Lahm T, McCaslin CA, Wozniak TC et al: Medical and surgical treatment of acute right ventricular failure. Journal of the American College of Cardiology 2010, 56(18):1435-1446.
209. Lemaire F, Teboul JL, Cinotti L et al: Acute left ventricular dysfunction during unsuccessful weaning from mechanical ventilation. Anesthesiology 1988, 69(2):171-179.
210. Teboul J-L: Weaning-induced cardiac dysfunction: where are we today? Intensive care medicine 2014, 40(8):1069-1079.
211. Tobin MJ: Extubation and the myth of "minimal ventilator settings". American journal of respiratory and critical care medicine 2012, 185(4):349-350.
212. Aaron EA, Johnson BD, Seow CK et al: Oxygen cost of exercise hyperpnea: measurement. J Appl Physiol (1985) 1992, 72(5):1810-1817.
213. Caille V, Amiel J-B, Charron C et al: Echocardiography: a help in the weaning process. Critical care 2010, 14(3):R120.
214. Richard C, Teboul J-L, Archambaud F et al: Left ventricular function during weaning of patients with chronic obstructive pulmonary disease. Intensive care medicine 1994, 20(3):181-186.
215. Moschietto S, Doyen D, Grech L et al: Transthoracic echocardiography with Doppler tissue imaging predicts weaning failure from mechanical ventilation: evolution of the left ventricle relaxation rate during a spontaneous breathing trial is the key factor in weaning outcome. Critical care 2012, 16(3):R81.
216. Nonogi H, Hess OM, Ritter M et al: Diastolic properties of the normal left ventricle during supine exercise. British heart journal 1988, 60(1):30-38.
217. Kasner M, Westermann D, Steendijk P et al: Left ventricular dysfunction induced by nonsevere idiopathic pulmonary arterial hypertension: a pressure-volume relationship study. American journal of respiratory and critical care medicine 2012, 186(2):181-189.
218. Dres M, Teboul J-L, Monnet X: Weaning the cardiac patient from mechanical ventilation. Current opinion in critical care 2014, 20(5):493-498.
219. Vieillard-Baron A, Prin S, Schmitt JM et al: Pressure-volume curves in acute respiratory distress syndrome: clinical demonstration of the influence of expiratory flow limitation on the initial slope. American journal of respiratory and critical care medicine 2002, 165(8):1107-1112.
220. Ishii M, Matsumoto N, Fuyuki T et al: Effects of hemodynamic edema formation on peripheral vs. central airway mechanics. J Appl Physiol (1985) 1985, 59(5):1578-1584.
221. Salome CM, King GG, Berend N: Physiology of obesity and effects on lung function. J Appl Physiol (1985) 2010, 108(1):206-211.
222. Harris P, Segel N, Green I et al: The influence of the airways resistance and alveolar pressure on the pulmonary vascular resistance in chronic bronhcitis. Cardiovascular research 1968, 2(1):84-92.
223. Butler J, Schrijen F, Henriquez A et al: Cause of the raised wedge pressure on exercise in chronic obstructive pulmonary disease. The American review of respiratory disease 1988, 138(2):350-354.
224. Liu J, Shen F, Teboul J-L et al: Cardiac dysfunction induced by weaning from mechanical ventilation: incidence, risk factors, and effects of fluid removal. Critical care 2016, 20(1):369.
225. Dres M, Teboul J-L, Anguel N et al: Passive leg raising performed before a spontaneous breathing trial predicts weaning-induced cardiac dysfunction. Intensive care medicine 2015, 41(3): 487-494.
226. Kuper M, Gunning M, Halder S et al: The short–term effect of hyperoncotic albumin, given alone or with furosemide, on oxygenation in sepsis–induced Acute Respiratory Distress Syndrome. Anaesthesia 2007, 62(3):259-263.
227. Woodcock T: Plasma volume, tissue oedema, and the steady-state Starling principle. Bja Education 2017, 17(2):74-78.
228. Michel CC, Woodcock TE, Curry FRE: Understanding and extending the Starling principle. Acta Anaesthesiologica Scandinavica 2020.
229. Levick JR, Michel CC: Microvascular fluid exchange and the revised Starling principle. Cardiovascular research 2010, 87(2):198-210.

230. Woodcock T, Woodcock TM: Revised Starling equation and the glycocalyx model of transvascular fluid exchange: an improved paradigm for prescribing intravenous fluid therapy. British journal of anaesthesia 2012, 108(3):384-394.
231. Nieuwdorp M, van Haeften TW, Gouverneur MC et al: Loss of endothelial glycocalyx during acute hyperglycemia coincides with endothelial dysfunction and coagulation activation in vivo. Diabetes 2006, 55(2):480-486.
232. Reed RK, Rubin K: Transcapillary exchange: role and importance of the interstitial fluid pressure and the extracellular matrix. Cardiovascular research 2010, 87(2):211-217.
233. Margarson M, Soni N: Changes in serum albumin concentration and volume expanding effects following a bolus of albumin 20% in septic patients. British journal of anaesthesia 2004, 92(6): 821-826.
234. Oczkowski SJ, Klotz L, Mazzetti I et al: Furosemide and albumin for diuresis of edema (fade): a parallel-group, blinded, pilot randomized controlled trial. Journal of critical care 2018, 48:462-467.
235. Mahmoodpoor A, Zahedi S, Pourakbar A et al: Efficacy of furosemide-albumin compared with furosemide in critically ill hypoalbuminemia patients admitted to intensive care unit: a prospective randomized clinical trial. DARU Journal of Pharmaceutical Sciences 2020:1-7.
236. Woodcock T: No more colloid trials! British journal of anaesthesia 2014, 112(4):761.
237. Woodcock T: Ernest Starling and the Colloid Delusion. fluidphysiology.org 2015.
238. Magder S: Phenylephrine and tangible bias. Anesthesia & Analgesia 2011, 113(2):211-213.
239. Magder SA: The highs and lows of blood pressure: toward meaningful clinical targets in patients with shock. Critical care medicine 2014, 42(5):1241-1251.
240. Magder S: The meaning of blood pressure. Critical Care 2018, 22(1):257.
241. Thiele RH, Nemergut EC, Lynch C: The physiologic implications of isolated alpha1 adrenergic stimulation. Anesthesia & Analgesia 2011, 113(2):284-296.
242. Thiele RH, Nemergut EC, Lynch C: The clinical implications of isolated alpha1 adrenergic stimulation. Anesthesia & Analgesia 2011, 113(2):297-304.
243. Nakashima T, Tanikawa J: A study of human aortic distensibility with relation to atherosclerosis and aging. Angiology 1971, 22(8):477-490.
244. Naeije R, Vachiery JL, Yerly P et al: The transpulmonary pressure gradient for the diagnosis of pulmonary vascular disease. The European respiratory journal 2013, 41(1):217-223.
245. Versprille A: Pulmonary vascular resistance. A meaningless variable. Intensive care medicine 1984, 10(2):51-53.
246. Naeije R: Pulmonary vascular resistance. A meaningless variable? Intensive care medicine 2003, 29(4):526-529.
247. Kelly RP, Tunin R, Kass D: Effect of reduced aortic compliance on cardiac efficiency and contractile function of in situ canine left ventricle. Circulation research 1992, 71(3):490-502.
248. Magder SA: The highs and lows of blood pressure: toward meaningful clinical targets in patients with shock. Critical care medicine 2014, 42(5):1241-1251.
249. Lamontagne F, Richards-Belle A, Thomas K et al: Effect of Reduced Exposure to Vasopressors on 90-Day Mortality in Older Critically Ill Patients With Vasodilatory Hypotension: A Randomized Clinical Trial. JAMA 2020.
250. Magder SA: The ups and downs of heart rate. Critical care medicine 2012, 40(1):239-245.
251. Magder S: Pressure-flow relations of diaphragm and vital organs with nitroprusside-induced vasodilatation. Journal of Applied Physiology 1986, 61(2):409-416.
252. Bennett VA, Vidouris A, Cecconi M: Effects of Fluids on the Macro-and Microcirculations. Critical Care 2018, 22(1):74.
253. Khanna A, English SW, Wang XS et al: Angiotensin II for the treatment of vasodilatory shock. New England Journal of Medicine 2017, 377(5):419-430.
254. Corrêa TD, Takala J, Jakob SM: Angiotensin II in septic shock. Critical care 2015, 19(1):98.
255. Persichini R, Silva S, Teboul J-L et al: Effects of norepinephrine on mean systemic pressure and venous return in human septic shock. Critical care medicine 2012, 40(12):3146-3153.
256. Marshall JC: Choosing the Best Blood Pressure Target for Vasopressor Therapy. JAMA 2020.
257. Giuntini C, Maseri A, Bianchi R: Pulmonary vascular distensibility and lung compliance as modified by dextran infusion and subsequent atropine injection in normal subjects. The Journal of clinical investigation 1966, 45(11):1770-1789.
258. Naeije R: Physiology of the pulmonary circulation and the right heart. Current hypertension reports 2013, 15(6):623-631.
259. Karam M, Wise RA, Natarajan TK et al: Mechanism of decreased left ventricular stroke volume during inspiration in man. Circulation 1984, 69(5):866-873.
260. Pinsky MR: Cardiovascular issues in respiratory care. Chest 2005, 128(5 Suppl 2):592S-597S.
261. Simon MA, Rajagopalan N, Mathier MA et al: Tissue Doppler imaging of right ventricular decompensation in pulmonary hypertension. Congest Heart Fail 2009, 15(6):271-276.
262. Dell'Italia LJ, Walsh RA: Application of a time varying elastance model to right ventricular performance in man. Cardiovascular research 1988, 22(12):864-874.
263. Yamaguchi S, Li KS, Harasawa H et al: The left ventricle affects the duration of right ventricular ejection. Cardiovascular research 1993, 27(2):211-215.
264. Sibbald WJ, Driedger AA: Right ventricular function in acute disease states: pathophysiologic considerations. Critical care medicine 1983, 11(5):339-345.

265. Maughan WL, Shoukas AA, Sagawa K et al: Instantaneous pressure-volume relationship of the canine right ventricle. Circulation research 1979, 44(3):309-315.
266. Mitzner W: Resistance of the pulmonary circulation. Clin Chest Med 1983, 4(2):127-137.
267. Lopez-Muniz R, Stephens NL, Bromberger-Barnea B et al: Critical closure of pulmonary vessels analyzed in terms of Starling resistor model. Journal of applied physiology 1968, 24(5):625-635.
268. McGregor M, Sniderman A: On pulmonary vascular resistance: the need for more precise definition. The American journal of cardiology 1985, 55(1):217-221.
269. Harvey RM, Enson Y, Ferrer MI: A reconsideration of the origins of pulmonary hypertension. Chest 1971, 59(1):82-94.
270. Milnor WR: Arterial impedance as ventricular afterload. Circulation research 1975, 36(5):565-570.
271. Saouti N, Westerhof N, Postmus PE et al: The arterial load in pulmonary hypertension. European respiratory review : an official journal of the European Respiratory Society 2010, 19(117):197-203.
272. Rodarte JR, Rehder K: Dynamics of respiration. Comprehensive Physiology 1986.
273. Yanof HM: Biomedical electronics: Davis, 1972.
274. Tedford RJ: Determinants of right ventricular afterload (2013 Grover Conference series). Pulmonary circulation 2014, 4(2):211-219.
275. Westerhof N, Elzinga G, Sipkema P: An artificial arterial system for pumping hearts. Journal of applied physiology 1971, 31(5):776-781.
276. Peters J, Kindred MK, Robotham JL: Transient analysis of cardiopulmonary interactions. II. Systolic events. J Appl Physiol (1985) 1988, 64(4):1518-1526.
277. Peters J, Kindred MK, Robotham JL: Transient analysis of cardiopulmonary interactions. I. Diastolic events. J Appl Physiol (1985) 1988, 64(4):1506-1517.
278. Robotham J, Peters J: Mechanical effects of intrathoracic pressure on ventricular performance. Heart/Lung Interactions 1989:251-283.
279. Gelb AF, Lyons HA, Fairshter RD et al: P pulmonale in status asthmaticus. The Journal of allergy and clinical immunology 1979, 64(1):18-22.
280. Jardin F, Farcot JC, Boisante L et al: Mechanism of paradoxic pulse in bronchial asthma. Circulation 1982, 66(4):887-894.
281. Naeije R, Maarek JM, Chang HK: Pulmonary vascular impedance in microembolic pulmonary hypertension: effects of synchronous high-frequency jet ventilation. Respiration physiology 1990, 79(3):205-217.
282. Muramoto A, Caldwell J, Albert RK et al: Nifedipine dilates the pulmonary vasculature without producing symptomatic systemic hypotension in upright resting and exercising patients with pulmonary hypertension secondary to chronic obstructive pulmonary disease. The American review of respiratory disease 1985, 132(5):963-966.
283. Robotham JL, Mays JB, Williams MA et al: Cardiorespiratory interactions in patients with an artificial heart. Anesthesiology 1990, 73(4):599-609.
284. Charlier AA, Jaumin PM, Pouleur H: Circulatory effects of deep inspirations, blocked expirations and positive pressure inflations at equal transpulmonary pressures in conscious dogs. The Journal of physiology 1974, 241(3):589-605.
285. Busch U, Renner U, Wirtzfeld A et al: Floating pulmonary embolus: unusual cause of recurrent syncope. European heart journal 1984, 5(7):602-605.
286. Prandoni P, Lensing AW, Prins MH et al: Prevalence of pulmonary embolism among patients hospitalized for syncope. New England Journal of Medicine 2016, 375(16):1524-1531.
287. Costantino G, Ruwald MH, Quinn J et al: Prevalence of pulmonary embolism in patients with syncope. JAMA internal medicine 2018, 178(3):356-362.
288. Demircan A, Aygencel G, Keles A et al: Pulmonary embolism presenting as syncope: a case report. Journal of medical case reports 2009, 3(1):7440.
289. Edelson G, Reis ND, Hettinger E: Syncope as a premonitory sign of fatal pulmonary embolism Two case reports. Acta Orthopaedica Scandinavica 1988, 59(1):71-73.
290. Thames MD, Alpert JS, Dalen JE: Syncope in patients with pulmonary embolism. Jama 1977, 238(23):2509-2511.
291. Simpson RJ, Podolak R, Mangano CA et al: Vagal syncope during recurrent pulmonary embolism. Jama 1983, 249(3):390-393.
292. Koutkia P, Wachtel TJ: Pulmonary embolism presenting as syncope: case report and review of the literature. Heart & lung 1999, 28(5):342-347.
293. Wood KE: Major pulmonary embolism: review of a pathophysiologic approach to the golden hour of hemodynamically significant pulmonary embolism. Chest 2002, 121(3):877-905.
294. Sharma G, McIntyre K, Sharma S et al: Clinical and hemodynamic correlates in pulmonary embolism. Clinics in chest medicine 1984, 5(3):421-437.
295. Prewitt RM: Hemodynamic management in pulmonary embolism and acute hypoxemic respiratory failure. Critical care medicine 1990, 18(1 Pt 2):S61-69.
296. Ducas J, Prewitt R: Pathophysiology and therapy of right ventricular dysfunction due to pulmonary embolism. Cardiovascular clinics 1987, 17(2):191-202.
297. Calvin Jr JE: Acute right heart failure: pathophysiology, recognition, and pharmacological management. Journal of cardiothoracic and vascular anesthesia 1991, 5(5):507-513.
298. McIntyre KM, Sasahara AA: The hemodynamic response to pulmonary embolism in patients without prior cardiopulmonary disease. The American journal of cardiology 1971, 28(3):288-294.

299. Calvin J, Quinn B: Right ventricular pressure overload during acute lung injury: Cardiac mechanics and the pathophysiology of right ventricular systolic dysfunction. Journal of Critical Care 1989, 4(4):251-265.
300. Calvin JE: Right ventricular afterload mismatch during acute pulmonary hypertension and its treatment with dobutamine: A pressure segment length analysis in a canine model. Journal of Critical Care 1989, 4(4):239-250.
301. Kontos HA, Levasseur JE, Richardson D et al: Comparative circulatory responses to systemic hypoxia in man and in unanesthetized dog. Journal of applied physiology 1967, 23(3):381-386.
302. Eckstein J, Horsley A: Effects of hypoxia on peripheral venous tone in man. The Journal of laboratory and clinical medicine 1960, 56:847-853.
303. Naeije R, Badagliacca R: The overloaded right heart and ventricular interdependence. Cardiovascular research 2017, 113(12):1474-1485.
304. Hamzaoui O, Monnet X, Teboul J-L: Pulsus paradoxus. In.: Eur Respiratory Soc; 2013.
305. Bove AA, Santamore WP: Ventricular interdependence. Progress in cardiovascular diseases 1981, 23(5):365-388.
306. Takata M, Harasawa Y, Beloucif S et al: Coupled vs. uncoupled pericardial constraint: effects on cardiac chamber interactions. Journal of Applied Physiology 1997, 83(6):1799-1813.
307. Calvin Jr JE, Langlois S, Garneys G: Ventricular interaction in a canine model of acute pulmonary hypertension and its modulation by vasoactive drugs. Journal of critical care 1988, 3(1): 43-55.
308. Kasner M, Westermann D, Steendijk P et al: Left ventricular dysfunction induced by nonsevere idiopathic pulmonary arterial hypertension: a pressure–volume relationship study. American journal of respiratory and critical care medicine 2012, 186(2):181-189.
309. Kingma I, Tyberg J, Smith ER: Effects of diastolic transseptal pressure gradient on ventricular septal position and motion. Circulation 1983, 68(6):1304-1314.
310. Watanabe J, Levine MJ, Bellotto F et al: Effects of coronary venous pressure on left ventricular diastolic distensibility. Circulation research 1990, 67(4):923-932.
311. Goswami N, Blaber AP, Hinghofer-Szalkay H et al: Orthostatic intolerance in older persons: etiology and countermeasures. Frontiers in physiology 2017, 8:803.
312. Castelli R, Tarsia P, Tantardini C et al: Syncope in patients with pulmonary embolism: comparison between patients with syncope as the presenting symptom of pulmonary embolism and patients with pulmonary embolism without syncope. Vascular Medicine 2003, 8(4):257-261.
313. Dalen JE, Mathur VS, Evans H et al: Pulmonary angiography in experimental pulmonary embolism. American heart journal 1966, 72(4):509-520.
314. Molloy WD, Lee K, Girling L et al: Treatment of shock in a canine model of pulmonary embolism. American Review of Respiratory Disease 1984, 130(5):870-874.
315. Ducas J, Duval D, Dasilva H et al: Treatment of canine pulmonary hypertension: effects of norepinephrine and isoproterenol on pulmonary vascular pressure-flow characteristics. Circulation 1987, 75(1):235-242.
316. Ghignone M, Girling L, Prewitt R: Volume expansion versus norepinephrine in treatment of a low cardiac output complicating an acute increase in right ventricular afterload in dogs. Anesthesiology 1984, 60(2):132-135.
317. Prewitt RM, Shiffman F, Greenberg D et al: Recombinant tissue-type plasminogen activator in canine embolic pulmonary hypertension. Effects of bolus versus short-term administration on dynamics of thrombolysis and on pulmonary vascular pressure-flow characteristics. Circulation 1989, 79(4):929-938.
318. Angle MR, Molloy DW, Penner B et al: The cardiopulmonary and renal hemodynamic effects of norepinephrine in canine pulmonary embolism. Chest 1989, 95(6):1333-1337.
319. Layish DT, Tapson VF: Pharmacologic hemodynamic support in massive pulmonary embolism. Chest 1997, 111(1):218-224.
320. Mitzner WA: Resistance of the pulmonary circulation. Clinics in chest medicine 1983, 4(2):127-137.
321. Ducas J, Schick U, Girling L et al: Effects of altered left atrial pressure on pulmonary vascular pressure-flow relationships. American Journal of Physiology-Heart and Circulatory Physiology 1988, 255(1):H19-H25.
322. Duval D, Ducas J, Molloy W et al: Effects of pulmonary (P) emboli (E) and noradrenaline (NE) on pulmonary pressure-flow relationships. Am Rev Respir Dis 1984, 129(4):A63.
323. Lopez-Muniz R, Stephens N, Bromberger-Barnea B et al: Critical closure of pulmonary vessels analyzed in terms of Starling resistor model. Journal of Applied Physiology 1968, 24(5):625-635.
324. Kerbaul F, Rondelet B, Motte S et al: Effects of norepinephrine and dobutamine on pressure load-induced right ventricular failure. Critical care medicine 2004, 32(4):1035-1040.
325. Brooks H, Kirk ES, Vokonas PS et al: Performance of the right ventricle under stress: relation to right coronary flow. The Journal of clinical investigation 1971, 50(10):2176-2183.
326. Spotnitz HM, Berman MA, Epstein SE: Pathophysiology and experimental treatment of acute pulmonary embolism. American heart journal 1971, 82(4):511-520.
327. McIntyre KM, Sasahara AA: Determinants of right ventricular function and hemodynamics after pulmonary embolism. Chest 1974, 65(5):534-543.
328. Lualdi JC, Goldhaber SZ: Right ventricular dysfunction after acute pulmonary embolism: pathophysiologic factors, detection, and therapeutic implications. American heart journal 1995, 130(6):1276-1282.

329. Douschan P, Kovacs G, Avian A et al: Mild elevation of pulmonary arterial pressure as a predictor of mortality. American journal of respiratory and critical care medicine 2018, 197(4): 509-516.
330. Tedford RJ: Determinants of right ventricular afterload (2013 Grover Conference series). Pulmonary circulation 2014, 4(2):211-219.
331. Schmitto JD, Doerge H, Post H et al: Progressive right ventricular failure is not explained by myocardial ischemia in a pig model of right ventricular pressure overload. European Journal of Cardio-Thoracic Surgery 2009, 35(2):229-234.
332. Mühlfeld C, Coulibaly M, Dörge H et al: Ultrastructure of right ventricular myocardium subjected to acute pressure load. The Thoracic and cardiovascular surgeon 2004, 52(06):328-333.
333. Vlahakes GJ, Turley K, Hoffman J: The pathophysiology of failure in acute right ventricular hypertension: hemodynamic and biochemical correlations. Circulation 1981, 63(1):87-95.
334. Gold FL, Bache RJ: Transmural right ventricular blood flow during acute pulmonary artery hypertension in the sedated dog. Evidence for subendocardial ischemia despite residual vasodilator reserve. Circulation research 1982, 51(2):196-204.
335. Coma-Canella I, Gamallo C, Onsurbe PM et al: Acute right ventricular infarction secondary to massive pulmonary embolism. European heart journal 1988, 9(5):534-540.

About the Author

Dr. Kenny obtained his B.Sc. at the University of British Columbia and M.D. at the University of Toronto. He completed his residency and chief residency in general internal medicine at NYU-Langone Medical Center and then moved to Palo Alto to complete his fellowship in pulmonary & critical care medicine at Stanford University Medical Center. As well, he has an M.Sc. in Medical Education from the Karolinska Institutet in Stockholm.

Dr. Kenny is the founder of heart-lung.org and a contributing editor to pulmccm.org. Previously a fixture on the High Line in Manhattan whilst dog-sitting his favourite Yorkie - Benjiboo Sprinkles - Dr. Kenny's time is now spent mostly in Toronto, Canada as Chief Medical Officer and co-founder of Flosonics Medical. His other time is usually lost searching for Proustian moments, the pre-reflective self and lobster rolls in Portland, Maine.

“But between the past which no longer is and the future which is not yet, this moment when he exists is nothing.”

-Simone De Beauvoir

SE
Publishing
House

325 Front Street W.
4th Floor
Toronto, ON. Canada
M5V 2Y1
se-ph.org
ISBN 978-1-7773232-0-2

ISBN 978-1-7773232-0-2